

Weak chelation assisted C-H bond activation via cobaltacycles: A sustainable approach towards the synthesis and functionalization of N-heterocycles

by

SHYAM KUMAR BANJARE

CHEM11201804007

**National Institute of Science Education and Research,
Bhubaneswar, Odisha**

*A thesis submitted to the
Board of Studies in Chemical Sciences
In partial fulfillment of requirements
for the Degree of*

DOCTOR OF PHILOSOPHY

of

HOMI BHABHA NATIONAL INSTITUTE



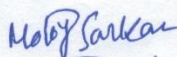
December, 2022

Homi Bhabha National Institute¹

Recommendations of the Viva Voce Committee

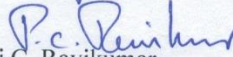
As members of the Viva Voce Committee, we certify that we have read the dissertation prepared by **Shyam Kumar Banjare** entitled “**Weak chelation assisted C-H bond activation via cobaltacycles: A sustainable approach towards the synthesis and functionalization of N-heterocycles**” and recommend that it may be accepted as fulfilling the thesis requirement for the award of Degree of Doctor of Philosophy.

Chairman – Dr. Moloy Sarkar



Date: 20.03.23

Guide / Convener - Dr. Ponneri C. Ravikumar



Date: 20/03/2023

Examiner – Prof. Ramakrishna G. Bhat



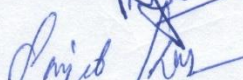
Date: 20/03/2023

Member 1- Dr. Sharanappa Nembenna



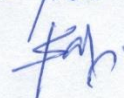
Date: 20/03/2023

Member 2- Dr. Sanjib Kar



Date: 20/03/2023

External Member 3- Dr. Shantanu Pal



Date: 20/03/2023

Final approval and acceptance of this thesis is contingent upon the candidate's submission of the final copies of the thesis to HBNI.

I/We hereby certify that I/we have read this thesis prepared under my/our direction and recommend that it may be accepted as fulfilling the thesis requirement.

Date: 20.03.2023


Signature

Place: NISER, Bhubaneswar

Guide

¹ This page is to be included only for final submission after successful completion of viva voce.

STATEMENT BY AUTHOR

This dissertation has been submitted in partial fulfillment of requirements for an advanced degree at Homi Bhabha National Institute (HBNI) and is deposited in the library to be made available to borrowers under rules of the HBNI.

Brief quotations from this dissertation are allowable without special permission, provided that accurate acknowledgement of source is made. Requests for permission for extended quotation from or reproduction of this manuscript in whole or in part may be granted by the Competent Authority of HBNI when in his or her judgment the proposed use of the material is in the interests of scholarship. In all other instances, however, permission must be obtained from the author.



Shyam Kumar Banjare

DECLARATION

I, hereby declare that the investigation presented in the thesis has been carried out by me. The work is original and has not been submitted earlier as a whole or in part for a degree / diploma at this or any other Institution/University.



Shaym Kumar Banjare

List of Publications

(A) Published Research Paper (#pertaining to thesis):

- #1) **Shyam Kumar Banjare**, Rajesh Chebolu, and P. C. Ravikumar. Cobalt Catalyzed Hydroarylation of Michael Acceptors with Indolines Directed by a Weakly Coordinating Functional Group, *Org. Lett.*, **2019**, 21, 4049.
- #2) **Shyam Kumar Banjare**, Tanmayee Nanda, and P. C. Ravikumar. Cobalt-Catalyzed Regioselective Direct C-4 Alkenylation of 3-Acetyindole with Michael Acceptors Using a Weakly Coordinating Functional Group, *Org. Lett.*, **2019**, 21, 8138.
- #3) **Shyam Kumar Banjare**, Pragati Biswal, P. C. Ravikumar. Cobalt-Catalyzed One-Step Access to Pyroquilon and C-7 Alkenylation of Indoline with Activated Alkenes Using Weakly Coordinating Functional Group, *J. Org. Chem.*, **2020**, 85, 5330.
- #4) **Shyam Kumar Banjare**[†], Tanmayee Nanda[†], Bedadyuti Vedvyas Pati, Gopal Krushna Das Adhikari, Juhi Dutta, and Ponneri C. Ravikumar. Breaking the Trend: Insight into Unforeseen Reactivity of Alkynes in Cobalt-Catalyzed Weak Chelation-Assisted Regioselective C(4)–H Functionalization of 3-Pivaloyl Indole. *ACS Catal.* **2021**, 11, 18, 11579. ([†]equal contribution).
- #5) **Shyam Kumar Banjare**, Annapurna Saxena, Tanmayee Nanda, Namrata Prusty, Sofaya Joshi and Ponneri C. Ravikumar. Weak-chelation assisted cobalt-catalyzed C-H bond activation: A sustainable approach towards regioselective ethynylation of *N*-aryl γ -lactam. *Org. Lett.* **2023**, 25, 251–255.

(B) Communicated Research Paper (# pertaining to thesis):

#6) **Shyam Kumar Banjare**, Saista Afreen, Tanmayee Nanda, Gopal Krusna Das Adhikari, Naupada Preeyanka, and Ponneri C. Ravikumar. Cobalt-Catalyzed Decarbonylative *Ips*o-C-C Bond Functionalization via Weak Coordination: An Approach Towards Indole-Acylolins and Its Photophysical Studies. DOI **10.26434/chemrxiv-2022-4kckr**. (*Manuscript submitted*).

#7) **Shyam Kumar Banjare**, Saista Afreen, Pranav Shridhar Mahulkar, Annapurna Saxena and Ponneri C. Ravikumar. Unveiling the Reactivity of Cobalt(III)-catalyst Towards Regioselective Hydroarylation of 1,6 Diyne via Weak-chelation Assisted C-H Bond Activation. (*Manuscript submitted*).

(C) Review (Highlight Articles):

8) **Shyam Kumar Banjare**, Pranav Shridhar Mahulkar, Tanmayee Nanda, Bedadyuti Vedvyas Pati, Lamphiza O Najjar and Ponneri C. Ravikumar. Diverse reactivity of alkynes with metal-carbon bond generated through C-H activation. *Chem. Commun.*, **2022**, 58, 10262-10289.

9) **Shyam Kumar Banjare**, Tanmayee Nanda, Bedadyuti Vedvyas Pati, Pragati Biswal, and Ponneri Chandrababu Ravikumar O-directed C–H functionalization via cobaltacycles: A sustainable approach for C–C and C–heteroatom bond formations, *Chem. Commun.*, **2021**, 57, 3630-3647.

(D) Book Chapter:

10) **Shyam Kumar Banjare**, Bedadyuti Vedvyas Pati, and Ponneri C. Ravikumar. Book Chapter: First-row transition metal (Mn, Fe, Co, Ni, Cu) catalyzed C- H bond functionalization through weak chelation. Handbook of C-H

Functionalizations (CHF), *Wiley-VCH Publishers*, **2021**, DOI:
10.1002/9783527834242.chf0220.

(E) Other Research Publications:

- 11) Namrata Prusty[†], **Shyam Kumar Banjare**[†], Smruti Ranjan Mohanty, Tanmayee Nanda, Komal Yadav, and Ponneri C. Ravikumar Synthesis and Photophysical Study of Heteropolycyclic and Carbazole Motif: Nickel-Catalyzed Chelate-Assisted Cascade C–H Activations/Annulations *Org. Lett.* **2021**, 23, 9041-9046.
([†]equal contribution).
- 12) Tanmayee Nanda, **Shyam Kumar Banjare**, Wang-Yeuk Kong, Wentao Guo, Pragati Biswal, Lokesh Gupta, Bedadyuti Vedvyas Pati, Smruti Ranjan Mohanty, Dean J Tantillo, Ponneri C. Ravikumar. Breaking The Monotony: Cobalt and Maleimide as a New Entrant to the Catellani Reaction. *ACS Catal.* **2022**, 12, 19, 11651–11659.
- 13) Bedadyuti Vedvyas Pati, **Shyam Kumar Banjare**, Gopal Krusna Das Adhikari, Tanmayee Nanda, Ponneri C. Ravikumar. Rhodium-Catalyzed Selective C(sp²)-H Activation/Annulation of tert- butyl benzoyloxycarbamates with 1,3-Diynes: A one Step Access to Alkynylated Isocoumarins and Bis-Isocoumarins. *Org. Lett.* **2022**, 24, 31, 5651–5656.
- 14) Pragati Biswal, **Shyam Kumar Banjare**, Bedadyuti Vedvyas Pati, Smruti Ranjan Mohanty, and P. C. Ravikumar Rhodium-Catalyzed One-Pot Access to N-Polycyclic Aromatic Hydrocarbons from Aryl Ketones through Triple C–H Bond Activations, *J. Org. Chem.* **2021**, 86, 1, 1108–1117.
- 15) Smruti Ranjan Mohanty, Bedadyuti Vedvyas Pati, **Shyam Kumar Banjare**, Gopal Krushna Das Adhikari, and Ponneri Chandrababu Ravikumar Redox-

-
- Neutral Cobalt(III)-Catalyzed C–H Activation/Annulation of α,β -Unsaturated Oxime Ether with Alkyne: One-Step Access to Multisubstituted Pyridine, *J. Org. Chem.* **2021**, 86, 1, 1074–1083.
- 16) Smruti Ranjan Mohanty, Namrata Prusty, **Shyam Kumar Banjare**, Tanmayee Nanda, and Ponneri C. Ravikumar. Overcoming the Challenges toward Selective C(6)–H Functionalization of 2-Pyridone with Maleimide through Mn(I)-Catalyst: Easy Access to All-Carbon Quaternary Center. *Org. Lett.* **2022**, 24, 848–852.
- 17) Namrata Prusty, Smruti Ranjan Mohanty, **Shyam Kumar Banjare**, Tanmayee Nanda, and Ponneri C. Ravikumar. Switching the Reactivity of the Nickel-Catalyzed Reaction of 2-Pyridones with Alkynes: Easy Access to Polyaryl/Polyalkyl Quinolinones. *Org. Lett.* **2022**, 24, 6122–6127.
- 18) Tanmayee Nanda, Pragati Biswal, Bedadyuti Vedvyas Pati, **Shyam Kumar Banjare**, and Ponneri Chandrababu Ravikumar Palladium-Catalyzed C–C Bond Activation of Cyclopropanone: Modular Access to Trisubstituted α,β -Unsaturated Esters and Amides. *J. Org. Chem.* **2021**, 86, 3, 2682–2695.
- 19) Bedadyuti Vedvyas Pati, Asit Ghosh, Komal Yadav, **Shyam Kumar Banjare**, Shalini Pandey, Upakarasamy Lourderaj, and Ponneri C. Ravikumar Palladium-Catalyzed Selective C–C Bond Cleavage and Stereoselective Alkenylation between Cyclopropanol and 1,3-Diyne: One-Step Synthesis of Diverse Conjugated Enynes. *Chem. Sci.*, **2022**, 13, 2692–2700.
- 20) Smruti Ranjan Mohanty, Namrata Prusty, Tanmayee Nanda, **Shyam Kumar Banjare**, and Ponneri C. Ravikumar. Pyridone Directed Ru-Catalyzed

-
- Olefination of $\text{sp}^2(\text{C-H})$ Bond Using Michael Acceptors: Creation of Drug Analogues. *J. Org. Chem.* **2022**, 87, 6189–6201.
- 21) Tanmayee Nanda, Muhammed Fastheem, Astha Linda, Bedadyuti Vedvyas Pati, **Shyam Kumar Banjare**, Pragati Biswal and Ponneri C Ravikumar. Recent Advancement in Palladium Catalysed CC bond Activation of Strained Ring Systems: Three and four-membered carbocycles as prominent C3/C4 building blocks. *ACS Catal.* **2022**, 12, 13247–13281.
- 22) Gopal Krushna Das Adhikari, Bedadyuti Vedvyas Pati, Tanmayee Nanda, Pragati Biswal, **Shyam Kumar Banjare**, and Ponneri C. Ravikumar. Co(II)-Catalyzed C–H/N–H Annulation of Cyclic Alkenes with Indole-2-carboxamides at Room Temperature: One-Step Access to β -Carboline-1-one Derivatives. *J. Org. Chem.* **2022**, 87, 6, 4438–4448.
- 23) Pragati Biswal[†], Tanmayee Nanda[†], **Shyam Kumar Banjare**, Smruti Ranjan Mohanty, Ponneri C. Ravikumar. *N*-allylbenzimidazole as a strategic surrogate in Rh-catalyzed stereoselective trans-propenylation of aryl $\text{C}(\text{sp}^2)\text{-H}$ bond. *Chem. Commun.*, **2022**, Accepted Manuscript. *Chem. Commun.*, **2023**, 59, 199–202. ([†]equal contribution).
- 24) Gopal Krushna Das Adhikari, Smruti Ranjan Mohanty, **Shyam Kumar Banjare**, Namrata Prusty Gaji Ram Murmu, and Ponneri C. Ravikumar. Ruthenium indole. *J. Org. Chem.* **2023**, 88, 952–959.
- 25) Bedadyuti Vedvyas Pati, Nitha Nahan Puthalath, **Shyam Kumar Banjare**, Tanmayee Nanda, Ponneri C. Ravikumar. Transition Metal-catalyzed C–H /C–C Activation and Coupling with 1, 3-diyne. *Org. Biomol. Chem.*, **2023**, (Accepted Manuscript) DOI <https://doi.org/10.1039/D3OB00238A>
-

(F) Other Manuscript under preparation:

- 26) Sofaya Joshi, **Shyam Kumar Banjare**, Riya Dutta and Ponneri C. Ravikumar.
Weak-Chelation Assisted Generation of Cyclic Six-membered Cobalt-Intermediate: A Potential Approach Towards Functionalization of N-Heterocycles. (*Manuscript under preparation*)
- 27) Pranav Shridhar Mahulkar, **Shyam Kumar Banjare**, Sofaya Joshi and Ponneri C. Ravikumar. Cobalt catalyzed keto-alkylation of 3-pivaloyl indole through weak coordination. (*Manuscript under preparation*).
- 28) Saista Afreen, Abhipsa Ghosh, **Shyam Kumar Banjare**, and Ponneri C. Ravikumar. Cobalt catalysed hetero-arylation of 1,6-diyne. (*Manuscript under preparation*)
- 29) T. Nanda, M. Fastheem, **Shyam Kumar Banjare**, and Ponneri C. Ravikumar. Palladium-Catalyzed Cascade C–C Bond Activation of Cyclopropanone: A strategic approach towards the synthesis of pyrrolo-quinolinedione and anticancer drug mitomycin skeleton. (*Manuscript under preparation*)
- 30) Sofaya Joshi, Riya Dutta, **Shyam Kumar Banjare**, and Ponneri C. Ravikumar. Weak-Chelation Assisted Regioselective Ethynylation of Indole at C4-position. (*Manuscript under preparation*)

Conferences:

1. ‘Cobalt catalyzed C–H functionalization of indole and indolines through weakly coordinating directing group’; **Shyam Kumar Banjare**, R. Chebolu, and Ponneri. C. Ravikumar*; in National Conference on Organic Synthesis (NCOS-2020), Organized by PG Department of Chemistry, Berhampur University,

-
- Odisha. during 02-03 March, 2020. (**In-person poster and Short oral presentation**).
2. ‘Development of Cobalt Catalyzed Benzenoid C–H Bond activation of Indole and Indoline using Weakly Coordinating Directing Group’; **Shyam Kumar Banjare**, T. Nanda and Ponneri C. Ravikumar*; 1st International Conferences on “Recent Advances in Material Science and Organic Synthesis” (**RAMSOS-2021**), India during October 20-21–Dec. 2021. (**Virtual oral presentation**).
3. ‘Weak chelation-assisted cobalt catalyzed benzenoid C–H bond functionalizations of indoles and indolines’; **Shyam Kumar Banjare**, R. Chebolu, T. Nanda and Ponneri C. Ravikumar; The biannual national meeting of the American Chemical Society (ACS) (**ACS Fall-2021**)’ held at the India during 22-26 August 2021. (**Virtual oral presentation**).
4. ‘Regioselective C-H/C-C Bond Functionalization of Heterocycles: Uncovering the Reactivity of Cobalt(III)-catalyst through Weak Chelation’; **Shyam Kumar Banjare**, T. Nanda and Ponneri C. Ravikumar*; “Chemical Research Society of India 28th National Symposium in Chemistry (CRSI NSC-28), India during 4-6 February 2022” (**In-person oral presentation**).



Shyam Kumar Banjare

Dedicated to
My Family, Friends
&
all My Teachers

ACKNOWLEDGEMENTS

I would like to express my sincere gratitude to my thesis supervisor **Dr. Ponneri C. Ravikumar**, for his insightful advice, constant encouragement, and patience guidance during my Ph.D. studies.

I take this opportunity to thank my doctoral committee members, Dr. Moloy Sarkar (chairperson of doctoral committee members), Dr. Sharanappa Nembenna (member), Dr. Sanjib Kar (member), and Dr. Shantanu Pal (External member from IIT, Bhubaneswar) for their valuable suggestions.

I would like to acknowledge my thesis reviewers (i) Prof. Ramakrishna G. Bhat, IISER Pune, India (External examiner) (ii) Prof. Ramesh Ramapanicker, IIT Kanpur, India (iii) Prof. Poisson Thomas, INSA Rouen Normandie, France.

I would like to acknowledge my course Instructors: Prof. A Srinivasan, Dr. U. Lourderaj, Dr. N. K. Sharma, and Dr. Bidraha Bagh, School of Chemical Sciences, NISER, Bhubaneswar.

I would like to acknowledge PGCSC convener: Dr. C. Gunanathan (Present), Dr. Bidraha Bagh, and Dr. N. K. Sharma (Former), School of Chemical Sciences, NISER, Bhubaneswar.

I would like to acknowledge Dr. Prasenjit Mal for his needful help and suggestions. I am grateful to all the faculties and staff of the School of Chemical Sciences, NISER, Bhubaneswar.

I would like to acknowledge NISER for giving the laboratory facilities and DAE financial support.

I am grateful to my lab-members: Dr. Rajesh, Tanmayee, Dr. Pragati, Dr. Smruti, Namrata, Vedvyas, Dr. Gopal, Saista, Annapurna, Pranav, Sofaya, Shubham, Abhipsa, Arijit, Lipsa, Lam, Nitha, Fastheem, Ashish, Astha, Lokesh, Rohit, Gaji, Dr. Laxman, Dr. Asit and other for their help in experiments and valuable discussions.

I acknowledge our collaborator co-authors: Juhi Dutta, N. Preeyanka and Komal Yadav, for their contributions.

I would like to acknowledge Dr. Shreenibas Sa, Dr. Shyamashrit, Dr. Kashturi Sahu, and Dr. Narayan Ch. Jana for helping with single-crystal X-ray data.

I am also grateful to my friends Dr. Shyaml, Dr. Sudip, Tanmoy, Sahadev, Abhishek, Akshay Kumar, Siddharth, Deepsagar, Lalmani Roy, Naveen Sahu, Heera, Vashuraman, Shyamsundar, Leena Patel, Divya Patel, Radha Patel, Anjali Patel, Mamta Patel, Poonam Verma, Bharti Dewangan, Priyanka Gupta, Rahul, Sahu, Fakirchand, Laxmi, Deepak, Jagjiwan, Gangaram, Suraj, Khagraz, Dilesh, Rajendra Sahu, Kamlesh, Umashankar, Arvind, Ghanshyam, Jugal, Jiwan, Omprakash, Mahesh, Raju, and all other friends.

I would like to acknowledge my school teachers: Mrs. Khalkho mam and Mr. Tuleshwar Sahu.

I would like to acknowledge my college teachers: Dr. A.L.S. Chandel, Dr. Neeta Gupta, Dr. D.P. Sahu, Autonomous Science College, Bilaspur C.G.

My special thanks to my teachers and well-wishers: Prof. G. K. Patra, Dr. Subhash Banerjee, Dr. Pathik Maji, Dr. S. K. Singh, Dr. S. S. Thakur, Dr. V.K. Rai, Dr. Charu Arora, Dr. Arti Shrivastava, Dr. B. Sharma, Dr. Manorama, Guru Ghasidas Central University, Bilaspur C.G.

My special thanks to my well-wisher: Mr. Firat Ram Chauhan (Bade Papa), for his support and motivation to archive my goal.

I deeply thank my parents and family members: Mr. Dileram Banjare (Dada), Mrs. Ramkuwar Banjare (Dadi), Mr. Bhudh Ram Banjare (Father), Mrs. Roopa Bai Banjare (Mother), Mr. Shail Kumar Banjare (Younger brother), Ms. Sheela Banjare (Younger sister) for their unconditional love, blessings, patience, and support in my life.

Lastly, “I would like to thank all the beautiful souls who have helped me in my journey so far.”



Shyam Kumar Banjare

CONTENTS

	Page No.
Thesis title	i
Recommendations of the viva-voce committee	ii
Statement by author	iii
Declaration	iv
List of publications	v-x
Conferences	x-xi
Dedications	xii
Acknowledgements	xiii-xiv
Contents	xv
Division of chapters	xvi
Synopsis	xvii-xxi
List of Figures	xxi-xxii
List of Schemes	xxiii-xxv
List of Tables	xxv-xxvi
List of Abbreviations	xxvi-xxvii

(This thesis has been organized into seven chapters)

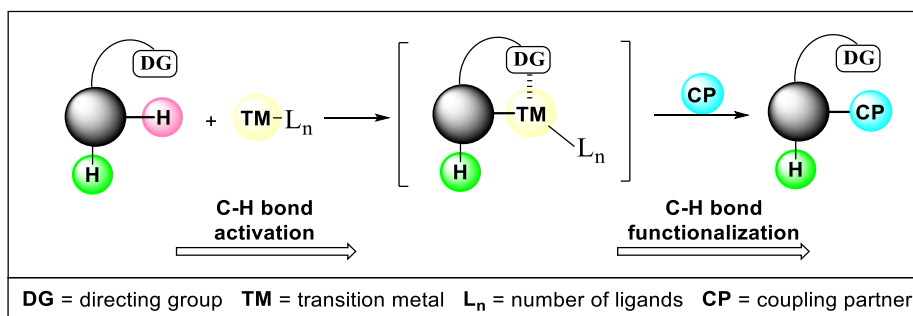
Chapter 1:	Introduction to directed C-H functionalization	1
Chapter 2:	Cobalt catalyzed hydroarylation of Michael acceptors with indolines directed by a weakly coordinating functional group	19
Chapter 3:	Cobalt-Catalyzed One-Step Access to Pyroquilon and C-7 Alkenylation of Indoline with Activated Alkenes Using Weakly Coordinating Functional Groups	49
Chapter 4:	Cobalt-Catalyzed Regioselective Direct C-4 Alkenylation of 3-Acetylindole with Michael Acceptors Using a Weakly Coordinating Functional Group	92
Chapter 5:	Breaking the Trend: Insight into Unforeseen Reactivity of Alkynes in Cobalt-Catalyzed Weak Chelation-Assisted Regioselective C(4)-H Functionalization of 3-Pivaloyl Indole	126
Chapter 6:	Cobalt-Catalyzed Decarbonylative <i>Ips</i> o C-C Bond Functionalization via Weak Coordination: An Approach Towards Indole-Acyloins and Its Photophysical Studies	189
Chapter 7a:	Unveiling the Reactivity of Cobalt(III)-catalyst Towards Regioselective Hydroarylation of 1,6 Diyne via Weak-chelation Assisted C-H Bond Activation	232
Chapter 7b:	Weak-chelation assisted regioselective <i>ortho</i> -(<i>sp</i> ²)-H ethynylation of <i>N</i> -aryl γ -lactam utilizing cobalt(III)-catalyst	260
Summary		289

SYNOPSIS

(This thesis has been organized into seven chapters)

Chapter 1. A brief introduction to directed C-H bond functionalization's:

Abstract: The transition metal-catalyzed C-H bond activation has enabled useful retrosynthetic disconnections using inert C-H bonds (Scheme 1). Nevertheless, reactions in this field are still dominated by precious 4d or 5d metals using strong coordination. Extensive use of heavy metals is not sustainable as it raises several problems, such as limited resources, high cost, and environmental impact. Therefore, 3d transition metal-catalyzed C-H functionalization through weak chelation is gaining immense attention.



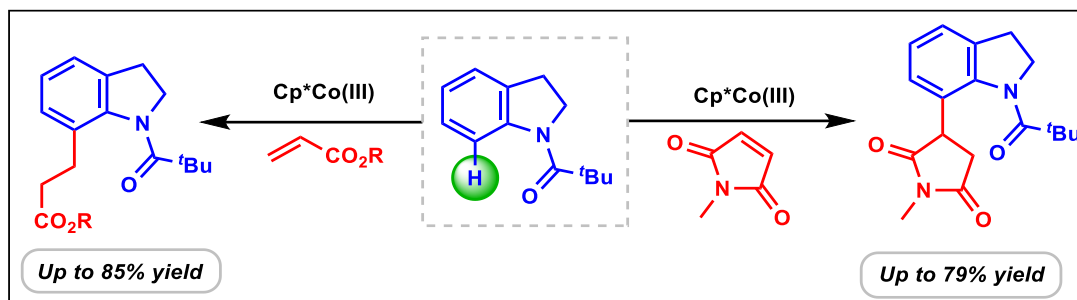
Scheme 1: Schematic representation of transition-metal catalyzed directed C-H functionalization

It is a highly sustainable approach because it is less expensive, eco-friendly, and commonly available directing groups such as aldehyde, ketone, and ester could be used. Moreover, the weakly coordinating directing group is easily removable or modifiable, which considerably enhances the synthetic scope.

Chapter 2. Cobalt catalyzed hydroarylation of Michael acceptors with indolines

directed by a weakly coordinating functional group:

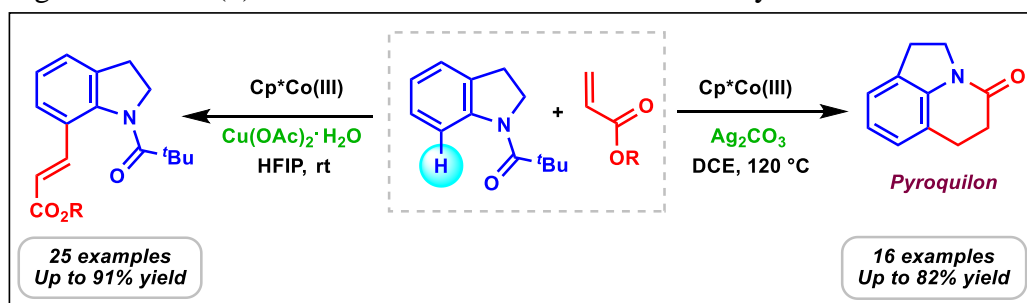
Abstract: The cobalt(III) catalyzed hydroarylation of Michael acceptors using indolines, selectively at the C-7 position, has been reported. For the selective C-7 functionalization of indoline, we have used a weakly coordinating amide carbonyl group. During the process of optimization, we also discovered the unusual co-catalytic activity of zinc triflate in the C-H functionalization reaction. Hydroarylation of unprotected maleimide using indolines was a challenging substrate and had never been accomplished before, and we were able to achieve this with our methodology in good yields.



Scheme 2: Cobalt(III)-catalyzed selective C(7)-alkylation of indoline.

Chapter 3. Cobalt-Catalyzed One-Step Access to Pyroquilon and C-7 Alkenylation of Indoline with Activated Alkenes Using Weakly Coordinating Functional Groups:

Abstract: A new strategy for the C(7)-H functionalization of indoline derivatives using first-row transition-metal cobalt has been demonstrated wherein the pivaloyl group acts as a weakly coordinating directing group. Biologically important pyroquilon (tetrahydropyroquinolinone) derivatives have been synthesized in a one-pot manner through selective C(7)-H functionalization and concomitant cyclization.

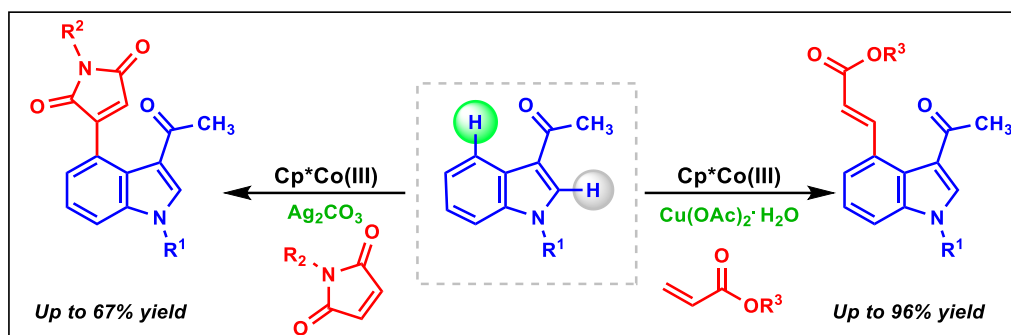


Scheme 3: Cobalt(III)-catalyzed selective synthesis of pyroquilon and C(7)-olefination of indoline.

In this process, aromatic C–H and amidic C–N bonds are cleaved, and new C–C and C–N bonds are formed step-economically. Further, selective C(7)-H alkenylation of indoline derivatives has also been accomplished using activated alkenes by varying the reaction conditions.

Chapter 4. Cobalt-Catalyzed Regioselective Direct C-4 Alkenylation of 3-Acetylindole with Michael Acceptors Using a Weakly Coordinating Functional Group:

Abstract: Herein, we disclosed the first report on the selective C(4)-H functionalization of 3-acetylindole derivatives using first-row transition metal cobalt, where an acetyl group is acting as a weakly coordinating directing group. Selective C(4)-H functionalization has been achieved using diverse Michael acceptors (acrylate and maleimide) simply by switching the additive from copper acetate to silver carbonate.

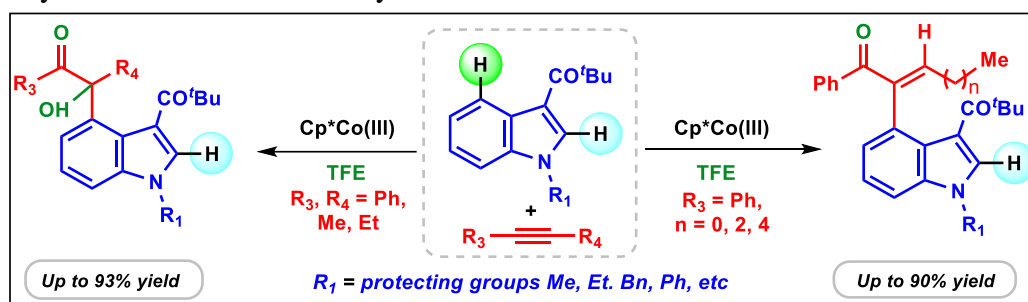


Scheme 4: Cobalt(III)-catalyzed regioselective C(4)-olefination of 3-acetyl indole.

Further, the formation of a cobaltacycle intermediate was also detected through HRMS for mechanistic insight.

Chapter 5. Breaking the Trend: Insight into Unforeseen Reactivity of Alkynes in Cobalt-Catalyzed Weak Chelation-Assisted Regioselective C(4)–H Functionalization of 3-Pivaloyl Indole:

Abstract: The unique reactivity of diphenylacetylene has been uncovered through weak chelation-assisted cobalt-catalyzed regioselective C(4)–H activation of 3-pivaloyl indole. α -Hydroxy ketone and α, β -unsaturated ketone derivatives have been synthesized in good yields from indole and alkynes.

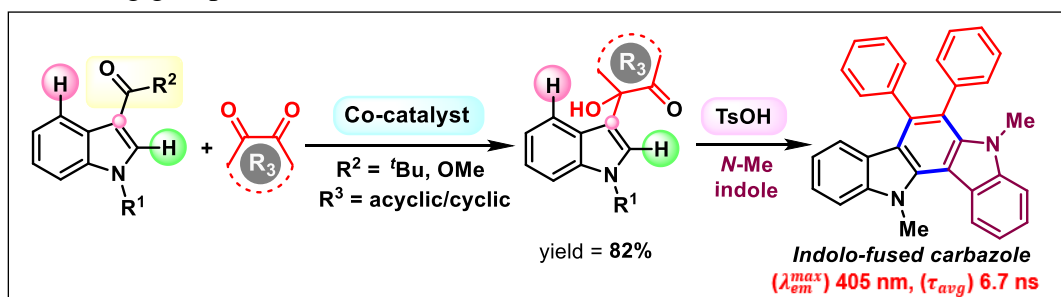


Scheme 5: Cobalt(III)-catalyzed regioselective C(4)- α -hydroxy ketone 3-acetyl indole.

Notably, the indole C(4)–H-functionalized α, β -unsaturated ketone product was obtained with high stereo- and regioselectivity simply by changing the coupling partner from symmetrical alkynes to unsymmetrical aromatic-aliphatic alkynes. Most importantly, trifluoroethanol is the sole water source for this conversion. Quantitative detection of bis(2,2,2-trifluoroethyl) ether from dry trifluoroethanol through ^{19}F NMR and LCMS studies indirectly confirms the in-situ formation of water.

Chapter 6. Cobalt-Catalyzed Decarbonylative *Ipso* C-C Bond Functionalization via Weak Coordination: An Approach Towards Indole-Acyloins and Its Photophysical Studies:

Abstract: Selective functionalization of indole C₃-C bond with aromatic/heteroaromatic 1,2-diketones has been uncovered for the first time. Earth crust abundant first-row transition metal cobalt-catalyst has been demonstrated as an effective catalyst for this unusual transformation. Furthermore, using easily available weakly coordinating groups such as ketone and ester were found to be effective.

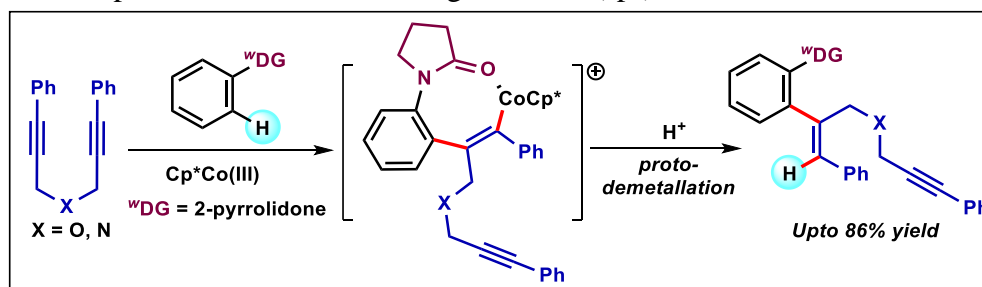


Scheme 6: Cobalt(III)-catalyzed regioselective C(3)C-*ipso* bond functionalization of indole.

The in-situ generation of water from hexafluoro-2-propanol and removal of the pivaloyl/ester group in a decarbonylative manner at a lower temperature is the key feature of this methodology.

Chapter 7a. Unveiling the Reactivity of Cobalt(III)-catalyst Towards Regioselective Hydroarylation of 1,6 Diyne via Weak-chelation Assisted C-H Bond Activation:

Abstract: Herein, we report the reactivity of cobalt(III)-catalyst towards hydroarylation of 1,6 diyne, which was never explored before. The *N*-aryl γ -lactam is the prime substrate that undergoes *ortho*-(sp²)-H bond activation.



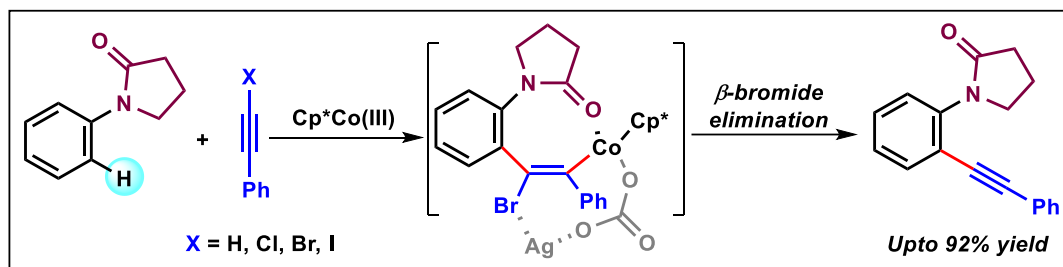
Scheme 7: Cobalt(III)-catalyzed regioselective hydroarylation of 1,6-diyne using weak chelation.

The reaction mechanism reveals the in-situ formation of a six-membered cobaltacycle which undergoes further functionalization with 1,6 diyne.

Chapter 7b. Weak-chelation assisted cobalt-catalysed C-H bond activation: A sustainable approach towards regioselective ethynylation of *N*-aryl γ -lactam:

Abstract: The sustainable C-H bond functionalization of *N*-aryl γ -lactam has been achieved in highly regioselective manner. In this protocol, earth-abundant cobalt(III)-

catalyst was found to be effective, triggering the C-H metallation using a weakly coordinating lactam group. Herein, the *ortho*-(sp²)-H ethynylation has been obtained regioselectively.



Scheme 8: Cobalt(III)-catalyzed regioselective ethynylation of *N*-aryl γ -lactam.

However, the parallel kinetic isotope experiment suggests that the C-H bond activation is involved in the rate-determining step. Moreover, the synthetic utility of ethynylated *N*-aryl γ -lactam has been demonstrated for many useful transformations.

List of figures

1	Figure 1.1	Basic modes of catalytic transition metal-catalyzed C-H bond activation.	4
2	Figure 1.2	Well explore transition metals in C-H activation and their cost.	5
3	Figure 1.3	3d-transition metals in C-H bond functionalization.	6
4	Figure 1.4	Energy profile diagram: strong vs weak coordination assisted C-H bond activation.	8
5	Figure 1.5	Sustainable approach towards olefination of arene	9
6	Figure 2.1	C(7)-H functionalization of indolines catalyzed by first-row transition metals.	21
7	Figure 1.7	Proposed Catalytic Cycle for the Cobalt Catalyzed Hydroarylation of Michael Acceptors.	28
8	Figure 2.3	Crystal structure of 3a (50% ellipsoid probability).	45

9	Figure 3.1	Selective examples of bioactive compound bearing pyrroloquinolinone skeleton.	51
10	Figure 3.3	Crystal structure of 3ia (50% ellipsoid probability).	87
11	Figure 3.4	Crystal structure of 4aa (50% ellipsoid probability)..	88
12	Figure 4.1	C–H functionalization of 3-acylindole.	94
13	Figure 4.2	Mechanistic studies.	102
14	Figure 4.3	Crystal structure of 3ia (50% ellipsoid probability)	122
15	Figure 4.4	Crystal structure of 3bd (50% ellipsoid probability)	123
16	Figure 5.1	Transition metal-catalyzed C–H functionalizations of indole.	129
17	Figure 5.2	Detection of bis(2,2,2-trifluoroethyl) ether formation in the reaction mixture through ¹⁹ F NMR.	142
18	Figure 5.3	Crystal structure of 3aa (50% ellipsoid probability).	183
19	Figure 5.3	Optimized structures of (a) 6-membered, and (b) 5-membered cobaltacycle intermediates with their relative energies.	184
20	Figure 5.4	Crystal structure of 3be (50% ellipsoid probability).	185
21	Figure 6.1	Overview and challenges of transition metal catalyzed C–H/C–C bond functionalization of indole.	192
22	Figure 6.2	Computational studies	201
23	Figure 6.3	The fluorescence decay curves of 3aa (in chloroform) and 4aa (in dichloromethane).	204
24	Figure 6.4	Crystal structure of 3fa (50% ellipsoid probability).	227
25	Figure 6.5	Crystal structure of 3ga (50% ellipsoid probability).	228

26	Figure 7a.1	Overview and Challenges of C-Metal Bond towards Reactivity of 1,6 diyne.	235
27	Figure 7b.1	Reactivity of transition metals towards ethynylation using various alkynylating agents.	262
28	Figure 7b.2	Crystal structure of 3ca (50% ellipsoid probability).	286

List of schemes

1	Scheme 1.1	C-H functionalization via strongly coordinating directing group.	7
2	Scheme 1.2	C-H functionalization via weakly coordinating directing group.	7
3	Scheme 1.3	Cobalt-catalysed hydroarylation cyclization of enynes via aldehydes wDG.	10
4	Scheme 1.4	Cobalt-catalyzed annulation of salicylaldehydes utilizing alkyne.	11
5	Scheme 1.5	Cobalt-catalysed hydroarylation cyclization of enynes and aromatic ketones.	11
6	Scheme 1.7	Cobalt catalyzed annulation utilizing carboxylic ester wDG.	12
7	Scheme 1.8	Scope of Cp*Co(III)-catalyzed C-H annulation and alkenylation.	13
8	Scheme 1.9	Alkyne scope for the three-component addition cascade.	13
9	Scheme 1.10	Cobalt catalyzed C-H/OH annulation using alkyne.	14

10	Scheme 2.1	Evaluation of Various of Indolines and Michael Acceptors for the Hydroarylation Reaction	25
11	Scheme 2.2	Evaluation of Various Indolines with the Acyclic Michael Acceptors	26
12	Scheme 2.3	Mechanistic studies.	27
13	Scheme 3.1	Scope of tetrahydropyrroloquinolinone	56
14	Scheme 3.2	Scope of Indoline C-7 Alkenylation with Acylates	59
15	Scheme 3.3	Mechanistic Studies.	61
16	Scheme 3.4	Proposed Catalytic Cycle.	63
17	Scheme 3.5	Synthetic Applications.	64
18	Scheme 4.1	Scope of C-4 Alkenylation of Indole with Acrylates	99
19	Scheme 4.2	Scope of C-4 Alkenylation of Indole with Maleimide.	100
20	Scheme 4.3	Proposed Catalytic Cycle	103
21	Scheme 5.1	Substrate Scope of Indole Derivatives with Various Alkynes	134
22	Scheme 5.2	Substrate Scopes of Indole and Unsymmetrical Alkyne	136
23	Scheme 5.3	Mechanistic Studies and Control Experiments	139
24	Scheme 5.4	Control Experiment and Isotope Labeling Experiment	141
25	Scheme 5.5	Proposed Mechanism Catalytic Cycle	144
26	Scheme 5.6	Synthetic Utility of the Indole C4-Derived Product	146
27	Scheme 6.1	Screening of weakly coordinating directing groups	196
28	Scheme 6.2	Scopes of various indole substituents for cobalt(III)-catalyzed decarbonylative indole(3)-acyloination.	197
29	Scheme 6.3	Mechanistic studies	199
30	Scheme 6.4	Synthetic utility of the developed method.	203
31	Scheme 7a.1	Scope of Various Substituted 1-phenylpyrrolidin-2-one and 1,6 diyne.	239

32	Scheme 7a.2	Mechanistic Experiments.	241
33	Scheme 7a.3	Detection of Intermediates through LCMS.	242
34	Scheme 7a.4	Plausible Catalytic Pathway for Cobalt Catalyzed Hydroarylation Functionalization of 1,6 diyne.	243
35	Scheme 7b.1.	Scope of various substrate and reacting partners towards cobalt catalyzed ethynylation	167
36	Scheme 7b.2	Mechanistic studies and control experiments	269
37	Scheme 7b.3	Catalytic cycle for regioselective Co(III)-catalysed ethynylation	271
38	Scheme 7b.4	Synthetic utilization.	272

List of tables

1	Table 2.1	Optimization of the Hydroarylation Reaction	23
2	Table 2.2	Scope of Various Directing Groups for the Hydroarylation of <i>N</i> -Methylmaleimides	24
3	Table 3.1	Optimization of the tetrahydropyrroloquinolinone	54
4	Table 3.2	Screening of directing groups for indoline C-7 alkenylation and cyclization.	55
5	Table 3.3	Scope of tetrahydropyrroloquinolinone with various Acrylates	57
6	Table 4.1	Optimization table	96
	Table 4.2	Screening of various directing groups	98
7	Table 5.1	Optimization of Reaction Conditions	132
8	Table 6.1	Overview and challenges of transition metal catalyzed C-H/C-C bond functionalization of indole	195

9	Table 6.2	Fluorescence decay parameters of 3aa (in chloroform) and 4aa (in dichloromethane)	204
10	Table 7a.1	Optimization Studies for Hydroarylation of 1,6-diyne	237
11	Table 7b.1	Optimization of reaction condition towards ethynylation.	265

List of Abbreviations

THF	Tetrahydrofuran
DMSO	Dimethyl sulfoxide
NMR	Nuclear magnetic resonance
¹ H NMR	Proton nuclear magnetic resonance
¹³ C NMR	Carbon nuclear magnetic resonance
IR	Infrared
DCM/CH ₂ Cl ₂	Dichloromethane
CHCl ₃	Chloroform
HRMS	High resolution mass spectrometry
GC	Gas chromatography
DMF	Dimethylformamide
2D	Two dimensional
AgOAc	Silver acetate
LiClO ₄	Lithium perchlorate
NaH	Sodium hydride
MW	Molecular weight
EtOAc	Ethyl acetate
CDCl ₃	Chloroform-d
TM	Transition metal
DEPT-135	Distortionless enhancement by polarization transfer
Pd(OAc) ₂	Palladium acetate
DG	Directing group
FG	Functional group
DCE	1,2-dichloroethane

HFIP	1,1,1,3,3,3-Hexafluoro isopropanol
NBS	N-Bromosuccinimide
HMBC	¹ H- ¹³ C Heteronuclear Multiple Bond Correlation Spectroscopy
OA	Oxidative addition
S _E Ar	Aromatic electrophilic substitution
CH ₃ CN	Acetonitrile
CMD	Concerted metalation deprotonation
BIES	Base-assisted intramolecular electrophilic substitution
TDG	Transient directing group
AgTFA	Silver trifluoroacetate
DG ^{OX}	Redox neutral directing group
OLED	Organic light emitting diode
K ₂ CO ₃	Potassium carbonate
Na ₂ SO ₄	Sodium sulphate
HOSA	Hydroxylamine- <i>O</i> -Sulfonic Acid
PAHs	Polycyclic aromatic hydrocarbons
KIE	Kinetic Isotope Effect
AcOH	Acetic acid
ⁿ BuLi	<i>n</i> -Butyllithium
TFA	Trifluoroacetic acid
TEMPO	(2,2,6,6-Tetramethylpiperidin-1-yl)oxyl
BHT	Butylated hydroxytoluene
Zn(OAc) ₂	Zinc acetate
MeOH	Methanol
Cu(OAc) ₂	Copper(II) acetate
TFE	Trifluoroethanol
CD ₃ OD	d ₄ -methanol

Chapter 1

Introduction to directed C-H bond activation

1.1 Abstract

1.2 Introduction

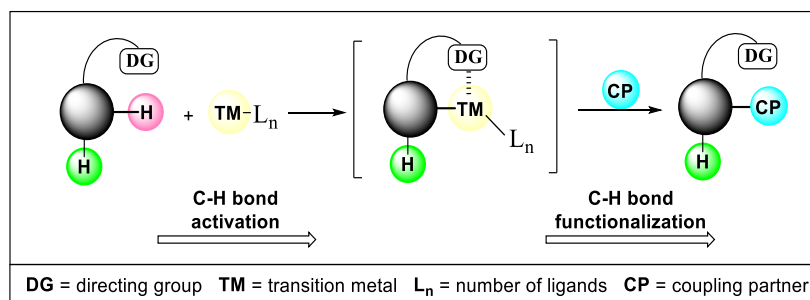
1.3 Literature survey

1.4 Conclusion

1.5 References

Chapter 1

Introduction to directed C-H bond activation



1.1 ABSTRACT

The transition metal-catalyzed C-H bond functionalization strategy has opened up a wide range of opportunities to develop organic transformations in a step and atom-economical manner. The use of earth-abundant 3d transition metals further translates these transformations into a cost-effective as well as eco-friendly approach. The selective C-H bond activation could be achieved by utilizing the proximal directing group present in a molecule. In this regard, strongly chelating N-directing groups (8-aminoquinoline, pyrimidine, pyridine) were well explored. However, the use of readily available and weakly coordinating O-directing groups (aldehyde, ketone, ester substituted amide) are underdeveloped. Thus, synthetic transformations that utilize earth abundance 3d transition metal catalysts along with easily available weakly coordinating directing groups are highly sustainable, especially for the large-scale production of chemicals in industries.

1.2 INTRODUCTION

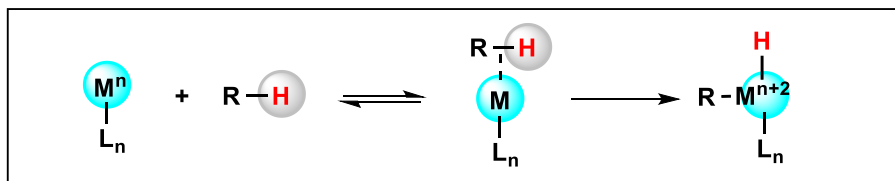
Synthesis of organic molecules that have applications in medicine and agriculture is of great value to human life¹. The classical organic synthesis relies on functional

group manipulations through multiple steps. One of the major drawbacks of the multistep approach is that it takes a lot of time and energy and generates a lot of wasteful by-products.² Then, cross-coupling reactions became more popular in organic synthesis on account of operational simplicity and easy adaptability in industries³. In cross-coupling reactions, the C(sp²)-X bonds can be transformed into C-C bonds using appropriate metal-catalyzed coupling methods (Kumada coupling, Heck reaction, Sonogashira coupling, Negishi coupling, Stille cross-coupling, Suzuki reaction, etc).⁴ However, these cross-coupling reactions have some inherent limitations, such as (i) the requirement of pre-functionalized substrates, (ii) compounds having C(sp³)-X bonds with a β -hydrogen cannot undergo coupling reactions. As opposed to pre-functionalized substrates (C-X) the use of the C-H bond as a functional group for synthetic transformations is an attractive proposition. It prevents lengthy functional group interconversions and significantly reduces the generation of wasteful by-products.

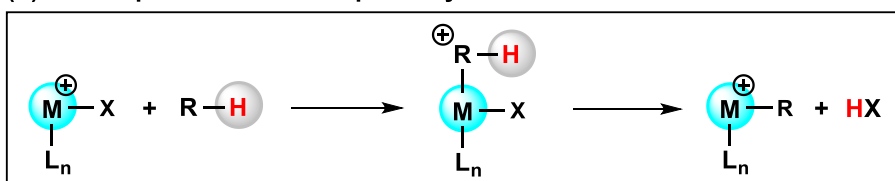
In this regard, the transition metal-catalyzed C-H bond activation and functionalization have gained enormous significance.⁵ However, at the beginning of this century, the inert C-H bond functionalization reaction through metal-catalyzed C-H bond activation almost seemed very difficult to achieve. Some of the significant challenges associated with C-H bond activation are (i) low reactivity,⁶ (ii) higher bond dissociation energies (BDE), and (iii) the generally non-polar nature of the isolated C-H bonds.⁷ However, over the last two decades, it has become one of the most explored areas in catalysis, thus broadening the scope of organometallic and synthetic chemistry.⁸ Furthermore, metal-catalyzed C-H functionalization has emerged as a powerful tool, as it provides easy access to the synthesis of valuable carbon-carbon (C-C) and carbon-hetero (e.g., C-N, C-O) bonds.⁹ This approach is not only useful for the synthesis of

complex molecular entities but also contributes to a paradigm shift in the way chemists think about chemical reactivity and chemical synthesis.¹⁰ The common pathways through which selective C–H functionalization operates are represented in figure 1.1.¹¹

(a) Oxidative addition pathway:



(b) Electrophilic metallation pathway:



(c) Concerted metalation-deprotonation (CMD) pathway:

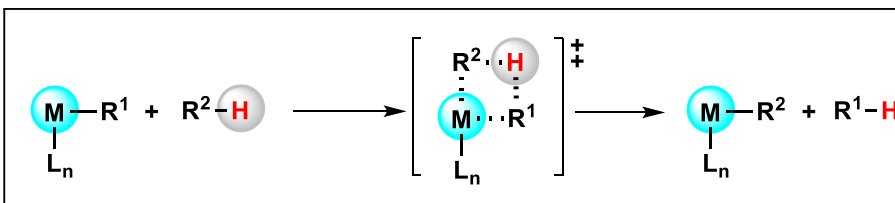


Figure 1.1. Basic modes of catalytic transition metal-catalyzed C–H bond activation.

In the oxidative pathway, the oxidative addition of the metal into the inert C–H bond through agostic interaction results in the formation of the C–M bond. Generally, transition metals with low oxidation state favours oxidative addition pathways toward C–H activation (Figure 1.1a). Further, the metal with a high oxidation state prefers to follow the electrophilic pathway, where the C–M bond has been generated through electrophilic metallation into the C–H bond (Figure 1.1b). Also, the C–M bond could be generated through concerted metallation followed by a deprotonation pathway. Generally, high valent late transition metals favours this transformation (Figure 1.1c). After the generation of the C–M bond through these catalytic pathways, it further

transformed into new C–C, C–N, or C–X bonds in the presence of appropriate coupling partners.

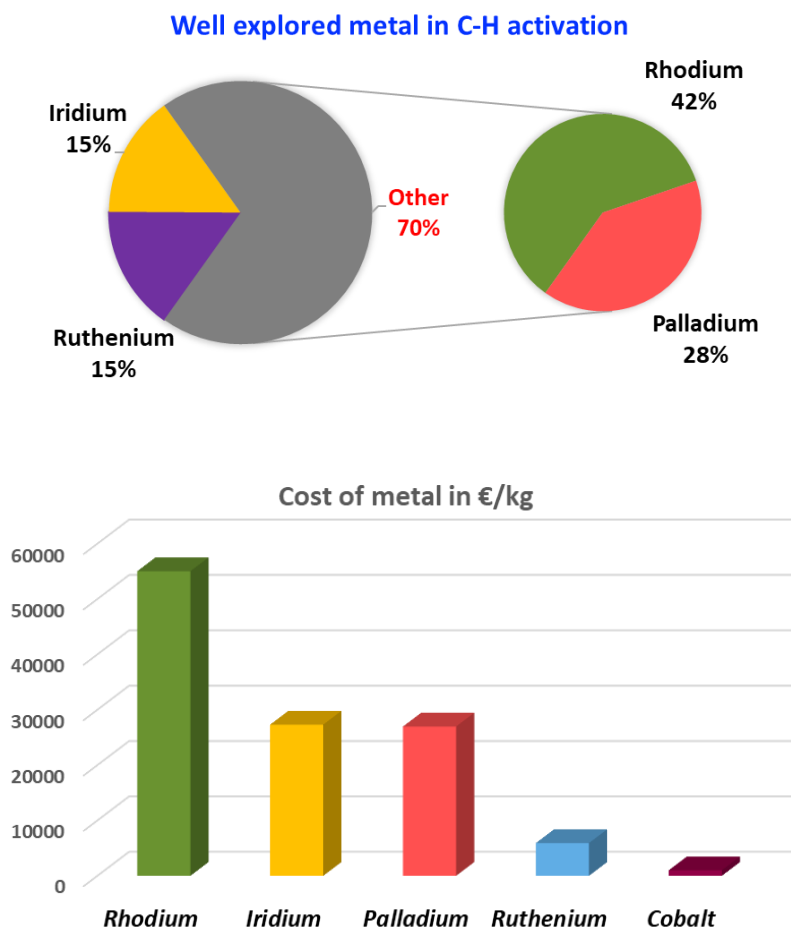


Figure 1.2. Well-explored transition metals in C-H activation and their cost.

Noble metals, such as ruthenium,¹² palladium,¹³ rhodium,¹⁴ and iridium¹⁵ have been extensively used for C–H bond functionalizations. However, these metals have high costs and low natural abundance, making them less sustainable (Figure 1.2).¹⁶ Hence, using first-row 3d-transition metals offers an economical and sustainable alternative to their higher congeners. The high natural abundance of the first-row transition metals renders the catalytic process cost-effective. The number of publications in the advancement of C–H bond functionalizations by exploiting 3d metals is depicted in Figure 1.3.¹⁷ Among the 3d metals, cobalt has emerged as a versatile and efficient metal-

catalyst for C–H activation, where both low and high valent cobalt catalysts have been employed. The reactivity of cobalt is comparable to that of 2nd and 3rd-row metal catalysts.¹⁸

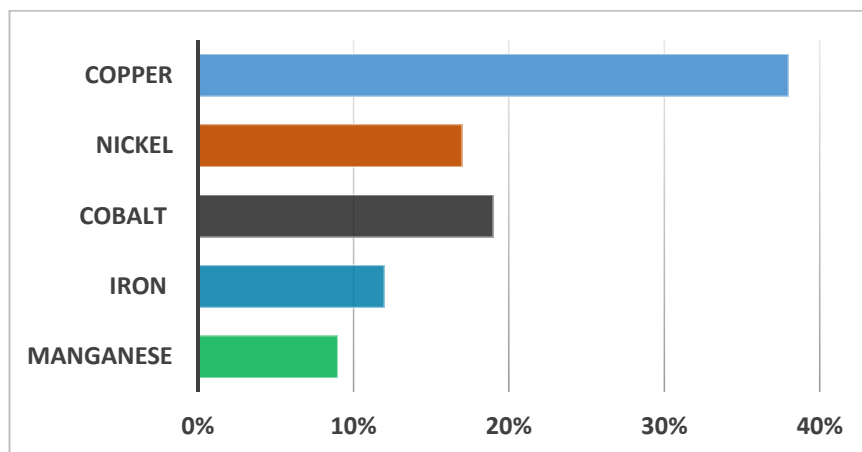
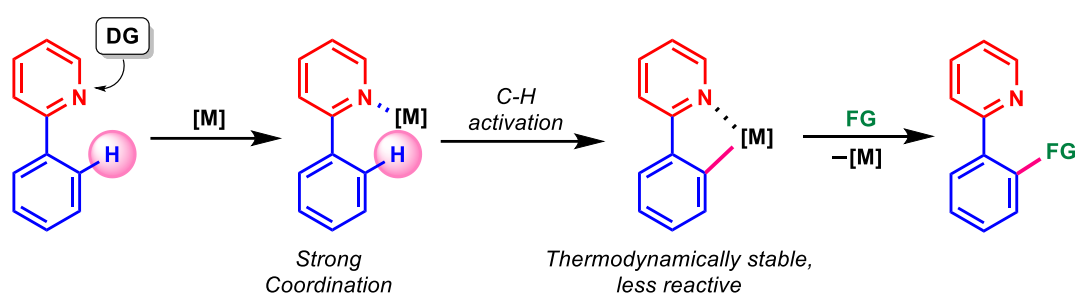


Figure 1.3. 3d-transition metals in C–H bond functionalization.

However, cobalt significantly differs in spin-orbit couplings and electronegativity from those of 4d or 5d homologue catalysts.¹⁹ Furthermore, cobalt is a less electronegative metal among the group IX elements. This translates into a more nucleophilic organometallic intermediate.²⁰ Thus, some unprecedented reactions have been uncovered in cobalt-catalyzed C–H functionalizations (e.g., for the nucleophilic attack of the C–Co intermediate on electrophilic sites after the C–H activation step).²¹ Also, cobalt is underdeveloped and isoelectronic with rhodium, which is well explored in C–H activation, so it can also lead to good reactivity and unusual transformation. Therefore, we have chosen a cobalt catalyst to study its reactivity toward C–H/C–C bond functionalization.²² Critical challenges in this chemistry are the selective C–H functionalization in the presence of several C–H bonds.²³ Thus, the ubiquitous nature of the C–H bonds in organic molecules makes it necessary to distinguish between similar but inequivalent sites. The selectivity issue has been addressed by directing groups that can coordinate with the metal and assist in activating the proximal C–H

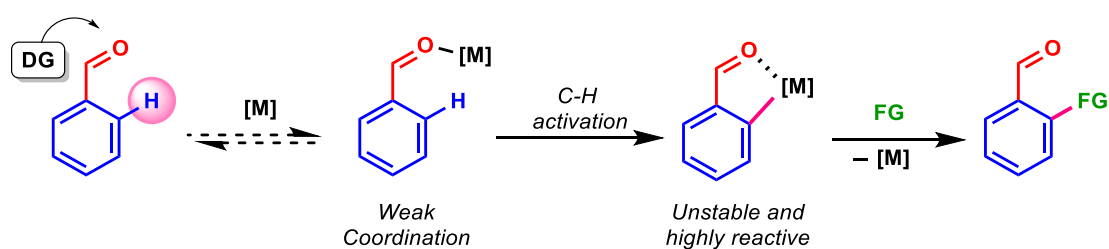
bond.²⁴ Traditionally, the C–H bond functionalizations have been accomplished by utilizing strongly coordinating atoms, such as nitrogen (e.g., pyrimidine, pyridine, aminoquinoline, oxazoline), which are well known as strong σ -donors (Scheme 1.1).²⁵

Scheme 1.1. C-H functionalization via strongly coordinating directing group.



Due to strong coordination, the metalation step is easier; therefore, this method was well utilized in C-H activation. However, further functionalization requires a high energy barrier to give the product (Figure 1.4).²² Most importantly, the *N*-coordinating directing groups have to be installed on the substrate before the C–H functionalization step. Also, often *N*-coordinating directing groups cannot be modifiable, so their removal requires harsh reaction conditions.

Scheme 1.2. C-H functionalization via weakly coordinating directing group.



In contrast, cyclometalation using *O*-coordinating directing groups (e.g., aldehyde, ketones, carboxylic acids, ester, and amides) is a better approach, which has been less studied (Scheme 1.2). The advantage of weak coordination is the formation of a thermodynamically less stable cobaltacycle resulting from the weak σ -donor nature of the oxygen atom, which can easily undergo further functionalizations (Figure 1.4).²²

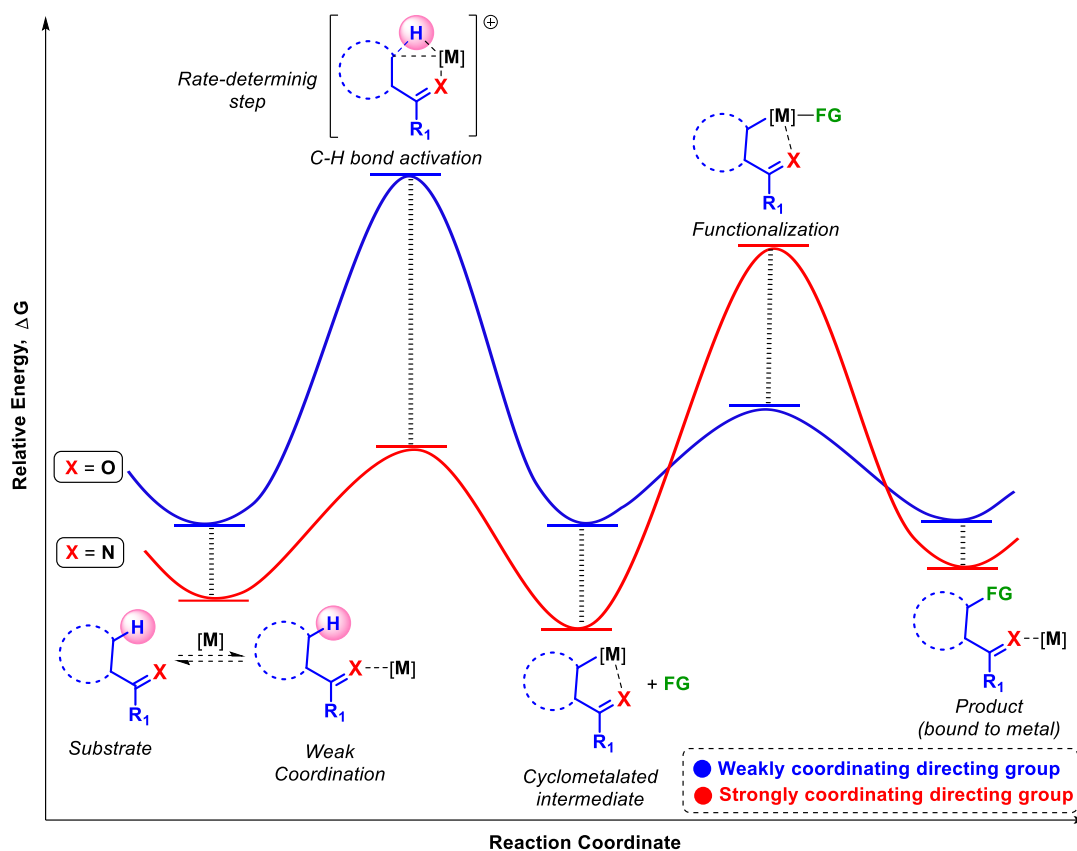


Figure 1.4. Energy profile diagram: strong vs. weak coordination assisted C-H bond activation.

Another advantage of this approach is the synthetic availability of the weakly coordinating functional groups, such as aldehydes, ketones, carboxylic acids, and esters, which are mostly part of the substrate or can be easily modified after functionalization.²⁶

The combination of 3d transition metal and weakly coordinating directing group are more sustainable approaches toward C-H bond functionalization (Figure 1.5). Because 3d transition metals are abundantly present in the earth's crust and weakly coordinating directing groups are easily modifiable and often part of organic molecules, reducing synthetic steps such as installation and removal of directing groups.

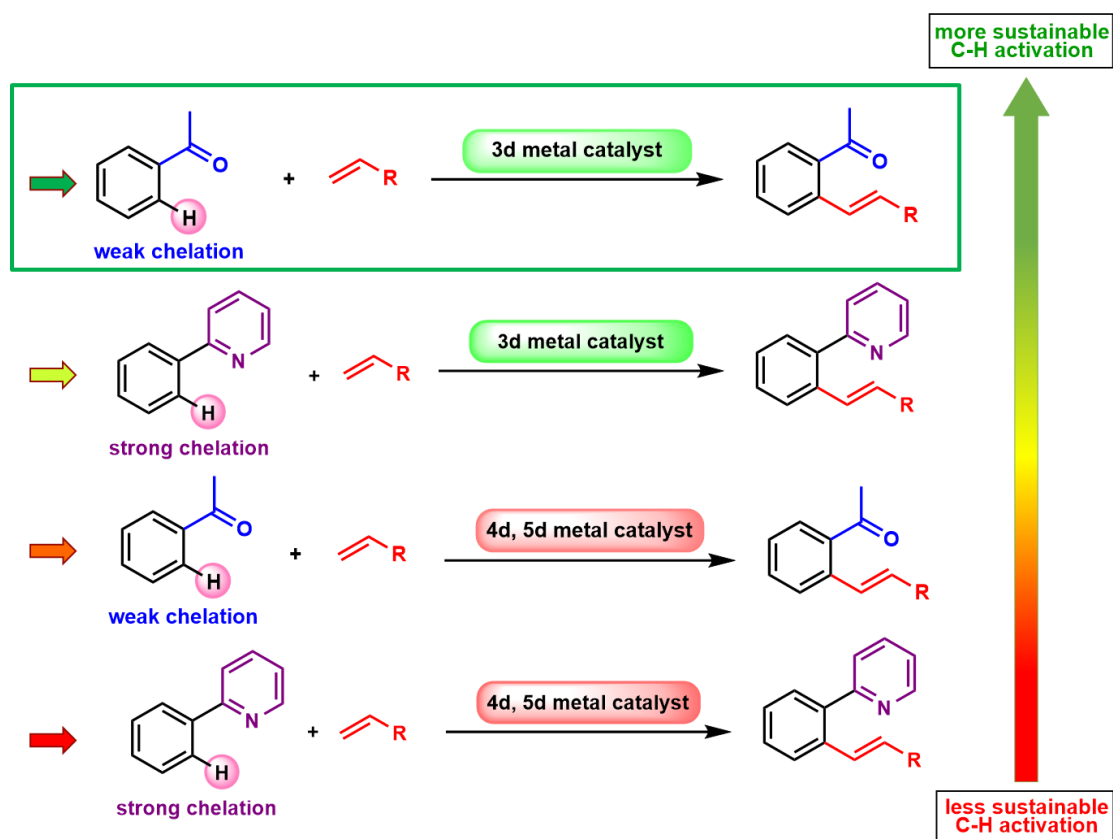


Figure 1.5. Sustainable approach towards olefination of the arene.^{16,22}

The well-explored transition metal-catalyzed olefination has been depicted in Figure 1.5, wherein the combination of 4d and 5d transition metals along with strongly coordinating directing group pyridine are less sustainable as it is non-modifiable. This could also be achieved by utilizing 3d transition metal with a weakly coordinating directing group that is highly sustainable in terms of the metal catalyst and versatility of the directing group.

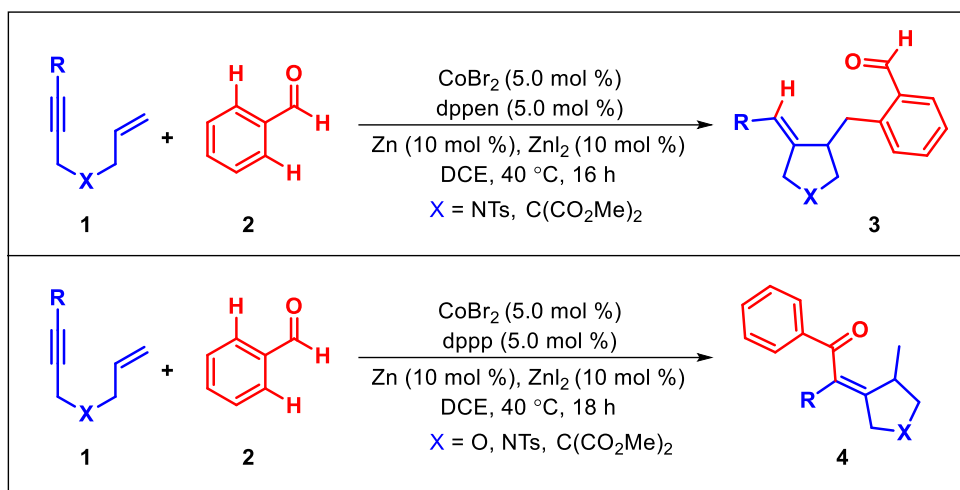
1.3. LITRATURE SURVEY

Further literature survey shows that there are only a limited number of reports on cobalt-catalyzed C–H bond functionalizations by utilizing weakly coordinating directing groups. Thus, we have segregated the developed examples of cobalt-catalyzed C–H bond functionalization assisted through weak coordination.

(i) Aldehyde-directed C-H bond activation:

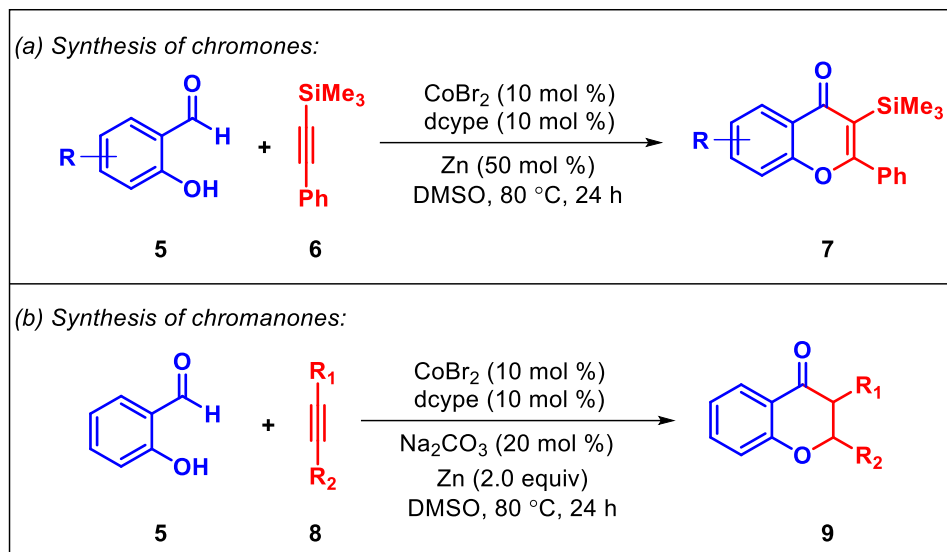
Aldehyde is one of the commonly available functional groups in organic molecules. As a functional group, it has some basic challenges, such as it can easily get oxidized to acid. Also, the aldehydic C-H bond could be activated using transition metal; despite having these challenges, aldehyde has been utilized as a weakly coordinated directing group.

Scheme 1.3. Cobalt-catalyzed cyclization of enynes via aldehyde directed C-H bond activation.



In this series, Cheng *et al.* reported cobalt-catalyzed hydroarylation and acylation reaction of enynes **1** with aldehydes **2**, affording functionalized pyrrolidines **3** and dihydrofurans **4** in high chemo and stereoselectivity (Scheme 1.3).²⁷ A switchable C–H bond functionalization was observed depending on changing the ligands dppen to dppp. Further, In 2016, Yoshikai *et al.* demonstrated cobalt-catalyzed annulation **7** of salicylaldehydes **5** with alkynes **6**.²⁸

Scheme 1.4. Cobalt-catalyzed annulation of salicylaldehydes utilizing alkyne.

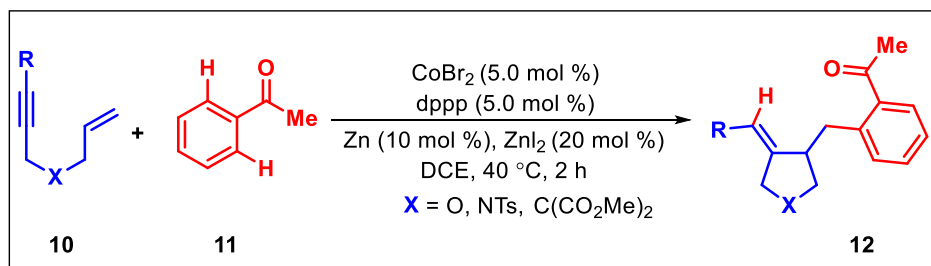


Depending on the substituent pattern of alkynes **6**, **8**, chromones **7**, and 4-chromanones **9** have been synthesized through dehydrogenative annulation of salicylaldehydes **5**.

(ii) Ketone-directed C-H bond activation:

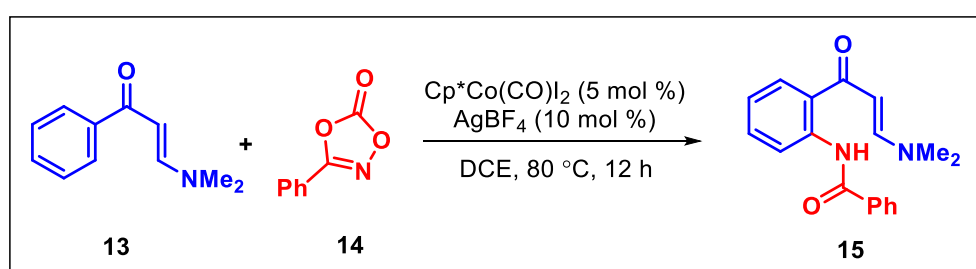
Ketones are commonly used as weakly coordinating directing groups in transition metal-catalyzed C–H bond functionalization. They are found in various bioactive molecules and can be easily transformed into various other functional groups, thus employed as synthetic intermediates. In this context, ketone-directed C–H functionalizations have higher synthetic utility, especially in C–C bond formation reactions.²⁹

Scheme 1.5. Cobalt-catalyzed hydroarylation cyclization of enynes and aromatic ketones.



In 2014, Cheng *et al.* reported the ketone-directed cobalt-catalyzed hydroarylation cyclization **12** (Scheme 1.5)³⁰ The in situ generated cobalt cycle from enyne **10** triggers the C–H functionalization reaction, affording functionalized pyrrolidines and dihydrofurans. Further, Zhu *et al.* developed cobalt-catalyzed *ortho*-C–H amidation of aryl enones **13** with dioxazolones **14** in the presence of enaminone as directing group (Scheme 1.6).³¹

Scheme 1.6. Substrate scope for enaminones and synthesis of quinolones.

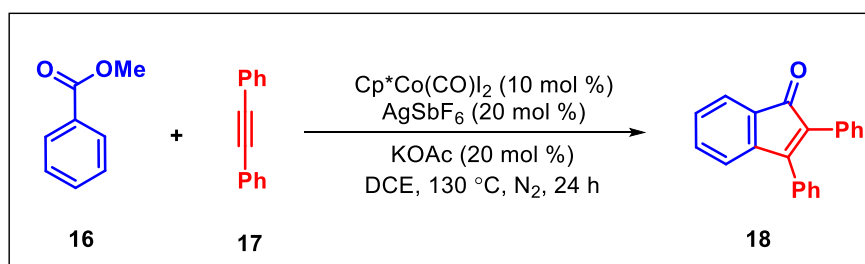


Herein, $\text{Cp}^*\text{Co}(\text{III})$ -catalyst has been utilized for the regioselective amidation of aryl enones **15**.

(iii) Carboxylic esters directed C–H bond activation:

Carboxylic ester is essential to various bioorganic molecules like fatty acids and lipids. Esters usually have a sweet smell, are commonly used as fragrances, and are found in essential oils and pheromones. Limited reports exist employing ester functionalities as a directing group in cobalt catalysis. Utilizing the weakly coordinating ability of esters,

Scheme 1.7. Cobalt catalyzed annulation utilizing carboxylic ester wDG.

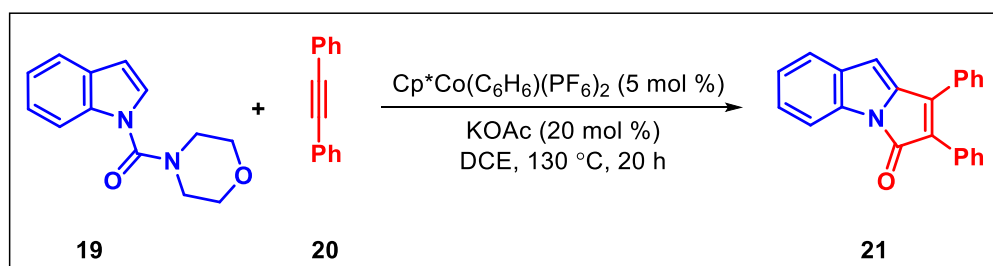


Zhang *et al.* synthesized indenones **18** through the annulation of benzoic esters **16** and internal alkynes **17** by exploiting cobalt catalysis (Scheme 1.7).³²

(iv) Substituted amide-directed C-H bond activation:

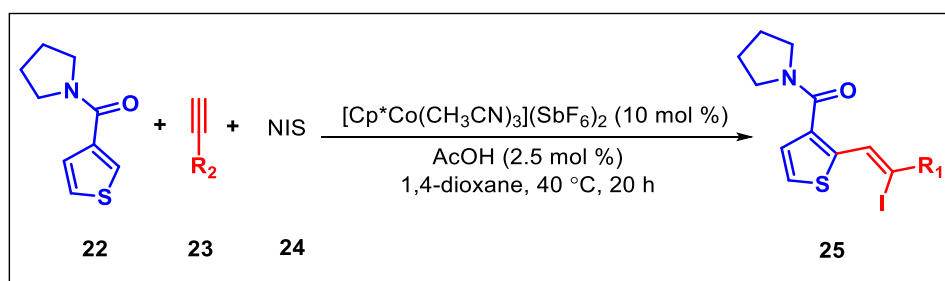
Amides are an essential class of organic compounds. Therefore selective synthesis and further derivatization of the amide is a crucial pursuit in synthetic methodology. Matsunaga *et al.* described the synthesis of indole-derived C-2 annulated product **21**, using the unique synthetic utility of Cp*Co(III) catalyst (Scheme 1.8).³³

Scheme 1.8. Scope of Cp*Co(III)-catalyzed C-H annulation and alkenylation.



Further, Ellman *et al.* have developed the synthesis of functionalized alkenyl halides **25** via weakly coordinating directing group **22** using cobalt(III)-catalyzed C-H functionalization/addition of alkyne **23** and halogens **24** in a domino reaction sequence (Scheme 1.9).³⁴ This reaction goes through the multicomponent pathway, which is quite challenging using weakly coordinating directing groups.

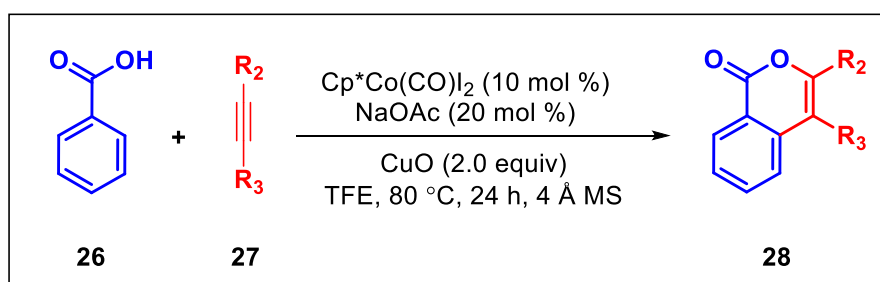
Scheme 1.9. Alkyne scope for the three-component addition cascade.



(v) Carboxylic acid group directed C-H activation:

Carboxylate groups are prevalent in organic molecules and can be removed easily by decarboxylation or transformed into various functionalities. Weak coordinating carboxylic acids have been well explored with 4d transition metal-catalyzed C–H functionalization reactions. However, there are only a few reports on carboxylic acid as a directing group in cobalt-catalyzed C–H functionalization reactions.

Scheme 1.10. Cobalt catalyzed C-H/OH annulation using alkyne.



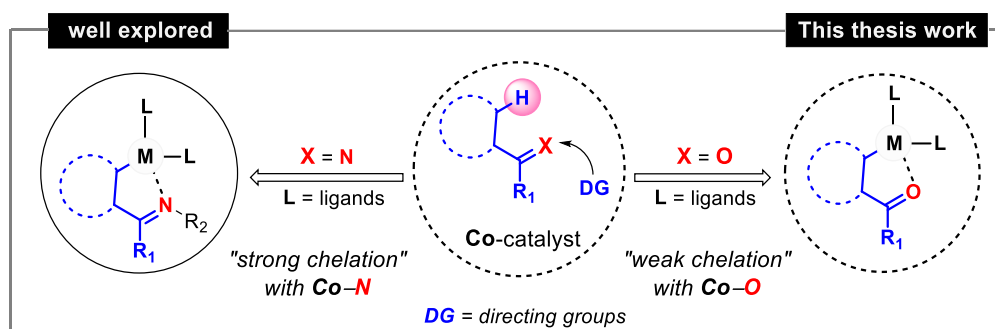
In 2017, Sundararaju *et al.* explored carboxylic acids as directing group for the synthesis of isocoumarins **28** through the annulation of aromatic carboxylic acids **26** with alkynes **27** using cobalt (III) catalysis.³⁵

In summary of these reported transformations, the cobalt catalyst has been well utilized for C-C and C-X bond formation. However, there is plenty of scopes to study this sustainable cobalt-weak chelation combination towards C-H/C-C bond functionalization.

1.4. CONCLUSION

This thesis thoroughly covers the development of C-H/C-C bond functionalization assisted by 3d transition metals cobalt using weakly coordinating directing groups. Researchers are now switching to use first-row transition metal catalysts in C-H bond functionalization reactions. Using earth's abundant, less toxic,

and economic 3d transition metals adds to sustainability. It has unique catalytic activities compared to its 4d and 5d congeners in C-H bond activation chemistry.



The utilization of weak coordinating groups for cobalt-catalyzed C-H functionalization is emerging as a powerful tool for developing synthetically versatile transformations, thus expanding the chemist's toolbox. Due to lower electronegativity, the unique reactivity of cobalt such as nucleophilic Co-C bond, enabled the synthesis of various skeletons that are otherwise not easily accessible. The combination of weak coordination and cobalt catalyst is environmentally benign, therefore, more sustainable for large-scale production of chemicals in pharmaceutical industries. Moreover, this combination has emerged unique reactivities towards C-H bond functionalization, which can be seen in the upcoming thesis chapters.

1.5 REFERENCES

1. (a) Nicolaou, K. C.; Bulger, P. G.; Sarlah, D. Palladium-catalyzed cross-coupling reactions in total synthesis. *Angew. Chem., Int. Ed.* **2005**, *44*, 4442–4489. (b) Magano, J.; Dunetz, J. R. Large-Scale Applications of Transition Metal-Catalyzed Couplings for the Synthesis of Pharmaceuticals. *Chem. Rev.* **2011**, *111*, 2177–2250. (c) Ruiz-Castillo, P.; Buchwald, S. L. Applications of Palladium-Catalyzed C–N Cross-Coupling Reactions. *Chem. Rev.* **2016**, *116*, 12564–12649.
2. Larock, R. C. Comprehensive organic transformations: a guide to functional group preparations; Wiley-VCH: **1999**. DOI: 10.1002/9781118662083. Online ISBN: 9781118662083.
3. (a) Miyaura, N.; Suzuki, A. Palladium-catalyzed cross-coupling reactions of organoboron compounds. *Chem. Rev.* **1995**, *95*, 2457. (b) De Meijere, A.; Diederich, F., Eds.; Metal-Catalyzed Cross-Coupling Reactions. Wiley-VCH: Weinheim, **2004**.
4. (a) Miyaura, N.; Yamada, K.; Suzuki, A. A New Stereospecific Cross-Coupling by the Palladium-Catalyzed Reaction of 1-Alkenylboranes with 1-Alkenyl or 1-Alkynyl Halides. *Tetrahedron Lett.* **1979**, *20*, 3437–3440. (b) Miyaura, N.; Suzuki, A. Stereoselective Synthesis of Arylated (E)-Alkenes by the Reaction of Alk-1-Enylboranes with Aryl Halides in the Presence of Palladium Catalyst. *J. Chem. Soc., Chem. Commun.* **1979**, 866–867. (c) Thorand, S.; Krause, N. Improved Procedures for the Palladium-Catalyzed Coupling of Terminal Alkynes with Aryl Bromides (Sonogashira Coupling). *J. Org. Chem.* **1998**, *63*, 8551–8553.
5. (a) Ding, K.; Dai, L.-X. Transition Metal-Catalyzed C–H Functionalization: Synthetically Enabling Reactions for Building Molecular Complexity. Organic Chemistry-Breakthroughs and Perspectives; Wiley-VCH: Weinheim, **2012** (b) Yu, J.-Q.; Shi, Z. C–H Activation. Topics in Current Chemistry; Springer-Verlag: Heidelberg, **2010**; Vol. 292.
6. Roudesly, F.; Oble, J.; Poli, G. Metal-Catalyzed C–H Activation/ Functionalization: The Fundamentals. *J. Mol. Catal. A: Chem.* **2017**, *426*, 275–296.
7. Bordwell, F. G. Equilibrium Acidities in Dimethyl Sulfoxide Solution. *Acc. Chem. Res.* **1988**, *21*, 456–463. (b) M. B. Smith, March’s Advanced Organic Chemistry, Wiley, New York, 7th Edn, **2013**, pp. 314–318.
8. (a) Chen, Z.; Rong, M.-Y.; Nie, J.; Zhu, X.-F.; Shi, B.-F.; Ma, J.-A. Catalytic alkylation of unactivated C(sp³)–H bonds for C(sp³)–C(sp³) bond formation. *Chem. Soc. Rev.* **2019**, *48*, 4921–4942. (b) Abrams, D. J.; Provencher, P. A.; Sorensen, E. J. Recent Applications of C–H Functionalization in Complex Natural Product Synthesis. *Chem. Soc. Rev.* **2018**, *47*, 8925–8967. (c) Liu, C.; Yuan, J.; Gao, M.; Tang, S.; Li, W.; Shi, R.; Lei, A. Oxidative Coupling between Two Hydrocarbons: An Update of Recent C–H Functionalizations. *Chem. Rev.* **2015**, *115*, 12138–12204.
9. (a) Cernak, T.; Dykstra, K. D.; Tyagarajan, S.; Vachal, P.; Krska, S. W. The Medicinal Chemist’s Toolbox for Late Stage Functionalization of Drug-Like Molecules. *Chem. Soc. Rev.* **2016**, *45*, 546–576. (b) Wencel-Delord, J.; Glorius, F. C–H Bond Activation Enables the Rapid Construction and Late-Stage Diversification of Functional Molecules. *Nat. Chem.* **2013**, *5*, 369–375. (c) Okamoto, K.; Zhang, J.; Housekeeper, J. B.; Marder, S. R.; Luscombe, C. K. C–H Arylation Reaction: Atom Efficient and Greener Syntheses of π -Conjugated Small Molecules and Macromolecules for Organic Electronic Materials. *Macromolecules* **2013**, *46*, 8059–8078.
10. (a) Yang, Y.; Lan, J.; You, J. Oxidative C–H/C–H Coupling Reactions between Two (Hetero)Arenes. *Chem. Rev.* **2017**, *117*, 8787–8863. (b) Liu, B.; Romine, A. M.; Rubel, C. Z.; Engle, K. M.; Shi, B.-F. Transition-Metal-Catalyzed, Coordination-Assisted Functionalization of Nonactivated C(sp³)–H Bonds. *Chem. Rev.* **2021**, *121*, 14957–15074.
11. (a) Gallego, D.; Baquero, E. A. Recent Advances on Mechanistic Studies on C–H Activation Catalyzed by Base Metals. *Open Chem.* **2018**, *16*, 1001–1058. (b) Carvalho, R.-L.; Dias, G.-

- G.; Pereira, C-L. M.; Ghosh, P.; Maiti, D.; da Silva Junior, E.-N. A' Catalysis Guide Focusing on C-H Activation Processes. *J. Braz. Chem. Soc.* **2021**, *32*, 917–952.
12. (a) Duarah, G.; Kaishap, P. P.; Begum, T.; Gogoi, S. Recent Advances in Ruthenium(II)-Catalyzed C-H Bond Activation and Alkyne Annulation Reactions. *Adv. Synth. Catal.* **2019**, *361*, 654–672. (b) Arockiam, P. B.; Bruneau, C.; Dixneuf, P. H. Ruthenium(II)-Catalyzed C-H Bond Activation and Functionalization. *Chem. Rev.* **2012**, *112*, 5879–5918.
 13. (a) Ramachandiran, K.; Sreelatha, T.; Lakshmi, N. V. T.; Babu, T. H.; Muralidharan, D.; Perumal, P. T. Palladium Catalyzed C-H Activation and its Application to Multi-bond Forming Reactions. *Curr. Org. Chem.* **2013**, *17*, 2001. (b) Li, H.; Li, B.-J.; Shi, Z. – J. Challenge and progress: palladium-catalyzed sp³ C-H activation. *Catal. Sci. Technol.* **2011**, *1*, 191.
 14. (a) Yang, Z.; Yu, J.-T.; Pan, C. Recent advances in rhodium-catalyzed C(sp²)-H (hetero)arylation. *Org. Biomol. Chem.* **2021**, *19*, 8442–8465. (b) Colby, D. A.; Bergman, R. G.; Ellman, J. A. Rhodium-Catalyzed C-C Bond Formation via Heteroatom-Directed C-H Bond Activation. *Chem. Rev.* **2010**, *110*, 624–655.
 15. (a) Nishimura, T. Iridium-Catalyzed Hydroarylation via C-H Bond Activation. *Chem. Rec.* **2021**, *21*, 3532–3545. (b) Wu, X.; Sun, S.; Yu, J.- T.; Cheng, J. Recent Applications of α -Carbonyl Sulfoxonium Ylides in Rhodium and Iridium-Catalyzed C-H Functionalizations. *Synlett* **2019**, *30*, 21–29.
 16. Dalton, T.; Faber, T.; Glorius, F. C-H Activation: Toward Sustainability and Applications. *ACS Cent. Sci.* **2021**, *7*, 245–261.
 17. Gandeepan, P.; Müller, T.; Zell, D.; Cera, G.; Warratz, S.; Ackermann, L. 3d Transition Metals for C-H Activation. *Chem. Rev.* **2019**, *119*, 2192–2452.
 18. (a) Baccalini, A.; Vergura, S.; Dolui, P.; Zannoni, G.; Maiti, D. Recent Advances in Cobalt-Catalysed C-H Functionalizations. *Org. Biomol. Chem.* **2019**, *17*, 10119–10141. (b) Liu, Y.; You, T.; Wang, H.-X.; Tang, Z.; Zhou, C.-Y.; Che, C.- M. Iron- and Cobalt-Catalyzed C(sp³)-H Bond Functionalization Reactions and Their Application in Organic Synthesis. *Chem. Soc. Rev.* **2020**, *49*, 5310–5358.
 19. CRC Handbook of Chemicals and Physics, ed. W. M. Haynes, CRC Press/Taylor and Francis, Boca Raton, 95th edn, **2015**.
 20. (a) Tanaka, R.; Kojima, M.; Yoshino, T.; Matsunaga, S. Cobaltcatalyzed Synthesis of Homoallylic Amines from Imines and Terminal Alkenes. *Chem. Lett.* **2019**, *48*, 1046–1049. (b) Lorion, M. M.; Kaplaneris, N.; Son, J.; Kuniyil, R.; Ackermann, L. Late-Stage Peptide Diversification through CobaltCatalyzed C-H Activation: Sequential Multicatalysis for Stapled Peptides. *Angew. Chem., Int. Ed.* **2019**, *58*, 1684–1688.
 21. Ikemoto, H.; Yoshino, T.; Sakata, K.; Matsunaga, S.; Kanai, M. Pyrroloindolone Synthesis via a Cp*CoIII-Catalyzed Redox-Neutral Directed C-H Alkenylation/Annulation Sequence. *J. Am. Chem. Soc.* **2014**, *136*, 5424–5431.
 22. Banjare, S. K.; Nanda, T.; Pati, B. V.; Biswal, P.; Ravikumar, P. C. O-Directed C-H Functionalization via Cobaltacycles: A Sustainable Approach for C-C and C-Heteroatom Bond Formations. *Chem. Commun.* **2021**, *57*, 3630–3647.
 23. (a) Ackermann, L.; Vicente, R.; Kapdi, A. R. Transition-metal-catalyzed direct arylation of (hetero) arenes by C-H bond cleavage. *Angew. Chem., Int. Ed.* **2009**, *48*, 9792–9826. (b) Chen, X.; Engle, K. M.; Wang, D.-H.; Yu, J.- Q. Palladium (II)-catalyzed C-H activation/C-C cross-coupling reactions: versatility and practicality. *Angew. Chem., Int. Ed.* **2009**, *48*, 5094–5115.
 24. (a) Ros, A.; Fernandez, R.; Lassaletta, J. M. Functional Group Directed C-H Borylation. *Chem. Soc. Rev.* **2014**, *43*, 3229–3243. (b) Das, R.; Kumar, G. S.; Kapur, M. Amides as Weak Coordinating Groups in Proximal C-H Bond Activation. *Eur. J. Org. Chem.* **2017**, *2017*, 5439–5459. (c) Rej, S.; Ano, Y.; Chatani, N. Bidentate Directing Groups: An Efficient Tool in C-H Bond Functionalization Chemistry for the Expedient Construction of C-C Bonds. *Chem. Rev.* **2020**, *120*, 1788–1887.

-
25. Zhang, M.; Zhang, Y.; Jie, X.; Zhao, H.; Li, G.; Su, W. Recent Advances in Directed C-H Functionalizations Using Monodentate Nitrogen-Based Directing Groups. *Org. Chem. Front.* **2014**, *1*, 843–895.
 26. (a) Yao, Q.-J.; Zhang, S.; Zhan, B.-B.; Shi, B.-F. Atroposelective Synthesis of Axially Chiral Biaryls by Palladium-Catalyzed Asymmetric C–H Olefination Enabled by a Transient Chiral Auxiliary. *Angew. Chem., Int. Ed.* **2017**, *56*, 6617–6621. (b) Liao, G.; Yao, Q.-J.; Zhang, Z.-Z.; Wu, Y.-J.; Huang, D.-Y.; Shi, B.-F. Scalable, Stereocontrolled Formal Syntheses of (+)-Isoschizandrin and (+)-Steganone: Development and Applications of Palladium- (II)-Catalyzed Atroposelective C–H Alkynylation. *Angew. Chem., Int. Ed.* **2018**, *57*, 3661–3665.
 27. Santhoshkumar, R.; Mannathan, S.; Cheng, C.-H. LigandControlled Divergent C-H Functionalization of Aldehydes with Enynes by Cobalt Catalysts. *J. Am. Chem. Soc.* **2015**, *137*, 16116–16120.
 28. Yang, J.; Yoshikai, N. Cobalt-Catalyzed Annulation of Salicylaldehydes and Alkynes to Form Chromones and 4-Chromanones. *Angew. Chem., Int. Ed.* **2016**, *55*, 2870–2874.
 29. (a) Huang, Z.; Lim, H. N.; Mo, F.; Young, M. C.; Dong, G. Transition Metal-Catalyzed Ketone-Directed or Mediated C–H Functionalization. *Chem. Soc. Rev.* **2015**, *44*, 7764–7786. (b) Zheng, Q. Z.; Jiao, N. Transition-metal-catalyzed ketone-directed *ortho*-C–H functionalization reactions. *Tetrahedron Lett.* **2014**, *55*, 1121–1126.
 30. Santhoshkumar, R.; Mannathan, S.; Cheng, C.-H. CobaltCatalyzed Hydroarylatve Cyclization of 1,6-Enynes with Aromatic Ketones and Esters via C–H Activation. *Org. Lett.* **2014**, *16*, 4208–4211.
 31. Shi, P.; Wang, L.; Chen, K.; Wang, J.; Zhu, J. Co(III)-Catalyzed Enaminone-Directed C–H Amidation for Quinolone Synthesis. *Org. Lett.* **2017**, *19*, 2418.
 32. Yu, W. L.; Zhang, W.; Liu, Z. X.; Zhang, Y. H. Cobalt(III)- Catalyzed Annulation of Esters and Alkynes: a Facile Route to Indenones. *Chem. Commun.* **2016**, *52*, 6837–6840.
 33. Ikemoto, H.; Yoshino, T.; Sakata, K.; Matsunaga, S.; Kanai, M. Pyrroloindolone Synthesis Via a Cp*Co-III-Catalyzed Redox-Neutral Directed C-H Alkenylation/Annulation Sequence. *J. Am. Chem. Soc.* **2014**, *136*, 5424–5431.
 34. Boerth, J. A.; Ellman, J. A. A Convergent Synthesis of Functionalized Alkenyl Halides through Cobalt(III)–Catalyzed Three-Component C–H Bond Addition. *Angew. Chem., Int. Ed.* **2017**, *56*, 9976–9980.
 35. Mandal, R.; Sundararaju, B. Cp*Co(III)-Catalyzed Annulation of Carboxylic Acids with Alkynes. *Org. Lett.* **2017**, *19*, 2544–2547.

Chapter 2

Cobalt Catalyzed Hydroarylation of Michael Acceptors with Indolines Directed by a Weakly Coordinating Functional Group

2.1 Abstract

2.2 Introduction

2.3 Results and Discussions

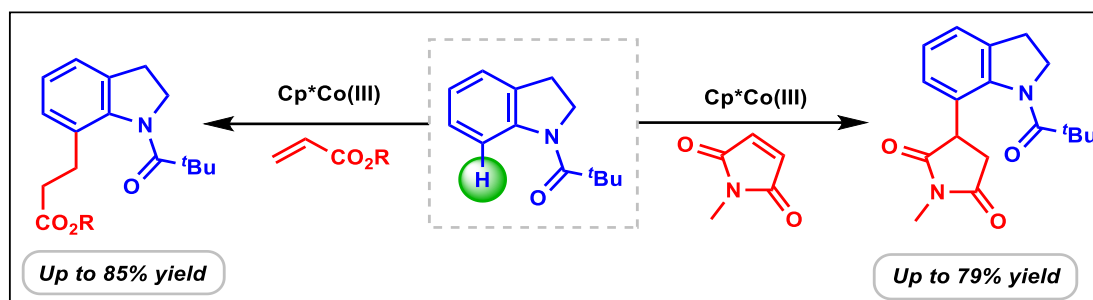
2.4 Conclusions

2.5 Experimental Section

2.6 References

Chapter 2

Cobalt Catalyzed Hydroarylation of Michael Acceptors with Indolines Directed by a Weakly Coordinating Functional Group



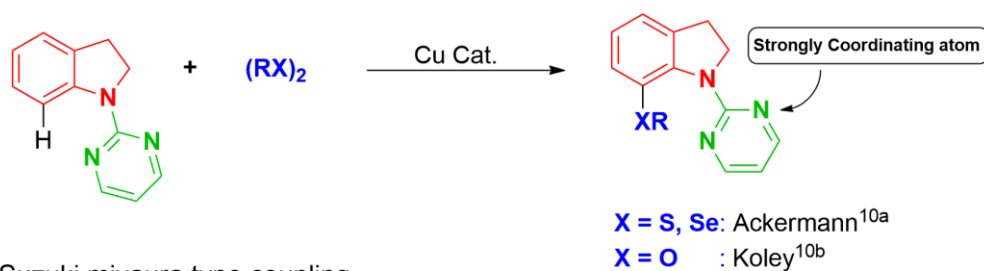
2.1 ABSTRACT: A cobalt(III) catalyzed hydroarylation of Michael acceptors using indolines, selectively at the C-7 position, has been reported. For the selective C-7 functionalization of indoline, we have used a weakly coordinating amide carbonyl group. During the optimization process, we also discovered zinc triflate's unusual co-catalytic activity in the C-H functionalization reaction. Hydroarylation of unprotected maleimide using indolines was a challenging substrate and had never been accomplished before. We were able to achieve this with our methodology in good yields.

2.2 INTRODUCTION

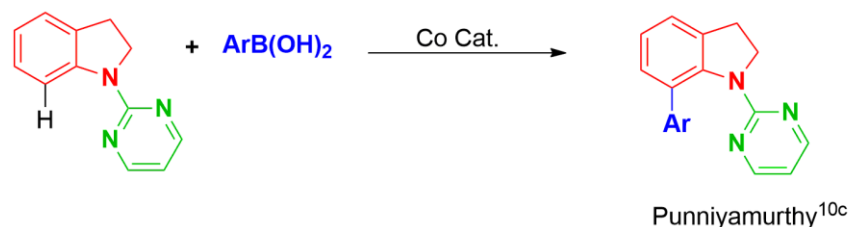
The ubiquitous nature of indole and indoline structural motifs in numerous bioactive natural products and pharmaceuticals has drawn considerable attention to their synthesis and structural modification. It has become an essential area for drug discovery.¹ The direct transition metal catalyzed C-H bond functionalization has proven to be the most elegant approach for structural modification of indoles. It offers

advantages like simple precursors without any prerequisite, functional groups, and step and atom economy.² Due to the inherent reactivity of the pyrrole core in indole, the direct C(2)–H and C(3)–H functionalization of indoles has been well explored.³ In contrast, the direct C–H functionalization at the C₇ position of the indole ring is less explored.⁴ Installation of the functional group at the C(7)–H of indoles can be achieved by the directing group assisted C(7)–H functionalization of indolines, followed by dehydrogenation. Significant efforts have been dedicated to developing efficient and practical strategies for the regioselective functionalization of indolines at the C₇ position using second- and third-row transition elements (mainly Ru,⁵ Rh,⁶ Pd,⁷ and Ir⁸).

a) Carbon-hetero bond formation



b) Suzuki miyaura type coupling



c) This work (Hydroarylation)

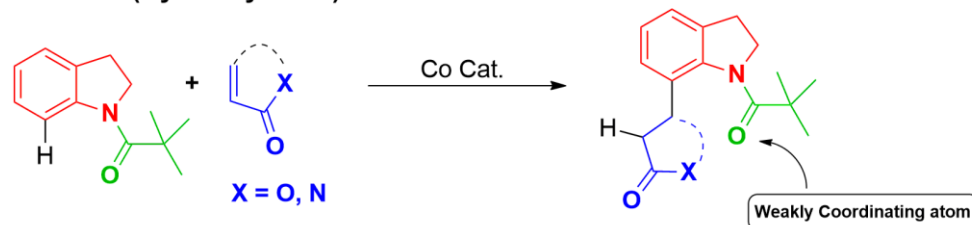


Figure 2.1: C(7)–H functionalization of indolines catalyzed by first-row transition metals.

In the recent decade, a paradigm shift has been observed toward the development of earth-abundant and environmentally benign first-row transition metal-catalyzed reactions.⁹ In this regard, Ackermann^{10a} and Koley^{10b} groups, have reported copper-catalyzed C–S/C–Se and C–O bond formation of indolines at the C₇ position, respectively, using the strong nitrogen donor, i.e., pyrimidyl directing group. Recently, the Punniyamurthy^{10c} group also exploited the strongly coordinating pyrimidyl directing group for the cobalt-catalyzed Suzuki–Miyaura type coupling of indolines at the C₇ position with aryl boronic acid. Weakly coordinating directing groups are gaining importance due to their weak coordination with the metal catalyst facilitating the reaction at faster rates with higher selectivities.¹¹ In this regard, we report a cobalt-catalyzed hydroarylation of Michael acceptors with indolines at the C₇ position through a weakly coordinating amide directing group (Figure 2.1). Hydroarylation reactions are generally challenging due to a competing β -hydride elimination pathway.

2.3 RESULTS AND DISCUSSION

We chose a model reaction using 1-(indolin-1-yl)-2,2-dimethylpropan-1-one **1a** and 1-methyl-1H-pyrrole-2,5-dione **2a** to investigate various reaction parameters for the cobalt-catalyzed hydroarylation of Michael acceptors. Initially, we screened various carboxylic acids as additives, which showed inferior results except for the sterically bulky adamantane-carboxylic acid (40%) (Table 2.1). Then, we switched to screening various base additives; it showed satisfactory and intriguing results. In this study, we observed that the anion and its counteranion influence hydroxylation. It was observed from the result in using CsOAc, NaOAc, and LiOAc that with the increase in counteranion charge density (charge/size), the yield of hydroarylation product

increases since the cation possessing higher charge density could act as a better Lewis acid to activate the Michael acceptor as well as the active catalyst. Next, we screened various carbonate bases, among which Li_2CO_3 showed the best result in the presence of $\text{Zn}(\text{OTf})_2$ and produced 76% of hydroarylation product **3a** in trifluoroethanol at 80 °C.¹²

Table 2.1: Optimization of the Hydroarylation Reaction^{a,b}

entry	Ag salt	Additive/variations	Yield (%) ^b
1	AgSbF_6	--	0
2	AgSbF_6	PivOH	0
3	AgSbF_6	Glycine	0
4	AgSbF_6	Isoleucine	0
5	AgSbF_6	Adamantyl acid	36
6	AgSbF_6	Adamantyl acid, 36h	40
7	AgNTf_2	Adamantyl acid	40
8	AgSbF_6	CsOPiv	30
9	AgSbF_6	CsOAc	0
10	AgSbF_6	NaOAc	51
11	AgSbF_6	LiOAc	61
12	AgSbF_6	Cs_2CO_3	23
13	AgSbF_6	Na_2CO_3	38
14	AgSbF_6	$\text{Na}_2\text{CO}_3 + \text{Zn}(\text{OTf})_2$	37
15	AgSbF_6	$\text{Na}_2\text{CO}_3 + \text{Zn}(\text{OTf})_2$, TFE	54
16	AgSbF_6	$\text{Li}_2\text{CO}_3 + \text{Zn}(\text{OTf})_2$	66
17	AgSbF_6	$\text{Li}_2\text{CO}_3 + \text{Zn}(\text{OTf})_2$, TFE	73
18	AgSbF_6	$\text{Li}_2\text{CO}_3 + \text{Zn}(\text{OTf})_2$, TFE, 80 °C	76
19	--	$\text{Li}_2\text{CO}_3 + \text{Zn}(\text{OTf})_2$, TFE, 80 °C	0
20	AgNTf_2	$\text{Li}_2\text{CO}_3 + \text{Zn}(\text{OTf})_2$, TFE, 80 °C	68

^aReaction conditions: **1a** (0.25 mmol), **2a** (2 equiv), $\text{Cp}^*\text{Co}(\text{CO})\text{I}_2$ (10 mol %), Ag salt (20 mol %), additive (20 mol %), trifluoroethanol (0.1 M) as a solvent, 120 °C, 24 h.

^bIsolated yields.

The optimized conditions were evaluated with various *N*-substituted indolines (Table 2.2), among which *N*-pivaloyl (76%) and *N*-acetyllindolines (**3x**, 62) showed positive results; *N*-pivaloyllindoline produced a better yield of the C(7) hydroarylation product. It might be due to the presence of peripheral interactions between the bulky *t*-butyl group of *N*-pivaloyl and C(7)–H, which makes the oxygen donor atom of *N*-pivaloyl orient toward the C(7) position more conveniently than in *N*-acetyllindoline. With the optimization condition, the substrate scope was examined with various indolines and Michael acceptors (Schemes 2.1 and 2.2). Various *N*-substituted (free *NH*, methyl, ethyl, benzyl, and phenyl) maleimides were tested with electronically different indolines, giving the hydroarylated products at the C(7) of indolines in good yields with high positional selectivities. The *N*-alkyl substituents produced better yields than the *N*-phenylmaleimide.

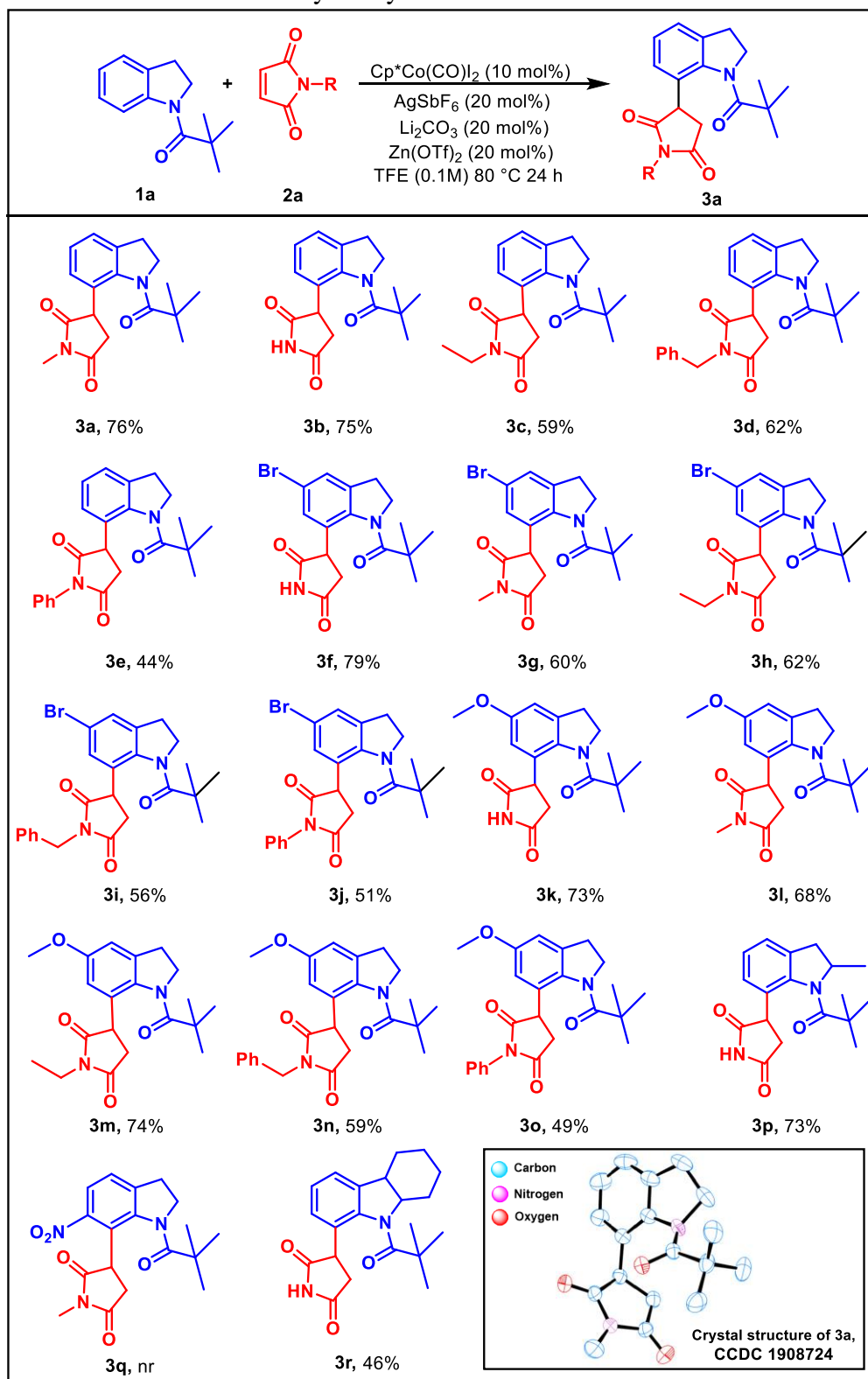
Table 2.2: Scope of Various Directing Groups for the Hydroarylation of *N*-Methylmaleimides^{a,b}

entry	R	Yield (%) ^b
1	H	0
2	Ac	62
3	Boc	0
4	Piv	76

^aReaction conditions: **1a** (0.25 mmol), **2a** (2 equiv), Cp*Co(CO)I₂ (10 mol %), Ag salt (20 mol %), additive (20 mol %), trifluoroethanol (0.1 M) as a solvent, 120 °C, 24 h.

^bIsolated yields.

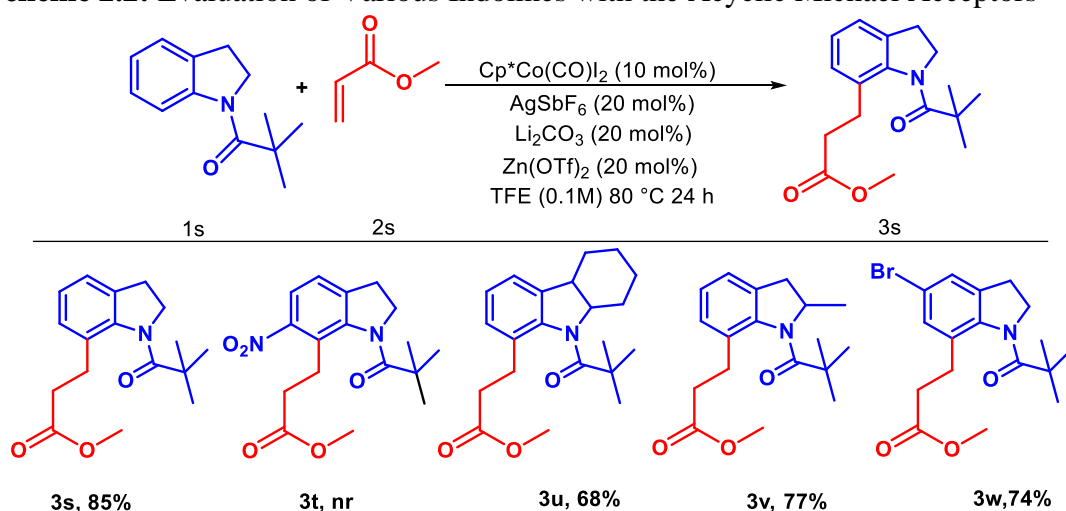
Scheme 2.1: Evaluation of Various Indolines and Michael Acceptors for the Hydroarylation Reaction^{a,b}



^aReaction conditions: **1** (0.25 mmol), **2** (2 equiv), $\text{CoCp}^*(\text{CO})\text{I}_2$ (10 mol %), AgSbF_6 (20 mol %), Li_2CO_3 (20 mol %), $\text{Zn}(\text{OTf})_2$ (20 mol %), trifluoroethanol (TFE) (0.1 M) as a solvent, 80 °C, 12–24 h. ^bIsolated yields.

The cobalt-catalyzed hydroarylation of indolines was compatible with methoxy and bromo substituents (**3f–3o**), which could be useful for further transformations. Even the sterically hindered 2-methyl indoline and hexahydro carbazole produced the desired products **3p** and **3r**, respectively, in good yields. The electron-withdrawing indolines showed insignificant results (**3q**, **3t**). The present protocol also worked with the acyclic Michael acceptors and afforded good yields (**3s–3w**).

Scheme 2.2: Evaluation of Various Indolines with the Acyclic Michael Acceptors^{a,b}

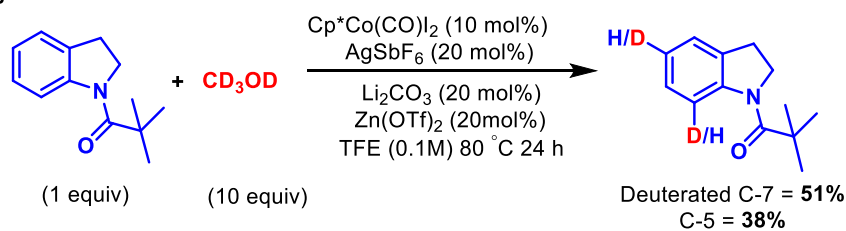


^aReaction conditions: **1** (0.25 mmol), **2** (2 equiv), $\text{CoCp}^*(\text{CO})\text{I}_2$ (10 mol %), AgSbF_6 (20 mol %), Li_2CO_3 (20 mol %), $\text{Zn}(\text{OTf})_2$ (20 mol %), trifluoroethanol (TFE) (0.1 M) as a solvent, 80 °C, 12–24 h. ^bIsolated yields.

In the absence of the Michael acceptor, *N*-pivalylindoline, under the same reaction conditions with 10 equiv of methanol-*d*₄, gave us C-7 and C-5 deuterated compounds in 51% and 38%, respectively (Scheme 2.3a). The ratios did not change much even after continuing for long hours, confirming that the first step might be in reversible equilibrium. In the presence of radical quenchers such as TEMPO and BHT (Scheme 2.3b), the reaction yield decreases but is not completely quenched, which confirms that the reaction is going through the ionic mechanism.

Scheme 2.3: Mechanistic studies.

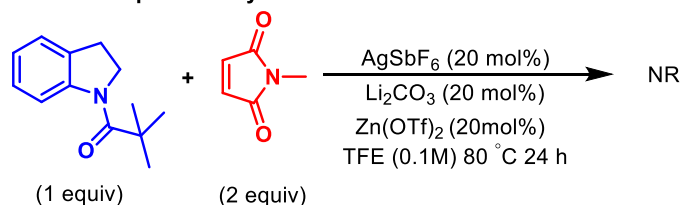
(a) H/D exchange studies:



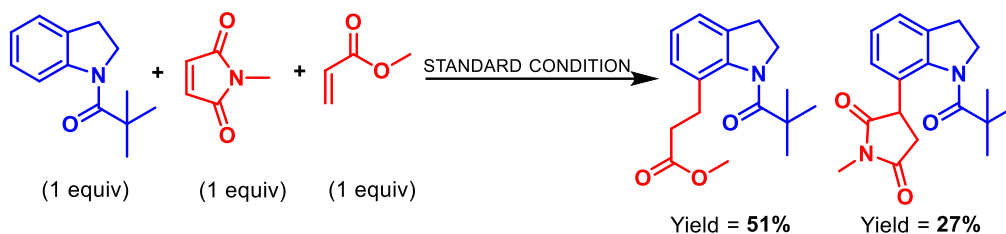
(b) Reaction with radical scavengers:



(c) Reaction in absence of Cp^*Co catalyst :



(d) Competition studies with coupling partners:



We did a control reaction to understand the influence of Cp^*Co ; the reaction did not give us any product, which confirms the critical role of cobalt in this reaction (Scheme 2.3c). Competition reaction between the two coupling partners, maleimide and methyl acrylate, gave us the corresponding products in 27% and 51% yield, which confirms that the sterically less hindered acrylate reacts at almost twice the rate as that of maleimide derivatives (Scheme 3d). An intermolecular competitive study was performed between electronically diverse indolines (Scheme 2.3d). Only the electron-rich ($-\text{OMe}$) indoline produced 57% of the hydroarylation product, whereas the

electron-poor ($-\text{CN}$) substituted indoline afforded an insignificant result. This might be due to the poor nucleophilicity of the $\text{Co}-\text{C}$ bond in the electron-withdrawing ($-\text{CN}$) substrate making it less prone to undergo olefin insertion from the intermediate **III**.

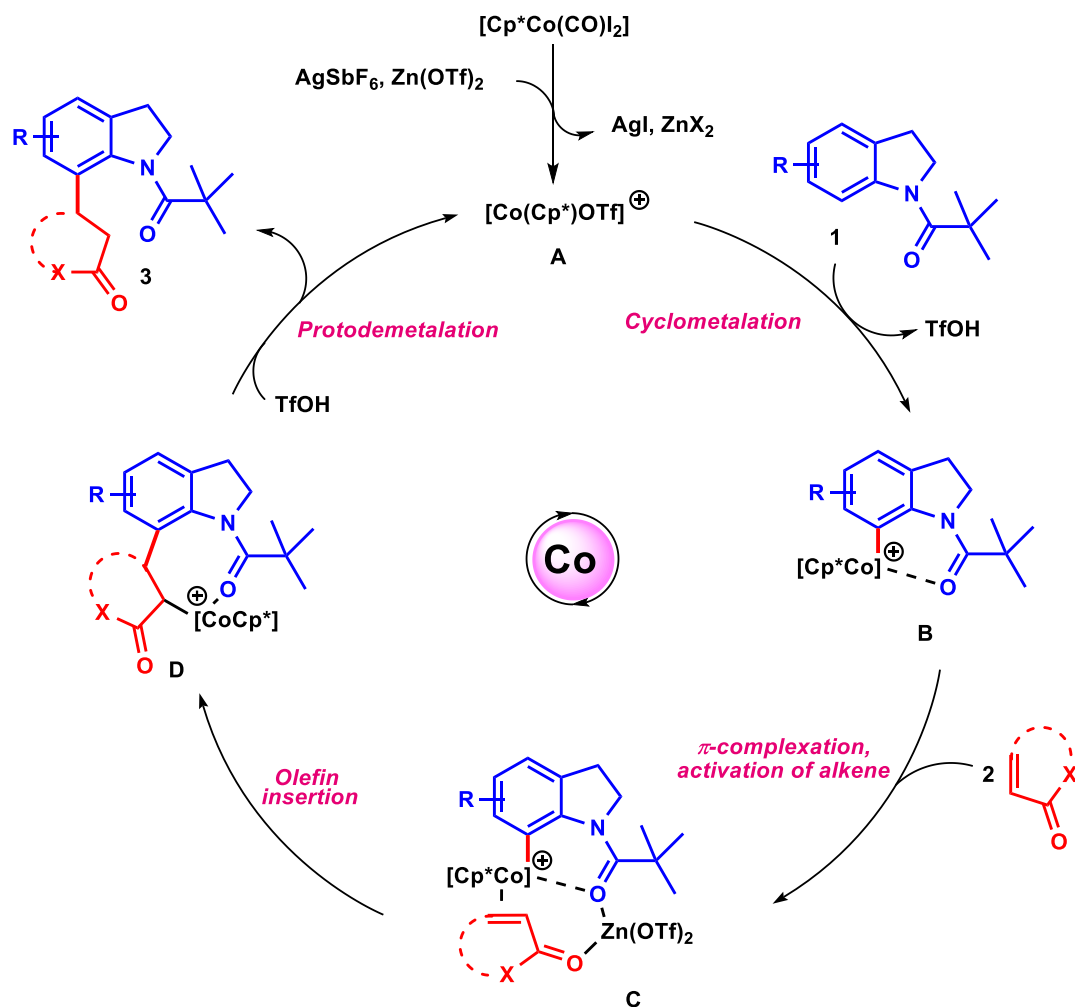


Figure 2.2: Proposed Catalytic Cycle for the Cobalt Catalyzed Hydroarylation of Michael Acceptors.

A plausible mechanism was depicted based on the experimental observations and precedent reports (Figure 2.2).^{11,12,13} We presume that, initially, an active cationic cobalt complex **I** is formed with AgSbF_6 and $\text{Zn}(\text{OTf})_2$, followed by the C–H functionalization of indoline **1** to yield cyclometalation intermediate **II**. Then, the formation of π -complex **III** occurs with Michael acceptor **2**. The subsequent olefin

insertion step provides intermediate **IV**, which undergoes proto-demetalation to complete the catalytic cycle and gives the desired hydroarylation product.

2.4 CONCLUSION

In summary, using a weakly coordinating directing group, we developed the cobalt catalyzed regioselective C(7) hydroarylation of indolines with activated olefins. We have also uncovered the remarkable role of Lewis acids in facilitating the reaction. The developed protocol works well with various Michael acceptors and indolines. Our methodology works well even with unprotected maleimides, which were a difficult substrate based on previous reports.

Limitations: Electron-withdrawing substituted arenes such as -NO₂ are incompatible with optimized reaction conditions. Because electron-withdrawing groups decrease the nucleophilicity of Co-C bond towards olefin insertion.

2.5 EXPERIMENTAL SECTION

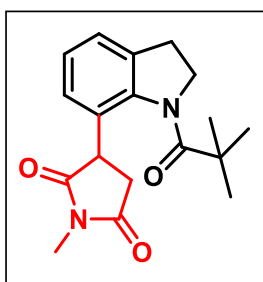
Reactions were performed using borosil sealed tube vial under an N₂ atmosphere. Column chromatography was done by using 100-200 & 230-400 mesh size silica gel of Merck Company. Gradient elution was performed by using distilled petroleum ether and ethyl acetate. TLC plates were detected under UV light at 254 nm. ¹H NMR, ¹³C NMR, recorded on Bruker AV 400,700 MHz spectrometer using CDCl₃ as internal standards the residual CHCl₃ for ¹H NMR (δ = 7.26 ppm) and the deuterated solvent signal for ¹³C NMR (δ = 77.36 ppm) is used on reference.¹⁴ Multiplicity (s = single, d = doublet, t = triplet, q = quartet, m = multiplet, dd = double doublet), integration, and coupling constants (*J*) in hertz (Hz). HRMS signal analysis was performed using a

micro TOF Q-II mass spectrometer, and X-ray analysis was recorded at SCS, NISER. Reagents and starting materials were purchased from Sigma Aldrich, Alfa Aesar, TCI, Avra, Spectrochem, and other commercially available sources and used without further purification unless otherwise noted.

(a) General reaction procedure for C-7 functionalization of indoline:

Under N₂, the mixture of *N*-pivaloyl indoline **1a** (0.1 mmol), maleimide **2a** (0.2 mmol), [Cp*Co(CO)I₂] (10 mol%), AgSbF₆ (20 mol%), Li₂CO₃ (20 mol%), Zn(OTf)₂ (20 mol%) and TFE (1 mL) were added into the tube and sealed. The reaction mixture was vigorously stirred at 80 °C on the preheated aluminum block for 24 h. After 24 h (completion of the reaction as monitored by TLC analysis), the reaction mixture was cooled to room temperature and diluted with ethyl acetate and passed through a short celite pad, the solvent was evaporated under reduced pressure, and the residue was purified by column chromatography to give the pure product **3a** light yellow solid (24 mg, 76% yield) R_f: 0.42 (in 30% EtOAc/Hexane).

(b) Experimental characterization data of products:



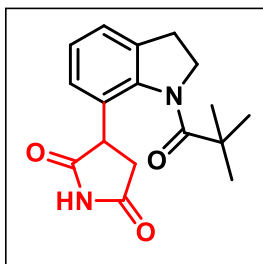
3-(1-pivaloyl indolin-7-yl)-1-methylpyrrolidine-2,5-dione

(3a): was prepared according to general procedure (2.5a).

The crude reaction mixture was purified by column chromatography using silica gel (100-200 mesh size), giving a light yellow solid (24 mg, 76% yield) R_f: 0.42 (in

30% EtOAc/Hexane): ¹H NMR (CDCl₃, 400 MHz): δ 7.17 (d, *J* = 6.8 Hz, 1H), 7.09 (t, *J* = 7.6 Hz, 1H), 6.93 (d, *J* = 7.6 Hz, 1H), 4.34-4.29 (m, 1H), 4.06-3.98 (m, 2H), 3.39-3.32 (m, 1H), 3.15-3.09 (m, 1H), 3.06 (s, 3H), 2.97-2.91 (m, 1H), 2.86-2.80 (m,

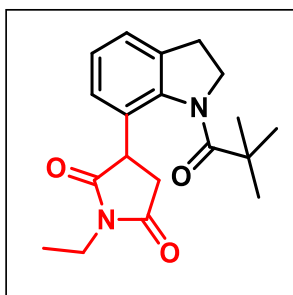
1H), 1.36 (s, 9H). **¹³C NMR (CDCl₃, 100 MHz):** δ 179.2, 178.9, 177.6, 143.2, 135.5, 129.6, 126.7, 126.2, 124.1, 51.3, 44.8, 40.1, 36.8, 31.2, 28.7, 25.3. **HRMS (ESI) m/z** calcd for C₁₈H₂₂N₂O₃Na [M+Na]⁺: 337.1523; found: 337.1520.



3-(1-pivaloylindolin-7-yl) pyrrolidine-2,5-dione (3b): was prepared according to the general procedure (2.5a). The crude reaction mixture was purified by column chromatography using silica gel (100-200 mesh size), giving a light yellow solid (22 mg, 75% yield) R_f: 0.30 (in

40% EtOAc/Hexane).

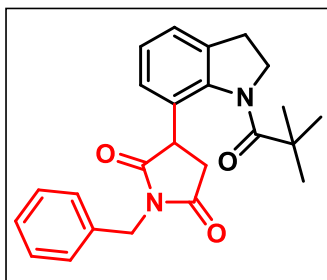
¹H NMR (CDCl₃, 700 MHz): δ 8.70 (brs, 1H), 7.18 (d, *J* = 7.7 Hz, 1H), 7.11 (t, *J* = 7.7 Hz, 1H), 7.00 (d, *J* = 7.7 Hz, 1H), 4.32-4.29 (m, 1H), 4.05-4.01 (m, 2H), 3.41-3.37 (m, 1H), 3.13-3.08 (m, 1H), 2.95-2.92 (m, 1H), 2.90-2.86 (m, 1H), 1.37 (s, 9H). **¹³C NMR (CDCl₃, 175 MHz):** δ 179.4, 179.2, 177.8, 143.1, 135.6, 129.2, 126.7, 126.3, 124.2, 51.3, 46.0, 40.0, 38.0, 31.1, 28.6. **HRMS (ESI) m/z** calcd for C₁₇H₂₀N₂O₃Na [M+Na]⁺: 295.1053; found: 295.1052.



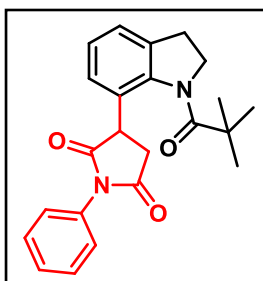
1-ethyl-3-(1-pivaloylindolin-7-yl) pyrrolidine-2,5-dione (3c): was prepared according to general procedure (2.5a). The crude reaction mixture was purified by column chromatography using silica gel (100-200 mesh size), giving a colorless oil (20 mg, 60% yield) R_f: 0.40 (in 30%

EtOAc/Hexane). **¹H NMR (CDCl₃, 400 MHz):** δ 7.17 (d, *J* = 7.2 Hz, 1H), 7.09 (t, *J* = 7.6 Hz, 1H), 6.93 (d, *J* = 7.6 Hz, 1H), 4.35-4.29 (m, 1H), 4.04-3.95 (m, 2H), 3.62 (q, *J* = 7.2 Hz, 2H), 3.36-3.29 (m, 1H), 3.15-3.07 (m, 1H), 2.96-2.93 (m, 1H), 2.81-2.75

(m, 1H), 1.36 (s, 9H), 1.22 (t, $J = 7.2$ Hz, 3H) **^{13}C NMR (CDCl_3 , 175 MHz):** δ 179.3, 178.7, 177.5, 143.3, 135.5, 130.0, 126.4, 126.3, 124.1, 51.4, 44.5, 40.1, 36.9, 34.2, 31.2, 28.7, 13.4. **HRMS (ESI)** m/z calcd for $\text{C}_{19}\text{H}_{24}\text{N}_2\text{O}_3\text{Na}$ $[\text{M}+\text{Na}]^+$: 351.1679; found: 351.1690.

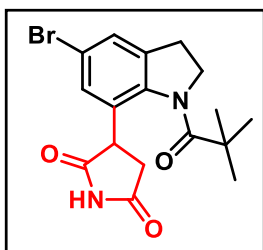


1-benzyl-3-(1-pivaloylindolin-7-yl)pyrrolidine-2,5-dione (3d): was prepared according to general procedure (2.5a). The crude reaction mixture was purified by column chromatography using silica gel (100-200 mesh size), giving a white solid (23.6 mg, 62% yield) Rf: 0.40 (in 30% EtOAc/Hexane). **^1H NMR (CDCl_3 , 400 MHz):** δ 7.43 (d, $J = 7.2$ Hz, 2H), 7.31 (q, $J = 6.4$ Hz, 3H), 7.16 (d, $J = 7.2$ Hz, 1H), 7.04 (t, $J = 7.6$ Hz, 1H), 6.83 (d, $J = 7.6$ Hz, 1H), 4.71 (q, $J = 8.8$ Hz, 2H), 4.34-4.29 (m, 1H), 4.03-3.96 (m, 2H), 3.39-3.32 (m, 1H), 3.14-3.06 (m, 1H), 2.95-2.89 (m, 1H), 2.83-2.77 (m, 1H), 1.33 (s, 9H). **^{13}C NMR (CDCl_3 , 175 MHz):** δ 179.2, 178.5, 177.1, 143.2, 136.3, 135.5, 129.9, 129.3, 128.9, 128.2, 126.4, 126.3, 124.1, 51.4, 44.6, 42.9, 40.1, 37.0, 31.2, 28.7. **HRMS (ESI)** m/z calcd for $\text{C}_{24}\text{H}_{26}\text{N}_2\text{O}_3\text{Na}$ $[\text{M}+\text{Na}]^+$: 413.1836; found: 413.1848.



1-phenyl-3-(1-pivaloylindolin-7-yl)pyrrolidine-2,5-dione (3e): was prepared according to general procedure (2.5a). The crude reaction mixture was purified by column chromatography using silica gel (100-200 mesh size), giving a yellow solid (17 mg, 44% yield) Rf: 0.30 (in 30% EtOAc/Hexane). **^1H NMR (CDCl_3 , 700 MHz):** δ 7.49-7.46 (m, 2H), 7.40-7.37 (m, 3H), 7.21 (d, $J = 6.8$ Hz, 1H), 7.16-7.10 (m, 2H), 4.40-4.34 (m, 1H), 4.22-4.19 (m, 1H),

4.06-3.98 (m, 1H), 3.48-3.41 (m, 1H), 3.18-3.10 (m, 1H) 3.05-2.99 (m, 1H), 2.97-2.92 (m, 1H), 1.38 (s, 9H). **¹³C NMR (CDCl₃, 175 MHz):** δ 179.3, 177.6, 176.5, 143.1, 135.7, 132.6, 129.4, 128.8, 127.4, 127.0, 126.3, 124.3, 53.8, 51.4, 45.2, 40.2, 36.2, 31.1, 28.8. **HRMS (ESI)** m/z calcd for C₂₃H₂₄N₂O₃Na [M+Na]⁺: 399.1679; found: 399.1688.

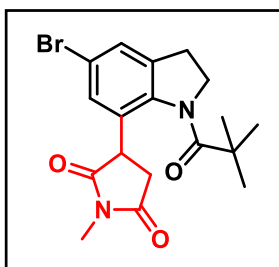


3-(5-bromo-1-pivaloylindolin-7-yl)pyrrolidine-2,5-dione

(3f): was prepared according to general procedure (2.5a).

The crude reaction mixture was purified by column chromatography using silica gel (100-200 mesh size),

giving a light yellow solid (20 mg, 73% yield) R_f: 0.40 (in 30% EtOAc/Hexane). **¹H NMR (CDCl₃, 400 MHz):** δ 8.34 (brs, 1H), 7.31 (s, 1H), 7.15 (s, 1H), 4.33-4.27 (m, 1H), 4.07-4.00 (m, 2H), 3.39-3.32 (m, 1H), 3.14-3.06 (m, 1H), 2.98-2.91 (m, 1H), 2.90-2.83 (m, 1H), 1.36 (s, 9H). **¹³C NMR (CDCl₃, 100 MHz):** δ 179.4, 178.0, 176.9, 142.5, 137.8, 130.7, 129.6, 127.4, 118.9, 51.4, 45.9, 40.1, 37.7, 30.9, 28.6. **HRMS (ESI)** m/z calcd for C₁₇H₁₉BrN₂O₃Na [M+Na]⁺: 401.0471; found: 401.0484.



3-(5-bromo-1-pivaloylindolin-7-yl)-1-methylpyrrolidine-

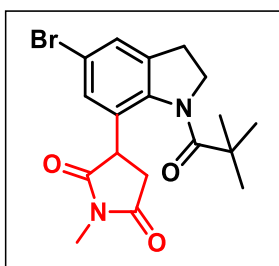
2,5-dione (3g): was prepared according to the general procedure (2.5a). The crude reaction mixture was purified

by column chromatography using silica gel (100-200 mesh

size), giving a light yellow solid (19 mg, 68% yield) R_f: 0.42 (in 30% EtOAc/Hexane).

¹H NMR (CDCl₃, 400 MHz): δ 7.30 (s, 1H), 7.08 (s, 1H), 4.33-4.27 (m, 1H), 4.14-3.09 (m, 1H), 3.98-3.95 (m, 1H), 3.35-3.28 (m, 1H), 3.14-3.08 (m, 1H), 3.06 (s, 3H), 2.98-2.90 (m, 1H), 2.82-2.76 (m, 1H), 1.35 (s, 9H). **¹³C NMR (CDCl₃, 100 MHz):** δ 179.2, 178.0, 177.1, 142.6, 137.8, 131.1, 129.6, 127.3, 118.9, 51.4, 44.5, 40.1, 36.5,

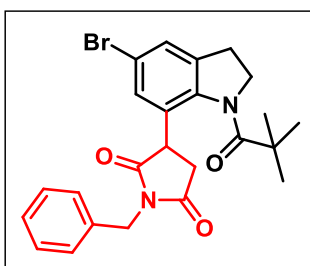
30.9, 28.6, 25.4. **HRMS (ESI)** m/z calcd for $C_{18}H_{21}BrN_2O_3Na$ $[M+Na]^+$: 415.0628; found: 415.0626.



3-(5-bromo-1-pivaloylindolin-7-yl)-1-ethylpyrrolidine-2,5-dione (3h): was prepared according to the general procedure (2.5a). The crude reaction mixture was purified by column chromatography using silica gel (100-200 mesh size), giving a colourless oil (21.8 mg, 74% yield) R_f : 0.40

(in 30% EtOAc/Hexane)

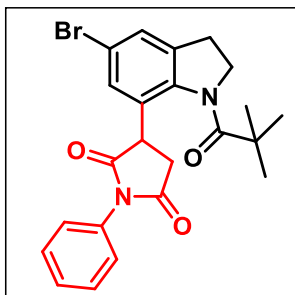
1H NMR ($CDCl_3$, 700 MHz): δ 7.30 (s, 1H), 7.06 (s, 1H), 4.32-4.29 (m, 1H), 4.05-4.01 (m, 1H), 3.94-3.92 (m, 1H), 3.63 (q, J = 7.0 Hz, 2H), 3.31-3.27 (m, 1H), 3.15-3.07 (m, 1H), 2.95-2.91 (m, 1H), 2.76-2.73 (m, 1H), 1.35 (s, 9H) 1.32 (t, J = 7.0 Hz, 3H). **^{13}C NMR ($CDCl_3$, 175 MHz):** δ 179.2, 177.9, 176.9, 142.6, 137.8, 131.5, 129.4, 127.3, 119.0, 51.4, 44.4, 40.2, 36.5, 34.4, 31.1, 28.7, 13.4. **HRMS (ESI)** m/z calcd for $C_{19}H_{23}BrN_2O_3Na$ $[M+Na]^+$: 429.0784; found: 429.0795.



1-benzyl-3-(5-bromo-1-pivaloylindolin-7-yl)pyrrolidine-2,5-dione (3i): was prepared according to general procedure (2.5a). The crude reaction mixture was purified by column chromatography using silica gel (100-200 mesh size) giving a white solid (16.4 mg, 60%

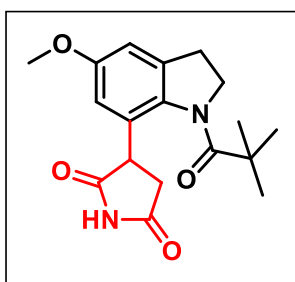
yield) R_f : 0.40 (in 30% EtOAc/Hexane). **1H NMR ($CDCl_3$, 700 MHz):** δ 7.42 (d, J = 7.0 Hz, 2H), 7.33 (t, J = 7.0 Hz, 2H), 7.30-7.28 (m, 2H), 6.96 (t, J = 1.4 Hz, 1H), 4.76-4.68 (m, 2H), 4.32-4.29 (m, 1H), 4.02-4.00 (m, 1H) 3.98-3.92 (m, 1H), 3.38-3.29 (m, 1H), 3.11-3.06 (m, 1H), 2.94-2.90 (m, 1H), 2.78-2.75 (m, 1H), 1.33 (s, 9H). **^{13}C NMR ($CDCl_3$, 175 MHz):** δ 179.3, 177.8, 176.7, 142.5, 137.7, 136.2, 131.5, 129.3, 129.1,

128.4, 127.3, 119.1, 51.4, 44.4, 43.0, 40.1, 36.7, 31.0, 28.7. **HRMS (ESI)** m/z calcd for $C_{24}H_{25}BrN_2O_3Na$ $[M+Na]^+$: 491.0941; found: 491.0941.



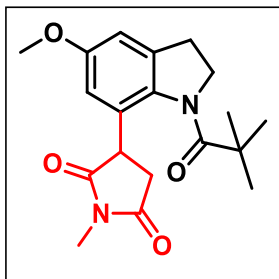
3-(5-bromo-1-pivaloylindolin-7-yl)-1-phenylpyrrolidine-2,5-dione (3j): was prepared according to general procedure (2.5a). The crude reaction mixture was purified by column chromatography using silica gel (100-200 mesh size), giving a yellow solid (15.8

mg, 49% yield) R_f : 0.45 (in 30% EtOAc/Hexane). **1H NMR ($CDCl_3$, 700 MHz):** δ 7.49-7.47 (m, 2H), 7.41-7.37 (m, 3H), 7.37 (s, 1H), 7.24 (d, $J = 2.1$ Hz, 1H), 4.37-4.34 (m, 1H), 4.17-4.15 (m, 1H), 4.06-4.02 (m, 1H), 3.43-3.39 (m, 1H), 3.14-3.10 (m, 1H), 3.00-2.97 (m, 1H), 2.96-2.93 (m, 1H), 1.37 (s, 9H). **^{13}C NMR ($CDCl_3$, 175 MHz):** δ 179.3, 176.9, 175.9, 142.5, 138.1, 132.5, 130.8, 130.3, 129.5, 129.1, 127.5, 127.1, 119.0, 82.4, 51.5, 45.1, 40.2, 36.1, 31.1, 28.7. **HRMS (ESI)** m/z calcd for $C_{23}H_{23}BrN_2O_3Na$ $[M+Na]^+$: 477.0784; found: 477.0774.



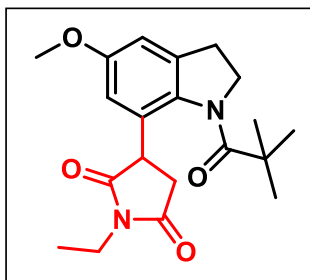
3-(5-methoxy-1-pivaloylindolin-7-yl)pyrrolidine-2,5-dione (3k): was prepared according to general procedure (2.5a). The crude reaction mixture was purified by column chromatography using silica gel (100-200 mesh size), giving a colourless oil (23 mg, 79% yield) R_f : 0.42 (in 30% EtOAc/Hexane). **1H NMR ($CDCl_3$, 400 MHz):** δ 8.67 (brs, 1H) 6.76 (d, $J = 2$ Hz, 1H), 6.53 (d, $J = 2$ Hz, 1H), 4.27-4.14 (m, 2H), 4.12-4.03 (m, 1H), 3.75 (s, 3H), 3.34-3.27 (m, 1H), 3.08-3.27 (m, 1H), 2.97-2.90 (m, 1H), 2.85-2.79 (m, 1H), 1.35 (s, 9H). **^{13}C NMR ($CDCl_3$, 100 MHz):** δ 179.5, 177.7, 171.6, 158.4, 137.3, 136.4,

129.8, 111.9, 110.3, 56.1, 51.6, 46.1, 40.0, 38.1, 31.5, 28.7. **HRMS (ESI)** m/z calcd for $C_{18}H_{22}N_2O_4Na$ $[M+Na]^+$: 353.1472; found: 353.1480.



3-(5-methoxy-1-pivaloylindolin-7-yl)-1-methylpyrrolidine-2,5-dione (3l): was prepared according to general procedure (2.5a). The crude reaction mixture was purified by column chromatography using silica gel (100-200 mesh size) giving a colourless oil (18 mg, 60 %

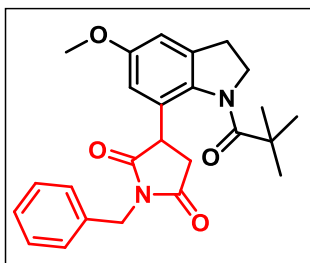
yield) R_f : 0.40 (in 30% EtOAc/Hexane). **1H NMR ($CDCl_3$, 400 MHz):** δ 6.75 (d, J = 1.6 Hz, 1H), 6.47 (d, J = 2.0 Hz, 1H), 4.32-4.26 (m, 1H), 4.05-3.98 (m, 2H), 3.75 (s, 3H), 3.35-3.28 (m, 1H), 3.11-3.06 (m, 1H), 3.05 (s, 3H), 2.93-2.87 (m, 1H), 2.85-2.79 (m, 1H), 1.34 (s, 9H). **^{13}C NMR ($CDCl_3$, 100 MHz):** δ 178.9, 178.6, 177.5, 158.2, 137.0, 136.5, 130.2, 112.1, 110.1, 56.1, 51.5, 44.8, 39.9, 36.7, 31.5, 28.7, 25.3. **HRMS (ESI)** m/z calcd for $C_{19}H_{24}N_2O_4Na$ $[M+Na]^+$: 367.1628; found: 367.1643.



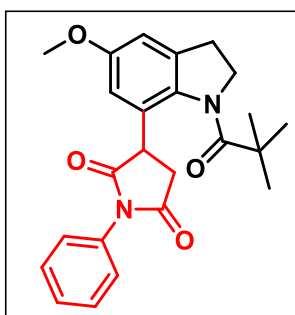
1-ethyl-3-(5-methoxy-1-pivaloylindolin-7-yl)pyrrolidine-2,5-dione (3m): was prepared according to the general procedure (2.5a). The crude reaction mixture was purified by column chromatography using silica gel (100-200 mesh size), giving a colourless oil (19 mg, 62%

yield) R_f : 0.40 (in 30% EtOAc/Hexane). **1H NMR ($CDCl_3$, 700 MHz):** δ 6.74 (d, J = 2.1 Hz, 1H), 6.46 (d, J = 2.8 Hz, 1H), 4.32-4.29 (m, 1H), 4.02-3.97 (m, 2H), 3.74 (s, 3H), 3.62 (q, J = 7.0 Hz, 2H), 3.31-3.27 (m, 1H), 3.09-3.04 (m, 1H), 2.91-2.88 (m, 1H), 2.79-2.76 (m, 1H), 1.35 (s, 9H), 1.22 (t, J = 7.7 Hz, 3H). **^{13}C NMR ($CDCl_3$, 175 MHz):** δ 179.1, 178.4, 177.4, 158.2, 137.0, 136.7, 131.0, 111.7, 110.1, 56.1, 51.6, 44.6, 40.1,

36.8, 34.3, 31.6, 28.8, 13.4. **HRMS (ESI)** m/z calcd for $C_{20}H_{26}N_2O_4Na$ $[M+Na]^+$: 381.1785; found: 381.1798.

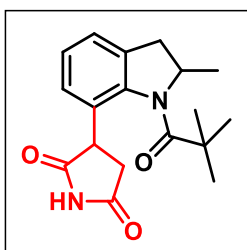


1-benzyl-3-(5-methoxy-1-pivaloylindolin-7-yl)pyrrolidine-2,5-dione (3n): was prepared according to general procedure (2.5a). The crude reaction mixture was purified by column chromatography using silica gel (100-200 mesh size), giving a white solid (20 mg, 56% yield) R_f : 0.35 (in 30% EtOAc/Hexane). **1H NMR ($CDCl_3$, 700 MHz):** δ 7.44 (d, J = 7.0 Hz, 2H), 7.31 (t, J = 7.0 Hz, 2H), 7.26 (t, J = 8.4 Hz, 1H) 6.71 (d, J = 2.8 Hz, 1H) 6.29 (d, J = 2.1 Hz, 1H) 4.74-4.69 (m, 2H), 4.31-4.28 (m, 1H), 4.00-3.96 (m, 2H), 3.59 (s, 3H), 3.36-3.32 (m, 1H), 3.08-3.03 (m, 1H), 2.89-2.85 (m, 1H), 2.81-2.78 (m, 1H), 1.34 (s, 9H). **^{13}C NMR ($CDCl_3$, 175 MHz):** δ 179.1, 178.4, 177.1, 158.3, 137.1, 136.5, 136.4, 130.5, 129.3, 129.1, 128.2, 110.7, 110.6, 55.8, 51.6, 44.6, 42.8, 40.0, 37.1, 31.5, 28.7. **HRMS (ESI)** m/z calcd for $C_{25}H_{28}N_2O_4Na$ $[M+Na]^+$: 421.2122; found: 421.2148.



3-(5-methoxy-1-pivaloylindolin-7-yl)-1-phenylpyrrolidine-2,5-dione (3o): was prepared according to general procedure (2.5a). The crude reaction mixture was purified by column chromatography using silica gel (100-200 mesh size), giving a white liquid (17 mg, 51% yield) R_f : 0.35 (in 30% EtOAc/Hexane). **1H NMR ($CDCl_3$, 400 MHz):** δ 7.52-7.48 (m, 2H), 7.42-7.39 (m, 3H), 6.80 (d, J = 2.0 Hz, 1H), 6.68 (d, J = 2.4 Hz, 1H), 4.40-4.35 (m, 1H), 4.26-4.21 (m, 1H), 4.07-4.00 (m, 1H), 3.80 (s, 3H), 3.46-3.39 (m, 1H), 3.16-3.10 (m, 1H), 3.08-3.00 (m, 1H), 2.97-2.90 (m, 1H) 1.38 (s, 9H). **^{13}C NMR ($CDCl_3$, 175 MHz):** δ 179.0, 177.4, 176.4, 158.2, 137.3, 136.5, 132.6, 129.7,

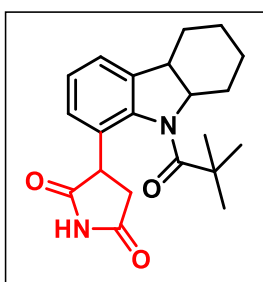
129.4, 128.8, 127.0, 112.8, 110.2, 56.0, 53.8, 51.6, 45.3, 40.0, 36.0, 31.5, 28.8. **HRMS** (ESI) m/z calcd for $C_{24}H_{26}N_2O_4Na$ $[M+Na]^+$: 429.1785; found: 429.1786.



3-(2-methyl-1-pivaloylindolin-7-yl)pyrrolidine-2,5-dione

(3p): (inseparable diastereomeric mixture 6:4) was prepared according to general procedure (2.5a). The crude reaction mixture was purified by column chromatography using silica gel (100-200 mesh size), giving a light yellow

solid (21.2 mg, 73% yield) R_f : 0.30 (in 40% EtOAc/Hexane). **1H NMR ($CDCl_3$, 700 MHz):** δ 8.52 (brs, 1H), 7.31 (d, $J = 7.7$ Hz, 0.46H), 7.20 (t, $J = 7.0$ Hz, 1H), 7.15-7.10 (m, 1H) 6.99 (d, $J = 7.7$ Hz, 1H), 4.86-4.81 (m, 1H), 4.57-4.55 (m, 0.43H), 4.13-4.10 (m, 0.36H), 3.97-3.95 (m, 0.61H), 3.46-3.38 (m, 1H), 3.30-3.26 (m, 1H), 2.99-2.94 (m, 1H), 2.74-2.70 (m, 0.45H), 2.54-2.50 (m, 1H), 1.37 (s, 9H), 1.27 (d, $J = 6.3$ Hz, 2H), 1.22 (d, $J = 6.3$ Hz, 1H). **^{13}C NMR ($CDCl_3$, 175 MHz):** δ 179.3, 179.1, 178.0, 177.0, 177.5, 177.0, 142.2, 141.3, 135.4, 134.9, 130.8, 129.9, 126.8, 126.7, 126.1, 124.9, 124.7, 60.7, 57.8, 57.7, 46.1, 45.4, 40.5, 38.2, 38.0, 37.8, 28.99, 28.97, 21.3, 20.6, 20.2, 14.5. **HRMS (ESI) m/z calcd for $C_{18}H_{22}N_2O_3Na$ $[M+Na]^+$:** 337.1523; found: 337.1539.

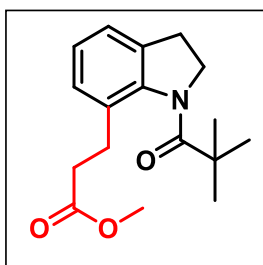


3-(9-pivaloyl-2,3,4,4a,9,9a-hexahydro-1H-carbazol-8-yl)pyrrolidine-2,5-dione (3r): (inseparable diastereomeric mixture 7:4) was prepared according to general procedure

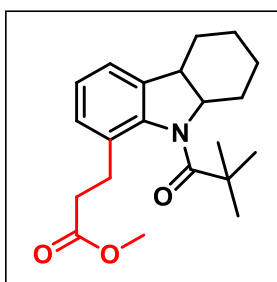
(2.5a). The crude reaction mixture was purified by column chromatography using silica gel (100-200 mesh size),

giving a colourless liquid (13 mg, 46% yield) R_f : 0.35 (in 30% EtOAc/Hexane). **1H NMR ($CDCl_3$, 400 MHz):** δ 8.39 (brs, 1H), 7.30 (d, $J = 7.2$ Hz, 0.45H), 7.20-7.11 (m, 2H) 6.98 (d, $J = 8.0$ Hz, 1H), 4.60-4.51 (m, 2H), 4.14-4.09 (m, 1H), 3.99-3.96 (m, 1H),

3.47-3.38 (m, 2H), 3.00-2.92 (m, 1H), 2.75-2.69 (m, 0.47H), 4.65 (d, $J = 14.0$ Hz, 1H), 2.06-2.00 (m, 2H), 1.85-1.49 (m, 6H), 1.37 (s, 9H), 1.32-1.05 (m, 6H). **^{13}C NMR (CDCl₃, 175 MHz):** δ 179.1, 179.0, 177.9, 177.8, 177.5, 177.4, 176.94, 176.91, 143.8, 142.9, 141.3, 138.5, 138.1, 131.0, 130.1, 126.8, 126.6, 126.3, 126.2, 122.4, 122.3, 63.8, 63.6, 46.0, 45.3, 42.5, 42.3, 40.47, 40.45, 37.7, 29.04, 29.01, 27.6, 27.5, 25.0, 23.63, 23.61, 20.7, 20.6, 14.5. **HRMS (ESI)** m/z calcd for C₂₁H₂₆N₂O₃Na [M+Na]⁺: 377.1836; found: 377.1849.

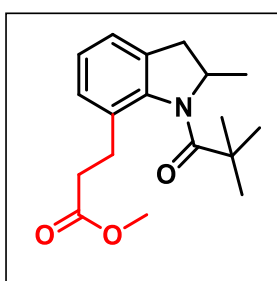


Methyl 3-(1-pivaloylindolin-7-yl)propanoate (3s): was prepared according to the general procedure (2.5b). The crude reaction mixture was purified by column chromatography using silica gel (100-200 mesh size), giving a light yellow liquid (24 mg, 85% yield) R_f : 0.50 (in 20% EtOAc/Hexane). **^1H NMR (CDCl₃, 400 MHz):** δ 7.08 (dd, $J = 8.4$ Hz, 1H), 7.03 (t, $J = 4.4$ Hz, 2H), 4.10 (t, $J = 14.8$ Hz, 2H), 3.63 (s, 3H), 3.01 (t, $J = 14.8$ Hz, 2H), 2.85 (t, $J = 15.6$ Hz, 2H), 2.59 (t, $J = 15.6$ Hz, 2H), 1.39 (s, 9H). **^{13}C NMR (CDCl₃, 100 MHz):** δ 179.0, 174.1, 143.1, 134.8, 132.0, 128.3, 125.5, 122.6, 51.8, 51.6, 40.3, 33.3, 31.5, 29.1, 28.8. **HRMS (ESI)** m/z calcd for C₁₇H₂₃NO₃Na [M+Na]⁺: 312.1570; found: 312.1567.



Methyl 3-(9-pivaloyl-2,3,4,4a,9,9a-hexahydro-1H-carbazol-8-yl)propanoate (3u): was prepared according to general procedure (2.5b). The crude reaction mixture was purified by column chromatography using silica gel (100-200 mesh size), giving a colourless oil (18 mg, 68% yield)

R_f: 0.40 (in 20% EtOAc/Hexane). **¹H NMR (CDCl₃, 400 MHz):** δ 7.11-7.08 (m, 1H) 7.04-7.01 (m, 2H) 4.53-4.48 (m, 1H), 3.62 (s, 3H), 3.48-3.45 (m, 1H), 3.01-2.92 (m, 1H) 2.82-2.75 (m, 1H) 2.65-2.50 (m, 2H) 2.31 (d, *J* = 14.4 Hz, 1H), 2.00-1.97 (m, 1H), 1.83-1.73 (m, 1H), 1.58-1.55 (m, 1H) 1.49 (d, *J* = 12.8 Hz, 1H) 1.39 (s, 9H) 1.25-1.05 (m, 3H). **¹³C NMR (CDCl₃, 100 MHz):** δ 178.7, 174.2, 143.5, 137.4, 133.9, 127.9, 125.9, 120.9, 63.7, 51.7, 42.7, 40.6, 33.4, 29.2, 29.0, 27.6, 25.0, 23.8, 20.8. **HRMS (ESI)** m/z calcd for C₂₁H₂₉NO₃Na [M+Na]⁺: 366.2040; found: 366.2049.

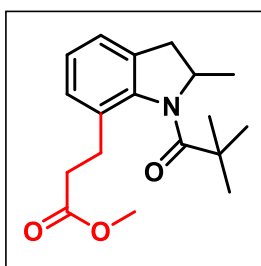


Methyl 3-(2-methyl-1-pivaloylindolin-7-yl)propanoate

(3v): was prepared according to general procedure (2.5b).

The crude reaction mixture was purified by column chromatography using silica gel (100-200 mesh size), giving a colourless oil (22 mg, 77% yield) R_f: 0.45 (in 20%

EtOAc/Hexane). **¹H NMR (CDCl₃, 400 MHz):** δ 7.11-7.07 (m, 1H) 7.05-7.02 (m, 2H) 4.79-4.73 (m, 1H), 3.61 (s, 3H), 3.28 (dd, *J* = 14.8 Hz, *J* = 7.2 Hz, 1H), 2.99-2.92 (m, 1H), 2.83-2.75 (m, 1H), 2.66-2.45 (m, 3H) 1.39 (s, 9H) 1.56 (d, *J* = 6.0 Hz, 3H). **¹³C NMR (CDCl₃, 100 MHz):** δ 179.1, 174.1, 142.0, 134.4, 133.7, 128.1, 126.0, 123.3, 57.7, 51.8, 40.6, 38.4, 33.5, 29.2, 29.1, 20.5. **HRMS (ESI)** m/z calcd for C₁₈H₂₃NO₃Na [M+Na]⁺: 326.1727; found: 326.1734.

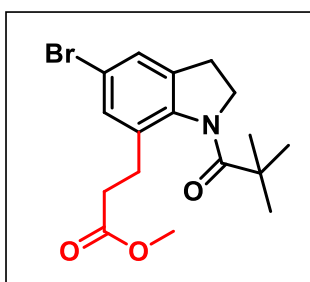


Methyl 3-(5-bromo-1-pivaloylindolin-7-yl)propanoate

(3w): was prepared according to general procedure (2.5b).

The crude reaction mixture was purified by column chromatography using silica gel (100-200 mesh size) giving a colourless oil (19 mg, 74% yield) R_f: 0.45 (in 20%

EtOAc/Hexane). **¹H NMR (CDCl₃, 400 MHz):** δ 7.21 (s, 1H), 7.17 (s, 1H), 4.10 (t, J = 14.4 Hz, 2H), 3.65 (s, 3H), 3.00 (t, J = 14.4 Hz, 2H), 2.79 (t, J = 15.6 Hz, 2H), 2.27 (t, J = 15.6 Hz, 2H), 1.38 (s, 9H). **¹³C NMR (CDCl₃, 100 MHz):** δ 179.1, 173.8, 142.5, 137.0, 133.9, 131.0, 125.7, 118.3, 53.8, 51.9, 51.6, 40.4, 33.0, 31.3, 28.9. **HRMS (ESI)** m/z calcd for C₁₇H₂₂BrNO₃Na [M+Na]⁺: 390.0675; found: 390.0679.

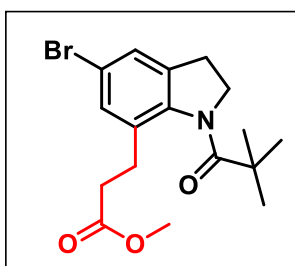


Methyl 3-(5-bromo-1-pivaloylindolin-7-yl)propanoate

(3w): was prepared according to general procedure (2.5b).

The crude reaction mixture was purified by column chromatography using silica gel (100-200 mesh size), giving a colourless oil (19 mg, 74% yield) R_f: 0.45 (in 20%

EtOAc/Hexane). **¹H NMR (CDCl₃, 400 MHz):** δ 7.21 (s, 1H), 7.17 (s, 1H), 4.10 (t, J = 14.4 Hz, 2H), 3.65 (s, 3H), 3.00 (t, J = 14.4 Hz, 2H), 2.79 (t, J = 15.6 Hz, 2H), 2.27 (t, J = 15.6 Hz, 2H), 1.38 (s, 9H). **¹³C NMR (CDCl₃, 100 MHz):** δ 179.1, 173.8, 142.5, 137.0, 133.9, 131.0, 125.7, 118.3, 53.8, 51.9, 51.6, 40.4, 33.0, 31.3, 28.9. **HRMS (ESI)** m/z calcd for C₁₇H₂₂BrNO₃Na [M+Na]⁺: 390.0675; found: 390.0679.



3-(1-acetylinolin-7-yl)-1-methylpyrrolidine-2,5-dione

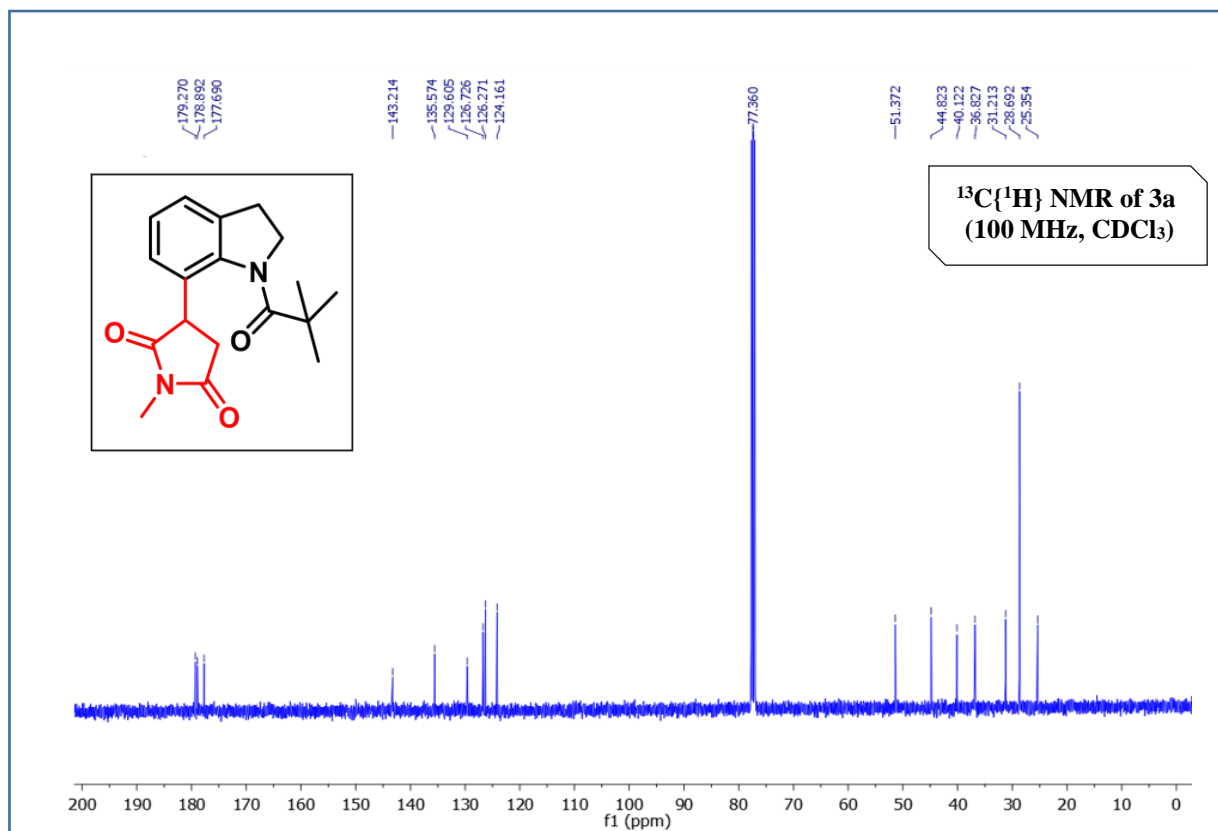
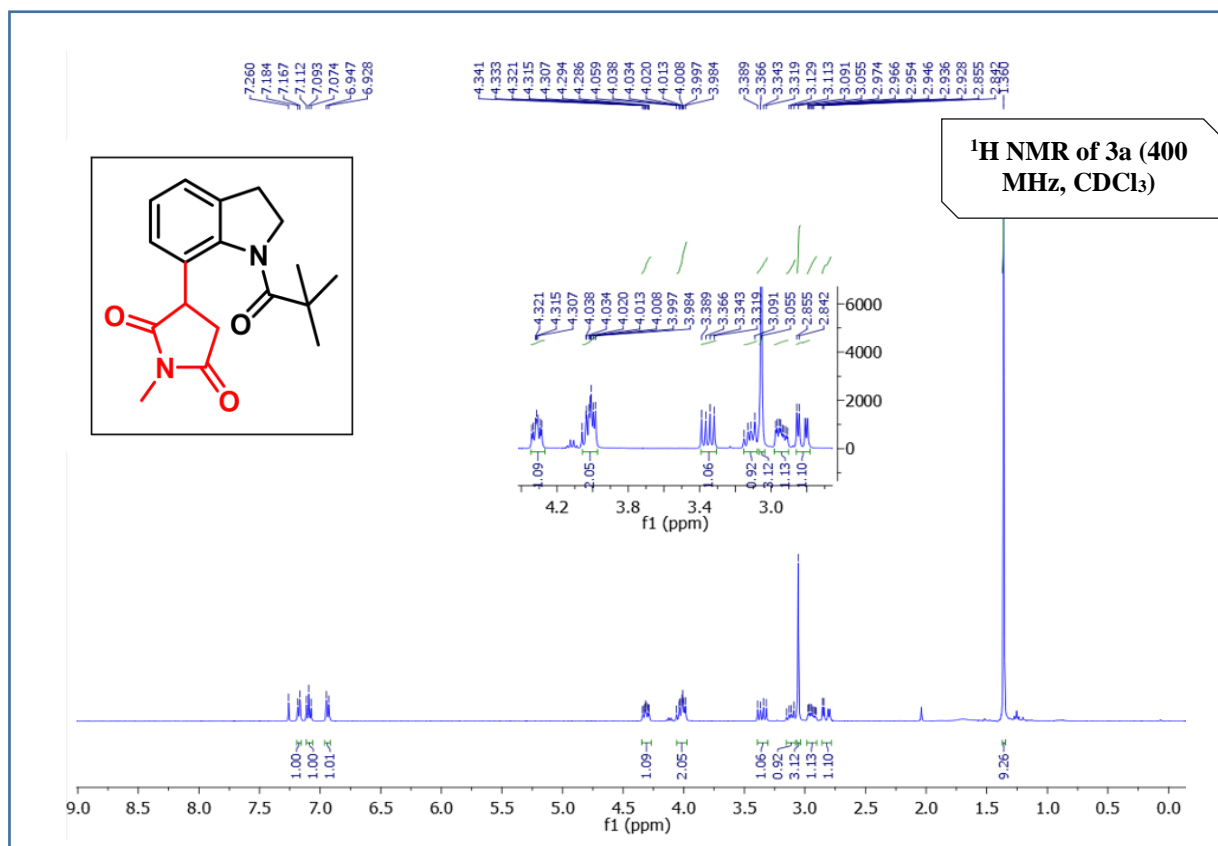
(3x): was prepared according to general procedure (2.5b).

The crude reaction mixture was purified by column chromatography using silica gel (100-200 mesh size) giving a white liquid (21 mg, 62% yield) R_f: 0.42 (in 60%

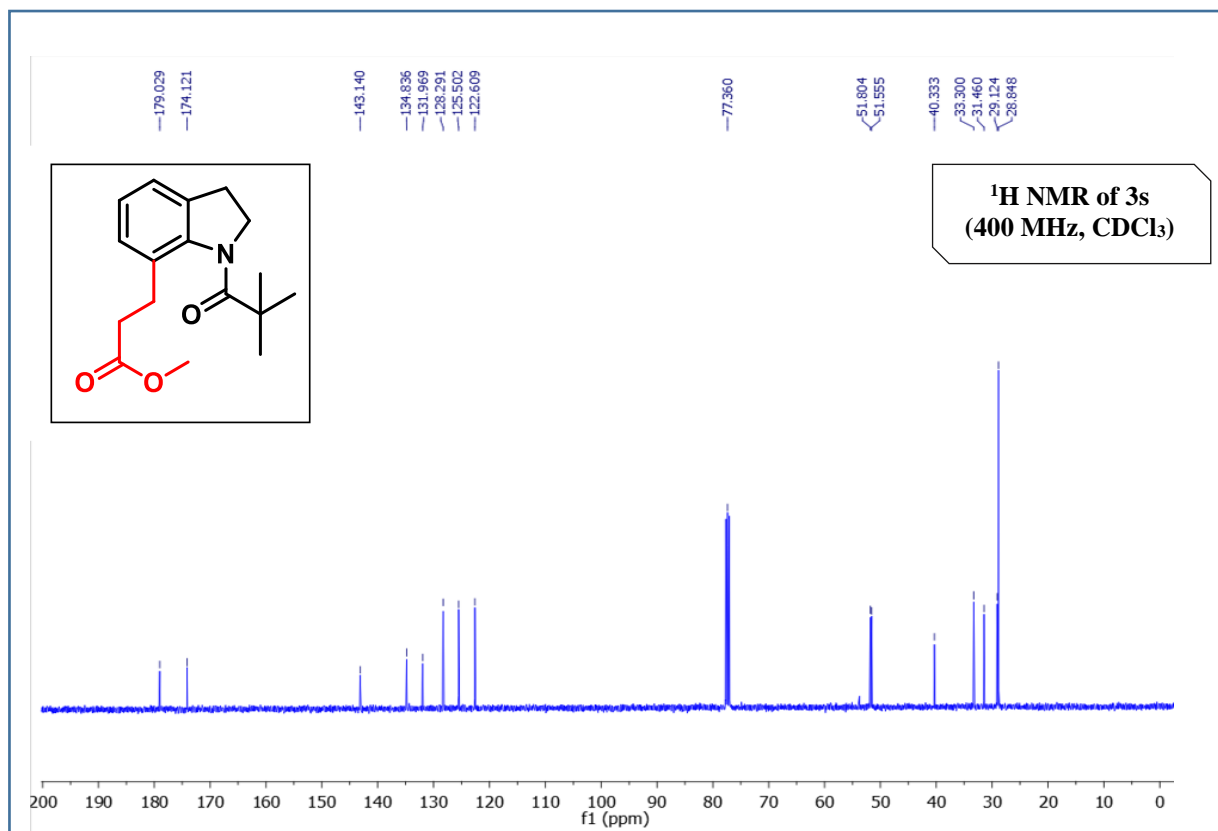
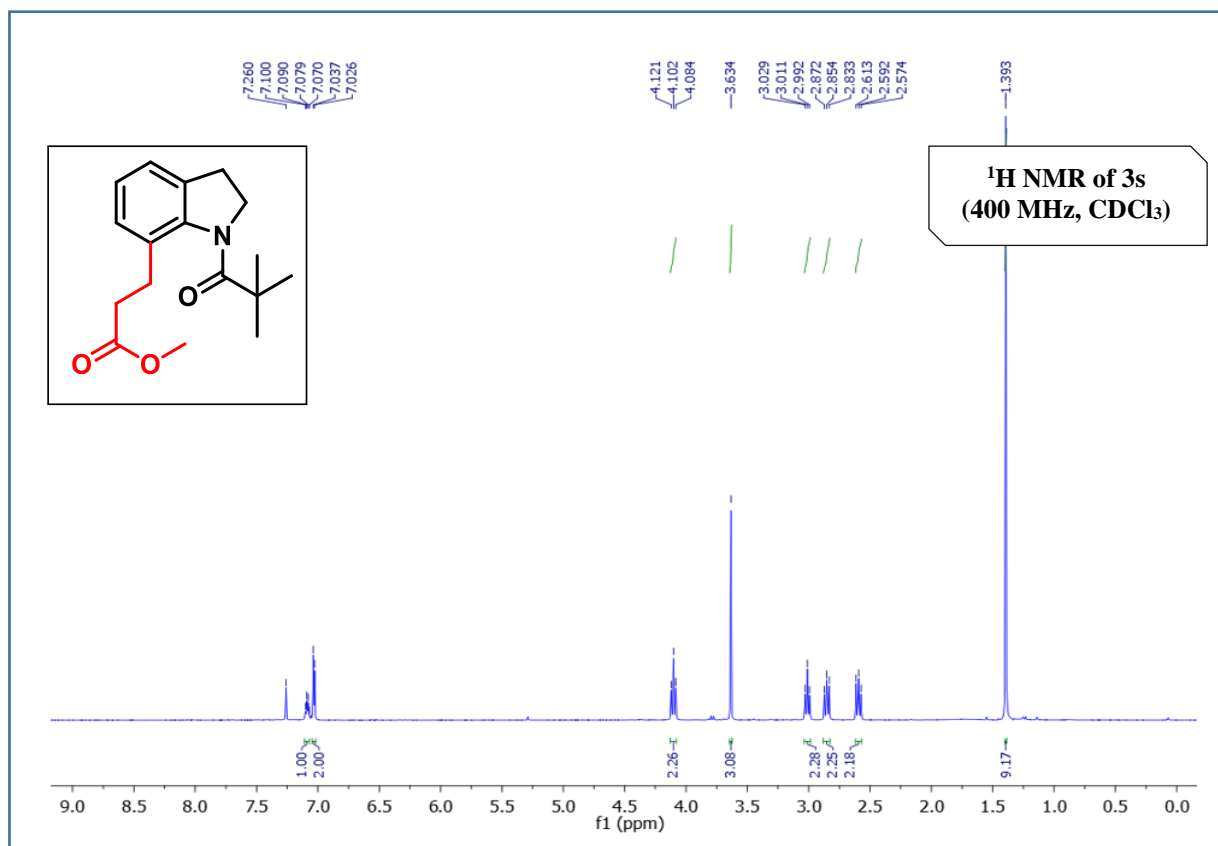
EtOAc/Hexane). **¹H NMR (CDCl₃, 400 MHz):** δ 7.16 (d, J = 7.2 Hz, 1H), 7.10 (t, J = 7.6 Hz, 1H), 6.89 (d, J = 7.6 Hz, 1H), 4.37-4.33 (m, 1H), 4.18-4.04 (m, 2H), 3.47-3.40 (m, 1H), 3.21-3.13 (m, 1H), 3.05 (s, 3H), 3.01-2.95 (m, 1H), 2.84-2.70 (m, 1H), 2.28

(s, 3H). **¹³C NMR (CD₂Cl₂, 175 MHz):** δ 179.4, 177.8, 170.8, 140.8, 136.0, 128.9, 126.5, 126.1, 123.7, 51.0, 44.5, 36.7, 29.2, 23.8, 22.4. **HRMS (ESI)** m/z calcd for C₁₅H₁₆N₂O₃Na [M+Na]⁺: 371.1366; found: 371.1361.

NMR spectra of 1-methyl-3-(1-pivaloylindolin-7-yl)pyrrolidine-2,5-dione (3a):



NMR spectra of methyl 3-(1-pivaloylindolin-7-yl)propanoate (3s):



(c) **Crystals of the compounds 3a:** (1-methyl-3-(1-pivaloylindolin-7-yl)pyrrolidine-2,5-dione) were obtained after slow evaporation of ethyl acetate.

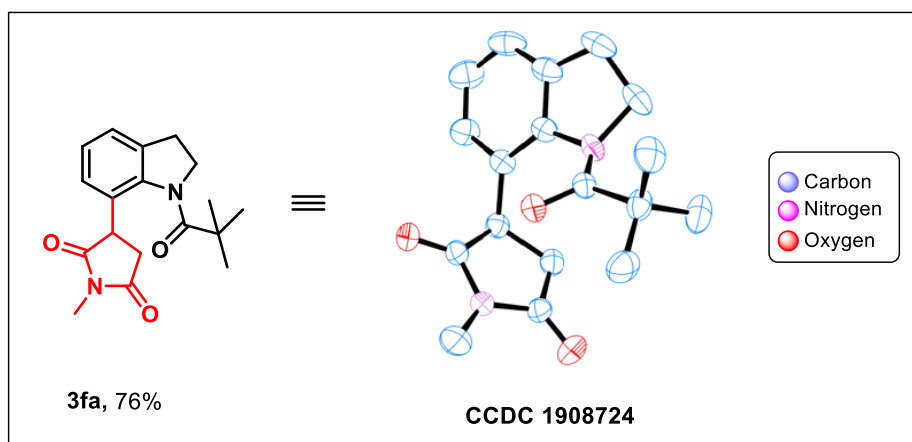
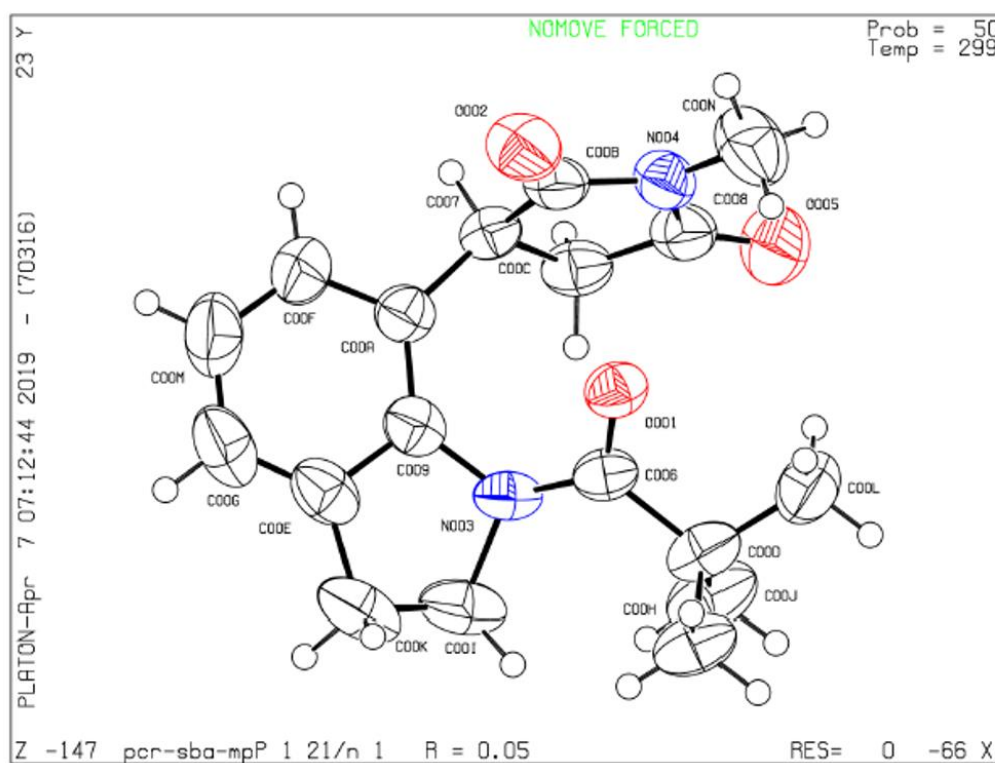


Figure 2.3: Crystal structure of **3a** (50% ellipsoid probability).



2.6 REFERENCES

1. (a) Sundberg, R. J. *Indoles*; Academic Press: *San Diego, CA*, **1996**. (b) Kochanowska-Karamyan, A. J.; Hamann, M. T. Marine Indole Alkaloids: Potential New Drug Leads for the Control of Depression and Anxiety. *Chem. Rev.* **2010**, *110*, 4489–4497. (c) Williams, R. M.; Cox, R. J. Paraherquarides, Brevianamides, and Asperparalines: Laboratory Synthesis and Biosynthesis. An Interim Report. *Acc. Chem. Res.* **2003**, *36*, 127–139. (d) Podoll, J. D.; Liu, Y.; Chang, L.; Walls, S.; Wang, W.; Wang, X. Bio-Inspired Synthesis Yields a Tricyclic Indoline That Selectively Resensitizes Methicillin-Resistant Staphylococcus Aureus (MRSA) to β -Lactam Antibiotics. *Proc. Natl. Acad. Sci. U. S. A.* **2013**, *110*, 15573–15578. (e) Horton, D. A.; Bourne, G. T.; Smythe, M. L. The Combinatorial Synthesis of Bicyclic Privileged Structures or Privileged Substructures. *Chem. Rev.* **2003**, *103*, 893–930.
2. (a) Ping, L.; Chung, D. S.; Bouffard, J.; Lee, S. G. Transition Metal-Catalyzed Site- and Regio-Divergent C–H Bond Functionalization. *Chem. Soc. Rev.* **2017**, *46*, 4299–4328. (b) Vorobyeva, D.; Osipov, S. Selective Synthesis of 2- and 7-Substituted Indole Derivatives via Chelation-Assisted Metallocarbenoid C–H Bond Functionalization. *Synthesis* **2018**, *50*, 227–240. (c) Agasti, S.; Dey, A.; Maiti, D. Palladium-Catalyzed Benzofuran and Indole Synthesis by Multiple C–H Functionalizations. *Chem. Commun.* **2017**, *53*, 6544–6556. (d) Kalepu, J.; Gandeepan, P.; Ackermann, L.; Pilarski, L. T. C4-H Indole Functionalisation: Precedent and Prospects. *Chem. Sci.* **2018**, *9*, 4203–4216.
3. (a) Cacchi, S.; Fabrizi, G. Update 1 of: Synthesis and Functionalization of Indoles Through Palladium-Catalyzed Reactions. *Chem. Rev.* **2011**, *111*, PR215–PR283. (b) Sinha, A. K.; Equbal, D.; Uttam, M. R. Metal-Catalyzed Privileged 2- and 3-Functionalized Indole Synthesis. *Chem. Heterocycl. Compd.* **2018**, *54*, 292–301. (c) Bandini, M.; Eichholzer, A. Catalytic Functionalization of Indoles in a New Dimension. *Angew. Chem., Int. Ed.* **2009**, *48*, 9608–9644. (d) Joucla, L.; Djakovitch, L. Transition Metal-Catalysed, Direct and Site-Selective N1-, C2- or C3-Arylation of the Indole Nucleus: 20 Years of Improvements. *Adv. Synth. Catal.* **2009**, *351*, 673–714.
4. (a) Leitch, J. A.; Bhonoah, Y.; Frost, C. G. Beyond C2 and C3: Transition-Metal-Catalyzed C–H Functionalization of Indole. *ACS Catal.* **2017**, *7*, 5618–5627. (b) Ping, L.; Chung, D. S.; Bouffard, J.; Lee, S. Transition Metal-Catalyzed Site- and Regio-Divergent C–H Bond Functionalization. *Chem. Soc. Rev.* **2017**, *46*, 4299–4328. (c) Yang, Y.; Shi, Z. Regioselective Direct Arylation of Indoles on the Benzenoid Moiety. *Chem. Commun.* **2018**, *54*, 1676–1685.
5. (a) Pan, C.; Abdukader, A.; Han, J.; Cheng, Y.; Zhu, C. Ruthenium-Catalyzed C7 Amidation of Indoline C–H Bonds with Sulfonyl Azides. *Chem. Eur. J.* **2014**, *20*, 3606–3609. (b) Zhang, L.; Chen, C.; Han, J.; Huang, Z.-B.; Zhao, Y. Ru-Catalyzed Selective C–H Oxidative Olefination with N-Heteroarenes Directed by Pivaloyl Amide. *Org. Chem. Front.* **2016**, *3*, 1271–1275. (c) Jo, H.; Park, J.; Choi, M.; Sharma, S.; Jeon, M.; Mishra, N. K.; Jeong, T.; Han, S.; Kim, I. S. Ruthenium(II)- or Rhodium(III)-Catalyzed Grignard-Type Addition of Indolines and Indoles to Activated Carbonyl Compounds. *Adv. Synth. Catal.* **2016**, *358*, 2714–2720. (d) De, P. B.; Banerjee, S.; Pradhan, S.; Punniyamurthy, T. Ru(II)-Catalyzed C7-Acyloxylation of Indolines with Carboxylic Acids. *Org. Biomol. Chem.* **2018**, *16*, 5889–5898.
6. (a) Song, Z.; Samanta, R.; Antonchick, A. P. Rhodium(III)-Catalyzed Direct Regioselective Synthesis of 7-Substituted Indoles. *Org. Lett.* **2013**, *15*, 5662–5665. (b) Yang, X.-F.; Hu, X.-H.; Feng, C.; Loh, T.-P. Rhodium(III)-Catalyzed C7-Position C–H Alkenylation and Alkynylation of Indolines. *Chem. Commun.* **2015**, *51*, 2532–2535. (c) Park, J.; Mishra, N. K.; Sharma, S.; Han, S.; Shin, Y.; Jeong, T.; Oh, J. S.; Kwak, J. H.; Jung, Y. H.; Kim, I. S. Mild Rh(III)-Catalyzed C7-Allylation of Indolines with Allylic Carbonates. *J. Org. Chem.* **2015**, *80*, 1818–1827. (d) Jeon, M.; Mishra, N. K.; De, U.; Sharma, S.; Oh, Y.; Choi, M.; Jo, H.; Sachan, R.; Kim, H. S.; Kim, I. S. Rh(III)-Catalyzed C–H Functionalization of Indolines with Readily Accessible Amidating Reagent:

- Synthesis and Anticancer Evaluation. *J. Org. Chem.* **2016**, *81*, 9878–9885. (e) Zhou, X.; Yu, S.; Qi, Z.; Kong, L.; Li, X. Rhodium(III)-Catalyzed Mild Alkylation of (Hetero)Arenes with Cyclopropanols via C–H Activation and Ring Opening. *J. Org. Chem.* **2016**, *81*, 4869–4875. (f) Pan, C.; Wang, Y.; Wu, C.; Yu, J.-T. Rhodium-Catalyzed C7-Alkylation of Indolines with Maleimides. *Org. Biomol. Chem.* **2018**, *16*, 693–697.
7. (a) Kim, M.; Kumar Mishra, N.; Park, J.; Han, S.; Shin, Y.; Sharma, S.; Lee, Y.; Lee, E.-K.; Kwak, J. H.; Kim, I. S. Decarboxylative Acylation of Indolines with α -Keto Acids under Palladium Catalysis: A Facile Strategy for the Synthesis of 7-Substituted Indoles. *Chem. Commun.* **2014**, *50*, 14249–14252. (b) Jiao, L.-Y.; Smirnov, P.; Oestreich, M. Exceptionally Mild Palladium(II)-Catalyzed Dehydrogenative C–H/C–H Arylation of Indolines at the C-7 Position under Air. *Org. Lett.* **2014**, *16*, 6020–6023. (c) Shin, Y.; Sharma, S.; Mishra, N. K.; Han, S.; Park, J.; Oh, H.; Ha, J.; Yoo, H.; Jung, Y. H.; Kim, I. S. Direct and Site-Selective Palladium-Catalyzed C-7 Acylation of Indolines with Aldehydes. *Adv. Synth. Catal.* **2015**, *357*, 594–600. (d) Luo, H.; Liu, H.; Zhang, Z.; Xiao, Y.; Wang, S.; Luo, X.; Wang, K. Direct and Site-Selective Pd(II)-Catalyzed C-7 Arylation of Indolines with Arylsilanes. *RSC Adv.* **2016**, *6*, 39292–39295. (e) Wang, P.-L.; Li, Y.; Ma, L.; Luo, C.-G.; Wang, Z.-Y.; Lan, Q.; Wang, X.-S. Palladium-Catalyzed C-7 Selective C–H Carbonylation of Indolines for Expedient Synthesis of Pyrroloquinazolinones. *Adv. Synth. Catal.* **2016**, *358*, 1048–1053.
 8. (a) Shin, K.; Chang, S. Iridium(III)-Catalyzed Direct C-7 Amination of Indolines with Organic Azides. *J. Org. Chem.* **2014**, *79*, 12197–12204. (b) Pan, S.; Wakaki, T.; Ryu, N.; Shibata, T. Ir(III)-Catalyzed C7-Position-Selective Oxidative C–H Alkenylation of Indolines with Alkenes in Air. *Chem. - Asian J.* **2014**, *9*, 1257–1260. (c) Wu, Y.; Yang, Y.; Zhou, B.; Li, Y. Iridium(III)-Catalyzed C-7 Selective C–H Alkynylation of Indolines at Room Temperature. *J. Org. Chem.* **2015**, *80*, 1946–1951. (d) Vorobyeva, D.; Osipov, S. Selective Synthesis of 2- and 7-Substituted Indole Derivatives via Chelation-Assisted Metallocarbenoid C–H Bond Functionalization. *Synthesis* **2018**, *50*, 227–240.
 9. (a) Kulkarni, A. A.; Daugulis, O. Direct conversion of Carbon–Hydrogen into Carbon–Carbon Bonds by First-Row Transition-Metal Catalysis. *Synthesis* **2009**, *41*, 4087–4109. (b) Su, B.; Cao, Z.-C.; Shi, Z.-J. Exploration of Earth-Abundant Transition Metals (Fe, Co, and Ni) as Catalysts in Unreactive Chemical Bond Activations. *Acc. Chem. Res.* **2015**, *48*, 886–896. (c) Pototschnig, G.; Maulide, N.; Schnürch, M. Direct Functionalization of C–H Bonds by Iron, Nickel, and Cobalt Catalysis. *Chem. Eur. J.* **2017**, *23*, 9206–9232. (d) Liu, J.; Chen, G.; Tan, Z. Copper-Catalyzed or -Mediated C–H Bond Functionalizations Assisted by Bidentate Directing Groups. *Adv. Synth. Catal.* **2016**, *358*, 1174–1194. (e) Liu, W.; Ackermann, L. Manganese-Catalyzed C–H Activation. *ACS Catal.* **2016**, *6*, 3743–3752. (f) Gandeepan, P.; Müller, T.; Zell, D.; Cera, G.; Warratz, S.; Ackermann, L. 3d Transition Metals for C–H Activation. *Chem. Rev.* **2019**, *119*, 2192–2452.
 10. (a) Gandeepan, P.; Koeller, J.; Ackermann, L. Expedient C–H Chalcogenation of Indolines and Indoles by Positional-Selective Copper Catalysis. *ACS Catal.* **2017**, *7*, 1030–1034. (b) Ahmad, A.; Dutta, H. S.; Khan, B.; Kant, R.; Koley, D. Cu(I)-Catalyzed Site-Selective Acyloxylation of Indoline Using O₂ as the Sole Oxidant. *Adv. Synth. Catal.* **2018**, *360*, 1644–1649. (c) De, P. B.; Pradhan, S.; Banerjee, S.; Punniyamurthy, T. Expedient Cobalt(I)-Catalyzed Site-Selective C7-Arylation of Indolines with Arylboronic Acids. *Chem. Commun.* **2018**, *54*, 2494–2497.
 11. (a) Engle, K. M.; Mei, T.-S.; Wasa, M.; Yu, J.-Q. Weak Coordination as a Powerful Means for Developing Broadly Useful C–H Functionalization Reactions. *Acc. Chem. Res.* **2012**, *45*, 788–802. (b) De Sarkar, S.; Liu, W.; Kozhushkov, S. I.; Ackermann, L. Weakly Coordinating Directing Groups for Ruthenium(II)-Catalyzed C–H Activation. *Adv. Synth. Catal.* **2014**, *356*, 1461–1479. (c) Das, R.; Kumar, G. S.; Kapur, M. Amides as Weak Coordinating Groups in Proximal C–H Bond Activation. *Eur. J. Org. Chem.* **2017**, *2017*, 5439–5459.
 12. The standard reaction conditions showed similar results even with higher scale, i.e., 1 mmol scale reaction of **1a**, and afforded the respective hydro-arylated product in 71% yield.

-
13. (a) Mandal, R.; Emayavaramban, B.; Sundararaju, B. Cp*Co- (III)-Catalyzed C-H Alkylatioin with Maleimides Using Weakly Coordinating Carbonyl Directing Groups. *Org. Lett.* **2018**, *20*, 2835–2838. (b) Muniraj, N.; Prabhu, K. R. Cobalt(III)-Catalyzed [4+2] Annulation of N-Chlorobenzamides with Maleimides. *Org. Lett.* **2019**, *21*, 1068–1072. (c) Kumar, R.; Kumar, R.; Chandra, D.; Sharma, U. Cp*CoIII-Catalyzed Alkylation of Primary and Secondary C(sp³)-H Bonds of 8-Alkylquinolines with Maleimides. *J. Org. Chem.* **2019**, *84*, 1542–1552. (d) Jeganmohan, M.; Manoharan, R. Alkylation, Annulation and Alkenylation of Organic Molecules with Maleimides via Transition-Metal-Catalyzed C-H Bond. *Asian J. Org. Chem.* **2019**, *8*, 1949-1969.
14. 14. Hugo E. Gottlieb, Vadim Kotlyar, and Abraham Nudelman, NMR Chemical Shifts of Common Laboratory Solvents as Trace Impurities *J. Org. Chem.* **1997**, *62*, 7512–7515.

Chapter 3

Cobalt-Catalyzed One-Step Access to Pyroquilon and C-7 Alkenylation of Indoline with Activated Alkenes Using Weakly Coordinating Functional Groups

3.1 Abstract

3.2 Introduction

3.3 Results and Discussions

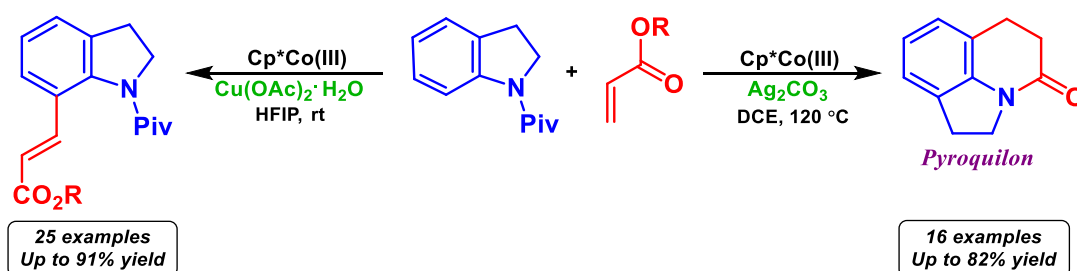
3.4 Conclusions

3.5 Experimental Section

3.6 References

Chapter 3

Cobalt-Catalyzed One-Step Access to Pyroquilon and C-7 Alkenylation of Indoline with Activated Alkenes Using Weakly Coordinating Functional Groups



3.1 ABSTRACT: A new strategy for the C(7)-H functionalization of indoline derivatives using first-row transition-metal cobalt has been demonstrated wherein the pivaloyl group acts as a weakly coordinating directing group. Biologically important pyroquilon (tetrahydropyroquinolinone) derivatives have been synthesized in a one-pot manner through selective C(7)-H functionalization and concomitant cyclization. In this process, aromatic C–H and amidic C–N bonds are cleaved, and new C–C and C–N bonds are formed step-economically. Further, selective C(7)-H alkenylation of indoline derivatives has also been accomplished using activated alkenes by varying the reaction conditions.

3.2 INTRODUCTION

The indoline and pyrroloquinolinone skeleton exists in numerous pharmaceuticals, biologically active molecules,¹ and several drugs.^{2a,b} Because of its pharmacological activity toward Alzheimer's disease, obesity, asthma, and epilepsy,

synthesizing pyrroloquinoline and its derivatives has attracted significant interest from synthetic and medicinal chemists (Figure 3.1).²

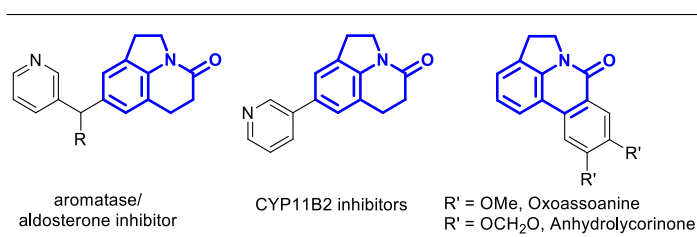


Figure 3.1. Selective examples of bioactive compounds bearing pyrroloquinolinone skeleton.

Traditionally, pyrroloquinolinone derivatives have been synthesized by Fischer indole cyclization,^{3a} radical cyclization,^{3b} Michael addition-type cyclization,^{3c} and sigmatropic rearrangement.^{3d,e} However, these processes suffer from many drawbacks, such as more synthetic operations, harsh reaction conditions, and functional group incompatibility. Thus, a straightforward synthetic procedure that can overcome these challenges is needed.⁴ In recent years, transition-metal-catalyzed C–H bond activation has been considered one of the most powerful synthetic protocols due to its step- and atom-economical properties. A few research groups have reported the synthesis of the pyrroloquinolinone skeleton by intermolecular annulation of indoline derivatives with triple bonds using second- and third-row transition metals (Re, Rh, Ru).⁵ Also, there are a few reports on the C-7 alkenylation of indoline using second- and third-row transition metals (Pd, Ru, Rh, Ir).⁶ However, there is no report on the synthesis of pyrroloquinolinone and C-7 alkenylation of indoline using first-row transition metals. In recent years, the first-row transition-metal-catalyzed organic transformation has increasingly become popular due to its low cost, lower toxicity, and easy availability.⁷ In this regard, Ackermann's^{8a}, and Koley's^{8b} groups have reported the copper-catalyzed

formation of C–S/Se and C–O bonds on indolines at the C-7 position, respectively, using a strongly coordinating pyrimidyl directing group (Figure 2.2a).

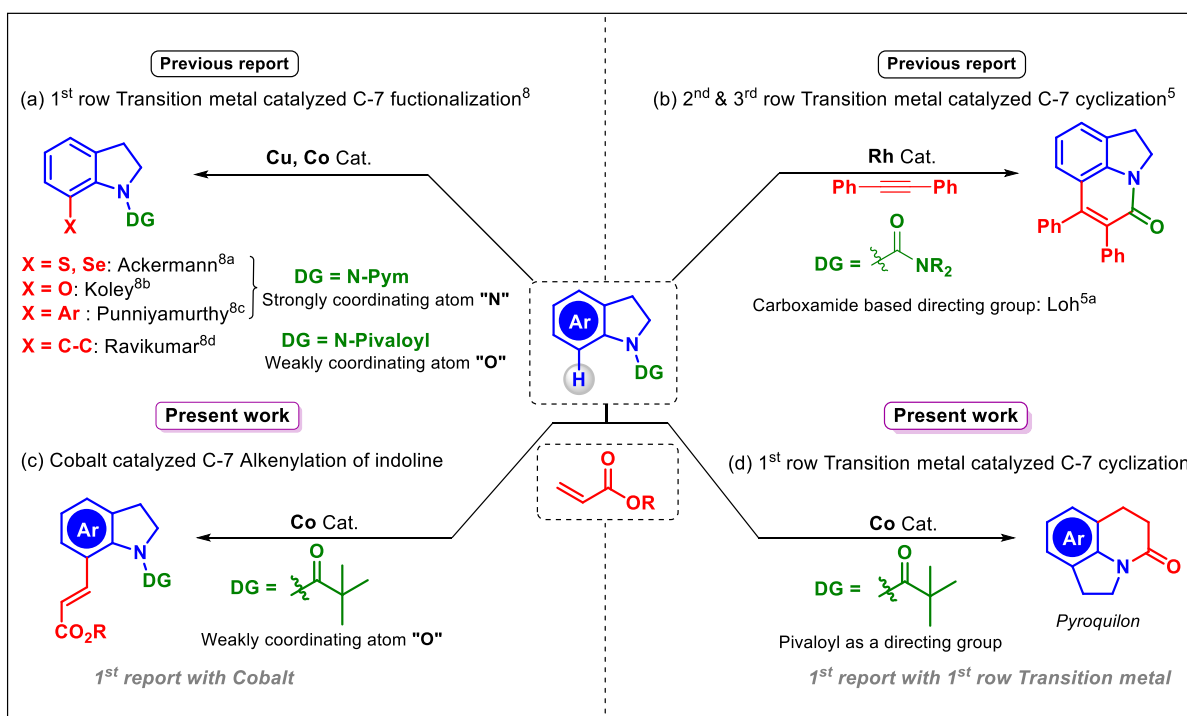


Figure 2.2. Transition metal-catalyzed C(7)–H functionalization of indoline.

Punniyamurthy's^{8c} group has also exploited the strongly coordinating pyrimidyl directing group for the cobalt-catalyzed Suzuki–Miyaura-type coupling of indolines at the C-7 position with aryl boronic acid. Recently, we have reported cobalt-catalyzed hydroarylation at the C-7 position of indoline using weakly coordinating directing groups (Figure 3.2a).^{8d} The use of weakly coordinating directing groups has gained significant importance compared to strongly coordinating directing groups because of their unique reactivity and selectivity.^{8d,9} To the best of our knowledge, there is no report on the C-7 alkenylation of indoline and the one-step synthesis of pyroquilon (tetrahydropyrroloquinolinones) using first-row transition metals. According to the literature, urea-based directing groups are well known for C–H functionalization/annulation to build a pyrroloquinolinone framework (Figure

3.2b).^{5,6,10} Herein, we introduce one-step access to the tetrahydropyrroloquinolinone framework by intermolecular annulation of indoline (bearing pivaloyl as the weakly coordinating directing group) with acrylates using the Cp*Co catalyst (Figure 3.2d). With a simple modification of conditions, this strategy also gives direct access to the C-7 alkenylated indoline, which has the potential for further transformation into desired products (Figure 3.2c).

3.3 RESULTS AND DISCUSSION

To test the feasibility of selective C-7 functionalization of indoline, *N*-pivaloyl indoline **1a**, and methyl-acrylate **2a** were reacted with the Cp*Co(CO)I₂/AgSbF₆/Ag₂CO₃/Cu(OAc)₂ catalytic system using various solvents such as 1,4-dioxane, toluene, and THF (Table 3.1, entries 1, 2, and 3). Gratifyingly, we got pyroquilon in a 40% isolated yield with THF (Table 3.1, entry 3). Then, we tested this reaction with a polar protic solvent such as methanol; we did not observe the desired product **3aa** (Table 3.1, entry 4). The use of fluorinated solvents such as trifluoroethanol and hexafluoroisopropanol gave a moderate yield, whereas using trifluorotoluene (TFT) raised the yield of **3aa** to 77% (Table 3.1, entries 5, 6, and 7). Then, we screened the reaction in different chlorinated solvents such as dichloromethane (DCM), 1,2-dichlorobenzene (DCB), and 1,2-dichloroethane (DCE) (Table 1, entries 8, 9, and 10). Interestingly, with DCE, the yield improved to 82%. To improve the yield further, we changed the silver salt to AgNTf₂, but no improvement in the yield was observed (Table 3.1, entry 11). To understand the role of the base, we performed a reaction without AgCO₃ and obtained only a 12% yield. This result suggests that the base plays a crucial

role in this reaction. To understand the essential role of the catalyst, another reaction has been performed without the $\text{Cp}^*\text{Co}(\text{CO})\text{I}_2$ catalyst.

Table 3.1. Optimization of the tetrahydropyrroloquinolinone^{a,b}

entry	solvent	Ag salt	yield (%) ^b
1	1,4-dioxane	AgSbF_6	0
2	toluene	AgSbF_6	0
3	THF	AgSbF_6	40
4	MeOH	AgSbF_6	0
5	TFE	AgSbF_6	46
6	HFIP	AgSbF_6	43
7	TFT	AgSbF_6	77
8	DCM	AgSbF_6	21
9	1,2-DCB	AgSbF_6	33
10	DCE	AgSbF_6	82
11	DCE	AgNTf_2	80
12	DCE	without Ag_2CO_3	12
13	DCE	without $\text{Cp}^*\text{Co}(\text{CO})\text{I}_2$	0

^aReaction conditions: **1a** (0.1 mmol), **2a** (4 equiv), $\text{Cp}^*\text{Co}(\text{CO})\text{I}_2$ (10 mol %), Ag salt (20 mol %), Ag_2CO_3 (1 equiv), solvent (0.1 M), 120 °C, 24 h. ^bIsolated yields.

In that case, we did not observe the formation of any products, which confirms that this reaction is catalyzed by the $\text{Cp}^*\text{Co}(\text{CO})\text{I}_2$ catalyst. Various *N*-substituted indolines were screened under the optimized reaction conditions to further optimize the reaction in terms of directing groups with **2a** (Table 3.2, entries 1–5). Among all these directing groups, pivaloyl **1a** afforded an excellent yield of **3aa** and **4aa** (Table 3.2, entry 1), whereas acetyl- and benzoyl-substituted indolines gave good yields of **4aa** (Table 3.2, entries 3 and 4). Indoline bearing free $-\text{NH}$ and *tert*-butoxycarbonyl directing groups

could not lead to the formation of products **3aa** and **4aa**, respectively (Table 3.2, entries 2 and 5).

Table 3.2. Screening of directing groups for indoline C-7 alkenylation and cyclization^{a,b}

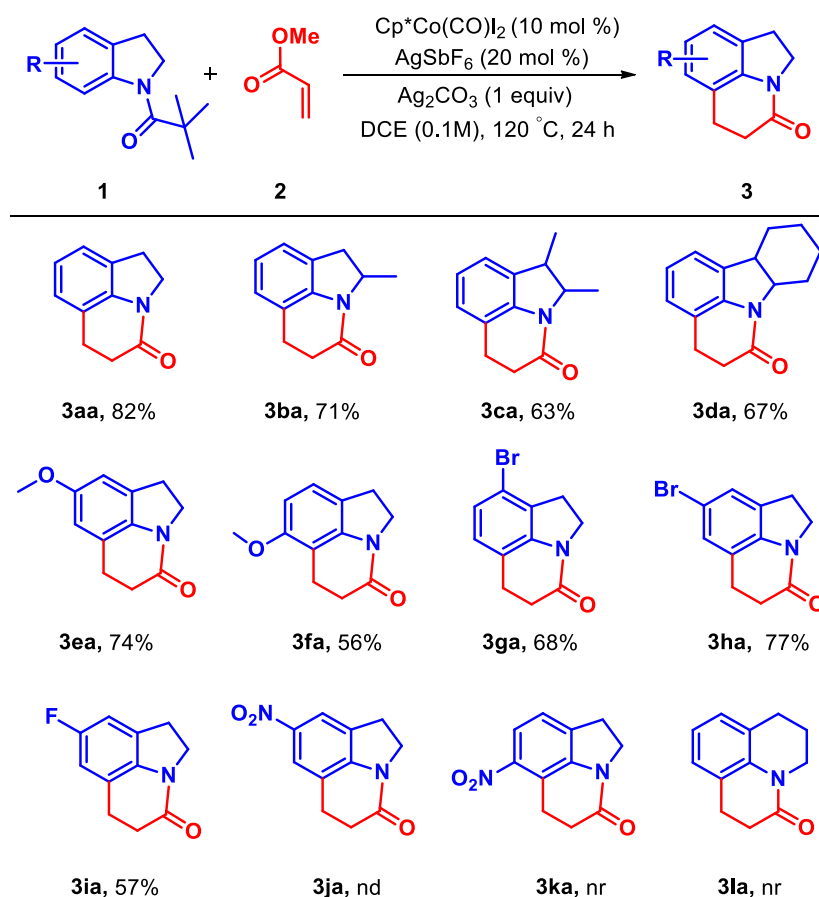
entry	yield of alkenylated product (%)	R	yield of pyroquilon 3aa (%)
1	4aa , 84%	Piv 1a	82%
2	4a'a , nr	H 1a'	nr
3	4la , 68%	Ac 1l	nr
4	4ma , 54%	Bz 1m	nr
5	4na , nr	Boc 1n	nd

^aReaction conditions: **1a** (0.1 mmol), **2a** (4 equiv), Cp*Co(CO)I₂ (10 mol %), Ag salt (20 mol %), Ag₂CO₃/Cu(OAc)₂ (1 equiv), solvent (0.1 M), 120 °C, 24 h. ^bIsolated yields.

With the optimized reaction condition in hand, the substrate scope of indolines **1** with methyl acrylate **2a** was investigated (Scheme 3.1). The developed methodology worked well with 2-methyl indoline, 2,3-methyl indoline, and 2,3-fused indoline, giving a good yield of the corresponding products (Scheme 3.1, **3ba**, **3ca**, and **3da**). Methoxy-substituted indolines gave moderate to good yields (Scheme 3.1, **3ea** and **3fa**). Halogen (F, Cl, and Br)-substituted indolines also gave moderate to good yields of the corresponding products (Scheme 3.1, **3ia**, **3iia**, **3ga**, and **3ha**). In contrast, only a trace amount of the desired product was formed from iodo-substituted indoline (Scheme 3.1, **3iia**). The structure of **3ia** was further confirmed by single-crystal X-ray analysis, whereas the electron-poor indolines provided an irrelevant result (Scheme 3.1, **3ja**, and **3ka**). This might be due to the poor nucleophilicity of the Co–C bond in the electron-

withdrawing group ($-\text{NO}_2$)-substituted indoline, making it less prone to olefin insertion from intermediate **III** (Scheme 3.4).

Scheme 3.1. Scope of tetrahydropyrroloquinolinone^{a,b}



^aReaction conditions: **1a** (0.1 mmol), **2a** (4 equiv), $\text{CoCp}^*(\text{CO})\text{I}_2$ (10 mol %), AgSbF_6 (20 mol %), Ag_2CO_3 (1 equiv), 1,2-Dichloroethane (0.1 M) as a solvent, 120 °C, 24 h.

^bIsolated yields.

We also allowed them to react with *N*-pivaloyl tetrahydroquinoline, but their reaction failed to give the desired annulated product under the reaction conditions (Scheme 3.1, **3la**). Next, to know the effect of alkoxy substituents, various *O*-substituted acrylates such as methyl acrylate **2a**, ethyl acrylate **2b**, *n*-butyl acrylate **2c**, *tert*-butyl acrylate **2d**, acrylic acid **2e**, and phenyl acrylate **2f** were reacted with the indolines under the optimized reaction conditions (Table 3.3). Except for acrylic acid **2e**, **3aa** was found to

decrease gradually with an increase in the chain length of the alkoxide unit. This might be due to their decreasing ability to act as leaving groups and steric factors. To further optimize the C-7 alkenylation reaction of indolines, we performed the same reaction. Still, the additive was changed from silver carbonate to copper acetate in the presence of dichloromethane at room temperature. We obtained a 54% yield of alkenylated product **4aa** without any trace of **3aa** (hydroarylation and cyclization product). For further confirmation of **4aa**, we performed a single-crystal X-ray analysis. Encouraged by this intriguing observation, we have screened other chlorinated and fluorinated solvents, out of which HFIP was found to be the best solvent to drive the reaction to be C-7 alkenylation, giving an 84% yield of the desired product. After establishing the optimal reaction conditions for the cobalt-catalyzed C-7 alkenylation of indolines, we evaluated the substrate scope of various indoline derivatives.

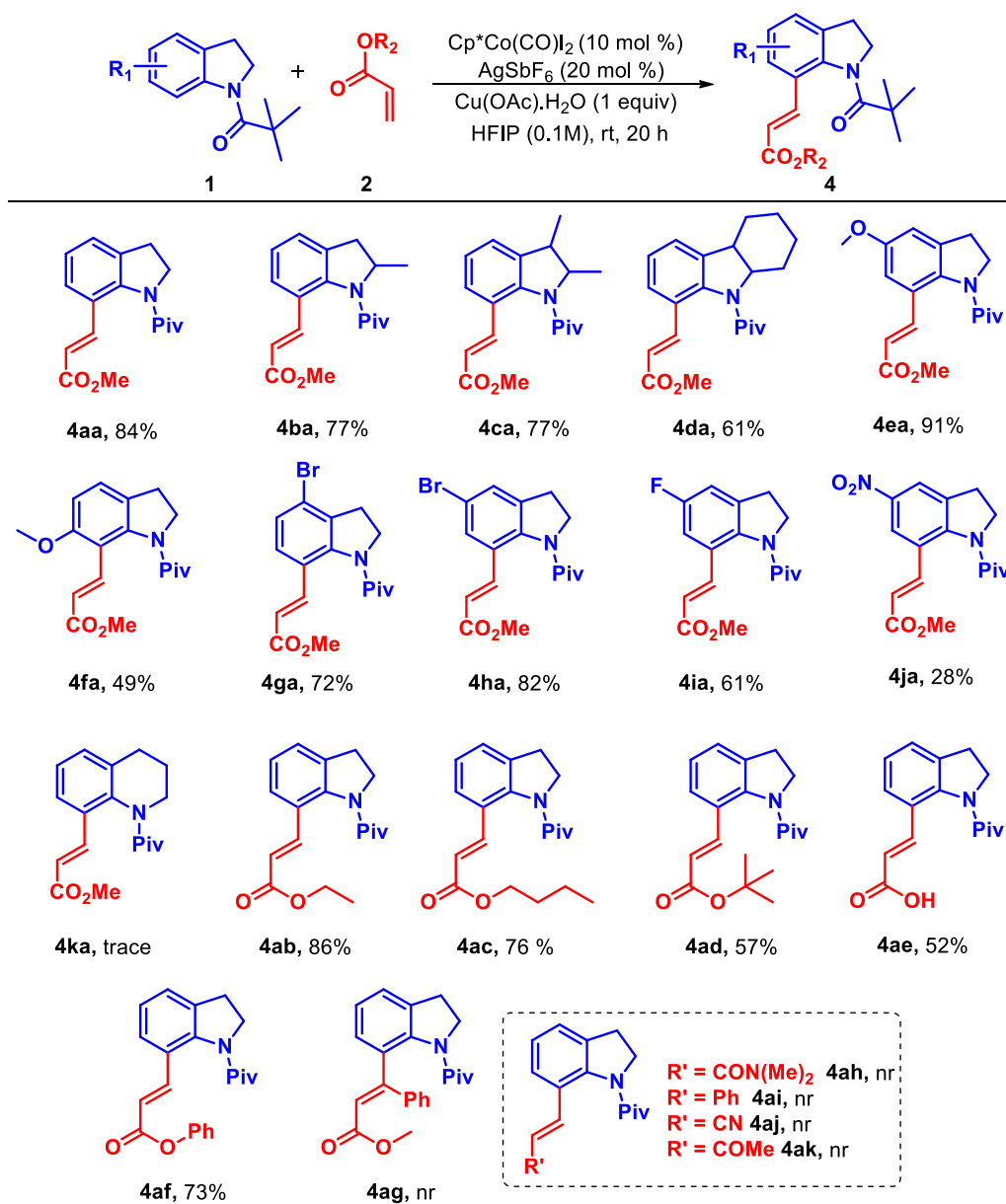
Table 3.3. Scope of tetrahydropyrroloquinolinone with various Acrylates

R			yield of 3aa ^b
R = methyl	(Me)	2a	82%
R = ethyl	(Et)	2b	58%
R = <i>n</i> -butyl	(ⁿ Bu)	2c	53%
R = <i>tert</i> -butyl	(^t Bu)	2d	37%
R = hydrogen	(H)	2e	24%
R = phenyl	(Ph)	2f	64%

At first, we tested them with *N*-pivaloylindoline bearing 2-methyl and 2,3-dimethyl groups under the conditions. In both cases, we got a good yield of the C-7 alkenylated product (Scheme 3.2, **4ba**, and **4ca**). 2,3-Fused indolines also gave a good yield

(Scheme 3.2, **4da**). While indoline with electron-donating methoxy substituents at C-5 gave a 91% yield (Scheme 3.2, **4ea**), C-6 methoxy-substituted indolines gave only a 49% yield (Scheme 3.2, **4fa**), possibly due to steric hindrance by the methoxy group. The halogenated indolines (bromo, fluoro, chloro, and iodo) gave good yields (Scheme 3.2, **4ga–4iia**), whereas electron-withdrawing 5-NO₂-substituted indoline gave a low yield (Scheme 3.2, **4ja**) and 6-NO₂-substituted indoline failed to produce the desired product (Scheme 3.2, **4ka**). Also, *N*-pivaloyl tetrahydroquinoline afforded a trace amount of the desired product (Scheme 3.2, **4la**). To understand the reactivity of the indolines with various alkoxy substituents with acrylates, we performed their reaction with various acrylates (Scheme 3.2). We obtained the corresponding alkenylated products in moderate to good yields (Scheme 3.2, **4aa**, **4ab**, **4ac**, **4ad**, and **4af**). Notably, acrylic acid showed good reactivity with the present catalytic system (Scheme 3.2, **4ae**). When (*Z*)-methyl 3-phenylacrylate as a coupling partner was reacted with the indolines under the standard reaction conditions, it failed to give the desired product (Scheme 3.2, **4ag**). It appears that the bulky phenyl group at the C-3 position of the acrylate contributes steric resistance, hindering its reactivity. Moreover, to understand the reactivity of the indolines in C-7 alkenylation, we performed the reaction with various olefins under standard conditions, revealing that only olefins bear ester and acid substituents work well (Scheme 3.2, **4ah–4ak**).

Scheme 3.2. Scope of Indoline C-7 Alkenylation with Acrylates^{a,b}



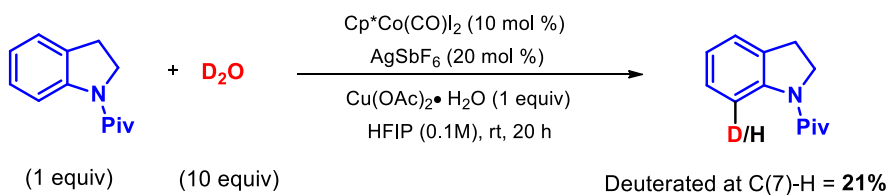
^aReaction conditions: **1a** (0.1 mmol), **2a** (4 equiv), $\text{CoCp}^*(\text{CO})\text{I}_2$ (10 mol %), AgSbF_6 (20 mol %), $\text{Cu}(\text{OAc})_2 \cdot \text{H}_2\text{O}$ (1 equiv), Hexafluoroisopropanol (0.1 M) as a solvent, rt, 20 h. ^bIsolated yield.

We have performed various control experiments to gain insight into the reaction mechanism (Scheme 3.3). A deuterium exchange study was conducted using *N*-pivaloyl indoline **1a** in the absence of Michael acceptor **2a** with 10 equiv of D_2O under the alkenylation conditions. We observed 21% deuteration at the C-7 position (Scheme

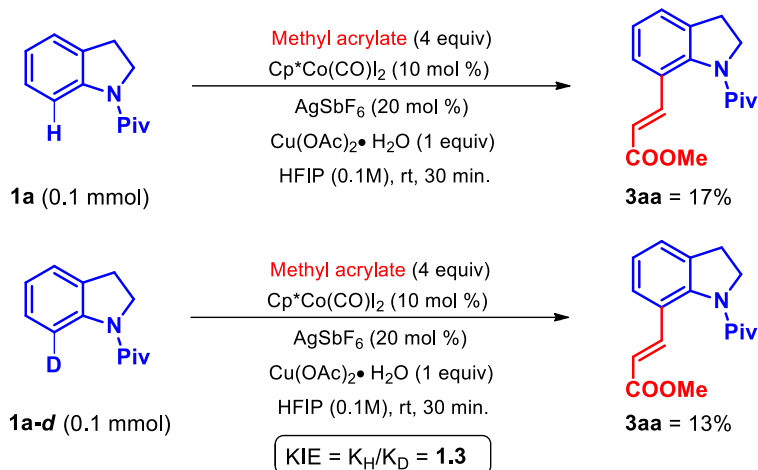
3.3a). The ratio of deuterated C(7)-H did not change much even after continuing the reaction for a longer time, suggesting that the first step might be reversible. Further, we have performed intermolecular parallel experiments for the kinetic isotope effect (Scheme 3.3b), resulting in $KIE = 1.3$, which confirms that the C–H bond activation step is not the rate-determining step. The use of radical scavengers such as TEMPO and BHT (Scheme 3.3c) did not quench the reaction altogether; this indicates that the reaction proceeds via the ionic mechanism. In addition, we have performed a competition study between 1-(5-fluoroindolin-1-yl)-2,2-dimethylpropan-1-one and 1-(5-methoxyindolin-1-yl)-2,2-dimethylpropan-1-one substrates, which gave almost the exact yield as those of the respective C-7 alkenylated products (Scheme 3.3d). Competitive studies for the cyclization reaction were performed between 5-methoxy- and 5-fluoroindolines (Scheme 3.3e). They reveal that electron-rich indolines react faster than electron-poor ones. Moreover, to understand the role of Ag_2CO_3 in the cyclization reaction, **VI** was heated at 120 °C in DCE in the absence of the catalyst and $AgSbF_6$, giving a 21% yield of **3aa** (Scheme 3.3f); also, 60% of the **VI** was recovered. Meanwhile, when **VI** was heated at 120 °C in DCE without Ag_2CO_3 , the catalyst, and $AgSbF_6$, a trace amount of **3aa** was observed. In addition, the alkylated species **VI** was subjected to cyclization reactions under the standard conditions, which resulted in a 92% isolated yield of pyroquilon **3aa** within 2 h (Scheme 3.3g). These control experiments confirm that the formation of **3aa** goes through the alkylated intermediate **VI** (Scheme 3.3f,g) and the Co catalyst enhances the rate of cyclization. Meanwhile, when **4aa** was subjected to cyclization under the standard conditions, we did not observe any cyclized product (Scheme 3.3g).

Scheme 3.3. Mechanistic Studies.

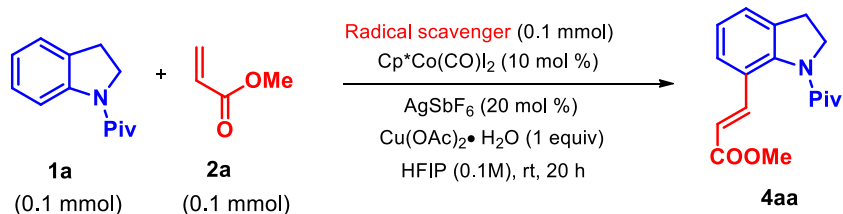
(a) H/D exchange studies:



(b) Inter molecular parallel experiment for kinetic isotope effect:

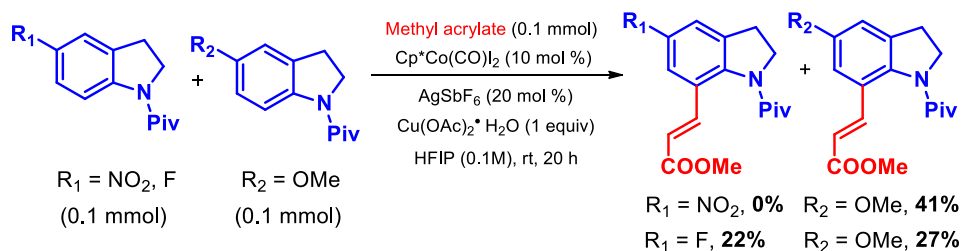


(c) Reaction with radical scavengers:

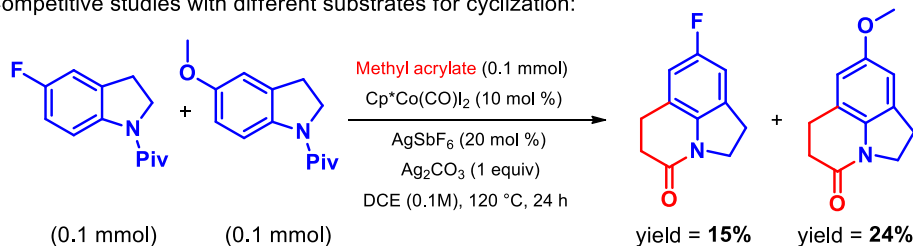


entry	radical scavengers	yield of 4aa	yield of recovered 1a
1.	TEMPO	36%	57%
2.	BHT	43%	49%

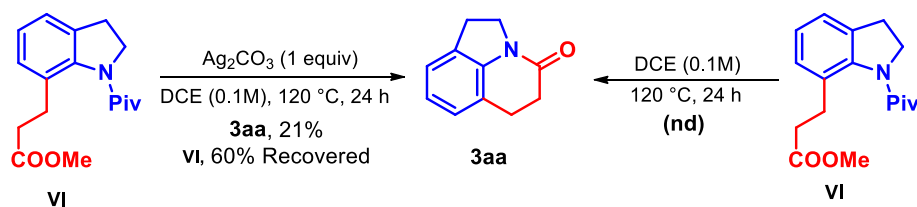
(d) Competitive studies with different substrates for C-7 alkenylation:



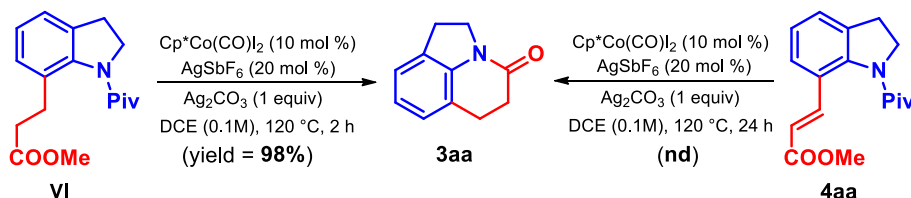
(e) Competitive studies with different substrates for cyclization:



(f)

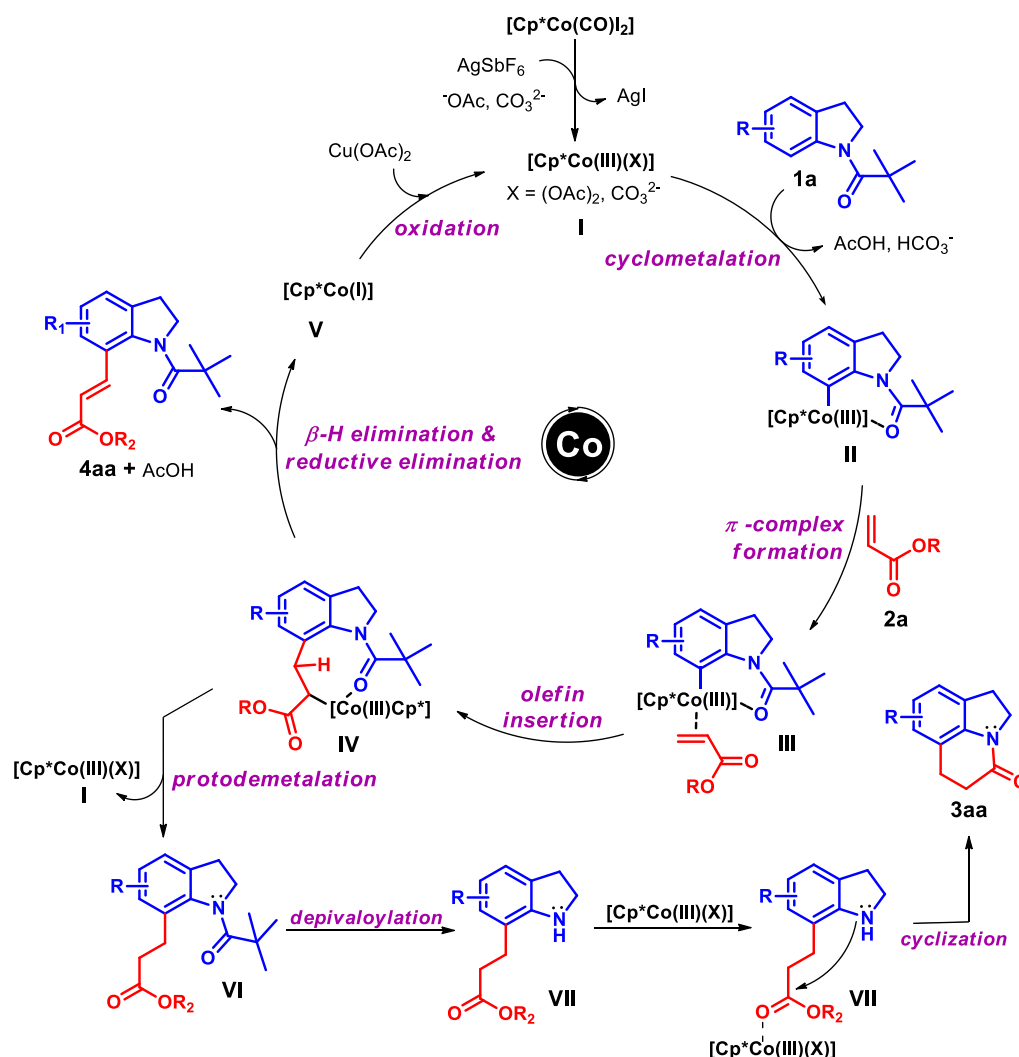


(g)



his might be due to the trans-geometry of the olefin in **4aa**. Based on kinetic studies and literature reports,^{11,12} we proposed a plausible catalytic cycle (Scheme 3.4) where $\text{Cp}^*\text{Co}(\text{CO})\text{I}_2$ reacts with AgSbF_6 to generate an active catalyst **I** that forms a six-membered cyclometalated species **II** in the presence of **1a**. The cationic cobalt(III) species undergoes π -complexation with the Michael acceptor **2a** and gives intermediate **III**, which then undergoes olefin insertion to give intermediate **IV**. Then, β -hydride elimination followed by reductive elimination gives the desired product **4aa** and cobalt(I) complex **V**, which is further oxidized by copper acetate to regenerate the active

Scheme 3.4. Proposed Catalytic Cycle.

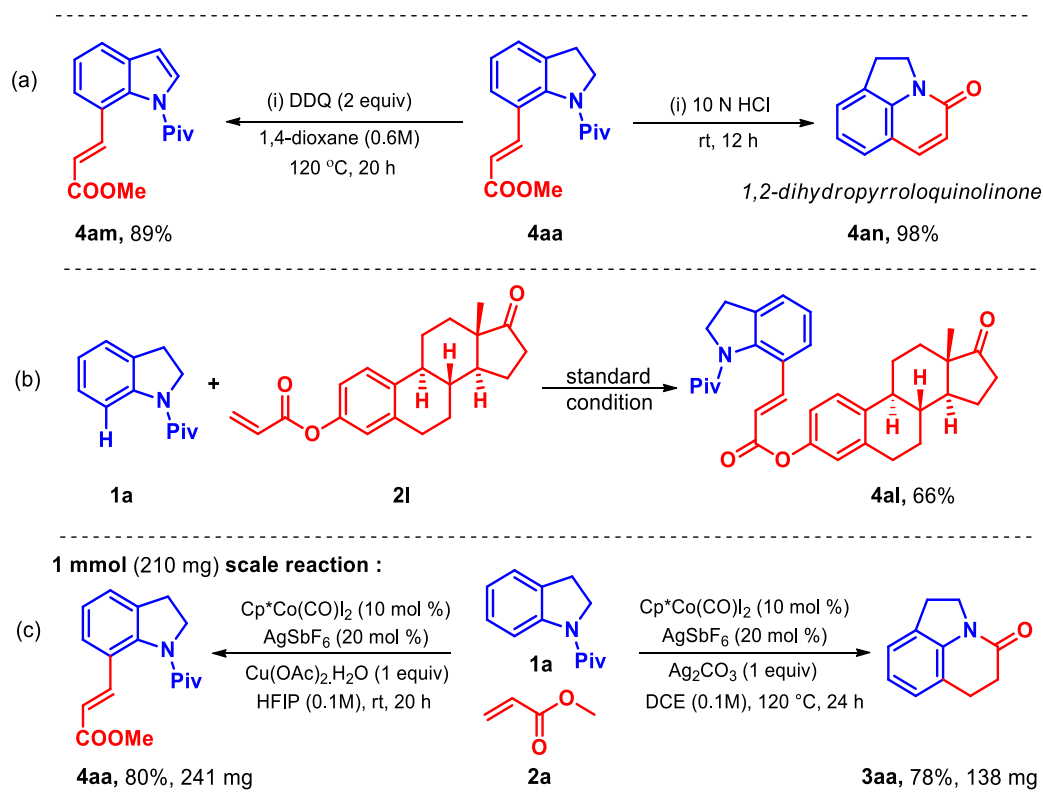


cobalt(III) catalyst **I** for the next catalytic cycle. In another pathway, intermediate **IV** undergoes protodemetalation giving intermediate **VI**, which undergoes depivaloylation followed by cyclization of **VII**, giving the desired cyclized product **3aa**. This might be due to the Lewis acidic nature of the Co catalyst, which coordinates with the alkylated carbonyl **VII**, increasing the electrophilicity of the carbonyl carbon and making it likely to undergo cyclization via nucleophilic substitution.^{12d}

To check the applicability of this transformation, we have performed the oxidation reaction of C-7-olefinated indoline **4aa** to get C-7-olefinated indole **4am** in

89% yield (Scheme 3.5a). Interestingly, when **4aa** was treated with 10 N HCl, it led to multiple events in one pot, such as (i) deprotection of the pivaloyl directing group, (ii) hydrolysis of ester, (iii) isomerization of trans-olefins to cis-olefins, and (iv) intramolecular amidation, giving an excellent yield of 1,2-dihydropyrroloquinolinone **4an** (Scheme 3.5a). This one-pot process in itself is a new method for the synthesis of 1,2-dihydropyrroloquinolinone.

Scheme 3.5. Synthetic Applications.



This C–H activation methodology also worked well with acrylate **2l** derived from the biologically active molecule estrone to give a good yield of **4al** (Scheme 3.5b). To know the synthetic applicability on a larger scale, we performed a 1 mmol-scale reaction, which gave **3aa** and **4aa** in 78% and 80% yields, respectively.

3.4 CONCLUSION

In summary, we have developed a cobalt-catalyzed one-step synthesis of tetrahydropyrroloquinolinone and C-7 alkenylated indolines using a weakly coordinating directing group for the first time. By simply modifying the reaction conditions, we could achieve either C(7)-H alkenylation or the formation of tetrahydropyrroloquinolinones. The control experiment confirmed that the C-7 alkylated indoline is the active intermediate for the formation of pyroquilon. In addition, this methodology is further useful for synthesizing 1,2-dihydropyrroloquinolinone from C-7 alkenylated indoline just by treatment with 10 N HCl, which is a new method. The developed protocol works well for a wide range of indolines and acrylates

Limitations: Electron-withdrawing substituted arenes such as -NO₂ is incompatible with alkylation process. Because electron-withdrawing groups decreases the nucleophilicity of Co-C bond towards olefin insertion giving moderate yield for olefination.

3.5 EXPERIMENTAL SECTION

Reactions were performed using a Borosil-sealed tube vial under an N₂ atmosphere. Column chromatography was done using 100–200 and 230–400 mesh silica gels from Acme Synthetic Chemicals Company. Gradient elution using distilled petroleum ether and ethyl acetate. TLC plates were detected under UV light at 254 nm. ¹H NMR and ¹³C NMR spectroscopy was performed using Bruker AV 400 and 700 MHz spectrometers with CDCl₃ and DMSO-*d*₆ as the deuterated solvents.¹³ Multiplicity (s = single, d = doublet, t = triplet, q = quartet, m = multiplet, dd = doublet of doublet), integration, and coupling constants (*J*) in hertz (Hz) are presented. HRMS signal

analysis was performed using a micro TOF Q-II mass spectrometer, and X-ray analysis was conducted at SCS, NISER. Reagents and starting materials were purchased from Sigma Aldrich, TCI, Avra, and CDCl₃ (77.36 ppm). Spectrochem and other commercially available sources and used without further purification unless otherwise noted.

(a) General procedure for rhodium-catalyzed annulation reaction (a):

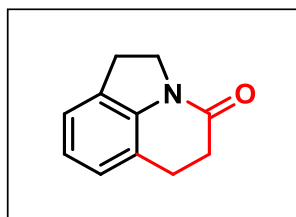
To a pre-dried sealed tube under N₂, a mixture of *N*-pivaloyl indoline **1** (0.1 mmol), acrylate **2** (0.4 mmol), [Cp*Co(CO)I₂] (10 mol %), AgSbF₆ (20 mol %), Ag₂CO₃ (1 equiv), and DCE (1 mL) was added and sealed. The reaction mixture was vigorously stirred at 120 °C in a heating aluminum block for 24 h. After 24 h (completion of the reaction as monitored by TLC analysis), the reaction mixture was cooled to room temperature, diluted with diethyl ether/ dichloromethane, and passed through a short celite pad; the solvent was evaporated under reduced pressure, and the residue was purified by column chromatography using an EtOAc/hexane mixture on silica gel to give the pure product **3**.

(b) General procedure for rhodium-catalyzed annulation reaction (b):

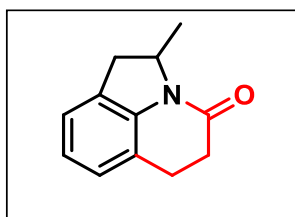
To a pre-dried sealed tube under N₂, a mixture of *N*-pivaloyl indoline **1** (0.1 mmol), acrylate **2** (0.4 mmol), [Cp*Co(CO)I₂] (10 mol %), AgSbF₆ (20 mol %), Cu(OAc)₂·H₂O (1 equiv), and HFIP (1 mL) was added and sealed. The reaction mixture was vigorously stirred at room temperature for 20 h. After 20 h (completion of the reaction as monitored by TLC analysis), the reaction mixture was cooled to room temperature, diluted with diethyl ether/dichloromethane, and passed through a short celite pad; the solvent was

evaporated under reduced pressure, and the residue was purified by column chromatography using an EtOAc/hexane mixture on silica gel to give the pure product **4**.

(c) Experimental characterization data of products:

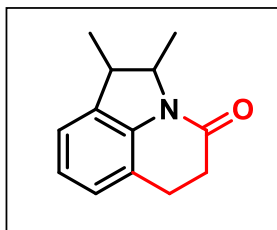


5,6-Dihydro-1H-pyrrolo[3,2,1-ij]quinolin-4(2H)-one (3aa)^{6e} was prepared according to general procedure (3.5a). The crude reaction mixture was purified by column chromatography using silica gel (100–200 mesh size), giving a white solid (14 mg, 82% yield). R_f: 0.35 (in 30% EtOAc/hexane), mp 113–115 °C. **¹H NMR (CDCl₃, 400 MHz):** δ 7.07 (d, *J* = 7.2 Hz, 1H), 7.01 (d, *J* = 7.2 Hz, 1H), 6.92 (t, *J* = 7.2 Hz, 1H), 4.08 (t, *J* = 8.4 Hz, 2H), 3.19 (t, *J* = 8.4 Hz, 2H), 2.97 (t, *J* = 7.6 Hz, 2H), 2.68 (t, *J* = 7.6 Hz, 2H). **¹³C{¹H} NMR (CDCl₃, 100 MHz):** δ 168.0, 141.6, 129.3, 125.7, 123.6, 123.6, 120.6, 45.5, 32.0, 28.1, 24.7. **HRMS (ESI) m/z** calcd for C₁₁H₁₁NONa [M + Na]⁺: 196.0738; found: 196.0734. **IR (KBr, cm⁻¹):** 1654.

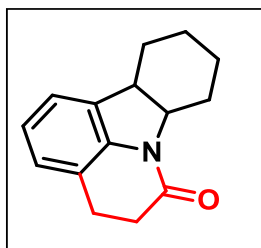


2-Methyl-5,6-dihydro-1H-pyrrolo[3,2,1-ij]quinolin-4(2H)-one (3ba) was prepared according to general procedure (3.5a). The crude reaction mixture was purified by column chromatography using silica gel (100–200 mesh size) giving a colorless liquid (12 mg, 71% yield). R_f: 0.30 (in 20% EtOAc/hexane). **¹H NMR (CDCl₃, 700 MHz):** δ 7.04 (d, *J* = 7.0 Hz, 1H), 6.98 (d, *J* = 7.7 Hz, 1H), 6.92 (t, *J* = 7.7 Hz, 1H), 4.68–4.64 (m, 1H), 3.41 (dd, *J* = 16.1, 6.3 Hz, 1H), 3.04–2.99 (m, 1H), 2.92–2.88 (m, 1H), 2.72–2.63 (m, 3H), 1.43 (d, *J* = 6.3 Hz, 3H). **¹³C{¹H} NMR (CDCl₃, 175 MHz):** δ 168.0, 141.1, 127.9, 125.6, 123.7, 123.6, 120.6, 54.6, 37.0, 32.3, 24.8, 21.4.

HRMS (ESI) m/z calcd for $C_{12}H_{14}NO$ $[M + H]^+$: 188.1075; found: 188.1071. **IR (KBr, cm^{-1}):** 1667.

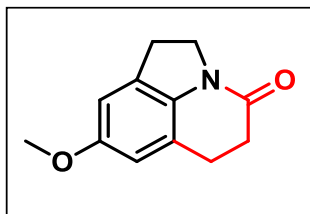


1,2-Dimethyl-5,6-dihydro-1H-pyrrolo[3,2,1-ij]quinolin-4(2H)-one (3ca) was prepared according to general procedure (3.5a). The crude reaction mixture was purified by column chromatography using silica gel (100–200 mesh size), giving a colorless liquid (11 mg, 63% yield). R_f : 0.35 (in 20% EtOAc/hexane). **1H NMR ($CDCl_3$, 400 MHz):** δ 7.04–7.699 (m, 2H), 6.95–6.92 (m, 1H), 4.15–4.10 (m, 1H), 3.06–2.97 (m, 3H), 2.73–2.59 (m, 2H), 1.46 (d, J = 6.5 Hz, 3H), 1.29 (d, J = 7.5 Hz, 3H). **$^{13}C\{^1H\}$ NMR ($CDCl_3$, 100 MHz):** δ 168.2, 140.5, 133.3, 125.8, 123.7, 122.7, 120.5, 63.0, 44.7, 32.3, 24.7, 21.0, 20.5. **HRMS (ESI)** m/z calcd for $C_{13}H_{16}NO$ $[M + H]^+$: 202.1226; found: 202.1231. **IR (KBr, cm^{-1})** 1669.

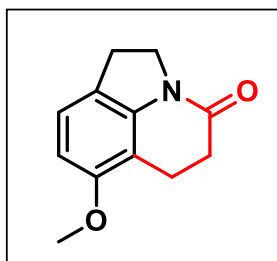


7a,8,9,10,11,11a-Hexahydro-4H-pyrido[3,2,1-jk]carbazol-6(5H)-one (3da)^{14a} was prepared according to general procedure (3.5a). The crude reaction mixture was purified by column chromatography using silica gel (100–200 mesh size) giving a yellow liquid (14 mg, 67% yield). R_f : 0.35 (in 20% EtOAc/hexane). **1H NMR ($CDCl_3$, 700 MHz):** δ 7.03 (d, J = 7.7 Hz, 1H), 7.0 (d, J = 7.7 Hz, 1H), 6.96 (t, J = 7.7 Hz, 1H), 4.58–4.55 (m, 1H), 3.49 (t, J = 9.8 Hz, 1H), 3.03–2.98 (m, 1H), 2.93–2.89 (m, 1H), 2.69–2.64 (m, 2H), 2.26–2.23 (m, 1H), 2.12–2.08 (m, 1H), 1.91–1.86 (m, 1H), 1.57–1.55 (m, 2H), 1.36–1.25 (m, 3H). **$^{13}C\{^1H\}$ NMR ($CDCl_3$, 175 MHz):** δ 167.3, 141.1, 132.2, 125.6, 123.7, 122.0, 120.9, 58.9, 40.6, 32.2, 26.8, 24.8, 24.7, 21.2, 20.9.

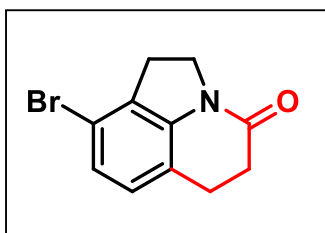
HRMS (ESI) m/z calcd for $C_{15}H_{18}NO$ $[M + H]^+$: 228.1388; found: 228.1386. **IR (KBr, cm^{-1}):** 1667.



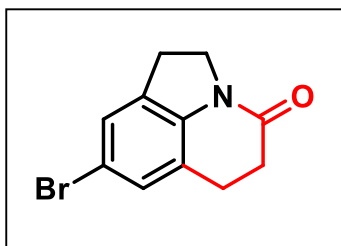
8-Methoxy-5,6-dihydro-1H-pyrrolo[3,2,1-ij]quinolin-4(2H)-one (3ea) was prepared according to general procedure (3.5a). The crude reaction mixture was purified by column chromatography using silica gel (100–200 mesh size) giving a brown solid (10 mg, 74% yield). R_f : 0.25 (in 40% EtOAc/hexane), mp 121–123 °C. **1H NMR ($CDCl_3$, 400 MHz):** δ 6.59 (s, 1H), 6.49 (s, 1H), 4.01 (t, J = 8.4 Hz, 2H), 3.70 (s, 3H), 3.09 (t, J = 8.3 Hz, 2H), 2.87 (t, J = 7.7 Hz, 2H), 2.59 (t, J = 7.7 Hz, 2H). **$^{13}C\{^1H\}$ NMR ($CDCl_3$, 100 MHz):** δ 157.2, 135.2, 130.2, 121.0, 111.4, 109.6, 56.2, 45.6, 31.7, 28.2, 24.9. **HRMS (ESI)** m/z calcd for $C_{12}H_{13}NO_2Na$ $[M + Na]^+$: 226.0844; found: 226.0843. **IR (KBr, cm^{-1}):** 1659.



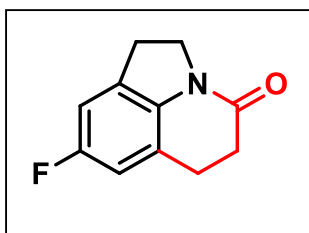
7-Methoxy-5,6-dihydro-1H-pyrrolo[3,2,1-ij]quinolin-4(2H)-one (3fa) 14b was prepared according to general procedure (3.5a). The crude reaction mixture was purified by column chromatography using silica gel (100–200 mesh size), giving a brown solid (12 mg, 56% yield). R_f : 0.35 (in 30% EtOAc/hexane), mp 129–131 °C. **1H NMR ($CDCl_3$, 400 MHz):** δ 6.99 (d, J = 8.0 Hz, 1H), 6.46 (d, J = 8.0 Hz, 1H), 4.06 (t, J = 8.4 Hz, 2H), 3.81 (s, 3H), 3.10 (t, J = 8.0 Hz, 2H), 2.91 (t, J = 7.6 Hz, 2H), 2.46 (t, J = 8.0 Hz, 2H). **$^{13}C\{^1H\}$ NMR ($CDCl_3$, 100 MHz):** δ 168.1, 156.3, 143.2, 124.0, 122.1, 109.2, 106.1, 56.0, 46.2, 31.4, 27.3, 19.4. **HRMS (ESI)** m/z calcd for $C_{12}H_{14}NO_2$ $[M + H]^+$: 204.1019; found: 204.1008. **IR (KBr, cm^{-1}):** 1662.



9-Bromo-5,6-dihydro-1H-pyrrolo[3,2,1-ij]quinolin-4(2H)-one (3ga) was prepared according to general procedure (3.5a). The crude reaction mixture was purified by column chromatography using silica gel (100–200 mesh size), giving a colorless solid (17 mg, 68% yield). R_f: 0.35 (in 30% EtOAc/hexane), mp 117–119 °C. **¹H NMR (CDCl₃, 400 MHz):** δ 7.04 (d, *J* = 8.0 Hz, 1H), 6.87 (d, *J* = 8 Hz, 1H), 4.1 (t, *J* = 8.4 Hz, 2H), 3.16 (t, *J* = 8.4 Hz, 2H), 2.92 (t, *J* = 8 Hz, 2H), 2.6 (t, *J* = 8 Hz, 2H). **¹³C{¹H} NMR (CDCl₃, 100 MHz):** δ 168.0, 142.7, 130.1, 127.6, 126.1, 119.3, 117.7, 45.1, 31.6, 29.4, 24.4. **HRMS (ESI)** *m/z* calcd for C₁₁H₁₀BrNONa [M + Na]⁺: 273.9838; found: 273.9842. **IR (KBr, cm⁻¹):** 1667.

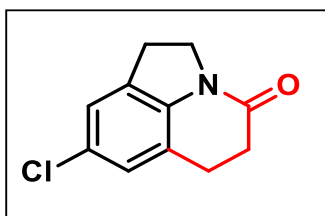


8-Bromo-5,6-dihydro-1H-pyrrolo[3,2,1-ij]quinolin-4(2H)-one (3ha) was prepared according to the general procedure (3.5a). The crude reaction mixture was purified by column chromatography using silica gel (100–200 mesh size), giving a yellow solid (13 mg, 77% yield). R_f: 0.32 (in 30% EtOAc/hexane), mp 122–124 °C. **¹H NMR (CDCl₃, 400 MHz):** δ 7.13 (s, 1H), 7.07 (s, 1H), 4.01 (t, *J* = 8.4 Hz, 2H), 3.10 (t, *J* = 8.5 Hz, 2H), 2.88 (t, *J* = 7.8 Hz, 2H), 2.59 (t, *J* = 7.8 Hz, 2H). **¹³C{¹H} NMR (CDCl₃, 100 MHz):** δ 167.6, 140.8, 131.2, 128.6, 126.7, 122.0, 115.8, 45.6, 31.6, 27.8, 24.5. **HRMS (ESI)** *m/z* calcd for C₁₁H₁₀BrNONa [M + Na]⁺: 273.9843; found: 273.9843. **IR (KBr, cm⁻¹):** 1667.



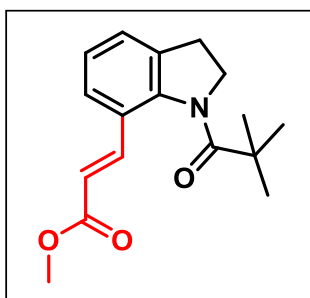
8-Fluoro-5,6-dihydro-1H-pyrrolo[3,2,1-ij]quinolin-4(2H)-one (3ia) was prepared according to general Procedure (3.5a). The crude reaction mixture was purified by column chromatography using silica gel (100–200

mesh size), giving a pale-yellow liquid (11 mg, 57% yield). *R*_f: 0.30 (in 30% EtOAc/hexane). **¹H NMR (CDCl₃, 400 MHz):** δ 6.79 (d, *J* = 8.4 Hz, 1H), 6.71 (d, *J* = 9.2 Hz, 1H), 4.09 (t, *J* = 8.4 Hz, 2H), 3.17 (t, *J* = 8.4 Hz, 2H), 2.94 (t, *J* = 7.6 Hz, 2H), 2.66 (t, *J* = 7.6 Hz, 2H). **¹³C{¹H} NMR (CDCl₃, 175 MHz):** δ 167.5, 160.7, 159.3, 137.6, 130.5 (d, *J* = 8.7 Hz), 121.3 (d, *J* = 8.4 Hz), 112.6 (d, *J* = 24.7 Hz), 111.0 (d, *J* = 24.8 Hz), 45.7, 31.5, 28.1 (d, *J* = 1.7 Hz), 24.7 (d, *J* = 1 Hz). **HRMS (ESI)** *m/z* calcd for C₁₁H₁₁FNO [M + H]⁺: 192.0819; found: 192.0829. **IR (KBr, cm⁻¹):** 1676.



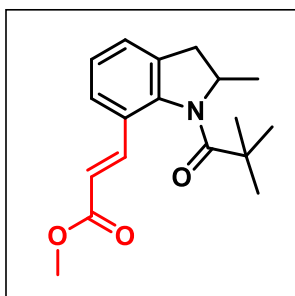
8-Chloro-5,6-dihydro-1H-pyrrolo[3,2,1-ij]quinolin-4(2H)-one (3iia) was prepared according to general procedure (3.5a). The crude reaction mixture was purified by column chromatography using silica gel

(100–200 mesh size), giving a white solid (5 mg, 34% yield). *R*_f: 0.35 (in 40% EtOAc/hexane), mp 113–115 °C. **¹H NMR (CDCl₃, 400 MHz):** δ 7.20 (s, 1H), 7.13 (s, 1H), 4.08 (t, *J* = 8.4 Hz, 2H), 3.17 (t, *J* = 8.4 Hz, 2H), 2.94 (t, *J* = 8.0 Hz, 2H), 2.66 (t, *J* = 8.0 Hz, 2H). **¹³C{¹H} NMR (CDCl₃, 100 MHz):** δ 168.0, 140.4, 131.3, 128.7, 126.8, 122.1, 116.2, 45.8, 31.2, 27.8, 24.3. **HRMS (ESI)** *m/z* calcd for C₁₁H₁₀ClNONa [M + Na]⁺: 230.0343; found: 230.0342. **IR (KBr, cm⁻¹):** 1739.



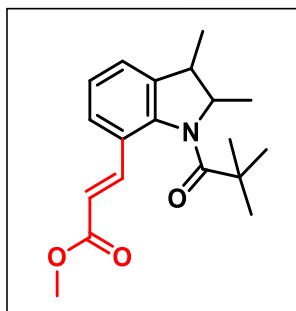
(E)-Methyl 3-(1-pivaloylindolin-7-yl)acrylate (**4aa**) was prepared according to general procedure (3.5b). The crude reaction mixture was purified by column chromatography using silica gel (100–200 mesh size), giving a white solid (24 mg, 84% yield). R_f: 0.40 (in 20% EtOAc/hexane), mp

125–127 °C. ¹H NMR (CDCl₃, 700 MHz): δ 7.45 (d, *J* = 16.1 Hz, 1H), 7.40 (d, *J* = 7.7 Hz, 1H), 7.23 (d, *J* = 7.7 Hz, 1H), 7.09 (t, *J* = 7.7 Hz, 1H), 6.31 (d, *J* = 16.1 Hz, 1H), 4.17 (t, *J* = 7.4 Hz, 2H), 3.77 (s, 3H), 3.06 (t, *J* = 7.4 Hz, 2H), 1.42 (s, 9H). ¹³C{¹H} NMR (CDCl₃, 175 MHz): δ 180.0, 168.0, 144.0, 143.1, 135.0, 126.1, 125.6, 125.3, 117.1, 51.8, 51.4, 40.5, 31.1, 29.1. HRMS (ESI) *m/z* calcd for C₁₇H₂₁NO₃Na [M + Na]⁺: 310.1419; found: 310.1424. IR (KBr, cm⁻¹): 1715, 1652.



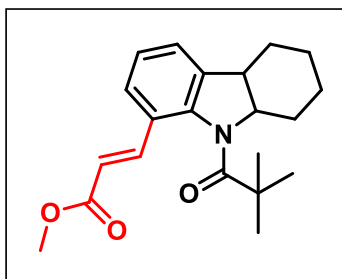
(E)-Methyl 3-(2-methyl-1-pivaloylindolin-7-yl)acrylate (**4ba**) was prepared according to general procedure (3.5b). The crude reaction mixture was purified by column chromatography using silica gel (100–200 mesh size), giving a yellow liquid (22 mg, 77% yield). R_f: 0.45 (in 20%

EtOAc/hexane). ¹H NMR (CDCl₃, 700 MHz): δ 7.47 (d, *J* = 16.1 Hz, 1H), 7.43 (d, *J* = 7.7 Hz, 1H), 7.25 (d, *J* = 5.6 Hz, 1H), 7.12 (t, *J* = 7.7 Hz, 1H), 6.34 (d, *J* = 16.1 Hz, 1H), 4.84–4.81 (m, 1H), 3.76 (s, 3H), 3.31–3.28 (m, 1H), 2.54 (d, *J* = 14.7 Hz, 1H), 1.41 (s, 9H), 1.26 (d, *J* = 6.3 Hz, 3H). ¹³C{¹H} NMR (CDCl₃, 175 MHz): δ 179.4, 168.2, 143.1, 142.8, 134.7, 127.6, 127.7, 125.8, 125.4, 116.8, 57.8, 51.9, 50.0, 38.4, 29.1, 21.0. HRMS (ESI) *m/z* calcd for C₁₈H₂₃NO₃Na [M + Na]⁺: 324.1576; found: 324.1577. IR (KBr, cm⁻¹): 1734, 1653.



(E)-Methyl-3-(2,3-dimethyl-1-pivaloylindolin-7-yl)acrylate (4ca) was prepared according to the general procedure (3.5b). The crude reaction mixture was purified by column chromatography using silica gel (100–200 mesh size), giving a yellow liquid (24 mg, 77% yield). R_f: 0.30 (in

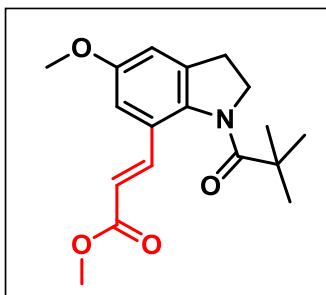
10% EtOAc/hexane). **¹H NMR (CDCl₃, 400 MHz):** δ 7.51–7.43 (m, 2H), 7.23 (d, *J* = 7.2 Hz, 1H), 7.12 (t, *J* = 7.6 Hz, 1H), 6.34 (d, *J* = 16.0 Hz, 1H), 4.36 (q, *J* = 6.4 Hz, 1H), 3.8 (s, 3H), 2.78 (q, *J* = 7.2 Hz, 1H), 1.41 (s, 9H), 1.26 (d, *J* = 6.4 Hz, 3H), 1.17 (d, *J* = 7.2 Hz, 3H). **¹³C{¹H} NMR (CDCl₃, 100 MHz):** δ 180.0, 168.1, 142.8, 142.2, 140.0, 127.6, 126.0, 125.8, 125.7, 116.8, 64.6, 51.9, 45.6, 41.0, 29.4, 21.0, 20.4. **HRMS (ESI)** *m/z* calcd for C₁₉H₂₆NO₃ [M + H]⁺: 316.1907; found: 316.1914. **IR (KBr, cm⁻¹):** 1700, 1653.



(E)-Methyl-3-(9-pivaloyl-2,3,4,4a,9,9a-hexahydro-1H-carbazol-8-yl)acrylate (4da) was prepared according to the general procedure (3.5b). The crude reaction mixture was purified by column chromatography using silica gel (100–200 mesh size),

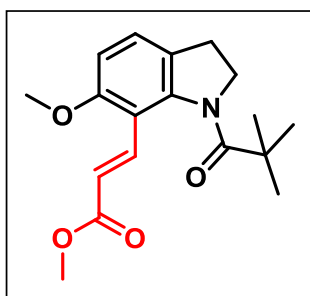
giving a colorless liquid (17 mg, 61% yield). R_f: 0.40 (in 20% EtOAc/hexane). **¹H NMR (CDCl₃, 700 MHz):** δ 7.49 (d, *J* = 16.1 Hz, 1H), 7.43–7.42 (m, 1H), 7.18–7.15 (m, 2H), 6.33 (d, *J* = 16.1 Hz, 1H), 4.59–4.55 (m, 1H), 3.76 (s, 3H), 3.48 (t, *J* = 5.5 Hz, 1H), 2.32 (d, *J* = 14.7 Hz, 1H), 2.07–2.04 (m, 1H), 1.84–1.78 (m, 1H), 1.53 (d, *J* = 12.6 Hz, 1H), 1.41 (s, 9H), 1.25–1.19 (m, 3H), 1.12–1.06 (m, 1H). **¹³C{¹H} NMR (CDCl₃, 175 MHz):** δ 179.0, 168.1, 144.5, 143.0, 138.0, 127.8, 125.8, 125.1, 124.2, 116.8, 63.7, 52.0, 42.6,

40.7, 29.2, 28.1, 24.9, 23.7, 20.8. **HRMS (ESI)** m/z calcd for $C_{21}H_{28}NO_3$ $[M + H]^+$: 342.2069; found: 342.2065. **IR (KBr, cm^{-1})**: 1717, 1652.



(E)-Methyl-3-(5-methoxy-1-pivaloylindolin-7-yl)acrylate (4ea) was prepared according to the general procedure (3.5b). The crude reaction mixture was purified by column chromatography using silica gel (100–200 mesh size), giving a yellow solid (24 mg, 91% yield). Rf:

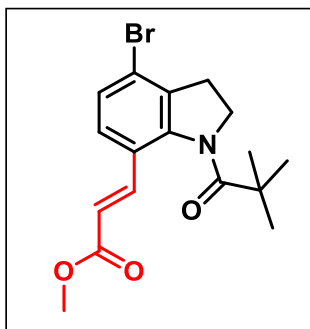
0.35 (in 30% EtOAc/hexane), mp 114–116 °C. **1H NMR ($CDCl_3$, 700 MHz)**: δ 7.45 (d, $J = 16.1$ Hz, 1H), 6.89 (d, $J = 2.1$ Hz, 1H), 6.83 (d, $J = 0.7$ Hz, 1H), 6.28 (d, $J = 16.1$ Hz, 1H), 4.16 (t, $J = 7.4$ Hz, 2H), 3.79 (s, 3H), 3.76 (s, 3H), 3.00 (d, $J = 7.4$ Hz, 2H), 1.40 (s, 9H). **$^{13}C\{^1H\}$ NMR ($CDCl_3$, 175 MHz)**: δ 179.6, 167.8, 157.8, 142.7, 137.6, 136.6, 126.4, 117.0, 113.0, 109.6, 56.0, 52.0, 51.6, 40.4, 31.3, 29.0. **HRMS (ESI)** m/z calcd for $C_{18}H_{23}NO_4Na$ $[M + Na]^+$: 340.1525; found: 340.1527. **IR (KBr, cm^{-1})**: 1717, 1652.



(E)-Methyl 3-(6-methoxy-1-pivaloylindolin-7-yl)acrylate (4fa) was prepared according to the general procedure (3.5b). The crude reaction mixture was purified by column chromatography using silica gel (100–200 mesh size), giving a yellow solid (15 mg, 49% yield). Rf:

0.30 (in 20% EtOAc/hexane), mp 109–112 °C. **1H NMR ($CDCl_3$, 400 MHz)**: δ 7.41 (d, $J = 16.4$ Hz, 1H), 7.14 (d, $J = 8.4$ Hz, 1H), 6.64 (d, $J = 8.4$ Hz, 1H), 6.58 (d, $J = 16.4$ Hz, 1H), 4.18 (t, $J = 7.6$ Hz, 2H), 3.85 (s, 3H), 3.75 (s, 3H), 2.98 (t, $J = 7.2$ Hz, 2H), 1.39 (s, 9H). **$^{13}C\{^1H\}$ NMR ($CDCl_3$, 100 MHz)**: δ 179.9, 168.9, 158.7, 145.7, 139.2, 126.9,

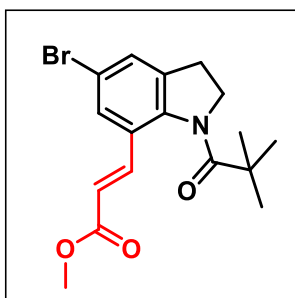
125.6, 119.8, 115.6, 107.8, 56.2, 52.1, 51.7, 40.6, 30.6, 28.7. **HRMS (ESI)** m/z calcd for $C_{18}H_{24}NO_4$ $[M + H]^+$: 318.1700; found: 318.1689. **IR (KBr, cm^{-1}):** 1713, 1651.



(E)-Methyl 3-(4-bromo-1-pivaloylindolin-7-yl)acrylate

(4ga) was prepared according to the general procedure (3.5b). The crude reaction mixture was purified by column chromatography using silica gel (100–200 mesh size), giving a brown solid (18 mg, 72% yield). R_f : 0.55 (in 20%

EtOAc/hexane), mp 147–149 °C. **1H NMR ($CDCl_3$, 400 MHz):** δ 7.34 (d, J = 16.0 Hz, 1H), 7.29–7.22 (m, 2H), 6.29 (d, J = 16 Hz, 1H), 4.2 (t, J = 7.6 Hz, 2H), 3.76 (s, 3H), 3.1 (t, J = 7.6 Hz, 2H), 1.4 (s, 9H). **$^{13}C\{^1H\}$ NMR ($CDCl_3$, 100 MHz):** δ 180.1, 167.7, 144.8, 141.9, 135.7, 128.3, 127.1, 125.0, 120.7, 117.2, 51.9, 50.7, 40.7, 32.6, 28.8. **HRMS (ESI)** m/z calcd for $C_{17}H_{21}BrNO_3$ $[M + H]^+$: 366.0699; found: 366.0703. **IR (KBr, cm^{-1}):** 1709, 1657.

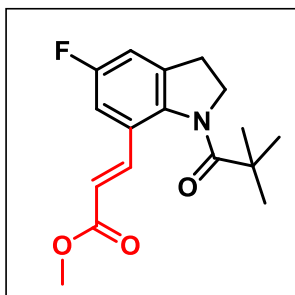


(E)-Methyl-3-(5-bromo-1-pivaloylindolin-7-yl)acrylate

(4ha) was prepared according to the general procedure (3.5b). The crude reaction mixture was purified by column chromatography using silica gel (100–200 mesh size), giving a yellow solid (21 mg, 82% yield). R_f : 0.35 (in 20%

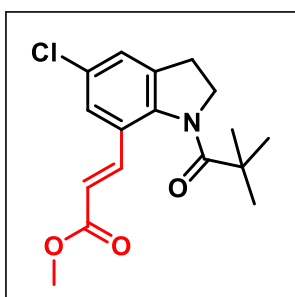
EtOAc/hexane), mp 132–134 °C. **1H NMR ($CDCl_3$, 700 MHz):** δ 7.51 (d, J = 1.4 Hz, 1H), 7.34–7.32 (m, 2H), 6.27 (d, J = 15.4 Hz, 1H), 4.17 (t, J = 7.7 Hz, 2H), 3.76 (s, 3H), 3.05 (t, J = 7.7 Hz, 2H), 1.40 (s, 9H). **$^{13}C\{^1H\}$ NMR ($CDCl_3$, 175 MHz):** δ 180.0, 167.6, 143.1, 141.5, 137.2, 128.8, 128.3, 127.5, 118.2, 117.9, 52.0, 51.4, 40.6, 30.9, 28.7.

HRMS (ESI) m/z calcd for $C_{17}H_{21}BrNO_3$ $[M + H]^+$: 366.0705; found: 366.0707. **IR** (**KBr**, cm^{-1}): 1699, 1653.



(E)-Methyl-3-(5-fluoro-1-pivaloylindolin-7-yl)acrylate (**4ia**) was prepared according to the general procedure (3.5b). The crude reaction mixture was purified by column chromatography using silica gel (100–200 mesh size), giving a yellow liquid (18 mg, 61% yield). R_f : 0.45 (in 20%

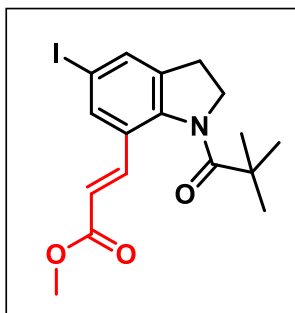
EtOAc/hexane). **1H NMR** ($CDCl_3$, 400 MHz): δ 7.38 (d, J = 15.6 Hz, 1H), 7.07 (d, J = 10.0 Hz, 1H), 6.95 (d, J = 6.8 Hz, 1H), 6.26 (d, J = 16.0 Hz, 1H), 4.2 (t, J = 7.6 Hz, 2H), 3.76 (s, 3H), 3.04 (t, J = 7.6 Hz, 2H), 1.4 (s, 9H). **$^{13}C\{^1H\}$ NMR** ($CDCl_3$, 175 MHz): δ 180.0, 167.7, 160.7 (d, J = 242.2 Hz), 141.7 (d, J = 1.9 Hz), 140.1 (d, J = 1.9 Hz), 137.2 (d, J = 8.9 Hz), 126.9 (d, J = 8.2 Hz), 117.8, 113.4 (d, J = 24.1 Hz), 111.6 (d, J = 24 Hz), 52.0, 51.6, 40.5, 31.2 (d, J = 1.4 Hz), 28.8. **HRMS (ESI)** m/z calcd for $C_{17}H_{20}FNO_3Na$ $[M + Na]^+$: 328.1319; found: 328.1342. **IR** (**KBr**, cm^{-1}): 1717, 1653.



(E)-Methyl-3-(5-chloro-1-pivaloylindolin-7-yl)acrylate (**4iia**) was prepared according to the general procedure (3.5b). The crude reaction mixture was purified by column chromatography using silica gel (100–200 mesh size), giving a brown solid (17 mg, 73% yield). R_f : 0.40 (in 20%

EtOAc/hexane), mp 121–123 °C. **1H NMR** (400 MHz, $CDCl_3$): δ 7.37 (s, 1H), 7.34 (d, J = 16.0 Hz, 1H), 7.26 (s, 1H), 6.28 (d, J = 16.0 Hz, 1H), 4.18 (t, J = 7.6 Hz, 2H), 3.76 (s, 3H), 3.04 (t, J = 7.6 Hz, 2H), 1.40 (s, 9H). **$^{13}C\{^1H\}$ NMR** (100 MHz, $CDCl_3$): δ

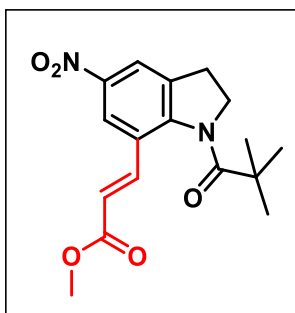
179.8, 167.5, 142.6, 141.5, 136.9, 130.6, 127.0, 125.9, 125.3, 117.8, 51.9, 51.4, 40.6, 30.9, 28.7. **HRMS (ESI)** m/z calcd for $C_{17}H_{20}ClNO_3Na$ $[M + Na]^+$: 344.1024; found: 344.1029. **IR (KBr, cm^{-1}):** 1739, 1403.



(E)-Methyl-3-(5-iodo-1-pivaloylindolin-7-yl)acrylate

(4iiia) was prepared according to the general procedure (3.5b). The crude reaction mixture was purified by column chromatography using silica gel (100–200 mesh size), giving a brown solid (16 mg, 69% yield). R_f : 0.45 (in 20%

EtOAc/hexane), mp 130–132 °C. **1H NMR (400 MHz, $CDCl_3$):** δ 7.69 (s, 1H) 7.53 (s, 1H), 7.30 (m, 1H), 6.27 (d, $J = 16.0$ Hz, 1H) 6.27 (d, $J = 16.0$ Hz, 1H), 4.15 (t, $J = 7.6$ Hz, 2H), 3.76 (s, 3H), 3.04 (t, $J = 7.6$ Hz, 2H), 1.39 (s, 9H). **$^{13}C\{^1H\}$ NMR (100 MHz, $CDCl_3$):** δ 179.7, 167.5, 143.9, 141.3, 137.4, 134.5, 134.3, 127.9, 117.7, 88.7, 51.9, 51.3, 40.6, 30.6, 28.7. **HRMS (ESI)** m/z calcd for $C_{17}H_{21}INO_3$ $[M + H]^+$: 414.0561; found: 414.0543. **IR (KBr, cm^{-1}):** 1741, 1367.

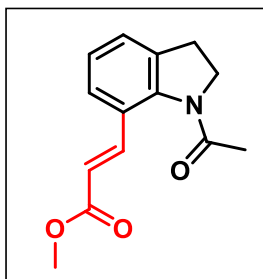


(E)-Methyl-3-(5-nitro-1-pivaloylindolin-7-yl)acrylate

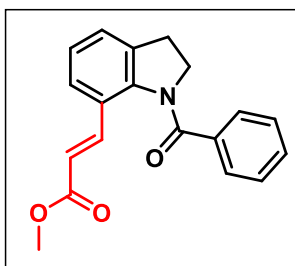
(4ja) was prepared according to general procedure (3.5b). The crude reaction mixture was purified by column chromatography using silica gel (100–200 mesh size) giving a yellow solid (8 mg, 28% yield). R_f : 0.40 (in 30%

EtOAc/hexane), mp 145–147 °C. **1H NMR ($CDCl_3$, 400 MHz):** δ 8.32 (d, $J = 2.1$ Hz, 1H), 8.07 (s, 1H), 7.32 (d, $J = 15.9$ Hz, 1H), 6.42 (d, $J = 15.9$ Hz, 1H), 4.28 (t, $J = 7.8$ Hz, 2H), 3.80 (s, 3H), 3.19 (t, $J = 7.8$ Hz, 2H), 1.43 (s, 9H). **$^{13}C\{^1H\}$ NMR ($CDCl_3$, 100**

MHz): δ 180.2, 167.2, 149.4, 145.3, 140.6, 136.4, 125.9, 122.3, 120.5, 119.1, 52.1, 51.72, 40.99, 30.5, 28.7. **HRMS (ESI)** m/z calcd for $C_{17}H_{20}N_2O_5Na$ $[M+Na]^+$: 355.1264; found: 355.1246. **IR (KBr, cm^{-1}):** 1716, 1668, 1524, 1295.

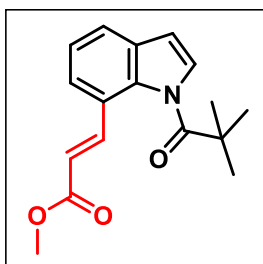


(E)-Methyl-3-(1-acetyllindolin-7-yl)acrylate (4ma)^{15a} was prepared according to the general procedure (3.5b). The crude reaction mixture was purified by column chromatography using silica gel (100–200 mesh size), giving a colorless liquid (20.4 mg, 68% yield). R_f : 0.40 (in 30% EtOAc/hexane). **1H NMR ($CDCl_3$, 400 MHz):** δ 7.68 (d, J = 16.0 Hz, 1H), 7.42 (d, J = 7.6 Hz, 1H), 7.24 (d, J = 7.2 Hz, 1H), 7.11 (t, J = 7.6 Hz, 1H), 6.34 (d, J = 16.0 Hz, 1H), 4.16 (br, 2H), 3.78 (s, 3H), 3.04 (t, J = 7.2 Hz, 2H), 2.20 (br, 3H). **$^{13}C\{^1H\}$ NMR ($CDCl_3$, 100 MHz):** δ 167.7, 143.3, 143.2, 143.1, 126.2, 125.8, 125.6, 116.9, 116.8, 51.9, 51.2, 29.6, 23.8. **HRMS (ESI)** m/z calcd for $C_{14}H_{15}NO_3Na$ $[M+Na]^+$: 268.0944; found: 268.0951. **IR (KBr, cm^{-1}):** 1714, 1667.



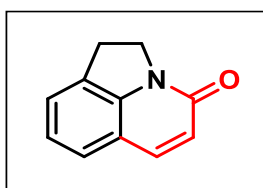
(E)-Methyl-3-(1-benzoyllindolin-7-yl)acrylate (4na) was prepared according to the general procedure (3.5b). The crude reaction mixture was purified by column chromatography using silica gel (100–200 mesh size), giving a yellow liquid (15 mg, 54% yield). R_f : 0.35 (in 20% EtOAc/hexane). **1H NMR ($CDCl_3$, 400 MHz):** δ 7.64 (d, J = 7.6 Hz, 1H), 7.51 (d, J = 16.0 Hz, 1H), 7.50–7.46 (m, 1H), 7.40 (t, J = 8.0 Hz, 3H), 7.26 (d, J = 8.4 Hz, 1H), 7.14 (t, J = 7.6 Hz, 1H), 6.20 (d, J = 16.0 Hz, 1H), 4.20 (t, J = 7.6 Hz, 2H), 3.71 (s, 3H), 3.05 (t, J = 7.6 Hz, 2H). **$^{13}C\{^1H\}$**

NMR (CDCl₃, 100 MHz): δ 170.9, 167.8, 142.4, 142.3, 135.4, 135.2, 131.8, 129.1, 128.7, 126.4, 125.9, 125.4, 117.9, 53.9, 51.9, 30.0. **HRMS (ESI)** m/z calcd for C₁₉H₁₇NO₃Na [M+Na]⁺: 330.1101; found: 330.1094. **IR (KBr, cm⁻¹):** 1715, 1653.



(E)-Methyl-3-(1-pivaloyl-1H-indol-7-yl)acrylate (4am)^{15b}

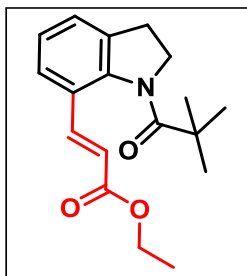
was prepared according to the reported procedure. The crude reaction mixture was purified by column chromatography using silica gel (100–200 mesh size), giving a brown solid (18 mg, 89% yield). R_f: 0.50 (in 20% EtOAc/hexane), mp 102–104 °C. **¹H NMR (CDCl₃, 400 MHz):** δ 7.82 (d, J = 15.6 Hz, 1H), 7.59 (m, 2H), 7.46 (d, J = 7.6 Hz, 1H), 7.27 (t, J = 7.6 Hz, 1H), 6.63 (d, J = 3.6 Hz, 1H), 6.29 (d, J = 15.6 Hz, 1H), 3.80 (s, 3H), 1.55 (s, 9H). **¹³C{¹H} NMR (CDCl₃, 100 MHz):** δ 179.8, 167.7, 143.7, 135.2, 131.6, 126.8, 124.4, 123.8, 123.6, 122.7, 117.5, 107.8, 51.9, 42.3, 29.3. **HRMS (ESI)** m/z calcd for C₁₇H₁₉NO₃Na [M + Na]⁺: 308.1257; found: 308.1264. **IR (KBr, cm⁻¹):** 1710, 1640.



1H-Pyrrolo[3,2,1-ij]quinolin-4(2H)-one (4an) was prepared

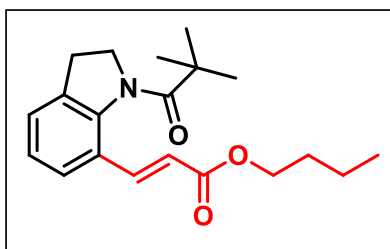
according to reported procedure. The crude reaction mixture was purified by column chromatography using silica gel (100–200 mesh size), giving a yellow solid (25 mg, 98% yield). R_f: 0.45 (in 40% EtOAc/hexane), mp 157–159 °C. **¹H NMR (CDCl₃, 400 MHz):** δ 7.70 (d, J = 9.6 Hz, 1H), 7.39 (t, J = 8.0 Hz, 1H), 7.34 (d, J = 6.8 Hz, 1H), 7.14 (t, J = 7.6 Hz, 1H), 6.67 (d, J = 9.6 Hz, 1H), 4.46 (t, J = 8.0 Hz, 2H), 3.43 (t, J = 8.0 Hz, 2H). **¹³C{¹H} NMR (CDCl₃, 100 MHz):** δ 161.4, 142.8, 137.5, 130.9, 125.3, 123.9, 123.8, 123.5, 118.0, 47.3, 27.4.

HRMS (ESI) m/z calcd for $C_{11}H_{11}NO_2Na$ $[M + Na]^+$: 194.0574; found: 194.0582. **IR** (KBr, cm^{-1}): 1648.



(E)-Ethyl 3-(1-pivaloylindolin-7-yl)acrylate (4ab)6e was prepared according to the general procedure (3.5b). The crude reaction mixture was purified by column chromatography using silica gel (100–200 mesh size), giving a yellow solid (24 mg, 86% yield). R_f : 0.40 (in 20% EtOAc/hexane), mp

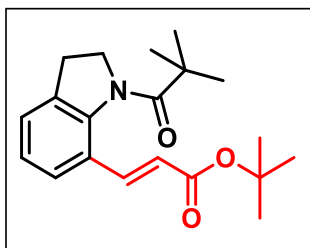
119–121 °C. **1H NMR** ($CDCl_3$, 400 MHz): δ 7.46–7.39 (m, 2H), 7.26–7.22 (m, 1H), 7.10 (t, J = 7.6 Hz, 1H), 6.26 (d, J = 16.0 Hz, 1H), 4.24–4.14 (m, 4H), 3.05 (t, J = 7.6 Hz, 2H), 1.41 (s, 9H), 1.30 (t, J = 7.2 Hz, 3H). **$^{13}C\{^1H\}$ NMR** ($CDCl_3$, 100 MHz): δ 180.1, 167.0, 144.1, 142.4, 135.0, 126.3, 125.5, 125.4, 117.2, 60.5, 51.4, 40.5, 31.1, 29.1, 15.5. **HRMS (ESI)** m/z calcd for $C_{18}H_{23}NO_3Na$ $[M + Na]^+$: 324.1576; found: 324.1575. **IR** (KBr, cm^{-1}): 1705, 1652.



(E)-Butyl-3-(1-pivaloylindolin-7-yl)acrylate (4ac) was prepared according to the general procedure (3.5b). The crude reaction mixture was purified by column chromatography using silica gel (100–200

mesh size), giving a colorless liquid (23 mg, 76% yield). R_f : 0.30 (in 20% EtOAc/hexane). **1H NMR** ($CDCl_3$, 400 MHz): δ 7.45–7.40 (m, 2H), 7.23 (d, J = 7.6 Hz, 1H), 7.09 (t, J = 7.6 Hz, 1H), 6.30 (d, J = 16.0 Hz, 1H), 4.17 (t, J = 7.2 Hz, 4H), 3.06 (t, J = 7.6 Hz, 2H), 1.69–1.63 (m, 2H), 1.45–1.42 (m, 11H), 0.95 (t, J = 7.6 Hz, 3H). **$^{13}C\{^1H\}$ NMR** ($CDCl_3$, 100 MHz): δ 180.0, 168.1, 144.0, 142.2, 135.0, 126.0,

125.8, 125.5, 125.3, 117.2, 64.5, 51.4, 40.5, 31.09, 31.05, 29.1, 19.5, 14.1. **HRMS (ESI)** m/z calcd for $C_{20}H_{27}NO_3Na$ $[M + Na]^+$: 352.1889; found: 352.1896. **IR (KBr, cm^{-1}):** 1706, 1653.

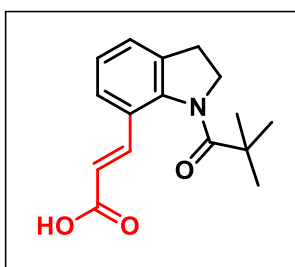


(E)-tert-Butyl 3-(1-pivaloylindolin-7-yl)acrylate (4ad)^{6e}

was prepared according to the general procedure (3.5b).

The crude reaction mixture was purified by column chromatography using silica gel (100–200 mesh size),

giving a yellow solid (17 mg, 57% yield). R_f : 0.30 (in 20% EtOAc/hexane), mp 134–136 °C. **1H NMR ($CDCl_3$, 400 MHz):** δ 7.39 (d, J = 7.6 Hz, 1H), 7.32 (d, J = 16.0 Hz, 1H), 7.20 (d, J = 7.2 Hz, 1H), 7.07 (t, J = 7.6 Hz, 1H), 6.22 (d, J = 16 Hz, 1H), 4.15 (t, J = 7.6 Hz, 2H), 3.04 (t, J = 7.6 Hz, 2H), 1.50 (s, 9H), 1.41 (s, 9H). **$^{13}C\{^1H\}$ NMR ($CDCl_3$, 100 MHz):** δ 180.0, 167.1, 144.0, 141.2, 135.1, 126.4, 126.1, 125.5, 125.3, 119.4, 80.3, 51.4, 40.5, 31.2, 29.1, 28.5. **HRMS (ESI)** m/z calcd for $C_{20}H_{27}NO_3Na$ $[M + Na]^+$: 352.1889; found: 352.1892. **IR (KBr, cm^{-1}):** 1706, 1652.

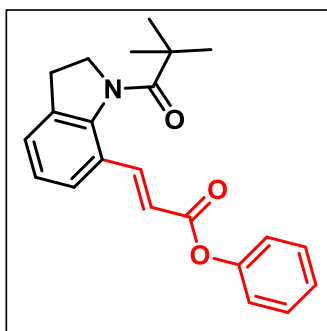


(E)-3-(1-Pivaloylindolin-7-yl)acrylic acid (4ae) was

prepared according to the general procedure (3.5b). The crude reaction mixture was purified by column chromatography using silica gel (100–200 mesh size),

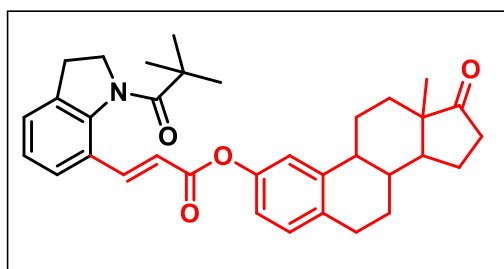
giving a yellow solid (12 mg, 52% yield). R_f : 0.30 (in 20% EtOAc/hexane), mp 204–206 °C. **1H NMR ($CDCl_3$, 700 MHz):** δ 7.54 (d, J = 16.1 Hz, 1H), 7.41 (d, J = 7.7 Hz, 1H), 7.25 (d, J = 7.7 Hz, 1H), 7.10 (t, J = 7.7 Hz, 1H), 6.28 (d, J = 15.4 Hz, 1H), 4.18 (t, J = 7.0 Hz, 2H), 3.06 (t, J = 7.0 Hz, 2H), 1.41 (s, 9H). **$^{13}C\{^1H\}$ NMR ($CDCl_3$,**

175 MHz): δ 180.0, 172.1, 145.0, 144.1, 135.0, 126.3, 125.8, 125.7, 125.4, 116.2, 51.4, 40.6, 31.1, 29.1. **HRMS (ESI)** m/z calcd for $C_{16}H_{20}NO_3$ $[M + H]^+$: 274.1443; found: 274.1441. **IR (KBr, cm^{-1}):** 1700, 1652.



(E)-Phenyl 3-(1-pivaloylindolin-7-yl)acrylate (4af) was prepared according to the general procedure (3.5b). The crude reaction mixture was purified by column chromatography using silica gel (100–200 mesh size), giving a white solid (22 mg, 73% yield). R_f : 0.35 (in 20%

EtOAc/hexane), mp 159–161 °C. **1H NMR ($CDCl_3$, 400 MHz):** δ 7.62 (d, J = 16.0 Hz, 1H), 7.48 (d, J = 8.0 Hz, 1H), 7.38 (t, J = 7.6 Hz, 2H), 7.27–7.20 (m, 2H), 7.17–7.10 (m, 3H), 6.48 (d, J = 16.0 Hz, 1H), 4.18 (t, J = 7.6 Hz, 2H), 3.07 (t, J = 7.6 Hz, 2H), 1.40 (s, 9H). **$^{13}C\{^1H\}$ NMR ($CDCl_3$, 100 MHz):** δ 179.9, 165.9, 151.2, 144.4, 144.2, 135.1, 129.6, 126.3, 125.8, 125.7, 125.6, 125.4, 122.0, 116.0, 51.3, 40.6, 31.1, 28.8. **HRMS (ESI)** m/z calcd for $C_{22}H_{23}NO_3K$ $[M + K]^+$: 388.1315; found: 388.1337. **IR (KBr, cm^{-1}):** 1726, 1652.

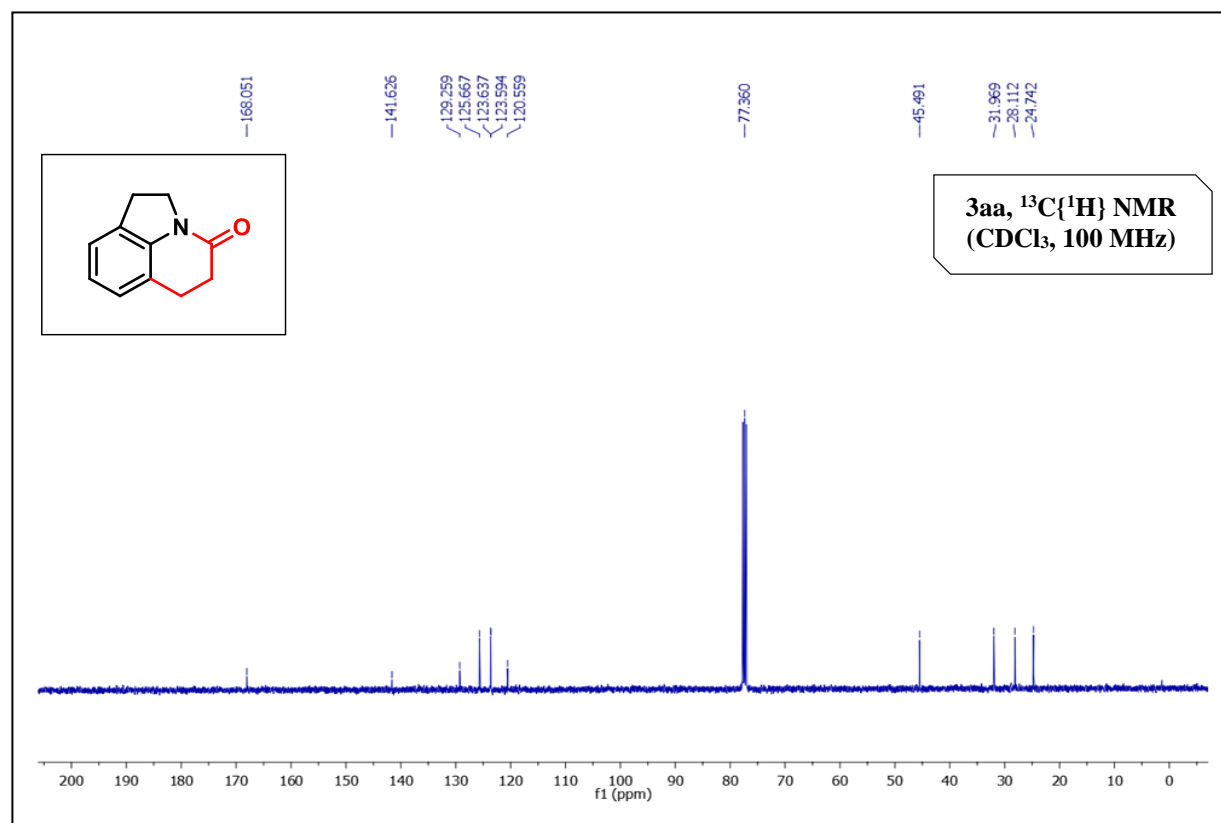
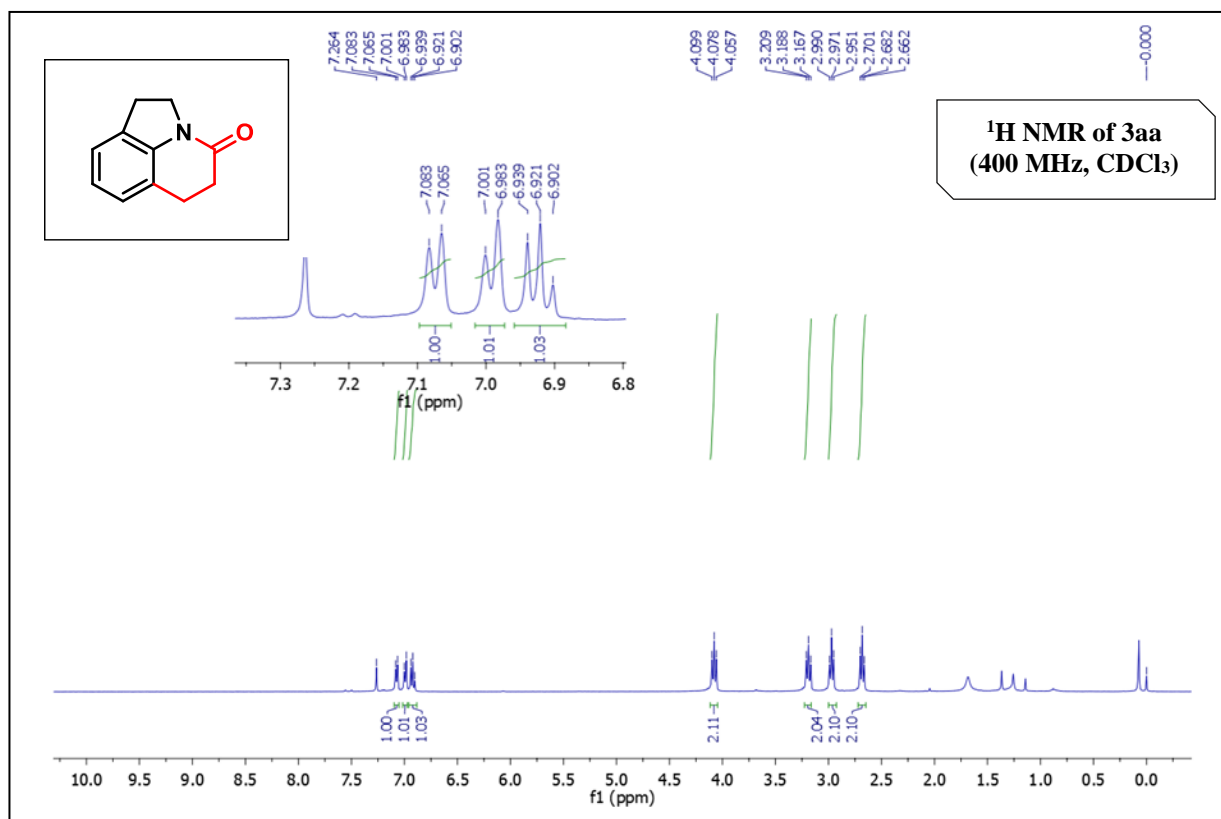


(E)-13-Methyl-17-oxo-7,8,9,11,12,13,14,15,16,17-decahydro-6Hcyclopenta[a]phenanthren-2-yl 3-(1-pivaloylindolin-7-yl)acrylate (4al) was

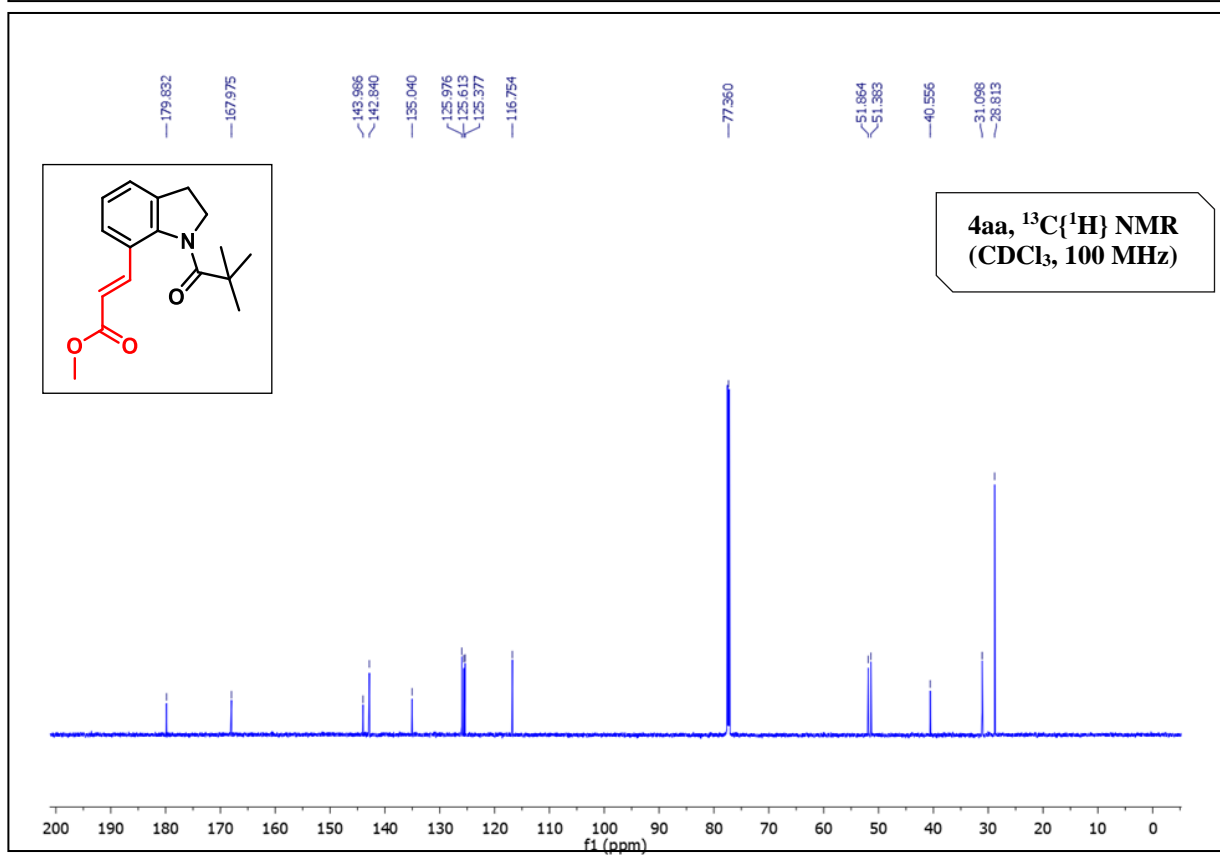
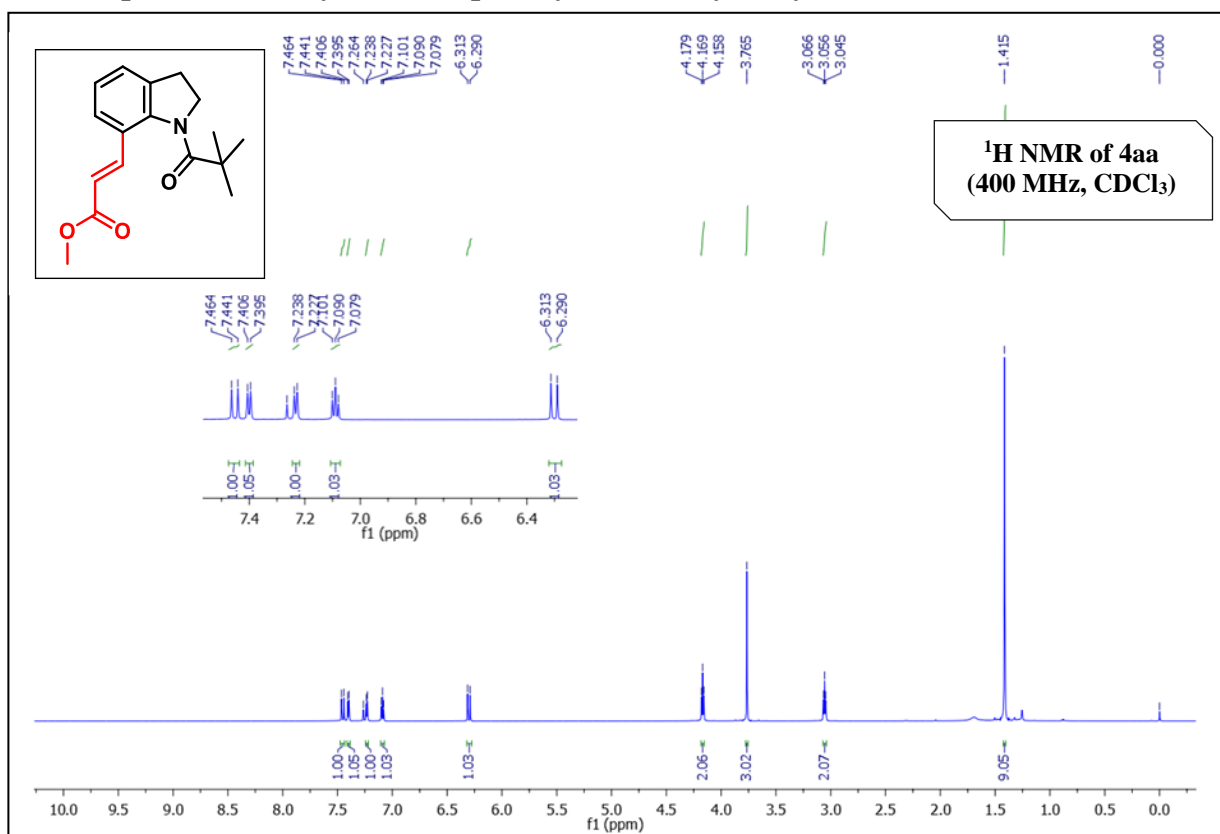
prepared according to the general procedure (3.5b). The crude reaction mixture was purified by column chromatography using silica gel (100–200 mesh size), giving a white solid (33 mg, 66% yield). R_f : 0.30 (in 40% EtOAc/hexane), mp 258–260 °C. **1H NMR ($CDCl_3$, 400 MHz):** δ 7.60 (d, J = 16.0 Hz, 1H), 7.47 (d, J = 7.6 Hz, 1H), 7.29 (d, J =

8.8 Hz, 1H), 7.12 (t, $J = 7.6$ Hz, 1H), 6.92 (d, $J = 8.4$ Hz, 1H), 6.89 (s, 1H), 6.48 (d, $J = 16.0$ Hz, 1H), 4.18 (t, $J = 7.6$ Hz, 2H), 3.08 (t, $J = 7.6$ Hz, 2H), 2.93–2.90 (m, 2H), 2.54–2.47 (m, 1H), 2.43–2.39 (m, 1H), 2.31–2.26 (m, 1H), 2.19–1.95 (m, 5H), 1.68–1.60 (m, 2H), 1.54–1.45 (m, 3H), 1.40 (s, 9H), 0.91 (s, 9H). **$^{13}\text{C}\{^1\text{H}\}$ NMR (CDCl₃, 100 MHz):** δ 221.2, 180.0, 166.2, 149.1, 144.3, 144.2, 138.2, 137.4, 135.1, 126.6, 126.3, 125.7, 125.6, 125.4, 122.1, 119.2, 116.1, 51.3, 50.7, 48.3, 44.5, 40.6, 38.3, 36.2, 31.9, 31.1, 29.7, 28.8, 26.7, 26.1, 29.9, 14.1. **HRMS (ESI)** m/z calcd for C₃₄H₃₉NO₄ Na [M + Na]⁺: 548.2771; found: 548.2784. **IR (KBr, cm⁻¹):** 1735, 1659, 1493.

NMR spectra of 1,2,5,6-tetrahydro-4H-pyrrolo[3,2,1-ij]quinolin-4-one (3aa):



NMR spectra of methyl (E)-3-(1-pivaloylindolin-7-yl)acrylate (4aa):



(d) Crystal structure of 8-fluoro-1,2,5,6-tetrahydro-4*H*-pyrrolo[3,2,1-*ij*]quinolin-4-one (**3ia**):

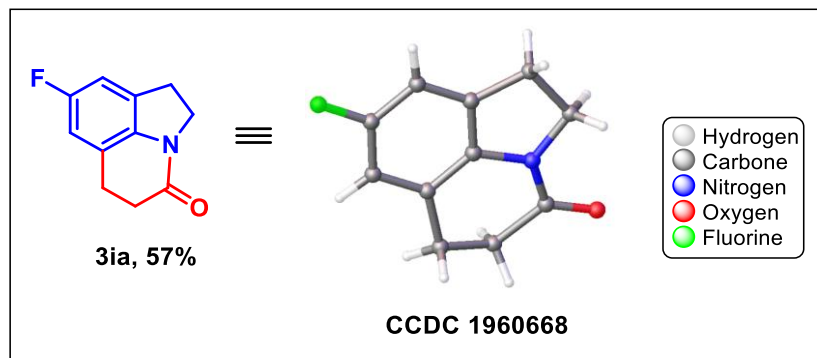
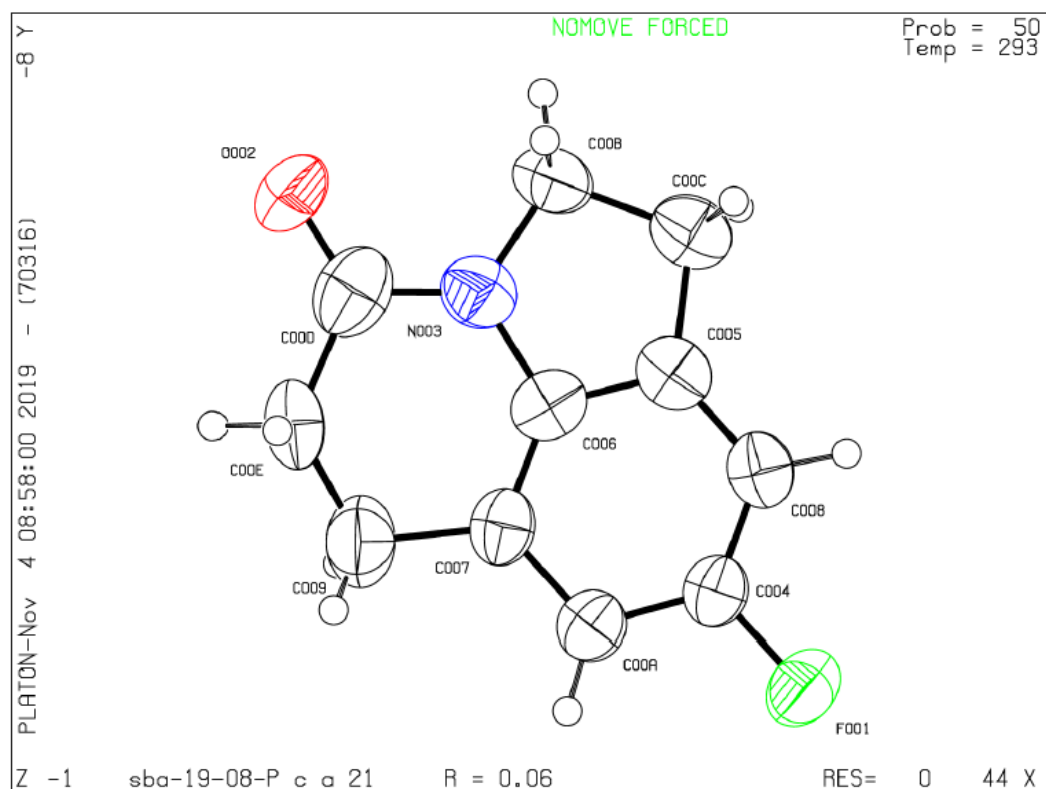


Figure 3.3. Crystal structure of **3ia** (50% ellipsoid probability).

Datablock: sba-19-08-19 - ellipsoid plot



(e) Crystal structure of (*E*)-methyl 3-(1-pivaloylindolin-7-yl)acrylate (**4aa**):

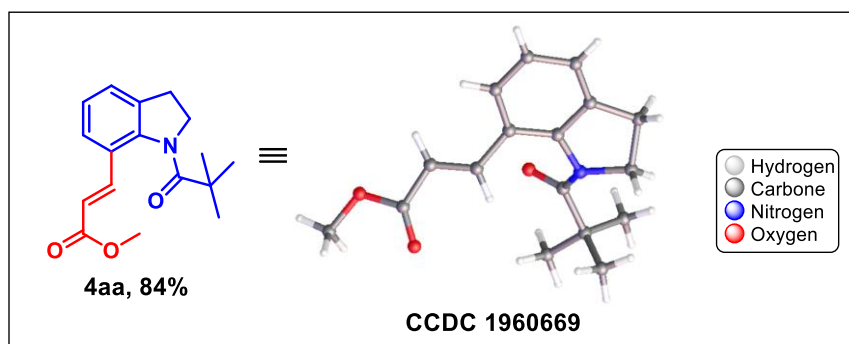
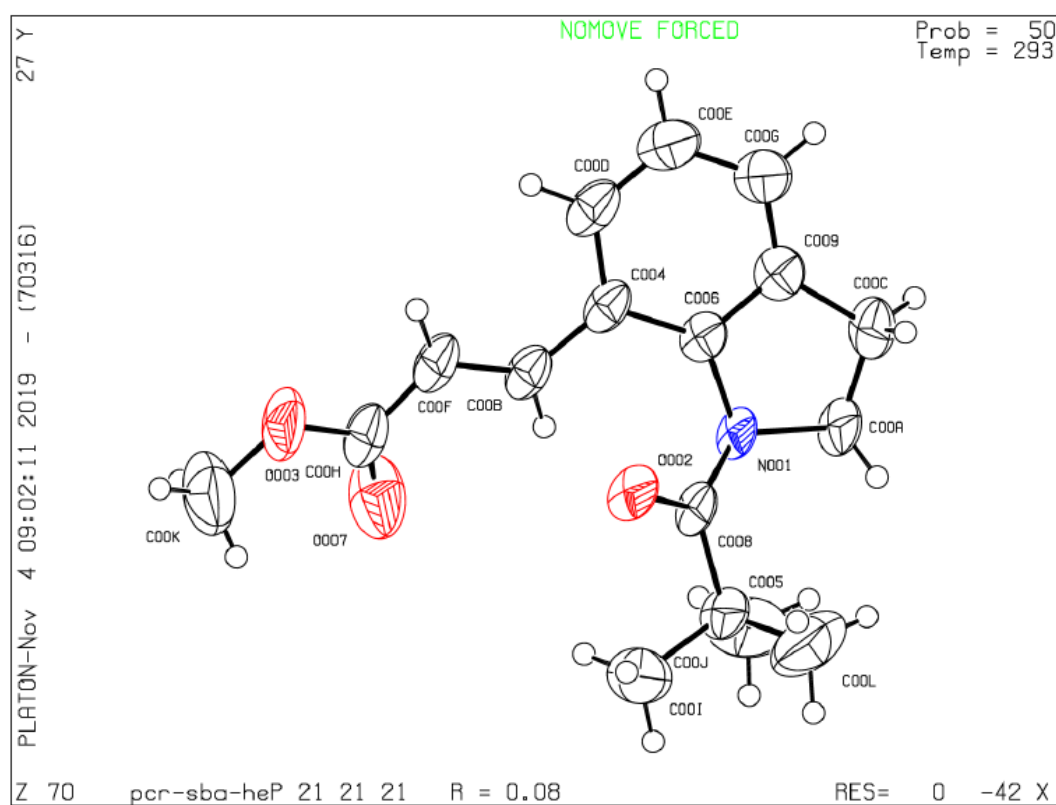


Figure 3.4. Crystal structure of 4aa (50% ellipsoid probability).

Datablock pcr-sba-heck - ellipsoid plot



3.6 REFERENCES

1. (a) Sundberg, R. J. *Indoles*; Academic Press: San Diego, CA, **1996**. (b) Kochanowska-Karamyan, A. J.; Hamann, M. T. Marine Indole Alkaloids: Potential New Drug Leads for the Control of Depression and Anxiety. *Chem. Rev.* **2010**, *110*, 4489–4497. (c) Williams, R. M.; Cox, R. J. Paraherquamides, Brevianamides, and Asperparalines: Laboratory Synthesis and Biosynthesis. An Interim Report. *Acc. Chem. Res.* **2003**, *36*, 127–139. (d) Podoll, J. D.; Liu, Y.; Chang, L.; Walls, S.; Wang, W.; Wang, X. Bio-Inspired Synthesis Yields a Tricyclic Indoline That Selectively Resensitizes Methicillin-Resistant *Staphylococcus Aureus* (MRSA) to β -Lactam Antibiotics. *Proc. Natl. Acad. Sci. U. S. A.* **2013**, *110*, 15573–15578. (e) Horton, D. A.; Bourne, G. T.; Smythe, M. L. The Combinatorial Synthesis of Bicyclic Privileged Structures or Privileged Substructures. *Chem. Rev.* **2003**, *103*, 893–930. (f) Taylor, R. D.; MacCoss, M.; Lawson, A. D. G. Rings in drugs. *J. Med. Chem.* **2014**, *57*, 5845–5859.
2. (a) Lucas, S.; Negri, M.; Heim, R.; Zimmer, C.; Hartmann, R. W. Fine-Tuning the Selectivity of Aldosterone Synthase Inhibitors: Structure-Activity and Structure-Selectivity Insights from Studies of Heteroaryl Substituted 1,2,5,6-Tetrahydropyrrolo[3,2, 1-Ij]Quinolin- 4-One Derivatives. *J. Med. Chem.* **2011**, *54*, 2307–2319. (b) Dorow, R. L.; Herrinton, P. M.; Hohler, R. A.; Maloney, M. T.; Mauragis, M. A.; McGhee, W. E.; Moeslein, J. A.; Strohbach, J. W.; Velez, M. F. Development of an Efficient Synthesis of the Pyrrolquinolone PHA- 529311. *Org. Process Res. Dev.* **2006**, *10*, 493–499. (c) Isaac, M.; Slassi, A.; O'Brien, A.; Edwards, L.; MacLean, N.; Bueschkens, D.; Lee, D. K. H.; McCallum, K.; De Lannoy, I.; Demchyshyn, L.; et al. Pyrrolo[3,2,1-Ij]Quinoline Derivatives, a 5-HT(2c) Receptor Agonist with Selectivity over the 5-HT(2a) Receptor: Potential Therapeutic Applications for Epilepsy and Obesity. *Bioorg. Med. Chem. Lett.* **2000**, *10*, 919–921. (d) Tsotinis, A.; Panoussopoulou, M.; Eleutheriades, A.; Davidson, K.; Sugden, D. Design, Synthesis and Melatoninergic Activity of New Unsubstituted and β , β' -Difunctionalised 2,3- Dihydro-1H-Pyrrolo[3,2,1-Ij]Quinolin-6-Alkanamides. *Eur. J. Med. Chem.* **2007**, *42*, 1004–1013. (e) Ishichi, Y.; Sasaki, M.; Setoh, M.; Tsukamoto, T.; Miwatashi, S.; Nagabukuro, H.; Okanishi, S.; Imai, S.; Saikawa, R.; Doi, T.; et al. Novel Acetylcholinesterase Inhibitor as Increasing Agent on Rhythmic Bladder Contractions: SAR of 8-{3-[1- (3-Fluorobenzyl)Piperidin-4-Yl]Propanoyl}-1,2,5,6-Tetrahydro-4HPyrrolo[3,2,1-Ij]Quinolin-4-One (TAK-802) and Related Compounds. *Bioorg. Med. Chem.* **2005**, *13*, 1901–1911. (f) Paris, D.; Cottin, M.; Demonchaux, P.; Augert, G.; Dupassieux, P.; Lenoir, P.; Peck, M. J.; Jasserand, D. Synthesis, Structure-Activity Relationships, and Pharmacological Evaluation of Pyrrolo[3,2,1-ij] Quinoline Derivatives: Potent Histamine and Platelet Activating Factor Antagonism and 5-Lipoxygenase Inhibitory Properties. Potential Therapeutic Application in Asthma. *J. Med. Chem.* **1995**, *38*, 669–685.
3. (a) Steck, E. A.; Fletcher, L. T.; Carabateas, C. D. Some 5,6- dihydro-4H-pyrrolo[3,2,1-i,j]quinolines. *J. Heterocycl. Chem.* **1974**, *11*, 387–393. (b) Padwa, A.; Rashatasakhon, P.; Ozdemir, A. D.; Willis, J. A Study of Vinyl Radical Cyclization Using N-Alkenyl-7-Bromo- Substituted Hexahydroindolinones. *J. Org. Chem.* **2005**, *70*, 519–528. (c) Rajput, S.; Leu, C. W.; Wood, K.; Black, D. S.; Kumar, N. Facile Syntheses of 7,9-Dimethoxypyrrolo[3,2,1-Ij]Quinolin-6-Ones. *Tetrahedron Lett.* **2011**, *52*, 7095–7098. (d) Zimmermann, T. Ring Transformations of Heterocyclic Compounds. XXIV [1]. 1',2',5',6'- Tetrahydro-4'H-Spiro[Cyclohexa-2, 4-Diene-1,2'-Pyrrolo[3,2,1-Ij]- Quinoline] and 1,2,4,5,6,7- Hexahydrospiro[Azepino[3,2,1-Hi]- Indole-2,1'-Cyclo-Hexa[2,4]Diene] - Two New Spiro- [Cyclohexadiene-Azaheterocycles] Easily Accessible by Pyrylium Ring Transformation. *J. Heterocycl. Chem.* **2004**, *41*, 691–695. (e) Prasada Rao Lingam, V. S.; Thomas, A.; Mukkanti, K.; Gopalan, B. Simple and Convenient Approach for Synthesis of Tetrahydroquinoline Derivatives and Studies on Aza-Cope Rearrangement. *Synth. Commun* **2011**, *41*, 1809–1828.
4. Selected reviews: (a) Ackermann, L.; Vicente, R.; Kapdi, A. R. Transition-Metal-Catalyzed Direct Arylation of (Hetero)Arenes by CH Bond Cleavage. *Angew. Chem., Int. Ed.* **2009**, *48*, 9792. (b)

- Lyons, T. W.; Sanford, M. S. Palladium-catalyzed ligand-directed C–H functionalization reactions. *Chem. Rev.* **2010**, *110*, 1147. (c) Liu, C.; Zhang, H.; Shi, W.; Lei, A. Bond formations between two nucleophiles: transition metal catalyzed oxidative cross-coupling reactions. *Chem. Rev.* **2011**, *111*, 1780. (d) Kuhl, N.; Hopkinson, M. N.; Wencel-Delord, J.; Glorius, F. Beyond Directing Groups: Transition-Metal-Catalyzed C–H Activation of Simple Arenes. *Angew. Chem., Int. Ed.* **2012**, *51*, 10236. (g) Song, G.; Wang, F.; Li, X. C–C, C–O and C–N bond formation via rhodium (iii)-catalyzed oxidative C–H activation. *Chem. Soc. Rev.* **2012**, *41*, 3651. (h) Arockiam, P. B.; Bruneau, C.; Dixneuf, P. H. Ruthenium (II)-catalyzed C–H bond activation and functionalization. *Chem. Rev.* **2012**, *112*, 5879. (j) Rouquet, G.; Chatani, N. Catalytic Functionalization of C(sp²)-H and C(sp³)-H Bonds by Using Bidentate Directing Groups. *Angew. Chem., Int. Ed.* **2013**, *52*, 11726.
5. (a) Yang, X. F.; Hu, X. H.; Loh, T. P. Expedient Synthesis of Pyrroloquinolinones by Rh-Catalyzed Annulation of *n*-Carbamoyl Indolines with Alkynes through a Directed C–H Functionalization/CN Cleavage Sequence. *Org. Lett.* **2015**, *17*, 1481–1484. (b) Manoharan, R.; Jeganmohan, M. Ruthenium-Catalyzed Cyclization of N-Carbamoyl Indolines with Alkynes: An Efficient Route to Pyrroloquinolinones. *Org. Biomol. Chem.* **2015**, *13*, 9276–9284. (c) Zhou, T.; Wang, Y.; Li, B.; Wang, B. Rh(III)-Catalyzed Carbocyclization of 3-(Indolin-1-yl)-3-Oxopropanenitriles with Alkynes and Alkenes through C–H Activation. *Org. Lett.* **2016**, *18*, 5066–5069. (d) Han, L.; Zhang, X.; Wang, X.; Zhao, F.; Liu, S.; Liu, T. Mechanistic Insights into the Selective Cyclization of Indolines with Alkynes and Alkenes to Produce Six- and Seven-Membered 1,7- Fused Indolines: Via Rh(III) Catalysis: A Theoretical Study. *Org. Biomol. Chem.* **2017**, *15*, 3938–3946. (e) Yang, Y.; Wang, C. Re- Catalyzed Annulations of Weakly Coordinating N-Carbamoyl Indoles/Indolines with Alkynes via C–H/C–N Bond Cleavage. *Chem. – Eur. J.* **2019**, *25*, 8245–8248.
 6. (a) Song, Z.; Samanta, R.; Antonchick, A. P. Rhodium(III)- Catalyzed Direct Regioselective Synthesis of 7-Substituted Indoles. *Org. Lett.* **2013**, *15*, 5662–5665. (b) Jiao, L. Y.; Oestreich, M. Oxidative Palladium(II)-Catalyzed C-7 Alkenylation of Indolines. *Org. Lett.* **2013**, *15*, 5374–5377. (c) Pan, S.; Wakaki, T.; Ryu, N.; Shibata, T. Ir(III)-Catalyzed C7-Position-Selective Oxidative C–H Alkenylation of Indolines with Alkenes in Air. *Chem. Asian J.* **2014**, *9*, 1257–1260. (d) Yang, X. F.; Hu, X. H.; Feng, C.; Loh, T. P. Rhodium(III)-Catalyzed C7-Position C–H Alkenylation and Alkynylation of Indolines. *Chem. Commun.* **2015**, *51*, 2532–2535. (e) Pan, S.; Ryu, N.; Shibata, T. Iridium(I)-Catalyzed Direct C–H Bond Alkylation of the C-7 Position of Indolines with Alkenes. *Adv. Synth. Catal.* **2014**, *356*, 929–933.
 7. (a) Kulkarni, A. A.; Daugulis, O. Direct conversion of Carbon-Hydrogen into Carbon-Carbon Bonds by First-Row Transition-Metal Catalysis. *Synthesis* **2009**, 4087–4109. (b) Su, B.; Cao, Z.-C.; Shi, Z.-J. Exploration of Earth-Abundant Transition Metals (Fe, Co, and Ni) as Catalysts in Unreactive Chemical Bond Activations. *Acc. Chem. Res.* **2015**, *48*, 886–896. (c) Pototschnig, G.; Maulide, N.; Schnürch, M. Direct Functionalization of C –H Bonds by Iron, Nickel, and Cobalt Catalysis. *Chem. – Eur. J.* **2017**, *23*, 9206–9232. (d) Liu, J.; Chen, G.; Tan, Z. Copper-Catalyzed or -Mediated C–H Bond Functionalizations Assisted by Bidentate Directing Groups. *Adv. Synth. Catal.* **2016**, *358*, 1174–1194. (e) Liu, W.; Ackermann, L. Manganese-Catalyzed C –H Activation. *ACS Catal.* **2016**, *6*, 3743– 3752. (f) Gandeepan, P.; Müller, T.; Zell, D.; Cera, G.; Warratz, S.; Ackermann, L. 3d Transition Metals for C–H Activation. *Chem. Rev.* **2019**, *119*, 2192–2452.
 8. (a) Gandeepan, P.; Koeller, J.; Ackermann, L. Expedient C – H Chalcogenation of Indolines and Indoles by Positional-Selective Copper Catalysis. *ACS Catal.* **2017**, *7*, 1030–1034. (b) Ahmad, A.; Dutta, H. S.; Khan, B.; Kant, R.; Koley, D. Cu(I)-Catalyzed Site-Selective Acyloxylation of Indoline Using O as the Sole Oxidant. *Adv. Synth. Catal.* **2018**, *360*, 1644–1649. (c) De, P. B.; Pradhan, S.; Banerjee, S.; Punniyamurthy, T. Expedient Cobalt(II)-Catalyzed Site- Selective C7-Arylation of Indolines with Arylboronic Acids. *Chem. Commun.* **2018**, *54*, 2494–2497. (d) Banjare, S. K.; Chebolu, R.; Ravikumar, P. C. Cobalt Catalyzed Hydroarylation of Michael Acceptors with Indolines Directed by a Weakly Coordinating Functional Group. *Org. Lett.* **2019**, *21*, 4049–4053. (e) Moselage, M.; Li, J.; Ackermann, L. Cobalt-Catalyzed C–H Activation. *ACS Catal.* **2016**, *6*, 498–525. (f)

- Ujwaldev, S. M.; Harry, N. A.; Divakar, M. A.; Anilkumar, G. Cobalt-catalyzed C–H activation: recent progress in heterocyclic chemistry. *Catal. Sci. Technol.* **2018**, *8*, 5983–6018.
9. (a) Engle, K. M.; Mei, T.-S.; Wasa, M.; Yu, J.-Q. Weak Coordination as a Powerful Means for Developing Broadly Useful C – H Functionalization Reactions. *Acc. Chem. Res.* **2012**, *45*, 788–802. (b) de Sarkar, S.; Liu, W.; Kozhushkov, S. I.; Ackermann, L. Weakly Coordinating Directing Groups for Ruthenium(II)-Catalyzed C-H Activation. *Adv. Synth. Catal.* **2014**, *356*, 1461–1479. (c) Das, R.; Kumar, G. S.; Kapur, M. Amides as Weak Coordinating Groups in Proximal C-H Bond Activation. *Eur. J. Org. Chem.* **2017**, 5439–5459.
 10. (a) Houlden, C. E.; Bailey, C. D.; Ford, J. G.; Gagné, M. R.; Lloyd-Jones, G. C.; Booker-Milburn, K. I. Distinct Reactivity of Pd(OTs)₂: The Intermolecular Pd(II)-Catalyzed 1,2-Carboamination of Dienes. *J. Am. Chem. Soc.* **2008**, *130*, 10066. (b) Houlden, C. E.; Hutchby, M.; Bailey, C. D.; Ford, J. G.; Tyler, S. N. G.; Gagné, M. R.; Lloyd-Jones, G. C.; Booker-Milburn, K. I. Room-Temperature Palladium-Catalyzed C-H Activation: *Ortho*-Carbonylation of Aniline Derivatives. *Angew. Chem., Int. Ed.* **2009**, *48*, 1830.
 11. (a) Sk, M. R.; Bera, S. S.; Maji, M. S. Cp*Co(III)-Catalyzed C–H Alkenylation of Aromatic Ketones with Alkenes. *Adv. Synth. Catal.* **2019**, *361*, 585–590. (b) Sherikar, M. S.; Kapaniaiah, R.; Lanke, V.; Prabhu, K. R. Rhodium(III)-Catalyzed C-H Activation at the C4- Position of Indole: Switchable Hydroarylation and Oxidative Heck- Type Reactions of Maleimides. *Chem. Commun.* **2018**, *54*, 11200–11203. (c) Feng, R.; Yu, W.; Wang, K.; Liu, Z.; Zhang, Y. Ester- Directed Selective Olefination of Acrylates by Rhodium Catalysis. *Adv. Synth. Catal.* **2014**, *356*, 1501–1508. (d) Yokoyama, Y.; Unoh, Y.; Hirano, K.; Satoh, T.; Miura, M. Rhodium(III)-Catalyzed Regioselective C–H Alkenylation of Phenylphosphine Sulfides. *J. Org. Chem.* **2014**, *79*, 7649–7655. (e) Patureau, F. W.; Besset, T.; Glorius, F. Rhodium-Catalyzed Oxidative Olefination of C-H Bonds in Acetophenones and Benzamides. *Angew. Chem., Int. Ed.* **2011**, *50*, 1064–1067. (f) Padala, K.; Jeganmohan, M. Ruthenium-Catalyzed *ortho*-Alkenylation of Aromatic Ketones with Alkenes by C–H Bond Activation. *Org. Lett.* **2011**, *13*, 6144–6147. (g) Grigorjeva, L.; Daugulis, O. Cobalt-Catalyzed, Aminoquinoline-Directed Coupling of sp² C–H Bonds with Alkenes. *Org. Lett.* **2014**, *16*, 4684–4687. (h) Suzuki, Y.; Sun, B.; Yoshino, T.; Kanai, M.; Matsunaga, S. Cp* Co (III)-catalyzed oxidative C–H alkenylation of benzamides with ethyl acrylate. *Tetrahedron* **2015**, *71*, 4552–4556. (i) Zhang, J.; Xie, H.; Zhang, S.; Lonka, M. R.; Zou, H. Chameleon-like Behavior of the Directing Group in the Rh(III)-Catalyzed Regioselective C–H Amidation of Indole: An Experimental and Computational Study. *ACS Catal.* **2019**, *9*, 10233–10244.
 12. (a) Mandal, R.; Emayavaramban, B.; Sundararaju, B. Cp*Co(III)-Catalyzed C-H Alkylation with Maleimides Using Weakly Coordinating Carbonyl Directing Groups. *Org. Lett.* **2018**, *20*, 2835–2838. (b) Muniraj, N.; Prabhu, K. R. Cobalt(III)-Catalyzed [4 + 2] Annulation of N-Chlorobenzamides with Maleimides. *Org. Lett.* **2019**, *21*, 1068–1072. (c) Kumar, R.; Kumar, R.; Chandra, D.; Sharma, U. Cp*Co(III)-Catalyzed Alkylation of Primary and Secondary C(sp³)-H Bonds of 8-Alkylquinolines with Maleimides. *J. Org. Chem.* **2019**, *84*, 1542–1552. (d) Zhao, D.; Kim, J. H.; Stegemann, L.; Strasser, C. A.; Glorius, F. Cobalt(III)-Catalyzed Directed C-H Coupling with Diazo Compounds: Straightforward Access towards Extended π -Systems. *Angew. Chem., Int. Ed.* **2015**, *54*, 4508–4511.
 13. (a) Gottlieb, H. E.; Kotlyar, V.; Nudelman, A. NMR chemical shifts of common laboratory solvents as trace impurities. *J. Org. Chem.* **1997**, *62*, 7512–7515. (b) Stuart, D. R.; Villemure, E.; Fagnou, K. Elements of regiocontrol in palladium-catalyzed oxidative arene crosscoupling. *J. Am. Chem. Soc.* **2007**, *129*, 12072–12073. (c) Cornella, J.; Lu, P.; Larrosa, L. Intermolecular decarboxylative direct C-3 arylation of indoles with benzoic acids. *Org. Lett.* **2009**, *11*, 5506–5509. (d) Ruiz, M.; Sánchez, J. D.; López-Alvarado, P.; Menéndez, J. C. A systematic study of two complementary protocols allowing the general, mild and efficient deprotection of N-pivaloylindoles. *Tetrahedron* **2012**, *68*, 705–710. (e) Gribble, G. W.; Hoffman, J. H. Reactions of sodium borohydride in acidic media; VI. Reduction of indoles with cyanoborohydride in acetic acid. *Synthesis* **1977**, 859–860. (f) Dankwardt,

-
- J. W.; Flippin, L. A. Palladium-mediated 6-endotrig intramolecular cyclization of *N*-acryloyl-7-bromoindolines. A regiochemical variant of the intramolecular Heck reaction. *J. Org. Chem.* **1995**, *60*, 2312–2313.
14. (a) Goto, G.; Ishihara, Y.; Miyamoto, M. From Eur. *Pat. Appl.* (**1995**), EP 655451 A1. 19950531. (b) Takeshiba, H.; Imai, T.; Ohta, H.; Kato, S. From Jpn. Kokai Tokkyo Koho (**1999**), JP 11222407 A. 19990817.
15. (a) Somei, M.; Saida, Y.; Funamoto, T.; Ohta, T. A Facile Synthetic Method for 7-Substituted Indoles. *Chem. Pharm. Bull.* **1987**, *35*, 3146. (b) Xu, L.; Zhang, C.; He, Y.; Tan, L.; Ma, D. Rhodiumcatalyzed regioselective C7-olefination of *N*-pivaloylindoles. *Angew. Chem., Int. Ed.* **2016**, *55*, 321–325. (c) Fosu, S. C.; Hambira, C. M.; Chen, A. D.; Fuchs, J. R.; Nagib, D. A. Site-Selective C-H Functionalization of (Hetero)Arenes via Transient, Non-symmetric Iodanes. *Chem* **2019**, *5*, 417–428.

Chapter 4

Cobalt-Catalyzed Regioselective Direct C-4 Alkenylation of 3-Acetylundole with Michael Acceptors Using a Weakly Coordinating Functional Group

4.1 Abstract

4.2 Introduction

4.3 Results and Discussions

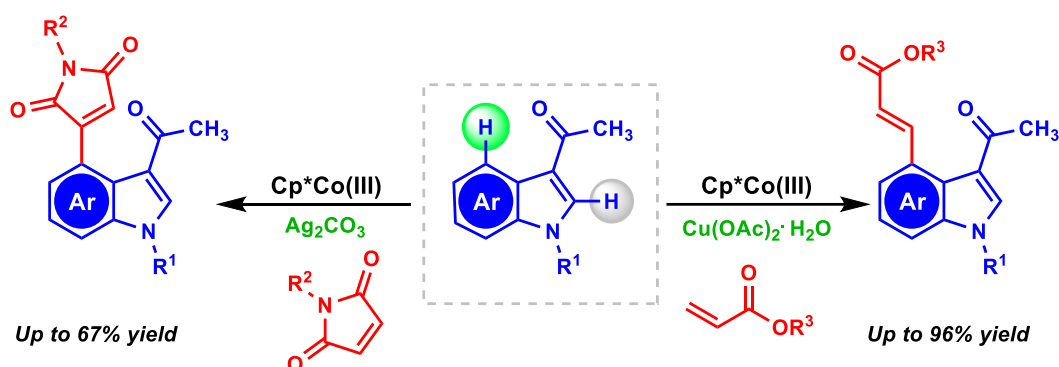
4.4 Conclusions

4.5 Experimental Section

4.6 References

Chapter 4

Cobalt-Catalyzed Regioselective Direct C-4 Alkenylation of 3-Acetylindole with Michael Acceptors Using a Weakly Coordinating Functional Group



4.1 ABSTRACT

Herein, we disclosed the first report on the selective C(4)-H functionalization of 3-acetylindole derivatives using first-row transition metal cobalt, where an acetyl group is acting as a weakly coordinating directing group. Selective C(4)-H functionalization has been achieved using diverse Michael acceptors (acrylate and maleimide) simply by switching the additive from copper acetate to silver carbonate. Further, the formation of a cobaltacycle intermediate was also detected through HRMS for mechanistic insight.

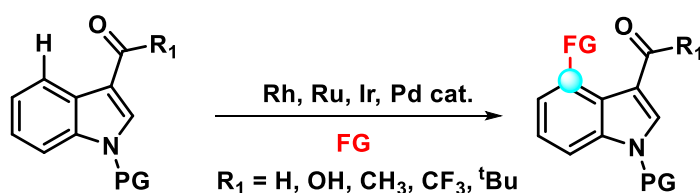
4.2 INTRODUCTION

The heteroaromatic indole moiety is present in numerous marketed drugs such as Ondansetron (nausea), Sumatriptan (migraine), and Indomethacin (anti-inflammatory). It is considered the fourth most commonly prevalent heteroaromatic skeleton among the currently marketed drugs.¹ Owing to its biological significance, synthetic

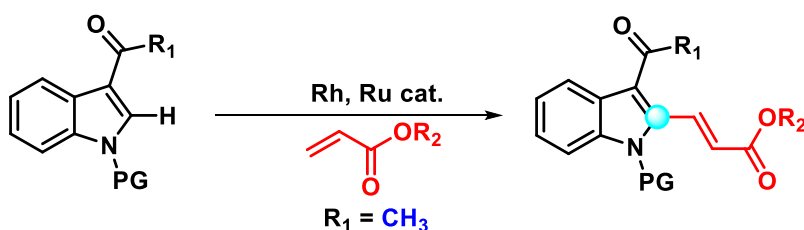
modification of indole has been one of the frontline areas of research for a long time. The C-2 and C-3 functionalizations of indoles were well explored due to the inherent reactivity of *N*-heterocycle.² Traditionally, functionalization at indole's benzenoid (C-4 to C-7) ring was performed through a metal-catalyzed coupling reaction using functionalized substrates.³

1. Previous work

(a) 2nd & 3rd row Transition metal catalysed **C-4** functionalization at indole^{5a}

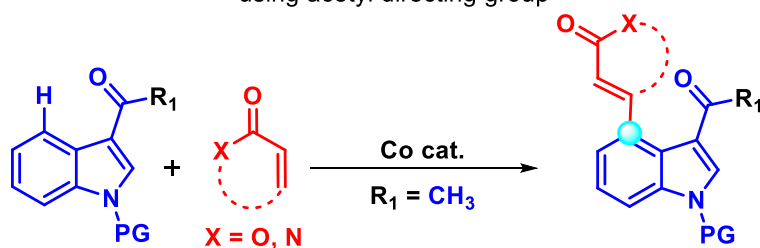


(b) 2nd row Transition metal catalysed selectively **C-2** functionalization at indole^{5b}



2. Present work

1st row Transition metal catalysed selectively **C-4** functionalization at indole using acetyl directing group



First report with 1st row transition metal

Figure 4.1. C–H functionalization of 3-acylindole.

Recent advancements in metal-catalyzed C–H activation/ functionalization reactions led to an intense exploration of direct C–H activation methods at the relatively less explored C-4 and C-7 positions.⁴ Functionalization at the C-4 position of indole is quite

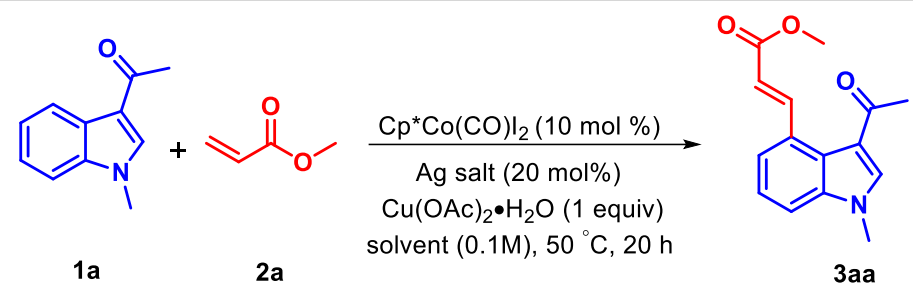
challenging due to the favorable five-membered cyclometalation step at C-2 as compared to the high energy six-membered cyclometalation step at C-4. During the past decade, several research groups have made phenomenal progress on selective C-4 functionalization of indole via C–H activation using second- and third-row transition metals such as Rh, Ru, Ir, and Pd (Figure 4.1).⁵ However, there is no report on the selective C-4 functionalization with first-row transition metals. In recent years there has been an impetus for mimicking the reactivity of noble metals (Rh, Ru, Ir, and Pd) through a first-row transition metal due to its low toxicity, easy availability, and low cost.⁶ In addition, C–H activation reaction through weakly coordinating directing groups has recently gained considerable attention. In continuation of our efforts to synthesize functionalized indole with a first-row transition metal using simple and weakly coordinating directing groups, we envisaged synthesizing C-4 functionalized indole⁷ with commonly used Michael acceptors such as acrylates⁸ and maleimides.⁹ We have successfully achieved our desired cobalt-catalyzed C-4 functionalization of indoles with those Michael acceptors.

4.3 RESULTS AND DISCUSSION

To test our hypothesis, we chose indole **1a** and methyl acrylate **2a** as the model substrates in the presence of Cp^{*}Co catalyst, silver hexafluoroantimonate (AgSbF₆) additive, and copper acetate as an oxidant. For the optimization of C-4 alkenylation initially, we started with a hydrocarbon and an oxygenated solvent such as toluene, tetrahydrofuran, and 1,4-dioxane, but the reaction failed in those solvents. However, when we used a chlorinated solvent such as dichloromethane, 1,2-dichloroethane, and 1,2-dichlorobenzene for the reaction, it produced a moderate to a good yield of the desired product **3aa** (Table 4.1, entries 4–6). To further improve the product yield, we

next focused on fluorinated solvents. A slight yield enhancement was observed when we performed the reaction in trifluoroethanol (TFE) (Table 4.1, entry 7).

Table 4.1 Optimization table^{a,b}

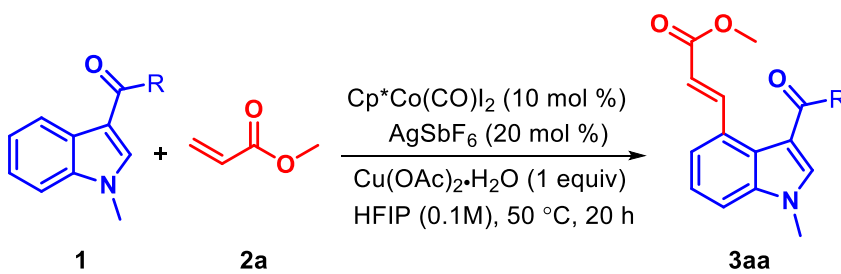
			
entry	solvent	Ag salt	yield (%) ^b
1	toluene	AgSbF ₆	0
2	THF	AgSbF ₆	0
3	1,4-dioxane	AgSbF ₆	0
4	DCM	AgSbF ₆	55
5	DCE	AgSbF ₆	62
6	1,2-DCB	AgSbF ₆	41
7	TFE	AgSbF ₆	69
8	TFT	AgSbF ₆	22
9	HFIP	AgSbF₆	88
10	HFIP	AgSbF ₆ , rt	56
11	HFIP	-	24
12	HFIP	AgBF ₄	44
13	HFIP	AgNTF ₂	80
14	HFIP	Ag ₂ O	38
15	HFIP	AgSbF ₆ , without Cu(OAc) ₂ •H ₂ O	16
16	HFIP	AgSbF ₆ , without Cp*Co(CO)I ₂	0

^aReaction conditions: **1a** (0.1 mmol), **2a** (4 equiv), Cp*Co(CO)I₂ (10 mol %), Ag salt (20 mol %), additive (1 equiv), hexafluoroisopropanol (0.1 M) as a solvent, 50 °C, 20 h. ^bIsolated yields.

This result encouraged us to check this transformation in fluorinated solvents, such as hexafluoroisopropanol (HFIP) and trifluorotoluene (TFT). Interestingly HFIP turned out to be the best solvent for the titled transformation resulting in an 88% yield of **3aa** (Table 4.1, entry 9). To investigate the role of the silver additive, we performed this reaction in the absence of AgSbF₆. Still, the reaction failed to yield significantly, and

we recovered the starting material (Table 4.1, entry 11). This implies that AgSbF₆ plays a crucial role in the alkenylation reaction. Motivated by this outcome we envisioned that screening the other silver salts might improve the yield. Hence, different silver salts such as AgBF₄, Ag₂O, and AgNTf₂ were used. Still, no improvement in the yield of **3aa** was observed (Table 1.1, entries 12–14). Thus, the combination of AgSbF₆ as the silver salt and HFIP as the solvent proved to be the conditions for the C-4 alkenylation reaction (Table 1.1, entry 9). To understand the influence of the Cp^{*}Co catalyst on the titled reaction, we carried out the reaction without the catalyst, which failed to give the adduct (Table 1.1, entry 16).

Table 4.2 Screening of various directing groups^{a,b}



entry	R	yield (%) ^b
1	CH ₃	88 (3aa)
2	H	33 (3aa1)
3	CF ₃	52 (3aa2)
4	^t Bu	81 (3aa3)
5	OH	0 (3aa4)
6	OMe	23 (3aa5)
7	NH ₂ CH ₃	38 (3aa6)

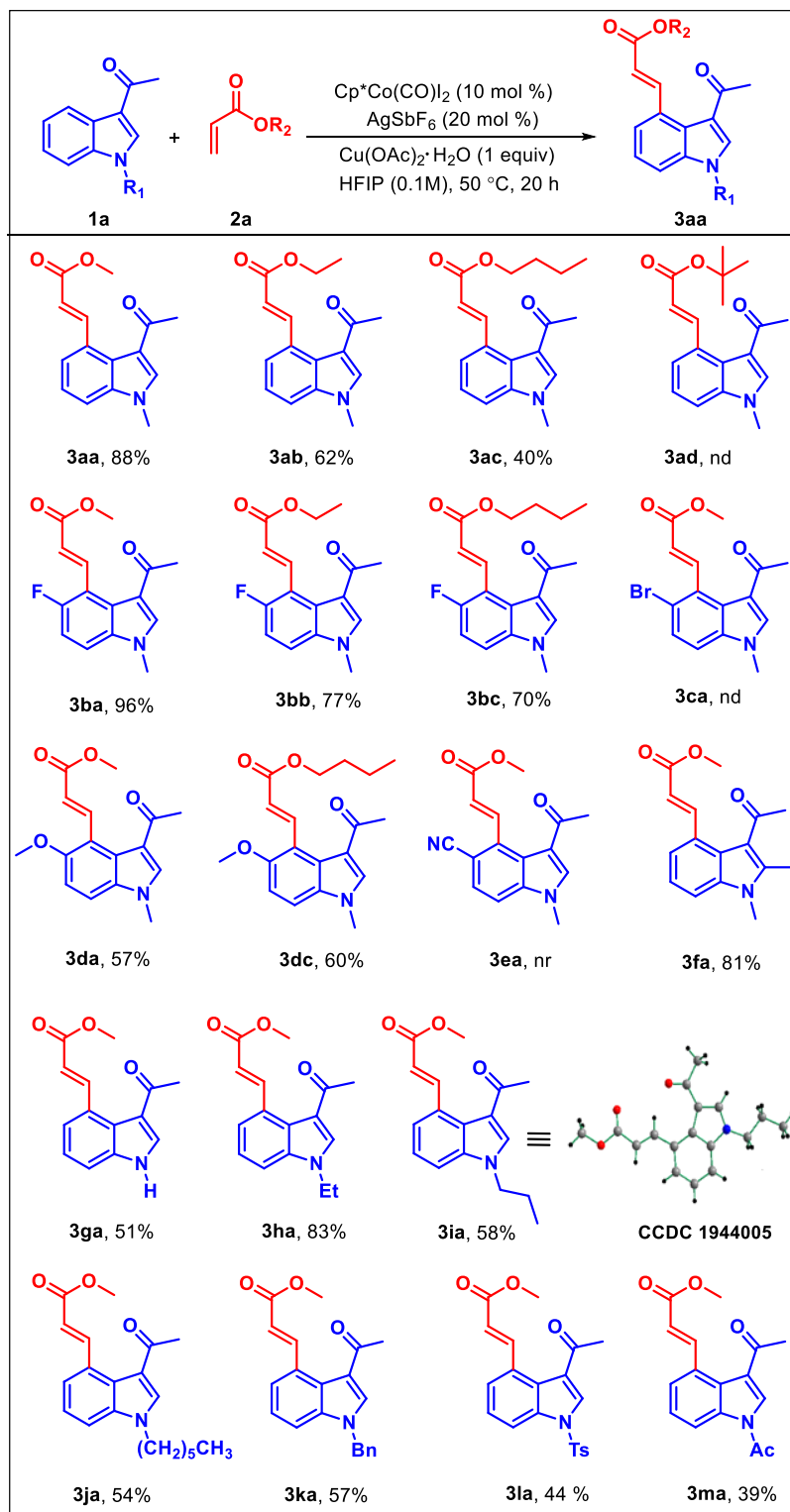
^bReaction conditions: **1a** (0.1 mmol), **2a** (4 equiv), Cp^{*}Co(CO)I₂ (10 mol %), Ag salt (20 mol %), additive (1 equiv), hexafluoroisopropanol (0.1 M) as a solvent, 50 °C, 20 h. ^bIsolated yields.

To further optimize the reaction in terms of directing groups, we planned to examine the reaction with different electron-rich and electron-poor directing groups while maintaining the same coupling partner **2a**. We checked our optimized reaction

conditions with acetyl, trifluoroacetyl, pivaloyl, carboxaldehyde, carboxylic acid, and acid derivative substituted indoles (Table 4.2, entries 1–7). Among these substrates, acetyl- and pivaloyl-substituted indoles gave excellent yields of **3aa** and **3aa3** (Table 4.2, entries 1 and 4). However, moderate yields were obtained in the case of indole bearing carboxaldehyde and a trifluoroacetyl directing group (Table 4.2, entries 2 and 3). Also, we screened acid and ester as a directing group, and the result was insignificant (Table 4.2, entries 5 and 6). In the case of an amide-directing group, both C-4 and C-2 alkenylated adducts **3aa6** and **3aa7** obtained a moderate yield (Table 4.2, entry 7). In contrast to the earlier reports,^{5a,b} an electron-rich directing group such as acetyl- and pivaloyl-substituted indoles, gave a C-4 regioselective adduct with a cobalt catalyst. This complementary nature of cobalt catalyst could be useful for the selective synthesis of C-4 functionalized indoles containing electron-rich directing groups.

With the optimized conditions in hand, we proceeded to screen the generality of this catalytic reaction with various indoles and acrylates to obtain an array of diversely functionalized C-4 alkenylated indoles. The steric and electronic influence of the alkyl substituent of acrylate for the designed catalytic transformation was first tested with **1a**. It was observed that with the increasing chain length of the alkyl group, the yield of the corresponding alkenylated product decreased (Scheme 4.1, **3aa–3ac**). This indicates that an electron-rich alkyl substituent on the ester group of acrylates retards the catalytic reaction.

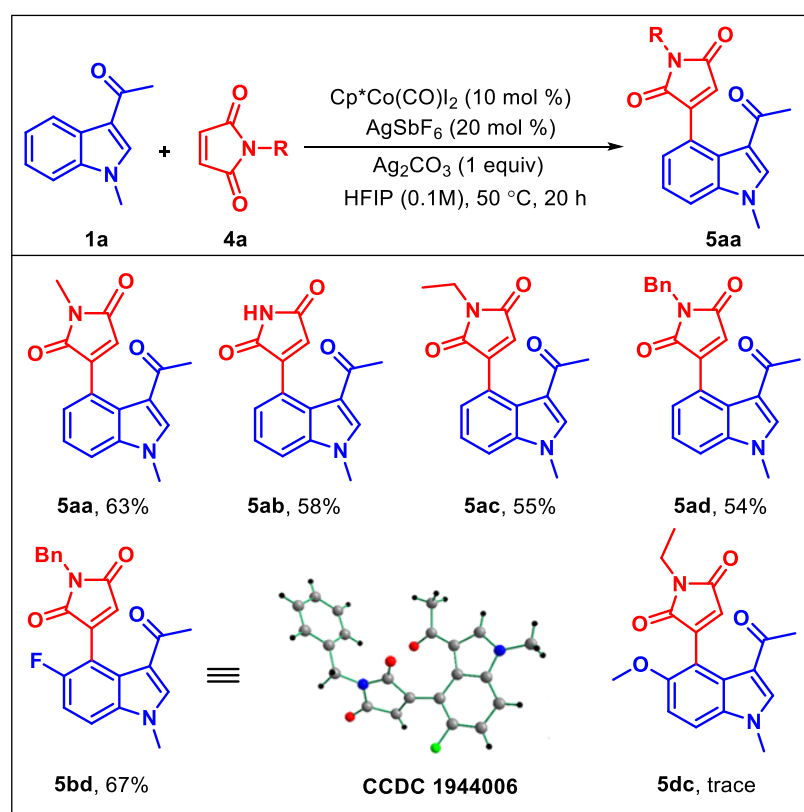
Scheme 4.1. Scope of C-4 Alkenylation of Indole with Acrylates^{a,b}



^aReaction conditions: **1a** (0.1 mmol), **2a** (4 equiv), $\text{CoCp}^*(\text{CO})\text{I}_2$ (10 mol %), AgSbF_6 (20 mol %), $\text{Cu}(\text{OAc})_2 \cdot \text{H}_2\text{O}$ (1 equiv), hexafluoroisopropanol (0.1 M) as a solvent, 50 °C, 20 h. ^bIsolated yields.

In the case of the bulkier tert-butyl (Scheme 4.1, **3ad**) substituent, the reaction failed under the optimized reaction conditions. Overall, it implies that the reaction seems highly sensitive to the steric and electronic nature of the alkyl substituents in acrylates. However, it is encouraging to note that C-5 substituted indoles such as 5-fluoro indole reacted with different acrylates resulting in excellent yields of desired products **3ba** (96%), **3bb** (77%), and **3bc** (70%). In contrast, bromo-substituted indole (1, **3ca**) did not react. It is possibly due to steric hindrance near the reaction site. Indole bearing a methoxy group at the C-5 position provided the desired products **3da** and **3dc** in good yields. However, electron-deficient indole (5-cyanoindole, **1e**) showed insignificant results (**3ea**).

Scheme 4.2. Scope of C-4 Alkenylation of Indole with Maleimides^a,



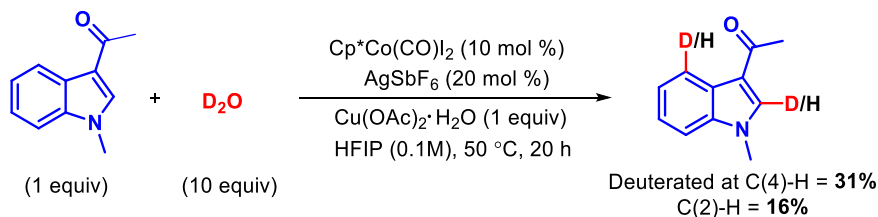
^aReaction conditions: **1a** (0.1 mmol), **2a** (4 equiv), $\text{CoCp}^*(\text{CO})\text{I}_2$ (10 mol %), AgSbF_6 (20 mol %), Ag_2CO_3 (1 equiv), hexafluoroisopropanol (0.1 M) as a solvent, 50 °C, 20 h. ^bIsolated yields.

Besides C-5 substituted indole, the C-2 substituted indole was also compatible with the reaction conditions leading to the formation of respective adduct **3fa** in 81% yield. Moreover, many *N*-protected indoles were effective, including alkyl, benzyl, tosyl, and acetyl groups giving the product (Scheme 4.1, **3ha–3ma**) moderate to excellent yields. It is worth mentioning that even though **3la** and **3ma** were obtained in diminished yields, 2-alkylated indole derivatives were not obtained as side products. Notably, the unprotected 3-acetyl indole showed good reactivity for the present catalytic system (Scheme 4.1, **3ga**). Further, to show the diversity of the reaction, we utilized *N*-methyl maleimide as a coupling partner and subjected it to the same reaction conditions. Unfortunately, we observed only a 38% yield of desired product **5aa**. Hence, we explored different additives and oxidants to enhance the product yield. A better yield was obtained with Ag₂CO₃. It is noteworthy that with *N*-substituted maleimides, the reaction worked well (Scheme 4.2, **5aa**, **5ac**, and **5ad**). A significant reactivity difference was observed in the case of C-5 substituted indoles. Fluoro-substituted indole **2b** reacted efficiently to give the desired adduct **5bd** in 67% yield, while methoxy-substituted indole **2d** was less prone to react under the same reaction conditions. To check the feasibility of the transformation on a large scale, we also performed the reaction in 1 mmol scale and obtained an excellent yield of **3aa**.¹⁰ In the absence of the Michael acceptor, both C(2)–H and C(4)–H of 3-acetyl indole under the same reaction conditions became deuterated by 16% and 31%, respectively, with 10 equiv of D₂O (Figure 4.2a). The ratio of C(2)–H and C(4)–H deuteration did not change notably after continuing the reaction for a longer time, revealing that the first step might be reversible. In addition, we also performed a competition study between an electron-rich (1-(1-methyl-1H-indol-3-yl)ethanone) and an electron-poor (2,2,2-trifluoro-1-(1-methyl-1H-

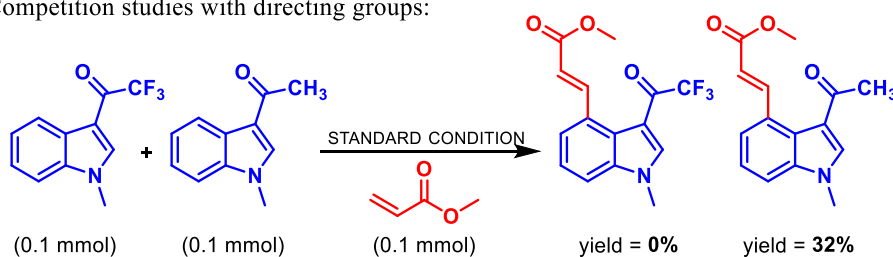
indol-3-yl)- ethanone) substrate. We found that the catalytic C-4 alkenylation is selective to electron-rich indole leading to the formation of the respective C-4 alkenylated adduct as the exclusive product (Figure 4.2b).

Figure 4.2. Mechanistic studies.

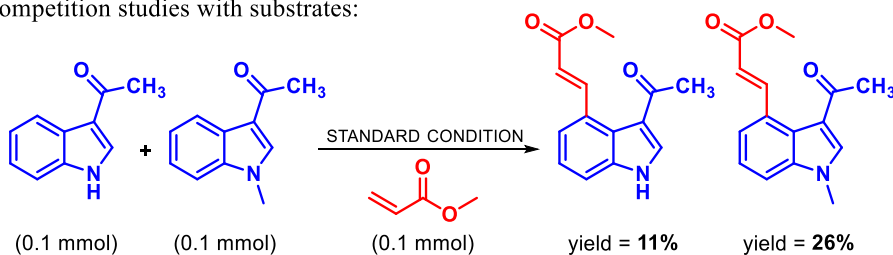
(a) H/D exchange studies:



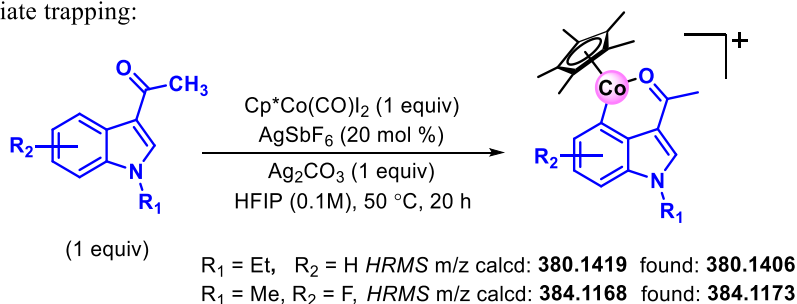
(b) Competition studies with directing groups:



(c) Competition studies with substrates:



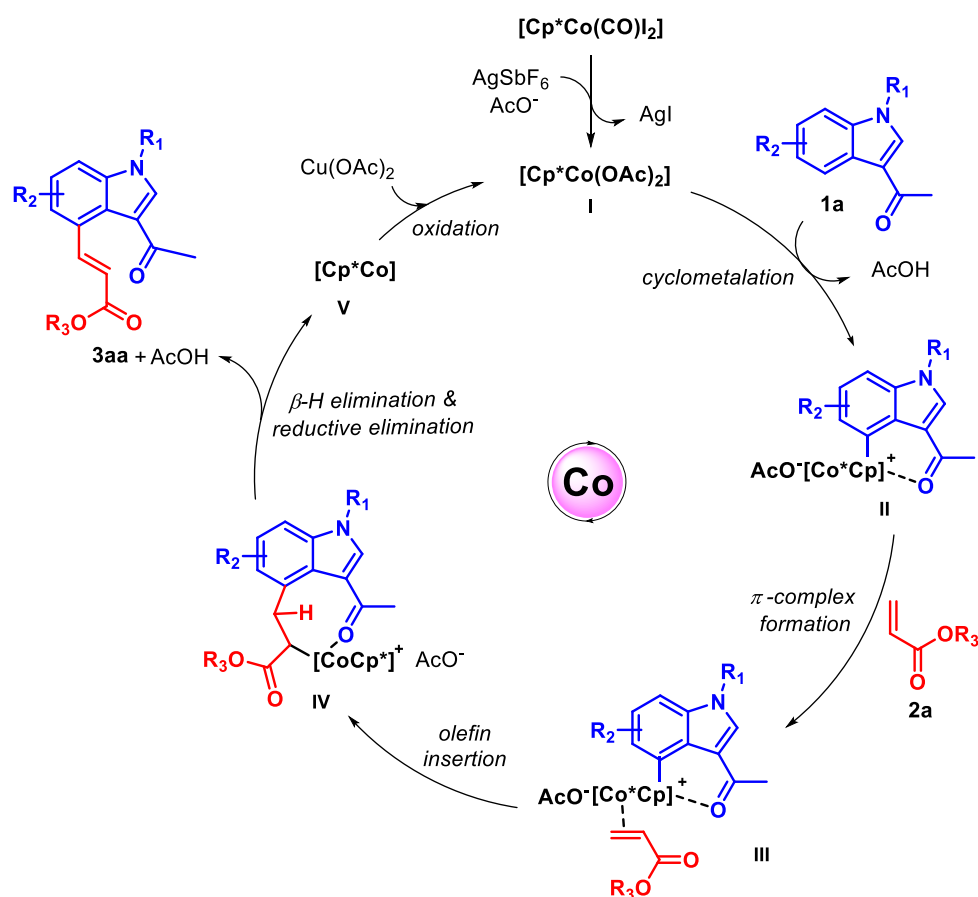
(d) Intermediate trapping:



Likewise, to examine the effect of the *N*-protecting group in the catalytic reaction, another competition study was accomplished between 1-(1H-indol-3-yl)ethanone and 1-(1-methyl-1H-indol-3-yl)ethanone. The catalytic C-4 alkenylation was found to be

more facile, with the N-protected indole producing a higher yield of the alkenylated compound (Figure 4.2c). Further, we have performed the stoichiometric reaction with a cobalt catalyst to trap the cobaltacycle intermediate, whereby the six-membered intermediate has been detected through HRMS for different indole derivatives (Figure 4.2d).

Scheme 4.3. Proposed Catalytic Cycle



Based on kinetic studies and literature precedents,¹¹ we proposed a plausible catalytic cycle (Scheme 4.3) where $\text{Cp}^*\text{Co}(\text{CO})\text{I}_2$ reacts with AgSbF_6 to generate an active catalyst **I** that forms a six-membered cyclometalated species **II** in the presence of **1a** which was detected in HRMS (Figure 4.2d). Then, the cationic cobalt(III) species undergoes π -complexation with the Michael acceptor **2a**, followed by olefin insertion to give intermediate **IV**. Then β -hydride elimination followed by reductive elimination

gives the desired product **3aa** and cobalt(I) complex **V**, which is further oxidized by copper acetate to regenerate the active cobalt(III) catalyst **I** for the next catalytic cycle.

4.4 CONCLUSION

In summary, using a weakly coordinating directing group, we developed cobalt-catalyzed regioselective C-4 alkenylation of indole with activated olefins. We also detected the six-membered cobaltacycle through HRMS, which supports our proposed mechanism. The developed protocol works well with various Michael acceptors and indoles. Further work regarding the origin of C-4 selectivity is being carried out in our laboratory.

Limitations: Electron-withdrawing substituted arenes such as -CN is incompatible with optimized reaction condition. Because electron-withdrawing groups decreases the nucleophilicity of Co-C bond towards olefin insertion.

4.5 EXPERIMENTAL SECTION

Reactions were performed using sealed tube vial under an N₂ atmosphere. Column chromatography was done using 100-200 & 230-400 mesh silica gel of Acme synthetic chemicals company. Gradient elution was performed by using distilled petroleum ether and ethyl acetate. TLC plates were detected under UV light at 254 nm. ¹H NMR, ¹³C NMR, recorded on Bruker AV 400 and 700 MHz spectrometers using CDCl₃ & DMSO-d₆ as the deuterated solvent.¹³ Multiplicity (s = singlet, d= doublet, t = triplet, q = quartet, m = multiplet, dd = double doublet), integration, and coupling constants (*J*) in hertz (Hz). HRMS signal analysis was performed using a micro TOF Q-II mass

spectrometer, and X-ray analysis was recorded at SCS, NISER. Reagents and starting materials were purchased from Sigma Aldrich, TCI, Avra, Spectrochem, and other commercially available sources and used without further purification unless otherwise noted.

(a) General reaction procedure for C-4 alkenylation of 3-acetyl indole with acrylates:

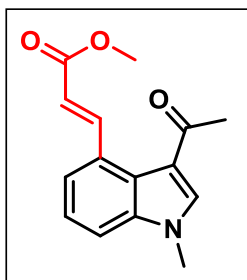
To a pre-dried sealed tube under N₂, the mixture of *N*-methyl 3-acetyl indole **1** (0.1 mmol), acrylate **2** (0.4 mmol), [Cp*Co(CO)I₂] (10 mol %), AgSbF₆ (20 mol %), Cu(OAc)₂.H₂O (0.1 mmol) and HFIP (1.1 mL) were added and sealed. The reaction mixture was vigorously stirred at 50 °C for 20 h. After 20 h (completion of the reaction as monitored by TLC analysis), the reaction mixture was cooled to room temperature and diluted with diethyl ether/ dichloromethane, and passed through a short celite pad, the solvent was evaporated under reduced pressure, and the residue was purified by column chromatography using EtOAc/hexane mixture on silica gel to give the pure product **3**.

(b) General reaction procedure for C-4 Alkenylation of 3-acetyl indole with maleimides:

To a pre-dried sealed tube under N₂, the mixture of *N*-methyl 3-acetyl indole **1** (0.1 mmol), maleimide **4** (0.2 mmol), [Cp*Co(CO)I₂] (10 mol %), AgSbF₆ (20 mol %), Ag₂CO₃ (0.1 mmol) and HFIP (1.1 mL) were added and sealed. The reaction mixture was vigorously stirred at 50 °C for 20 h. After 20 h (completion of reaction monitored by TLC), the reaction mixture was cooled to room temperature and diluted with diethyl

ether/ dichloromethane, and passed through a short celite pad, the solvent was evaporated under reduced pressure, and the residue was purified by column chromatography using EtOAc/hexane mixture on silica gel to give the pure product **5**.

Experimental characterization data of products:



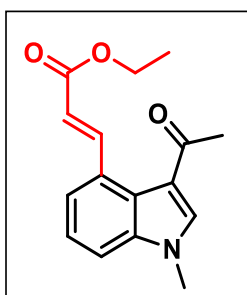
(E)-methyl 3-(3-acetyl-1-methyl-1H-indol-4-yl)acrylate (**3aa**):

was prepared according to general procedure (4.5a).

The crude reaction mixture was purified by column chromatography using silica gel (100-200 mesh), giving a white solid (26 mg, 88% yield) R_f: 0.42 (in 50%

EtOAc/hexane). **¹H NMR (CDCl₃, 400 MHz):** δ 9.34 (d, *J* = 16.0 Hz, 1H), 7.81 (s, 1H), 7.53-7.51 (m, 1H), 7.35-7.26 (m, 2H), 6.32 (d, *J* = 16.0 Hz, 1H), 3.84 (s, 6H), 2.53 (s, 3H). **¹³C NMR (CDCl₃, 100 MHz):** δ 168.3, 168.2, 147.4, 139.1, 139.0, 130.4, 125.1, 124.1, 122.4, 118.0, 112.1, 52.1, 34.1, 29.1. **IR (KBr, cm⁻¹):** 1718.10, 1670.27.

HRMS (ESI) m/z calcd for C₁₅H₁₅NO₃Na [M+Na]⁺: 280.0944; found: 280.0962.

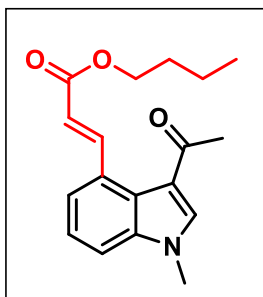


(E)-ethyl 3-(3-acetyl-1-methyl-1H-indol-4-yl)acrylate (**3ab**):

was prepared according to general procedure (4.5a). The crude reaction mixture was purified by column chromatography using silica gel (230-400 mesh), giving a pale white solid (19 mg, 62% yield) R_f: 0.6 (in 60% EtOAc/hexane). **¹H NMR**

(CDCl₃, 400 MHz): δ 9.32 (d, *J* = 16.0 Hz, 2H), 7.79 (s, 1H), 7.54 (d, *J* = 6.5 Hz, 1H), 7.34-7.29 (m, 2H), 6.33 (d, *J* = 16.0 Hz, 2H), 4.30 (q, *J* = 7.0 Hz, 2H), 3.84 (s, 3H), 2.53 (s, 3H), 1.37 (t, *J* = 7.0 Hz, 3H). **¹³C NMR (CDCl₃, 100 MHz):** δ 191.9, 167.7, 147.1, 138.9, 138.8, 130.5, 124.8, 123.9, 121.5, 118.6, 118.5, 111.4, 60.6, 34.0, 28.5,

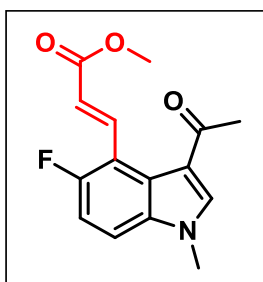
14.7. **IR (KBr, cm⁻¹):** 1709.55, 1651.03. **HRMS (ESI) m/z** calcd for C₁₆H₁₇NO₃Na [M+Na]⁺: 294.1101; found: 294.1086.



(E)-butyl 3-(3-acetyl-1-methyl-1H-indol-4-yl)acrylate (3ac):

was prepared according to general procedure (4.5a). The crude reaction mixture was purified by column chromatography using silica gel (230-400 mesh), giving a pale white solid (13 mg, 40% yield) R_f: 0.5 (in 50% EtOAc/hexane).

¹H NMR (CDCl₃, 400 MHz): δ 9.32 (d, *J* = 16.0 Hz, 2H), 7.79 (s, 1H), 7.54 (d, *J* = 6.5 Hz, 1H), 7.36-7.29 (m, 2H), 6.34 (d, *J* = 16.0 Hz, 2H), 4.25 (t, *J* = 6.7 Hz, 2H), 3.84 (s, 3H), 2.53 (s, 3H), 1.73 (m, 3H), 1.48 (m, 2H), 0.97 (t, *J* = 7.4 Hz, 3H). **¹³C NMR (CDCl₃, 100 MHz):** δ 191.9, 167.8, 147.0, 139.0, 138.6, 130.6, 124.8, 123.9, 121.5, 118.7, 118.5, 111.3, 64.5, 34.0, 31.2, 28.5, 19.5, 14.1. **IR (KBr, cm⁻¹):** 1704.99, 1661.97. **HRMS (ESI) m/z** calcd for C₁₈H₂₁NO₃Na [M+Na]⁺: 322.1414; found: 322.1423.

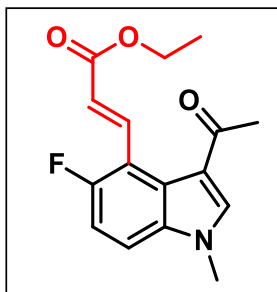


(E)-methyl 3-(3-acetyl-5-fluoro-1-methyl-1H-indol-4-yl)acrylate (3ba):

was prepared according to general procedure (4.5a). The crude reaction mixture was purified by column chromatography using silica gel (100-200 mesh),

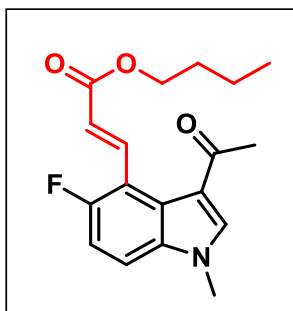
giving a light-yellow solid (27 mg, 96% yield) R_f: 0.35 (in 60% EtOAc/hexane). **¹H NMR (DMSO-*d*₆, 400 MHz):** δ 9.05 (d, *J* = 16.0 Hz, 1H), 8.58 (s, 1H), 7.66 (dd, *J* = 8.8, 4.4, Hz, 1H), 7.32-7.27 (m, 1H), 6.45 (d, *J* = 16.0 Hz, 1H), 3.91 (s, 3H), 3.78 (s, 3H), 2.54 (s, 3H). **¹³C NMR (DMSO-*d*₆, 100 MHz):** δ 199.2, 172.1, 163.0 (d, *J* = 239.3 Hz), 145.3, 145.4, 139.9, 129.7 (d, *J* = 5.1 Hz), 125.9 (d, *J* = 16.1 Hz), 122.2 (d, *J* = 4.2 Hz), 119.6 (d, *J* = 13.4 Hz), 118.5 (d, *J* = 11.1 Hz), 116.9 (d, *J* = 28.2 Hz), 56.3, 38.4,

33.2. **IR (KBr, cm⁻¹):** 1646.81, 1404.46. **HRMS (ESI)** m/z calcd for C₁₅H₁₄FN₃Na [M+Na]⁺: 298.0850; found: 298.0858.



(E)-ethyl 3-(3-acetyl-5-fluoro-1-methyl-1H-indol-4-yl)acrylate (3bb): was prepared according to general procedure (4.5a). The crude reaction mixture was purified by column chromatography using silica gel (230-400 mesh), giving a yellow solid (22 mg, 77% yield) R_f: 0.3 (in 60%

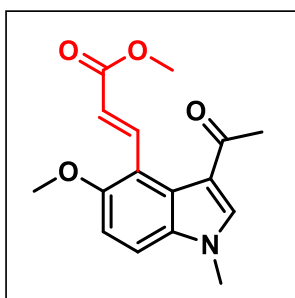
EtOAc/hexane). **¹H NMR (DMSO-*d*₆, 400 MHz):** δ 8.98 (d, *J* = 16.0 Hz, 1H), 7.80 (s, 1H), 7.23 (dd, *J* = 8.8, 4.4 Hz, 1H), 7.12-7.07 (m, 1H), 6.56 (d, *J* = 16.0 Hz, 1H), 4.31 (q, *J* = 7.2 Hz, 2H), 3.84 (s, 3H), 2.53 (s, 3H), 1.36 (t, *J* = 7.2 Hz, 3H). **¹³C NMR (DMSO-*d*₆, 175 MHz):** δ 191.8, 168.0, 158.9 (d, *J* = 245 Hz), 140.2, 139.4, 135.1, 125.9 (d, *J* = 5.2 Hz), 122.7 (d, *J* = 15.7 Hz), 119.2 (d, *J* = 5.2 Hz), 116.8 (d, *J* = 12.2 Hz), 113.0 (d, *J* = 28 Hz), 111.6 (d, *J* = 10.5 Hz), 60.6, 34.1, 28.6, 14.7. **IR (KBr, cm⁻¹):** 1711.18, 1647.00, 1556.76. **HRMS (ESI)** m/z calcd for C₁₆H₁₆NFO₃Na [M+Na]⁺: 312.1006; found: 312.1030.



(E)-butyl 3-(3-acetyl-5-fluoro-1-methyl-1H-indol-4-yl)acrylate (3bc): was prepared according to general procedure (4.5a). The crude reaction mixture was purified by column chromatography using silica gel (230-400 mesh), giving a pale white solid (22 mg, 70% yield) R_f:

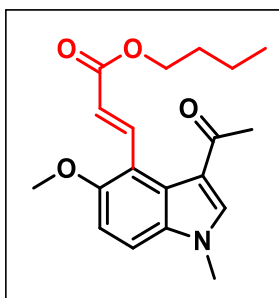
0.4 (in 60% EtOAc/hexane). **¹H NMR (DMSO-*d*₆, 400 MHz):** δ 9.05 (d, *J* = 16.0 Hz, 1H), 8.58 (s, 1H), 7.66 (dd, *J* = 8.8, 4.4 Hz, 1H), 7.32-7.27 (m, 1H), 6.43 (d, *J* = 16.0 Hz, 1H), 4.18 (t, *J* = 6.4 Hz, 2H), 3.91 (s, 3H), 2.53 (s, 3H), 1.67 (m, 2H), 1.44 (m, 2H),

0.96 (t, $J = 7.2$ Hz, 3H). ^{13}C NMR (DMSO- d_6 , 100 MHz): δ 192.2, 167.5, 159.0 (d, $J = 242.0$ Hz), 143.2, 141.2, 135.9, 125.8 (d, $J = 5.0$ Hz), 122.2 (d, $J = 17.0$ Hz), 118.2 (d, $J = 4.0$ Hz), 115.7 (d, $J = 13.0$ Hz), 114.5 (d, $J = 12.0$ Hz), 112.9 (d, $J = 28$ Hz), 64.5, 34.4, 31.3, 29.3, 19.6, 14.5. IR (KBr, cm^{-1}): 1705.14, 1659.89, 1525.25. HRMS (ESI) m/z calcd for $\text{C}_{18}\text{H}_{20}\text{NFO}_3\text{Na}$ $[\text{M}+\text{Na}]^+$: 340.1319; found: 340.1341.



(E)-methyl 3-(3-acetyl-5-methoxy-1-methyl-1H-indol-4-yl)acrylate (**3da**): was prepared according to general procedure (4.5a). The crude reaction mixture was purified by column chromatography using silica gel (100-200 mesh), giving a yellow solid 15 mg, 57% yield) R_f : 0.45

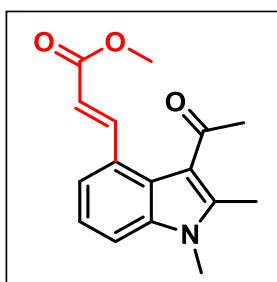
(in 50% EtOAc/hexane). ^1H NMR (DMSO- d_6 , 400 MHz): δ 9.09 (d, $J = 16.0$ Hz, 1H), 8.47 (s, 1H), 7.61 (d, $J = 9.2$, Hz, 1H), 7.21 (d, $J = 8.8$, 1H), 6.67 (d, $J = 16.0$ Hz, 1H), 3.93 (s, 3H), 3.87 (s, 3H), 3.73 (s, 3H), 2.51 (s, 3H). ^{13}C NMR (DMSO- d_6 , 100 MHz): δ 192.1, 169.1, 157.0, 143.3, 143.1, 134.4, 127.0, 120.2, 118.1, 116.2, 114.0, 110.2, 57.4, 52.0, 34.2, 29.4. IR (KBr, cm^{-1}): 1695.79, 1654.42. HRMS (ESI) m/z calcd for $\text{C}_{16}\text{H}_{17}\text{NO}_4\text{Na}$ $[\text{M}+\text{Na}]^+$: 310.1050; found: 310.1050.



((E)-butyl 3-(3-acetyl-5-methoxy-1-methyl-1H-indol-4-yl)acrylate (3dc)): was prepared according to general procedure (4.5a). The crude reaction mixture was purified by column chromatography using silica gel (230-400 mesh), giving a yellow solid (18 mg, 60% yield) R_f : 0.2 (in 60%

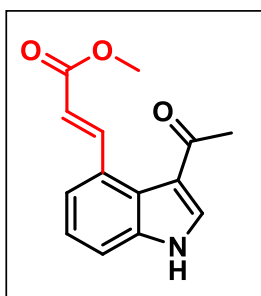
EtOAc/hexane). ^1H NMR (DMSO- d_6 , 400 MHz): δ 9.08 (d, $J = 16.0$ Hz, 1H), 8.47 (s, 1H), 7.61 (d, $J = 9.2$ Hz, 1H), 7.21 (d, $J = 9.2$ Hz, 1H), 6.66 (d, $J = 16.0$ Hz, 1H), 4.15

(t, $J = 6.4$ Hz, 2H), 3.93 (s, 3H), 3.87 (s, 3H), 2.51 (s, 3H), 1.67 (m, 2H), 1.39 (m, 2H), 0.96 (t, $J = 7.6$ Hz, 3H). **^{13}C NMR (DMSO- d_6 , 100 MHz):** δ 191.9, 168.5, 156.8, 143.2, 142.5, 134.4, 126.9, 120.5, 117.8, 116.2, 114.0, 110.2, 64.1, 57.4, 34.2, 31.4, 29.5, 19.6, 14.6. **IR (KBr, cm^{-1}):** 1705.12, 1643.40. **HRMS (ESI)** m/z calcd for $\text{C}_{19}\text{H}_{23}\text{NO}_4\text{Na}$ $[\text{M}+\text{Na}]^+$: 352.1519; found: 352.1528.



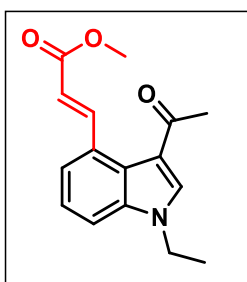
((E)-methyl 3-(3-acetyl-1,2-dimethyl-1H-indol-4-yl)acrylate (3fa): was prepared according to general procedure (4.5a). The crude reaction mixture was purified by column chromatography using silica gel (100-200 mesh),

giving a yellow solid (20 mg, 81% yield) R_f : 0.40 (in 40% EtOAc/hexane). **^1H NMR (CDCl_3 , 400 MHz):** δ 8.14 (d, $J = 16.0$ Hz, 1H), 7.41 (d, $J = 7.2$ Hz, 1H), 7.32 (d, $J = 7.2$ Hz, 1H), 7.26-7.22 (m, 1H), 6.41 (d, $J = 16.0$ Hz, 1H), 3.81 (s, 3H), 3.69 (s, 3H), 2.57 (s, 3H), 2.49 (s, 3H). **^{13}C NMR (CDCl_3 , 100 MHz):** δ 198.0, 168.1, 146.0, 143.1, 138.0, 128.1, 125.1, 123.1, 121.2, 117.9, 117.6, 111.1, 52.1, 32.2, 30.1, 12.2. **IR (KBr, cm^{-1}):** 1703.93, 1637.41. **HRMS (ESI)** m/z calcd for $\text{C}_{16}\text{H}_{17}\text{NO}_3\text{Na}$ $[\text{M}+\text{Na}]^+$: 294.1101; found: 294.1091.



(E)-methyl 3-(3-acetyl-1H-indol-4-yl)acrylate (3ga): was prepared according to general procedure (4.5a). The crude reaction mixture was purified by column chromatography using silica gel (100-200 mesh), giving a yellow solid (15 mg, 51% yield) R_f : 0.45 (in 50% EtOAc/hexane). **^1H NMR (DMSO- d_6 , 400 MHz):** δ 12.26 (s, 1H), 9.38 (d, $J = 16.0$ Hz 1H), 8.52 (d, $J = 3.2$ Hz,

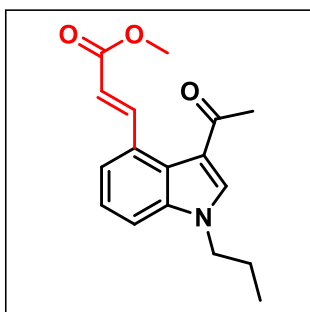
1H), 7.65 (d, $J = 7.6$ Hz, 1H), 7.59 (d, $J = 8.0$ Hz, 1H), 7.308 (t, $J = 8.0$ Hz, 1H), 6.43 (d, $J = 16.0$ Hz, 1H), 3.76 (s, 3H), 2.56 (s, 3H). **^{13}C NMR (DMSO- d_6 , 100 MHz):** δ 193.0, 168.0, 148.0, 139.2, 139.1, 129.1, 125.1, 124.1, 121.4, 119.0, 117.4, 115.2, 52.2, 29.2. **IR (KBr, cm^{-1}):** 1747.12, 1615.09. **HRMS (ESI)** m/z calcd for $\text{C}_{14}\text{H}_{13}\text{NO}_3\text{Na}$ $[\text{M}+\text{Na}]^+$: 266.0788; found: 266.0787.



(*E*)-methyl 3-(3-acetyl-1-ethyl-1H-indol-4-yl)acrylate (3ha):

was prepared according to general procedure (4.5a). The crude reaction mixture was purified by column chromatography using silica gel (100-200 mesh), giving a pale yellow solid (24 mg, 83% yield) R_f : 0.40 (in 50% EtOAc/hexane). **^1H NMR**

(CDCl_3 , 400 MHz): δ 9.36 (d, $J = 16.0$ Hz, 1H), 7.99 (s, 1H), 7.52 (d, $J = 7.6$ Hz, 1H), 7.42 (d, $J = 7.6$ Hz, 1H), 7.32 (t, $J = 7.6$ Hz, 1H), 6.32 (d, $J = 16.0$ Hz, 1H), 4.25 (q, $J = 7.2$ Hz, 2H) 3.82 (s, 3H), 2.56 (s, 3H), 1.54 (t, $J = 7.2$ Hz, 3H). **^{13}C NMR (CDCl_3 , 100 MHz):** δ 192.1, 168.0, 147.3, 138.1, 138.0, 130.1, 125.0, 123.4, 121.1, 118.0, 118.0, 117.1, 115.5, 51.5, 42.1, 28.2, 15.2. **IR (KBr, cm^{-1}):** 1708.92, 1648.19. **HRMS (ESI)** m/z calcd for $\text{C}_{16}\text{H}_{17}\text{NO}_3\text{Na}$ $[\text{M}+\text{Na}]^+$: 294.1101; found: 294.1126.



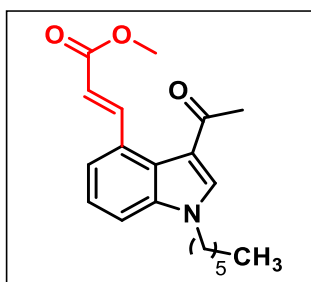
((*E*)-methyl 3-(3-acetyl-1-propyl-1H-indol-4-yl)acrylate

(3ia): was prepared according to general procedure (4.5a).

The crude reaction mixture was purified by column chromatography using silica gel (100-200 mesh), giving a yellow solid (16 mg, 58% yield) R_f : 0.30 (in 50%

EtOAc/hexane). **^1H NMR (CDCl_3 , 400 MHz):** δ 9.32 (d, $J = 16.0$ Hz, 1H), 7.84 (s, 1H),

7.51 (d, $J = 7.2$ Hz, 1H), 7.37 (d, $J = 7.2$ Hz, 1H), 7.30 (d, $J = 7.6$ Hz, 1H), 6.32 (d, $J = 16.0$ Hz, 1H), 4.12 (d, $J = 7.2$ Hz, 2H), 3.84 (s, 3H), 2.55 (s, 3H), 194-1.89 (m, 2H), 0.97 (d, $J = 7.2$ Hz, 3H). ^{13}C NMR (CDCl_3 , 100 MHz): δ 192.1, 168.1, 147.4, 138.3, 138.2, 131.0, 125.1, 124.5, 122.3, 118.5, 118.1, 112.1, 52.0, 49.2, 28.5, 23.4, 12.1. IR (KBr, cm^{-1}): 1711.51, 1644.11. HRMS (ESI) m/z calcd for $\text{C}_{17}\text{H}_{19}\text{NO}_3\text{Na}$ $[\text{M}+\text{Na}]^+$: 308.1257; found: 308.1284.

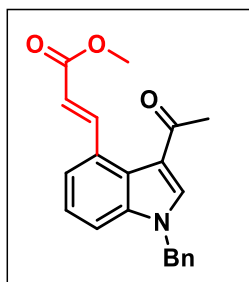


(E)-methyl 3-(3-acetyl-1-hexyl-1H-indol-4-yl)acrylate

(3ja): was prepared according to general procedure (4.5a).

The crude reaction mixture was purified by column chromatography using silica gel (100-200 mesh) given as pale-yellow liquid (15 mg, 54% yield) R_f : 0.45 (in 60% EtOAc/hexane).

^1H NMR (CDCl_3 , 400 MHz): δ 9.32 (d, $J = 16.0$ Hz, 1H), 7.83 (s, 1H), 7.51 (d, $J = 7.2$ Hz, 1H), 7.36 (d, $J = 8.0$ Hz, 1H), 7.30 (t, $J = 7.6$ Hz, 1H), 6.32 (d, $J = 16.0$ Hz, 1H), 4.25 (t, $J = 7.2$ Hz, 2H), 3.84 (s, 3H), 2.56 (s, 3H), 1.87 (t, $J = 6.8$ Hz, 2H), 1.32 (s, 6H), 0.88 (t, $J = 6.4$ Hz, 3H). ^{13}C NMR (CDCl_3 , 100 MHz): δ 192.1, 168.1, 147.4, 138.3, 138.0, 131.0, 125.1, 124.1, 122.0, 119.0, 118.1, 112.1, 52.0, 48.0, 32.0, 30.1, 29.1, 27.1, 23.1, 14.2. IR (KBr, cm^{-1}): 1705.40, 1652.55. HRMS (ESI) m/z calcd for $\text{C}_{20}\text{H}_{25}\text{NO}_3\text{Na}$ $[\text{M}+\text{Na}]^+$: 350.1727; found: 350.1730.

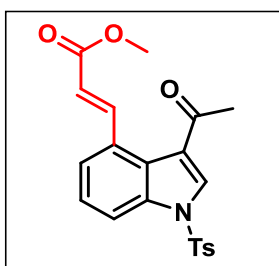


(E)-methyl 3-(3-acetyl-1-benzyl-1H-indol-4-yl)acrylate (3ka):

was prepared according to general procedure (4.5a). The crude reaction mixture was purified by column chromatography using silica gel (100-200 mesh), giving as colorless liquid (16

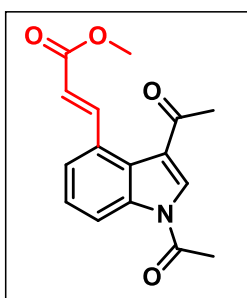
mg, 57% yield) R_f : 0.35 (in 50% EtOAc/hexane). ^1H NMR (CDCl_3 , 400 MHz): δ 9.31

(d, $J = 16.0$ Hz, 1H), 7.86 (s, 1H), 7.52 (d, $J = 7.2$ Hz, 1H), 7.35-7.24 (m, 5H), 7.13 (d, $J = 7.6$ Hz, 2H), 6.33 (d, $J = 16.0$ Hz, 1H), 5.36 (s, 2H), 3.84 (s, 3H), 2.54 (s, 3H). **^{13}C NMR** (CDCl_3 , **100 MHz**): δ 192.3, 168.1, 147.3, 139.1, 138.1, 136.0, 131.1, 129.4, 129.0, 127.1, 125.0, 124.1, 122.1, 119.2, 118.3, 112.0, 52.0, 51.2, 29.0. **IR** (KBr , cm^{-1}): 1696.05, 1649.30. **HRMS** (**ESI**) m/z calcd for $\text{C}_{21}\text{H}_{19}\text{NO}_3\text{Na}$ $[\text{M}+\text{Na}]^+$: 356.1257; found: 356.1244.



***(E)*-methyl 3-(3-acetyl-1-tosyl-1H-indol-4-yl)acrylate (3la):**

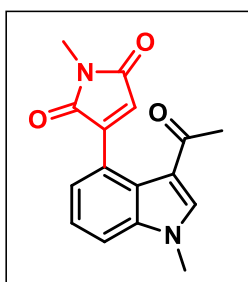
was prepared according to general procedure (4.5a). The crude reaction mixture was purified by column chromatography using silica gel (100-200 mesh), giving a yellow solid (11 mg, 44% yield) R_f : 0.40 (in 30% EtOAc/hexane). **^1H NMR** (CDCl_3 , **400 MHz**): δ 8.85 (d, $J = 16.0$ Hz, 1H), 8.31 (s, 1H), 7.97 (d, $J = 8.4$ Hz, 1H), 7.82 (d, $J = 8.0$ Hz, 2H), 7.52 (d, $J = 7.6$ Hz, 1H), 7.37 (t, $J = 8.0$ Hz, 1H), 7.30 (d, $J = 8.0$ Hz, 2H), 6.26 (d, $J = 16.0$ Hz, 1H), 3.82 (s, 3H), 2.63 (s, 3H), 2.38 (s, 3H). **^{13}C NMR** (CDCl_3 , **175 MHz**): δ 193.1, 168.0, 147.0, 146.0, 136.2, 135.5, 135.5, 131.1, 131.0, 128.1, 126.3, 126.1, 124.0, 123.4, 119.3, 115.1, 52.1, 29.1, 22.0. **IR** (KBr , cm^{-1}): 1707.11, 1663.05. **HRMS** (**ESI**) m/z calcd for $\text{C}_{21}\text{H}_{19}\text{NO}_5\text{SNa}$ $[\text{M}+\text{Na}]^+$: 420.0876; found: 420.0841.



***(E)*-methyl 3-(1,3-diacetyl-1H-indol-4-yl)acrylate (3ma):**

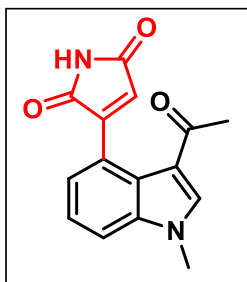
was prepared according to general procedure (4.5a). The crude reaction mixture was purified by column chromatography using silica gel (100-200 mesh), giving a yellow solid (12 mg, 39% yield) R_f : 0.45 (in 50% EtOAc/hexane). **^1H NMR**

(CDCl₃, 400 MHz): δ 8.68 (d, J = 15.6 Hz, 1H), 8.52 (d, J = 8.4 Hz, 1H), 8.11 (s, 1H), 7.58 (d, J = 7.6 Hz, 1H), 7.43 (t, J = 8.0 Hz, 1H), 6.33 (d, J = 15.6 Hz, 1H), 3.84 (s, 3H), 2.75 (s, 3H), 2.63 (s, 3H). ¹³C NMR (CDCl₃, 175 MHz): δ 193.3, 169.1, 168.1, 146.2, 137.4, 133.3, 130.4, 127.1, 126.1, 124.3, 124.1, 119.1, 118.0, 52.1, 29.1, 24.4. IR (KBr, cm⁻¹): 1730.21, 1698.78, 1668.74. HRMS (ESI) m/z calcd for C₁₆H₁₅NO₄Na [M+Na]⁺: 308.0893; found: 308.0903.



3-(3-acetyl-1-methyl-1H-indol-4-yl)-1-methyl-1H-pyrrole-2,5-dione (5aa): was prepared according to the general procedure (4.5b). The crude reaction mixture was purified by column chromatography using silica gel (230-400 mesh),

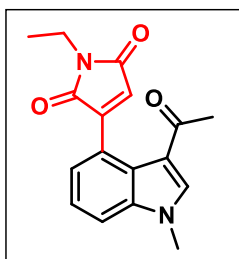
giving a green solid (20 mg, 63% yield) R_f: 0.3 (in 60% EtOAc/hexane). ¹H NMR (DMSO-*d*₆, 400 MHz): δ 8.47 (s, 1H), 7.71 (d, J = 8.4 Hz, 1H), 7.39 (t, J = 7.6 Hz, 1H), 7.20 (d, J = 7.2 Hz, 1H), 7.24 (d, J = 7.2 Hz, 1H), 6.66 (s, 1H), 3.94 (s, 3H), 2.96 (s, 3H), 2.38 (s, 3H). ¹³C NMR (DMSO-*d*₆, 100 MHz): δ 192.1, 172.3, 171.5, 150.9, 140.7, 138.8, 124.8, 124.0, 123.8, 12.7, 123.6, 117.3, 113.3, 34.2, 28.3, 24.4. IR (KBr, cm⁻¹): 1700.28, 1645.93, 1531.92. HRMS (ESI) m/z calcd for C₁₆H₁₄N₂O₃Na [M+Na]⁺: 283.1077; found: 283.1075.



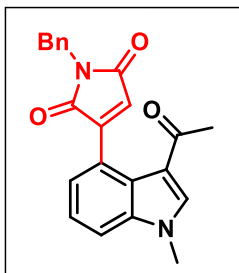
3-(3-acetyl-1-methyl-1H-indol-4-yl)-1H-pyrrole-2,5-dione (5ab): was prepared according to the general procedure (4.5b). The crude reaction mixture was purified by column chromatography using silica gel (230-400 mesh), giving a

green solid (16 mg, 58% yield) R_f: 0.2 (in 60% EtOAc/hexane).

¹H NMR (DMSO-*d*₆, 400 MHz): δ 10.70 (s, 1H), 8.45 (s, 1H), 7.69 (d, *J* = 8.4 Hz, 1H), 7.38 (t, *J* = 7.6 Hz, 1H), 7.19 (d, *J* = 7.2, 1H), 6.55 (s, 1H), 3.92 (s, 3H), 2.38 (s, 3H). **¹³C NMR (DMSO-*d*₆, 100 MHz):** δ 192.1, 173.7, 172.8, 151.4, 140.5, 138.8, 124.9, 124.4, 124.2, 123.9, 123.6, 117.5, 113.2, 34.2, 28.3. **IR (KBr, cm⁻¹):** 1653.18, 1613.56, 1400.58. **HRMS (ESI)** *m/z* calcd for C₁₅H₁₂N₂O₃Na [M+Na]⁺: 291.0740; found: 291.0763.

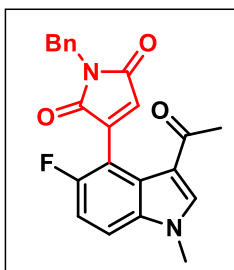


3-(3-acetyl-1-methyl-1H-indol-4-yl)-1-ethyl-1H-pyrrole-2,5-dione (5ac): was prepared according to the general procedure (4.5b). The crude reaction mixture was purified by column chromatography using silica gel (230-400 mesh), giving a green solid (18 mg, 55% yield) *R*_f: 0.2 (in 60% EtOAc/hexane). **¹H NMR (DMSO-*d*₆, 400 MHz):** δ 8.45 (s, 1H), 7.71 (d, *J* = 8.4 Hz, 1H), 7.39 (t, *J* = 8.0 Hz, 1H), 7.21 (d, *J* = 7.2, 1H), 6.67 (s, 1H), 3.93 (s, 3H), 3.50 (q, *J* = 7.2 Hz, 2H), 2.38 (s, 3H), 1.16 (t, *J* = 7.2 Hz, 3H). **¹³C NMR (DMSO-*d*₆, 100 MHz):** δ 192.2, 172.1, 171.3, 150.7, 140.7, 138.8, 124.8, 124.1, 123.9, 123.7, 123.6, 117.5, 113.4, 34.3, 33.0, 28.4, 14.5. **IR (KBr, cm⁻¹):** 1695.86, 1647.99, 1533.42. **HRMS (ESI)** *m/z* calcd for C₁₇H₁₆N₂O₃Na [M+Na]⁺: 319.1053; found: 319.1043.

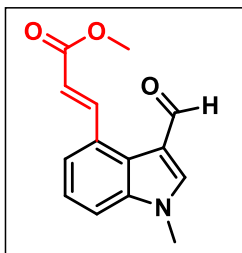


3-(3-acetyl-1-methyl-1H-indol-4-yl)-1-benzyl-1H-pyrrole-2,5-dione (5ad): was prepared according to general procedure (4.5b). The crude reaction mixture was purified by column chromatography using silica gel (230-400 mesh), giving a green solid (20 mg, 54% yield) *R*_f: 0.4 (in 50% EtOAc/hexane). **¹H NMR (DMSO-*d*₆,**

400 MHz): δ 8.47 (s, 1H), 7.72 (d, $J = 8.4$ Hz, 1H), 7.38 (t, $J = 7.6$ Hz, 1H), 7.42-7.35 (m, 1H), 7.30 (t, $J = 7.2$ Hz, 1H), 7.24 (d, $J = 7.2$ Hz), 6.76 (s, 1H), 4.67 (s, 2H), 3.94 (s, 3H), 2.38 (s, 3H). **^{13}C NMR (DMSO- d_6 , 100 MHz):** δ 192.3, 172.1, 171.3, 151.0, 140.6, 138.8, 137.7, 129.3, 128.0, 125.0, 123.9, 123.7, 123.6, 117.5, 113.6, 41.5, 34.3, 28.4. **IR (KBr, cm^{-1}):** 1695.72, 1635.60, 1560.04. **HRMS (ESI) m/z calcd for $\text{C}_{22}\text{H}_{18}\text{N}_2\text{O}_3\text{Na}$ $[\text{M}+\text{Na}]^+$:** 381.1210; found: 381.1215



3-(3-acetyl-5-fluoro-1-methyl-1H-indol-4-yl)-1-benzyl-1H-pyrrole-2,5-dione (5bd): was prepared according to general procedure (4.5b). The crude reaction mixture was purified by column chromatography using silica gel (230-400 mesh), giving a green solid (22 mg, 67% yield) R_f : 0.4 (in 60% EtOAc/hexane). **^1H NMR (Acetone- d_6 , 400 MHz):** δ 8.33 (s, 1H), 7.68 (dd, $J = 9.2$, $J = 4.4$ Hz, 1H), 7.51 (d, $J = 7.2$ Hz, 2H), 7.37 (t, $J = 6.0$ Hz, 1H), 7.31-7.23 (m, 2H), 6.68 (s, 1H), 4.00 (s, 2H), 3.14 (s, 3H), 2.38 (s, 3H). **^{13}C NMR (Acetone- d_6 , 100 MHz):** δ 192.6, 172.3, 171.8, 158.2 (d, $J = 237.0$ Hz), 144.3, 141.6, 138.9, 136.3, 129.9, 129.1, 128.3, 127.8 (d, $J = 4.0$ Hz), 126.3 (d, $J = 3.0$ Hz), 119.2 (d, $J = 4.0$ Hz), 115.0 (d, $J = 11.0$ Hz), 112.7 (d, $J = 27.0$ Hz), 111.2 (d, $J = 18.0$ Hz), 42.6, 34.7, 28.3. **IR (KBr, cm^{-1}):** 1712.36, 1682.72, 1574.90. **HRMS (ESI) m/z calcd for $\text{C}_{22}\text{H}_{17}\text{FN}_2\text{O}_3\text{Na}$ $[\text{M}+\text{Na}]^+$:** 399.1115; found: 399.1099.

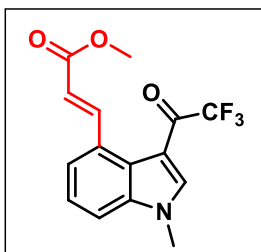


(E)-methyl 3-(3-formyl-1-methyl-1H-indol-4-yl)acrylate

(3aa1): was prepared according to general procedure (4.5a).

The crude reaction mixture was purified by column chromatography using silica gel (100-200 mesh), giving a

brown solid (10 mg, 33% yield) Rf: 0.45 (in 50% EtOAc/hexane). **¹H NMR (Acetone-*d*₆, 400 MHz):** δ 9.91(s, 1H), 9.51 (d, *J* = 16.0 Hz, 1H), 8.32 (s, 1H) 7.80 (d, *J* = 7.6 Hz, 1H), 7.67 (d, *J* = 8.4 Hz, 1H), 7.45 (d, *J* = 7.6 Hz, 1H), 6.54 (d, *J* = 16.0 Hz, 1H), 4.05 (s, 3H). **¹³C NMR (DMSO-*d*₆, 175 MHz):** δ 184.1, 168.2, 148.0, 147.1, 140.3, 129.1, 125.1, 125.0, 122.2, 119.0, 118.4, 114.0, 52.2, 34.5. **IR (KBr, cm⁻¹):** 1715.01, 1647.31. **HRMS (ESI) m/z** calcd for C₁₄H₁₃NO₃Na [M+Na]⁺: 266.0788; found: 266.0770.

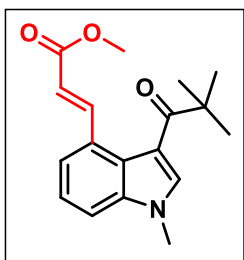


(E)-methyl 3-(1-methyl-3-(2,2,2-trifluoroacetyl)-1H-indol-4-yl)acrylate

(3aa2): was prepared according to general procedure (4.5a). The crude reaction mixture was purified by

column chromatography using silica gel (100-200 mesh),

giving a white solid (15 mg, 52% yield) Rf: 0.35 (in 20% EtOAc/hexane). **¹H NMR (CDCl₃, 400 MHz):** δ 9.51 (d, *J* = 16.0 Hz, 1H), 8.02 (s, 1H), 7.57 (dd, *J* = 6.0, 2.0 Hz, 1H), 7.42-7.37 (m, 2H), 6.32 (d, *J* = 16.0 Hz, 1H), 3.92 (s, 3H), 3.84 (s, 3H). **¹³C NMR (CDCl₃, 100 MHz):** δ 174.0 (d, *J* = 33.9 Hz), 167.8, 146.1, 141.2 (q, *J* = 6.0 Hz), 138.7, 130.7, 125.3, 125.1, 123.1, 119.2, 116.4, 111.9, 110.4, 52.1, 34.6. **IR (KBr, cm⁻¹):** 1718.05, 1559.94, 1401.28. **HRMS (ESI) m/z** calcd for C₁₅H₁₂F₃NO₃Na [M+Na]⁺: 334.0661; found: 334.0672.

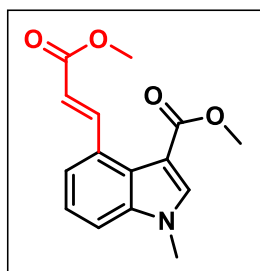


(E)-methyl 3-(1-methyl-3-pivaloyl-1H-indol-4-yl)acrylate

(3aa3): was prepared according to general procedure (4.5a).

The crude reaction mixture was purified by column chromatography using silica gel (100-200 mesh), giving pale

white liquid (23 mg, 81% yield) Rf: 0.5 (in 40% EtOAc/hexane). **¹H NMR (CDCl₃, 400 MHz):** δ 8.31 (d, *J* = 16.0 Hz, 1H), 7.52 (s, 1H), 7.44 (d, *J* = 7.2 Hz, 1H), 7.34-7.26 (m, 2H), 6.32 (d, *J* = 16.0 Hz, 1H), 3.80 (s, 6H) 1.39 (s, 9H). **¹³C NMR (CDCl₃, 100 MHz):** δ 206.1, 168.0, 145.0, 138.0, 132.1, 129.3, 126.2, 123.3, 121.1, 118.0, 116.0, 111.2, 52.1, 45.1, 34.0, 28.4. **IR (KBr, cm⁻¹):** 1713.64, 1644.60. **HRMS (ESI) m/z** calcd for C₁₈H₂₁NO₃Na [M+Na]⁺: 322.1414; found: 322.1429.



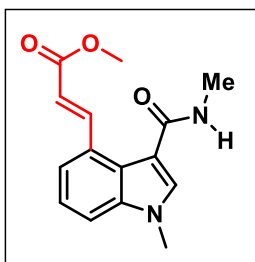
(E)-methyl 4-(3-methoxy-3-oxoprop-1-en-1-yl)-1-methyl-

1H-indole-3-carboxylate (3aa5): was prepared according to

general procedure (4.5a). The crude reaction mixture was purified by column chromatography using silica gel (100-200

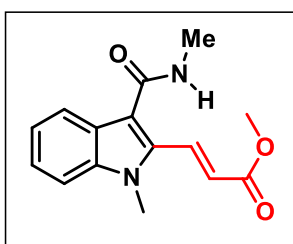
mesh), giving a brown solid (6 mg, 23% yield) Rf: 0.40 (in

30% EtOAc/hexane). **¹H NMR (CDCl₃, 400 MHz):** δ 9.31 (d, *J* = 16.0 Hz, 1H), 7.90 (s, 1H), 7.53 (d, *J* = 7.2, 1H), 7.36 (d, *J* = 7.6, 1H), 7.29 (t, *J* = 7.6 Hz, 1H), 6.39 (d, *J* = 16.0 Hz, 1H), 3.89 (s, 3H), 3.84 (s, 3H) 3.82(s, 3H). **¹³C NMR (CDCl₃, 100 MHz):** δ 168.1, 165.2, 146.6, 138.6, 138.2, 129.4, 125.2, 123.2, 121.1, 118.0, 111.7, 107.9, 51.9, 51.7, 33.9. **IR (KBr, cm⁻¹):** 1634.62, 1401.14, 1134.71. **HRMS (ESI) m/z** calcd for C₁₅H₁₅NO₄Na [M+Na]⁺: 296.0893; found: 296.0906.



(E)-methyl 3-(1-methyl-3-(methylcarbamoyl)-1H-indol-4-yl)acrylate (**3aa6**): was prepared according to general procedure (4.5a). The crude reaction mixture was purified by column chromatography using silica gel (100-200 mesh)

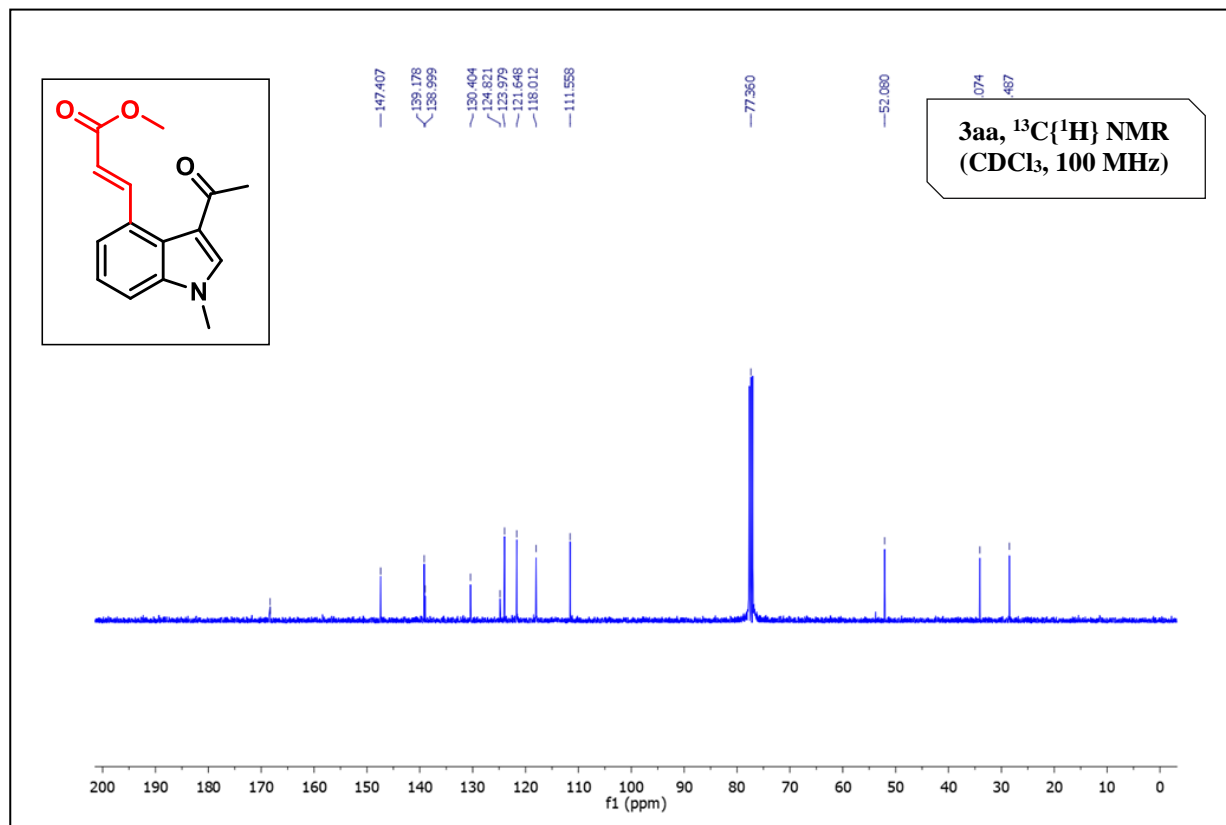
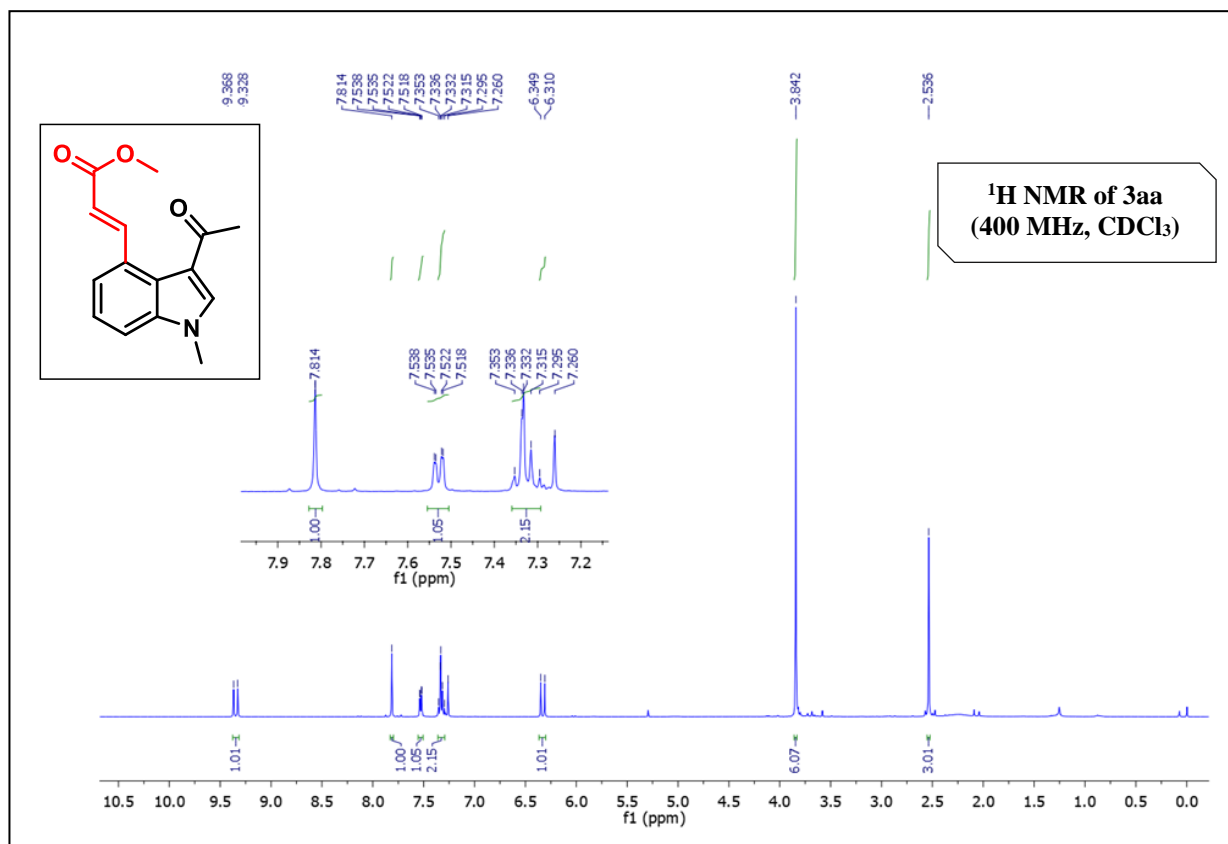
giving as pale white liquid (11 mg, 38% yield) R_f: 0.3 (in 90% EtOAc/hexane). **¹H NMR (DMSO-*d*₆, 400 MHz)**: δ 9.02 (d, *J* = 16.0 Hz, 1H), 8.08 (brs, 1H), 7.88 (s, 1H), 7.62 (d, *J* = 8.0 Hz, 2H), 7.30 (d, *J* = 8.0 Hz, 1H), 6.49 (d, *J* = 16.0 Hz, 1H), 3.85 (s, 3H) 3.74 (s, 3H) 2.80 (d, *J* = 4.4 Hz, 3H). **¹³C NMR (DMSO-*d*₆, 100 MHz)**: δ 167.8, 166.4, 146.3, 138.5, 134.3, 128.3, 125.3, 123.1, 120.2, 117.7, 113.3, 112.7, 52.2, 33.9, 27.0. **IR (KBr, cm⁻¹)**: 1636.12, 1404.74, 1026.56. **HRMS (ESI)** *m/z* calcd for C₁₅H₁₆N₂O₃Na [M+Na]⁺: 295.1053; found: 295.1020.



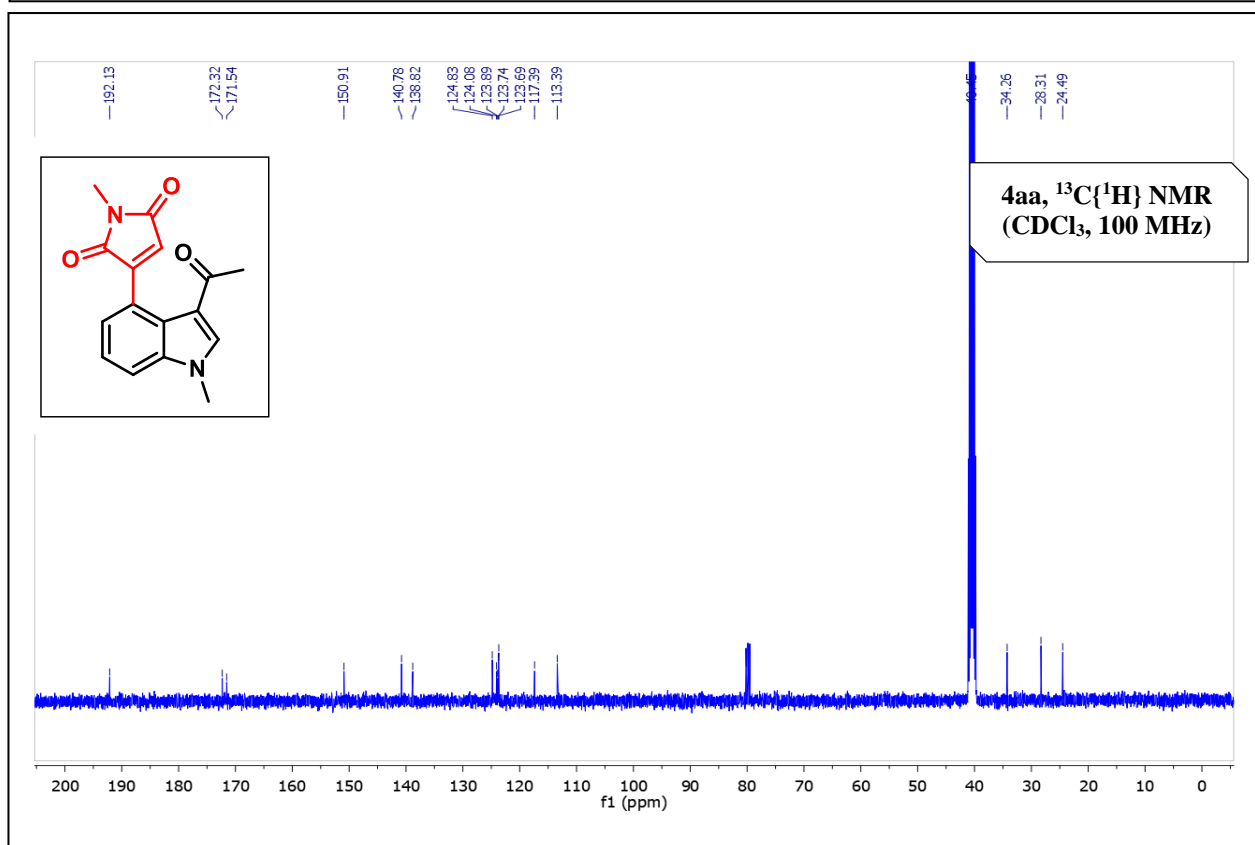
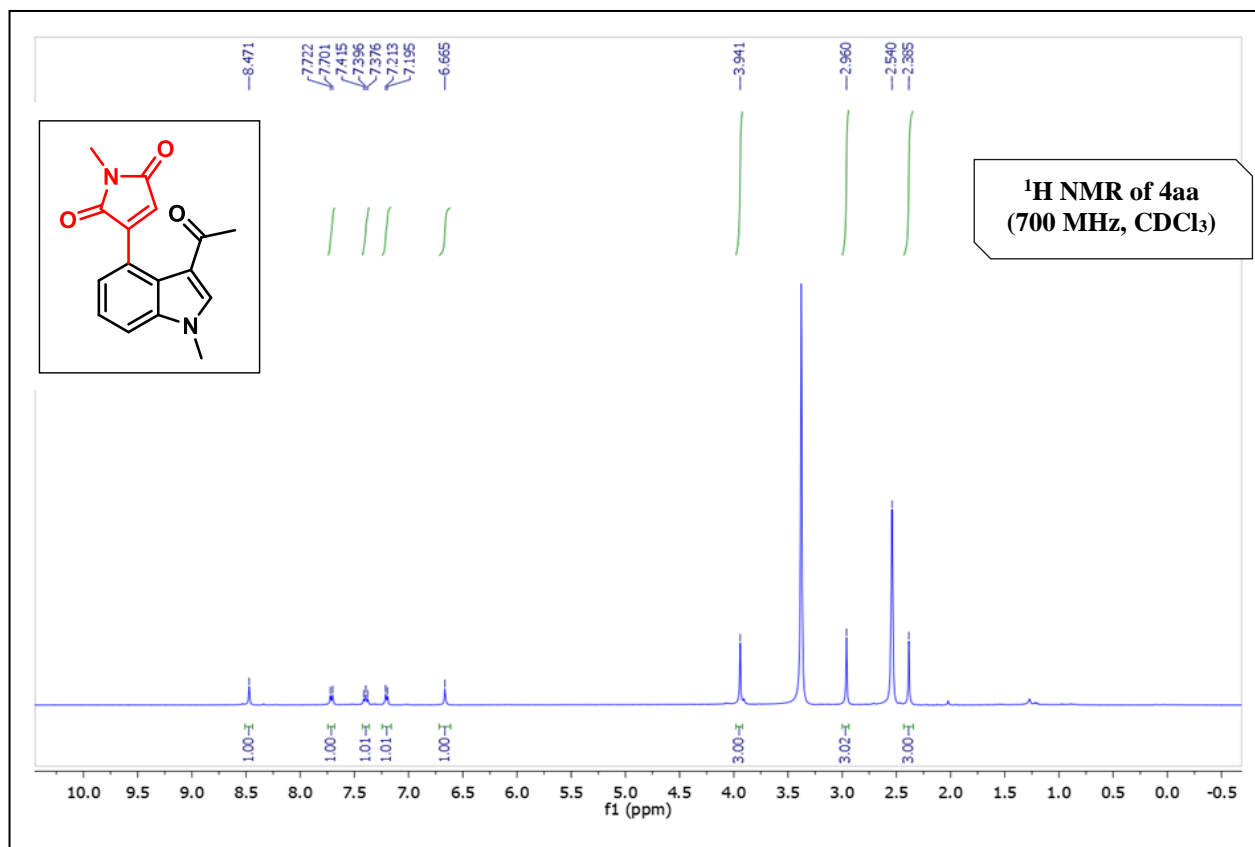
(E)-methyl 3-(1-methyl-3-(methylcarbamoyl)-1H-indol-2-yl)acrylate (**3aa7**): was prepared according to general procedure (4.5a). The crude reaction mixture was purified by column chromatography using silica gel (100-200

mesh), giving as pale white liquid (13 mg, 45% yield) R_f: 0.3 (in 90% EtOAc/hexane). **¹H NMR (DMSO-*d*₆, 400 MHz)**: δ 8.11 (d, *J* = 16.0 Hz, 1H), 8.06 (brs, 1H), 7.77 (d, *J* = 8.4 Hz, 1H), 7.63 (d, *J* = 8.4 Hz, 1H), 7.35 (d, *J* = 7.2 Hz, 1H), 7.21 (d, *J* = 7.2 Hz, 1H), 6.63 (d, *J* = 16.0 Hz, 1H) 3.92 (s, 3H) 1.79 (s, 3H), 2.86 (d, *J* = 4.4 Hz, 3H). **¹³C NMR (DMSO-*d*₆, 100 MHz)**: δ 167.6, 165.8, 138.9, 134.7, 133.6, 125.5, 125.2, 122.0, 121.7, 121.6, 115.9, 111.6, 52.7, 32.5, 27.2. **IR (KBr, cm⁻¹)**: 1637.35, 1400.78, 1025.62. **HRMS (ESI)** *m/z* calcd for C₁₅H₁₇N₂O₃ [M+H]⁺: 273.1234; found: 273.1244

NMR spectra of methyl (E)-3-(3-acetyl-1-methyl-1H-indol-4-yl)acrylate (3aa):



NMR spectra of 3-(3-acetyl-1-methyl-1H-indol-4-yl)-1-methyl-1H-pyrrole-2,5-dione (4aa):



(b) X-ray data of 3-(3-acetyl-5-fluoro-1-methyl-1H-indol-4-yl)-1-benzyl-1H-pyrrole-2,5-dione (5bd):

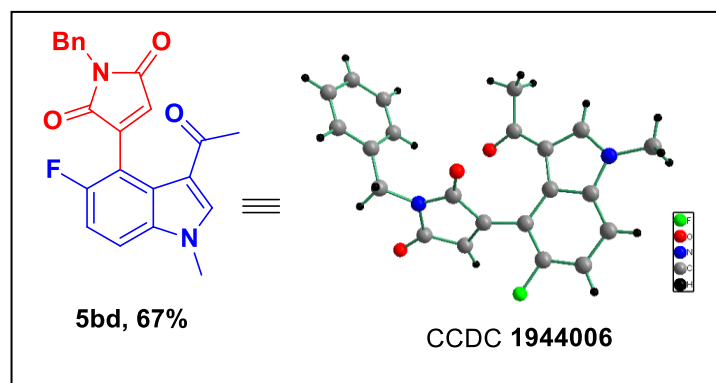
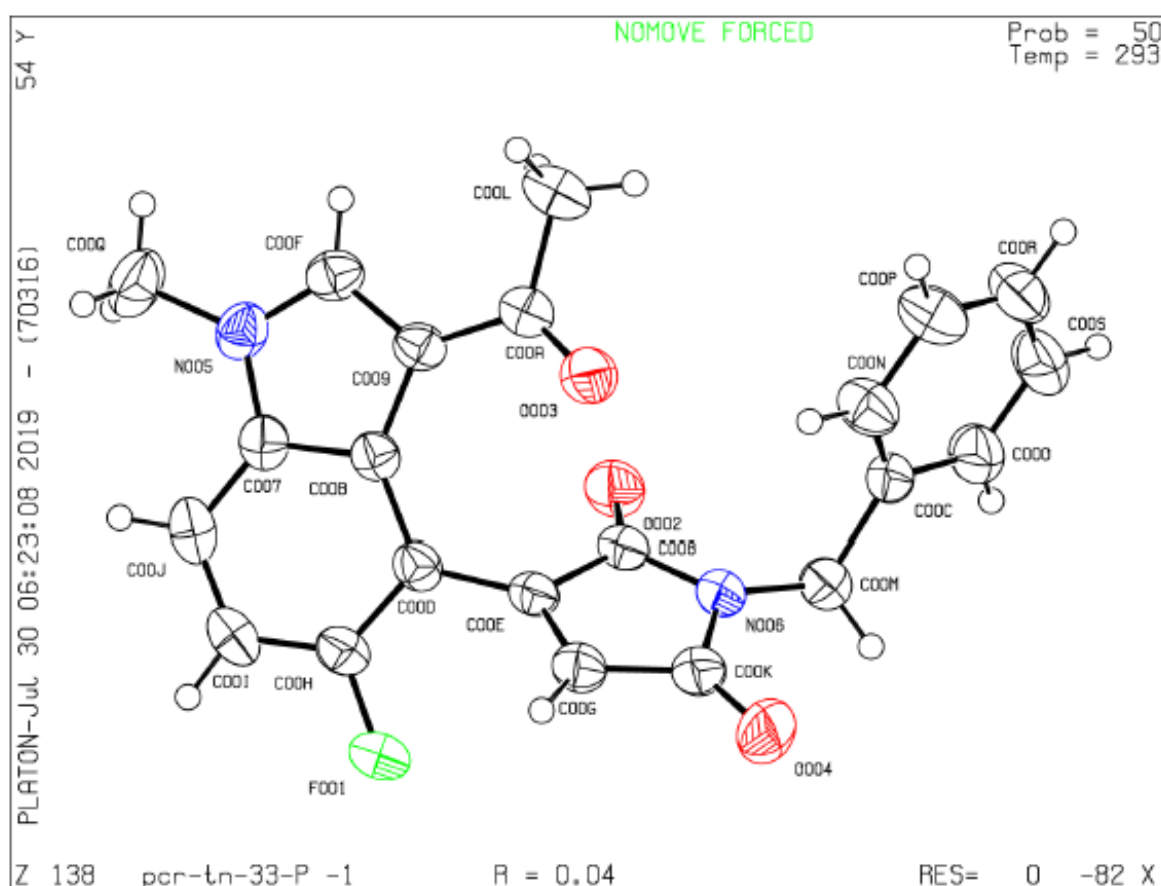


Figure 4.4. Crystal structure of 3bd (50% ellipsoid probability).



4.6 REFERENCES

1. (a) Taylor, R. D.; MacCoss, M.; Lawson, A. D. G. *J. Med. Chem.* **2014**, *57*, 5845–5859. (b) For recent reviews on synthesis of ergot alkaloids, see: (c) Liu, H.; Jia, Y. Ergot alkaloids: synthetic approaches to lysergic acid and clavine alkaloids. *Nat. Prod. Rep.* **2017**, *34*, 411–432. (d) McCabe, S. R.; Wipf, P. Total Synthesis, Biosynthesis and Biological Profiles of Clavine Alkaloids. *Org. Biomol. Chem.* **2016**, *14*, 5894–5913.
2. For a review, see: (a) Sandtorv, A. H. Transition Metal-Catalyzed C-H Activation of Indoles. *Adv. Synth. Catal.* **2015**, *357*, 2403–2435. For key seminal publications, see: (b) Wang, X.; Lane, B. S.; Sames, D. Direct C-Arylation of Free (NH)-Indoles and Pyrroles Catalyzed by Ar-Rh(III) Complexes Assembled in Situ. *J. Am. Chem. Soc.* **2005**, *127*, 4996–4997. (c) Stuart, D. R.; Villemure, E.; Fagnou, K. Elements of Regiocontrol in Palladium-Catalyzed Oxidative Arene Cross-Coupling. *J. Am. Chem. Soc.* **2007**, *129*, 12072–12073. (d) Deprez, N. R.; Kalyani, D.; Krause, A.; Sanford, M. S. Room Temperature Palladium-Catalyzed 2-Arylation of Indoles. *J. Am. Chem. Soc.* **2006**, *128*, 4972–4973. (e) Lebrasseur, N.; Larrosa, I. Room Temperature and Phosphine Free Palladium Catalyzed Direct C-2 Arylation of Indoles. *J. Am. Chem. Soc.* **2008**, *130*, 2926–2927.
3. (a) Hollins, R. A.; Colnago, L. A.; Salin, V. M.; Seidl, M. C. Thallation-iodination studies of heterocyclic systems *J. Heterocycl. Chem.* **1979**, *16*, 993–996. (b) S. Picard.; F.; Lecornu'e and G. Bashiardes, Synthesis of Unique Analogues of the Ergoline Skeleton Using Intramolecular [3+2] Cycloaddition. *Synlett*, **2014**, *25*, 1106–1110. (c) Düfert, M. A.; Billingsley, K. L.; Buchwald, S. L. Suzuki-Miyaura Cross-Coupling of Unprotected, Nitrogen-Rich Heterocycles: Substrate Scope and Mechanistic Investigation. *J. Am. Chem. Soc.* **2013**, *135*, 12877–12885. (d) Hartung, C. G.; Fecher, A.; Chapell, B.; Snieckus, V. Directed *ortho*-Metalation Approach to C-7-Substituted Indoles. Suzuki-Miyaura Cross Coupling and the Synthesis of Pyrrolophenanthridone Alkaloids. *Org. Lett.* **2003**, *5*, 1899–1902. (e) Alberico, D.; Scott, M. E.; Lautens, M. Aryl-Aryl Bond Formation by Transition-Metal-Catalyzed Direct Arylation. *Chemical Reviews*. **2007**, *107*, 174. (f) Brückl, T.; Baxter, R. D.; Ishihara, Y.; Baran, P. S. Innate and Guided C-H Functionalization Logic. *Acc. Chem. Res.* **2012**, *45* (6), 826–839.
4. (a) Yang, J. Transition Metal Catalyzed Meta-C-H Functionalization of Aromatic Compounds. *Organic and Biomolecular Chemistry*. **2015**, *13*, 1930–1941 (b) Dey, A.; Agasti, S.; Maiti, D. Palladium Catalysed: Meta -C-H Functionalization Reactions. *Org. Biomol. Chem.* **2016**, *14*, 5440–5453. (c) Frost, C. G.; Paterson, A. J. Directing Remote Meta-C-H Functionalization with Cleavable Auxiliaries. *ACS Central Science*. **2015**, *1*, 418–419 (d) Ackermann, L.; Li, J. C-H Activation: Following Directions. *Nature Chemistry*. **2015**, *7*, 686–687. (e) Banjare, S. K.; Chebolu, R.; Ravikumar, P. C. Cobalt Catalyzed Hydroarylation of Michael Acceptors with Indolines Directed by a Weakly Coordinating Functional Group. *Org. Lett.* **2019**, *21*, 4049–4053.
5. (a) Kalepu, J.; Gandeepan, P.; Ackermann, L.; Pilarski, L. T. C4-H Indole Functionalisation: Precedent and Prospects. *Chem. Sci.* **2018**, *9*, 4203–4216. (b) Leitch, J. A.; Bhonoah, Y.; Frost, C. G. Beyond C2 and C3: Transition-Metal-Catalyzed C-H Functionalization of Indole. *ACS Catalysis*. **2017**, *7*, 5618–5627. (c) Lanke, V.; Bettadapur, K. R.; Prabhu, K. R. Electronic Nature of Ketone Directing Group as a Key to Control C-2 vs C-4 Alkenylation of Indoles. *Org. Lett.* **2016**, *18* (21), 5496–5499. (d) Yang, Y.; Qiu, X.; Zhao, Y.; Mu, Y.; Shi, Z. Palladium-Catalyzed C-H Arylation of Indoles at the C7 Position. *J. Am. Chem. Soc.* **2016**, *138*, 495–498.
6. For a review, see: (a) Gandeepan, P.; Müller, T.; Zell, D.; Cera, G. Warratz, S.; Ackermann, L. 3d Transition Metals for C-H Activation. *Chem. Rev.* **2019**, *119*, 2192–2452. (b) Kulkarni, A. A.; Daugulis, O. Direct Conversion of Carbon-Hydrogen into Carbon-Carbon Bonds by First-Row Transition-Metal Catalysis. *Synthesis*. **2009**, *24*, 4087–4109. (c) Su, B.; Cao, Z.-C.; Shi, Z.-J. Exploration of Earth-Abundant Transition Metals (Fe, Co, and Ni) as Catalysts in Unreactive Chemical Bond Activations. *Acc. Chem. Res.* **2015**, *48*, 886–896. (d) Pototschnig, G.; Maulide, N.; Schnürch, M. Direct Functionalization of C–H Bonds by Iron, Nickel, and Cobalt Catalysis. *Chemistry - A European Journal*. **2017**, *23*, 9206–9232. (e) Liu, J.; Chen, G.; Tan, Z. Copper-Catalyzed or -Mediated C-H Bond Functionalizations Assisted by Bidentate Directing Groups. *Adv. Synth. Catal.* **2016**, *358* (8), 1174–1194 (f) Liu, W.; Ackermann, L. Manganese-Catalyzed C-H Activation. *ACS Catal.* **2016**, *6*, 3743–3752. (g)

- Yoshino, S.; Matsunaga, S. High-Valent Cobalt-Catalyzed C-H Bond Functionalization *Adv. Organomet. Chem.* **2017**, *68*, 197–247. (h) Yoshino, T.; Ikemoto, H.; Matsunaga, S.; Kanai, M. A Cationic High-Valent Cp*Co(III) Complex for the Catalytic Generation of Nucleophilic Organometallic Species: Directed C-H Bond Activation. *Angew. Chem., Int. Ed.* **2013**, *52*, 2207–2211. (i) Wang, S.; Chen, S.-Y.; Yu, X.-Q. C-H Functionalization by High-Valent Cp*Co(III) Catalysis. *Chem. Commun.* **2017**, *53*, 3165–3180.
7. (a) Engle, K. M.; Mei, T. S.; Wasa, M.; Yu, J. Q. Weak Coordination as a Powerful Means for Developing Broadly Useful C-H Functionalization Reactions. *Acc. Chem. Res.* **2012**, *45*, 788–802. (b) De Sarkar, S.; Liu, W.; Kozhushkov, S. I.; Ackermann, L. Weakly Coordinating Directing Groups for Ruthenium (II)-Catalyzed C-H Activation. *Adv. Synth. Catal.* **2014**, *356*, 1461–1479. (c) Das, R.; Kumar, G. S.; Kapur, M. Amides as Weak Coordinating Groups in Proximal C-H Bond Activation. *Eur. J. Org. Chem.* **2017**, *37*, 5439–5459. (d) Kim, J.; Kim, J.; Chang, S. Ruthenium-Catalyzed Direct C-H Amidation of Arenes Including Weakly Coordinating Aromatic Ketones. *Chem. - A Eur. J.* **2013**, *19*, 7328–7333.
 8. (a) Koubachi, J.; El Brahmi, N.; Guillaumet, G.; El Kazzouli, S. Oxidative Alkenylation of Fused Bicyclic Heterocycles. *European Journal of Organic Chemistry*. **2019**, 2568–2586. (b) Koubachi, J.; Berteina-Raboin, S.; Mouaddib, A.; Guillaumet, G. Pd/Cu-Catalyzed Oxidative C-H Alkenylation of Imidazo[1,2-*a*]Pyridines. *Synthesis (Stuttg.)*. **2009**, *2*, 271–276. (c) Kim, D. S.; Park, W. J.; Jun, C. H. Metal-Organic Cooperative Catalysis in C-H and C-C Bond Activation. *Chemical Reviews*. **2017**, *117*, 8977–9015. (d) Padala, K.; Jeganmohan, M. Ruthenium-Catalyzed *Ortho*-Alkenylation of Aromatic Ketones with Alkenes by C-H Bond Activation. *Org. Lett.* **2011**, *13*, 6144–6147.
 9. (a) Muniraj, N.; Prabhu, K. R. Cobalt(III)-Catalyzed C-H Activation: Azo Directed Selective 1,4-Addition of *ortho*-C-H Bond to Maleimides. *J. Org. Chem.* **2017**, *82*, 6913–6921. (b) Zhang, Z.; Han, S.; Tang, M.; Ackermann, L.; Li, J. C-H Alkylations of (Hetero) Arenes by Maleimides and Maleate Esters through Cobalt(III) Catalysis. *Org. Lett.* **2017**, *19*, 3315–3318. (c) Chen, X.; Ren, J.; Xie, H.; Sun, W.; Sun, M.; Wu, B. Cobalt(III)-catalyzed 1,4-addition of C-H bonds of oximes to maleimides. *Org. Chem. Front.* **2018**, *5*, 184–188. (d) Mandal, R.; Emayavaramban, B.; Sundararaju, B. Cp*Co(III)-Catalyzed C-H Alkylation with Maleimides Using Weakly Coordinating Carbonyl Directing Groups. *Org. Lett.* **2018**, *20*, 2835–2838. (e) Muniraj, N.; Prabhu, K. R. Cobalt(III)-Catalyzed [4 + 2] Annulation of N-Chlorobenzamides with Maleimides. *Org. Lett.* **2019**, *21*, 1068–1072. (f) Jeganmohan, M.; Manoharan, R. Alkylation, Annulation and Alkenylation of Organic Molecules with Maleimides via Transition-Metal-Catalyzed C-H Bond. *Asian J. Org. Chem.* **2019** in press. DOI: 10.1002/ajoc.201900054.
 10. The standard reaction conditions showed similar results even with higher scale, i.e., 1 mmol scale reaction of **1a**, and afforded the respective C-4 alkenylated product **3aa** in 82% yield.
 11. (a) Sk, M. R.; Bera, S. S.; Maji, M. S. Cp*Co(III)-Catalyzed C-H Alkenylation of Aromatic Ketones with Alkenes. *Adv. Synth. Catal.* **2019**, *361*, 585–590. (b) Sherikar, M. S.; Kapaniaiah, R.; Lanke, V.; Prabhu, K. R. Rhodium(III)-Catalyzed C-H Activation at the C4-Position of Indole: Switchable Hydroarylation and Oxidative Heck-Type Reactions of Maleimides. *Chem. Commun.* **2018**, *54*, 11200–11203. (c) Feng, R.; Yu, W.; Wang, K.; Liu, Z.; Zhang, Y. Ester-Directed Selective Olefination of Acrylates by Rhodium Catalysis. *Adv. Synth. Catal.* **2014**, *356*, 1501–1508. (d) Yokoyama, Y.; Unoh, Y.; Hirano, K.; Satoh, T.; Miura, M. Rhodium(III)-Catalyzed Regioselective C-H Alkenylation of Phenylphosphine Sulfides. *J. Org. Chem.* **2014**, *79*, 7649–7655. (e) Patureau, F. W.; Besset, T.; Glorius, F. *Angew. Chem., Int. Ed.* **2011**, *50*, 1064–1067. (f) Padala, K.; Jeganmohan, M. Ruthenium-Catalyzed *ortho*-Alkenylation of Aromatic Ketones with Alkenes by C-H Bond Activation. *Org. Lett.* **2011**, *13*, 6144–6147. (g) Grigorjeva, L.; Daugulis, O. *Org. Lett.* **2014**, *16*, 4684–4687. (h) Suzuki, Y.; Sun, B.; Yoshino, T.; Kanai, M.; Matsunaga, S. *Tetrahedron* **2015**, *71*, 4552–4556. (i) Graczyk, K.; Ma, W.; Ackermann, L. Oxidative Alkenylation of Aromatic Esters by Ruthenium-Catalyzed Twofold C-H Bond Cleavages. *Org. Lett.* **2012**, *14*, 4110–4113. (j) Kozhushkov, S. I.; Ackermann, L. Ruthenium-Catalyzed Direct Oxidative Alkenylation of Arenes Through Twofold C-H Bond Functionalization. *Chem. Sci.* **2013**, *4*, 886–896.
 12. Hugo E. Gottlieb, Vadim Kotlyar, and Abraham Nudelman, NMR chemical shifts of common laboratory solvents as trace impurities. *J. Org. Chem.* **1997**, *62*, 7512–7515.

Chapter 5

Breaking the Trend: Insight into Unforeseen Reactivity of Alkynes in Cobalt-Catalyzed Weak Chelation-Assisted Regioselective C(4)–H Functionalization of 3-Pivaloyl Indole

5.1 Abstract

5.2 Introduction

5.3 Results and Discussions

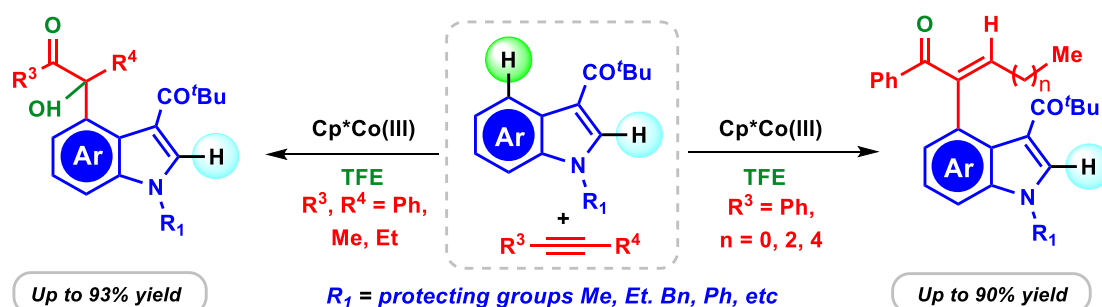
5.4 Conclusions

5.5 Experimental Section

5.6 References

Chapter 5

Breaking the Trend: Insight into Unforeseen Reactivity of Alkynes in Cobalt-Catalyzed Weak Chelation-Assisted Regioselective C(4)–H Functionalization of 3-Pivaloyl Indole



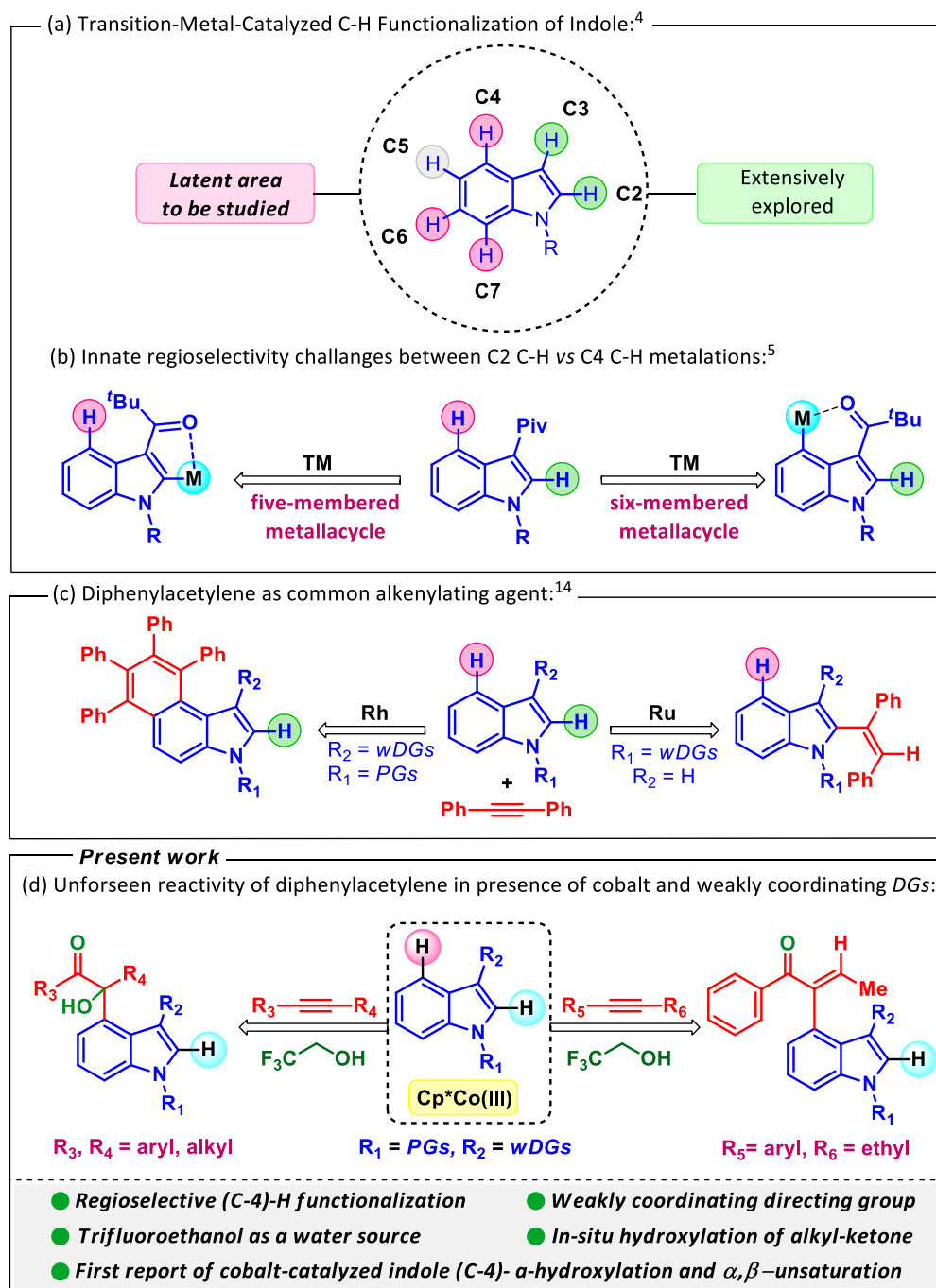
5.1 ABSTRACT

The unique reactivity of diphenylacetylene has been uncovered through weak chelation-assisted cobalt-catalyzed regioselective C(4)–H activation of 3-pivaloyl indole. α -hydroxy and α,β -unsaturated ketone derivatives have been synthesized in good yields from indole and alkynes. Notably, the indole C(4)–H-functionalized α,β -unsaturated ketone product was obtained with high stereo- and regioselectivity simply by changing the coupling partner from symmetrical alkynes to unsymmetrical aromatic-aliphatic alkynes. Most importantly, trifluoroethanol is the sole water source for this conversion. Quantitative detection of bis(2,2,2-trifluoroethyl) ether from dry trifluoroethanol through ^{19}F NMR and LCMS studies indirectly confirms the in situ formation of water. A six-membered cobaltacycle intermediate was detected in HRMS, and also, this was further confirmed by the quantum mechanical calculations, which account for the highly regioselective C(4)–H functionalization.

5.2 INTRODUCTION

The increasing demand for *N*-heterocyclic scaffolds in the pharmaceutical industry makes it a highly attractive target for synthetic and medicinal chemists.¹ In this regard, indoles, and indolines are one of the most admired skeletons because their derivatives exhibit significant biological activities such as antibacterial, anticancer, antioxidant, anti-inflammatory, antidiabetic, antiviral, and antispermatogenic activity.² The wide applications of the indole systems were well documented by Lawson et al. in 2014 and by Manju et al. in 2016.³ Functionalization of indole C–H bonds assumes significance due to its potential application in medicinal chemistry. The selective C–H functionalization of indole at the C2 or C3 position has been well explored due to the high reactivity of the pyrrole ring in indole (Figure 5.1a).⁴ Nevertheless, in recent years, various methods have been developed for benzenoid C–H functionalization at the C6 and C7 positions of indole using *N*-protected directing groups.⁵ However, selective C(4)–H functionalization is an underdeveloped and challenging task, which can be addressed by installing a directing group at the C3 position of indole.⁶ Despite the proximal directing group, the inherent challenge that makes the functionalization of indole C(4)–H difficult is the formation of a five-membered metallacycle at the C2 position, as compared to six-membered metallacycle at the C4 position (Figure 5.1b). Furthermore, the stronger σ donor *N*-coordinating directing groups (pyridine, pyrimidine, 8-amino quinoline, etc.) have been extensively used for C2–C7 C–H functionalization in indoles and indolines. However, the installation and removal of such directing groups limit their application. This opens up a vast opportunity to use easily modifiable *O*-coordinating functional groups (aldehyde, ketone, ester, etc.) as directing groups in such functionalizations.⁷

Figure 5.1. Transition metal-catalyzed C–H functionalizations of indole.



Recently, few research groups have demonstrated methodologies on selective C(4)–H functionalization of indole via C–H activation using noble transition metals such as Ir, Rh, Ru, and Pd.⁸ The exuberant cost of such metals limits their applications in industries; therefore, a cheaper and more abundant catalytic system needs to be

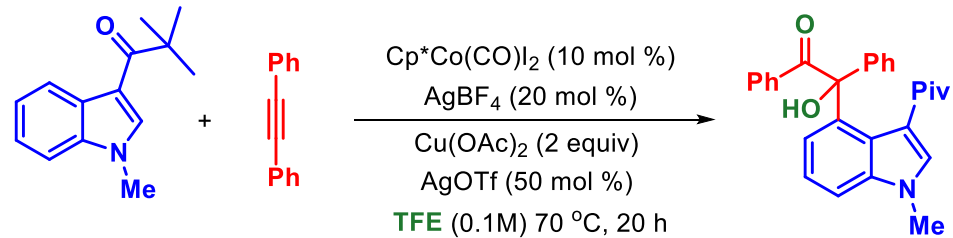
developed for sustainable synthesis. In this vein, exploiting the reactivity of first-row transition metals is gaining much attention in recent years due to their high abundance, low cost, and less exploration.⁹ Among the first-row metals, cobalt-catalyzed C–H functionalization has become an active research area in recent years.¹⁰ Cobalt’s ability to mimic rhodium in reactivity and selectivity has brought huge success to various pioneering research groups.¹¹ Though cobalt-catalyzed C–H activation with a variety of *N*-coordinating directing groups (strong coordination) were well studied, only limited reports are available on exploiting the *O*-coordinating ability (weak coordination) of commonly prevailing directing groups such as aldehyde, ketone, ester, carboxylic acid, etc.¹² This provides an eccentric opportunity to fine-tune the combination of “cobalt-weak coordination” to address the previous issues. In this regard, we have successfully demonstrated indole C(4)–H and indoline C(7)–H functionalization using various weak coordinating directing groups employing cobalt as the first-row transition metal catalyst.¹³ For over a decade, diphenylacetylene has been the most successful alkenylating agent through C–H activation.¹⁴ In this context, regioselective indole C(2)-alkenylation^{14a} and C(4)–C(5)-alkenylation followed by annulation^{14b} have been reported using ruthenium and rhodium catalysts, respectively (Figure 5.1c). Notably, with our key strategy (cobalt-weak coordination), when alkyne was chosen as the coupling partner, completely new reactivity was achieved, delivering regioselective C(4)–H functionalized α -hydroxy ketone and α,β -unsaturated ketones (Figure 5.1d). The product selectivity depends upon the type of alkyne chosen for the reaction. Thus, we have revealed the synthesis of α -hydroxy ketone and α,β -unsaturated ketone derivatives in a controlled manner. The key features of this protocol are (i) regioselective C(4)–H activation of indole, (ii) use of weakly coordinating directing

groups, (iii) in situ generations of water from trifluoroethanol, (iv) cobalt as a sustainable catalyst, (v) synthesis of α -hydroxy ketone and α,β -unsaturated ketone derivatives from indole and alkynes for the first time, and (vi) observation of a single stereoisomer with an unsymmetrical alkyne (1-phenyl-butyne).

5.3 RESULTS AND DISCUSSION

We started our study with *N*-methyl 3-pivaloyl indole **1a** and diphenylacetylene **2a** in the presence of cobalt catalysts, silver salts, and copper acetate. After extensive investigation^{15a} of different reaction parameters, a composition containing Cp*Co-(CO)I₂ (10 mol %) as the catalyst, AgBF₄ (20 mol %) as the additive, Ag(OTf) (50 mol %) as the promoter, and Cu(OAc)₂ (2 equiv) as the oxidant in dry 2,2,2-trifluoroethanol (TFE) as a solvent as well as the oxygen source at 70 °C facilitated the formation of the desired product **3aa** in 93% isolated yields (Table 5.1, entry 1). Deviations from the standard condition were performed by changing different reaction parameters to validate the versatility of the optimized condition. We have screened other oxygenated, hydrocarbon, and chlorinated solvents such as methanol, tetrahydrofuran, 1,4-dioxane, benzene, toluene, dichloromethane, and acetonitrile instead of dry TFE, but these solvents seem unsuitable for the transformation (Table 5.1, entry 2). However, hexafluoroisopropanol (HFIP) was found to deliver the expected product **3aa** in 72% yield (Table 5.1, entry 3). Further screening of mixture solvents like TFE: HFIP (1:1) decreases the product yield (Table 5.1, entry 4). A detrimental effect on the product yield was observed while screening of different silver salts such as AgSbF₆, AgNTf₂, and Ag₂O instead of AgBF₄ (Table 5.1, entries 5–7). When one equivalent of Cu(OAc)₂ was used instead of two equivalents, product yield was reduced (Table 5.1, entry 8).

Table 5.1. Optimization of Reaction Conditions^{a,b,c}

<div></div>		
1a (1 equiv)	2a (4 equiv)	3aa
entry	deviation from the standard conditions	yield of 3aa (%) ^b
1	none	93
2 ^c	other solvents instead of TFE	0
3	HFIP as a solvent instead of TFE	72
4	mixture solvents TFE:HFIP (1:1)	47
5	AgSbF ₆ instead of AgBF ₄ as a additive	46
6	AgNTf ₂ instead of AgBF ₄ as a additive	10
7	AgO instead of AgBF ₄ as a silver salt	trace
8	1 equiv instead of 2 equiv of Cu(OAc) ₂	74
9	Cu ₂ O instead of Cu(OAc) ₂ as a additive	24
10	LiOAc instead of Cu(OAc) ₂ as a additive	33
11	Zn(OTf) ₂ instead of AgOTf	48
12	NaOTf instead of AgOTf	66
13	Co(acac) ₂ instead of Cp*Co(CO)I ₂ as a catalyst	0
14	Co ₂ (CO) ₈ instead of Cp*Co(CO)I ₂ as a catalyst	0
15	2 equiv instead of 4 equiv of 2a	57
16	3 equiv instead of 4 equiv of 2a	76
17	temperature 50 °C instead of 70 °C	43
18	temperature 90 °C instead of 70 °C	82
19	without Cu(OAc) ₂ as a additive	32
20	without Cp*Co(CO)I ₂ as a catalyst	0
21	other directing groups instead of pivaloyl	0

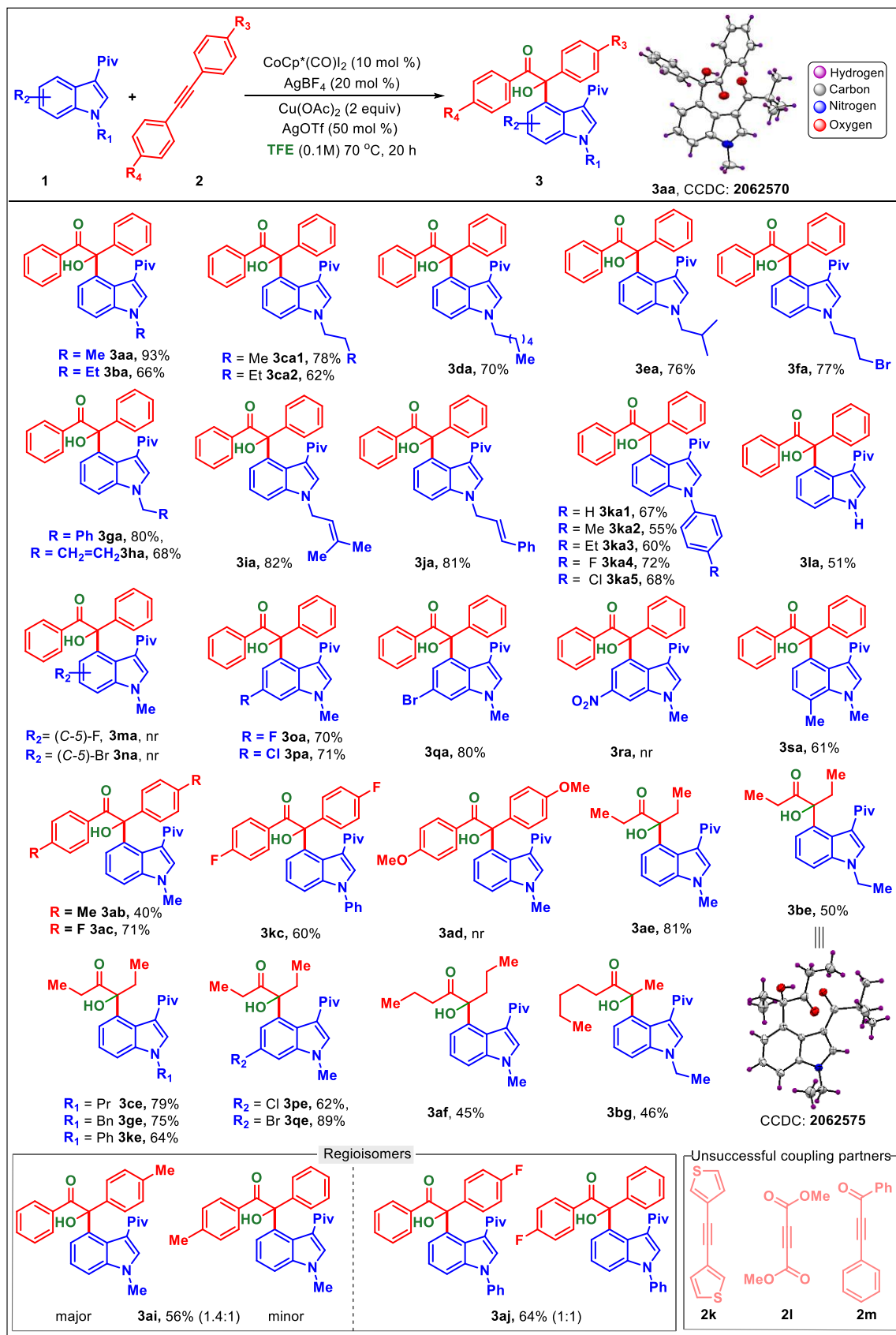
^aReaction conditions: **1a** (0.1 mmol), **2a** (0.4 mmol), Cp*Co(CO)I₂ (10 mol %), Ag salt (20 mol %), Lewis acids (50 mol %), additive (2 equiv), dry solvents (1 mL), 70 °C, N₂.

^bIsolated yield. ^cMethanol, tetrahydrofuran, 1,4-dioxane, benzene, toluene, dichloromethane, and acetonitrile.

When Cu₂O was used as the oxidant, a 24% yield of product **3aa** was formed, whereas LiOAc gave the desired product a reasonable yield (Table 5.1, entries 9 and 10). To check the effect of other metal triflates, Zn(OTf)₂ and NaOTf were explored; this led to lower yields (Table 5.1, entries 11 and 12). Changing the catalyst from Cp^{*}Co to simple cobalt salt could not assist the designed C–H activation reaction, which indicates the unique reactivity of the Cp^{*}Co catalyst (Table 5.1, entries 13 and 14). Decreasing the equivalents of diphenylacetylene **2a** reduces the product yield **3aa** (Table 1, entries 15 and 16). It is worth mentioning that under the standard reaction conditions, we also observed the diphenylacetylene-derived side product 1,2 diphenylethanone **2a***. Therefore, excess alkyne (4 equivalents) is crucial for this transformation. The product formation seems to be facilitated by increased equivalents of the alkyne coupling partner. Further physical deviations, such as temperature, did not produce any positive result (Table 5.1, entries 17 and 18). Therefore, it is clear that 70 °C is the optimum temperature for this transformation. Reaction performed without copper acetate resulted in a reduced yield (Table 5.1, entry 19), which tells us that copper acetate plays an essential role in this transformation. To understand the influence of Cp^{*}Co(III), we carried out the reaction without the cobalt catalyst, which resulted in no reaction (Table 5.1, entry 20). After stabilizing standard reaction conditions, further, we screened other *O*-coordinating directing groups such as *N*-methyl indole-(C-3)-CHO, (C-3)-COCH₃, (C-3)-CO₂H, and (C-3)-CO₂CH₃. We found the pivaloyl group as the best for this transformation (Table 5.1, entry 21).

Next, we scrutinized the optimized condition's general applicability by varying indoles **1** and alkynes **2** to synthesize highly desirable α- hydroxy ketone derivatives (Scheme 5.1).

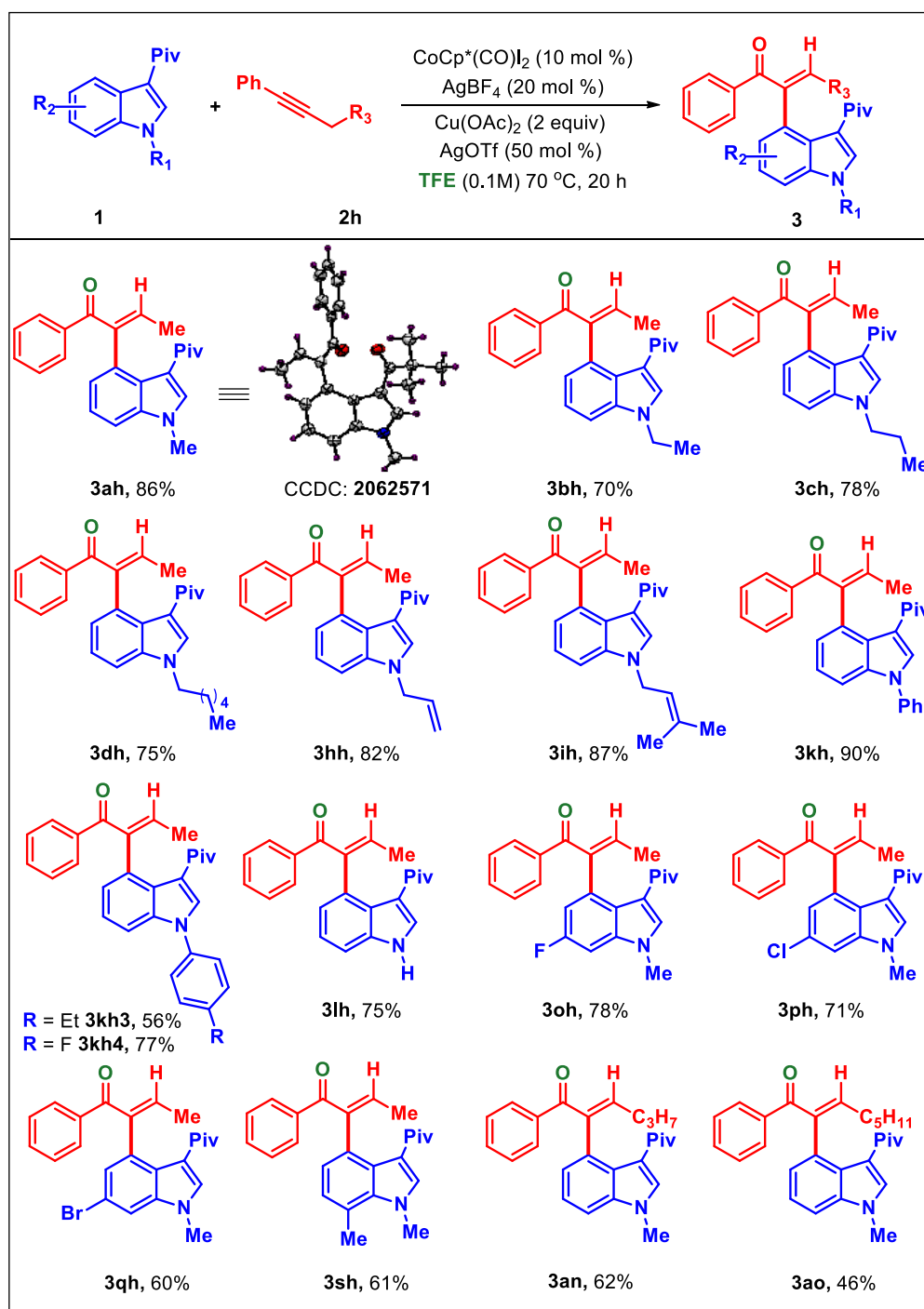
Scheme 5.1. Substrate Scope of Indole Derivatives with Various Alkynes



We have taken various *N*-protected indoles and subjected to standard reaction conditions. When the alkyl chain length was varied, good to excellent product conversion was observed, delivering 62–93% of the desired product (Scheme 5.1, **3aa–3da**). Furthermore, switching to isobutyl, bromo propyl, and benzyl protection of indole showed good compatibility with the reaction condition (Scheme 5.1, **3ea–3ga**). *N*-allyl protected indoles were well tolerated in the reaction condition giving 68–82% yield of the desired α -hydroxy ketone derivatives (Scheme 5.1, **3ha–3ja**). Further screening of various *N*-phenyl-substituted indoles gave the expected products **3ka1–3ka5** in 55–70% yields. Synthetically useful *NH* indole also gave the product in 51% yield, which is usually less reactive (Scheme 5.1, **3la**). The steric effect on the C5 position of indole was tested by varying different substituents. When C5-fluoro- and bromo-substituted indoles were tested, no reactivity was observed, which signifies that steric hindrance at the C5 position retards the reaction (Scheme 5.1, **3ma**, **3na**). C6 halo-substituted indoles gave good yields of the α -hydroxy ketone, which can be further functionalized to different synthetically useful skeletons (Scheme 5.1, **3oa–3qa**). In most of the weak chelation-directed cobalt-catalyzed C–H activation reactions, the presence of an electron-withdrawing group in the substrate results in no product formation¹³. As expected, we observed no reactivity of **2ra** under our reaction conditions (Scheme 5.1, **3ra**). C7- methylated indole gave the desired product **3sa** in 61% yield. A variety of aromatic alkyne was also tested, which gave us the desired products in moderate to good yields (Scheme 5.1, **3ab**, **3ac**, and **3kc**). Surprisingly, the electron-donating group containing alkyne did not yield the desired product **3ad**. We presume that the C–Co bond generated after the C–H activation step might be very nucleophilic due to the electronegativity of cobalt, and hence the addition to an electron-

rich alkyne is hampered. Moreover, the literature has reported that the C–Co bond is known to react as a nucleophile.^{15d}

Scheme 5.2. Substrate Scopes of Indole and Unsymmetrical Alkyne



Given the intriguing reactivity of diphenyl acetylene in cobalt-catalyzed C–H functionalization, we chose aliphatic alkynes to show the diversity in alkyne scope.

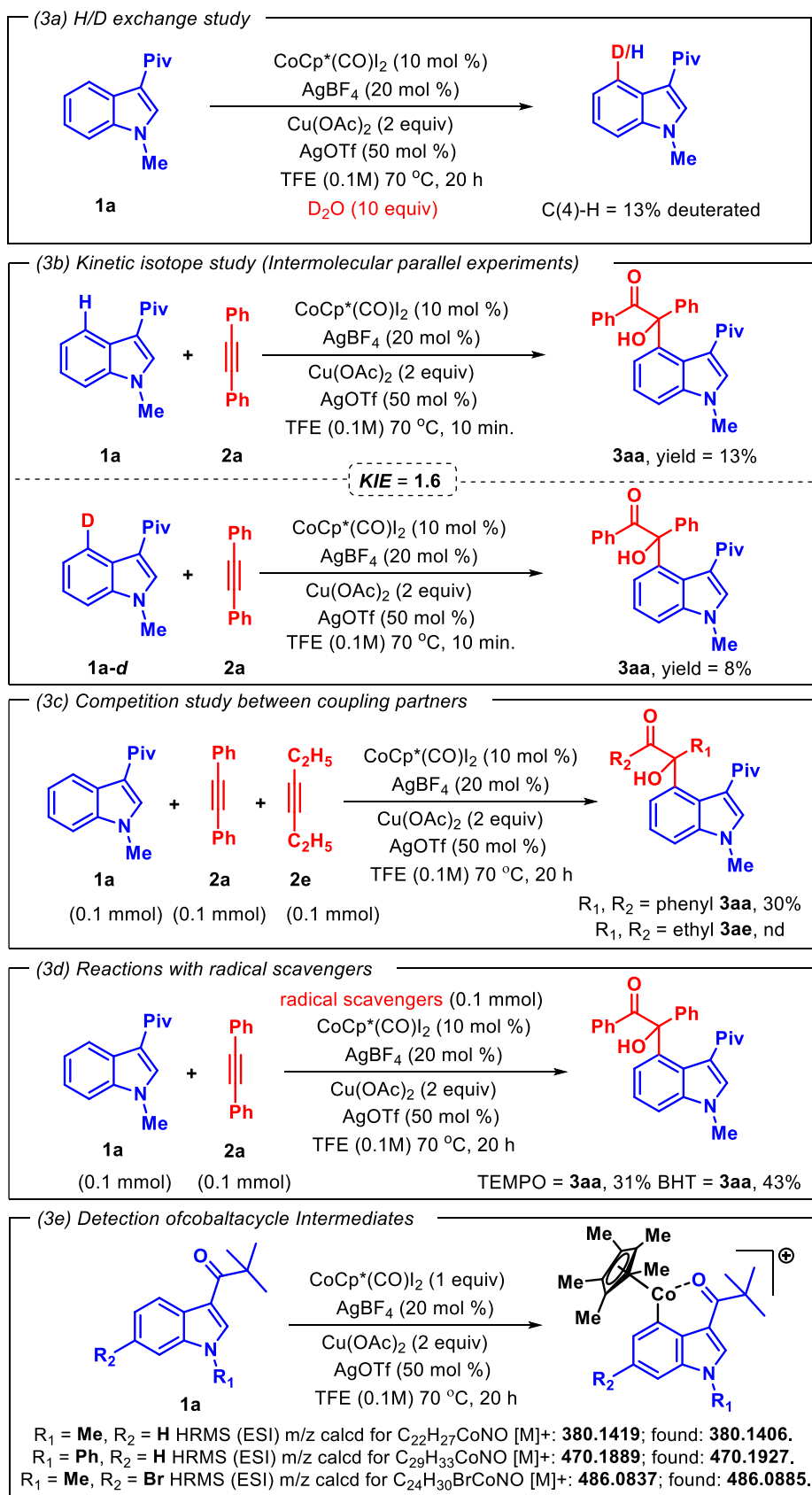
Synthesis of the α -hydroxy ketone is tricky with aliphatic alkynes due to the possibility of an elimination pathway leading to α,β -unsaturated ketone derivatives. Despite this limitation, we successfully synthesized numerous α -hydroxy ketone derivatives from aliphatic alkynes. Various indole derivatives were screened by taking 3-hexyne as the α -hydroxy ketone surrogate. *N*-Me, Et, and propyl 3-pivaloyl indoles gave us the desired product in moderate to good yields (Scheme 5.1, **3ae**– **3ce**). Furthermore, *N*-benzyl and phenyl 3-pivaloyl indoles worked well under the optimized condition giving 75–64% yield of the targeted product (Scheme 5.1, **3ge**, and **3ke**). Moreover, C6 halo-substituted indoles were well tolerated under the reaction condition (Scheme 5.1, **3pe**, and **3qe**). Switching to 4-octyne also gave the product in 45% yield (Scheme 5.1, **3af**). Notably, unsymmetrical 2-octyne gave the desired product with high regioselectivity, preferring the ketone on the more substituted side (Scheme 5.1, **3bg**). Furthermore, screening of unsymmetrical aromatic alkynes has given both regioisomers of their products **3ai**–**3ji**. In contrast, the heteroaromatic alkyne and other carbonyl substituted alkynes have failed to give desired products (Scheme 5.1, **2k**, **2i**, and **2m**).

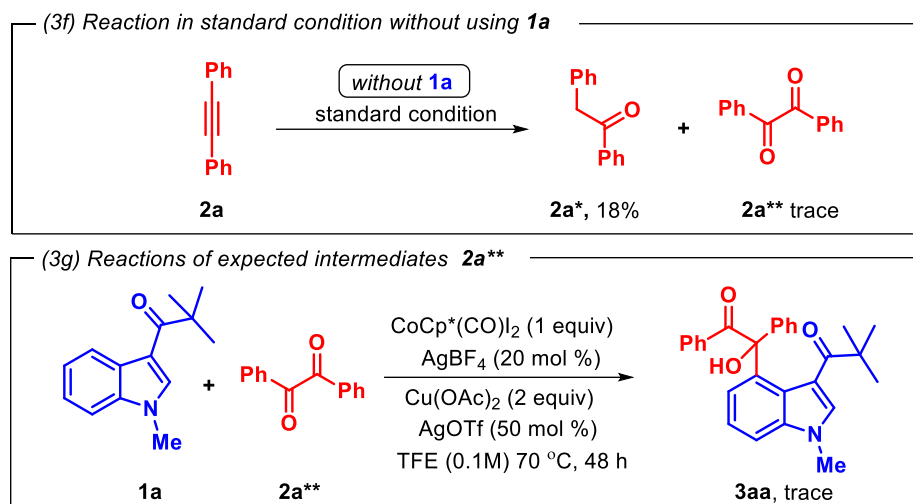
The scope of the alkyne was further extended to unsymmetrical 1-phenyl butyne **2h** (Scheme 5.2). Interestingly, in this case, a concomitant elimination pathway ensued C4- α,β -unsaturated ketone derivatives **3** (Scheme 5.2). Subjecting differently decorated indoles with **2h** delivered the product in good to excellent yields, thereby illustrating the functional group tolerance of this mild transformation. Notably, the complete compatibility of valuable functionalities such as alkyl, allyl, phenyl, and halo offers a convenient handle for potential synthetic elaboration (Scheme 5.2). It is worth noting that high regio- and stereoselectivity have been observed in the product. The selective

reaction at the keto group and the selective formation of the *E*-isomer (trans) suggest that the thermodynamic stability of the products controls this reaction.

A series of mechanistic studies were performed to understand the mechanism of this reaction. In this series, first, a deuterium exchange study was conducted using *N*-pivaloyl indole **1a** with D₂O under standard conditions, which resulted in 13% deuteration at the C4 position (Scheme 5.3a). This suggests that the first step might be reversible. Furthermore, we have performed intermolecular parallel experiments to study the kinetic isotope effect (Scheme 5.3b). We obtained a *KIE* value of 1.6, which confirms that the C–H bond activation step is not the rate-determining step.^{16a} To gain insight into the effect of electronics on the reaction rate, a competition experiment was performed between diphenylacetylene **2a** and 3-hexyne **2e** with indole **1a**. Product **3aa** observed in 30% yield, whereas hexyne failed to deliver the expected product **3ae** (Scheme 5.3c). This shows that aromatic internal alkyne reacts much faster than aliphatic internal alkyne. The addition of radical scavengers such as TEMPO and BHT under optimized reaction conditions failed to prevent the product formation, indicating a nonradical pathway for the reaction (Scheme 5.3d). To detect the active cobaltacycle intermediate, we have performed the stoichiometric parallel reactions by taking various substituted 3-pivaloyl indoles such as **1a**, **1k**, **1q**, and Cp^{*}Co in a 1:1 ratio. We have detected cationic cobaltacycle intermediates through high-resolution mass spectrometry (HRMS) (Scheme 5.3e). To identify the active coupling partner inside the reaction vessel, we performed a standard reaction without using substrate **1a**, wherein we isolated 1,2-diphenylethanone **2a*** in 18% yield along with detection of benzil **2a**** in HRMS (Scheme 5.3f).

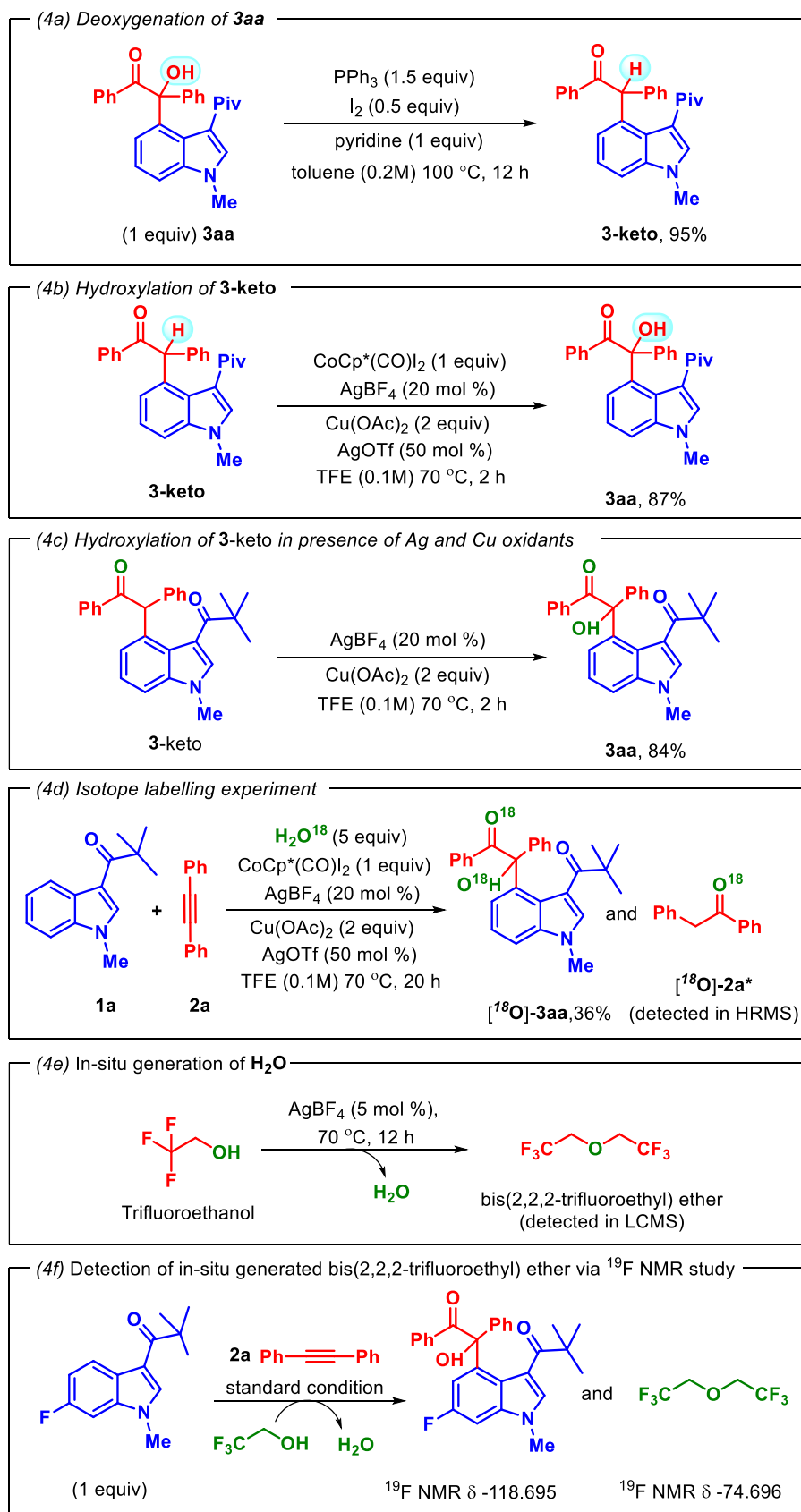
Scheme 5.3. Mechanistic Studies and Control Experiments





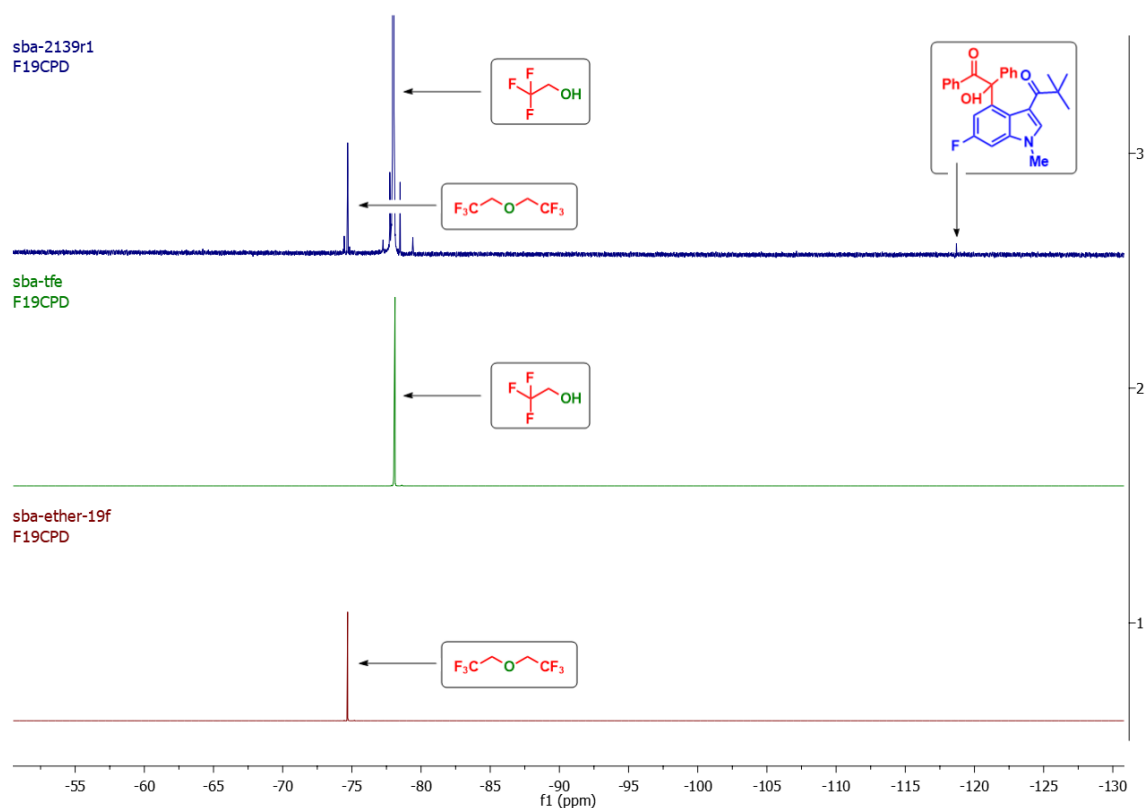
Considering the structure of the product **3aa**, initially, we presumed that benzil **2a**** is the active coupling partner. However, when the standard reaction was performed directly using benzil **2a**** (2 equivalents) as a coupling partner, it failed to give prominent results even after a long time (Scheme 5.3g). These experiments confirm that benzil **2a**** is not the actual reacting partner for this transformation. When we tried this reaction with 1,2-diphenylethanone **2a***, it was unreactive in the reaction mixture. Therefore, we thought that this reaction might go through a stepwise process and that oxidation may be the last step in this reaction; therefore, we prepared dehydroxylated compound 3-keto from the product **3aa** using PPh₃ and I₂ (Scheme 5.4a). When we subjected this dehydroxylated product 3-keto under the standard reaction condition, we obtained the hydroxylated product **3aa** in very good yield (87%) within 2 h (Scheme 5.4b), which means 3-keto is the intermediate product in this reaction. Furthermore, to know the role of actual oxidants in this transformation, another reaction has been performed using 3-keto in the presence of copper and silver salts in trifluoroethanol (Scheme 5.4c). As predicted, a good amount (84%) of **3aa** was obtained, thus indicating the role of Cu and Ag salts as oxidants.

Scheme 5.4. Control Experiment and Isotope Labeling Experiment



Yet another aspect that puzzled us was the oxygen source in the product **3aa** and diphenylacetylene-derived 1,2-diphenylethanone **2a***. obtained ^{18}O -labeled product $[^{18}\text{O}]\text{-3aa}$ (Scheme 5.4d). To understand this, we performed a series of experiments and concluded that oxygen distinctly comes from the dry solvent TFE. To confirm this, we deliberately added 5 equivalents of ^{18}O -labeled water in the standard reaction, and delightfully, from this experiment, it is clear that the water generated in situ from dry TFE is responsible for the source of oxygen in the product $[^{18}\text{O}]\text{-3aa}$. Also, we observed an increase in mass values of in situ generated 1,2-diphenylethanone $[^{18}\text{O}]\text{-2a}$ through HRMS when we added ^{18}O -labeled water to this reaction.

Figure 5.2. Detection of bis(2,2,2-trifluoroethyl) ether formation in the reaction mixture through ^{19}F NMR.

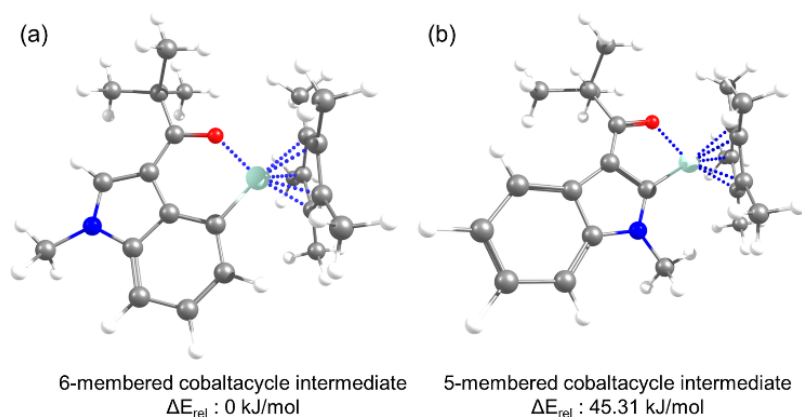


To ascertain the reaction responsible for the in situ generations of water, we tested a reaction of silver tetrafluoroborate with dry TFE (Scheme 5.4e). The liquid

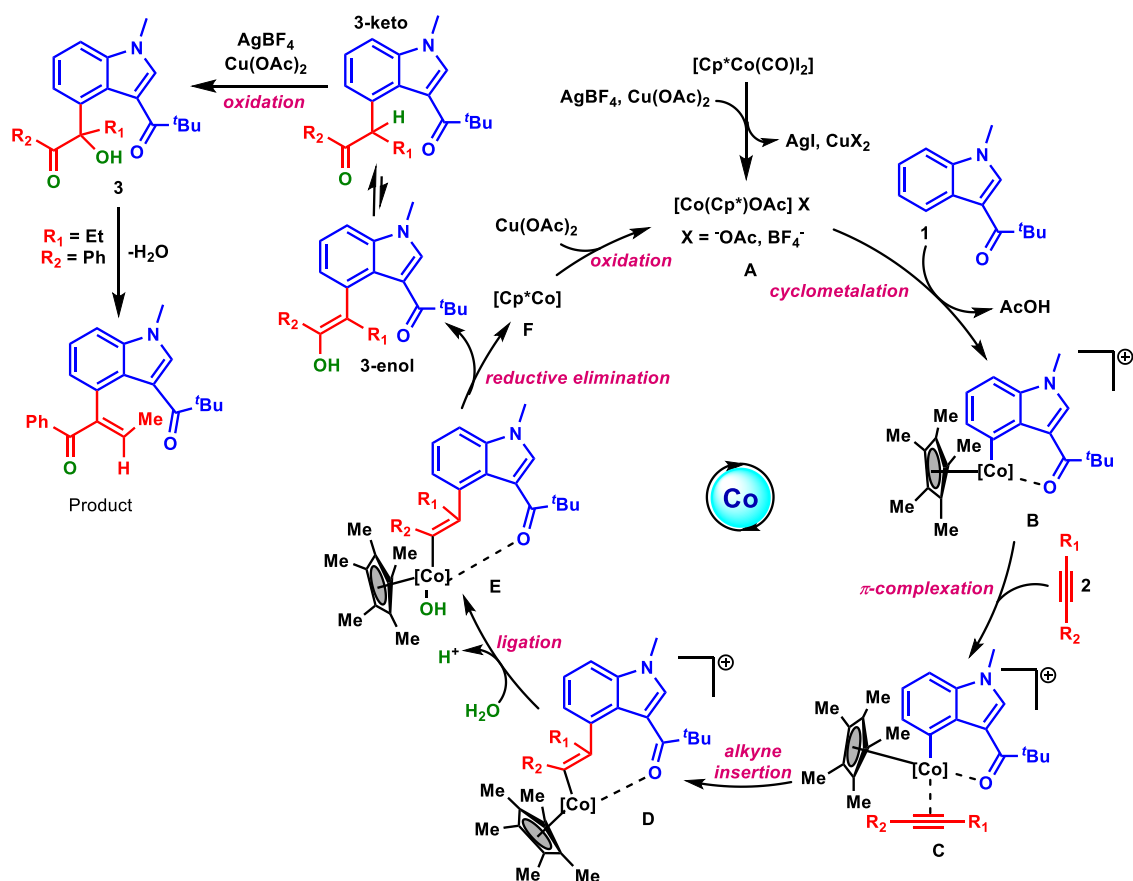
chromatography–mass spectrometry (LCMS) study of this reaction indicated the formation of bis(2,2,2-trifluoroethyl) ether in the reaction, which also indirectly indicates the formation of water as the byproduct (Scheme 5.4e). Furthermore, quantitative ^{19}F NMR studies^{15e} substantiated the formation of bis(2,2,2-trifluoroethyl) ether, which is indirect evidence for water formation in the reaction (Scheme 5.4f). The formation of bis(2,2,2-trifluoroethyl) ether is four times greater than the product **3aa** in the reaction mixture (Figure 5.2). As there was a decrease in the yield of **3aa** (36%) when we used 5 equivalents of ^{18}O -labeled water (Scheme 5.4d), in order to understand the compatibility threshold limit for the presence of water in this reaction. Accordingly, when we performed a reaction with 10 equivalents of water, we observed only a trace amount of product **3aa**. This confirms that the controlled release of water is another key factor for the success of this reaction.

Computational Studies. The exclusive formation of the C(4)–H-functionalized product could be explained by comparing the relative energies of the metallacycle intermediate through quantum mechanical calculations. The optimized geometry with their relative energies is depicted in Figure 5.3. We have taken both six- and five-membered cyclic intermediates and optimized them in RI-B97-D3/def2-TZVPP level of theory using the Turbomole-6.5 software package. This level of theory is already benchmarked, and it was used for transition metals.^{16a–c} The relative electronic energies unveil that the six-membered cobaltacycle intermediate is stabilized by 45.31 *kJ/mol* from the other five-membered cobaltacycle intermediate.

Figure 5.3. Optimized structures of (a) 6-membered, and (b) 5-membered cobaltacycle intermediates with their relative energies.



Scheme 5.5. Proposed Mechanism Catalytic Cycle

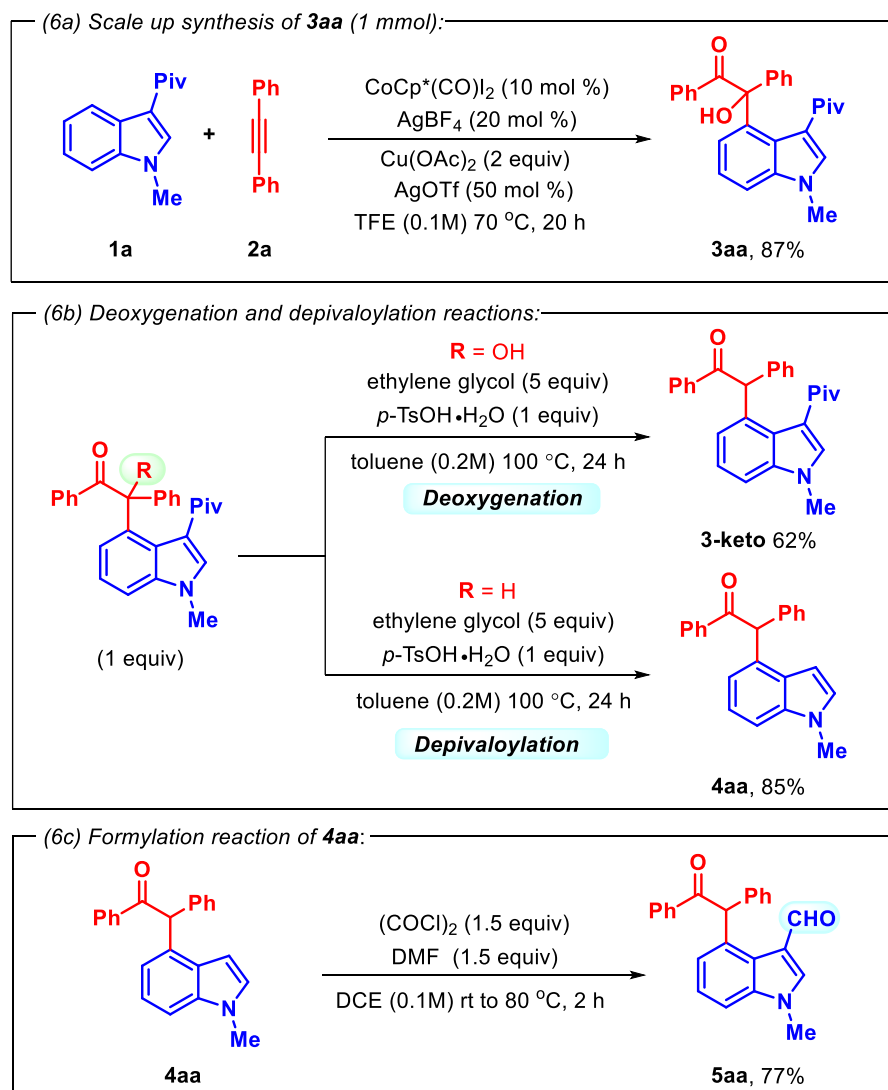


Based on our mechanistic studies, computational experiments, and literature reports,^{16,17} a plausible catalytic cycle has been proposed in scheme 5.5. Initially, $\text{Cp}^*\text{Co}(\text{CO})\text{I}_2$ reacts with AgBF_4 to generate an active catalyst **A**. Then, the C–H

metalation of **1** leads to the formation of the six-membered cobaltacycle species **B**, which was detected in HRMS and supported by computational experiments (Scheme 5.3e and Figure 5.3). Furthermore, the cationic cobalt(III) species undergo π -complexation with active coupling partner **2** followed by alkyne insertion to give intermediate **D**. Then, species **D** undergoes ligation with in situ generated H₂O to give intermediate **E**. Furthermore, the reductive elimination of intermediate **E** gives intermediate **F** and the production of **3-enol**, which after tautomerization, gives **3-keto**. Then, the oxidation of intermediate **F** regenerates the active catalyst **A** for the further catalytic cycle. In the other pathway, the oxidation of product **3-keto** occurs in the presence of copper and silver salts to furnish the desired product **3**. Furthermore, dehydration of **3** gives **3ah** if it is unsymmetrical alkyne (1-phenyl-1-butyne).

To demonstrate the versatility of the developed protocol in large scales, a 1 mmol scale reaction was performed, which also produced a near-excellent yield (Scheme 5.6a). Furthermore, to demonstrate the synthetic utility of the reaction, we attempted a depivaloylation reaction of **3aa**, and interestingly, we obtained the selective deoxygenated product **3-keto** (Scheme 5.6b). Further treatment of **3-keto** with *p*-TsOH gave us the depivaloylated product **4aa** (Scheme 5.6b). In view of the wide application of the formyl functional group in organic synthesis, as well as to diversify the synthetic product usefulness, we have performed the formylation reaction of **4aa**, which has given the indole C3-formylated product **5aa** in good yields (Scheme 5.6c). The formyl group can be used as a handle for further modifications.

Scheme 5.6. Synthetic Utility of the Indole C4-Derived Product.



5.4 CONCLUSION

In conclusion, we have developed weak coordination directed C–H activation with the more abundant first-row transition metal cobalt, which is an active and growing branch of research on the aspects of sustainability. This methodology gives access to highly regioselective C(4)–H-functionalized α -hydroxy ketone and α,β -unsaturated ketone-derived products efficiently, wherein we have observed unique reactivity of diphenylacetylene for the first time. Further, we have observed the in-situ generation of

H₂O from trifluoroethanol in the presence of silver salts, which is more efficient for this conversion. Furthermore, we have performed control and mechanistic studies: (i) isotopic labeling experiments prove oxygen source as in situ generated water; (ii) the ¹⁹F NMR and LCMS studies of bis(2,2,2-trifluoroethyl) ether confirm the in situ generations of water; (iii) we have also detected the six-membered cobaltacycle through HRMS; and (iv) to verify the regioselective indole C(4)–H bond metalation, we have calculated the relative energies of six- and five-membered cyclic intermediates with the help of computational experiments, which further supports our proposed mechanism. The generality of the transformations has been demonstrated on a broad range of substrates, thus producing various indole C4-substituted α - hydroxy ketones and α,β -unsaturated ketones.

Limitations: Electron-withdrawing substituted arenes such as -NO₂ are incompatible with optimized reaction conditions. Because electron-withdrawing groups decreases the nucleophilicity of Co-C bond towards olefin insertion. Also, C5 substituted indoles were failed to give the desired product, which might be due to the steric hindrance.

5.5 EXPERIMENTAL SECTION¹⁸

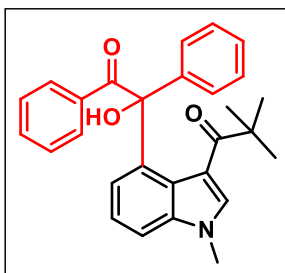
Reactions were performed using borosil schlenk tube vial under an N₂ atmosphere. Column chromatography was done by using 100-200 & 230-400 mesh size silica gel of Acme Chemicals. Gradient elution was performed by using distilled petroleum ether and ethyl acetate. TLC plates were detected under UV light at 254 nm. ¹H NMR and ¹³C NMR were recorded on Bruker AV 400, 700 MHz spectrometers using CDCl₃ as internal standards. The residual CHCl₃ for ¹H NMR (δ = 7.26 ppm) and the deuterated

solvent signal for ^{13}C NMR ($\delta = 77.36$ ppm) is used as reference.¹⁹ Multiplicity (s = single, d = doublet, t = triplet, q = quartet, m = multiplet, dd = double doublet), integration, and coupling constants (J) in hertz (Hz). HRMS signal analysis was performed using a micro TOF Q-II mass spectrometer. X-ray analysis was conducted using a Rigaku Smartlab X-ray diffractometer at SCS, NISER. Reagents and starting materials were purchased from Sigma Aldrich, Alfa Aesar, TCI, Avra, Spectrochem, and other commercially available sources and used without further purification unless otherwise noted.

(a) General reaction procedure for C-4 substitution of 3-pivaloyl indole with alkyne coupling partner:

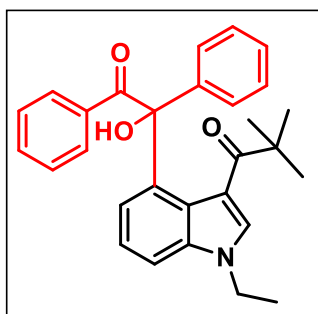
In a pre-dried sealed tube under N_2 , the mixture of *N*-methyl 3-pivaloyl indole **1** (0.1 mmol), diphenylacetylene **2** (0.4 mmol), $[\text{Cp}^*\text{Co}(\text{CO})\text{I}_2]$ (10 mol %), AgBF_4 (20 mol %), $\text{Cu}(\text{OAc})_2$ (0.2 mmol), AgOTf (50 mol %) and dry TFE (1 mL) were added and sealed inside the glove box. The reaction mixture was vigorously stirred at 70 °C on the preheated aluminum block for 20 h. After 20 h (completion of the reaction as monitored by TLC analysis), the reaction mixture was cooled to room temperature and diluted with ethyl acetate/dichloromethane, and passed through a short celite pad, the solvent was evaporated under reduced pressure, and the residue was purified by column chromatography using EtOAc/hexane mixture on silica gel to give the pure product **3**.

Experimental characterization data of products:



1-(4-(1-hydroxy-2-oxo-1,2-diphenylethyl)-1-methyl-1H-indol-3-yl)-2,2-dimethylpropan-1-one (3aa): was prepared according to general procedure (5.5a). The crude reaction mixture was purified by column chromatography using silica gel (100-200 mesh size), giving (39 mg) 93% yield.

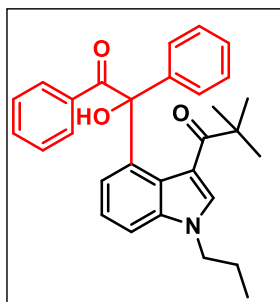
Physical State: solid brown m.p.: 226 – 228 °C R_f-value: 0.4 (20% EtOAc/hexane). **¹H NMR (CDCl₃, 400 MHz):** δ 8.82 (s, 1H), 8.26 – 8.25 (m, 2H), 7.88 (s, 1H), 7.65 (brs, 1H), 7.39-7.35 (m, 3H), 7.31-7.25 (m, 5H), 7.07 (t, *J* = 7.6 Hz, 1H), 6.50 (d, *J* = 7.6 Hz, 1H), 3.84 (s, 3H), 1.22 (s, 9H). **¹³C NMR (CDCl₃, 100 MHz):** δ 206.2, 198.1, 141.3, 141.1, 138.4, 135.6, 135.3, 132.2, 131.4, 128.6, 127.9, 127.8, 124.5, 124.4, 123.4, 115.8, 110.4, 87.3, 44.3, 34.2, 29.5. **IR (KBr, cm⁻¹):** 3166, 1671, 1620, 1525, 1398. **HRMS (ESI) m/z:** [M+Na]⁺ Calcd for C₂₈H₂₇NO₃Na 448.1883; Found 448.1879.



1-(1-ethyl-4-(1-hydroxy-2-oxo-1,2-diphenylethyl)-1H-indol-3-yl)-2,2-dimethylpropan-1-one (3ba): was prepared according to general procedure (5.5a). The crude reaction mixture was purified by column chromatography using silica gel (100-200 mesh size), giving (26 mg) 66% yield. Physical State: pale white

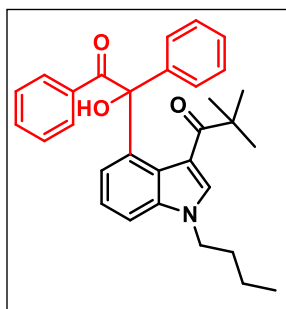
solid m.p.: 242 – 244 °C R_f-value: 0.3 (20% EtOAc/hexane). **¹H NMR (CDCl₃, 400 MHz):** δ 8.80 (s, 1H), 8.26 (d, *J* = 8.8 Hz, 2H), 7.91 (s, 1H), 7.65 (s, 1H), 7.35 (t, *J* = 7.2 Hz, 3H), 7.30-7.27 (m, 5H), 7.05 (t, *J* = 8.0 Hz, 1H), 6.48 (d, *J* = 7.6 Hz, 1H), 4.28-4.15 (m, 2H), 1.54 (t, *J* = 7.6 Hz, 3H), 1.21 (s, 9H). **¹³C NMR (CDCl₃, 100 MHz):** δ

206.3, 198.1, 141.4, 141.2, 137.5, 135.3, 133.8, 132.1, 131.41, 128.5, 127.8 (2C), 124.6, 124.4, 123.2, 116.0, 110.4, 87.3, 44.3, 42.2, 29.5, 15.3. **IR (KBr, cm⁻¹):** 3148, 1673, 1622, 1524, 1397. **HRMS (ESI) m/z:** [M+Na]⁺ Calcd for C₂₉H₂₉NO₃Na 462.2040; Found 462.2042.



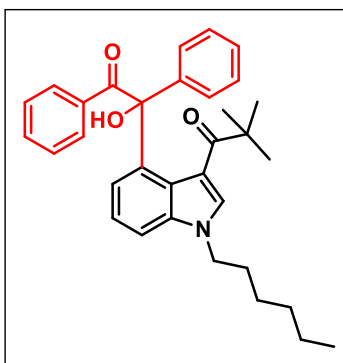
1-(4-(1-hydroxy-2-oxo-1,2-diphenylethyl)-1-propyl-1H-indol-3-yl)-2,2-dimethylpropan-1-one (3ca1): was prepared according to general procedure (5.5a). The crude reaction mixture was purified by column chromatography using silica gel (100-200 mesh size), giving (30 mg) 78% yield. Physical

State: solid brown m.p.: 229 – 231 °C Rf -value: 0.35 (10% EtOAc/hexane). **¹H NMR (CDCl₃, 400 MHz):** δ 8.86 (s, 1H), 8.27 – 8.25 (m, 2H), 7.90 (s, 1H), 7.66 (brs, 1H), 7.38-7.34 (m, 3H), 7.31-7.24 (m, 5H), 7.04 (t, *J* = 8.0 Hz, 1H), 6.47 (d, *J* = 8.0 Hz, 1H), 4.18-4.05 (m, 2H), 1.91 (sextet, *J* = 7.2 Hz, 2H), 1.21 (s, 9H), 0.99 (t, *J* = 7.2 Hz, 3H). **¹³C NMR (CDCl₃, 100 MHz):** δ 206.4, 198.1, 141.4, 141.2, 137.7, 135.3, 134.7, 132.1, 131.4, 129.9, 128.5, 127.9, 127.8, 124.6, 124.4, 123.2, 115.8, 110.5, 87.3, 49.2, 44.4, 29.5, 23.3, 118.8. **IR (KBr, cm⁻¹):** 3198, 2969, 1669, 1616, 1522, 1394. **HRMS (ESI) m/z:** [M+Na]⁺ Calcd for C₃₀H₃₁NO₃Na 476.2196; Found 476.2178.



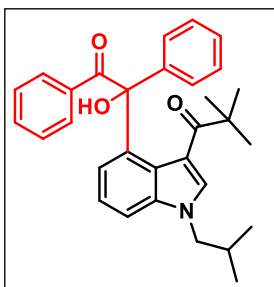
1-(1-butyl-4-(1-hydroxy-2-oxo-1,2-diphenylethyl)-1H-indol-3-yl)-2,2-dimethylpropan-1-one (3ca2): was prepared according to general procedure (5.5a). The crude reaction mixture was purified by column chromatography using silica gel (100-200 mesh size), giving (29 mg) 62%

yield. Physical State: colourless liquid R_f -value: 0.4 (10% EtOAc/hexane). **¹H NMR (CDCl₃, 700 MHz):** δ 8.85 (s, 1H), 8.26 (d, *J* = 7.7 Hz, 2H), 7.90 (s, 1H), 7.65 (brs, 1H), 7.36 (t, *J* = 7.0 Hz, 3H), 7.31-7.27 (m, 5H), 7.05 (t, *J* = 8.4 Hz, 1H), 6.47 (d, *J* = 7.7 Hz, 1H), 4.20-4.13 (m, 3H), 1.87 (pent, *J* = 7.7 Hz, 2H), 1.42-1.40 (m, 2H), 1.22 (s, 9H), 0.98 (t, *J* = 7.0 Hz, 3H). **¹³C NMR (CDCl₃, 100 MHz):** δ 206.4, 198.1, 141.4, 141.2, 137.7, 135.4, 134.7, 132.1, 131.4, 128.6 (2C), 127.9, 127.8, 124.6, 124.4, 123.2, 115.8, 110.5, 87.3, 47.4, 44.2, 32.0, 29.6, 20.5, 13.9. **IR (KBr, cm⁻¹):** 3438, 2991, 1633, 1377, 1242. **HRMS (ESI) m/z:** [M+Na]⁺ Calcd for C₃₁H₃₃NO₃Na 490.2353; Found 490.2337.



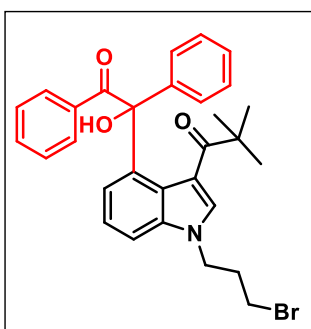
1-(1-hexyl-4-(1-hydroxy-2-oxo-1,2-diphenylethyl)-1H-indol-3-yl)-2,2-dimethylpropan-1-one (3da): was prepared according to general procedure (5.5a). The crude reaction mixture was purified by column chromatography using silica gel (100-200 mesh size), giving (25 mg) 70% yield. Physical State: yellow solid

m.p.: 174 – 176 °C R_f -value: 0.3 (10% EtOAc/hexane). **¹H NMR (CDCl₃, 400 MHz):** δ 8.86 (s, 1H), 8.26 (d, *J* = 8.0 Hz, 2H), 7.90 (s, 1H), 7.66 (s, 1H), 7.38-7.34 (m, 3H), 7.31-7.24 (m, 5H), 7.05 (t, *J* = 7.6 Hz, 1H), 6.47 (d, *J* = 7.6 Hz, 1H), 4.21-4.08 (m, 2H), 1.87 (pent, *J* = 7.2 Hz, 2H), 1.38-1.31 (m, 6H), 1.22 (s, 9H), 0.89 (t, *J* = 7.2 Hz, 3H). **¹³C NMR (CDCl₃, 100 MHz):** δ 206.3, 198.1, 141.4, 141.2, 137.7, 135.4, 134.7, 132.1, 131.4, 128.5, 127.9, 127.8, 124.6, 124.4, 123.2, 115.8, 110.5, 87.3, 47.6, 44.4, 31.6, 29.9, 29.6, 26.9, 22.8, 14.3. **IR (KBr, cm⁻¹):** 3145, 2929, 1675, 1626, 1523, 1398. **HRMS (ESI) m/z:** [M+Na]⁺ Calcd for C₃₃H₃₇NO₃Na 518.2666; Found 518.2670.



1-(4-(1-hydroxy-2-oxo-1,2-diphenylethyl)-1-isobutyl-1H-indol-3-yl)-2,2-dimethylpropan-1-one (3ea): was prepared according to general procedure (5.5a). The crude reaction mixture was purified by column chromatography using silica gel (100-200 mesh size), giving (27 mg) 76% yield. Physical

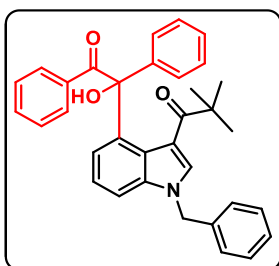
State: yellow solid m.p.: 205 – 207 °C *R_f*-value: 0.5 (10% EtOAc/hexane). **¹H NMR (CDCl₃, 400 MHz):** δ 8.88 (s, 1H), 8.26 (d, *J* = 8.0 Hz, 2H), 7.88 (s, 1H), 7.66 (brs, 1H), 7.37 (t, *J* = 6.8 Hz, 3H), 7.32-7.26 (m, 5H), 7.04 (t, *J* = 7.6 Hz, 1H), 6.46 (d, *J* = 7.6 Hz, 1H), 4.03-3.88 (m, 2H), 2.28-2.20 (m, 1H), 1.22 (s, 9H), 1.01-0.95 (m, 6H). **¹³C NMR (CDCl₃, 100 MHz):** δ 206.4, 198.1, 141.4, 141.2, 137.9, 135.4, 135.3, 132.1, 131.4, 128.5, 127.9 (2C), 127.8, 124.6, 124.4, 123.1, 115.6, 110.7, 87.3, 55.3, 44.4, 29.6, 29.1, 20.6, 20.5. **IR (KBr, cm⁻¹):** 3156, 1670, 1620, 1520, 1393. **HRMS (ESI) m/z:** [M+Na]⁺ Calcd for C₃₁H₃₃NO₃Na 490.2353; Found 490.2305.



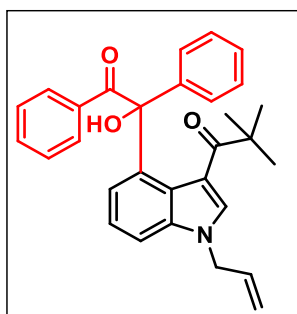
1-(1-(3-bromopropyl)-4-(1-hydroxy-2-oxo-1,2-diphenylethyl)-1H-indol-3-yl)-2,2-dimethylpropan-1-one (3fa): was prepared according to general procedure (5.5a). The crude reaction mixture was purified by column chromatography using silica gel (100-200 mesh

size), giving (28 mg) 77% yield. Physical State: solid brown m.p.: 168 – 170 °C *R_f*-value: 0.45 (10% EtOAc/hexane). **¹H NMR (CDCl₃, 400 MHz):** δ 8.83 (s, 1H), 8.27-8.25 (m, 2H), 8.03 (s, 1H), 7.66 (brs, 1H), 7.39-7.36 (m, 3H), 7.32-7.26 (m, 5H), 7.07 (t, *J* = 8.0 Hz, 1H), 6.48 (d, *J* = 7.6 Hz, 1H), 4.44-4.40 (m, 2H), 3.39-3.26 (m, 2H), 2.40-2.34 (m, 2H), 1.23 (s, 9H). **¹³C NMR (CDCl₃, 100 MHz):** δ 206.6, 198.1, 141.6, 141.0,

137.3, 135.2, 135.2, 132.2, 131.4, 128.6, 127.9, 127.9, 127.8, 124.7, 124.6, 123.5, 116.1, 110.3, 87.3, 45.0, 44.5, 31.7, 30.5, 29.5. **IR (KBr, cm⁻¹):** 3142, 1667, 1625, 1523, 1397. **HRMS (ESI) m/z:** [M+Na]⁺ Calcd for C₃₀H₃₀BrNO₃Na 554.1301; Found 554.1308.

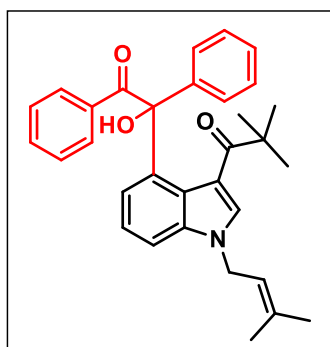


1-(1-benzyl-4-(1-hydroxy-2-oxo-1,2-diphenylethyl)-1H-indol-3-yl)-2,2-dimethylpropan-1-one (3ga): was prepared according to general procedure (5.5a). The crude reaction mixture was purified by column chromatography using silica gel (100-200 mesh size), giving (29 mg) 80% yield. Physical State: solid brown m.p.: 245 – 247 °C R_f-value: 0.4 (10% EtOAc/hexane). **¹H NMR (CDCl₃, 400 MHz):** δ 8.81 (s, 1H), 8.27-8.25 (m, 2H), 7.86 (s, 1H), 7.64 (brs, 1H), 7.37-7.32 (m, 6H), 7.31-7.21 (m, 6H), 7.17-7.15 (m, 3H), 6.99 (t, *J* = 8.0 Hz, 1H), 6.48 (d, *J* = 7.6 Hz, 1H), 1.17 (s, 9H). **¹³C NMR (CDCl₃, 100 MHz):** δ 206.6, 198.1, 141.3, 141.1, 138.0, 135.7, 135.6, 135.3, 134.8, 132.2, 131.4, 129.4, 128.6, 127.9, 127.8, 127.8, 127.3, 124.7, 124.6, 123.4, 116.3, 110.9, 87.3, 51.2, 44.4, 29.5. **IR (KBr, cm⁻¹):** 3138, 1673, 1629, 1400. **HRMS (ESI) m/z:** [M+Na]⁺ Calcd for C₃₄H₃₁NO₃Na 524.2196; Found 524.2154.



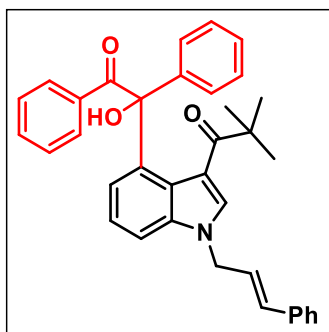
1-(1-allyl-4-(1-hydroxy-2-oxo-1,2-diphenylethyl)-1H-indol-3-yl)-2,2-dimethylpropan-1-one (3ha): was prepared according to the general procedure (5.5a). The crude reaction mixture was purified by column chromatography using silica gel (100-200 mesh size), giving (27 mg) 68% yield. Physical State: solid brown m.p.: 227 – 229 °C R_f-value: 0.5 (20% EtOAc/hexane). **¹H NMR (CDCl₃, 400 MHz):** δ 8.82 (s, 1H), 8.26 (d, *J* = 8.0 Hz, 2H), 7.90 (s, 1H), 7.65 (s, 1H), 7.38 - 7.34 (m, 3H), 7.31 - 7.25 (m, 5H), 7.04 (t, *J* = 8.0 Hz,

1H), 6.48 (d, $J = 7.2$ Hz, 1H), 6.06 - 5.96 (m, 1H), 5.33 – 5.20 (m, 1H), 4.81 – 4.71 (m, 3H), 1.21 (s, 9H). **^{13}C NMR (CDCl_3 , 100 MHz):** δ 206.5, 198.1, 141.3, 141.1, 137.8, 135.3, 134.4, 132.2, 132.1, 131.4, 128.6, 127.9, 127.8 (2C), 124.6, 124.5, 123.3, 119.3, 116.3, 110.7, 87.3, 49.8, 44.4, 29.5. **IR (KBr, cm^{-1}):** 3143, 1668, 1617, 1521, 1397. **HRMS (ESI) m/z :** $[\text{M}+\text{Na}]^+$ Calcd for $\text{C}_{30}\text{H}_{29}\text{NO}_3\text{Na}$ 474.2040; Found 474.2009.

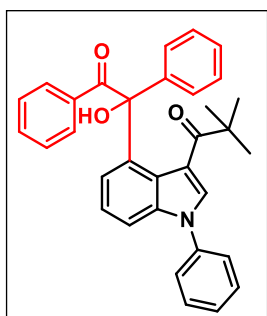


1-(4-(1-hydroxy-2-oxo-1,2-diphenylethyl)-1-(3-methylbut-2-en-1-yl)-1H-indol-3-yl)-2,2-dimethylpropan-1-one (3ia): was prepared according to general procedure (5.5a). The crude reaction mixture was purified by column chromatography using silica gel (100-200 mesh size), giving (31 mg) 82% yield.

Physical State: solid brown m.p.: 164 – 166 °C R_f -value: 0.3 (10% EtOAc/hexane). **^1H NMR (CDCl_3 , 400 MHz):** δ 8.88 (s, 1H), 8.26 (d, $J = 7.2$ Hz, 2H), 7.29 (s, 1H), 7.65 (brs, 1H), 7.38-7.35 (m, 3H), 7.31-7.25 (m, 5H), 7.04 (t, $J = 7.6$ Hz, 1H), 6.48 (d, $J = 7.6$ Hz, 1H), 5.41 (t, $J = 7.2$ Hz, 1H), 4.71 (d, 6.8 Hz, 2H), 1.82 (d, $J = 6.8$ Hz, 6H), 1.20 (s, 9H). **^{13}C NMR (CDCl_3 , 100 MHz):** δ 206.2, 198.1, 141.2, 141.1, 139.0, 137.8, 135.3, 134.3, 132.1, 131.4, 128.5, 127.9, 127.8, 124.7, 124.5, 123.1, 118.3, 115.7, 110.7, 87.3, 45.2, 44.3, 29.6, 25.9, 18.5. **IR (KBr, cm^{-1}):** 3137, 1673, 1615, 1523, 1397. **HRMS (ESI) m/z :** $[\text{M}+\text{Na}]^+$ Calcd for $\text{C}_{32}\text{H}_{33}\text{NO}_3\text{Na}$ 502.2352; Found 502.2380.

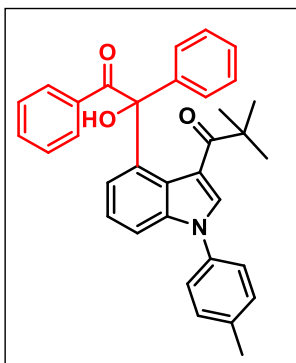


(E)-1-(1-cinnamyl-4-(1-hydroxy-2-oxo-1,2-diphenylethyl)-1H-indol-3-yl)-2,2-dimethylpropan-1-one (3ja): was prepared according to the general procedure (2.5). The crude reaction mixture was purified by column chromatography using silica gel (100-200 mesh size), giving (28 mg) 81% yield. Physical State: yellow solid m.p.: 216 – 218 °C R_f-value: 0.4 (10% EtOAc/hexane). **¹H NMR (CDCl₃, 400 MHz):** δ 8.85 (s, 1H), 8.29 – 8.26 (m, 2H), 7.96 (s, 1H), 7.66 (s, 1H), 7.38 – 7.24 (m, 13H), 7.05 (t, *J* = 8.0 Hz, 1H), 6.58 (d, *J* = 16.0 Hz, 1H), 6.49 (d, *J* = 7.2 Hz, 1H), 6.37 – 6.30 (m, 1H), 4.93 – 4.91 (m, 2H), 1.21 (s, 9H). **¹³C NMR (CDCl₃, 100 MHz):** δ 206.6, 198.1, 141.3, 141.1, 137.9, 136.0, 135.2, 134.4, 134.0, 132.2, 131.4, 129.0, 128.6 (2C), 127.9, 127.8, 126.9, 124.7, 124.6, 123.4, 123.2, 116.4, 110.8, 87.3, 49.5, 44.4, 29.5. **IR (KBr, cm⁻¹):** 3139, 1667, 1622, 1577, 1397. **HRMS (ESI) m/z:** [M+Na]⁺ Calcd for C₃₆H₃₃NO₃Na 550.2353; Found 550.2321.

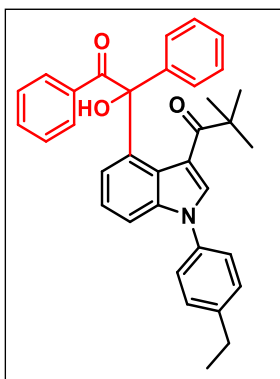


1-(4-(1-hydroxy-2-oxo-1,2-diphenylethyl)-1-phenyl-1H-indol-3-yl)-2,2-dimethylpropan-1-one (3ka1): was prepared according to general procedure (5.5a). The crude reaction mixture was purified by column chromatography using silica gel (100-200 mesh size), giving (24 mg) 67% yield. Physical State: solid brown m.p.: 139 – 141 °C R_f-value: 0.5 (10% EtOAc/hexane). **¹H NMR (CDCl₃, 400 MHz):** δ 8.77 (s, 1H), 8.32-8.30 (m, 2H), 8.05 (s, 1H), 7.68 (brs, 1H), 7.59-7.55 (m, 2H), 7.50-7.40 (m, 3H), 7.40-7.35 (m, 4H), 7.33-7.28 (m, 4H), 7.03 (t, *J* = 7.6 Hz, 1H), 6.52 (d, *J* = 7.6 Hz, 1H), 1.24 (s, 9H). **¹³C NMR (CDCl₃, 100 MHz):** δ 207.2,

198.2, 141.2, 141.1, 138.5, 138.4, 135.2, 134.4, 132.3, 131.5, 130.2, 128.7, 128.6, 127.9, 127.9, 127.8, 126.1, 125.0, 124.5, 123.8, 117.8, 111.6, 87.4, 44.6, 29.4. **IR (KBr, cm⁻¹):** 3145, 1675, 1636, 1596, 1402. **HRMS (ESI) m/z:** [M+Na]⁺ Calcd for C₃₃H₂₉NO₃Na 510.2040; Found 510.2043.



1-(4-(1-hydroxy-2-oxo-1,2-diphenylethyl)-1-(p-tolyl)-1H-indol-3-yl)-2,2-dimethylpropan-1-one (3ka2): was prepared according to general procedure (5.5a). The crude reaction mixture was purified by column chromatography using silica gel (100-200 mesh size), giving (28 mg) 55% yield. Physical State: solid brown m.p.: 233-235 °C R_f-value: 0.3 (10% EtOAc/hexane). **¹H NMR (CDCl₃, 400 MHz):** δ 8.75 (s, 1H), 8.29 (d, *J* = 8.8 Hz, 2H), 7.99 (s, 1H), 7.67 (brs, 1H), 7.40-7.35 (m, 5H), 7.29 (t, *J* = 8.0 Hz, 3H), 7.24 (d, *J* = 6.8 Hz, 2H), 7.06 (d, *J* = 9.2 Hz, 2H), 7.00 (t, *J* = 8.0 Hz, 1H), 6.51 (d, *J* = 6.8 Hz, 1H), 3.89 (s, 3H), 1.24 (s, 9H). **¹³C NMR (CDCl₃, 176 MHz):** δ 207.0, 198.2, 159.9, 141.2, 141.1, 138.9, 135.3, 134.8, 132.3, 131.5, 131.3, 128.6, 127.9 (2C), 127.8, 127.5, 124.9, 124.3, 123.7, 117.5, 115.3, 111.7, 87.4, 56.0, 44.5, 29.5. **IR (KBr, cm⁻¹):** 3425, 2991, 1631, 1519, 1445, 1263. **HRMS (ESI) m/z:** [M]⁺ Calcd for C₃₄H₃₁NO₃ 501.2298; Found 501.2276.



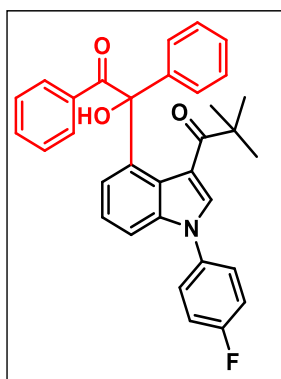
1-(1-(4-ethylphenyl)-4-(1-hydroxy-2-oxo-1,2-

diphenylethyl)-1H-indol-3-yl)-2,2-dimethylpropan-1-one

(3ka3): was prepared according to general procedure (5.5a).

The crude reaction mixture was purified by column chromatography using silica gel (100-200 mesh size), giving (30 mg) 60% yield. Physical State: brown liquid R_f-

value: 0.3 (20% EtOAc/hexane). **¹H NMR (CDCl₃, 700 MHz):** δ 8.78 (s, 1H), 8.30 (d, *J* = 7.7 Hz, 2H), 8.04 (s, 1H), 7.68 (brs, 2H), 7.40-7.37 (m, 7H), 7.32 (d, *J* = 8.4 Hz, 1H), 7.31-7.29 (m, 3H), 7.01 (t, *J* = 8.4 Hz, 1H), 6.51 (d, *J* = 7.7 Hz, 1H), 2.76 (q, *J* = 7.7 Hz, 2H), 1.32 (t, *J* = 7.0 Hz, 3H), 1.24 (s, 9H). **¹³C NMR (CDCl₃, 176 MHz):** δ 207.1, 198.2, 145.1, 141.2, 141.1, 138.5, 136.1, 135.3, 134.6, 132.3, 131.5, 129.6, 128.6, 127.9, 127.8 (2C), 126.0, 124.9, 124.4, 123.7, 117.5, 111.7, 87.4, 44.6, 29.5, 28.9, 15.8. **IR (KBr, cm⁻¹):** 3440, 1633, 1374, 1242, 1056. **HRMS (ESI) m/z:** [M+Na]⁺ Calcd for C₃₅H₃₃NO₃Na 538.2353; Found 538.2343.



1-(1-(4-fluorophenyl)-4-(1-hydroxy-2-oxo-1,2-

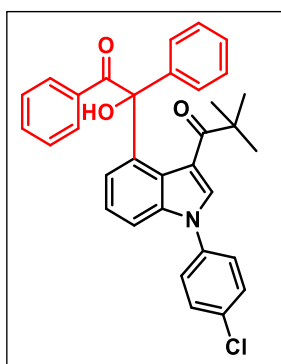
diphenylethyl)-1H-indol-3-yl)-2,2-dimethylpropan-1-one

(3ka4): was prepared according to general procedure (5.5a).

The crude reaction mixture was purified by column chromatography using silica gel (100-200 mesh size), giving (36 mg) 72% yield. Physical State: solid white m.p.: 257 –

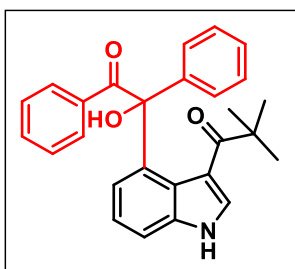
258 °C R_f-value: 0.2 (10% EtOAc/hexane). **¹H NMR (CDCl₃, 700 MHz):** δ 8.73 (s, 1H), 8.31 (d, *J* = 7.7 Hz, 2H), 8.00 (s, 1H), 7.67 (brs, 1H), 7.47-7.45 (m, 2H), 7.39-7.37 (m, 3H), 7.31-7.24 (m, 7H), 7.03 (t, *J* = 7.7 Hz, 1H), 6.52 (d, *J* = 7.7 Hz, 1H), 1.24 (s,

9H). **¹³C NMR (CDCl₃, 176 MHz):** δ 207.2, 198.2, 162.5 (d, *J*_{C-F} = 249.2 Hz), 141.3, 141.0, 138.6, 135.2, 134.5 (d, *J*_{C-F} = 3.1 Hz), 134.2, 132.4, 131.5, 128.6, 128.1 (d, *J*_{C-F} = 8.6 Hz), 127.9 (2C), 127.8, 125.1, 124.4, 124.0, 117.9, 117.2 (d, *J*_{C-F} = 22.8 Hz), 111.4, 87.4, 44.6, 29.4. **¹⁹F NMR (CDCl₃, 376 MHz):** δ -112.1. **IR (KBr, cm⁻¹):** 3439, 1660, 1625, 1522, 1448. **HRMS (ESI) m/z:** [M+Na]⁺ Calcd for C₃₃H₂₈FNO₃Na 528.1945; Found 528.1986.



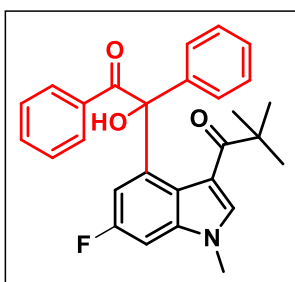
1-(1-(4-chlorophenyl)-4-(1-hydroxy-2-oxo-1,2-diphenylethyl)-1H-indol-3-yl)-2,2-dimethylpropan-1-one (3ka5): was prepared according to general procedure (5.5a). The crude reaction mixture was purified by column chromatography using silica gel (100-200 mesh size), giving (33 mg) 68% yield. Physical State: yellow solid m.p.: 229 –

231 °C *R_f*-value: 0.40 (10% EtOAc/hexane). **¹H NMR (CDCl₃, 700 MHz):** δ 8.70 (s, 1H), 8.31 (d, *J* = 7.7 Hz, 2H), 8.00 (s, 1H), 7.66 (s, 1H), 7.55 (d, *J* = 8.4 Hz, 2H), 7.44 (d, *J* = 9.1 Hz, 2H), 7.39-7.37 (m, 3H), 7.31-7.29 (m, 4H), 7.04 (t, *J* = 7.7 Hz, 1H), 6.53 (d, *J* = 7.7 Hz, 1H), 1.24 (s, 9H). **¹³C NMR (CDCl₃, 176 MHz):** δ 207.3, 198.2, 141.4, 141.0, 138.3, 137.0, 135.1, 134.6, 133.9, 132.4, 131.5, 130.5, 128.6, 128.0, 127.9, 127.8, 127.4, 125.2, 124.6, 124.1, 118.2, 111.3, 87.4, 44.6, 29.4. **IR (KBr, cm⁻¹):** 3427, 1630, 1265, 752. **HRMS (ESI) m/z:** [M+Na]⁺ Calcd for C₃₃H₂₈ClNO₃Na 544.1650; Found 544.1641.



71-(4-(1-hydroxy-2-oxo-1,2-diphenylethyl)-1H-indol-3-yl)-2,2-dimethylpropan-1-one (3la): was prepared according to general procedure (5.5a). The crude reaction mixture was purified by column chromatography using silica gel (100-200 mesh size), giving (22 mg) 51% yield.

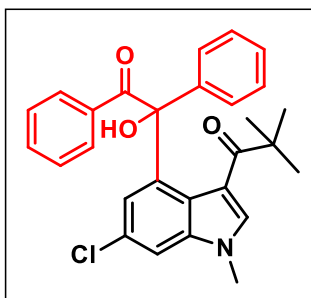
Physical State: solid brown m.p.: 246-248 °C R_f-value: 0.3 (20% EtOAc/hexane). **¹H NMR (CDCl₃, 400 MHz):** δ 8.93 (brs, 1H), 8.82 (s, 1H), 8.28-8.26 (m, 2H), 7.83 (d, *J* = 3.2 Hz, 1H), 7.64 (brs, 1H), 7.40-7.35 (m, 3H), 7.32-7.25 (m, 4H), 7.29-7.21 (m, 1H), 7.02 (t, *J* = 7.6 Hz, 1H), 6.48 (d, *J* = 7.6 Hz, 1H), 1.21 (s, 9H). **¹³C NMR (CDCl₃, 100 MHz):** δ 207.0, 198.5, 141.0, 140.9, 139.7, 137.5, 135.2, 132.4, 131.6, 131.4, 128.6, 127.9, 127.7, 124.5, 123.6, 123.5, 117.4, 112.4, 87.4, 44.4, 29.4. **IR (KBr, cm⁻¹):** 3155, 1677, 1600, 1400. **HRMS (ESI) m/z:** [M+Na]⁺ Calcd for C₂₇H₂₅NO₃Na 434.1727; Found 434.1697.



1-(6-fluoro-4-(1-hydroxy-2-oxo-1,2-diphenylethyl)-1-methyl-1H-indol-3-yl)-2,2-dimethylpropan-1-one (3oa): was prepared according to general procedure (5.5a). The crude reaction mixture was purified by column chromatography using silica gel (100-200 mesh size),

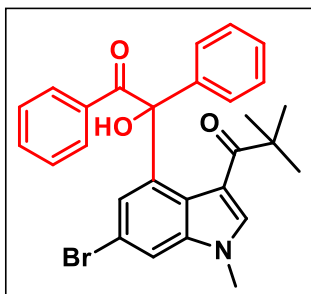
giving (28 mg) 70% yield. Physical State: orange solid m.p.: 225 – 227 °C R_f-value: 0.2 (10% EtOAc/hexane). **¹H NMR (CDCl₃, 400 MHz):** δ 8.83 (s, 1H), 8.24 (d, *J* = 7.6 Hz, 2H), 7.86 (s, 1H), 7.65 (s, 1H), 7.38-7.24 (m, 7H), 6.91 (d, *J* = 7.6 Hz, 1H), 6.26 (d, *J* = 7.6 Hz, 1H), 3.76 (s, 3H), 1.20 (s, 9H). **¹³C NMR (CDCl₃, 100 MHz):** δ 206.3, 197.7, 159.8 (d, *J*_{C-F} = 239.0 Hz), 143.5 (d, *J*_{C-F} = 8.0 Hz), 140.3, 138.7 (d, *J*_{C-F} = 11.0 Hz),

135.9 (d, $J_{\text{C-F}} = 2.0$ Hz), 135.0, 132.4, 131.3, 128.8, 128.2, 127.9, 127.6, 120.9, 116.1, 113.5 (d, $J_{\text{C-F}} = 26.0$ Hz), 96.3 (d, $J_{\text{C-F}} = 25.0$ Hz), 87.0, 44.4, 34.2, 29.4. **^{19}F NMR** (CDCl_3 , 376 MHz): δ -117.9. **IR** (KBr , cm^{-1}): 3195, 1661, 1633, 1531, 1403. **HRMS** (**ESI**) m/z : $[\text{M}+\text{Na}]^+$ Calcd for $\text{C}_{28}\text{H}_{26}\text{FNO}_3\text{Na}$ 466.1789; Found 466.1789.



1-(6-chloro-4-(1-hydroxy-2-oxo-1,2-diphenylethyl)-1-methyl-1H-indol-3-yl)-2,2-dimethylpropan-1-one (3pa):

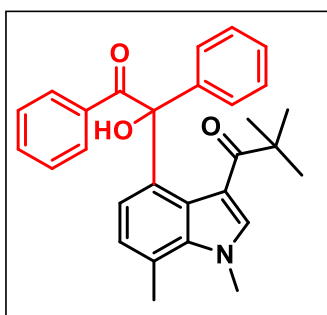
was prepared according to general procedure (5.5a). The crude reaction mixture was purified by column chromatography using silica gel (100-200 mesh size), giving (27 mg) 71% yield. Physical State: yellow solid m.p.: 230 – 232 °C R_f -value: 0.5 (20% EtOAc/hexane). **^1H NMR** (CDCl_3 , 400 MHz): δ 8.79 (s, 1H), 8.24 (d, $J = 7.2$ Hz, 2H), 7.85 (s, 1H), 7.64 (s, 1H), 7.40 - 7.33 (m, 4H), 7.31 - 7.25 (m, 4H), 6.44 (d, $J = 2.0$ Hz, 1H), 3.80 (s, 3H), 1.20 (s, 9H). **^{13}C NMR** (CDCl_3 , 100 MHz): δ 206.3, 197.7, 142.9, 140.1, 138.9, 135.9, 135.0, 132.4, 131.3, 129.5, 128.8, 128.2, 127.9, 127.7, 125.0, 123.2, 116.1, 110.2, 87.1, 44.5, 34.2, 29.4. **IR** (KBr , cm^{-1}): 3169, 1670, 1625, 1523, 1400. **HRMS** (**ESI**) m/z : $[\text{M}+\text{Na}]^+$ Calcd for $\text{C}_{28}\text{H}_{26}\text{ClNO}_3\text{Na}$ 482.1493; Found 482.1478.



1-(6-bromo-4-(1-hydroxy-2-oxo-1,2-diphenylethyl)-1-methyl-1H-indol-3-yl)-2,2-dimethylpropan-1-one (3qa):

was prepared according to general procedure (5.5a). The crude reaction mixture was purified by column chromatography using silica gel (100-200 mesh size), giving (29 mg) 80% yield. Physical State: yellow solid m.p.: 239 – 241 °C R_f -value: 0.4

(20% EtOAc/hexane). **¹H NMR (CDCl₃, 400 MHz):** δ 8.79 (s, 1H), 8.24 (d, *J* = 7.6 Hz, 2H), 7.83 (s, 1H), 7.62 (s, 1H), 7.42-7.37 (m, 4H), 7.35 - 7.25 (m, 4H), 6.56 (d, *J* = 1.6 Hz, 1H), 3.79 (s, 3H), 1.20 (s, 9H). **¹³C NMR (CDCl₃, 100 MHz):** δ 206.3, 197.6, 143.1, 140.1, 139.2, 135.8, 134.9, 132.4, 131.3, 128.8, 128.2, 127.9, 127.6 (2C), 123.6, 117.2, 116.1, 113.3, 87.0, 44.5, 34.2, 29.4. **IR (KBr, cm⁻¹):** 3147, 1674, 1623, 1525, 1404. **HRMS (ESI) m/z:** [M+Na]⁺ Calcd for C₂₈H₂₆BrNO₃Na 526.0988; Found 526.0989.

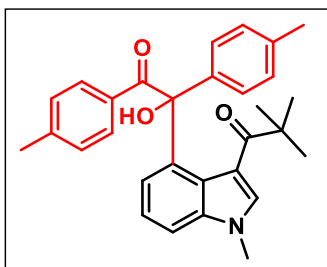


1-(4-(1-hydroxy-2-oxo-1,2-diphenylethyl)-1,7-

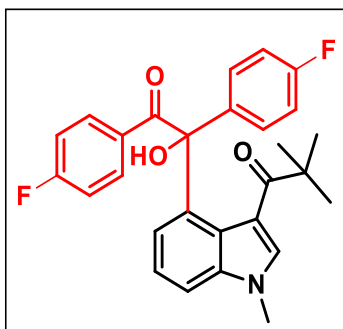
dimethyl-1H-indol-3-yl)-2,2-dimethylpropan-1-one

(3sa): was prepared according to general procedure (5.5a). The crude reaction mixture was purified by column chromatography using silica gel (100-200 mesh

size), giving (25 mg) 61% yield. Physical State: yellow solid m.p.: 223 – 225 °C *R_f*-value: 0.3 (20% EtOAc/hexane). **¹H NMR (CDCl₃, 400 MHz):** δ 8.74 (s, 1H), 8.27 (d, *J* = 7.6 Hz, 2H), 7.73 (s, 1H), 7.62 (s, 1H), 7.36-7.31 (m, 4H), 7.28 - 7.24 (m, 3H), 6.74 (d, *J* = 7.6 Hz, 1H), 6.33 (d, *J* = 8.0 Hz, 1H), 4.10 (s, 3H), 2.70 (s, 3H), 1.19 (s, 9H). **¹³C NMR (CDCl₃, 100 MHz):** δ 206.5, 198.1, 141.5, 139.3, 137.3 (2C), 135.6, 132.1, 131.4, 128.5, 128.0, 127.8, 127.7, 126.4, 125.8, 124.9, 121.9, 115.8, 87.5, 44.4, 38.7, 29.6, 20.3. **IR (KBr, cm⁻¹):** 3138, 1661, 1625, 1530, 1401. **HRMS (ESI) m/z:** [M+Na]⁺ Calcd for C₂₉H₂₉NO₃Na 462.2040; Found 462.2035.

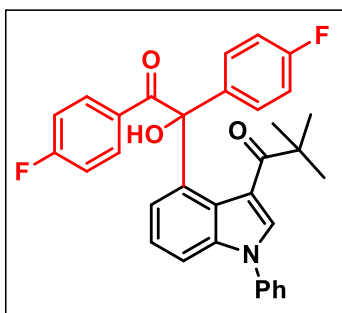


1-(4-(1-hydroxy-2-oxo-1,2-di-p-tolyloethyl)-1-methyl-1H-indol-3-yl)-2,2-dimethylpropan-1-one (3ab): was prepared according to general procedure (5.5a). The crude reaction mixture was purified by column chromatography using silica gel (100-200 mesh size), giving (18 mg) 40% yield. Physical State: solid brown m.p.: 247 – 249 °C R_f-value: 0.4 (10% EtOAc/hexane). **¹H NMR (CDCl₃, 400 MHz):** δ 8.74 (s, 1H), 8.17 (d, *J* = 8.4 Hz, 2H), 7.86 (s, 1H), 7.51 (brs, 1H), 7.27-7.25 (m, 2H), 7.16 (d, *J* = 7.2 Hz, 2H), 7.08 (d, *J* = 8.0 Hz, 3H), 6.51 (d, *J* = 7.6 Hz, 1H), 3.84 (s, 3H), 2.34 (s, 3H), 2.30 (s, 3H), 1.26 (s, 9H). **¹³C NMR (CDCl₃, 100 MHz):** δ 206.2, 197.8, 142.6, 141.6, 138.4, 138.2, 137.3, 135.3, 132.8, 131.5, 129.3, 128.6, 127.7, 124.5, 123.4, 116.0, 110.2, 87.2, 44.4, 34.2, 29.5, 21.9, 21.4. **IR (KBr, cm⁻¹):** 3153, 1664, 1621, 1526, 1400. **HRMS (ESI) m/z:** [M+Na]⁺ Calcd for C₃₀H₃₁NO₃Na 476.2196; Found 476.2178.



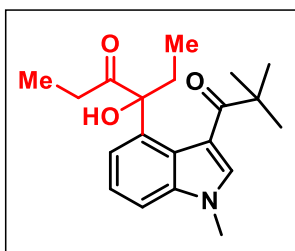
1-(4-(1,2-bis(4-fluorophenyl)-1-hydroxy-2-oxoethyl)-1-methyl-1H-indol-3-yl)-2,2-dimethylpropan-1-one (3ac): was prepared according to general procedure (5.5a). The crude reaction mixture was purified by column chromatography using silica gel (100-200 mesh size), giving (31 mg) 71% yield. Physical State: yellow solid m.p.: 239 – 241 °C R_f-value: 0.2 (20% EtOAc/hexane). **¹H NMR (CDCl₃, 400 MHz):** δ 8.82 (s, 1H), 8.33 – 8.29 (m, 2H), 7.89 (s, 1H), 7.60 (s, 1H), 7.29 – 7.27 (m, 1H), 7.11 – 7.03 (m, 3H), 6.98 – 6.94 (m, 3H), 6.47 (d, *J* = 8.0 Hz, 1H), 3.84 (s, 3H), 1.21 (s, 9H). **¹³C NMR (CDCl₃, 100 MHz):** δ 206.4, 196.6, 165.2 (d, *J*_{C-F} = 252.0 Hz), 162.6 (d, *J*_{C-F} = 245.0

Hz), 140.8, 138.4, 136.7 (d, J_{C-F} = 3.0 Hz), 135.7, 133.9 (d, J_{C-F} = 9.0 Hz), 131.6 (d, J_{C-F} = 3.0 Hz), 129.5 (d, J_{C-F} = 8.0 Hz), 124.4, 124.3, 123.4, 115.8, 115.5 (d, J_{C-F} = 21.0 Hz), 115.0 (d, J_{C-F} = 21.0 Hz), 110.6, 87.0, 44.4, 34.2, 29.5. **^{19}F NMR (CDCl₃, 376 MHz):** δ -106.9, -115.0. **IR (KBr, cm⁻¹):** 3156, 2980, 1674, 1626, 1527, 1400. **HRMS (ESI) m/z:** [M+Na]⁺ Calcd for C₂₈H₂₅F₂NO₃Na 484.1695; Found 484.1683.



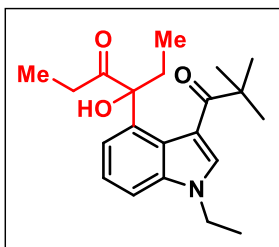
1-(4-(1,2-bis(4-fluorophenyl)-1-hydroxy-2-oxoethyl)-1-phenyl-1H-indol-3-yl)-2,2-dimethylpropan-1-one (3kc): was prepared according to general procedure (5.5a). The crude reaction mixture was purified by column chromatography using silica gel (100-200

mesh size), giving (23 mg) 60% yield. Physical State: pale white solid m.p.: 264 – 266 °C R_f -value: 0.6 (10% EtOAc/hexane). **^1H NMR (CDCl₃, 400 MHz):** δ 8.78 (s, 1H), 8.37 – 8.33 (m, 2H), 8.06 (s, 1H), 7.65 (s, 1H), 7.60 – 7.57 (m, 2H), 7.52 – 7.48 (m, 3H), 7.36 (d, J = 8.4 Hz, 1H), 7.09 – 6.96 (m, 6H), 6.49 (d, J = 7.6 Hz, 1H), 1.24 (s, 9H). **^{13}C NMR (CDCl₃, 100 MHz):** δ 207.4, 196.7, 165.3 (d, J_{C-F} = 252.0 Hz), 162.6 (d, J_{C-F} = 245.0 Hz), 140.8, 138.4 (d, J_{C-F} = 2.0 Hz), 136.7 (d, J_{C-F} = 3.0 Hz), 134.5, 134.1 (d, J_{C-F} = 9.0 Hz), 131.5 (d, J_{C-F} = 3.0 Hz), 130.3, 129.5 (d, J_{C-F} = 8.0 Hz), 128.8, 126.1, 124.8, 124.4, 124.3, 123.9, 117.7, 115.6 (d, J_{C-F} = 22.0 Hz), 115.1 (d, J_{C-F} = 21.0 Hz), 111.9, 87.1, 44.6, 29.4. **^{19}F NMR (CDCl₃, 376 MHz):** δ -106.5, -114.8. **IR (KBr, cm⁻¹):** 3140, 1676, 1635, 1523, 1401. **HRMS (ESI) m/z:** [M+Na]⁺ Calcd for C₃₃H₂₇F₂NO₃Na 522.1875; Found 522.1828.



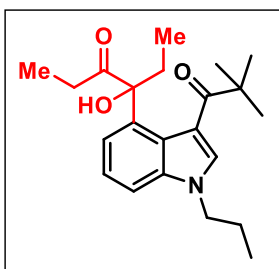
4-hydroxy-4-(1-methyl-3-pivaloyl-1H-indol-4-yl)hexan-3-one (3ae): was prepared according to general procedure (5.5a). The crude reaction mixture was purified by column chromatography using silica gel (100-200 mesh size),

giving (26 mg) 81% yield. Physical State: solid brown m.p.: 134 – 135 °C R_f-value: 0.45 (10% EtOAc/hexane). **¹H NMR (CDCl₃, 400 MHz):** δ 7.61 (s, 1H), 7.30 (s, 3H), 6.25 (s, 1H), 3.8 (s, 3H), 2.73-2.51 (m, 2H), 2.33-2.16 (m, 2H), 1.38 (s, 9H), 1.01 (t, *J* = 7.2 Hz, 3H), 0.86 (t, *J* = 7.2 Hz, 3H). **¹³C NMR (CDCl₃, 100 MHz):** δ 216.6, 207.4, 138.6, 135.9, 132.8, 124.3, 123.2, 121.8, 116.5, 110.1, 83.8, 44.5, 33.9, 31.3, 30.0, 2.4, 8.6, 8.3. **IR (KBr, cm⁻¹):** 3116, 1667, 1639, 1401. **HRMS (ESI) m/z:** [M+Na]⁺ Calcd for C₂₀H₂₇NO₃Na 352.1883; Found 352.1869.



4-(1-ethyl-3-pivaloyl-1H-indol-4-yl)-4-hydroxyhexan-3-one (3be): was prepared according to general procedure (5.5a). The crude reaction mixture was purified by column chromatography using silica gel (100-200 mesh size), giving

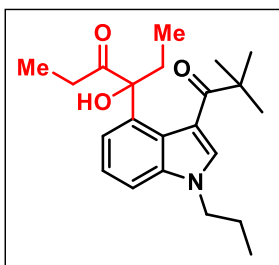
(17 mg) 50% yield. Physical State: yellow solid m.p.: 137 – 139 °C R_f-value: 0.6 (20% EtOAc/hexane). **¹H NMR (CDCl₃, 400 MHz):** δ 7.64 (s, 1H), 7.34 – 7.27 (m, 3H), 6.16 (s, 1H), 4.19 (q, *J* = 7.2 Hz, 2H), 2.73 – 2.51 (m, 2H), 2.33 – 2.14 (m, 2H), 1.50 (t, *J* = 7.2 Hz, 3H), 1.38 (s, 9H), 1.01 (t, *J* = 7.2 Hz, 3H), 0.87 (t, *J* = 7.2 Hz, 3H). **¹³C NMR (CDCl₃, 100 MHz):** δ 212.6, 207.5, 137.7, 136.0, 130.9, 124.5, 123.0, 121.7, 116.7, 110.1, 83.8, 44.5, 41.9, 31.4, 30.2, 29.4, 15.4, 8.6, 8.3. **IR (KBr, cm⁻¹):** 3139, 1653, 1619, 1401. **HRMS (ESI) m/z:** [M+Na]⁺ Calcd for C₂₁H₂₉NO₃Na 366.2040; Found 366.2003.



4-hydroxy-4-(3-pivaloyl-1-propyl-1H-indol-4-yl)hexan-

3-one (3ce): was prepared according to general procedure (5.5a). The crude reaction mixture was purified by column chromatography using silica gel (100-200 mesh size), giving (21 mg) 79% yield. Physical

State: solid brown m.p.: 110 – 112 °C R_f-value: 0.4 (10% EtOAc/hexane). **¹H NMR (CDCl₃, 400 MHz):** δ 7.66 (s, 1H), 7.23-7.19 (s, 2H), 6.91-6.89 (m, 1H), 4.75 (t, *J* = 7.6 Hz, 1H), 4.11 (t, *J* = 7.2 Hz, 2H), 2.49-2.43 (m, 2H), 2.12-2.01 (m, 1H), 1.96-1.87 (m, 2H), 1.67-1.51 (m, 2H), 1.42 (s, 9H), 1.01-0.94 (m, 6H), 0.79 (t, *J* = 7.6 Hz, 3H). **¹³C NMR (CDCl₃, 100 MHz):** δ 212.6, 206.1, 137.2, 134.9, 132.1, 126.7, 123.6, 120.9, 115.5, 108.6, 55.2, 48.9, 45.1, 35.7, 29.2, 26.3, 23.4, 12.6, 11.8, 8.4. **IR (KBr, cm⁻¹):** 3140, 1704, 1646, 1525, 1399. **HRMS (ESI) m/z:** [M+Na]⁺ Calcd for C₂₂H₃₁NO₃Na 380.2196; Found 380.2191.

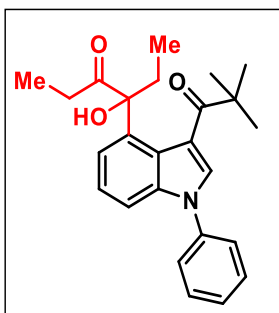


4-(1-benzyl-3-pivaloyl-1H-indol-4-yl)-4-hydroxyhexan-

3-one (3ge): was prepared according to general procedure (5.5a). The crude reaction mixture was purified by column chromatography using silica gel (100-200 mesh size), giving (22 mg) 75% yield. Physical

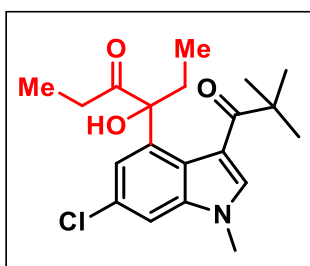
State: colourless liquid R_f-value: 0.4 (10% EtOAc/hexane). **¹H NMR (CDCl₃, 400 MHz):** δ 7.59 (s, 1H), 7.35-7.21 (m, 7H), 7.16-7.11 (m, 3H), 6.04 (s, 1H), 2.71-2.14 (m, 2H), 2.32-2.14 (m, 2H), 1.35 (s, 9H), 1.01 (t, *J* = 7.2 Hz, 3H), 0.87 (t, *J* = 7.2 Hz, 3H). **¹³C NMR (CDCl₃, 100 MHz):** δ 212.6, 207.8, 138.2, 136.0, 135.9, 131.7, 129.3, 128.5, 127.2, 124.5, 123.2, 121.9, 117.1, 110.5, 83.8, 50.9, 44.6, 31.5, 30.2, 29.3, 8.6,

8.2. **IR (KBr, cm⁻¹):** 3163, 1711, 1635, 1525, 1399. **HRMS (ESI) m/z:** [M+Na]⁺
Calcd for C₂₆H₃₁NO₃Na 428.2196; Found 428.2184.



4-hydroxy-4-(1-phenyl-3-pivaloyl-1H-indol-4-yl)hexan-3-one (3ke): was prepared according to general procedure (5.5a). The crude reaction mixture was purified by column chromatography using silica gel (100-200 mesh size), giving (19 mg) 64% yield. Physical State:

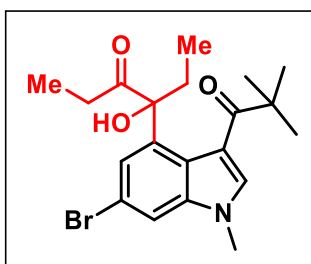
light yellow liquid R_f-value: 0.5 (10% EtOAc/hexane). **¹H NMR (CDCl₃, 400 MHz):** δ 7.70 (s, 1H), 7.58-7.52 (m, 2H), 7.47-7.45 (m, 3H), 7.42-7.39 (m, 1H), 7.34 (d, *J* = 7.2 Hz, 1H), 7.28-7.26 (m, 1H), 5.54 (s, 1H), 2.78-2.54 (m, 2H), 2.26-2.20 (m, 2H), 1.40 (s, 9H), 1.06 (t, *J* = 7.6 Hz, 3H), 0.89 (t, *J* = 7.6 Hz, 3H). **¹³C NMR (CDCl₃, 100 MHz):** δ 212.4, 208.2, 138.7, 138.3, 135.3, 130.4, 130.1, 128.3, 125.9, 124.6, 123.6, 122.4, 118.8, 111.2, 87.7, 44.6, 31.9, 30.2, 29.1, 8.4, 8.2. **IR (KBr, cm⁻¹):** 3139, 1710, 1630, 1524, 1398. **HRMS (ESI) m/z:** [M+Na]⁺ Calcd for C₂₅H₂₉NO₃Na 414.2040; Found 414.2026.



4-(6-chloro-1-methyl-3-pivaloyl-1H-indol-4-yl)-4-hydroxyhexan-3-one (3pe): was prepared according to general procedure (5.5a). The crude reaction mixture was purified by column chromatography using silica

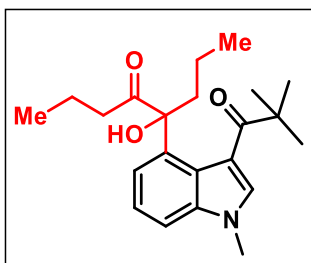
gel (100-200 mesh size) giving (18 mg) 62% yield. Physical State: yellow solid m.p.: 121 – 123 °C R_f-value: 0.6 (20% EtOAc/hexane). **¹H NMR (CDCl₃, 400 MHz):** δ 7.56 (s, 1H), 7.29 (d, *J* = 1.6 Hz, 1H), 7.27 (d, *J* = 2.0 Hz, 1H), 6.02 (s, 1H), 3.78 (s,

3H), 2.73 – 2.49 (m, 2H), 2.85 – 2.14 (m, 2H), 1.36 (s, 9H), 1.02 (t, $J = 7.2$ Hz, 3H), 0.86 (t, $J = 7.6$ Hz, 3H). **^{13}C NMR (CDCl_3 , 100 MHz):** δ 211.9, 207.2, 139.0, 137.3, 132.9, 129.3, 123.1, 122.5, 116.8, 109.9, 83.5, 44.6, 33.9, 31.4, 30.0, 29.2, 8.5, 8.2. **IR (KBr, cm^{-1}):** 3140, 1711, 1635, 1527, 1401. **HRMS (ESI) m/z :** $[\text{M}+\text{Na}]^+$ Calcd for $\text{C}_{20}\text{H}_{26}\text{ClNO}_3\text{Na}$ 386.1493; Found 386.1479.



4-(6-bromo-1-methyl-3-pivaloyl-1H-indol-4-yl)-4-hydroxyhexan-3-one (3qe): was prepared according to general procedure (5.5a). The crude reaction mixture was purified by column chromatography using silica gel (100-200 mesh size), giving (26 mg) 89% yield.

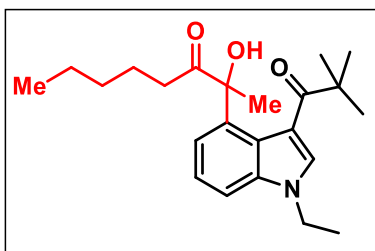
Physical State: yellow liquid R_f -value: 0.5 (20% EtOAc/hexane). **^1H NMR (CDCl_3 , 400 MHz):** δ 7.54 (s, 1H), 7.46 (d, $J = 1.6$ Hz, 1H), 7.40 (d, $J = 1.6$ Hz, 1H), 6.00 (s, 1H), 3.77 (s, 3H), 2.70 – 2.49 (m, 2H), 2.29 – 2.11 (m, 2H), 1.36 (s, 9H), 1.02 (t, $J = 7.2$ Hz, 3H), 0.86 (t, $J = 7.2$ Hz, 3H). **^{13}C NMR (CDCl_3 , 100 MHz):** δ 211.8, 207.2, 139.3, 137.5, 132.7, 125.1, 123.5, 116.9, 116.8, 113.0, 83.5, 44.6, 33.9, 31.4, 30.0, 29.2, 8.5, 8.2. **IR (KBr, cm^{-1}):** 3130, 1712, 1633, 1526, 1401. **HRMS (ESI) m/z :** $[\text{M}+\text{Na}]^+$ Calcd for $\text{C}_{20}\text{H}_{26}\text{BrNO}_3\text{Na}$ 430.0988; Found 430.0961.



5-hydroxy-5-(1-methyl-3-pivaloyl-1H-indol-4-yl)octan-4-one (3af): was prepared according to the general procedure (2.5). The crude reaction mixture was purified by column chromatography using silica gel (100-200 mesh size), giving (16 mg) 45% yield.

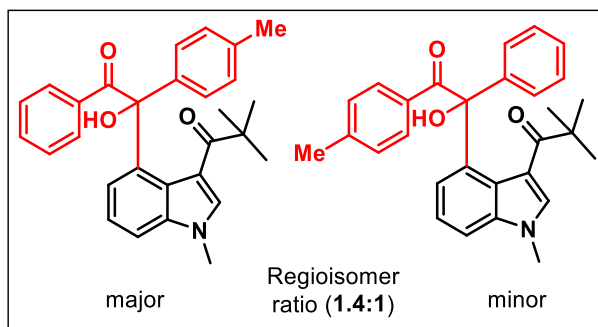
Physical State: colourless liquid R_f -value: 0.5 (20% EtOAc/hexane). **^1H NMR**

(CDCl₃, 400 MHz): δ 7.54 (s, 1H), 7.28 – 7.27 (m, 3H), 5.96 (s, 1H), 3.80 (s, 3H), 2.65 – 2.48 (m, 3H), 2.13 (t, J = 8.0 Hz, 2H), 1.62-1.53 (m, 3), 1.37 (s, 9H), 0.93 (t, J = 7.2 Hz, 3H), 0.85 (t, J = 7.2 Hz, 3H). ¹³C NMR (CDCl₃, 100 MHz): δ 211.9, 207.5, 141.4, 138.6, 136.1, 132.4, 123.1, 121.7, 116.6, 110.0, 83.5, 44.5, 40.9, 39.0, 33.9, 29.3, 17.4, 17.3, 14.7, 14.1. IR (KBr, cm⁻¹): 3131, 1700, 1621, 1530, 1402. HRMS (ESI) m/z: [M+Na]⁺ Calcd for C₂₂H₃₁NO₃Na 380.2196; Found 380.2180.



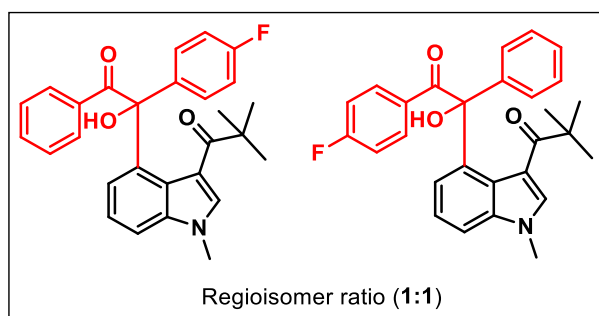
2-(1-ethyl-3-pivaloyl-1H-indol-4-yl)-2-hydroxyoctan-3-one (3bg): was prepared according to general procedure (5.5a). The crude reaction mixture was purified by column

chromatography using silica gel (100-200 mesh size), giving (16 mg) 46% yield. Physical State: colourless liquid R_f-value: 0.4 (20% EtOAc/hexane). ¹H NMR (CDCl₃, 400 MHz): δ 7.74 (s, 1H), 7.39 (d, J = 7.2 Hz, 1H), 7.34 (d, J = 7.2 Hz, 1H), 7.29 (d, J = 7.6 Hz, 1H), 6.63 (s, 1H), 4.20 (qd, J = 7.2 Hz, 2.0 Hz, 2H), 2.72 (td, J = 8.0 Hz, 1.6 Hz, 2H), 1.78 (s, 3H), 1.51 (t, J = 7.6 Hz, 3H), 1.37 (s, 9H), 1.30 – 1.21 (m, 6H), 0.85 (t, J = 7.2 Hz, 3H). ¹³C NMR (CDCl₃, 100 MHz): δ 213.3, 206.8, 137.6, 137.5, 132.1, 124.1, 123.3, 121.8, 116.0, 110.4, 81.1, 44.5, 42.1, 36.1, 31.8, 29.6, 26.7, 24.0, 22.8, 15.4, 14.3. IR (KBr, cm⁻¹): 3142, 1651, 1633, 1403. HRMS (ESI) m/z: [M+Na]⁺ Calcd for C₂₃H₃₃NO₃Na 394.2353; Found 394.2322.



1-(4-(1-hydroxy-2-oxo-2-phenyl-1-(p-tolylethyl)-1-methyl-1H-indol-3-yl)-2,2-dimethylpropan-1-one (3ai): was prepared according to general procedure

(5.5a). The crude reaction mixture was purified by column chromatography using silica gel (100-200 mesh size), giving (24 mg) 56% yield. Physical State: solid brown m.p.: 236 – 238 °C *R_f*-value: 0.30 (10% EtOAc/hexane). **¹H NMR (CDCl₃, 400 MHz):** δ 8.81 (s, 1.4H), 8.75 (s, 1H), 8.27 (d, *J* = 8.0 Hz, 2H), 8.16 (d, *J* = 8.0 Hz, 2.8H), 7.87 (s, 2.4H), 7.64 (s, 1.4H), 7.53 (s, 1H), 7.37-7.35 (m, 4H), 7.30-7.25 (m, 5H), 7.18-7.16 (m, 2H), 7.10-7.05 (m, 5H), 6.53 (d, *J* = 7.6 Hz, 1H), 6.48 (d, *J* = 7.6 Hz, 1.4H), 3.84 (s, 7.2H), 2.34 (s, 3H), 2.30 (s, 4.3H), 1.22 (s, 11.6H), 1.21 (s, 9H). **¹³C NMR (CDCl₃, 176 MHz):** δ 206.3, 206.1, 198.1, 197.8, 142.7, 141.5, 141.4, 138.4, 138.0, 137.4, 135.5, 135.4, 132.8, 132.1, 131.5, 131.4, 129.3, 128.6, 128.5, 128.5, 127.9, 127.8, 127.7, 124.5, 124.5, 123.4, 123.4, 116.0, 115.9, 110.3, 87.2, 44.4, 44.3, 34.2, 34.2, 29.5, 29.5, 21.9, 21.4. **IR (KBr, cm⁻¹):** 3439, 1763, 1632, 1257, 1055, 752. **HRMS (ESI) m/z:** [M+Na]⁺ Calcd for C₂₉H₂₉NO₃Na 462.2040; Found 462.2050.



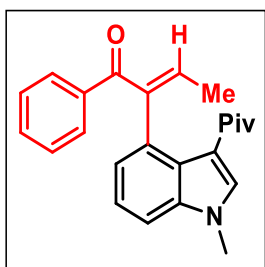
1-(4-(2-(4-fluorophenyl)-1-hydroxy-2-oxo-1-phenylethyl)-1-methyl-1H-indol-3-yl)-2,2-dimethylpropan-1-one (3aj):

was prepared according to

general procedure (5.5a). The crude reaction mixture was purified by column chromatography using silica gel (100-200 mesh size), giving (26 mg) 64% yield.

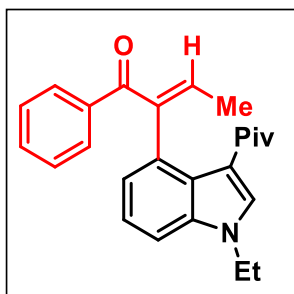
Physical State: yellow solid m.p.: 241 – 243 °C *R_f*-value: 0.35 (20% EtOAc/hexane).

¹H NMR (CDCl₃, 400 MHz): δ 8.84 (s, 1H), 8.80 (s, 1H), 8.34-8.30 (m, 3H), 8.25 (d, *J* = 8.0 Hz, 2H), 7.89 (s, 2H), 7.62 (s, 2H), 7.41-7.36 (m, 3H), 7.31-7.25 (m, 5H), 7.11-7.05 (m, 5H), 6.94 (t, *J* = 8.8 Hz, 2H), 6.49 (d, *J* = 7.2 Hz, 2H), 3.85 (s, 3H), 1.22 (s, 9H), 1.21 (s, 9H). **¹³C NMR (CDCl₃, 176 MHz):** δ 206.3, 206.3, 198.0, 196.6, 165.1 (d, *J_{C-F}* = 253.7 Hz), 162.6 (d, *J_{C-F}* = 246.2 Hz), 141.1 (d, *J_{C-F}* = 3.1 Hz), 140.9, 138.4 (d, *J_{C-F}* = 2.1 Hz), 136.9, 135.7, 135.6, 135.2, 134.0, (d, *J_{C-F}* = 3.8 Hz), 132.3, 131.7, 131.7, 131.3, 129.6, (d, *J_{C-F}* = 3.8 Hz), 128.6, 127.9, 127.8, 124.6, 124.4 (d, *J_{C-F}* = 2.1 Hz), 124.3, 123.4, 123.4, 115.9, 115.5 (d, *J_{C-F}* = 9.3 Hz), 115.0 (d, *J_{C-F}* = 9.1 Hz), 110.4 (d, *J_{C-F}* = 3.7 Hz), 87.3, 87.1, 44.4, 34.2, 29.5, 29.5. **¹⁹F NMR (CDCl₃, 376 MHz):** δ -107.1, -115.2. **IR (KBr, cm⁻¹):** 3145, 2929, 1675, 1626, 1523, 1398. **HRMS (ESI) m/z:** [M+Na]⁺ Calcd for C₂₈H₂₆FNO₃Na 466.1789; Found 466.1801.



(E)-2-(1-methyl-3-pivaloyl-1H-indol-4-yl)-1-phenylbut-2-en-1-one (3ah): was prepared according to general procedure (5.5a). The crude reaction mixture was purified by column chromatography using silica gel (100-200 mesh size), giving (26 mg) 86% yield. Physical State: solid

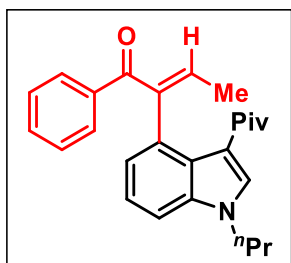
brown m.p.: 186 – 188 °C R_f-value: 0.3 (10% EtOAc/hexane). **¹H NMR (CDCl₃, 400 MHz):** δ 7.88 (dd, *J* = 7.6 Hz, 1.2 Hz, 2H), 7.63 (s, 1H), 7.48 – 7.38 (m, 3H), 7.33 – 7.32 (m, 2H), 7.01 – 6.97 (m, 1H), 6.77 (q, *J* = 7.2 Hz, 1H), 3.84 (s, 3H), 1.82 (d, *J* = 7.2 Hz, 3H), 1.26 (s, 9H). **¹³C NMR (CDCl₃, 100 MHz):** δ 203.0, 196.8, 145.0, 142.5, 139.9, 137.7, 132.7, 130.7, 130.3, 130.1, 127.9, 126.5, 125.6, 123.1, 115.8, 109.5, 44.3, 33.8, 29.1, 16.8. **IR (KBr, cm⁻¹):** 3143, 1648, 1572, 1530, 1400. **HRMS (ESI) m/z:** [M+Na]⁺ Calcd for C₂₄H₂₆NO₂ 360.1928; Found 360.1958.



(E)-2-(1-ethyl-3-pivaloyl-1H-indol-4-yl)-1-phenylbut-2-en-1-one (3bh): was prepared according to general procedure (5.5a). The crude reaction mixture was purified by column chromatography using silica gel (100-200 mesh size), giving (23 mg) 70% yield. Physical

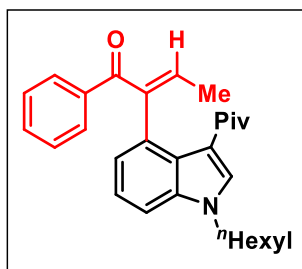
State: yellow solid m.p.: 181 – 183 °C R_f-value: 0.4 (10% EtOAc/hexane). **¹H NMR (CDCl₃, 400 MHz):** δ 7.88 (d, *J* = 8.0 Hz, 2H), 7.67 (s, 1H), 7.47 – 7.38 (m, 3H), 7.36 – 7.28 (m, 2H), 6.97 (d, *J* = 6.8 Hz, 1H), 6.76 (d, *J* = 7.2 Hz, 1H), 4.22 (q, *J* = 7.6 Hz, 2H), 1.82 (d, *J* = 7.2 Hz, 3H), 1.53 (t, *J* = 7.2 Hz, 3H), 1.26 (s, 9H). **¹³C NMR (CDCl₃, 100 MHz):** δ 203.2, 196.7, 145.0, 142.5, 139.9, 136.8, 130.9, 130.7, 130.4, 130.1, 127.9, 126.6, 125.5, 122.9, 115.9, 109.5, 44.3, 41.9, 29.1, 16.8, 15.5. **IR (KBr,**

cm^{-1}): 3142, 1642, 1599, 1435, 1367. **HRMS (ESI)** m/z : $[\text{M}+\text{Na}]^+$ Calcd for $\text{C}_{25}\text{H}_{28}\text{NO}_2$ 374.2115; Found 374.2094.



(E)-1-phenyl-2-(3-pivaloyl-1-propyl-1H-indol-4-yl)but-2-en-1-one (3ch): was prepared according to general procedure (5.5a). The crude reaction mixture was purified by column chromatography using silica gel (100-200 mesh size) giving (26 mg) 78% yield. Physical State:

brown liquid R_f -value: 0.5 (10% EtOAc/hexane). **^1H NMR (CDCl_3 , 400 MHz):** δ 7.89-7.87 (m, 2H), 7.66 (s, 1H), 7.47-7.38 (m, 3H), 7.35-7.28 (m, 2H), 6.98-6.96 (m, 1H), 6.77 (q, $J = 6.8$ Hz, 1H), 4.12 (t, $J = 7.2$ Hz, 2H), 1.97-1.88 (m, 2H), 1.83 (d, $J = 6.8$ Hz, 3H), 1.26 (s, 9H), 1.00 (t, $J = 7.2$ Hz, 3H). **^{13}C NMR (CDCl_3 , 100 MHz):** δ 203.2, 196.8, 145.0, 142.5, 139.9, 137.0, 131.8, 130.7, 130.3, 130.1, 127.9, 126.5, 125.4, 122.9, 115.6, 109.6, 49.0, 44.3, 29.1, 123.5, 16.8, 11.8. **IR (KBr, cm^{-1}):** 3135, 2965, 1647, 1598, 1525, 1398. **HRMS (ESI)** m/z : $[\text{M}+\text{Na}]^+$ Calcd for $\text{C}_{26}\text{H}_{29}\text{NO}_2\text{Na}$ 410.2091; Found 410.2113.

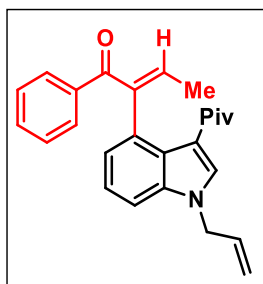


(E)-2-(1-hexyl-3-pivaloyl-1H-indol-4-yl)-1-phenylbut-2-en-1-one (3dh): was prepared according to general procedure (5.5a). The crude reaction mixture was purified by column chromatography using silica gel (100-200 mesh size), giving (24 mg) 75% yield.

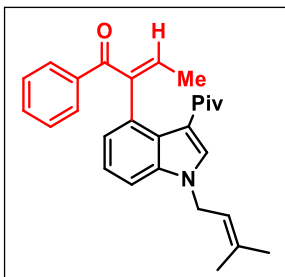
Physical State: yellow solid m.p.: 104 – 106 °C R_f -value: 0.3 (10% EtOAc/hexane).

^1H NMR (CDCl_3 , 400 MHz): δ 7.88 (dd, $J = 8.0$ Hz, 1.2 Hz, 2H), 7.65 (s, 1H),

7.47 – 7.38 (m, 3H), 7.35 – 7.28 (m, 2H), 6.97 (dd, $J = 6.8$ Hz, 1.2 Hz, 1H), 6.76 (q, $J = 7.2$ Hz, 1H), 4.15 (t, $J = 7.2$ Hz, 2H), 1.89 (pent, $J = 7.2$ Hz, 2H), 1.82 (d, $J = 7.2$ Hz, 3H), 1.40 – 1.31 (m, 6H), 1.26 (s, 9H), 0.89 (m, 3H). **^{13}C NMR (CDCl_3 , 100 MHz):** δ 203.2, 196.7, 145.0, 142.5, 139.9, 137.0, 131.7, 130.7, 130.3, 130.1, 127.9, 126.6, 125.4, 122.9, 115.7, 109.6, 47.3, 44.3, 31.6, 30.2, 29.1, 27.0, 22.8, 16.8, 14.3. **IR (KBr, cm^{-1}):** 3148, 1651, 1596, 1531, 1397. **HRMS (ESI) m/z :** $[\text{M}+\text{Na}]^+$ Calcd for $\text{C}_{29}\text{H}_{35}\text{NO}_2\text{Na}$ 452.2560; Found 452.2551.

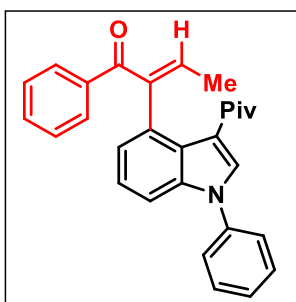


(*E*)-2-(1-allyl-3-pivaloyl-1H-indol-4-yl)-1-phenylbut-2-en-1-one (3hh): was prepared according to general procedure (5.5a). The crude reaction mixture was purified by column chromatography using silica gel (100-200 mesh size), giving (27 mg) 82% yield. Physical State: colourless liquid R_f -value: 0.2 (10% EtOAc/hexane). **^1H NMR (CDCl_3 , 400 MHz):** δ 7.88 (dd, $J = 8.0$ Hz, 1.2 Hz, 2H), 7.65 (s, 1H), 7.48 – 7.38 (m, 3H), 7.34 – 7.27 (m, 2H), 6.98 (dd, $J = 6.4$ Hz, 1.6 Hz, 1H), 6.77 (q, $J = 6.8$ Hz, 1H), 6.09 – 5.99 (m, 1H), 5.32 – 5.21 (m, 2H), 4.77 (d, $J = 5.2$ Hz, 2H), 1.83 (d, $J = 7.2$ Hz, 3H), 1.26 (s, 9H). **^{13}C NMR (CDCl_3 , 100 MHz):** δ 203.2, 196.7, 144.9, 142.6, 139.9, 137.1, 132.7, 131.4, 130.7, 130.3, 130.1, 127.9, 126.6, 125.6, 123.1, 118.8, 116.2, 109.8, 49.6, 44.3, 29.0, 16.8. **IR (KBr, cm^{-1}):** 3134, 1640, 1574, 1524, 1397. **HRMS (ESI) m/z :** $[\text{M}+\text{Na}]^+$ Calcd for $\text{C}_{26}\text{H}_{27}\text{NO}_2\text{Na}$ 408.1934; Found 408.1925.



(E)-2-(1-(3-methylbut-2-en-1-yl)-3-pivaloyl-1H-indol-4-yl)-1-phenylbut-2-en-1-one (3ih): was prepared according to general procedure (5.5a). The crude reaction mixture was purified by column chromatography using silica gel (100-200 mesh size),

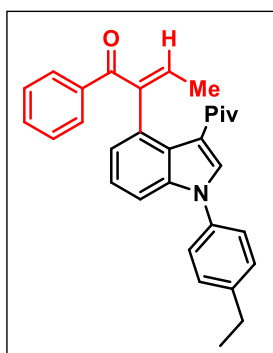
giving (28 mg) 87% yield. Physical State: solid brown m.p.: 123 – 124 °C R_f-value: 0.3 (10% EtOAc/hexane). **¹H NMR (CDCl₃, 400 MHz):** δ 7.90-7.87 (m, 2H), 7.66 (s, 1H), 7.47-7.38 (m, 3H), 7.34-7.27 (m, 2H), 6.98-6.96 (m, 1H), 6.77 (q, *J* = 7.2 Hz, 1H), 5.44-5.40 (m, 1H), 4.72 (d, *J* = 6.8 Hz, 2H), 1.84-1.81 (m, 9H), 1.25 (s, 9H). **¹³C NMR (CDCl₃, 100 MHz):** δ 203.1, 196.8, 145.0, 142.5, 139.9, 138.0, 137.1, 131.3, 130.7, 130.2, 130.1, 127.9, 126.7, 125.5, 122.8, 119.1, 115.7, 109.8, 45.0, 44.3, 29.1, 25.9, 18.5, 16.8. **IR (KBr, cm⁻¹):** 3133, 1646, 1576, 1523, 1401. **HRMS (ESI)** m/z: [M+Na]⁺ Calcd for C₂₈H₃₁NO₂Na 436.2247; Found 436.2251.



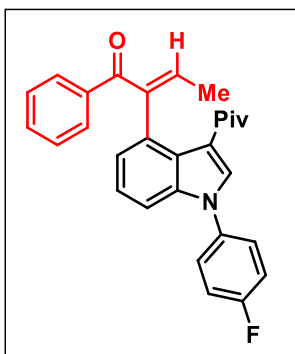
(E)-1-phenyl-2-(1-phenyl-3-pivaloyl-1H-indol-4-yl)but-2-en-1-one (3kh): was prepared according to general procedure (5.5a). The crude reaction mixture was purified by column chromatography using silica gel (100-200 mesh size), giving (29 mg) 90% yield.

Physical State: solid brown m.p.: 219 – 221 °C R_f-value: 0.4 (10% EtOAc/hexane). **¹H NMR (CDCl₃, 400 MHz):** δ 7.93-7.91 (m, 2H), 7.85 (s, 1H), 7.62-7.55 (m, 4H), 7.51-7.43 (m, 5H), 7.32 (t, *J* = 7.2 Hz, 1H), 7.05 (d, *J* = 6.8 Hz, 1H), 6.84 (q, *J* = 7.2 Hz, 1H), 1.91 (d, *J* = 6.8 Hz, 3H) 1.32 (s, 9H). **¹³C NMR (CDCl₃, 100 MHz):** δ 203.8, 196.8, 144.8, 143.1, 139.8, 139.0, 137.5, 131.4, 130.8, 130.3, 130.2, 130.1, 128.1,

128.0, 126.7, 126.1, 125.8, 123.7, 117.8, 110.7, 44.5, 29.0, 16.9. **IR (KBr, cm⁻¹):** 3415, 3138, 1653, 1595, 1527, 1401. **HRMS (ESI) m/z:** [M+Na]⁺ Calcd for C₂₉H₂₇NO₂Na 444.1934; Found 444.1917.

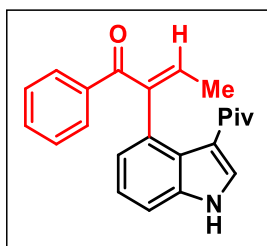


(E)-2-(1-(4-ethylphenyl)-3-pivaloyl-1H-indol-4-yl)-1-phenylbut-2-en-1-one (3kh3): was prepared according to general procedure (5.5a). The crude reaction mixture was purified by column chromatography using silica gel (100-200 mesh size), giving (25 mg) 56% yield. Physical State: colourless liquid R_f-value: 0.5 (30% EtOAc/hexane). **¹H NMR (CDCl₃, 700 MHz):** δ 7.89 (d, *J* = 7.7 Hz, 2H), 7.81 (s, 1H), 7.47 (t, *J* = 7.7 Hz, 1H), 7.44-7.42 (m, 5H), 7.39 (d, *J* = 8.4 Hz, 2H), 7.28 (t, *J* = 7.7 Hz, 1H), 7.01 (d, *J* = 7.0 Hz, 1H), 6.81 (q, *J* = 7.0 Hz, 1H), 2.77 (q, *J* = 7.7 Hz, 2H), 1.88 (d, *J* = 7.0 Hz, 3H), 1.32 (t, *J* = 7.7 Hz, 3H), 1.29 (s, 9H). **¹³C NMR (CDCl₃, 176 MHz):** δ 203.7, 196.8, 144.8, 144.5, 143.0, 139.8, 137.6, 136.6, 131.6, 130.8, 130.2, 130.1, 129.5, 128.0, 126.6, 126.0, 125.7, 123.5, 117.5, 110.8, 44.5, 29.0, 28.8, 16.9, 15.9. **IR (KBr, cm⁻¹):** 3453, 2993, 1637, 1424, 1264, 1045. **HRMS (ESI) m/z:** [M+H]⁺ Calcd for C₃₁H₃₂NO₂ 450.2428; Found 450.2412.



(E)-2-(1-(4-fluorophenyl)-3-pivaloyl-1H-indol-4-yl)-1-phenylbut-2-en-1-one (3kh4): was prepared according to the general procedure (5.5a). The crude reaction mixture was purified by column chromatography using silica gel (100-200 mesh size), giving (34 mg) 77% yield. Physical State: colourless

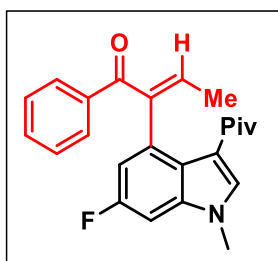
liquid R_f-value: 0.4 (30% EtOAc/hexane). **¹H NMR (CDCl₃, 700 MHz):** δ 7.89 (d, *J* = 7.0 Hz, 2H), 7.76 (s, 1H), 7.51-7.47 (m, 3H), 7.43 (t, *J* = 7.7 Hz, 2H), 7.36 (d, *J* = 7.7 Hz, 1H), 7.30 (t, *J* = 7.7 Hz, 1H), 7.27-7.25 (m, 3H), 7.02 (d, *J* = 7.0 Hz, 1H), 6.82 (q, *J* = 7.0 Hz, 1H), 1.88 (d, *J* = 7.0 Hz, 3H), 1.29 (s, 9H). **¹³C NMR (CDCl₃, 176 MHz):** δ 203.8, 196.8, 162.2 (d, *J*_{C-F} = 248.3 Hz), 144.6, 143.2, 139.7, 137.7, 135.0 (d, *J*_{C-F} = 2.9 Hz), 131.2, 130.9, 130.4, 130.1, 128.0, 127.7 (d, *J*_{C-F} = 8.6 Hz), 126.6, 126.1, 123.8, 117.8, 117.1 (d, *J*_{C-F} = 22.8 Hz), 110.4, 44.5, 28.9, 16.9. **¹⁹F NMR (CDCl₃, 376 MHz):** δ -113.1. **IR (KBr, cm⁻¹):** 3439, 2994, 1758, 1382, 1245. **HRMS (ESI) m/z:** [M+Na]⁺ Calcd for C₂₉H₂₆FO₂Na 462.1840; Found 462.1841.



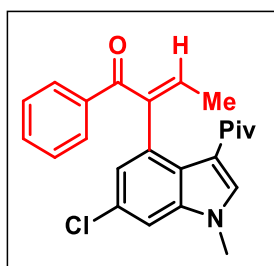
(Z)-1-phenyl-2-(3-pivaloyl-1H-indol-4-yl)but-2-en-1-one (3lh): was prepared according to the general procedure (5.5a). The crude reaction mixture was purified by column chromatography using silica gel (100-200 mesh size), giving

(27 mg) 75% yield. Physical State: brown solid m.p.: 198 – 200 °C R_f-value: 0.4 (20% EtOAc/hexane). **¹H NMR (CDCl₃, 400 MHz):** δ 9.02 (s, 1H), 7.93-7.91 (m, 2H), 7.52-7.42 (m, 4H), 7.14 (t, *J* = 7.6 Hz, 1H), 7.02 (d, *J* = 7.6 Hz, 1H), 6.92 (d, *J* = 7.2 Hz, 1H), 6.74 (q, *J* = 7.2 Hz, 1H), 1.69 (d, *J* = 6.8 Hz, 3H), 1.24 (s, 9H). **¹³C NMR**

(CDCl₃, 100 MHz): δ 203.9, 198.3, 145.0, 143.5, 139.8, 136.7, 130.9, 130.1, 129.4, 129.2, 128.0, 125.4, 125.0, 122.8, 116.0, 111.8, 44.3, 29.0, 16.6. **IR (KBr, cm⁻¹):** 3148, 1635, 1520, 1401. **HRMS (ESI) m/z:** [M+Na]⁺ Calcd for C₂₃H₂₃NO₂Na 368.1621; Found 368.1614.

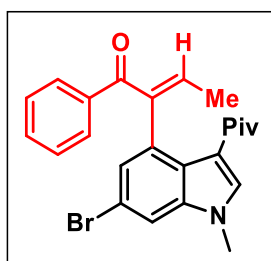


(Z)-2-(6-fluoro-1-methyl-3-pivaloyl-1H-indol-4-yl)-1-phenylbut-2-en-1-one (3oh): was prepared according to general procedure (5.5a). The crude reaction mixture was purified by column chromatography using silica gel (100-200 mesh size), giving (26 mg) 78% yield. Physical State: orange solid m.p.: 194 – 196 °C R_f-value: 0.3 (20% EtOAc/hexane). **¹H NMR (CDCl₃, 400 MHz):** δ 7.87 (d, *J* = 7.6 Hz, 2H), 7.61 (s, 1H), 7.49 – 7.37 (m, 3H), 7.00 (dd, *J* = 8.8 Hz, 2.4 Hz, 1H), 6.80 – 6.77 (m, 2H), 3.79 (s, 3H), 1.83 (d, *J* = 7.2 Hz, 3H), 1.25 (s, 9H). **¹³C NMR (CDCl₃, 100 MHz):** δ 202.9, 196.3, 160.0 (d, *J* = 239.0 Hz), 144.1, 143.0, 139.5, 137.9 (d, *J* = 13.0 Hz), 132.9 (d, *J* = 3.0 Hz), 132.6 (d, *J* = 3.0 Hz), 131.9 (d, *J* = 9.0 Hz), 130.9, 130.1, 128.0, 116.0, 113.9 (d, *J* = 24.0 Hz), 95.6 (d, *J* = 26.0 Hz), 44.4, 33.8, 29.0, 16.7. **¹⁹F NMR (CDCl₃, 376 MHz):** δ -119.8. **IR (KBr, cm⁻¹):** 3140, 1653, 1586, 1525, 1400. **HRMS (ESI) m/z:** [M+Na]⁺ Calcd for C₂₄H₂₄FNO₂Na 400.1683; Found 400.1688.



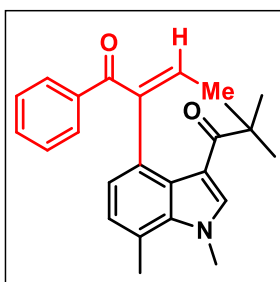
(Z)-2-(6-chloro-1-methyl-3-pivaloyl-1H-indol-4-yl)-1-phenylbut-2-en-1-one (3ph): was prepared according to general procedure (5.5a). The crude reaction mixture was purified by column chromatography using silica gel (100-200 mesh size), giving (23 mg) 71% yield. Physical State: yellow liquid R_f-value:

0.2 (10% EtOAc/hexane). **¹H NMR (CDCl₃, 400 MHz):** δ 7.86 (dd, J = 8.0 Hz, 1.2 Hz, 2H), 7.61 (s, 1H), 7.47 – 7.40 (m, 3H), 7.32 (brd, J = 2.0 Hz, 1H), 6.98 (d, J = 2.0 Hz, 1H), 6.79 (q, J = 7.2 Hz, 1H), 3.81 (s, 3H), 1.83 (d, J = 6.8 Hz, 3H), 1.25 (s, 9H). **¹³C NMR (CDCl₃, 100 MHz):** δ 202.9, 196.4, 143.9, 143.2, 139.5, 138.2, 133.0, 131.7, 130.9, 130.0, 129.0, 128.0, 125.6, 125.2, 116.0, 109.5, 44.4, 33.8, 28.9, 16.8. **IR (KBr, cm⁻¹):** 3131, 1644, 1598, 1524, 1401. **HRMS (ESI) m/z:** [M+Na]⁺ Calcd for C₂₄H₂₄ClNO₂Na 416.1388; Found 416.1376.



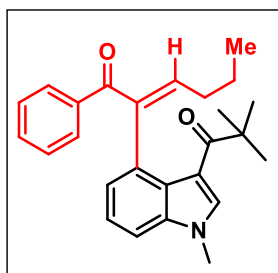
((Z)-2-(6-bromo-1-methyl-3-pivaloyl-1H-indol-4-yl)-1-phenylbut-2-en-1-one (3qh): was prepared according to general procedure (5.5a). The crude reaction mixture was purified by column chromatography using silica gel (100-

200 mesh size), giving (19 mg) 60% yield. Physical State: colourless liquid R_f-value: 0.4 (20% EtOAc/hexane). **¹H NMR (CDCl₃, 400 MHz):** δ 7.87-7.85 (m, 1H), 7.59 (s, 1H), 7.26 (s, 1H), 7.49-7.40 (m, 4H), 7.11 (d, J = 1.6 Hz, 1H), 6.79 (q, J = 7.2 Hz, 1H), 3.81 (s, 3H), 1.84 (d, J = 7.2 Hz, 3H), 1.24 (s, 9H). **¹³C NMR (CDCl₃, 100 MHz):** δ 202.9, 196.4, 143.8, 143.4, 139.4, 138.5, 132.9, 131.9, 130.1, 130.0, 128.1, 128.0, 125.6, 116.5, 116.0, 112.5, 44.4, 33.9, 28.9, 16.9. **IR (KBr, cm⁻¹):** 3391, 1712, 1698, 1523, 1397. **HRMS (ESI) m/z:** [M+Na]⁺ Calcd for C₂₄H₂₄BrNO₂Na 460.0883; Found 460.0881.



(E)-2-(1,7-dimethyl-3-pivaloyl-1H-indol-4-yl)-1-phenylbut-2-en-1-one (3sh): was prepared according to general procedure (5.5a). The crude reaction mixture was purified by column chromatography using silica gel (100-200 mesh size), giving (21 mg) 61% yield. Physical

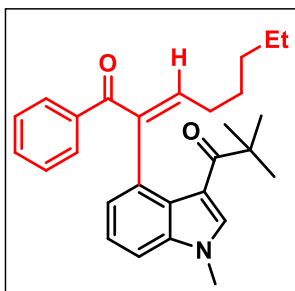
State: colourless liquid R_f -value: 0.30 (20% EtOAc/hexane). **^1H NMR (CDCl_3 , 400 MHz):** δ 7.86 (d, J = 8.0 Hz, 2H), 7.49 (s, 1H), 7.45-7.37 (m, 3H), 7.00 (d, J = 7.6 Hz, 1H), 6.81 (d, J = 7.2 Hz, 1H), 6.73 (q, J = 7.2 Hz, 1H), 4.10 (s, 3H), 2.79 (s, 3H), 1.82 (d, J = 7.2 Hz, 3H), 1.25 (s, 9H). **^{13}C NMR (CDCl_3 , 176 MHz):** δ 203.2, 196.7, 145.0, 142.5, 139.9, 136.4, 134.2, 130.7, 130.1, 128.1, 127.9, 127.4, 126.0, 125.7, 121.3, 115.6, 44.4, 38.1, 29.1, 20.2, 16.8. **IR (KBr, cm^{-1}):** 3439, 2360, 1636, 912, 744. **HRMS (ESI) m/z :** $[\text{M}+\text{Na}]^+$ Calcd for $\text{C}_{25}\text{H}_{27}\text{NO}_2\text{Na}$ 396.1934; Found 396.1941.



(E)-2-(1-methyl-3-pivaloyl-1H-indol-4-yl)-1-phenylhex-2-en-1-one (3an): was prepared according to general procedure (5.5a). The crude reaction mixture was purified by column chromatography using silica gel (100-200 mesh

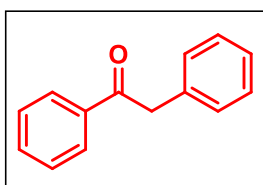
size), giving (24 mg) 62% yield. Physical State: brown colour liquid R_f -value: 0.30 (20% EtOAc/hexane). **^1H NMR (CDCl_3 , 700 MHz):** δ 7.91 (d, J = 7.7 Hz, 2H), 7.62 (s, 1H), 7.46 (t, J = 7.0 Hz, 1H), 7.41 (t, J = 7.7 Hz, 2H), 7.32 (d, J = 4.2 Hz, 2H), 6.98 (t, J = 4.2 Hz, 1H), 6.46 (t, J = 7.7 Hz, 1H) 3.84 (s, 3H), 2.17-2.10 (m, 2H), 1.47-1.40 (m, 2H), 1.25 (s, 9H), 0.85 (t, J = 7.0 Hz, 3H). **^{13}C NMR (CDCl_3 , 176 MHz):** δ 202.6, 197.0, 147.5 (2C), 143.8, 139.8, 137.7, 132.7, 130.8, 130.3, 127.9,

126.4, 125.6, 123.0, 115.7, 109.4, 44.2, 33.8, 32.9, 29.1, 22.5, 14.4. **IR (KBr, cm⁻¹):** 3440, 2958, 1645, 1528, 1443, 1279, 1112. **HRMS (ESI) m/z:** [M+H]⁺ Calcd for C₂₆H₃₀NO₂ 388.2271; Found 388.2260.



(E)-3-methyl-2-(1-methyl-3-pivaloyl-1H-indol-4-yl)-1-phenyloct-2-en-1-one (3ao): was prepared according to general procedure (5.5a). The crude reaction mixture was purified by column chromatography using silica gel (100-200 mesh size), giving (18 mg) 46% yield.

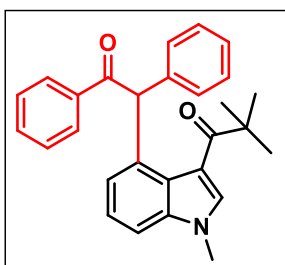
Physical State: colorless liquid *R_f*-value: 0.30 (10% EtOAc/hexane). **¹H NMR (CDCl₃, 400 MHz):** δ 7.91 (d, *J* = 7.6 Hz, 2H), 7.61 (s, 1H), 7.45-7.38 (m, 3H), 7.31-7.30 (m, 2H), 6.97 (t, *J* = 4.4 Hz, 1H), 6.63 (t, *J* = 7.6 Hz, 1H), 3.83 (s, 3H), 2.16-2.10 (m, 2H), 1.43-1.38 (m, 2H), 1.26 (s, 9H), 1.22-1.19 (s, 4H), 0.80 (t, *J* = 7.2 Hz, 3H). **¹³C NMR (CDCl₃, 176 MHz):** δ 202.6, 197.0, 147.8, 143.6, 139.9, 137.7, 132.7, 130.8, 130.7, 130.3, 127.9, 126.4, 125.6, 123.0, 115.6, 109.4, 44.2, 33.8, 32.0, 30.9, 29.1, 28.9, 22.7, 14.2. **IR (KBr, cm⁻¹):** 3441, 2957, 1645, 1529, 1443, 1366, 1265, 1113, 934, 755. **HRMS (ESI) m/z:** [M+H]⁺ Calcd for C₂₈H₃₄NO₂ 416.2584; Found 416.2564.



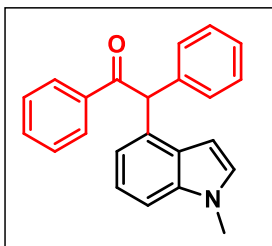
1,2-diphenylethanone (2a*): was prepared according to general procedure (5.5a). The crude reaction mixture was purified by column chromatography using silica gel (100-

200 mesh size), giving (21 mg) 52% yield. Physical State: yellow solid. m.p.: 68 – 70 °C *R_f*-value: 0.6 (05% EtOAc/hexane). **¹H NMR (CDCl₃, 400 MHz):** δ 8.02-8.00

(m, 2H), 7.5-7.512 (m, 1H), 7.47-7.43 (m, 2H), 7.34-7.30 (m, 2H), 7.27-7.24 (m, 3H), 4.28 (s, 2H). **¹³C NMR (CDCl₃, 100 MHz):** δ 197.9, 136.8, 134.8, 133.5, 129.7, 129.0, 128.97, 128.94, 127.2, 45.8. **IR (KBr, cm⁻¹):** 3146, 2918, 2849, 1737, 1586, 1402, 1020. **HRMS (ESI) m/z:** [M+Na]⁺ Calcd for C₁₄H₁₃O 197.0961; Found 197.0966.

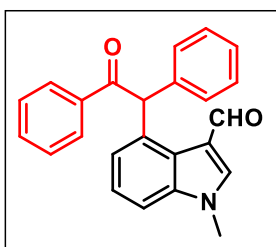


2,2-dimethyl-1-(1-methyl-4-(2-oxo-1,2-diphenylethyl)-1H-indol-3-yl)propan-1-one (3-keto): was prepared according to the reported procedure.²⁰ The crude reaction mixture was purified by column chromatography using silica gel (100-200 mesh size), giving (18 mg) 95% yield. Physical State: light brown solid m.p.: 202 – 204 °C R_f-value: 0.45 (20% EtOAc/hexane). **¹H NMR (CDCl₃, 400 MHz):** δ 8.19 (d, *J* = 7.6 Hz, 2H), 7.61 (s, 1H), 7.45-7.42 (m, 1H), 7.38-7.34 (m, 3H), 7.27-7.25 (m, 1H), 7.21-7.13 (m, 4H), 7.04 (d, *J* = 7.6 Hz, 2H), 6.88 (d, *J* = 7.2 Hz, 1H), 3.81 (s, 3H), 1.21 (s, 9H). **¹³C NMR (CDCl₃, 100 MHz):** δ 205.6, 199.6, 139.7, 138.0, 133.9, 132.8, 132.7, 130.3, 129.8, 128.7, 128.5, 126.9, 126.6, 123.7, 123.4, 116.5, 109.1, 56.6, 44.7, 33.8, 28.9. **IR (KBr, cm⁻¹):** 3440, 2966, 2922, 2848, 1679, 1640, 1524, 1494, 1444, 1364. **HRMS (ESI) m/z:** [M+Na]⁺ Calcd for C₂₈H₂₈NO₂ 410.2115; Found 410.2127.



(2-(1-methyl-1H-indol-4-yl)-1,2-diphenylethanone (4aa): was prepared according to reported procedure.²¹ The crude reaction mixture was purified by column chromatography using silica gel (100-200 mesh size),

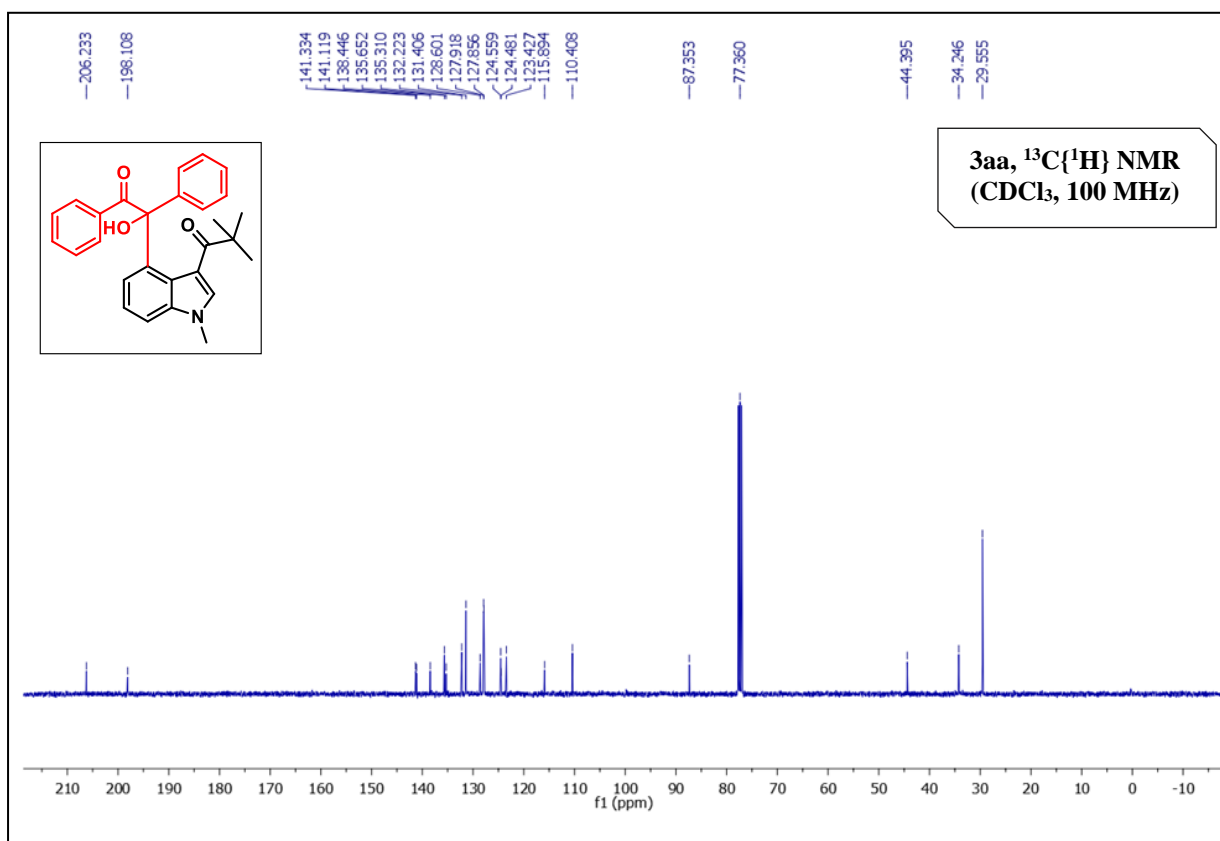
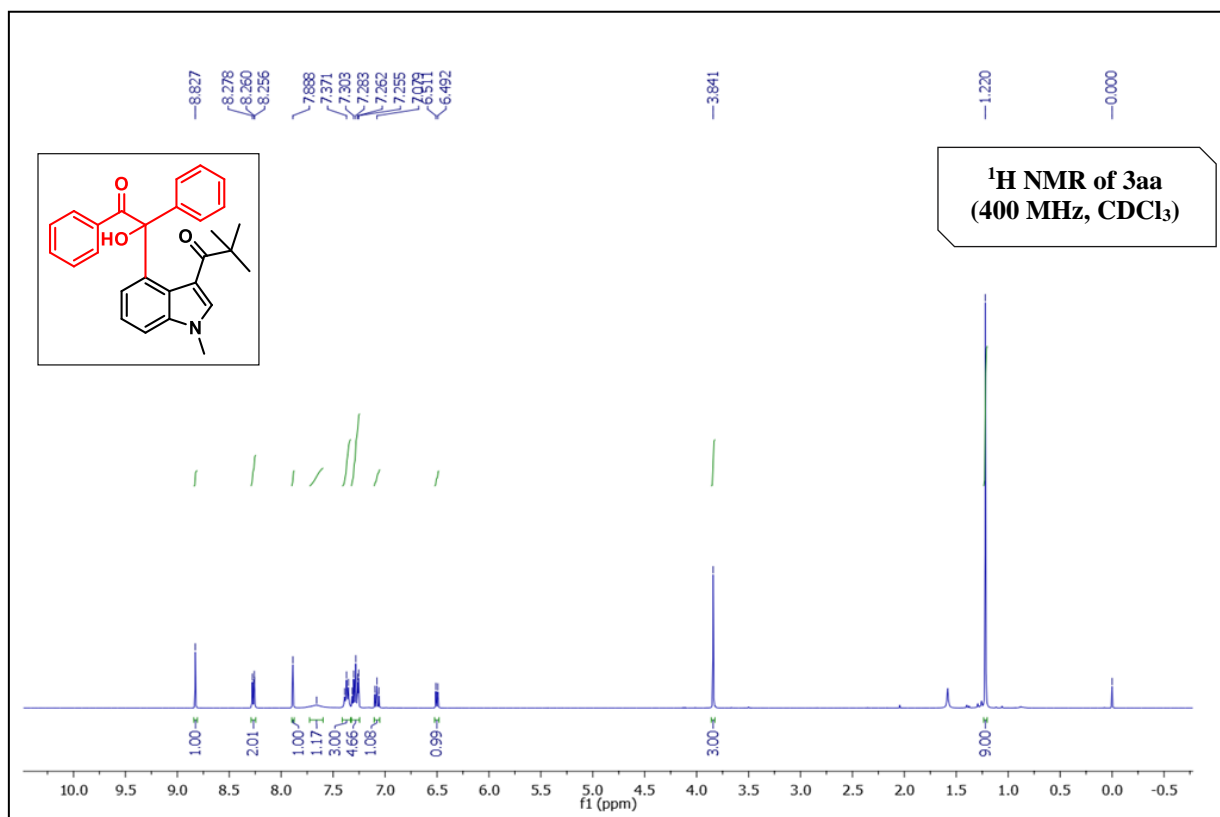
giving (13 mg) 85% yield. Physical State: solid brown m.p.: 217 – 219 °C R_f-value: 0.45 (20% EtOAc/hexane). **¹H NMR (CDCl₃, 400 MHz):** δ 8.00 (d, *J* = 8.0 Hz, 2H), 7.47 (t, *J* = 6.8 Hz, 1H), 7.38-7.28 (m, 6H), 7.24-7.21 (m, 2H), 7.15 (t, *J* = 7.2 Hz, 1H), 7.04 (d, *J* = 2.8 Hz, 1H), 6.92 (d, *J* = 7.2 Hz, 1H), 6.48 (d, *J* = 2.4 Hz, 1H), 6.41 (s, 1H), 3.78 (s, 3H). **¹³C NMR (CDCl₃, 176 MHz):** δ 198.5, 139.0, 137.4, 137.3, 133.1, 131.4, 129.8, 129.3, 129.1, 128.8, 128.7, 127.9, 127.3, 122.1, 119.8, 108.9, 99.4, 57.5, 33.3. **IR (KBr, cm⁻¹):** 3437, 1633, 1246, 751. **HRMS (ESI) m/z:** [M+Na]⁺ Calcd for C₂₃H₁₉NONa 348.1359; Found 348.1350.



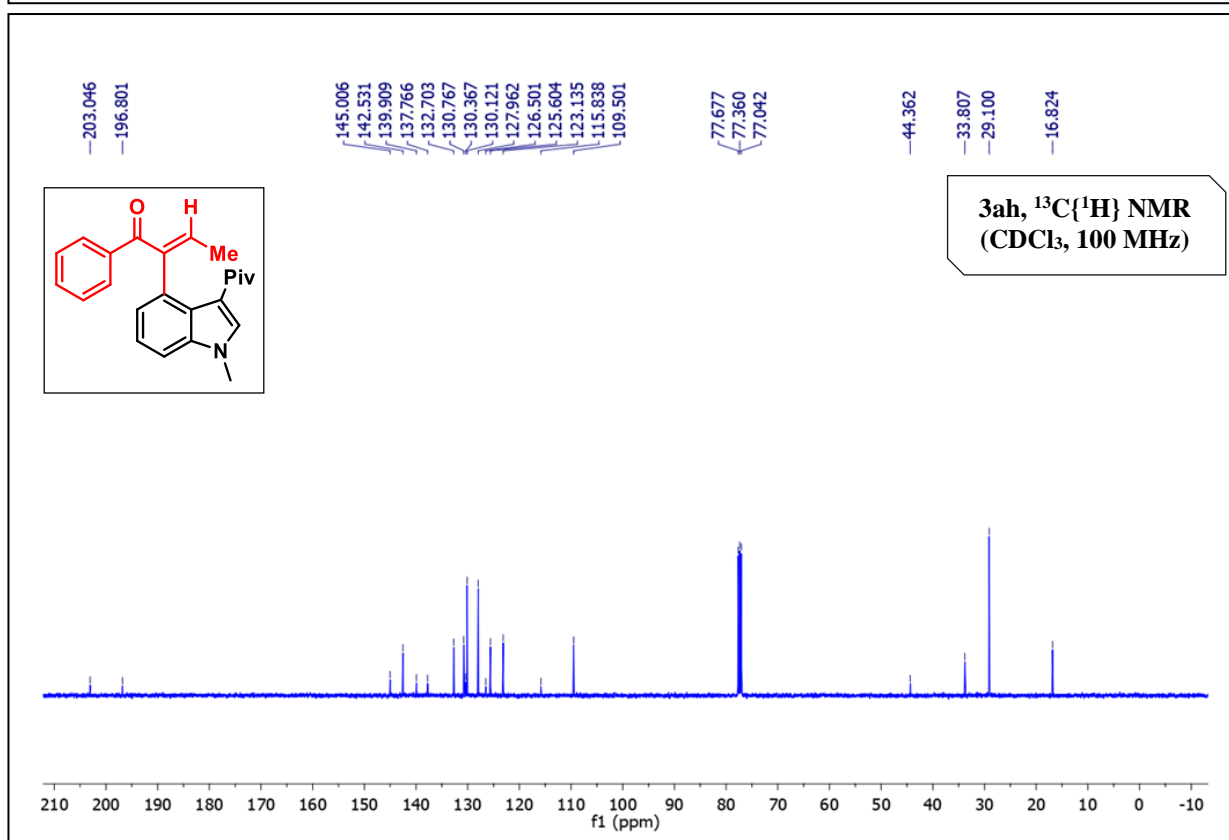
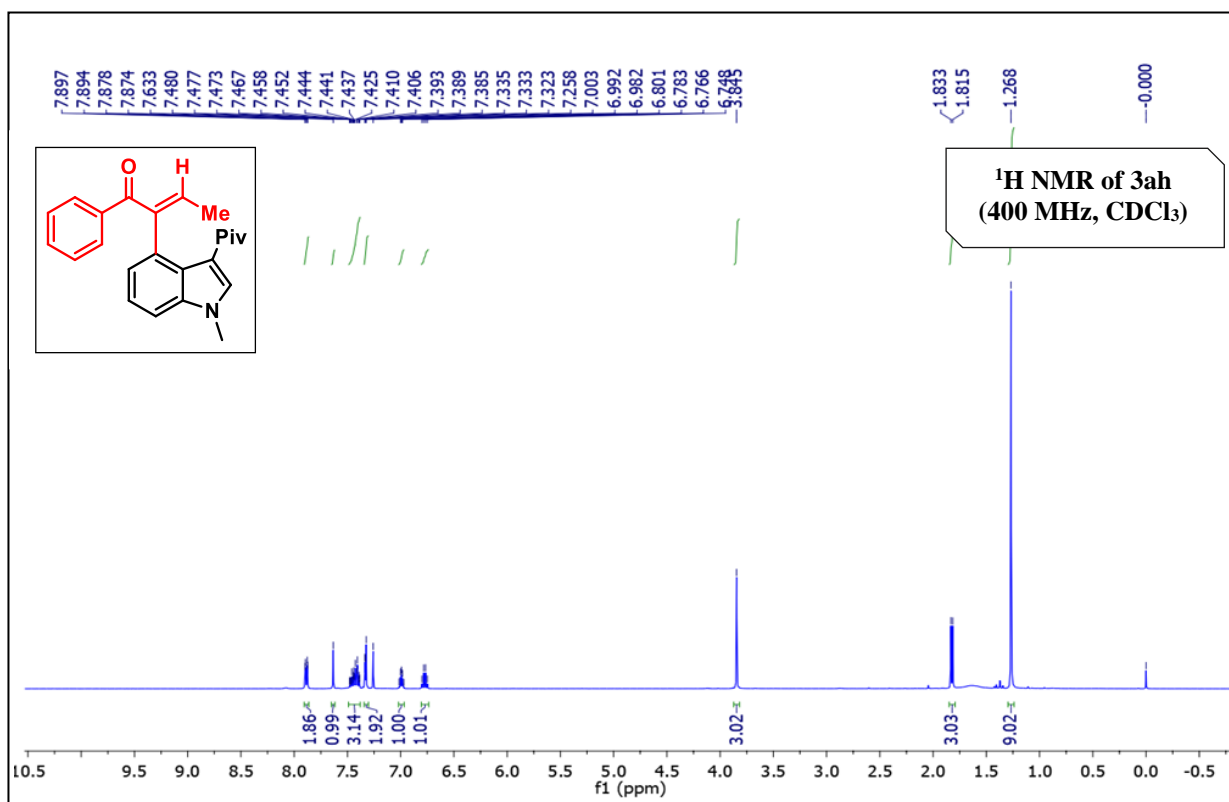
1-methyl-4-(2-oxo-1,2-diphenylethyl)-1H-indole-3-carbaldehyde (5aa): was prepared according to the general procedure.²² The crude reaction mixture was purified by column chromatography using silica gel (100-

200 mesh size), giving (16 mg) 77% yield. Physical State: solid brown m.p.: 211 – 213 °C R_f-value: 0.30 (30% EtOAc/hexane). **¹H NMR (CDCl₃, 700 MHz):** δ 9.81 (s, 1H), 8.13 (d, *J* = 7.7 Hz, 2H), 8.02 (s, 1H), 7.75 (s, 1H), 7.43-7.40 (m, 1H), 7.36-7.31 (m, 6H), 7.20-7.17 (m, 3H), 3.86 (s, 3H). **¹³C NMR (CDCl₃, 176 MHz):** δ 199.1, 183.8, 144.1, 140.2, 139.9, 137.3, 134.5, 132.7, 130.0, 129.8, 128.8, 128.6, 128.3, 127.0, 125.0, 124.7, 119.6, 109.3, 77.3, 57.6, 34.2. **IR (KBr, cm⁻¹):** 3439, 2358, 1634, 1266, 912, 745. **HRMS (ESI) m/z:** [M+Na]⁺ Calcd for C₂₄H₁₉NO₂Na 376.1308; Found 376.1304.

NMR spectra of 1-(4-(1-hydroxy-2-oxo-1,2-diphenylethyl)-1-methyl-1H-indol-3-yl)-2,2-dimethylpropan-1-one (3aa):



NMR spectra of (E)-2-(1-methyl-3-pivaloyl-1H-indol-4-yl)-1-phenylbut-2-en-1-one (3da):



- (b) **Crystals of the compounds 3aa** (1-(4-(1-hydroxy-2-oxo-1,2-diphenylethyl)-1-methyl-1H-indol-3-yl)-2,2-dimethylpropan-1-one) were obtained after slow evaporation of ethanol.

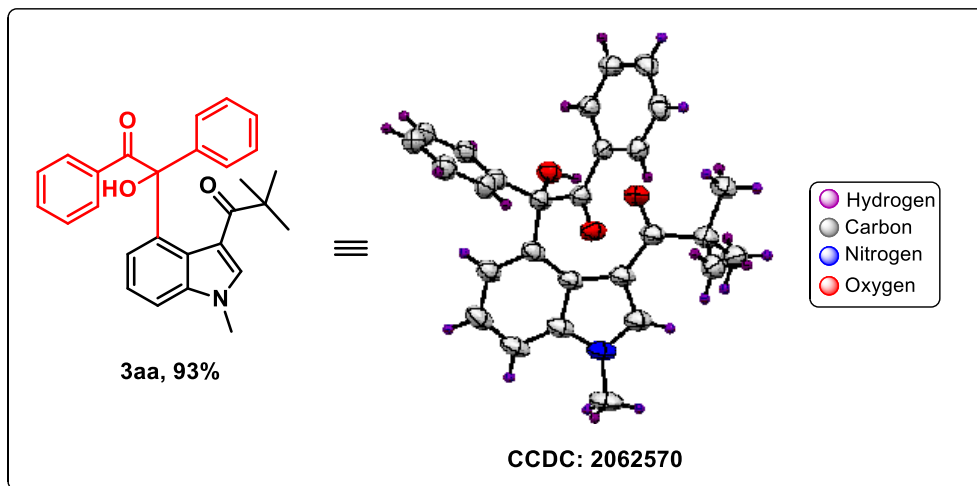
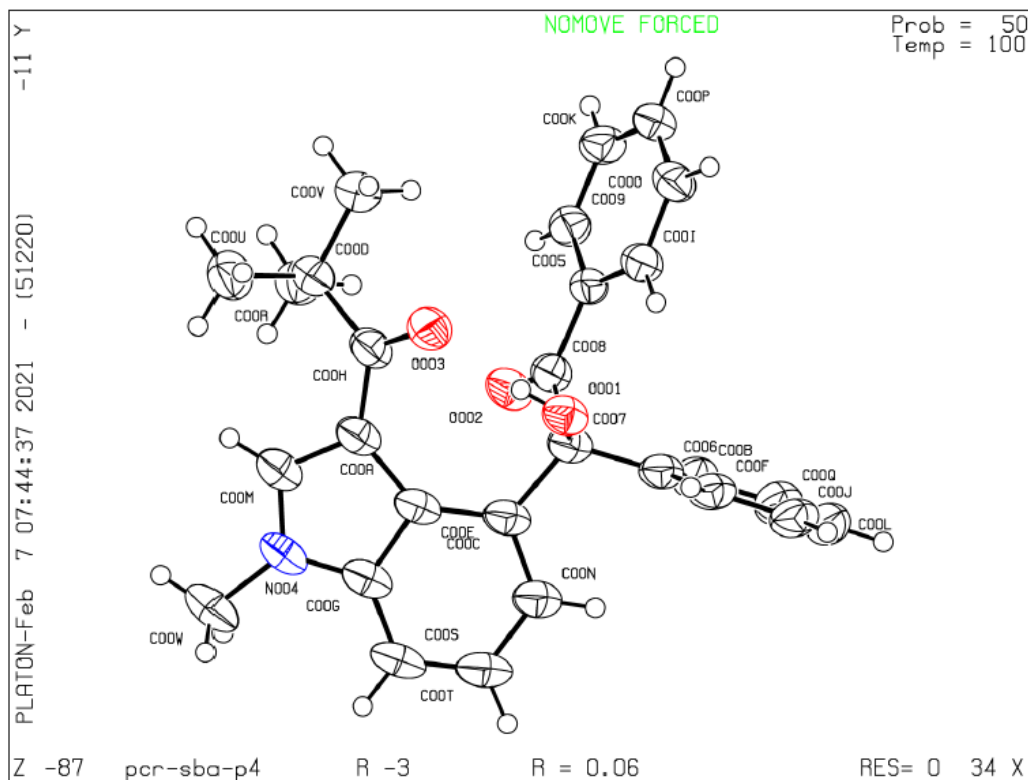


Figure 5.3. Crystal structure of **3aa** (50% ellipsoid probability).

Datablock pcr-sba-p4 - ellipsoid plot



(c) Crystals of the compounds **3be** (4-(1-ethyl-3-pivaloyl-1H-indol-4-yl)-4-hydroxyhexan-3-one) were obtained after slow evaporation of dichloromethane.

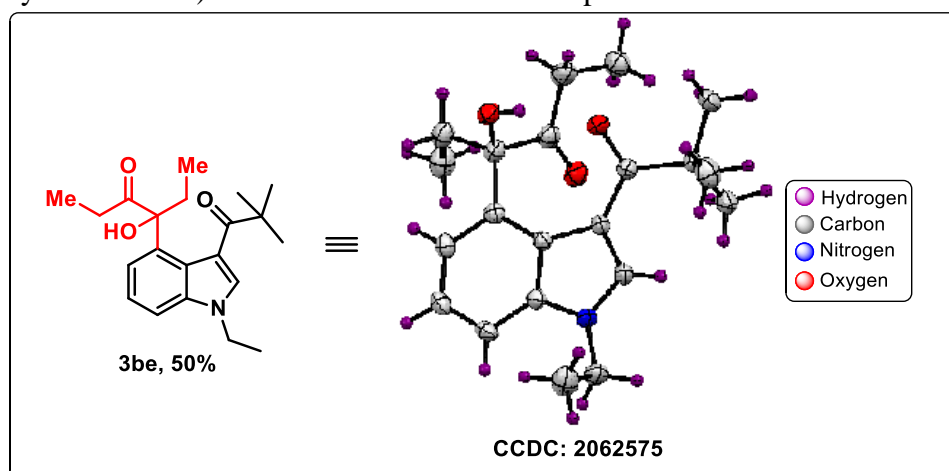
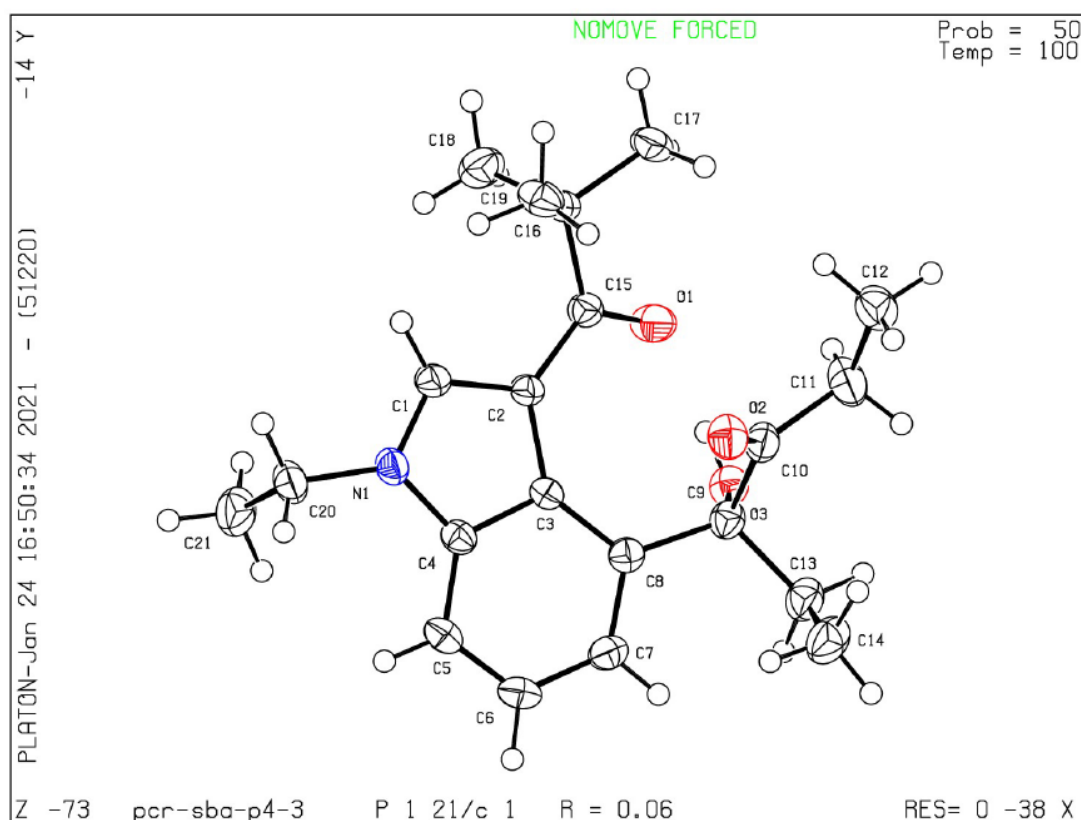


Figure 5.4. Crystal structure of **3be** (50% ellipsoid probability).



5.6 REFERENCES

1. (a) Sharma, V.; Kumar, P.; Pathak, D. Sharma, V.; Ku-mar, P.; Pathak, D. Biological importance of the indole nucleus in recent years: a comprehensive review. *J. Het-erocycl. Chem.* **2010**, *47*, 491–502. (b) Kochanowska-Karamyan, A. J.; Hamann, M. T. Marine Indole Alka-loids: Potential New Drug Leads for the Control of De-pression and Anxiety. *Chem. Rev.* **2010**, *110*, 4489–4497. For recent reviews on synthesis of ergot alkaloids, see: c) McCabe, S. R.; Wipf, Total synthesis, biosynthesis and biological profiles of clavine alkaloids. *P. Org. Biomol. Chem.* **2016**, *14*, 5894–5913. (d) Liu, H.; Jia, Y. Ergot alka-loids: synthetic approaches to lysergic acid and clavine alkaloids. *Nat. Prod. Rep.* **2017**, *34*, 411–432.
2. (a) Taylor, R. D.; Maccoss, M.; Lawson, A. D. Rings in Drugs. *J. Med. Chem.* **2014**, *57*, 5845–5859. (b) Zhang, M.-Z.; Chen, Q.; Yang, G.-F. A review on recent develop-ments of indole-containing antiviral agents. *Eur. J. Med. Chem.* **2015**, *89*, 421–441. (c) Chadha, N.; Silakari, O. In-doles as therapeutics of interest in medicinal chemistry: Bird's eye view. *Eur. J. Med. Chem.* **2017**, *134*, 159–184.
3. (a) Sravanthi, T. V.; Manju, S. L. Indoles a promising scaffold for drug development. *Eur. J. Pharm. Sci.* **2016**, *91*, 1–10. (b) de Sa Alves, F.; Barreiro, E.; Manssour Fraga, C. From nature to drug discovery: the indole scaffold as a 'privileged structure'. *Med. Chem.* **2009**, *9*, 782–793.
4. (a) Stuart, D. R.; Villemure, E.; Fagnou, K. Elements of regiocontrol in palladium-catalyzed oxidative arene cross-coupling. *J. Am. Chem. Soc.* **2007**, *129*, 12072–12073. (b) Lebrasseur, N.; Larrosa, I. Room temperature and phosphine free palladium catalyzed direct C-2 aryla-tion of indoles. *J. Am. Chem. Soc.* **2008**, *130*, 2926–2927. (c) Sandtorv, A. H. Transition Metal-Catalyzed C-H Acti-vation of Indoles. *Adv. Synth. Catal.* **2015**, *357*, 2403–2435.
5. (a) Hartung, C. G.; Fecher, A.; Chapell, B.; Snieckus, V. Directed *ortho*-Metalation Approach to C-7-Substituted Indoles. Suzuki–Miyaura Cross Coupling and the Syn-thesis of Pyrrolophenanthridone Alkaloids. *Org. Lett.* **2003**, *5*, 1899–1902. (b) Yang, G.; Lindovska, P.; Zhu, D.; Kim, J.; Wang, P.; Tang, R.-Y.; Movassaghi, M.; Yu, J.-Q. Pd(II)-Catalyzed meta-C–H Olefination, Arylation, and Acetoxylation of Indolines Using a U-Shaped Template. *J. Am. Chem. Soc.* **2014**, *136*, 10807–10813. (c) Yang, Y.; Qiu, X.; Zhao, Y.; Mu, Y.; Shi, Z. Palladium-catalyzed C–H ar-ylation of indoles at the C7 position. *J. Am. Chem. Soc.* **2016**, *138*, 495–498. (d) Leitch, J. A.; McMullin, C. L.; Mahon, M. F.; Bhonoah, Y.; Frost, C. G. Remote C6-selective ruthenium-catalyzed C–H alkylation of indole derivatives via σ -activation. *ACS Catal.* **2017**, *7*, 2616–2623. (e) Choi, I.; Messinis, A. M.; Ackermann, L. C7-Indole Sulfonamidations, Alkenylations by Rutheni-um(II) Catalysis. *Angew. Chem., Int. Ed.* **2020**, *59*, 12534–12540.
6. (a) Leitch, J. A.; Bhonoah, Y.; Frost, C. G. Beyond C2 and C3: transition-metal-catalyzed C–H functionalization of indole. *ACS Catal.* **2017**, *7*, 5618–5627. (b) Pradhan, S. De, P. B. Shah, T. A. Punniyamurthy T., Recent ad-vances in metal-catalyzed alkylation, alkenylation and alkynylation of indole/indoline benzenoid nucleus. *Chem Asian J.* **2020**, *15*, 4184–4198.
7. (a) K. M.; Mei, T.-S.; Wasa, M.; Yu, J.-Q. Weak Coordi-nation as a Powerful Means for Developing Broadly Use-ful C-H Functionalization Reactions. *Acc. Chem. Res.* **2012**, *45*, 788–802. (b) Chen, Z.; Wang, B.; Zhang, J.; Yu, W.; Liu, Z.; Zhang, Y. Transition Metal-Catalyzed C–H Bond Functionalizations by the use of Diverse Directing Groups. *Org. Chem. Front.* **2015**, *2*, 1107–1295. (c) Das, R.; Kumar, G. S.; Kapur, M. Amides as Weak Coordinating Groups in Proximal C–H Bond Activation. *Eur. J. Org. Chem.* **2017**, *2017*, 5439–5459.
8. (a) Lanke, V.; Bettadapur, K. R.; Prabhu, K. R. Electronic nature of ketone directing group as a key to control C-2 vs C-4 alkenylation of indoles. *Org. Lett.* **2016**, *18*, 5496–5499. (b) Chen, S.; Feng, B.; Zheng, X.; Yin, J.; Yang, S.; You, J. Iridium-catalyzed direct regioselective C4-amidation of indoles under mild conditions. *Org. Lett.* **2017**, *19*, 2502–2505. (c) Borah, A. J.; Shi, Z. Palladi-um-catalyzed regioselective C–H fluoroalkylation of in-doles at the C4-position. *Chem. Commun.* **2017**, *53*, 3945–3948. (d) Kalepu, J.; Gandeepan, P.; Ackermann, L.; Pilarski, L. T. C4-H Indole

- Functionalisation: Precedent and Prospects. *Chem. Sci.* **2018**, *9*, 4203–4216. (e) Chen, S.; Zhang, M.; Su, R.; Chen, X.; Feng, B.; Yang, Y.; You, J. C2/C4 Regioselective Heteroarylation of Indoles by Tuning C–H Metalation Modes. *ACS Catal.* **2019**, *9*, 6372–6379 (f) Kona, C. N.; Nishii, Y.; Miura, M. Thioether-Directed C4- Selective C–H Acylmethylation of Indoles Using α -Carbonyl Sulfoxonium Ylides. *Org. Lett.* **2020**, *22*, 4806–4811.
9. (a) Su, B.; Cao, Z.-C.; Shi, Z.-J. Su, Exploration of earth-abundant transition metals (Fe, Co, and Ni) as catalysts in unreactive chemical bond activations. *Acc. Chem. Res.* **2015**, *48*, 886–896. (b) Liu, W.; Ackermann, L. Manganese-Catalyzed C–H Activation. *ACS Catal.* **2016**, *6*, 3743–3752. (c) Gandeepan, P.; Müller, T.; Zell, D.; Cera, G.; Warratz, S.; Ackermann, L. 3d Transition Metals for C–H Activation. *Chem. Rev.* **2019**, *119*, 2192–2452.
 10. (a) Yoshino, T.; Ikemoto, H.; Matsunaga, S.; Kanai, M. A Cationic High-Valent Cp*Co^{III} Complex for the Catalytic Generation of Nucleophilic Organometallic Species: Directed C–H Bond Activation. *Angew. Chem., Int. Ed.* **2013**, *52*, 2207–2211. (b) Wang, S.; Chen, S.-Y.; Yu, X.-Q. C–H functionalization by high-valent Cp*Co (III) catalysis. *Chem. Commun.* **2017**, *53*, 3165–3180. (c) Han, J.-F.; Guo, P.; Zhang, X.-G.; Liao, J.-B.; Ye, K.-Y. Recent Advances in Cobalt-Catalyzed Allylic Functionalization. *Org. Biomol. Chem.* **2020**, *18*, 7740–7750 (d) Oliveira J. C. A., Dhawa U., Ackermann L. Insights into the Mechanism of Low-Valent Cobalt-Catalyzed C–H Activation. *ACS Catal.* **2021**, *11*, 1505–1515.
 11. (a) Park, J.; Chang, S. Comparative Catalytic Activity of Group 9 [Cp*M^{III}] Complexes: Cobalt-Catalyzed C–H Amidation of Arenes with Dioxazolones as Amidating Reagents. *Angew. Chem., Int. Ed.* **2015**, *54*, 14103–14107. (b) Wang, F.; Jin, L.; Kong, L.; Li, X. Cobalt (III)- and rhodium (III)-catalyzed C–H amidation and synthesis of 4-quinolones: C–H activation assisted by weakly coordinating and functionalizable enamines. *Org. Lett.* **2017**, *19*, 1812–1815. (c) Li, N.; Wang, Y.; Kong, L.; Chang, J.; Li, X. Cobalt(III)/Rhodium(III)-Catalyzed Regio- and Stereoselective Allylation of 8-methylquinoline via sp³ CH Activation. *Adv. Synth. Catal.* **2019**, *361*, 3880–3885.
 12. Banjare S. K.; Nanda T.; Pati B.V.; Biswal P.; Ravikumar P.C.; O-Directed C–H functionalization via cobaltacycles: a sustainable approach for C–C and C–heteroatom bond formations. *Chem. Commun.* **2021**, *57*, 3630–3647.
 13. (a) Banjare, S. K.; Chebolu, R.; Ravikumar, P. C. Cobalt Catalyzed Hydroarylation of Michael Acceptors with Indolines Directed by a Weakly Coordinating Functional Group. *Org. Lett.* **2019**, *21*, 4049–4053. (b) Banjare, S. K.; Nanda, T.; Ravikumar, P. C. Cobalt-Catalyzed Regioselective Direct C-4 Alkenylation of 3-Acetylindole with Michael Acceptors Using a Weakly Coordinating Functional Group. *Org. Lett.* **2019**, *21*, 8138–8143. (c) Banjare, S.-K.; Biswal, P.; Ravikumar, P.-C. Cobalt-Catalyzed One-Step Access to Pyroquilon and C-7 Alkenylation of Indoline with Activated Alkenes Using Weakly Coordinating Functional Groups. *J. Org. Chem.* **2020**, *85*, 5330–5341.
 14. (a) Zhang, W.; Wei, J.; Fu, S.; Lin, D.; Jiang, H.; Zeng, W. Highly Stereoselective Ruthenium(II)-Catalyzed Direct C2-syn-Alkenylation of Indoles with Alkynes. *Org. Lett.* **2015**, *17*, 1349. (b) Bettadapur, K. R.; Kapaniaiah, R.; Lan-ke, V.; Prabhu, R. Weak Directing Group Steered Formal Oxidative [2 + 2+2]-Cyclization for Selective Benzannulation of Indoles. *J. Org. Chem.* **2018**, *83*, 1810.
 15. (a) Wang C.; Chen F.; Qian P.; Cheng J.; Recent advances in the Rh-catalyzed cascade arene C–H bond activation/annulation toward diverse heterocyclic compounds. *Org. Biomol. Chem.*, **2021**, *19*, 1705–1721 (b) Sinha, S. K.; Bhattacharya, T.; Maiti, D. Role of Hexafluoroisopropanol in C–H Activation. *React. Chem. Eng.* **2019**, *4*, 244–253. (c) Bhattacharya, T.; Ghosh, A.; Maiti, D. Hexafluoroisopropanol: the magical solvent for Pd-catalyzed C–H activation. *Chem. Sci.* **2021**, *12*, 3857–3870. (d) Ikemoto, H.; Yoshino, T.; Sakata, K.; Matsunaga, S.; Kanai, M. Pyrroloindolone Synthesis via a Cp*Co-III-Catalyzed Redox-Neutral Directed C–H Alkenylation/Annulation Sequence. *J. Am. Chem. Soc.* **2014**, *136*, 5424–5431. (e) He, W. Y.; Du, F. P.; Wu, Y.; Wang, Y. H.; Liu, X.; Liu, H. Y.; Zhao, X. D. Quantitative ¹⁹F NMR method validation and application to the quantitative analysis of a fluoro-polyphosphates mixture. *J. Fluorine Chem.* **2006**, *127*, 809–815.

-
16. (a) TURBOMOLE V6.5 2013, A Development of University of Karlsruhe and Forschungszentrum Karlsruhe GmbH, TURBOMOLE V6.5, University of Karlsruhe and Forschungszentrum Karlsruhe GmbH, **1989-2007**. (b) Sa-hoo, D. K.; Jena, S.; Dutta, J.; Rana, A.; Biswal, H. S., Nature and Strength of M–H···S and M–H···Se (M = Mn, Fe, & Co) Hydrogen Bond. *J. Phys. Chem. A* **2019**, *123*, 2227–2236. (c) Dutta, J.; Sahoo, D. K.; Jena, S.; Tulsian, K. D.; Biswal, H. S., Non-covalent interactions with inverted carbon: a carbo-hydrogen bond or a new type of hydro-gen bond? *Phys. Chem. Chem. Phys.* **2020**, *22*, 8988–8997. (d) Simmons, E. M.; Hartwig, J. F. On the Interpretation of Deuterium Kinetic Isotope Effects in C–H Bond Functionalizations by Transition-Metal Complexes. *Angew. Chem., Int. Ed.* **2012**, *51*, 3066–3072. (e) Alexandropoulos, D. I.; Papatriantafyllopoulou, C.; Aromi, G.; Roubeau, O.; Teat, S. J.; Perlepes, S. P.; Christou, G.; Stamatatos, T. C. *Inorg. Chem.* **2010**, *49*, 3962–3964. (f) Vigato, P. A.; Peruzzo, V.; Tamburini, S. The evolution of β -diketone or β -diketophenol ligands and related complexes. *Coord. Chem. Rev.* **2009**, *253*, 1099–1201.
17. (a) Ganci, G.; Chisholm, J. D. Rhodium-catalyzed addition of aryl boronic acids to 1, 2-diketones and 1, 2-ketoesters. *Tetrahedron Lett.* **2007**, *48*, 8266–8269. (b) Yu, Y.; Wu, Q.; Liu, D.; Hu, L.; Yu, L.; Tan, Z.; Zhu, G. Synthesis of Benzofulvenes via $\text{Cp}^*\text{Co(III)}$ -Catalyzed C–H Activation and Carbocyclization of Aromatic Ketones with Internal Alkynes. *J. Org. Chem.* **2019**, *84*, 7449–7458 (c) Suslick, B. A.; Tilley, T. D. Mechanistic Interrogation of Alkyne Hydroarylations Catalyzed by Highly Reduced, Single-Component Cobalt Complexes. *J. Am. Chem. Soc.* **2020**, *142*, 11203–11218.
18. Banjare, S. K.; Biswal, P.; Ravikumar, P. C. Cobalt-Catalyzed One-Step Access to Pyroquilon and C-7 Alkenylation of Indoline with Activated Alkenes Using Weakly Coordinating Functional Groups. *J. Org. Chem.* **2020**, *85*, 5330–5341.
19. Gottlieb, H. E.; Kotlyar, V.; Nudelman, A. NMR Chemical Shifts of Common Laboratory Solvents as Trace Impurities. *J. Org. Chem.* **1997**, *62*, 7512–7515.
20. Pichon, M. M.; Stauffert, F.; Addante-Moya, L. G.; Bodlenner, A.; Compain, P. Metal-Free Iodine-Mediated Deoxygenation of Alcohols in the Position α to Electron-Withdrawing Groups. *Eur. J. Org. Chem.* **2018**, *2018*, 1538–1545.
21. Borah, A. J.; Shi, Z. Palladium-catalyzed regioselective C–H fluoroalkylation of indoles at the C4-position. *Chem. Commun.* **2017**, *53*, 3945–3948.
22. Yan, J.; Chen, J.; Zhang, S.; Hu, J.; Huang, L.; Li, X. Synthesis, evaluation, and mechanism study of novel indole-chalcone derivatives exerting effective antitumor activity through microtubule destabilization in vitro and in vivo. *J. Med. Chem.* **2016**, *59*, 5264–5283.
-

Chapter 6

Cobalt-Catalyzed Decarbonylative Ipso-C-C Bond

Functionalization via Weak Coordination: An Approach

Towards Indole-Acyloins and Its Photophysical Studies

4.1 Abstract

4.2 Introduction

4.3 Results and Discussions

4.4 Conclusions

4.5 Experimental Section

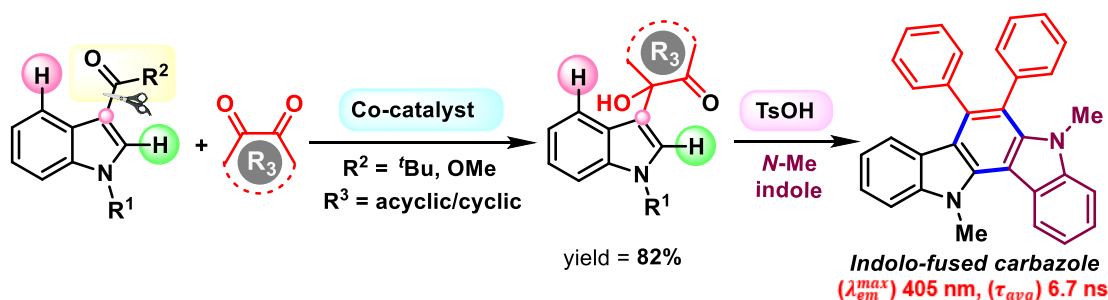
4.6 References

Chapter 6

Cobalt-Catalyzed Decarbonylative Ipso-C-C Bond

Functionalization via Weak Coordination: An Approach

Towards Indole-Acyloins and Its Photophysical Studies



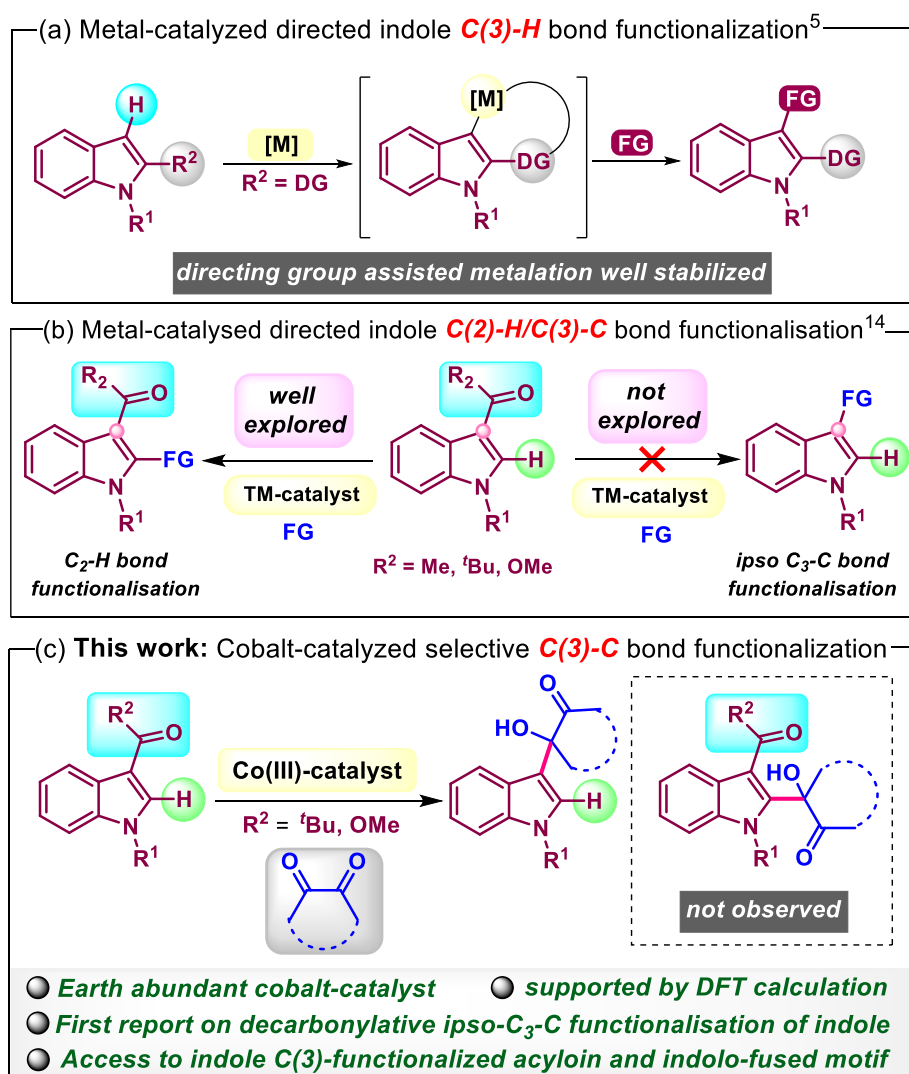
6.1 ABSTRACT

Selective functionalization of indole-C(3)-C bond with aromatic/heteroaromatic 1,2-diketones has been uncovered for the first time. Earth crust abundant first-row transition metal cobalt-catalyst has been demonstrated as an effective catalyst for this unusual transformation. Furthermore, using easily available weakly coordinating groups such as ketone and ester was found to be effective. The in-situ generation of water from hexafluoro-2-propanol and removal of the pivaloyl/ester group in a decarbonylative manner at a lower temperature is the key feature of this methodology. Notably, an unusual reactivity was observed with phenanthrene-9,10-dione as reacting partner, which gave a aromatized dispiro-polycyclic product with two contiguous quaternary carbons. The plausible mechanism has been supported by DFT calculation. In addition, photophysical studies show the potential utility of indole-(C3)-acyloin and indolo-fused carbazole in photovoltaic and optoelectronic applications.

6.2 INTRODUCTION

The structural modification and diversification of the indole moiety have been an active area of research, as it shows several biological activities such as antimicrobial, antifungal, antioxidant, anti-HIV, etc.¹ Moreover, the indole motifs are abundantly present in many alkaloid natural products (mitomycin, serotonin, and reserpine).² Therefore, indole-based transformations are always useful for drug development in pharmaceutical industries, as well as for the synthesis of many natural products. The transition metal-catalyzed C-H bond activation has been at the forefront of organic synthesis in recent years.³ The concept of C-H bond activation/functionalization has gained more attention in the scientific community due to its step and atom economical properties.⁴ In this context, the sp^2 C-H bond functionalization of indole at the C₃ position has been accomplished through directed (Figure 1a) and non-directed pathways.⁵ Among these two types of metalation, the directed sp^2 C-H functionalization has been explored by installing a directing group at the C₂ position. Benjamin Pelcman et al. have previously reported the palladium and platinum-catalyzed acetoxylation of indole at C₃ position using C₂ ester as coordinating group.⁶ Recently, the directed indole C(3)-H functionalization has been explored by Jian-Zhong Chen *et al.* where they have demonstrated copper-catalyzed C₃-arylation of indole using *N,N*-bidentate directing groups.⁷ Further, the metal-catalyzed non-directed C(3)-H bond functionalization of indole has been well documented in the literature.⁸ Also, the metal-catalyzed regioselective indole C(2)-H functionalization has been explored by installing a chelating group at the C₃-position of indole (Figure 6.1b).⁹ In recent years, base metals such as Mn, Fe, Co, Cu, and Ni are making a footprint in organic synthetic methodologies.¹⁰

Figure 6.1. Overview and challenges of transition metal-catalyzed C-H/C-C bond functionalization of indole.



The 3d transition metals are abundantly present in the earth's crust, which makes them cost-effective catalysts. Moreover, they are relatively eco-friendly compared to 4d and 5d metals. Further, the use of 3d metal-catalyst, along with commonly prevalent functional groups (aldehyde, ketone, ester, carboxylic acid) as a directing group, is synthetically more sustainable.¹¹ In this regard, low-valent Co(0)-catalyzed *N*-pyrimidine directed intramolecular indole C₂-C bond cleavage has been reported by H. Wei et al.¹² However, the development of intermolecular C-C bond functionalization

using aromatic 1,2-diketones as a coupling partner is undeveloped and a challenging task, as 1,2-diketones can bind with the metal through *O*-chelation and either activate the proximal C-H bond or quench the metal catalyst for further functionalization.¹³ Notably, all the metal-catalyzed indole C₃-functionalizations were achieved through C₃-H bond cleavage and not through *ipso*-decarbonylative C₃-C bond cleavage (Figure 6.1b).¹⁴ In the presence of C₃-C bond, regioselective indole C₃-functionalization was challenging and was never accomplished before through a metal-catalyzed decarbonylative pathway.¹⁵ In this regard, we have achieved the cobalt(III)-catalyzed decarbonylative C₃-C bond (*ipso*-) functionalization of indole using a weakly coordinating group in a highly regioselective manner (Figure 6.1c). As indicated, we have overcome many major challenges with our methodology, such as (i) the use of unexplored 1,2 diketones as a reacting partner with in situ generated C-M bond, (ii) the selective functionalization of indole C₃-C bond, (iii) use of earth-abundant and less expensive 3d transition metal, cobalt catalyst (iv) use of readily attachable weakly coordinating directing group, (v) decarbonylation transformation at moderate temperature and (vi) formation of highly selective acyloin product. The synthesis of α -hydroxylated ketones has considerable applications in natural product synthesis as well as in asymmetric synthesis.¹⁶

6.3 RESULTS AND DISCUSSION

Due to the described challenges above and in continuation of our studies with weakly chelating substrates in conjunction with sustainable 3d metal cobalt catalyst, we have initially chosen 3-pivaloyl indole **1a** as the substrate aryl 1,2-diketone **2a** as coupling partner. Along with cobalt(III)-catalyst, we have used AgBF₄ (40 mol %) and Cu(OAc)₂ (40 mol %) as additives in the presence of hexafluoroethanol (HFIP) solvent at 80 °C

(Table 6.1). Delightfully, we obtained an 82% yield of the indole (C₃)-acyloin product **3aa** instead of the indole (C₂)-acyloin product in the standard reaction conditions. It is interesting to note that C₃-C bond functionalization is preferred over C₂-H bond functionalization. Further, to enhance the yield and generality of the optimized reaction condition, several variations have been performed. Changing the solvent from HFIP to other solvents such as polar-protic methanol, aromatic hydrocarbons such as benzene and toluene, chlorinated solvents such as dichloromethane, and di-chloroethane did not provide the desired product (Table 6.1, entry 2). We obtained only 46% yield of **3aa** on choosing trifluoroethanol (TFE) as an alternative fluorinated solvent instead of HFIP (Table 6.1, entry 3). Whereas a mixture of both these fluorinated solvents resulted in only a slight improvement in the yield (Table 6.1, entry 4). Next, we varied the silver-based additives, such as AgSbF₆ and AgNTf₂ instead of AgBF₄, but no improvement in yield was observed (Table 6.1, entries 5-6). The amount of copper acetate and its variation from Cu(OAc)₂ to AgOAc was also not helpful in obtaining a better result (Table 6.1, entries 7-8). To know the actual catalytic activity of Cp*Co(III)-catalyst, we tried with Co(0)-catalyst in lieu of Co(III)-catalyst, but failed to produce the desired product (Table 6.1, entry 9). This implies that the Cp*Co(III)-catalyst plays a crucial role in this transformation with the optimized conditions. We then varied the equivalent of reacting partner **2a** from 2 equivalents to 1 and 3 equivalents and obtained 45 and 78% product yield, respectively. This further suggests 2 equivalents of the aromatic 1,2-diketone were optimal (Table 6.1, entry 10,11). Moreover, variations in the reaction temperature have also been performed, but none of the variations improved the yield (Table 6.1, entry 12-13).

Table 6.1. Overview and challenges of transition metal-catalyzed C-H/C-C bond functionalization of indole^{a,b,c}

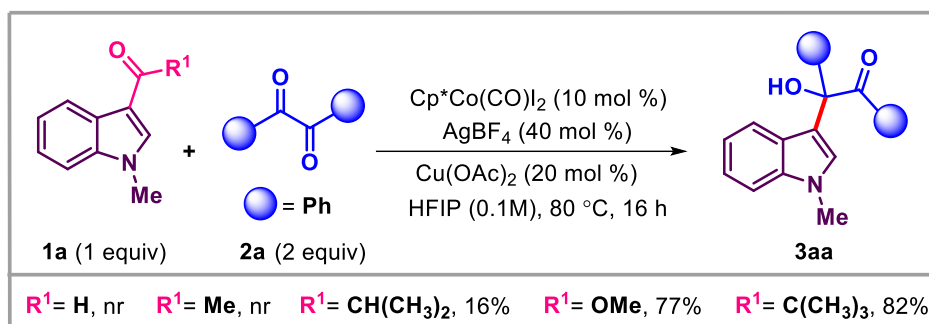
1a (1 equiv)	2a (2 equiv)	3aa
entry	deviation from the standard conditions	yield of 3aa (%) ^b
1	none	82
2 ^c	other solvents instead of HFIP	0
3	TFE as a solvent instead of HFIP	46
4	mixture solvents TFE:HFIP (1:1)	53
5	AgSbF ₆ instead of AgBF ₄ as a additive	22
6	AgNTf ₂ instead of AgBF ₄ as a additive	16
7	0.4 equiv instead of 0.2 equiv of Cu(OAc) ₂	67
8	AgOAc instead of Cu(OAc) ₂ as a additive	54
9	Co ₂ (CO) ₈ instead of Cp*Co(CO)I ₂ as a catalyst	0
10	1 equiv instead of 2 equiv of 2a	45
11	3 equiv instead of 2 equiv of 2a	78
12	temperature 60 °C instead of 80 °C	48
13	temperature 100 °C instead of 80 °C	71

^aReaction conditions: **1a** (0.1 mmol), **2a** (0.4 mmol), Cp*Co(CO)I₂ (10 mol %), Ag salts (40 mol %), additive (20 mol %), solvents (1 mL), 80 °C, N₂. ^bIsolated yield.

^cTetrahydrofuran, 1,4-dioxane, methanol, toluene, benzene, and acetonitrile.

With the optimized reaction condition, further screening of weakly coordinating directing groups was performed, where *N*-methyl indole-3-carbaldehyde and *N*-methyl indole-3-acetyl were not compatible with this decarbonylative C-C bond functionalization (Scheme 6.1). In contrast, *N*-methyl indole-3-dimethyl substituted acetyl has given the desired decarbonylated product **3aa** in 16% yield. Also, *N*-methyl indole 3-carboxylate (ester) as a directing group gave the product **3aa** in 77% yields.

Scheme 6.1. Screening of weakly coordinating directing groups^{a,b}



^aReaction conditions: **1a** (0.1 mmol), **2a** (0.4 mmol), $[\text{Cp}^*\text{Co}(\text{CO})\text{I}_2]$ (10 mol %), Ag salts (40 mol %), $\text{Cu}(\text{OAc})_2$ (20 mol %), HFIP (1 mL), 80 °C. ^bIsolated yield.

Notably, *N*-methyl indole-3-pivaloyl directing group gave an 82% yield of **3aa** through the decarbonylative pathway. After optimizing the reaction condition, we screened various substituted indoles. Initially, we chose the *N*-protected 3-pivaloyl indoles. Accordingly, *N*-methyl, -ethyl, -propyl, and -butyl were subjected to the optimized condition (Scheme 2, **3aa-3da**). We observed a decrease in yield (82-55%) with the increase in hydrocarbon chain length, possibly due to the increase in the steric crowding around the indole-pyrrole ring. Other *N*-protected variation, such as *N*-2-bromoethyl, *N*-phenyl, and *N*-benzyl substrates, also gave their respective products in good yields (Scheme 2, **3ea-3ga**). Next, we explored variations in the benzenoid ring system of indoles. C_4 -functionalized indoles with substituents such as -fluoro, -chloro, and -bromo also gave good yields of the desired products (Scheme 6.2, **3ha-3ja**). Generally, this is quite challenging due to the preferential insertion of metal into a weaker $\text{C}(\text{sp}^2)\text{-X}$ ($\text{X} = \text{Br}, \text{I}$) bond than an inert C-H bond. We then decided to screen the substituents at the C_5 position of indole.

Reaction Scheme:

Indole derivative **1** (with R^2 and R^1) reacts with 1,2-diketone **2** (where $\text{Ph} = \text{phenyl}$) in the presence of $\text{Cp}^*\text{Co}(\text{CO})\text{I}_2$ (10 mol %), AgBF_4 (40 mol %), $\text{Cu}(\text{OAc})_2$ (20 mol %), and HFIP (0.1M) at 80°C for 16 h to yield product **3**.

Variation in *N*-protection of indoles

Products **3a** and **3e** are shown with their respective yields and R^1 groups:

- $R^1 = \text{Me}$ **3aa**, 82% (1 mmol **3aa**, 73%)
- $R^1 = \text{Et}$ **3ba**, 80%
- $R^1 = \text{Pr}$ **3ca**, 72%
- $R^1 = \textit{n}\text{Bu}$ **3da**, 55%
- $R^1 = -(\text{CH}_2)_3\text{-Br}$ **3ea**, 64%
- $R^1 = \text{Ph}$ **3fa**, 69%
- $R^1 = \text{Bn}$ **3ga**, 68%

Crystal structure of **3fa**, CCDC 2152818.

Variation in benzenoid ring of indoles

Products **3a** and **3e** are shown with their respective yields and R^2 groups:

- $R^2 = \text{Me}$ **3ka**, 62%
- $R^2 = \text{OMe}$ **3la**, 87%
- $R^2 = \text{Cl}$ **3ma**, 72%
- $R^2 = \text{Br}$ **3na**, 76%
- $R^2 = \text{I}$ **3oa**, 69%
- $R^2 = \text{F}$ **3ha**, 64%
- $R^2 = \text{Cl}$ **3ia**, 73%
- $R^2 = \text{Br}$ **3ja**, 74%
- $R^2 = \text{Cl}$ **3qa**, 67%
- $R^2 = \text{Br}$ **3ra**, 86%
- $R^2 = \text{NO}_2$ **3sa**, 57%
- $R^2 = \text{Me}$ **3ta**, 84%
- $R^2 = \text{NO}_2$ **3ua**, 58%
- $R^2 = \text{F}$ **3pa**, 61%

Scope of 1,2 diketones

Products **3a** and **3e** are shown with their respective yields and R^3 groups:

- $R^3 = \text{Me}$ **3ab**, 54%
- $R^3 = \text{OMe}$ **3ac**, 68%
- $R^3 = \text{F}$ **3ad**, 50%
- $R^3 = \text{Cl}$ **3ae**, 56%
- $R^3 = \text{Me}$ **3af**, nr

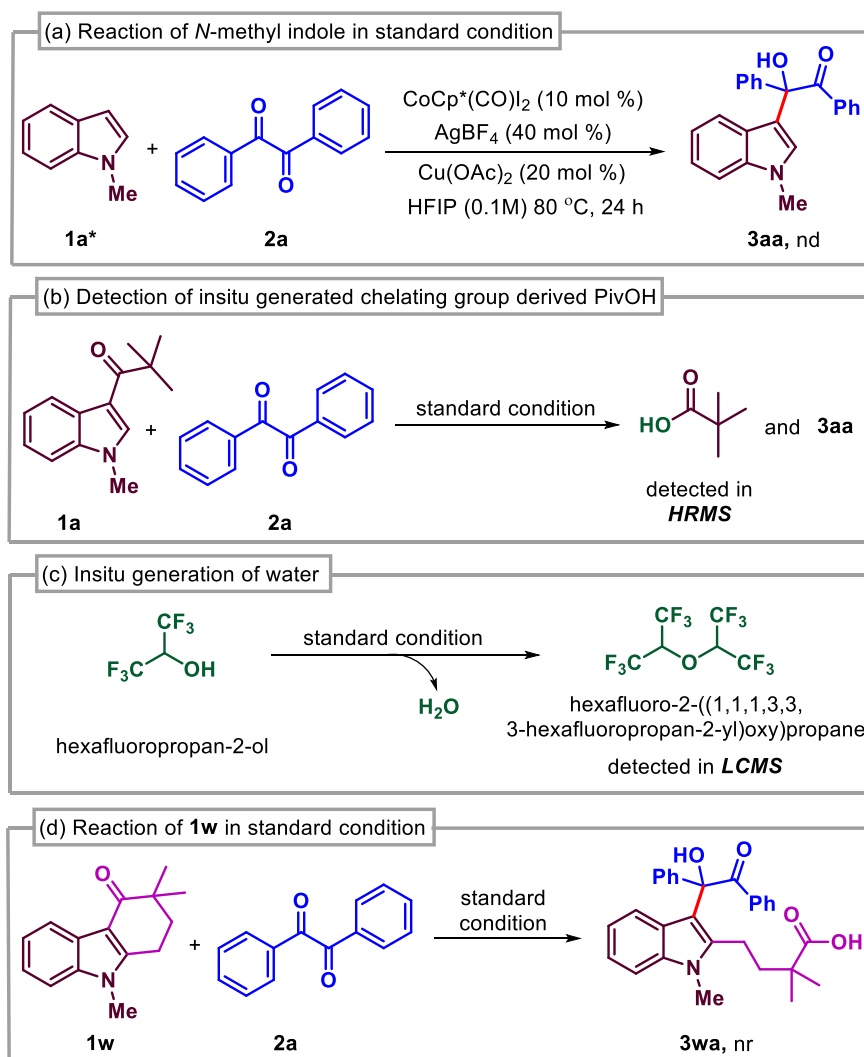
198

With C₅-methyl and -methoxy groups, we obtained 62% and 87% yield respectively (Scheme 6.2, **3ka**, **3la**). However, with this optimized reaction condition, we have observed good functional group tolerance. Further, with C₅-halogenated compounds, we obtained the desired products in good yields (Scheme 6.2, **3ma-3oa**). The C₆-substituted 3-acyl indole also showed good tolerance. C₆-halogenated indole with substituents such as -fluoro, -chloro, and -bromo gave their respective products **3pa** (61%), **3qa** (67%), and **3ra** (86%) in good yields. Notably, electron-withdrawing substituents such as nitro at the C₆-position also worked well and delivered 57% of product yield (Scheme 6.2, **3sa**). In many of the cobalt-catalyzed reports, we found that nitro-substituted substrates were incapable of forming the product, possibly due to the high electron-withdrawing nature of the -NO₂ group that decreases the nucleophilicity of the M-C bond.^{11b,17} Furthermore, substituents such as methyl and nitro groups at the C₇ position of 3-acyl indoles were also reactive and gave their respective products good yields (Scheme 6.2, **3ta-3ua**). Further, the scope of 1,2 diketone has been explored with various sterically and electronically diverse substituents. The electron-rich substituents such as methyl- and methoxy- worked well (Scheme 6.2, **3ab-3ac**), whereas moderate yields have been obtained with electron-withdrawing substituents like *para*-fluoro and chloro groups (Scheme 6.2, **3ad-3ae**). Contrary to our expectations, methyl-phenyl diketone failed to give the expected product (Scheme 6.2, **3af**). This result suggests that the aromatic 1,2-diketone is crucial for this transformation.

To better understand the reaction mechanism, some mechanistic studies have been carried out under standard reaction conditions. Initially, to ascertain whether the product **3aa** is formed through de-pivaloylation followed by nucleophilic attack of C₃-carbon on 1,2 diketones, we subjected the simple *N*-methyl indole **1a*** to standard reaction

condition, but it did not yield **3aa** (Scheme 6.3a). Instead, the decomposition of starting material was observed. This experiment highlighted the crucial role of the pivaloyl group as a weakly coordinating directing group.

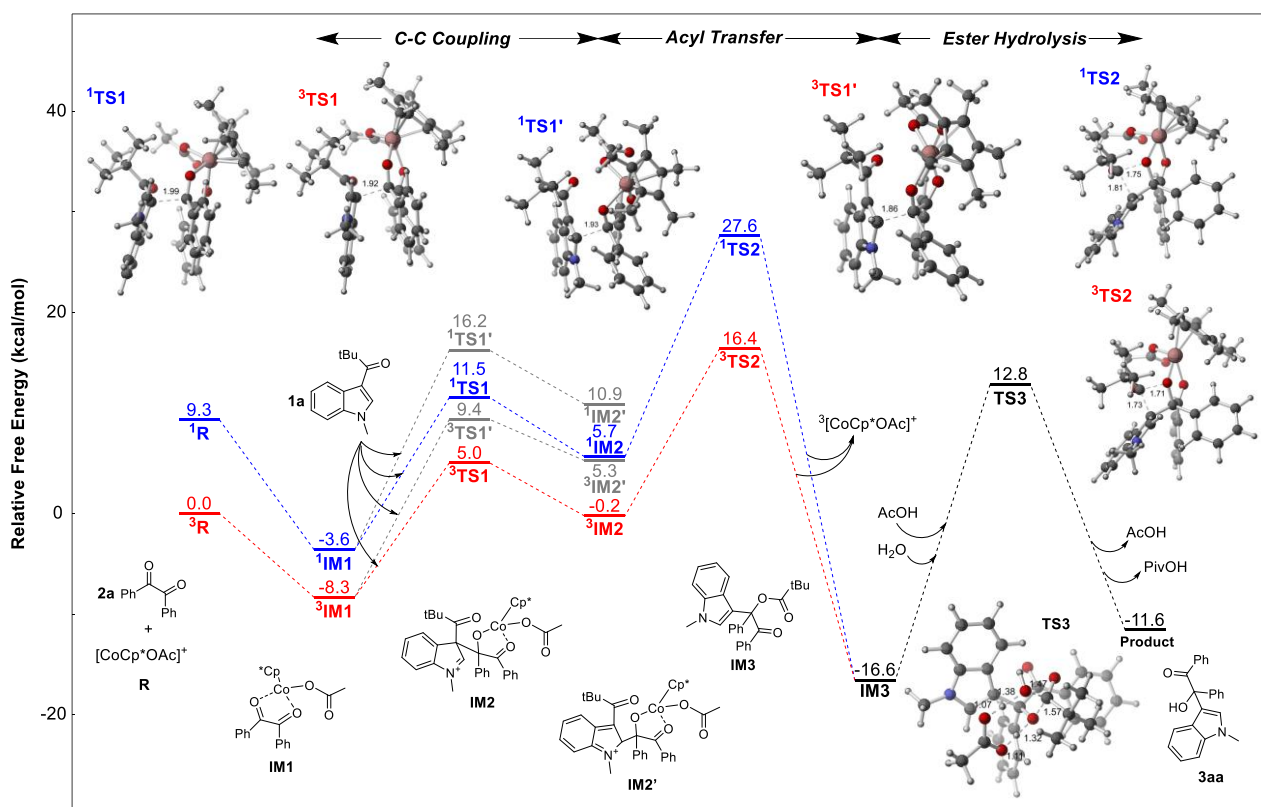
Scheme 6.3. Mechanistic studies



We presume that the pivaloyl group coordinates with the metal and brings the metal closer to the C₃-C bond for further functionalization. Further, the in-situ generation of pivalic acid has been detected in high-resolution mass spectrometer (Scheme 6.3b). This implies that the nucleophilic attack of water on the pivaloyl carbonyl group takes place, leading to the formation of pivalic acid through C-C bond cleavage. Aromatization of

the species involved in this process could be a driving force for this decarbonylation conversion through C-C cleavage. In-situ water generation from HFIP was indirectly confirmed by detecting the corresponding ether of HFIP through LCMS studies (Scheme 6.3c).^{11b} To track the mechanism, we designed a substrate C(3)-pivaloyl-derived cyclic ketone **1w** that would intramolecularly eliminate carboxylic acid, but we failed to observe any reactivity with this substrate (Scheme 6.3d). This suggests that steric and electronic balance is required at the C₂ position of indole for the metal insertion and further functionalization. This was also noticed during substrate scope; substrates with substituents at C(2)-position of indole failed to give the desired product. Based on mechanistic studies and literature precedence,¹⁸ to gain further insight regarding the reaction mechanism and the basis of the selectivity, we performed DFT calculations at the ω B97M-V/def2-TZVPP//SMD(HFIP)-PBE0-D3(BJ)/def2-SVP level of theory.¹⁹ We used the reaction between **1a** and **2a** as the representative reaction to be modelled. We began our modelling from **1a** and [Cp^{*}Co(OAc)]⁺, which was generated in-situ by the reaction of Cp^{*}Co(CO)I₂, Cu(OAc)₂, and AgBF₄. The predicted overall free energy profile is shown in Figure 6.2. Although both singlet and triplet states were considered, the reaction is predicted to proceed entirely on the triplet surface, which is the predicted ground state of the cationic cobalt species. Initial coordination of **2a** to [Cp^{*}Co(OAc)]⁺ forms **IM1**. An endergonic reversible ($\Delta G = +8$ kcal/mol, $\Delta G^\ddagger = 13$ kcal/mol) outer-sphere C(3)-C coupling of **1a** and **IM1** on the triplet surface is then predicted to result in complex **IM2** via transition structure TS1. Notably, an analogous transition structure for C(2)-C coupling is accompanied by a significantly higher activation barrier (via TS1') and leads to a higher energy intermediate (IM2'; $\Delta\Delta G^\ddagger = 4$ kcal/mol, $\Delta\Delta G = +5$ kcal/mol on the triplet surface).

Figure 6.2. Computed (ω B97M-V/def2-TZVPP//SMD(HFIP)-PBE0-D3(BJ)/def2-SVP) reaction profiles for $[\text{Cp}^*\text{Co}(\text{OAc})]^+$ -catalyzed coupling of in kcal/mol. Selected distances are shown in Å.



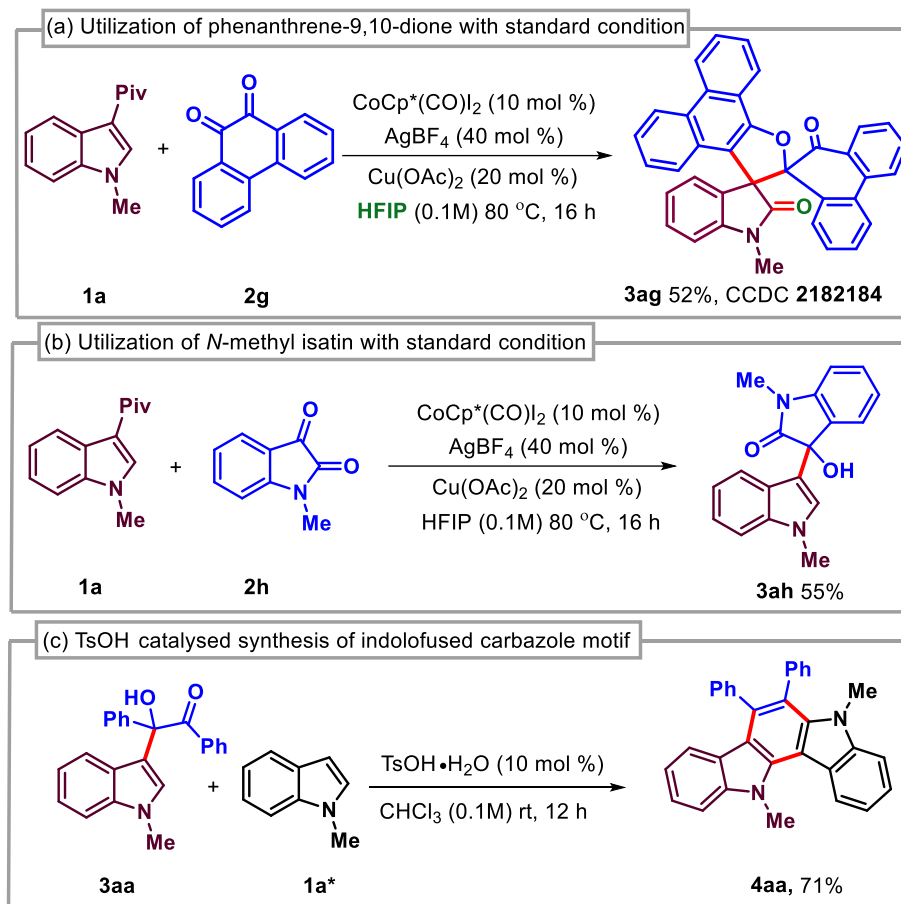
We also note a significantly larger maximum Bond Length Alternation in the fused benzene ring of the indole motif [1] at the energetically relevant **3IM2'** (0.08Å) compared to **3IM2** (0.01Å), indicating a significantly larger disruption of aromaticity at the unfavorable intermediate **3IM2'**. A facile ($\Delta G^\ddagger = 16$ kcal/mol; +24 kcal/mol from **3IM1**) C-to-O 1,3 acyl transfer of the pivaloyl group to the formally anionic oxygen followed by metal dissociation leads to ester **IM3** via TS2. An acid-catalyzed concerted ester hydrolysis affords the final product **3aa** via the liberation of pivalic acid (via TS3; $\Delta G^\ddagger = 28$ kcal/mol). Other means of pivalic acid release should also be reasonable and accessible given the protic solvent environment and high reaction temperature, which

drives equilibrium towards overall ester hydrolysis, but we show here one energetically viable possibility.

This mechanism is consistent with experimental observations, e.g., (i) The observation that *ipso*-C-C coupling prevailed over *para*-C-C coupling is consistent with our lower predicted barrier for coupling as well as facile acyl transfer, (ii) The observed lack of reactivity of **1w** can be explained by extra strain hindering the 1,3-acyl transfer step, and (iii) Substrate **1a*** lacks the acyl group needed to drive the reaction forward. Other mechanisms considered included processes first initiated by concerted metalation-deprotonation (CMD) activation of the indole C(2)-H and inner-sphere C-C coupling. All of these were found to be accompanied by high barriers ($\Delta G^\ddagger > 33$ kcal/mol).

Several reactions were performed to demonstrate this methodology's broad applicability (Scheme 6.4). At first, this methodology was tested using phenanthrene-9,10-dione **2g** with standard reaction conditions (Scheme 6.4a). Surprisingly, the completely diverse decarbonylative/dearomatized product **3ag** was obtained in synthetic, useful yields. This reaction open-up the new scope of our method towards synthesizing various 1-methyl-10''H-dispiro[indoline-3,3'-phenanthro[9,10-b] furan-2',9''-phenanthrene]-2,10''-dione. Further, we performed the reaction using isatin **2h** as a coupling partner, and to our delight, we obtained the corresponding product **3ah** in decent yield (Scheme 6.4b). This indicates that the synthetic applicability of cyclic 1,2-diketone systems can be extended further with this method. Notably, the highly conjugated indolo-fused carbazole derivatives **4aa**, **4sa** have been obtained from **3aa** and indole **1a*** in the presence of catalytic *p*-toluenesulfonic acid (Scheme 6.4c).

Scheme 6.4. The synthetic utility of the developed method.



This method is in itself a discovery for the synthesis of highly conjugated indolo-fused carbazoles, which can be extended further for the synthesis of derivatives of indolo-fused carbazole. These poly-aromatic heterocycles seem to have prominent photo-physical properties because of their extensive π -conjugation. Therefore, further photo-physical studies have been performed by taking **3aa** and **4aa**, which showed emission maxima ($\lambda_{\text{em}}^{\text{max}}$) of 425 nm and 405 nm, respectively (Figure 6.3).²⁰ We also observed promising time-resolved fluorescence average lifetime (τ_{avg}) of 1.61 ns and 6.7 ns for **3aa** and **4aa**, respectively (Table 6.2).²¹

Figure 6.3. The fluorescence decay curves of **3aa** (in chloroform) and **4aa** (in dichloromethane).

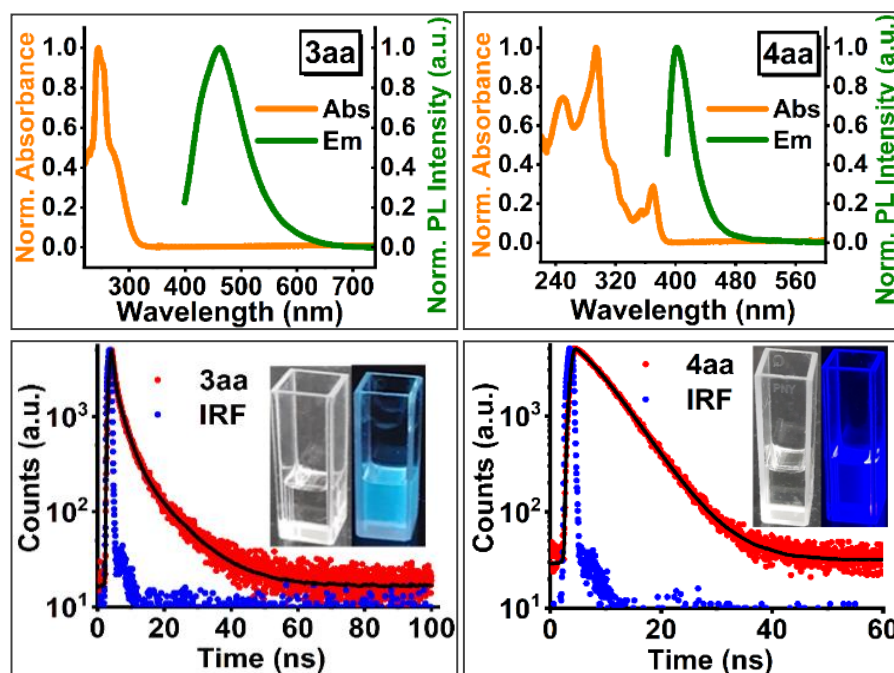


Table 6.2. Fluorescence decay parameters of **3aa** (in chloroform) and **4aa** (in dichloromethane).

system	τ_1	α_1	τ_2	α_2	τ_3	α_3	τ_{avg}
3aa	0.59	0.68	2.64	0.27	9.85	0.05	1.61
4aa	3.08	-1.09	4.81	2.09			6.70

6.4 CONCLUSION

In conclusion, the cobalt-catalyzed C₃-C bond functionalization of 3-pivaloyl indole has been demonstrated for the first time through a de-carbonylative pathway. High earth crust abundant and less expensive 3d-metal catalyst cobalt has been proven to be effective for this conversion. Notably, in this protocol, pivaloyl-ketone and ester have a crucial role in weakly coordinating directing groups. Aromatic 1,2-diketone has been

demonstrated as a coupling partner. It was never explored before as a cross-coupling partner due to the inherent challenge associated with its coordination with metal catalysts. This methodology was not limited to acyclic ketones. Even cyclic ketones such as isatin have been tolerated, which needs further exploration.

Most importantly, a de-aromatized cyclic product has been obtained with phenanthrene-9,10-dione, which reactivity could be further explored. The mechanism has been supported by DFT calculation. Photophysical studies of indole C₃-acyloin and poly-aromatic heterocycle products have been performed, showing promising results for its application in photovoltaics and optoelectronics. These molecules could also be used in other material chemistry applications. Further studies regarding the catalytic potential of metals in C-C bond functionalization are currently under progress in our lab.

Limitations: Aryl-alkyl 1,2-diketones is incompatible with the optimized reaction conditions. It might be due to aryl-alkyl 1,2-diketone has lower electrophilicity than aryl-aryl 1,2-diketones.

6.5 EXPERIMENTAL SECTION²²

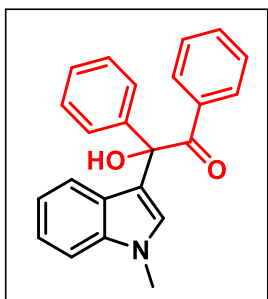
Reactions were performed using borosil schlenk tube vial under an N₂ atmosphere. Column chromatography was done by using 100-200 & 230-400 mesh size silica gel of Acme Chemicals. Gradient elution was performed by using distilled petroleum ether and ethyl acetate. TLC plates were detected under UV light at 254 nm. ¹H NMR and ¹³C NMR were recorded on Bruker AV 400, 700 MHz spectrometers using CDCl₃ as NMR solvents. The residual CHCl₃ for ¹H NMR (δ = 7.26 ppm) and the deuterated solvent signal for ¹³C NMR (δ = 77.36 ppm) is used as reference.²³ Multiplicity (s = single, d = doublet, t = triplet, q = quartet, m = multiplet, dd = double doublet),

integration, and coupling constants (J) in hertz (Hz). HRMS signal analysis was performed using a micro TOF Q-II mass spectrometer. X-ray analysis was conducted using a Rigaku Smartlab X-ray diffractometer at SCS, NISER. Reagents and starting materials were purchased from Sigma Aldrich, Alfa Aesar, TCI, Avra, Spectrochem, Carbanio, and other commercially available sources and used without further purification unless otherwise noted.

(a) General reaction procedure for C-3 substitution of 3-pivaloyl indole with diphenyl acetylene:

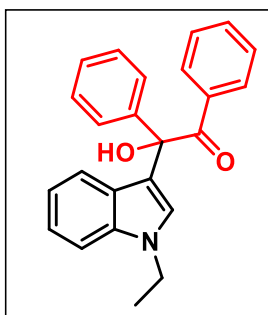
To a pre-dried sealed tube under N_2 , the mixture of *N*-protected 3-pivaloyl indole **1** (0.1 mmol), benzil **2** (0.4 mmol), $[Cp^*Co(CO)I_2]$ (10 mol %), $AgBF_4$ (40 mol %), $Cu(OAc)_2$ (20 mol %), and HFIP (1 mL) were added and sealed inside the glove box. The reaction mixture was vigorously stirred at 80 °C on the preheated aluminum block for 16 h. After 16 h (completion of the reaction as monitored by TLC analysis), the reaction mixture was cooled to room temperature and diluted with ethyl acetate/dichloromethane and passed through a short celite pad, the solvent was evaporated under reduced pressure, and the residue was purified by column chromatography using EtOAc/hexane mixture on silica gel to give the pure product **3**.

Experimental characterization data of products:



2-hydroxy-2-(1-methyl-1H-indol-3-yl)-1,2-diphenylethanone (3aa): was prepared according to general procedure (6.5a). The crude reaction mixture was purified by column chromatography using silica gel (100-200 mesh size), giving (28 mg in 0.1 mmol scale) 82% yield. **Physical**

State: brown solid. **m.p.:** 119–121 °C. **R_f-value:** 0.4 (10% EtOAc/hexane). **¹H NMR (CDCl₃, 400 MHz):** δ 7.86 (d, *J* = 8.0 Hz, 2H), 7.58–7.54 (m, 3H), 7.45–7.41 (m, 1H), 7.35–7.21 (m, 7H), 7.06 (t, *J* = 7.6 Hz, 1H), 6.63 (s, 1H), 4.82 (brs, 1H), 3.69 (s, 3H). **¹³C NMR {¹H} (CDCl₃, 100 MHz):** δ 200.6, 142.0, 137.8, 135.5, 133.2, 131.1, 129.2, 128.7, 128.4, 128.2, 127.9, 126.8, 122.6, 121.8, 120.1, 117.3, 109.8, 81.9, 33.2. **IR (KBr, cm⁻¹):** 3053, 1675, 1266, 748. **HRMS (ESI) m/z:** [M+Na]⁺ Calcd for C₂₃H₁₉NO₂Na: 364.1313; Found: 364.1315.

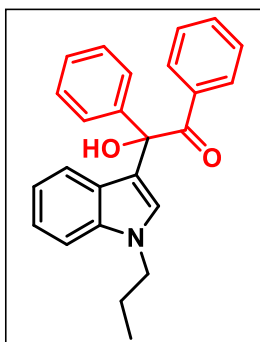


2-(1-ethyl-1H-indol-3-yl)-2-hydroxy-1,2-diphenylethanone (3ba): was prepared according to general procedure (6.5a). The crude reaction mixture was purified by column chromatography using silica gel (100-200 mesh size), giving (28 mg in 0.1 mmol scale) 80% yield. **Physical**

State: brown liquid. **R_f-value:** 0.4 (10% EtOAc/hexane). **¹H NMR (CDCl₃, 400 MHz):** δ 7.85 (d, *J* = 8.0 Hz, 2H), 7.56 (t, *J* = 8.0 Hz, 3H), 7.42 (t, *J* = 7.2 Hz, 1H), 7.33–7.19 (m, 7H), 7.05 (t, *J* = 7.6 Hz 1H), 6.69 (s, 1H), 4.84 (brs, 1H), 4.07 (q, *J* = 7.2 Hz, 2H), 1.37 (t, *J* = 7.2 Hz, 3H). **¹³C NMR {¹H} (CDCl₃, 100 MHz):** δ 200.7, 142.0, 136.8, 135.5, 133.1, 131.0, 128.6, 128.3, 128.2, 128.0, 127.6, 127.0 122.4

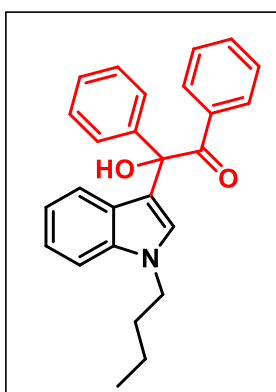
121.9, 120.1, 117.2, 109.8, 82.0, 41.4, 15.7. **IR** (KBr, cm^{-1}): 3052, 1671, 1274, 749.

HRMS (ESI) m/z: $[\text{M}+\text{Na}]^+$ Calcd for $\text{C}_{24}\text{H}_{21}\text{NO}_2\text{Na}$: 378.1470; Found: 378.1473.



2-hydroxy-1,2-diphenyl-2-(1-propyl-1H-indol-3-yl)ethanone (3ca): was prepared according to general procedure (6.5a). The crude reaction mixture was purified by column chromatography using silica gel (100-200 mesh size), giving (27 mg in 0.1 mmol scale) 72% yield. **Physical State:** colorless liquid. **R_f -value:** 0.45 (10% EtOAc/hexane). **^1H**

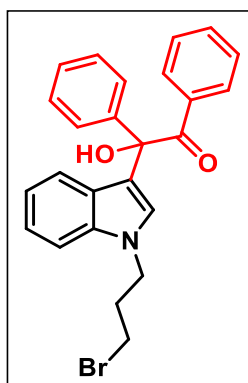
NMR (CDCl_3 , 400 MHz): δ 7.85 (d, J = 8.0 Hz, 2H), 7.56 (d, J = 6.4 Hz, 3H), 7.42 (t, J = 7.2 Hz, 1H), 7.34 -7.19 (m, 7H), 7.04 (t, J = 7.6 Hz, 1H), 6.69 (s, 1H), 4.90 (brs, 1H), 3.98 (t J = 7.2Hz, 2H) 1.82 -1.73(m, 2H), 0.85 (t, J = 7.6 Hz, 3H). **^{13}C NMR $\{^1\text{H}\}$ (CDCl_3 , 100 MHz):** δ 200.7, 142.1, 137.0, 135.5, 133.1, 131.1, 128.7, 128.4, 128.3, 128.2, 128.0, 127.0, 122.4, 121.9, 120.0, 116.9, 110.0, 81.9, 48.4, 23.7, 11.7. **IR** (KBr, cm^{-1}): 3053,1669, 1261, 749. **HRMS (ESI) m/z:** $[\text{M}+\text{Na}]^+$ Calcd for $\text{C}_{25}\text{H}_{23}\text{NO}_2\text{Na}$: 392.1626; Found: 392.1630.



2-(1-butyl-1H-indol-3-yl)-2-hydroxy-1,2-diphenylethanone (3da): was prepared according to general procedure (6.5a). The crude reaction mixture was purified by column chromatography using silica gel (100-200 mesh size), giving (21 mg in 0.1 mmol scale) 55% yield. **Physical State:** colorless liquid. **R_f -value:** 0.45 (10%

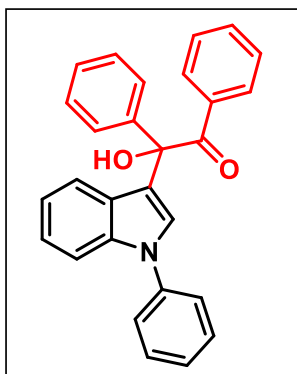
EtOAc/hexane). **^1H NMR (CDCl_3 , 400 MHz):** δ 7.85 (d, J = 8.0 Hz, 2H), 7.56 (d, J = 5.6 Hz, 3H), 7.43 (t, J = 7.2 Hz, 1H), 7.35-7.19 (m, 7H) 7.05 (t, J = 7.6 Hz, 1H),

6.68 (s 1H), 4.90 (brs, 1H), 4.02 (t, $J = 6.8$ Hz, 2H) 1.76-1.69 (m, 2H), 1.28-1.23 (m, 2H), 0.88 (t, $J = 7.2$ Hz, 3H). ^{13}C NMR $\{^1\text{H}\}$ (CDCl_3 , 100 MHz): δ 200.8, 142.2, 137.0, 135.6, 133.1, 131.1, 128.7, 128.4, 128.3, 128.2, 128.1, 127.0, 122.4, 121.9, 120.0, 116.9, 109.9, 82.0, 46.5, 32.5, 20.4, 13.9. IR (KBr, cm^{-1}): 3053, 1653, 1272, 749. HRMS (ESI) m/z : $[\text{M}+\text{Na}]^+$ Calcd for $\text{C}_{26}\text{H}_{25}\text{NO}_2\text{Na}$: 406.1783; Found: 406.1785.



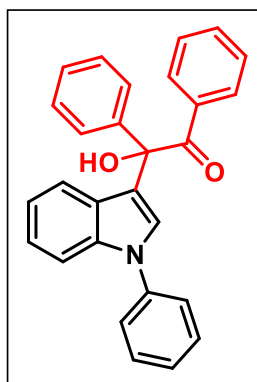
2-(1-(3-bromopropyl)-1H-indol-3-yl)-2-hydroxy-1,2-diphenylethanone (3ea): was prepared according to general procedure (6.5a). The crude reaction mixture was purified by column chromatography using silica gel (100-200 mesh size), giving (29 mg in 0.1 mmol scale) 64% yield. **Physical State:** brown solid, **m.p.:** 138–140 °C **R_f -value:** 0.4 (10%

EtOAc/hexane). ^1H NMR (CDCl_3 , 400 MHz): δ 7.84 (d, $J = 8.4$ Hz, 2H), 7.59-7.54 (m, 3H), 7.43 (t, $J = 7.6$ Hz, 1H), 7.37-7.20 (m, 7H), 7.07 (t, $J = 8.0$ Hz, 1H), 6.74 (s, 1H), 4.91 (brs, 1H), 4.23 (t, $J = 6.4$ Hz, 2H), 3.22 (t, $J = 6.0$ Hz, 2H) 2.30-2.24 (m, 2H). ^{13}C NMR $\{^1\text{H}\}$ (CDCl_3 , 100 MHz): δ 200.6, 142.1, 136.9, 135.4, 133.2, 131.0, 128.7, 128.5, 128.4, 128.3, 128.0, 127.2, 122.8, 122.1, 120.4, 117.5, 109.8, 81.9, 44.4, 32.7, 30.5. IR (KBr, cm^{-1}): 3053, 1653, 1261, 751. HRMS (ESI) m/z : $[\text{M}+\text{Na}]^+$ Calcd for $\text{C}_{25}\text{H}_{22}\text{BrNO}_2\text{Na}$: 470.0726; Found: 470.0758.



2-hydroxy-1,2-diphenyl-2-(1-phenyl-1H-indol-3-yl)ethanone (3fa): was prepared according to general procedure (6.5a). The crude reaction mixture was purified by column chromatography using silica gel (100-200 mesh size), giving (28 mg in 0.1 mmol scale) 69% yield. **Physical State:** white solid. **m.p.:** 128–130

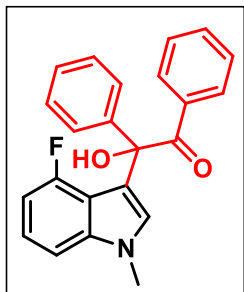
°C **R_f-value:** 0.5 (10% EtOAc/hexane). **¹H NMR (CDCl₃, 400 MHz):** δ 7.90 (d, *J* = 7.6 Hz, 2H), 7.62 (t, *J* = 7.6 Hz, 3H), 7.53 (d, *J* = 8.4 Hz, 1H), 7.48-7.38 (m, 5H), 7.37-7.26 (m, 6H), 7.24-7.21 (m, 1H), 7.12 (t, *J* = 7.6 Hz, 1H), 6.92 (s, 1H), 4.94 (brs, 1H). **¹³C NMR {¹H} (CDCl₃, 100 MHz):** δ 200.4, 141.7, 139.5, 137.0, 135.3, 133.3, 131.1, 129.9, 128.8, 128.4, 128.4, 128.3, 128.0, 127.7, 127.1, 124.8, 123.4, 122.1, 121.1, 119.7, 111.0, 81.9. **IR (KBr, cm⁻¹):** 3053, 1596, 1273, 749. **HRMS (ESI) m/z:** [M+Na]⁺ Calcd for C₂₈H₂₁NO₂Na: 426.1470; Found: 426.1472



2-hydroxy-1,2-diphenyl-2-(1-phenyl-1H-indol-3-yl)ethanone (3fa): was prepared according to general procedure (6.5a). The crude reaction mixture was purified by column chromatography using silica gel (100-200 mesh size), giving (28 mg in 0.1 mmol scale) 69% yield. **Physical State:** white solid. **m.p.:** 128–130 °C **R_f-value:**

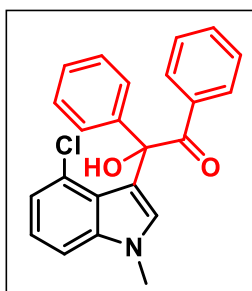
0.5 (10% EtOAc/hexane). **¹H NMR (CDCl₃, 400 MHz):** δ 7.90 (d, *J* = 7.6 Hz, 2H), 7.62 (t, *J* = 7.6 Hz, 3H), 7.53 (d, *J* = 8.4 Hz, 1H), 7.48-7.38 (m, 5H), 7.37-7.26 (m, 6H), 7.24-7.21 (m, 1H), 7.12 (t, *J* = 7.6 Hz, 1H), 6.92 (s, 1H), 4.94 (brs, 1H). **¹³C NMR {¹H} (CDCl₃, 100 MHz):** δ 200.4, 141.7, 139.5, 137.0, 135.3, 133.3, 131.1, 129.9, 128.8, 128.4, 128.4, 128.3, 128.0, 127.7, 127.1, 124.8, 123.4, 122.1, 121.1,

119.7, 111.0, 81.9. **IR** (KBr, cm^{-1}): 3053, 1596, 1273, 749. **HRMS (ESI) m/z**: $[\text{M}+\text{Na}]^+$ Calcd for $\text{C}_{28}\text{H}_{21}\text{NO}_2\text{Na}$: 426.1470; Found: 426.1472



2-(4-fluoro-1-methyl-1H-indol-3-yl)-2-hydroxy-1,2-diphenylethanone (3ha): was prepared according to general procedure (6.5a). The crude reaction mixture was purified by column chromatography using silica gel (100-200 mesh size), giving (23 mg in 0.1 mmol scale) 64% yield. **Physical**

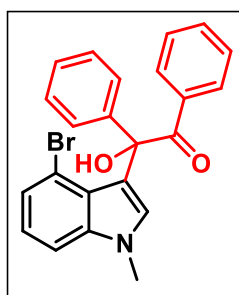
State: brown solid. **m.p.**: 126–128 °C **R_f-value**: 0.4 (20% EtOAc/hexane). **¹H NMR (CDCl₃, 400 MHz)**: δ 8.06 (d, J = 8.8 Hz, 2H), 7.50 (t, J = 7.2 Hz, 1H), 7.41 (t, J = 7.6 Hz, 4H), 7.33 (t, J = 7.6 Hz, 2H), 7.24 (brs, 1H), 7.10-7.02 (m, 2H), 6.74-6.69 (m, 2H), 6.50 (s, 1H), 3.69 (s, 3H). **¹³C NMR {¹H} (CDCl₃, 175 MHz)**: δ 198.8, 157.4 (d, $J_{\text{C-F}}$ = 246.2 Hz), 140.1 (d, $J_{\text{C-F}}$ = 11.6 Hz), 139.2, 137.1, 133.1, 129.3, 129.2, 129.1, 129.0, 128.9, 127.4, 122.6 (d, $J_{\text{C-F}}$ = 7.9 Hz), 116.0 (d, $J_{\text{C-F}}$ = 19.1 Hz), 112.4 (d, $J_{\text{C-F}}$ = 2.8 Hz), 105.9 (d, $J_{\text{C-F}}$ = 2.8 Hz), 104.8 (d, $J_{\text{C-F}}$ = 19.4 Hz), 51.5, 33.5. **¹⁹F NMR (CDCl₃, 376 MHz)** δ -123.9. **IR** (KBr, cm^{-1}): 3053, 1603, 1266, 748. **HRMS (ESI) m/z**: $[\text{M}+\text{Na}]^+$ Calcd for $\text{C}_{23}\text{H}_{18}\text{FNO}_2\text{Na}$: 382.1219; Found: 382.1221



2-(4-chloro-1-methyl-1H-indol-3-yl)-2-hydroxy-1,2-diphenylethanone (3ia): was prepared according to general procedure (6.5a). The crude reaction mixture was purified by column chromatography using silica gel (100-200 mesh size), giving (27 mg in 0.1 mmol scale) 73% yield. **Physical**

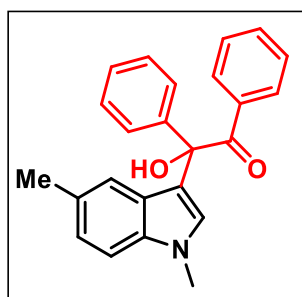
State: brown solid. **m.p.**: 118–119 °C **R_f-value**: 0.3 (10% EtOAc/hexane). **¹H NMR (CDCl₃, 400 MHz)**: δ 7.96 (d, J = 8.4 Hz, 2H), 7.74 (d, J = 6.8 Hz, 2H), 7.46-

7.39 (m, 4H) 7.31 (t, $J = 7.6$ Hz, 2H), 7.22-7.10 (m, 3H), 6.22 (s, 1H), 4.17 (brs, 1H), 3.62 (s, 3H). ^{13}C NMR $\{^1\text{H}\}$ (CDCl_3 , 100 MHz): δ 201.6, 140.6, 139.8, 136.1, 132.4, 132.0, 131.3, 128.7, 128.3, 128.1, 126.9, 124.6, 123.2, 123.0, 121.1, 119.9, 109.1, 82.4, 33.4. **IR** (KBr, cm^{-1}): 3053, 1635, 1273, 752. **HRMS (ESI) m/z :** $[\text{M}+\text{Na}]^+$ Calcd for $\text{C}_{23}\text{H}_{18}\text{ClNO}_2\text{Na}$: 398.0924; Found: 398.0931.



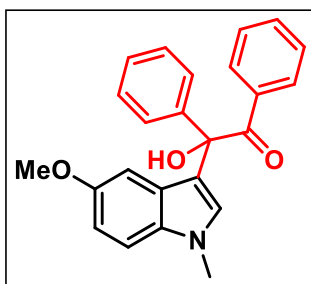
2-(4-bromo-1-methyl-1H-indol-3-yl)-2-hydroxy-1,2-diphenylethanone (3ja): was prepared according to general procedure (6.5a). The crude reaction mixture was purified by column chromatography using silica gel (100-200 mesh size) giving (31 mg in 0.1 mmol scale) 74% yield. **Physical State:**

white solid **m.p.:** 133–135 °C **R_f -value:** 0.3 (10% EtOAc/hexane). ^1H NMR (CDCl_3 , 400 MHz): δ 8.00 (d, $J = 8.0$ Hz, 2H), 7.73 (s, 1H), 7.46-7.38 (m, 4H), 7.35-7.25 (m, 5H), 7.09 (t, $J = 8.0$ Hz, 1H), 6.21 (s, 1H), 4.27 (brs, 1H), 3.61 (s, 3H). ^{13}C NMR $\{^1\text{H}\}$ (CDCl_3 , 100 MHz): δ 201.5, 140.7, 139.7, 136.0, 132.4, 131.5, 128.8, 128.7, 128.3, 128.1, 126.9, 124.8, 124.7, 123.3, 120.3, 113.4, 109.7, 82.4, 33.4. **IR** (KBr, cm^{-1}): 3053, 1693, 1275, 749. **HRMS (ESI) m/z :** $[\text{M}+\text{Na}]^+$ Calcd for $\text{C}_{23}\text{H}_{18}\text{BrNO}_2\text{Na}$: 442.0419; Found: 442.0423.



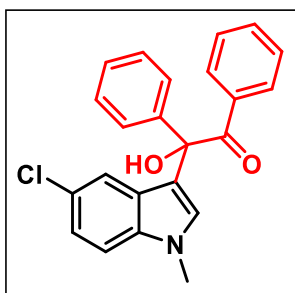
2-(1,5-dimethyl-1H-indol-3-yl)-2-hydroxy-1,2-diphenylethanone (3ka): was prepared according to general procedure (6.5a). The crude reaction mixture was purified by column chromatography using silica gel (100-200 mesh size), giving (22 mg in 0.1 mmol

scale) 62% yield. **Physical State:** brown solid, **m.p.:** 124–126 °C **R_f-value:** 0.5 (20% EtOAc/hexane). **¹H NMR (CDCl₃, 400 MHz):** δ 7.86 (d, *J* = 8.0 Hz, 2H), 7.55 (d, *J* = 7.6 Hz, 2H), 7.44 (t, *J* = 7.6 Hz, 1H), 7.35–7.25 (m, 6H), 7.19 (d, *J* = 8.4 Hz, 1H), 7.06 (d, *J* = 8.0 Hz, 1H), 6.55 (s, 1H), 4.82 (brs, 1H), 3.66 (s, 3H) 2.36 (s, 3H). **¹³C NMR {¹H} (CDCl₃, 100 MHz):** δ 200.6, 142.1, 136.2, 135.5, 133.1, 131.1, 129.5, 129.3, 128.7, 128.4, 128.2, 127.9, 127.1, 124.3, 121.3, 116.6, 109.5, 82.0, 33.2, 21.8. **IR (KBr, cm⁻¹):** 2987, 1635, 1274, 750. **HRMS (ESI) m/z:** [M+Na]⁺ Calcd for C₂₄H₂₁NO₂Na: 378.1470; Found: 478.1470.



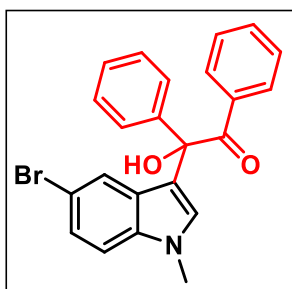
2-hydroxy-2-(5-methoxy-1-methyl-1H-indol-3-yl)-1,2-diphenylethanone (3la): was prepared according to general procedure (6.5a). The crude reaction mixture was purified by column chromatography using silica gel (100–200 mesh size), giving (32 mg in 0.1 mmol scales)

87% yield. **Physical State:** white solid. **m.p.:** 133–135 °C **R_f-value:** 0.3 (20% EtOAc/hexane). **¹H NMR (CDCl₃, 400 MHz):** δ 7.85 (d, *J* = 8.0 Hz, 2H), 7.55 (d, *J* = 7.6, 2H), 7.44 (t, *J* = 7.6 Hz, 1H), 7.33–7.28 (m, 5H), 7.19 (d, *J* = 8.8 Hz, 1H), 6.98 (s, 1H), 6.89 (d, *J* = 8.8 Hz, 1H), 6.60 (s, 1H), 4.88 (brs, 1H), 3.71 (s, 3H), 3.71 (s, 3H). **¹³C NMR {¹H} (CDCl₃, 175 MHz):** δ 200.7, 154.5, 142.0, 135.6, 133.2, 131.1, 129.6, 129.3, 128.7, 128.4, 128.2, 128.0, 127.3, 116.5, 113.1, 110.6, 103.3, 81.9, 56.1, 33.4. **IR (KBr, cm⁻¹):** 3053, 2304, 1635, 1421, 1260, 750. **HRMS (ESI) m/z:** [M-H]⁺ Calcd for C₂₄H₂₀NO₃: 370.1444; Found: 370.1438.



2-(5-chloro-1-methyl-1H-indol-3-yl)-2-hydroxy-1,2-diphenylethanone (3ma): was prepared according to general procedure 6.5a). The crude reaction mixture was purified by column chromatography using silica gel (100-200 mesh size), giving (27 mg in 0.1 mmol scale) 72%

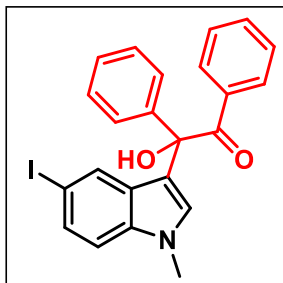
yield. **Physical State:** brown solid, **m.p.:** 126–128 °C **R_f -value:** 0.25 (20% EtOAc/hexane). **¹H NMR (DMSO-*d*₆, 400 MHz):** δ 8.33 (d, *J* = 2.8 Hz, 2H), 8.00 (d, *J* = 7.2 Hz, 2H), 7.52–7.47 (m, 3H), 7.42 (t, *J* = 7.2 Hz, 3H), 7.36 (d, *J* = 2.0 Hz, 1H), 7.17 (d, *J* = 8.0 Hz, 1H), 6.99 (s, 1H), 6.98 (s, 1H), 3.76 (s, 3H). **¹³C NMR {¹H} (DMSO-*d*₆, 100 MHz):** δ 200.7, 143.9, 136.7, 136.6, 133.3, 131.3, 129.1, 128.8, 128.3, 128.0, 127.3, 124.4, 122.1, 121.0, 119.2, 112.5, 83.2, 80.1, 33.6. **IR (KBr, cm⁻¹):** 3053, 1653, 1260, 750. **HRMS (ESI) m/z:** [M+Na]⁺ Calcd for C₂₃H₁₈ClNO₂Na: 398.0924; Found: 398.0927



2-(5-bromo-1-methyl-1H-indol-3-yl)-2-hydroxy-1,2-diphenylethanone (3na): was prepared according to general procedure (6.5a). The crude reaction mixture was purified by column chromatography using silica gel (100-200 mesh size), giving (32 mg in 0.1 mmol scale) 76%

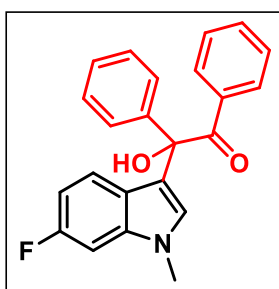
yield. **Physical State:** solid brown **m.p.:** 134–136 °C **R_f -value:** 0.3 (20% EtOAc/hexane). **¹H NMR (CDCl₃, 400 MHz):** δ 7.83 (d, *J* = 7.2 Hz, 2H), 7.71 (d, *J* = 1.6 Hz, 1H), 7.51 (d, *J* = 8.0 Hz, 2H), 7.45 (t, *J* = 7.6 Hz, 1H), 7.34–7.25 (m, 6H), 7.15 (d, *J* = 8.8 Hz, 1H), 6.61 (s, 1H), 4.82 (brs, 1H), 3.66 (s, 3H). **¹³C NMR {¹H} (CDCl₃, 100 MHz):** δ 200.2, 141.9, 136.5, 135.3, 133.3, 131.1, 130.2, 128.8, 128.5, 128.5, 128.4, 127.8, 125.6, 124.3, 116.9, 113.7, 111.2, 81.8, 33.4. **IR (KBr, cm⁻¹):** 2943,

1576, 1419, 749. **HRMS (ESI) m/z:** $[M+Na]^+$ Calcd for $C_{23}H_{18}BrNO_2Na$: 442.0419; Found: 442.0422.



2-hydroxy-2-(5-iodo-1-methyl-1H-indol-3-yl)-1,2-diphenylethanone (3oa): was prepared according to general procedure (6.5a). The crude reaction mixture was purified by column chromatography using silica gel (100-200 mesh size), giving (33 mg in 0.1 mmol scale) 69%

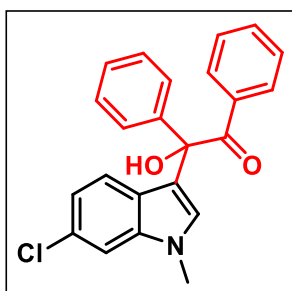
yield. **Physical State:** solid brown **m.p.:** 137–139 °C **R_f-value:** 0.4 (20% EtOAc/hexane). **¹H NMR (CDCl₃, 400 MHz):** δ 7.92 (s, 1H), 7.83 (d, J = 8.0 Hz, 2H), 7.51 – 7.44 (m, 4H), 7.36-7.27 (m, 5H) 7.07 (d, J = 8.8 Hz, 1H), 6.57 (s, 1H), 4.83 (brs, 1H), 3.66 (s, 3H). **¹³C NMR {¹H} (CDCl₃, 100 MHz):** δ 200.2, 141.8, 136.9, 135.3, 133.4, 131.1, 130.5, 130.3, 129.8, 129.3, 128.8, 128.5, 128.4, 127.8, 116.6, 111.8, 84.1, 81.8, 33.3. **IR (KBr, cm⁻¹):** 3053, 1653, 1272, 749. **HRMS (ESI) m/z:** $[M+Na]^+$ Calcd for $C_{23}H_{18}INO_2Na$: 490.0280; Found: 490.0243.



2-(6-fluoro-1-methyl-1H-indol-3-yl)-2-hydroxy-1,2-diphenylethanone (3pa): was prepared according to general procedure (6.5a). The crude reaction mixture was purified by column chromatography using silica gel (100-200 mesh size), giving (22 mg in 0.1 mmol scale) 61% yield. **Physical**

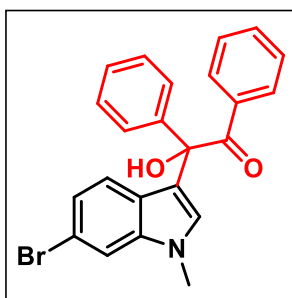
State: white solid, **m.p.:** 121–123 °C **R_f-value:** 0.45 (20% EtOAc/hexane). **¹H NMR (CDCl₃, 400 MHz):** δ 7.84 (d, J = 8.4 Hz, 2H), 7.53 (d, J = 8.0 Hz, 2H), 7.48-7.43 (m, 2H), 7.34-7.28 (m, 5H), 6.90 (d, J = 10.0 Hz, 1H), 6.85-6.79 (m, 1H), 6.60 (s, 1H), 4.85 (brs, 1H), 3.64 (s, 3H). **¹³C NMR {¹H} (CDCl₃, 175 MHz)** δ 200.4, 160.4 (d, J_{C-F} = 237.4 Hz), 141.9, 138.0, 135.4, 133.3, 131.1, 129.5 (d, J_{C-F} = 2.6 Hz), 129.3, 128.7,

128.4, 127.9, 123.4, 122.8 (d, J_{C-F} = 9.9 Hz), 117.6, 109.0 (d, J_{C-F} = 24.5 Hz), 96.1 (d, J_{C-F} = 25.9 Hz), 81.8, 33.3. **^{19}F NMR** (CDCl_3 , 376 MHz) δ -119.9. **IR** (KBr, cm^{-1}): 3054, 1635, 1273, 749. **HRMS (ESI) m/z:** $[\text{M}+\text{Na}]^+$ Calcd for $\text{C}_{23}\text{H}_{18}\text{FNO}_2\text{Na}$: 382.1219; Found: 382.1224.



2-(6-chloro-1-methyl-1H-indol-3-yl)-2-hydroxy-1,2-diphenylethanone (3qa): was prepared according to general procedure (6.5a). The crude reaction mixture was purified by column chromatography using silica gel (100-200 mesh size), giving (25 mg in 0.1 mmol scale) 67%

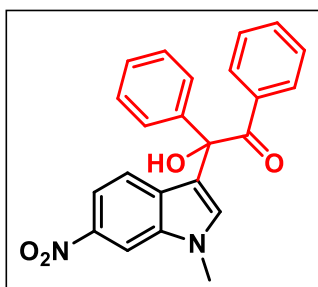
yield. **Physical State:** brown solid **m.p.:** 123–125 °C **R_f -value:** 0.3 (10% EtOAc/hexane). **^1H NMR** (CDCl_3 , 400 MHz): δ 7.83 (d, J = 8.0 Hz, 2H), 7.52 (d, J = 7.6 Hz 2H), 7.46-7.43 (m, 2H), 7.35-7.25 (m, 6H), 7.02 (d, J = 8.4 Hz, 1H), 6.62 (s, 1H), 4.86 (brs, 1H), 3.66 (s, 3H). **^{13}C NMR** $\{^1\text{H}\}$ (CDCl_3 , 100 MHz) δ 200.4, 141.9, 138.2, 135.3, 133.3, 131.1, 129.8, 128.8, 128.4 (2C), 128.4, 127.9, 125.5, 122.8, 120.9, 117.6, 109.8, 81.7, 33.3. **IR** (KBr, cm^{-1}): 3047, 1635, 1274, 749. **HRMS (ESI) m/z:** $[\text{M}+\text{Na}]^+$ Calcd for $\text{C}_{23}\text{H}_{18}\text{ClNO}_2\text{Na}$: 398.0918; Found: 398.0932.



2-(6-bromo-1-methyl-1H-indol-3-yl)-2-hydroxy-1,2-diphenylethanone (3ra): was prepared according to general procedure (6.5a). The crude reaction mixture was purified by column chromatography using silica gel (100-200 mesh size), giving (36 mg in 0.1 mmol scale) 86%

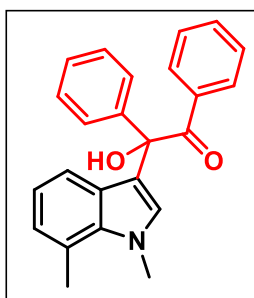
yield. **Physical State:** solid brown **m.p.:** 141–143 °C **R_f -value:** 0.4 (20% EtOAc/hexane). **^1H NMR** (CDCl_3 , 400 MHz): δ 7.83 (d, J = 8.0 Hz, 2H), 7.52 (d, J =

7.6 Hz, 2H), 7.46-7.40 (m, 3H), 7.33-7.25 (m, 5H), 7.15 (d, $J = 8.2$ Hz, 1H), 6.61 (s, 1H), 4.88 (brs, 1H), 3.65 (s, 3H). **^{13}C NMR** $\{^1\text{H}\}$ (CDCl_3 , 100 MHz): δ 200.3, 141.8, 138.6, 135.2, 133.4, 131.1, 129.7, 128.8, 128.4, 128.4, 127.9, 125.8, 123.4, 123.1, 117.5, 116.4, 112.8, 81.7, 33.3. **IR** (KBr, cm^{-1}): 3053, 1635, 1273, 749. **HRMS (ESI)** m/z : $[\text{M}+\text{Na}]^+$ Calcd for $\text{C}_{23}\text{H}_{18}\text{BrNO}_2\text{Na}$: 442.0413; Found: 442.0386.



2-hydroxy-2-(1-methyl-6-nitro-1H-indol-3-yl)-1,2-diphenylethanone (3sa): was prepared according to general procedure (6.5a). The crude reaction mixture was purified by column chromatography using silica gel (100-200 mesh size), giving (22 mg in 0.1 mmol scale)

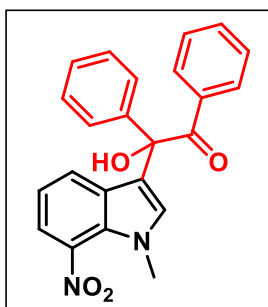
57% yield. **Physical State**: yellow solid **m.p.**: 152–154 °C **R_f -value**: 0.3 (30% EtOAc/hexane). **^1H NMR** (CDCl_3 , 400 MHz): δ 8.28 (d, $J = 1.6$ Hz, 1H), 7.94 (d, $J = 9.2$ Hz, 1H), 7.83 (d, $J = 8.8$ Hz, 2H), 7.62 (d, $J = 8.8$ Hz, 1H), 7.52-7.45 (m, 3H), 7.38 – 7.28 (m, 5H), 6.93 (s, 1H) 4.87 (brs, 1H), 3.80 (s, 3H). **^{13}C NMR** $\{^1\text{H}\}$ (CDCl_3 , 100 MHz): δ 199.9, 143.8, 141.6, 136.4, 135.0, 134.3, 133.6, 131.6, 131.0, 129.0, 128.7, 128.6, 127.7, 122.1, 118.6, 115.5, 106.8, 81.6, 33.7. **IR** (KBr, cm^{-1}): 3053, 1507, 1339, 749. **HRMS (ESI)** m/z : $[\text{M}+\text{Na}]^+$ Calcd for $\text{C}_{23}\text{H}_{18}\text{N}_2\text{O}_4\text{Na}$: 409.1159; Found: 409.1165.



2-(1,7-dimethyl-1H-indol-3-yl)-2-hydroxy-1,2-diphenylethanone (3ta): was prepared according to general procedure (6.5a). The crude reaction mixture was purified by column chromatography using silica gel (100-200 mesh size), giving (30 mg in 0.1 mmol scale) 84% yield. **Physical State**:

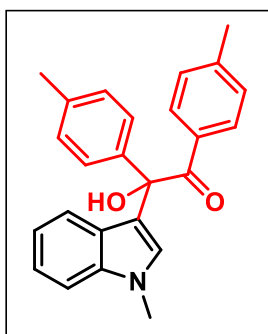
solid white **m.p.**: 118–120 °C **R_f -value**: 0.4 (20% EtOAc/hexane). **^1H NMR** (CDCl_3 ,

400 MHz): δ 7.86 (d, J = 8.0 Hz, 2H), 7.56 (d, J = 8.0 Hz, 2H), 7.43 (t, J = 7.6 Hz, 1H), 7.38-7.35 (m, 1H), 7.34-7.29 (m, 5H), 6.91 (d, J = 5.2 Hz, 2H), 6.49 (s, 1H), 4.71 (brs, 1H), 3.95 (s, 3H), 2.74 (s, 3H). **^{13}C NMR $\{^1\text{H}\}$ (CDCl_3 , 100 MHz):** δ 200.7, 141.9, 136.6, 135.6, 133.1, 131.1, 130.9, 128.6, 128.3, 128.2, 127.9, 127.9, 125.2, 121.7, 120.4, 119.9, 117.0, 81.8, 37.3, 20.1. **IR** (KBr, cm^{-1}): 3055, 1653, 1274, 749. **HRMS (ESI) m/z:** $[\text{M}-\text{H}]^+$ Calcd for $\text{C}_{24}\text{H}_{20}\text{NO}_2$: 354.1419; Found: 454.1507.



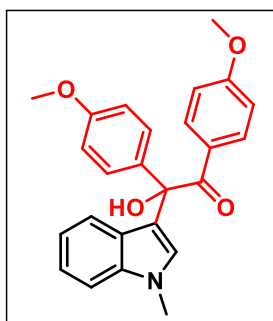
2-hydroxy-2-(1-methyl-7-nitro-1H-indol-3-yl)-1,2-diphenylethanone (3ua): was prepared according to general procedure (6.5a). The crude reaction mixture was purified by column chromatography using silica gel (100-200 mesh size scale), giving (22 mg in 0.1 mmol scale) 58% yield. **Physical**

State: yellow solid **m.p.:** 139–141 °C **R_f -value:** 0.3 (30% EtOAc/hexane). **^1H NMR (CDCl_3 , 400 MHz):** δ 7.88-7.80 (m, 4H), 7.51-7.46 (m, 3H), 7.36-7.29 (m, 5H), 7.09 (t, J = 8.0 Hz, 1H), 6.70 (s, 1H), 4.97 (brs, 1H) 3.73 (s, 3H). **^{13}C NMR $\{^1\text{H}\}$ (CDCl_3 , 100 MHz):** δ 199.9, 141.5, 137.0, 135.0, 133.7, 133.6, 131.8, 131.1, 128.9, 128.8, 128.6, 128.6, 128.2, 127.8, 120.6, 119.4, 118.6, 81.4, 37.8. **IR** (KBr, cm^{-1}): 3053, 1635, 1266, 749. **HRMS (ESI) m/z:** $[\text{M}+\text{Na}]^+$ Calcd for $\text{C}_{23}\text{H}_{18}\text{N}_2\text{O}_4\text{Na}$: 409.1159; Found: 409.1126.



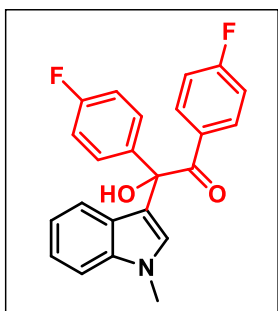
2-hydroxy-2-(1-methyl-1H-indol-3-yl)-1,2-di-p-tolyleanone (3ab): was prepared according to general procedure (6.5a). The crude reaction mixture was purified by column chromatography using silica gel (100-200 mesh size) giving (20 mg in 0.1 mmol scale) 54% yield. **Physical State:** solid white **m.p.:** 134–136 °C **R_f -value:** 0.3 (5%

EtOAc/hexane). **¹H NMR (CDCl₃, 700 MHz):** δ 7.80 (d, *J* = 8.4 Hz, 2H), 7.56 (d, *J* = 7.7 Hz, 1H), 7.42 (d, *J* = 7.7 Hz, 2H), 7.29 (d, *J* = 8.4 Hz, 1H), 7.22 (t, *J* = 7.7 Hz, 1H), 7.12 (d, *J* = 8.4 Hz, 2H), 7.07–7.80 (m, 3H), 6.64 (s, 1H), 4.97 (s, 1H), 3.69 (s, 3H), 2.33 (s, 3H), 2.31 (s, 3H). **¹³C NMR {¹H} (CDCl₃, 175 MHz):** δ 200.1, 144.1, 139.4, 137.8, 137.8, 132.7, 131.4, 129.3, 129.1, 129.1, 128.0, 127.0, 122.5, 122.0, 120.1, 117.5, 109.7, 81.5, 33.2, 21.9, 21.4. **IR (KBr, cm⁻¹):** 3053, 1653, 1266, 750. **HRMS (ESI) m/z:** [M+Na]⁺ Calcd for C₂₅H₂₃NO₂Na: 392.1627; Found: 392.1637.



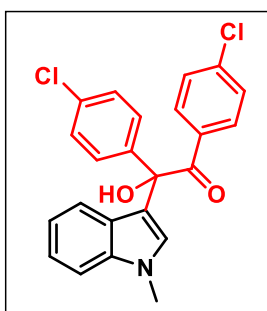
2-hydroxy-1,2-bis(4-methoxyphenyl)-2-(1-methyl-1H-indol-3-yl)ethanone (3ac): was prepared according to general procedure (6.5a). The crude reaction mixture was purified by column chromatography using silica gel (100–200 mesh size), giving (27 mg in 0.1 mmol scale) 68% yield.

Physical State: solid white **m.p.:** 129–131 °C **R_f-value:** 0.4 (20% EtOAc/hexane). **¹H NMR (CDCl₃, 400 MHz):** δ 7.92 (d, *J* = 8.8 Hz, 2H), 7.57 (d, *J* = 8.0 Hz, 1H), 7.45 (d, *J* = 8.0 Hz, 2H), 7.29 (d, *J* = 8.4 Hz, 1H), 7.22 (t, *J* = 7.2 Hz, 1H), 7.05 (t, *J* = 7.8 Hz, 1H), 6.83 (d, *J* = 8.8 Hz, 2H), 6.74 (d, *J* = 8.8 Hz, 2H), 6.63 (s, 1H), 5.16 (s, 1H), 3.78 (s, 6H), 3.69 (s, 3H). **¹³C NMR {¹H} (CDCl₃, 100 MHz):** δ 198.7, 163.6, 159.4, 137.8, 134.8, 133.8, 129.4, 129.0, 127.8, 127.1, 122.5, 122.1, 120.0, 117.6, 113.9, 113.6, 109.6, 80.9, 55.7, 55.5, 33.2. **IR (KBr, cm⁻¹):** 3053, 1635, 1274, 749. **HRMS (ESI) m/z:** [M+Na]⁺ Calcd for C₂₅H₂₃NO₄Na: 424.1525; Found: 424.1532.



1,2-bis(4-fluorophenyl)-2-hydroxy-2-(1-methyl-1H-indol-3-yl)ethanone (3ad): was prepared according to general procedure (6.5a). The crude reaction mixture was purified by column chromatography using silica gel (100-200 mesh size), giving (19 mg in 0.1 mmol scale) 50% yield. **Physical**

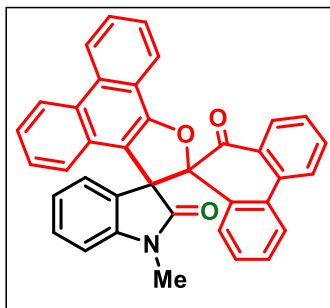
State: solid brown **m.p.:** 125–127 °C **R_f-value:** 0.45 (20% EtOAc/hexane). **¹H NMR (CDCl₃, 400 MHz):** δ 7.96-7.92 (m, 2H), 7.55-7.51 (m, 2H), 7.49 (d, *J* = 8.0 Hz, 1H), 7.32 (d, *J* = 8.4 Hz, 1H), 7.27-7.23 (m, 1H), 7.10-7.09 (m, 1H), 7.02 (t, *J* = 8.8 Hz, 2H), 6.97 (d, *J* = 8.8 Hz, 2H), 6.62 (s, 1H), 4.71 (s, 1H), 3.72 (s, 3H). **¹³C NMR {¹H} (CDCl₃, 100 MHz):** δ 198.7, 167.0, 164.2 (d, *J*_{C-F} = 212.0 Hz), 161.5, 137.8, 137.7 (d, *J*_{C-F} = 12.4 Hz), 133.9 (d, *J*_{C-F} = 36.8 Hz), 131.4, 129.7 (d, *J*_{C-F} = 32.4 Hz), 129.0, 126.5, 122.8, 121.5, 120.3, 117.1, 115.6 (d, *J*_{C-F} = 84.8 Hz), 109.9, 81.4, 33.2. **¹⁹F NMR {¹H} (CDCl₃, 376 MHz)** δ -104.3, -114.1 **IR (KBr, cm⁻¹):** 3004, 1653, 1275, 749. **HRMS (ESI) m/z:** [M+Na]⁺ Calcd for C₂₃H₁₇F₂NO₂Na: 400.1125; Found: 400.1140.



1,2-bis(4-chlorophenyl)-2-hydroxy-2-(1-methyl-1H-indol-3-yl)ethanone (3ae): was prepared according to general procedure (6.5a). The crude reaction mixture was purified by column chromatography using silica gel (100-200 mesh size), giving (23 mg in 0.1 mmol scale) 56% yield. **Physical**

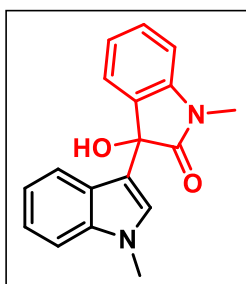
State: solid brown **m.p.:** 127–229 °C **R_f-value:** 0.4 (20% EtOAc/hexane) **¹H NMR (CDCl₃, 400 MHz):** δ 7.83 (d, *J* = 8.8 Hz, 2H), 7.51-7.46 (m, 3H), 7.33-7.30 (m, 3H), 7.28-7.25 (m, 3H), 7.07 (t, *J* = 8.0 Hz, 1H), 6.63 (s, 1H), 4.59 (s, 1H), 3.71 (s, 3H). **¹³C NMR {¹H} (CDCl₃, 100 MHz):** δ 199.0, 140.3, 139.9, 137.8, 134.4, 133.5, 132.5, 129.3, 129.1, 128.9, 128.8, 126.4, 122.9, 121.4, 120.4, 116.9, 110.0, 81.6, 33.3. **IR**

(KBr, cm^{-1}): 3009, 1652, 1274, 749. **HRMS (ESI) m/z :** $[\text{M}+\text{Na}]^+$ Calcd for $\text{C}_{23}\text{H}_{17}\text{Cl}_2\text{NO}_2\text{Na}$: 432.0534; Found: 432.0533.



1-methyl-10''H-dispiro[indoline-3,3'-phenanthro[9,10-b]furan-2',9''-phenanthrene]-2,10''-dione (3ag): was prepared according to reaction procedure (6.5a). The crude reaction mixture was purified by column chromatography using silica gel

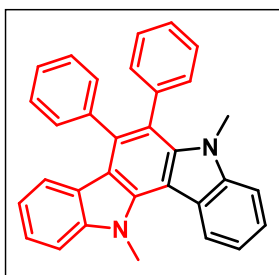
(100-200 mesh size), giving (15 mg in 0.1 mmol scale) 52% yield. **Physical State:** yellow solid **m.p.:** 256–258 °C **R_f -value:** 0.4 (40% EtOAc/hexane) **^1H NMR (CDCl_3 , 400 MHz):** δ 8.72-8.70 (m, 1H), 8.61-8.59 (m, 2H), 7.80-7.77 (m, 3H), 7.59 (d, $J = 7.6$ Hz, 1H), 7.43-7.28 (m, 5H), 7.24-7.19 (m, 2H), 7.13-7.07 (m, 2H) 6.51 (t, $J = 7.6$ Hz, 1H), 6.46 (d, $J = 8.0$ Hz, 1H), 6.41 (d, $J = 7.6$ Hz, 1H), 5.85 (d, $J = 6.8$ Hz, 1H), 2.82 (s, 3H). **^{13}C NMR $\{^1\text{H}\}$ (CDCl_3 , 175 MHz):** δ 194.8, 174.4, 156.7, 144.2, 137.1, 135.1, 134.3, 133.1, 132.7, 131.0, 129.8, 129.4, 128.9, 128.7, 128.6, 128.3, 128.3, 127.7, 127.6, 127.3, 126.9, 126.8, 126.7, 124.7, 124.4, 123.8, 123.6, 123.4, 122.4, 122.3, 121.9, 121.8, 112.5, 107.8, 99.1, 26.3. **IR (KBr, cm^{-1}):** 2993, 1768, 1693, 1385, 1244, 746. **HRMS (ESI) m/z :** $[\text{M}+\text{Na}]^+$ Calcd for $\text{C}_{37}\text{H}_{23}\text{NO}_2\text{Na}$: 552.1570; Found: 552.1559.



3-hydroxy-1-methyl-3-(1-methyl-1H-indol-3-yl)indolin-2-one (3ah): was prepared according to reaction procedure (6.5a). The crude reaction mixture was purified by column chromatography using silica gel (100-200 mesh size), giving (16 mg in 0.1 mmol scale) 55% yield. **Physical State:** solid

brown **m.p.:** 166–168 °C **R_f -value:** 0.3 (20% EtOAc/hexane). **^1H NMR (CDCl_3 , 400**

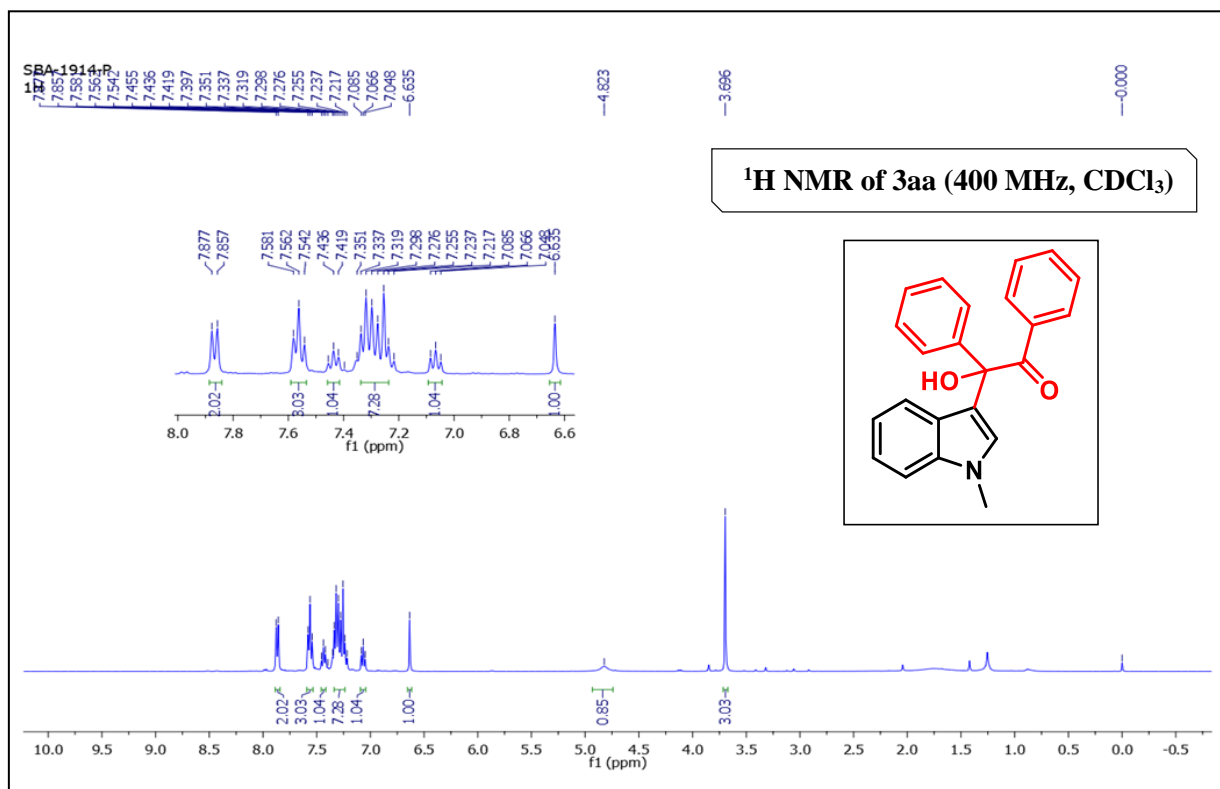
MHz): δ 7.69 (d, J = 8.0 Hz, 1H), 7.57 (d, J = 7.6 Hz, 1H), 7.36 (t, J = 7.6 Hz, 1H), 7.38-7.36 (m, 1H), 7.21 (t, J = 7.2 Hz, 1H), 7.08 (t, J = 7.6 Hz, 2H), 6.96 (s, 1H), 6.91 (t, J = 8.0 Hz, 1H), 3.76 (s, 3H), 3.26 (s, 3H), 3.23 (s, 1H). **^{13}C NMR $\{^1\text{H}\}$ (CDCl_3 , 100 MHz):** δ 177.4, 143.5, 138.0, 131.4, 130.1, 128.0, 125.6, 125.1, 123.5, 122.4, 121.1, 120.1, 114.0, 109.9, 108.8, 75.9, 33.1, 26.7. **IR** (KBr, cm^{-1}): 2925, 1717, 1329, 745. **HRMS (ESI) m/z :** $[\text{M}+\text{Na}]^+$ Calcd for $\text{C}_{18}\text{H}_{16}\text{N}_2\text{O}_2\text{Na}$: 315.1110; Found: 315.1112.



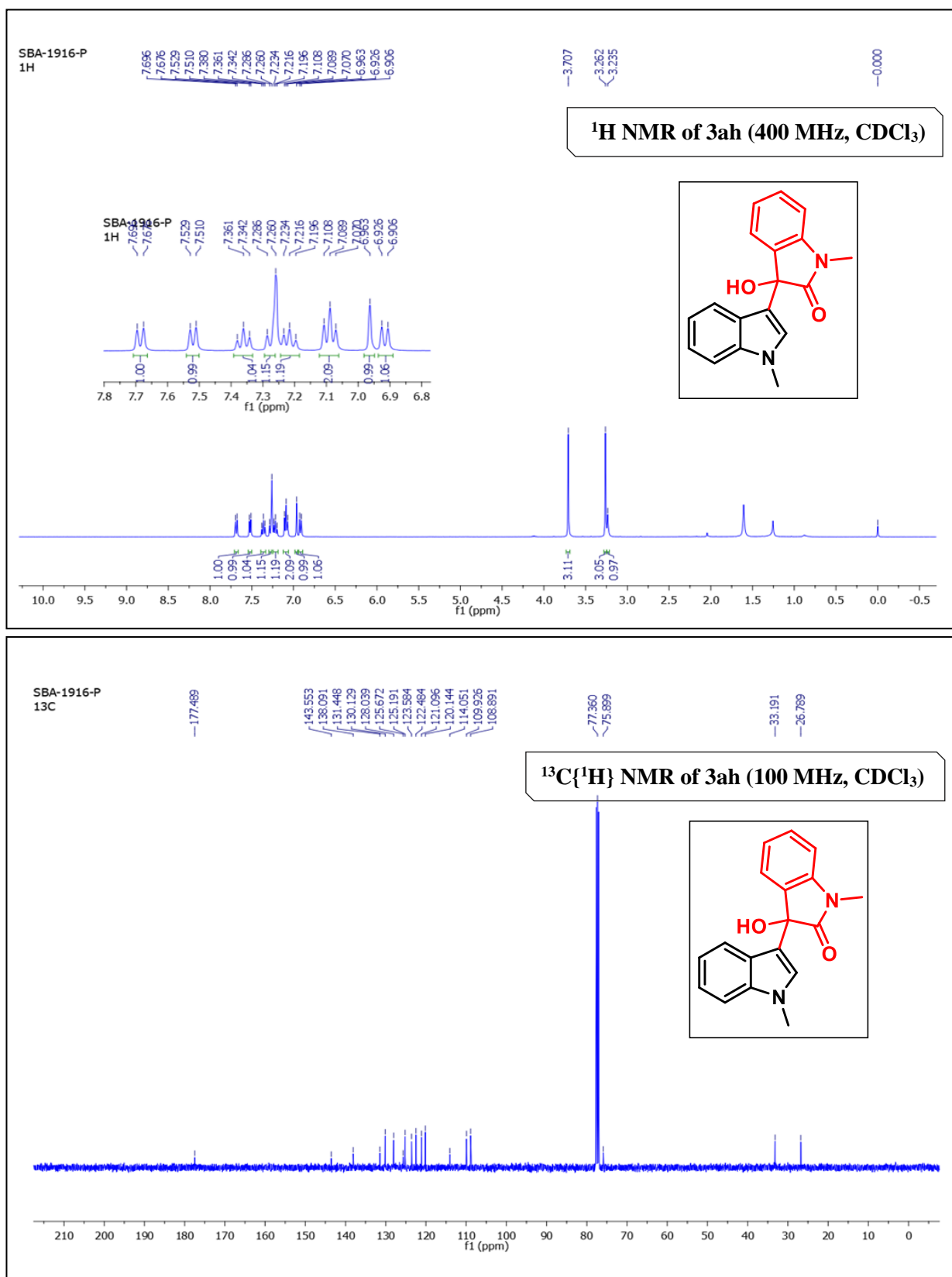
5,12-dimethyl-6,7-diphenyl-5,12-dihydroindolo[3,2-*a*]carbazole (4aa): was prepared according to reported procedure. The crude reaction mixture was purified by column chromatography using silica gel (100-200 mesh size), giving (31 mg in 0.1 mmol scale) 71% yield. **Physical**

State: solid brown **m.p.:** 248–250 °C **R_f -value:** 0.5 (10% EtOAc/hexane). **^1H NMR (CDCl_3 , 400 MHz):** δ 7.63 (d, J = 8.0 Hz, 1H), 7.50-7.46 (m, 2H), 7.41 (d, J = 8.0 Hz, 1H), 7.35-7.30 (m, 2H), 7.27-7.29 (m, 10H), 6.89 (t, J = 8.0 Hz, 1H), 6.27 (d, J = 8.0 Hz, 1H) 4.52 (s, 3H), 3.28 (s, 3H). **^{13}C NMR $\{^1\text{H}\}$ (CDCl_3 , 175 MHz):** δ 142.7, 142.1, 140.4, 139.6, 139.1, 137.3, 136.0, 132.6, 130.7, 128.2, 127.5, 126.9, 126.9, 124.8, 124.6, 124.1, 122.9, 121.4, 121.2, 119.6, 119.5, 118.6, 115.3, 109.5, 109.2, 107.5, 35.8, 33.3. **IR** (KBr, cm^{-1}): 3051, 1274, 895, 749. **HRMS (ESI) m/z :** $[\text{M}+\text{Na}]^+$ Calcd for $\text{C}_{32}\text{H}_{24}\text{N}_2\text{Na}$: 436.1934; Found: 436.1956.

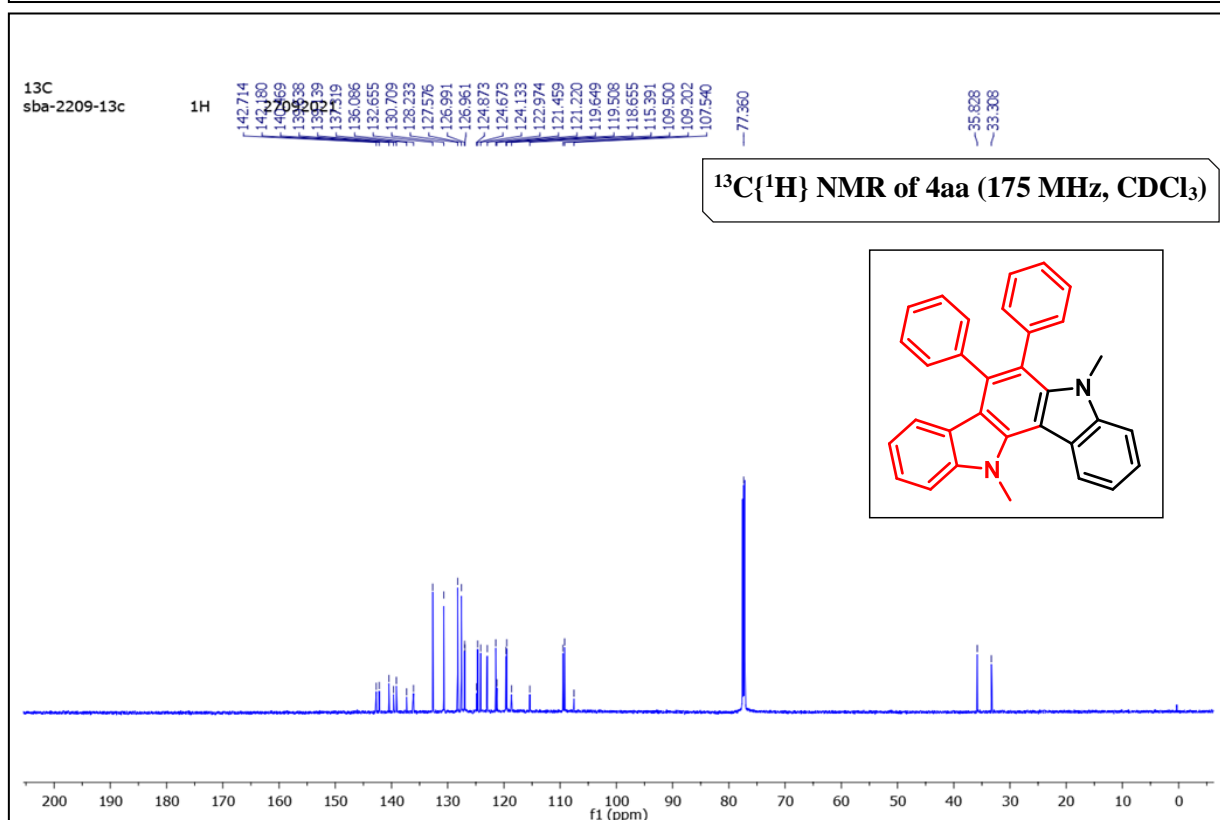
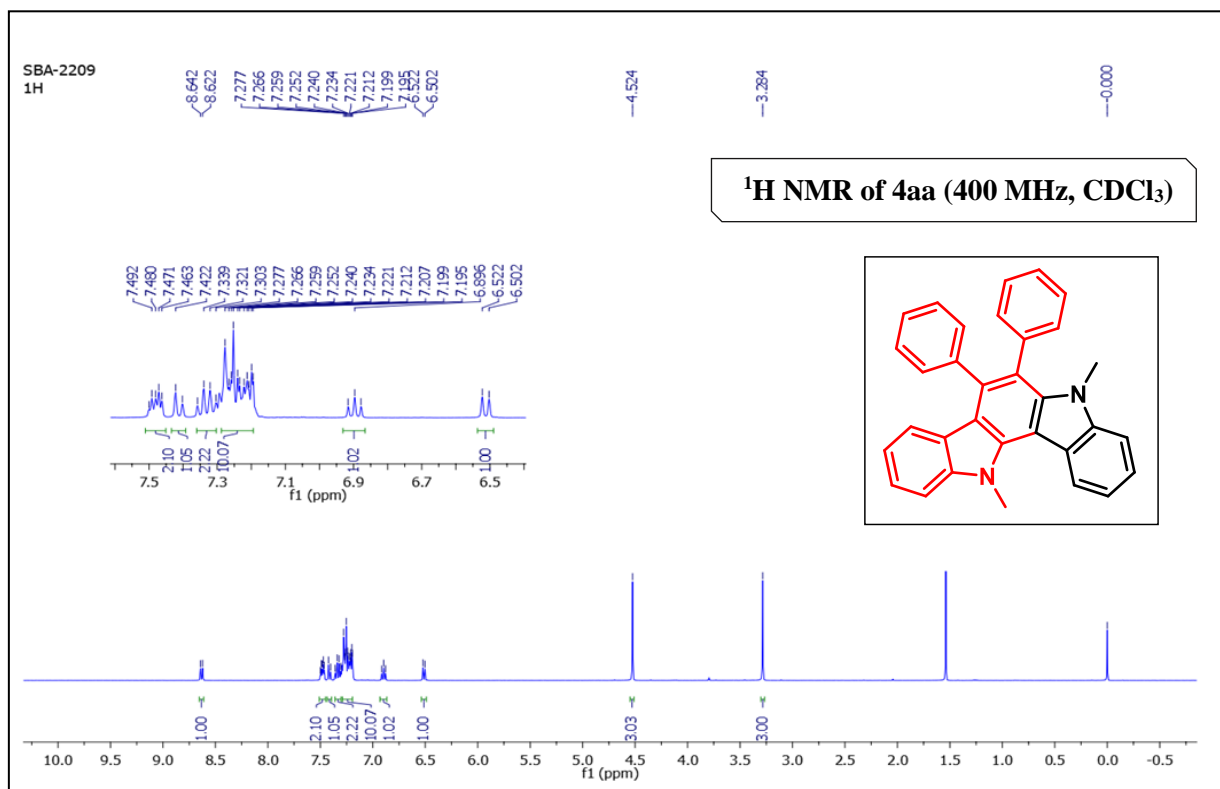
NMR spectra of 2-hydroxy-2-(1-methyl-1H-indol-3-yl)-1,2-diphenylethan-1-one (3aa):



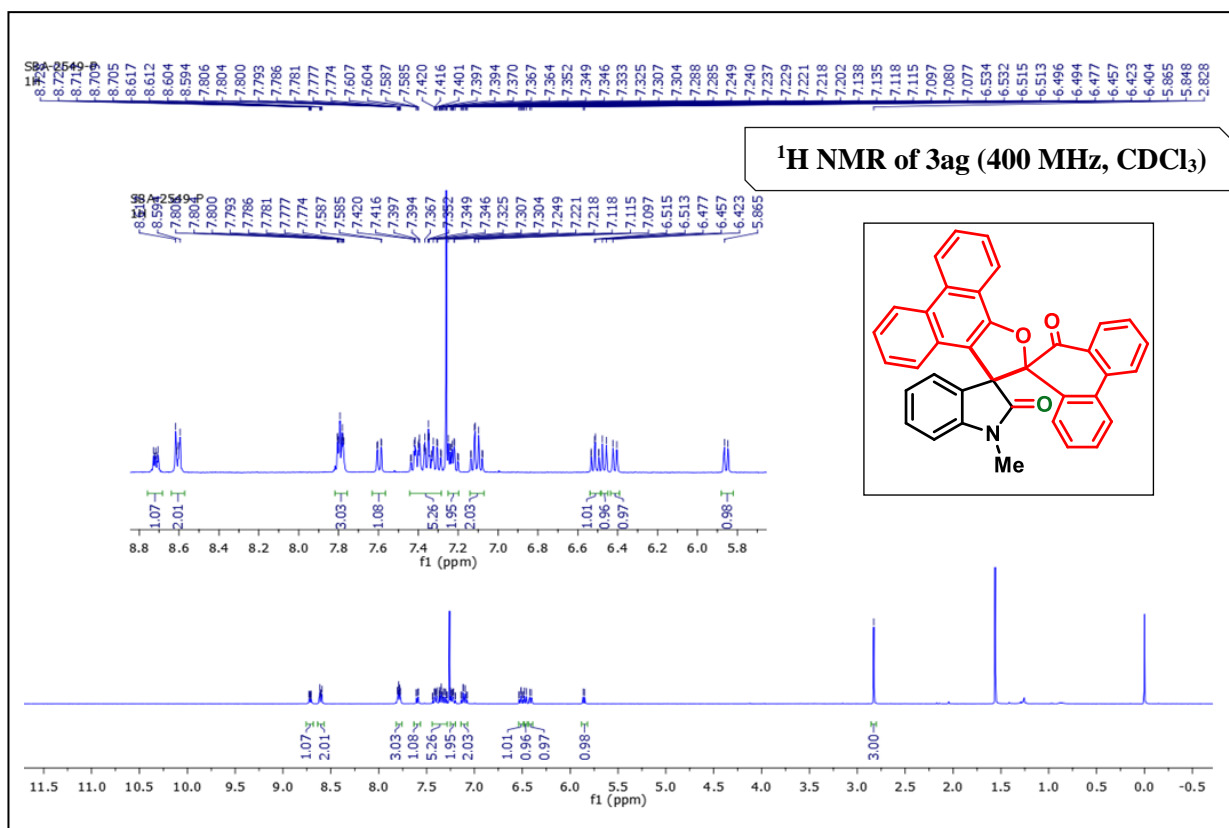
NMR spectra of 3-hydroxy-1-methyl-3-(1-methyl-1H-indol-3-yl)indolin-2-one (3da):



NMR spectra of 5,12-dimethyl-6,7-diphenyl-5,12-dihydroindolo[3,2-a]carbazole (3aa):



NMR spectra of 1-methyl-10''H-dispiro[indoline-3,3'-phenanthro[9,10-b]furan-2',9''-phenanthrene]-2,10''-dione (3da):



(b) Crystals of the compounds **3fa** (2-hydroxy-1,2-diphenyl-2-(1-phenyl-1H-indol-3-yl)ethan-1-one) were obtained after slow evaporation of methanol.

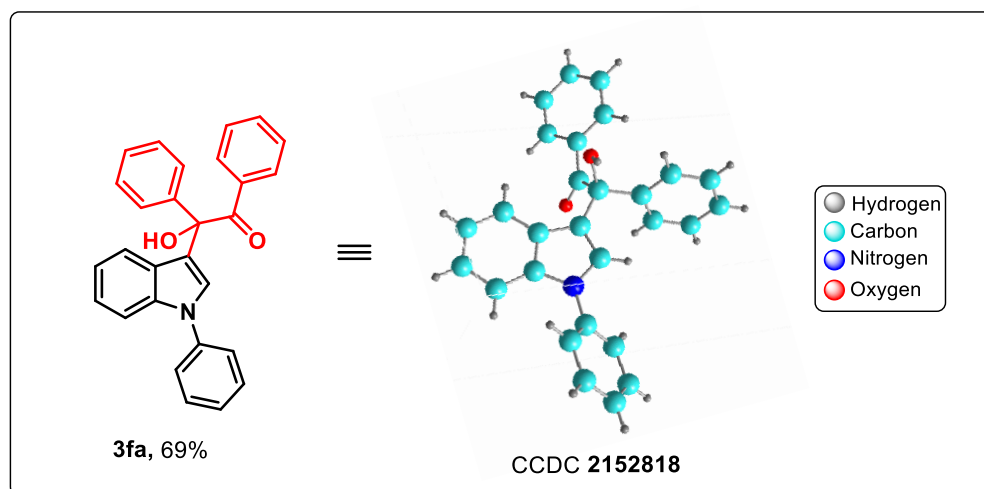
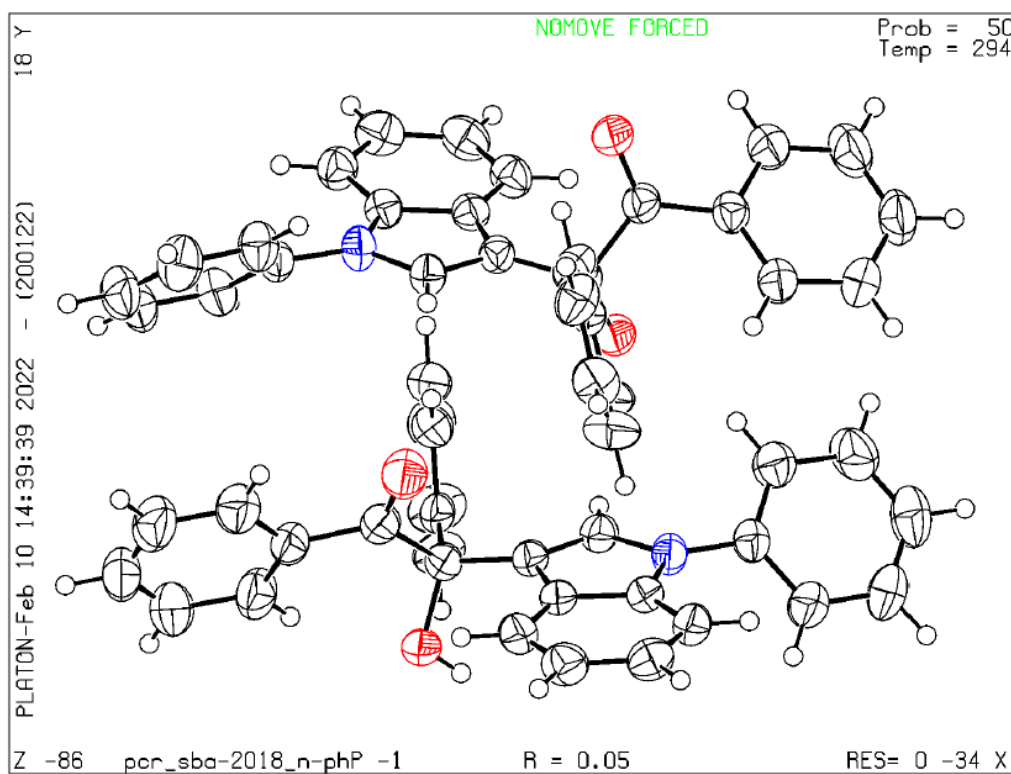


Figure 6.4. Crystal structure of **3fa** (50% ellipsoid probability).

Datablock pcr_sba-2018_n-phenyl - ellipsoid plot



(c) Crystals of the compounds **3ga** (2-hydroxy-1,2-diphenyl-2-(1-phenyl-1H-indol-3-yl)ethan-1-one) were obtained after slow evaporation of methanol.

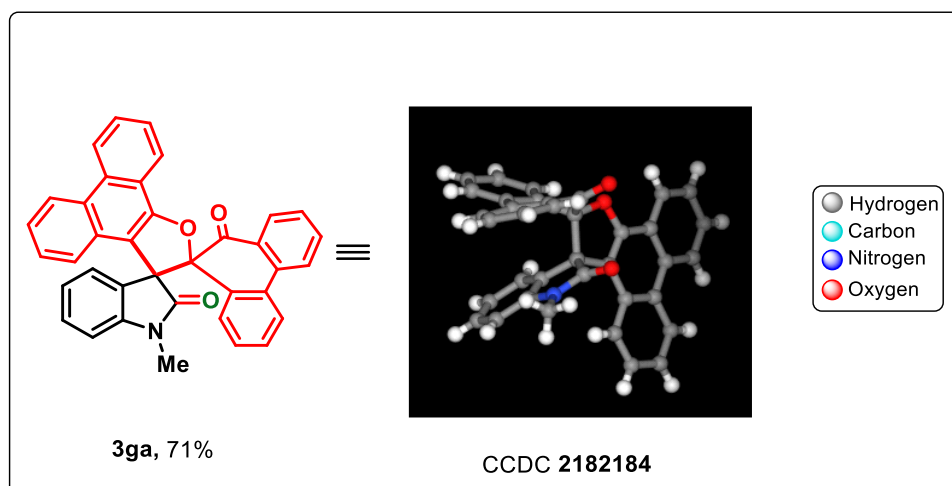
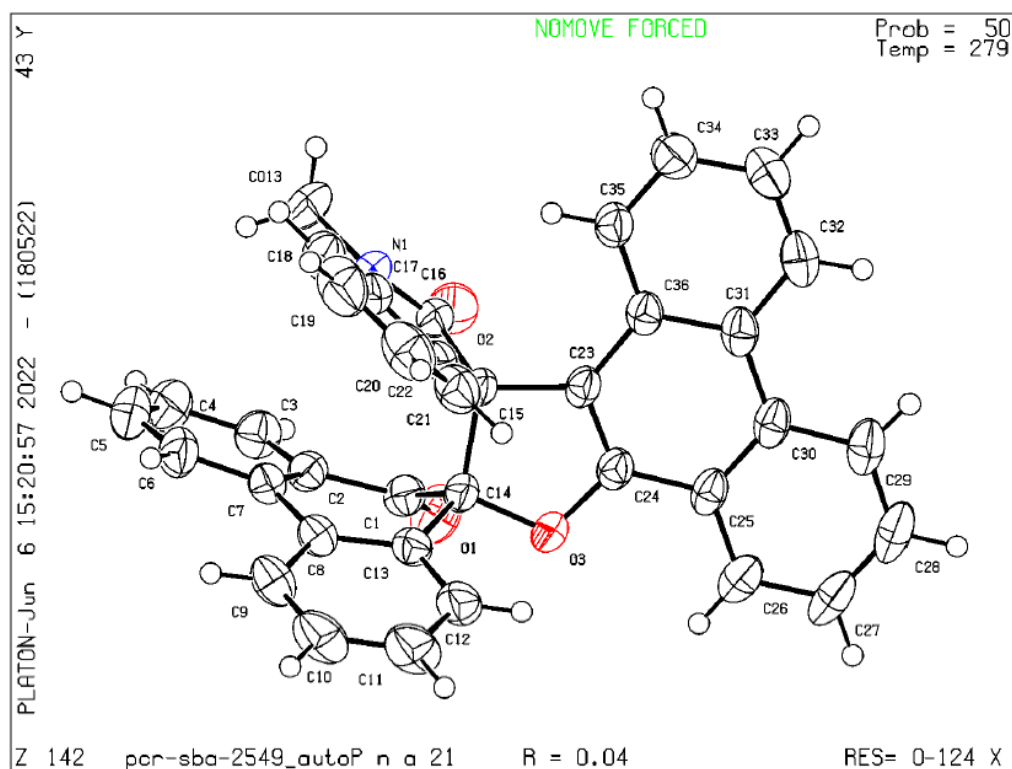


Figure 6.5. Crystal structure of **3ga** (50% ellipsoid probability).

Datablock pcr-sba-2549_auto - ellipsoid plot



REFERENCES

1. (a) Humphrey, G. R.; Kuethe, J. T. Practical Methodologies for the Synthesis of Indoles. *Chem. Rev.* **2006**, *106*, 2875–2911. (b) Taylor, R. D.; MacCoss, M.; Lawson, A. D. G. Rings in Drugs. *J. Med. Chem.* **2014**, *57*, 5845–5859. (c) Unzue, A.; Zhao, H.; Lolli, G.; Dong, J.; Zhu, J.; Zechner, M.; Dolbois, A.; Caflisch, A.; Nevado, C. The "Gatekeeper" Residue Influences the Mode of Binding of Acetyl Indoles to Bromodomains. *J. Med. Chem.* **2016**, *59*, 3087–97.
2. (a) Kochanowska-Karamyan, A. J.; Hamann, M. T. Marine Indole Alkaloids: Potential New Drug Leads for the Control of Depression and Anxiety. *Chem. Rev.* **2010**, *110*, 4489–4497. (b) McCabe, S. R.; Wipf, P. Total Synthesis, Biosynthesis and Biological Profiles of Clavine Alkaloids. *Org. Biomol. Chem.* **2016**, *14*, 5894–5913. (c) Liu, H.; Jia, Y. Ergot alkaloids: synthetic approaches to lysergic acid and clavine alkaloids. *Nat. Prod. Rep.* **2017**, *34*, 411–432.
3. (a) Seregin, I. V.; Gevorgyan, V. Direct Transition Metal-Catalyzed Functionalization of Heteroaromatic Compounds. *Chem. Soc. Rev.* **2007**, *36*, 1173–1193. (b) Ackermann, L.; Vicente, R.; Kapdi, A. R. Transition-metal-catalyzed direct arylation of (hetero) arenes by C-H bond cleavage *Angew. Chem., Int. Ed.* **2009**, *48*, 9792. (c) Baccalini, A.; Faita, G.; Zanon, G.; Maiti, D. Transition Metal Promoted Cascade Heterocycle Synthesis through C-H Functionalization. *Chem. Eur. J.* **2020**, *26*, 9749–9783.
4. (a) Gensch, T.; Hopkinson, M. N.; Glorius, F.; Wencel-Delord; Mild metal-catalyzed C–H activation: examples and concepts. *J. Chem. Soc. Rev.* **2016**, *45*, 2900–2936. (b) Davies, H. M. L.; Morton, D. Collective Approach to Advancing C–H Functionalization. *ACS Cent. Sci.* **2017**, *3*, 936–943. (c) Crabtree, R. H.; Lei, A. Introduction: C–H Activation. *Chem. Rev.* **2017**, *117*, 8481–8482 (d) Abrams, D. J.; Provencher, P. A.; Sorensen, E. J. Recent Applications of C–H Functionalization in Complex Natural Product Synthesis. *Chem. Soc. Rev.* **2018**, *47*, 8925–8967.
5. Kumar, P.; Naftalak P. J.; Kapur M. Transition metal-catalyzed C–H functionalizations of indoles. *New J. Chem.*, **2021**, *45*, 13692–13746.
6. Mutule, I.; Suna, E.; Olofsson, K.; Pelcman, B. Catalytic direct acetoxylation of indoles. *J. Org. Chem.* **2009**, *74*, 7195–7198.
7. Xu, H.; Pan, Y.; Li, G.; Hu, X.; Chen, J. Copper(II)-Catalyzed Direct C–H (Hetero)arylation at the C3 Position of Indoles Assisted by a Removable N,N-Bidentate Auxiliary Moiety. *J. Org. Chem.*, **2021**, *86*, 1789–1801.
8. (a) Choy, P. Y.; Wong, S. M.; Kapdi, A.; Kwong, F. Y. Recent developments in palladium-catalyzed non-directed coupling of (hetero)arene C–H bonds with C–Z (Z = B, Si, Sn, S, N, C, H) bonds in bi(hetero)aryl synthesis. *Org. Chem. Front.* **2018**, *5*, 288–321. (b) Khake, S. M.; Chatani, N. Nickel-Catalyzed C–H Functionalization Using A Non-Directed Strategy. *Chem.* **2020**, *6*, 1056–1081.
9. (a) Chai, X.-Y.; Xu, H.-B.; Dong, L.; Cascade Reaction to Selectively Synthesize Multifunctional Indole Derivatives by Ir(III)-Catalyzed C–H Activation. *Chem. Eur. J.* **2021**, *27*, 13123–13127. (b) Shi, X.; Xu, W.; Wang, R.; Zeng, X.; Qiu, H.; Wang, M.; Ketone-directed cobalt (III)-catalyzed regioselective C2 amidation of indoles. *J. Org. Chem.* **2020**, *85*, 3911–3920. (c) Ali, S.; Huo, J.; Wang, C. Manganese-Catalyzed Aromatic C–H Allylation of Ketones. *Org. Lett.* **2019**, *21*, 6961–6965. (d) Chen, S.; Zhang, M.; Su, R.; Chen, X.; Feng, B.; Yang, Y.; You, J. C2/C4 regioselective Heteroarylation of Indoles by Tuning C-H Metalation Modes. *ACS Catal.* **2019**, *9*, 6372–6379.
10. (a) Gandeepan, P.; Müller, T.; Zell, D.; Cera, G.; Warratz, S.; Ackermann, L. 3d Transition Metals for C–H Activation. *Chem. Rev.* **2019**, *119*, 2192–2452. (b) Dalton, T.; Faber, T.; Glorius, F. C-H Activation: Toward Sustainability and Applications. *ACS Cent. Sci.* **2021**, *7*, 245. (c) Banjare, S. K.; Nanda, T.; Ravikumar, P. C. Cobalt-Catalyzed Regioselective Direct C-4 Alkenylation of 3-

-
- Acetylintole with Michael Acceptors Using a Weakly Coordinating Functional Group. *Org. Lett.* **2019**, *21*, 8138–8143.
11. (a) Banjare, S. K.; Nanda, T.; Pati, B. V.; Biswal, P.; Ravikumar, P. C. O-Directed C–H functionalization via cobaltacycles: a sustainable approach for C–C and C–heteroatom bond formations. *Chem. Commun.* **2021**, *57*, 3630–3647. (b) Banjare, S. K.; Nanda, T.; Pati, B. V.; Adhikari, G. K. D.; Dutta, J.; Ravikumar, P. C. Breaking the Trend: Insight into Unforeseen Reactivity of Alkynes in Cobalt-Catalyzed Weak Chelation-Assisted Regioselective C(4)–H Functionalization of 3-Pivaloyl Indole. *ACS Catal.* **2021**, *18*, 11579–11587.
 12. Yu, T.-Y.; Xu, W.-H.; Lu, H.; Wei, H. Cobalt-catalyzed intramolecular decarbonylative coupling of acylindoles and diarylketones through the cleavage of C–C bonds. *Chem. Sci.* **2020**, *11*, 12336–12340.
 13. (a) Spikes, G. H.; Milsman, C.; Bill, E.; Weyhermüller, T.; Wieghardt, K. One- and Two-Electron Reduced 1,2-Diketone Ligands in $[\text{ZnII}(\text{L}^\bullet)_2(\text{Et}_2\text{O})]$, $[\text{CoII}(\text{L}^\bullet)_2(\text{Et}_2\text{O})]$, and $\text{Na}_2(\text{Et}_2\text{O})_4[\text{CoII}(\text{LRed})_2]$. *Inorg. Chem.* **2008**, *47*, 11745–11754. (b) Spikes, G. H.; Bill, E.; Weyhermüller, T.; Wieghardt, K. *Angew. Chem., Int. Ed.* **2008**, *47*, 2973–2977.
 14. (a) Dinda, E.; Bhunia, S. K.; Jana, R. Palladium-Catalyzed Cascade Reactions for Annulative π -Extension of Indoles to Carbazoles through C–H Bond Activation. *Curr. Org. Chem.*, **2020**, *24*, 2612–2633. (b) Liu, B.; Liu, M.; Li, Q.; Li, Y.; Feng, K.; Zhou, Y. Palladium Catalyzed Direct C3-Cyanation of Indoles Using Acetonitrile as the Cyanide Source. *Org. Biomol. Chem.* **2020**, *18*, 6108–6114. (c) Urbina, K.; Tresp, D.; Sipps, K.; Szostak, M.; Recent Advances in Metal-Catalyzed Functionalization of Indoles. *Adv. Synth. Catal.* **2021**, *363*, 2723–2739.
 15. Lu, H.; Yu, T. Y.; Xu, P. F.; Wei, H. Selective Decarbonylation via Transition-Metal-Catalyzed Carbon Carbon Bond Cleavage. *Chem. Rev.* **2020**, *121*, 365–411.
 16. (a) Hanessian, S. Total Synthesis of Natural Products: The Chiron Approach; Pergamon: Oxford, **1983**. (b) Palomo, C.; Oiarbide, M.; García, J. M. α -Hydroxy ketones as useful templates in asymmetric reactions. *Chem. Soc. Rev.* **2012**, *41*, 4150–4164. (c) De Luca, L.; Mezzetti, A. Base-Free Asymmetric Transfer Hydrogenation of 1,2-Di- and Monoketones Catalyzed by a (NH)₂P₂-Macrocyclic Iron(II) Hydride. *Angew. Chem., Int. Ed.* **2017**, *56*, 11949–11953.
 17. Banjare, S. K.; Biswal, P.; Ravikumar, P. C. Cobalt-Catalyzed One-Step Access to Pyroquilon and C-7 Alkenylation of Indoline with Activated Alkenes Using Weakly Coordinating Functional Groups. *J. Org. Chem.* **2020**, *85*, 5330–5341.
 18. (a) Zhao, D.; Kim, J. H.; Stegemann, L.; Strassert, C. A.; Glorius, F. Cobalt(III)-Catalyzed Directed C–H Coupling with Diazo Compounds: Straightforward Access towards Extended π -Systems. *Angew. Chem., Int. Ed.* **2015**, *54*, 4508–4511. (b) Guo, X.-K.; Zhang, L.-B.; Wei, D.; Niu, J.-L. Mechanistic Insights into Cobalt(II/III)-Catalyzed C–H Oxidation: A Combined Theoretical and Experimental Study. *Chem. Sci.* **2015**, *6*, 7059–7071. (c) Banjare, S. K.; Chebolu, R.; Ravikumar, P. C. Cobalt Catalyzed Hydroarylation of Michael Acceptors with Indolines Directed by a Weakly Coordinating Functional Group. *Org. Lett.* **2019**, *21*, 4049–4053. (d) Martínez de Salinas, S.; Sanjose-Orduna, J.; Odena, C.; Barranco, S.; Benet-Buchholz, J.; Perez-Temprano, M. H. Weakly Coordinated Cobaltacycles: Trapping Catalytically Competent Intermediates in Cp*CoIII Catalysis. *Angew. Chem., Int. Ed.* **2020**, *59*, 6239–6243.
 19. Krygowski, T. M.; Szatyłowicz, H.; Stasyuk, O. A.; Dominikowska, J.; Palusiak, M. Aromaticity from the Viewpoint of Molecular Geometry: Application to Planar Systems. *Chem. Rev.* **2014**, *114*, 6383–6422.
 20. Lakowicz, J. R. Principles of Fluorescence Spectroscopy; Plenum Press: New York, **1983**.
 21. Maroncelli, M.; Fleming, G. R. J. Picosecond solvation dynamics of coumarin 153: The importance of molecular aspects of solvation. *Chem. Phys.* **1987**, *86*, 6221.
 22. S. K. Banjare, P. Biswal, P. C. Ravikumar, Cobalt-Catalyzed One-Step Access to Pyroquilon and C-7 Alkenylation of Indoline with Activated Alkenes Using Weakly Coordinating Functional Groups. *J. Org. Chem.* **2020**, *85*, 5330–5341.
-

-
23. H. E. Gottlieb, V. Kotlyar, A. Nudelman, NMR Chemical Shifts of Common Laboratory Solvents as Trace Impurities. *J. Org. Chem.* **1997**, *62*, 7512 – 7515.

Chapter 7(A)

Unveiling the Reactivity of Cobalt(III)-catalyst Towards Regioselective Hydroarylation of 1,6 Diyne via Weak- chelation Assisted C-H Bond Activation

7a.1 Abstract

7a.2 Introduction

7a.3 Results and Discussions

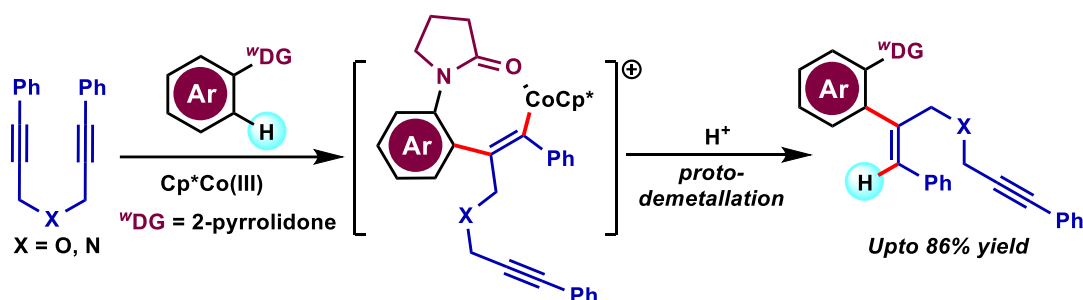
7a.4 Conclusions

7a.5 Experimental Section

7a.6 References

Chapter 7(A)

Unveiling the Reactivity of Cobalt(III)-catalyst Towards Regioselective Hydroarylation of 1,6 Diyne via Weak- chelation Assisted C-H Bond Activation



7a.1 ABSTRACT

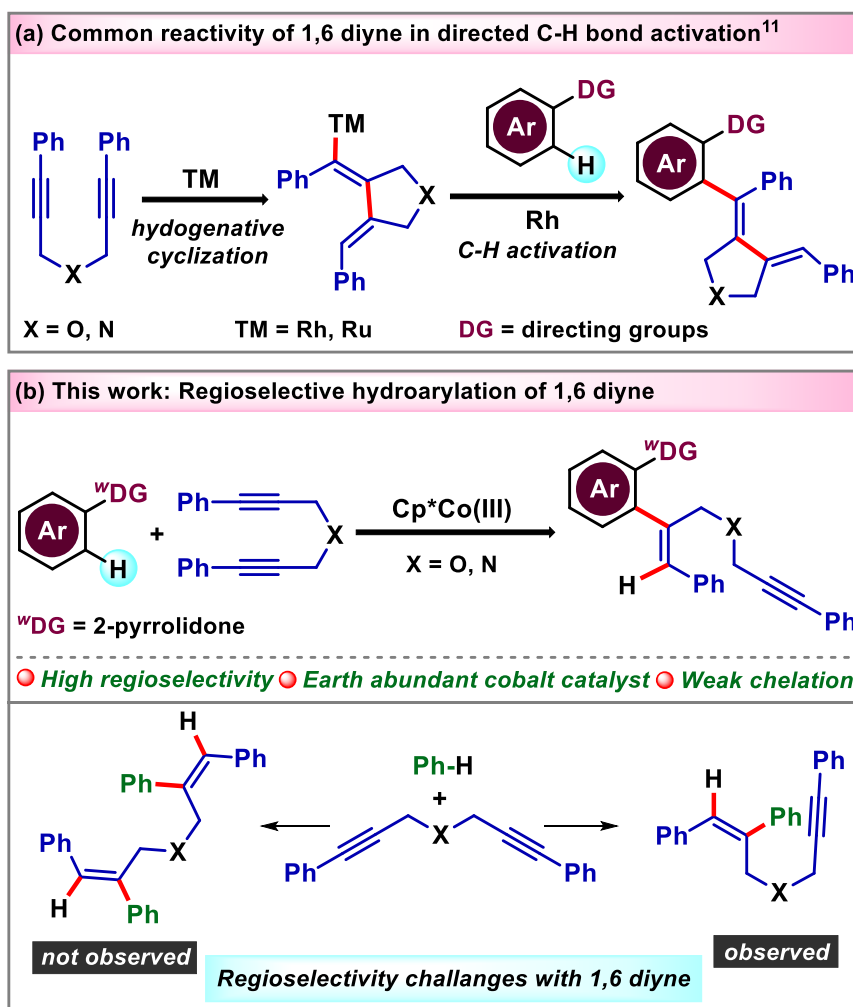
Herein, we report the reactivity of cobalt(III)-catalyst towards hydro-arylation functionalization of 1,6 diyne, which was never explored before. The N-aryl lactam is the prime substrate that undergoes sp^2 C-H bond activation. C-Co(III) bond formation occurs through weakly coordinating the pyrrolidinone group. The reaction mechanism reveals the in-situ formation of a six-membered cobaltacycle which undergoes further functionalization with 1,6 diyne. Also, radical quenching experiments suggest the involvement of the ionic pathway for this conversion. In addition, hydrogen scrambling and kinetic isotope experiments support the proposed mechanism. A wide range of electronically biased substrates and reacting partners work well with this method in a highly atom-economical fashion.

7a.2 INTRODUCTION

γ -Lactam is a useful scaffold, abundantly present in many drugs and natural products. The lactam ring-containing motifs are key substrates in organic synthesis.¹ Particularly *N*-aryl lactams are used as a starting material for the synthesis of many alkaloids and useful heterocycles.² *N*-aryl lactams are a unique class of compounds with several biological activities such as antimicrobial, anticancer, antidiabetic, etc.³ Therefore, further functionalization of *N*-aryl lactams is highly desirable from a medicinal chemistry point of view. Transition metal-catalyzed C-H bond functionalization is at the forefront of organic synthesis in recent years. It has provided an opportunity for selective C-H functionalization in the presence of several C-H bonds.⁴ In this vein, we have developed many methodologies until now, wherein several heterocyclic C-H bonds have been functionalized using weakly coordinating directing groups.⁵ The use of weakly coordinating directing groups such as aldehyde, ketone, and ester provides a powerful and step-economical platform in C-H activation methods on account of their wide prevalence and easy manipulation for further functionalization. Moreover, the use of base metals, such as cobalt, in conjunction with a weakly coordinating group is a significant step forward towards sustainable C-H activation, recently, we have covered a highlight article on this topic.⁶ The olefin-based coupling partners are quite reactive toward metal-carbon bonds generated through C-H activation.⁷ Therefore, a variety of π -systems such as acrylate, styrene, allene, and alkyne have been used as reacting partners, giving rise to many useful and unusual transformations.⁸ Among them, alkynes are prominent coupling partners widely explored in C-H activation reactions.⁹ However, there is no report to date for the concomitant C-H activation and regioselectively hydroarylation of 1,6 diyne using base metal along with weakly coordinating directing

group.¹⁰ In this regard, 1,6 diyne is a challenging and underdeveloped coupling partner compared to simple alkyne and other olefins.

Figure 7a.1. Overview and Challenges of C-Metal Bond towards Reactivity of 1,6 diyne.



Notably, controlling the regioselectivity (1,2 or 2,1 mono or di-functionalization) of 1,6 diyne is quite difficult and unexplored, making it a challenging and prominent coupling partner. The transition metal-catalyzed reductive cyclization and concomitant C-H bond activation have been well documented in the literature for 1,6 diyne (Figure 7a.1a).¹¹ Herein, we report a highly regioselective hydro-arylation of 1,6 diyne using base metal

cobalt(III)-catalyst, which is a completely different reactivity that was never reported before with 1,6 diynes (Figure 7a.1b). This protocol is more sustainable as well as atom economic due to the use of earth-abundant, cheap and eco-friendly 3d transition metal catalyst cobalt.¹² This methodology has several interesting features, such as (i) the unique reactivity of 3d metal cobalt catalyst with 1,6 diyne (ii) the first report on the hydro-arylation coupling of 1,6 diyne with arene instead of reductive cyclization, (iii) regioselective mono-hydroarylation of 1,6 diyne (iv) regioselective *ortho*-C-H bond functionalization of *N*-aryl γ -Lactam, (v) weakly coordinating 2-pyrrolidone as the directing group and (vi) utilization of several electronically diverse substrates with 1,6 diyne in a 100% atom economical manner.

7a.3 RESULTS AND DISCUSSION

To test the feasibility of this developed method, we have screened several parameters from standard reaction conditions (Scheme 7a.1). After extensive investigation of different reaction parameters, a composition containing 1-phenylpyrrolidin-2-one **1a** (1 equiv), (oxybis(prop-1-yne-3,1-diyl))dibenzene **2a** (2 equiv), Cp^{*}Co(CO)I₂ catalyst (10 mol %), AgSbF₆ (20 mol %), Cu(OAc)₂ (1.5 equiv) as an additive and 1,2-dichlorobenzene solvent (0.1M) at 80 °C facilitated the desired product **3aa** in 78% isolated yield (Scheme 7a.1, entry 1). We performed several deviation experiments from the standard condition. First, we tested a variety of solvents, such as methanol, benzene, tetrahydrofuran, dichloromethane, and acetonitrile, all of which failed to produce product **3aa** (Table 7a.1, entry 2). However, the chlorobenzene worked well, giving a 61% yield (Table 7a.1, entry 3). While screening the aryl-based mixture of chlorinated solvents, we observed that the 1:1 ratio of chlorobenzene and 1,2-dichlorobenzene gave **3aa** in 53% yield (Table 7a.1, entry 4). A detrimental effect on the product yield has

been observed while screening different silver salts such as AgBF₄ and AgNTf₂ (Table 7a.1, entries 5,6).

Table 7a.1. Optimization Studies Hydroarylation of 1,6-diyne^{a,b,c}

1a (1 equiv)	2a (2 equiv)	3aa
entry	deviation from the standard conditions	yield of 3aa (%) ^b
1	none	78
2 ^c	other solvents instead of 1,2-DCB	0
3	chlorobenzene as a solvent instead of 1,2-DCB	61
4	mixture solvents chlorobenzene:1,2-DCB (1:1)	53
5	AgBF ₄ instead of AgSbF ₆ as an additive	32
6	AgNTf ₂ instead of AgSbF ₆ as an additive	26
7	1 equiv instead of 1.5 equiv of Cu(OAc) ₂	57
8	2 equiv instead of 1.5 equiv of Cu(OAc) ₂	70
9	Cu ₂ O instead of Cu(OAc) ₂ as a additive	21
10	NaOAc instead of Cu(OAc) ₂ as a additive	42
11	Co(acac) ₂ instead of Cp*Co(CO)I ₂ as a catalyst	0
12	Co ₂ (CO) ₈ instead of Cp*Co(CO)I ₂ as a catalyst	0
13	1 equiv instead of 2 equiv of 2a	47
14	3 equiv instead of 2 equiv of 2a	56
15	temperature 70 °C instead of 80 °C	51
16	temperature 90 °C instead of 80 °C	66
17	0.2 M (1,2-DCB) instead of 0.1M	59
18	0.05 M (1,2-DCB) instead of 0.1M	44
19	without Cu(OAc) ₂ as a additive	22
20	without Cp*Co(CO)I ₂ as a catalyst	0

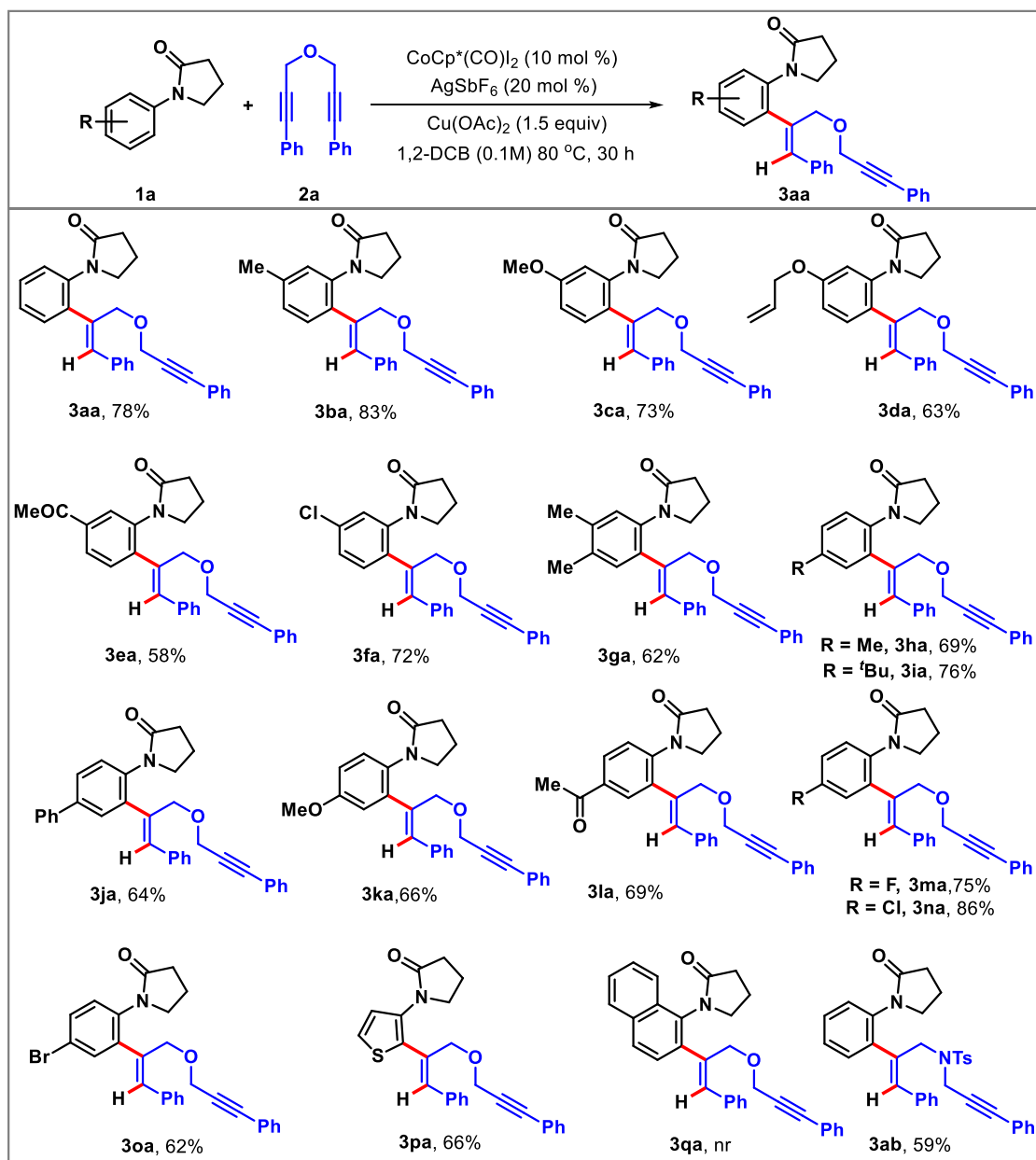
^aReaction conditions: **1a** (0.1 mmol), **2a** (0.2 mmol), Cp*Co(CO)I₂ (10 mol %), Ag salt (20 mol %), additive (1.5 equiv), solvents (1 mL), 80 °C, N₂, ^bIsolated yield, ^cmethanol, benzene, tetrahydrofuran, 1,4-dioxane, dichloromethane, acetonitrile.

Further, the amount of copper acetate has been screened from 1.5 equivalents to 1 and 2 equivalents, but the yield did not increase (Table 7a.1, entries 7,8). To check the feasibility of other metal salts, Cu₂O was tested instead of Cu(OAc)₂, and NaOAc was tested instead of Cu(OAc)₂. In both cases, **3aa** was obtained in a lower yield, which suggests that copper acetate is the most favorable additive for this conversion (Table 7a.1, entries 9, 10). To know the importance of Co(III)-catalyst, other cobalt-based catalysts have been tested, such as Co(acac)₂ and Co₂(CO)₈, but both failed to produce the desired product **3aa** (Table 7a.1, entries 11,12). Next, the equivalent of coupling partner **2a** has also been screened from 2 to 1 and 3 equivalents. However, no enhancement in yield was observed (Table 7a.1, entries 13,14). Further, physical deviations like temperature and concentration of solvents have varied from standard reaction conditions (Table 7a.1, entries 15-18). From these results, we concluded that a temperature of 80 °C and solvent concentration of 0.1M is optimal for this transformation. Control experiments revealed that copper acetate and cobalt(II)-catalyst is crucial for this methodology (Table 7a.1, entries 19,20).

Next, we scrutinized the general applicability of the optimized condition by varying different substrates (Scheme 7a.1). The transformation was very general and worked well with a broad range of substrates. It was observed that meta-substitution using electron-rich substituents such as methyl, methoxy, and allyloxy resulted in good yields **3ba-3da**. Out of these, the allyloxy substrate is of high significance as it can easily undergo further intramolecular cyclization to form a pyran derivative, but it preferentially gave the hydroarylated product. Acetyl group substituted **3ea** gave moderate results, whereas chloro-substitution **3fa** yielded a good yield. 3,4-dimethylphenyl pyrrolidinone **3ga** was also compatible and resulted in a good yield.

Next, we examined the effect of different substituents at the *para*-position of the phenyl ring. Electron-rich substituents offered good yields **3ha-3ka**, while electron-withdrawing ones gave good results **3la-3oa**. The success of both electronically rich and deficient substrates suggests electronics' minimal role in this transformation.

Scheme 7a. 1. Scope of Various Substituted 1-phenylpyrrolidin-2-one and 1,6 diyne.

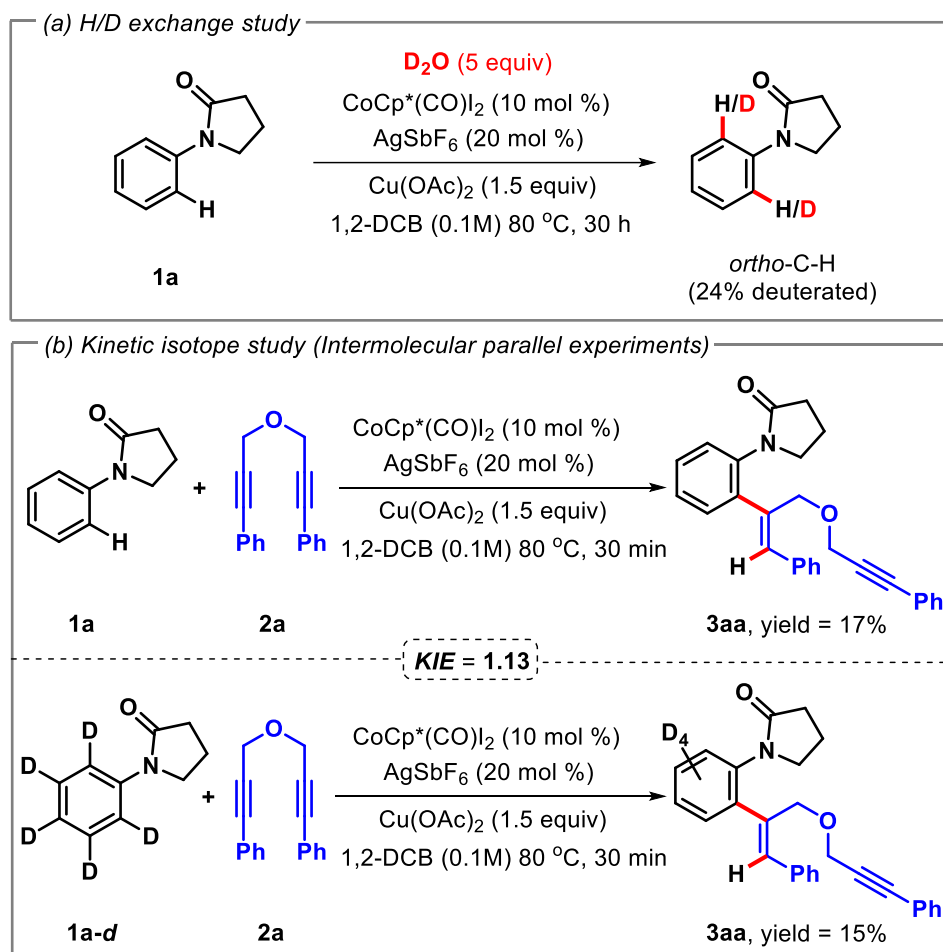


^aReaction conditions: **1a** (0.1 mmol), **2a** (0.2 mmol), $[\text{Cp}^*\text{Co}(\text{CO})\text{I}_2]$ (10 mol %), Ag salt (20 mol %), additive (1.5 equiv), solvents (1 mL), 80 °C, N_2 , ^bIsolated yield, ^cmethanol, benzene, tetrahydrofuran, 1,4-dioxane, dichloromethane, acetonitrile.

Notably, some synthetically valuable functionalities such as chloro, bromo, and carbonyl-based functional groups were amenable to the condition, which can be easily converted to other functionalities. Considering the synthetic significance of thiophene derivatives, we tried our condition on a thiophene-based substrate, which delightfully resulted in a good yield of product **3pa**. Unfortunately, *ortho*-substituted substrates could not withstand the condition, reflecting the operation of the steric factor. For the same reason, the naphthyl-based substrate **3qa** also resulted in no reaction as the *ortho*-position is blocked by the second benzene ring, resulting in steric hindrance towards the carbonyl group. Furthermore, apart from the oxygen-based 1,6 diyne, we also tried an *N*-protected 1,6 diyne as a coupling partner, which furnished the corresponding product **3ab** in good yield.

To understand the reaction mechanism and catalytic potential of the catalyst, several mechanistic and control studies have been carried out (Scheme 7a.2). Initially, the deuterium exchange experiment was performed with 1-phenylpyrrolidin-2-one **1a** using deuterium oxide as a deuterium source under standard conditions (Scheme 7a.2a). This resulted in 24% deuteration at the *ortho*-position of 1-phenylpyrrolidin-2-one **1a**, which suggests the reversibility of C-H bond activation step. To check the rate-determining step in the reaction, intermolecular parallel kinetic isotope experiments were performed using **1a** and **1a-d**, where the value of KIE was observed to be 1.13 (Scheme 7a.2b).

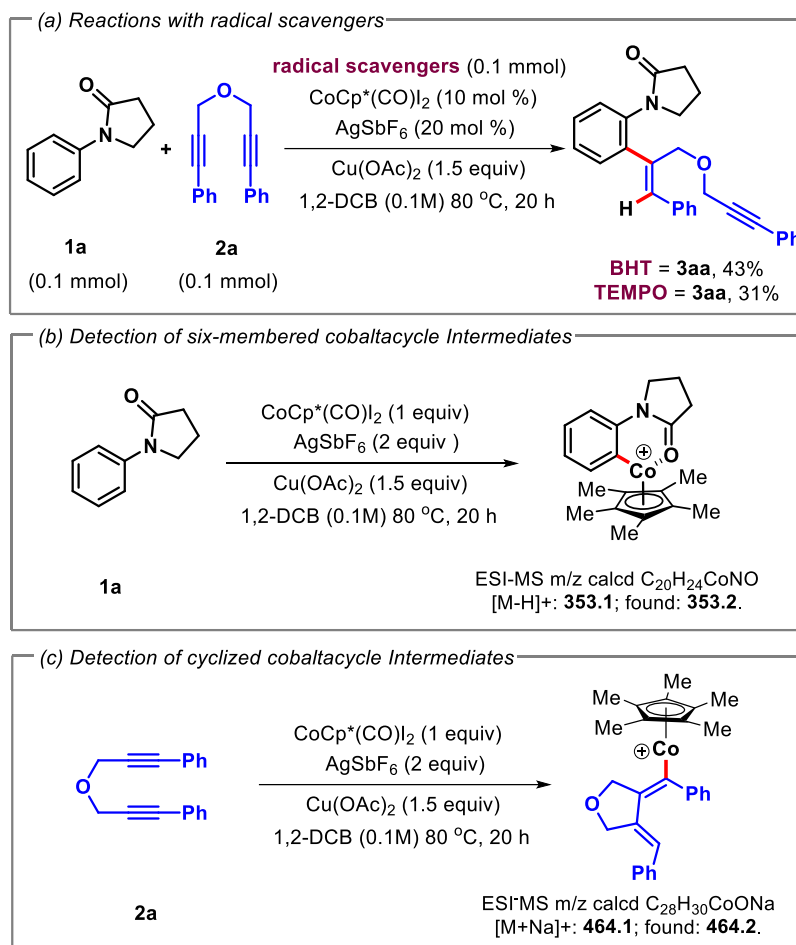
Scheme 2. Mechanistic Experiments.



These experiments suggest that the C-H bond activation step is not the rate-determining step. Further, to know the pathway of the reaction mechanism, the radical scavengers 2,2,6,6-tetramethylpiperidinyloxy (TEMPO) and butylated hydroxytoluene (BHT) have been subjected to the standard reaction, which resulted in a synthetically useful amount of the desired product **3aa** (Scheme 7a.3a). This indicates the non-involvement of a radical pathway for this conversion. Notably, the six-membered cobaltacycle intermediate (Scheme 7a.3b) has been detected through ESI-MS (Electrospray ionization mass spectrometry), indicating the C-metalation after C-H bond activation. Also, the coupling partner-derived intermediate has been detected in ESI-MS

(Electrospray ionization mass spectrometry), which suggests that there is a possibility that cobalt first coordinates through π -bond complexation followed by cyclization of 1,6 diyne (Scheme 7a.3c). However, it seems the reaction predominantly proceeds through C-H bond activation followed by an alkyne insertion pathway.

Scheme 7a.3. Detection of Intermediates through LCMS.

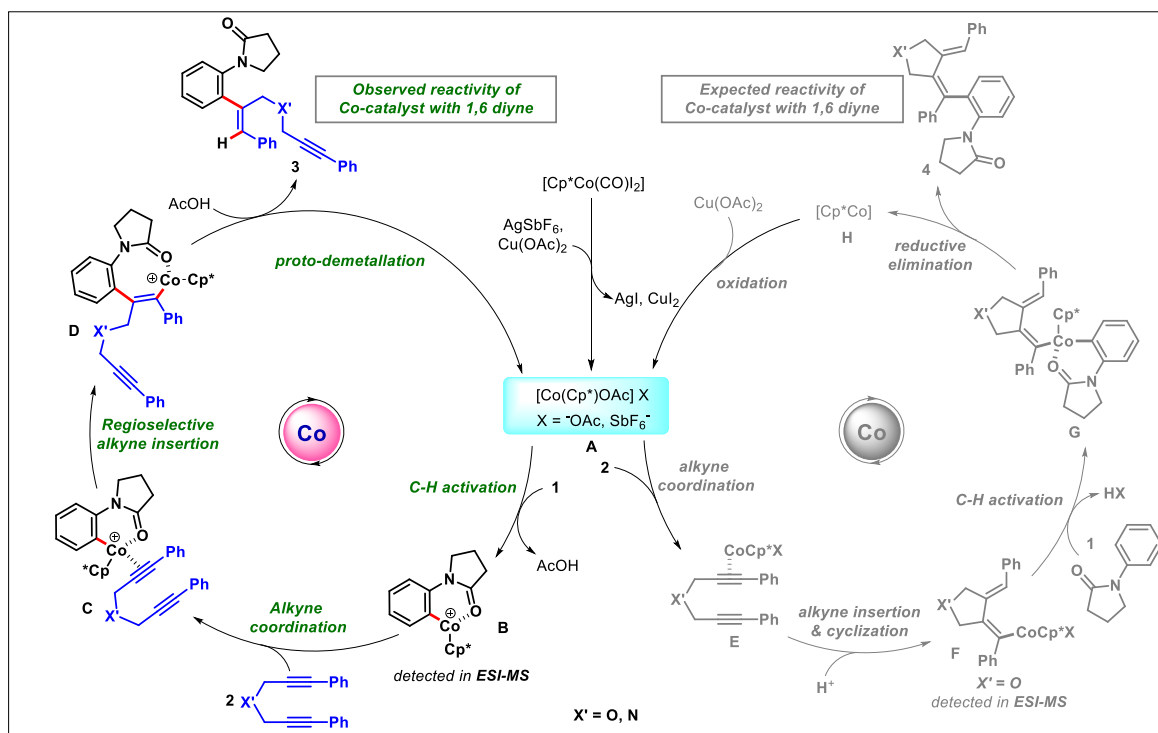


Based on these mechanistic studies, control experiments, and literature precedence,¹³ the plausible catalytic cycle has been depicted in Scheme 7a.4. Initially, the active cobalt catalyst **A** is generated in the presence of AgSbF₆ and Cu(OAc)₂, which drives both the proposed pathways. The active catalyst **A** coordinates with 1-phenylpyrrolidin-2-one **1** through weak coordination. After C-H activation, the six-membered cobaltacycle intermediate **B** is generated and detected through ESI-MS (Electrospray

ionization mass spectrometry). Further, alkyne **2** coordination gives intermediate **C**, which leads to the generation of intermediate **D** through alkyne insertion in a highly selective manner. Then, proto-demetallation gives the desired product **3**, along with the generation of active catalyst **A** for the next catalytic cycle.

Surprisingly, we did not observe the expected dehydrogenative cyclized product, even though 1,6 diyne is well-known for giving the cyclized product through a reductive elimination pathway. For this, the active catalyst **A** initially coordinates with coupling partner **2** to provide the intermediate **E**. Then, alkyne insertion, followed by reductive cyclization, leads to the generation of intermediate **F**, which has been detected through ESI-MS (Electrospray ionization mass spectrometry). Next, the cobalt catalyst from intermediate **F** coordinates with the 1-phenylpyrrolidin-2-one **1** and gives intermediate **G** through C-H bond activation.

Scheme 7a.4. Plausible Catalytic Pathway for Cobalt Catalyzed Hydro-arylativ Functionalization of 1,6 diyne.



Finally, reductive elimination could provide the final product **7a.4** along with the generation of reduced cobaltcatalyst **H**. Further active catalyst **A** could be re-generated via the oxidation of cobalt(0) in the presence of copper. Even though copper acetate has been used for this conversion, it acts as an additive rather than an oxidant.

7a.3 CONCLUSION

In conclusion, we have achieved highly regioselective hydroarylation of 1,6 diyne using first-row transition metal cobalt via weak coordination, which is sustainable and an active branch of research in catalysis. The regioselective C-H metalation and highly atom economic transformation is the key aspect of this methodology. The detection of six-membered cobaltcycle intermediate through ESI-MS (Electrospray ionization mass spectrometry) and cobalt-tetrahydrofuran intermediate supports the proposed catalytical cycle. The kinetic isotope experiments suggest that C-H bond activation is not involved in the rate-determining step. Also, the radical scavenger experiments rule out the possibility of having radical pathways in the mechanism. This method provides easy access to various sterically and electronically biased products in good yields.

Limitations: *Ortho*-substituted *N*-aryl γ -lactam is incompatible with optimized reaction conditions, most likely due to steric hindrance of the *ortho*-substituents.

7a.5 EXPERIMENTAL SECTION¹⁵

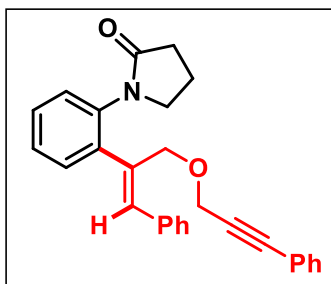
Reactions were performed using borosil Schlenk tube vial under an N₂ atmosphere. Column chromatography was done by using 100-200 & 230-400 mesh size silica gel of Acme Chemicals. Gradient elution was performed by using distilled petroleum ether and ethyl acetate. TLC plates were detected under UV light at 254 nm. ¹H NMR and ¹³C NMR were recorded on Bruker AV 400, 700 MHz spectrometers using CDCl₃ as

NMR solvents. The residual CHCl_3 for ^1H NMR ($\delta = 7.26$ ppm) and the deuterated solvent signal for ^{13}C NMR ($\delta = 77.36$ ppm) is used as reference.¹⁶ Multiplicity (s = single, d = doublet, t = triplet, q = quartet, m = multiplet, dd = double doublet), integration, and coupling constants (J) in hertz (Hz). HRMS signal analysis was performed using a micro TOF Q-II mass spectrometer. X-ray analysis was conducted using a Rigaku Smartlab X-ray diffractometer at SCS, NISER. Reagents and starting materials were purchased from Sigma Aldrich, Alfa Aesar, TCI, Avra, Spectrochem, Carbanio, and other commercially available sources and used without further purification unless otherwise noted.

(a) General reaction procedure for hydro-arylativ C-H bond functionalization:

To a pre-dried sealed tube under N_2 , the mixture of 1-phenylpyrrolidin-2-one **1** (0.1 mmol), (oxybis(prop-1-yne-3,1-diyl))dibenzene **2** (0.2 mmol), $[\text{Cp}^*\text{Co}(\text{CO})\text{I}_2]$ (10 mol %), AgSbF_6 (20 mol %), $\text{Cu}(\text{OAc})_2$ (1.5 equivalent), and 1,2-dichlorobenzene (1 mL) were added and sealed inside the glove box. The reaction mixture was vigorously stirred at $80\text{ }^\circ\text{C}$ on the preheated aluminum block for 30 h. After 30 h (completion of the reaction as monitored by TLC analysis), the reaction mixture was cooled to room temperature and diluted with ethyl acetate/dichloromethane and passed through a short celite pad, the solvent was evaporated under reduced pressure, and the residue was purified by column chromatography using EtOAc/hexane mixture on silica gel to give the pure product **3**.

Experimental characterization data of products:

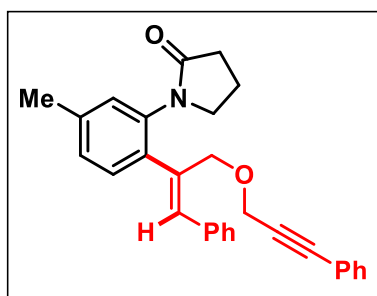


(Z)-1-(2-(1-phenyl-3-((3-phenylprop-2-yn-1-yl)oxy)prop-1-en-2-yl)phenyl)pyrrolidin-2-one (**3aa**):

was prepared according to the general procedure (7a.5a).

The crude reaction mixture was purified by column chromatography using silica gel (100-200 mesh size)

giving (32 mg, 0.1 mmol scale) 78% yield. **Physical State:** colourless liquid. **R_f-value:** 0.4 (30% EtOAc/hexane). **¹H NMR (CDCl₃, 400 MHz):** δ 7.50 – 7.44 (m, 3H), 7.38–7.33 (m, 6H), 7.32–7.22 (m, 5H), 6.77 (s, 1H), 4.51 (s, 2H), 4.36 (s, 2H), 3.78 (t, J = 7.2Hz, 2H), 2.48 (t, J = 8.0Hz, 2H), 2.12 – 2.05 (m, 2H). **¹³C NMR (CDCl₃, 100 MHz):** δ 175.7, 141.0, 136.9, 136.7, 135.4, 135.2, 132.0, 130.0, 129.3, 128.7, 128.5, 128.4, 128.0, 127.9, 122.9, 86.9, 85.3, 69.0, 59.1, 51.2, 31.7, 19.4. **IR (KBr, cm⁻¹):** 3461, 2984, 2313, 1734, 1244. **HRMS (ESI) m/z:** [M+Na]⁺ Calcd for C₂₈H₂₅NO₂Na 430.1778; Found 430.1746.



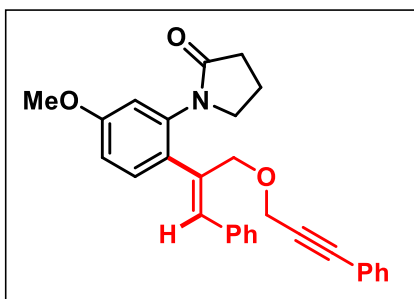
(Z)-1-(5-methyl-2-(1-phenyl-3-((3-phenylprop-2-yn-1-yl)oxy)prop-1-en-2-yl)phenyl)pyrrolidin-2-one (**3ba**):

was prepared according to the general procedure (7a.5a). The crude reaction mixture was

purified by column chromatography using silica gel

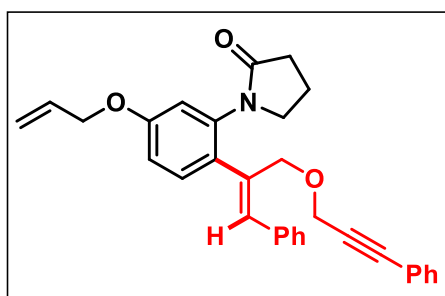
(100-200 mesh size) giving (35 mg, 0.1 mmol scale) 83% yield. **Physical State:** brown liquid **R_f-value:** 0.5 (30% EtOAc/hexane). **¹H NMR (CDCl₃, 700 MHz):** δ 7.44 (d, J = 7.0Hz, 2H), 7.38 – 7.36 (m, 3H), 7.33 – 7.28 (m, 6H), 7.13 (d, J = 7.7Hz, 1H), 7.08 (s, 1H), 6.75 (s, 1H), 4.50 (s, 2H), 4.35 (s, 2H), 3.76 (t, J = 7.0Hz, 2H), 2.47 (t, J = 8.4Hz, 2H), 2.36 (s, 3H) 2.10 – 2.06 (m, 2H). **¹³C NMR (CDCl₃, 176 MHz):** δ 175.79,

138.78, 138.05, 136.93, 136.81, 135.41, 135.02, 132.07, 129.80, 129.34, 129.11, 128.97, 128.76, 128.73, 128.60, 127.84, 122.99, 86.8, 85.44, 69.18, 59.19, 51.36, 31.80, 21.36, 19.49. **IR** (KBr, cm^{-1}): 3446, 1700, 1071, 697. **HRMS (ESI) m/z**: $[\text{M}+\text{Na}]^+$ Calcd for $\text{C}_{29}\text{H}_{27}\text{NO}_2\text{Na}$ 444.1934; Found 444.1938.



(Z)-1-(5-methoxy-2-(1-phenyl-3-((3-phenylprop-2-yn-1-yl)oxy)prop-1-en-2-yl)phenyl)pyrrolidin-2-one (3ca): was prepared according to the general procedure (7a.5a). The crude reaction mixture was purified by column

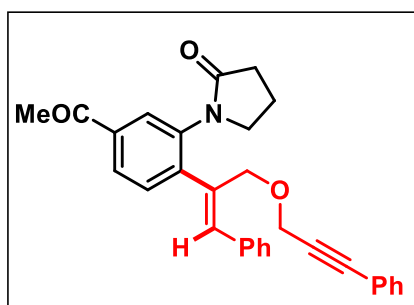
chromatography using silica gel (100-200 mesh size) giving (32 mg, 0.1 mmol scale) 73% yield. **Physical State**: colourless liquid **R_f-value**: 0.5 (30% EtOAc/hexane). **¹H NMR (DMSO-*d*₆, 400 MHz)**: δ 7.47-7.42 (m, 10H), 7.31 (t, $J = 7.2$ Hz, 1H), 6.93 (d, $J = 8.4$ Hz, 1H), 6.89 (d, $J = 2.0$ Hz, 1H), 6.65 (s, 1H), 4.44 (s, 2H), 4.41 (s, 2H), 3.81 (s, 3H), 3.75 (t, $J = 6.8$ Hz, 2H), 2.35 (t, $J = 8.0$ Hz, 2H), 2.05 (q, $J = 7.2$ Hz, 2H). **¹³C NMR (DMSO-*d*₆, 100 MHz)**: δ 174.8, 159.7, 138.8, 138.3, 137.2, 136.5, 136.1, 133.9, 133.5, 132.3, 131.1, 129.7, 129.6, 129.5, 129.3, 128.3, 127.3, 122.7, 113.9, 113.9, 86.9, 86.7, 68.9, 58.8, 56.3, 51.1, 40.4, 31.7, 19.6. **IR** (KBr, cm^{-1}): 3445, 1702, 1073, 689. **HRMS (ESI) m/z**: $[\text{M}+\text{Na}]^+$ Calcd for $\text{C}_{29}\text{H}_{27}\text{NO}_3\text{Na}$ 460.1883; Found 460.1903.



(Z)-1-(5-(allyloxy)-2-(1-phenyl-3-((3-phenylprop-2-yn-2-yl)oxy)prop-1-en-1-yl)phenyl)pyrrolidin-2-one (3da): was prepared according to the general procedure (7a.5a). The crude reaction mixture was

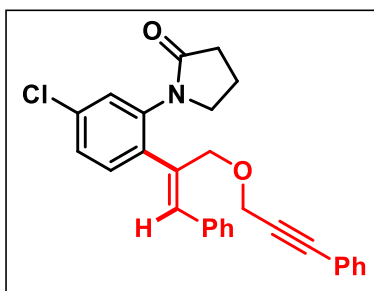
purified by column chromatography using silica gel (100-200 mesh size) giving (29 mg,

0.1 mmol scale) 63% yield. **Physical State:** brown liquid **R_f-value:** 0.35 (20% EtOAc/hexane). **¹H NMR (CDCl₃, 400 MHz):** δ 7.43 (d, J = 8.0Hz, 2H), 7.38 (t, J = 9.6Hz, 3H), 7.34– 7.29 (m, 6H), 6.88 (d, J = 8.4Hz, 1H), 6.82 (d, J = 2.4Hz, 1H), 6.73 (s, 1H), 6.08 – 6.01 (m, 1H), 5.42 (d, J = 17.2Hz, 1H), 5.29 (d, J = 10.4Hz, 1H), 4.53 (d, J = 5.2Hz, 2H), 4.48 (s, 2H), 4.36 (s, 2H), 3.77 (t, J = 7.2Hz, 2H), 2.47 (t, J = 8.4Hz, 2H), 2.12 – 2.04 (m, 2H). **¹³C NMR (CDCl₃, 100 MHz):** δ 175.6, 166.3, 158.7, 137.9, 136.9, 135.1, 134.9, 133.4, 133.3, 132.0, 130.8, 129.3, 128.7, 128.6, 127.8, 122.9, 118.1, 114.7, 114.4, 86.8, 85.4, 69.3, 69.2, 59.1, 51.2, 31.7, 19.4. **IR (KBr, cm⁻¹):** 3447, 1071, 1696, 699. **HRMS (ESI) m/z:** [M+Na]⁺ Calcd for C₃₁H₂₉NO₃Na 486.2136; Found 486.2136.



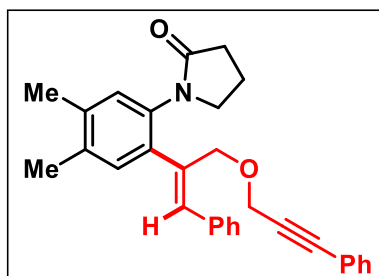
(Z)-1-(5-acetyl-2-(1-phenyl-3-((3-phenylprop-2-yn-1-yl)oxy)prop-1-en-2-yl)phenyl)pyrrolidin-2-one (3ea): was prepared according to the general procedure (7a.5a). The crude reaction mixture was purified by column

chromatography using silica gel (100-200 mesh size) giving (26 mg, 0.1 mmol scale) 58% yield. **Physical State:** yellow liquid **R_f-value:** 0.4 (30% EtOAc/hexane). **¹H NMR (DMSO-*d*₆, 400 MHz):** δ 7.91 (d, J = 8.4Hz, 1H), 7.86 (s, 1H), 7.66 (d, J = 8.0Hz, 1H), 7.44 (d, J = 7.6Hz, 2H), 7.41 – 7.32 (m, 8H), 6.73 (s, 1H), 4.48 (s, 2H), 4.38 (s, 2H), 3.76 (t, J = 6.8Hz, 2H), 2.59 (s, 3H), 2.36 (t, J = 8.0Hz, 2H), 2.10 – 2.03 (m, 2H). **¹³C NMR (CDCl₃, 176 MHz):** δ 175.9, 138.2, 137.3, 136.9, 136.7, 135.4, 134.9, 134.4, 132.0, 130.9, 129.4, 129.3, 128.7, 128.7, 128.5, 127.8, 123.0, 86.8, 85.4, 69.1, 59.1, 51.4, 31.7, 19.8, 19.4. **IR (KBr, cm⁻¹):** 3469, 2255, 1700, 1650, 1275, 1024 **HRMS (ESI) m/z:** [M+Na]⁺ Calcd for C₃₀H₂₇NO₃Na 472.1883; Found 472.1906.



(Z)-1-(5-chloro-2-(1-phenyl-3-((3-phenylprop-2-yn-1-yl)oxy)prop-1-en-2-yl)phenyl)pyrrolidin-2-one (3fa): was prepared according to the general procedure (7a.5a). The crude reaction mixture was purified by column chromatography using silica gel

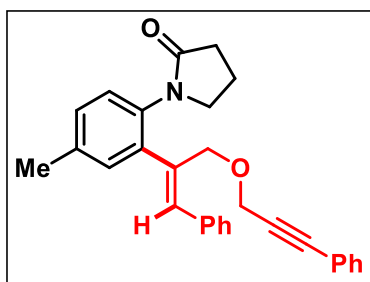
(100-200 mesh size) giving (32 mg, 0.1 mmol scale) 72% yield. **Physical State:** solid brown **m.p.:** 184–186 °C **R_f-value:** 0.45 (30% EtOAc/hexane). **¹H NMR (CDCl₃, 400 MHz):** δ 7.44-7.42 (m, 3H), 7.37–7.28 (m, 10H), 6.75 (s, 1H), 4.48 (s, 2H), 4.35 (s, 2H), 3.77 (t, *J* = 7.2Hz, 2H), 2.47 (t, *J* = 8.0Hz, 2H), 2.13 – 2.06 (m, 2H). **¹³C NMR (CDCl₃, 176 MHz):** δ 175.6, 139.5, 138.1, 136.5, 135.5, 134.6, 133.8, 132.0, 131.1, 129.3, 128.8, 128.8, 128.6, 128.2, 128.1, 122.8, 87.0, 85.2, 68.9, 59.2, 51.1, 31.6, 19.5. **IR (KBr, cm⁻¹):** 3447, 1714, 1070, 700. **HRMS (ESI) m/z:** [M+Na]⁺ Calcd for C₂₈H₂₄ClNO₂Na 464.1388; Found 464.1351.



(Z)-1-(4,5-dimethyl-2-(1-phenyl-3-((3-phenylprop-2-yn-1-yl)oxy)prop-1-en-2-yl)phenyl)pyrrolidin-2-one (3ga): was prepared according to the general procedure (7a.5a). The crude reaction mixture was purified by column

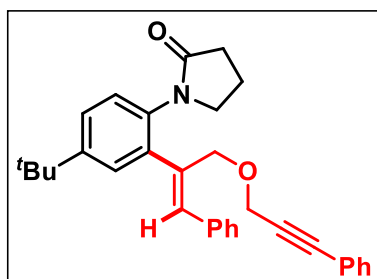
chromatography using silica gel (100-200 mesh size) giving (27 mg, 0.1 mmol scale) 62% yield. **Physical State:** colourless liquid **R_f-value:** 0.5 (40% EtOAc/hexane). **¹H NMR (CDCl₃, 400 MHz):** δ 7.44 (d, *J* = 7.6Hz, 2H), 7.36 (d, *J* = 7.2Hz, 2H), 7.33-7.29 (m, 4H), 7.24 (s, 3H), 7.03 (s, 1H), 6.75 (s, 1H), 4.49 (s, 2H), 4.36 (s, 2H), 3.74 (t, *J* = 7.2Hz, 2H), 2.47 (t, *J* = 8.4Hz, 2H), 2.25 (d, *J* = 4.8 Hz, 6H), 2.10 – 2.03 (m, 2H). **¹³C NMR (CDCl₃, 176 MHz):** δ 175.9, 138.2, 137.3, 136.9, 136.7, 135.4, 134.9, 134.4,

132.0, 130.9, 129.4, 129.3, 128.7, 128.7, 128.5, 127.8, 123.0, 86.8, 85.4, 69.1, 59.1, 51.4, 31.7, 19.8, 19.4. **IR** (KBr, cm^{-1}): 3420, 2843, 1684, 992, 767. **HRMS (ESI) m/z :** $[\text{M}+\text{Na}]^+$ Calcd for $\text{C}_{30}\text{H}_{29}\text{NO}_2\text{Na}$ 458.2091; Found 458.2108.



(Z)-1-(4-methyl-2-(1-phenyl-3-((3-phenylprop-2-yn-1-yl)oxy)prop-1-en-2-yl)phenyl)pyrrolidin-2-one (3ha): was prepared according to the general procedure (7a.5a). The crude reaction mixture was purified by column chromatography using silica gel

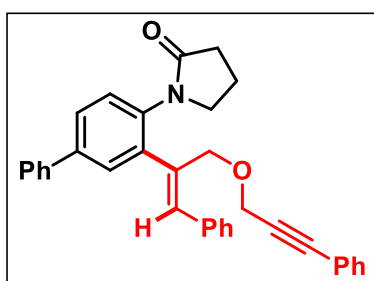
(100-200 mesh size) giving (29 mg, 0.1 mmol scale) 69% yield. **Physical State:** yellow liquid **R_f -value:** 0.4 (20% EtOAc/hexane). **^1H NMR (CDCl_3 , 400 MHz):** δ 7.45 (d, J = 7.6 Hz, 2H), 7.38 – 7.23 (m, 11H), 6.76 (s, 1H), 4.50 (s, 2H), 4.37 (s, 2H), 3.75 (t, J = 7.2 Hz, 2H), 2.47 (t, J = 8.2 Hz, 2H), 2.34 (s, 3H), 2.11 – 2.04 (m, 2H). **^{13}C NMR (CDCl_3 , 100 MHz):** δ 175.8, 140.7, 137.9, 136.8, 135.5, 135.1, 134.3, 132.0, 130.5, 129.5, 129.3, 128.7, 128.7, 128.5, 128.2, 127.8, 122.9, 86.9, 85.4, 69.0, 59.1, 51.3, 31.7, 21.4, 19.4. **IR** (KBr, cm^{-1}): 3447, 1696, 1180, 668. **HRMS (ESI) m/z :** $[\text{M}+\text{Na}]^+$ Calcd for $\text{C}_{29}\text{H}_{27}\text{NO}_2\text{Na}$ 444.1934; Found 444.1920.



(Z)-1-(4-(tert-butyl)-2-(1-phenyl-3-((3-phenylprop-2-yn-1-yl)oxy)prop-1-en-2-yl)phenyl)pyrrolidin-2-one (3ia): was prepared according to the general procedure (7a.5a). The crude reaction mixture was purified by column

chromatography using silica gel (100-200 mesh size) giving (35 mg, 0.1 mmol scale) 76% yield. **Physical State:** colourless liquid **R_f -value:** 0.5 (30% EtOAc/hexane). **^1H**

NMR (CDCl₃, 400 MHz): δ 7.48 (d, J = 8.8Hz, 3H), 7.38 – 7.33 (m, 5H), 7.31 – 7.27 (m, 4H), 7.18 (d, J = 8.4Hz, 1H), 6.78 (s, 1H), 4.51 (s, 2H), 4.37 (s, 2H), 3.76 (t, J = 7.2Hz, 2H), 2.48 (t, J = 8.0Hz, 2H), 2.12 – 2.04 (m, 2H), 1.32 (s, 9H). **¹³C NMR (CDCl₃, 100 MHz):** δ 175.83, 150.91, 140.40, 136.89, 135.86, 135.13, 134.20, 132.09, 129.37, 128.76, 128.74, 128.58, 127.89, 127.87, 126.94, 125.90, 122.97, 86.91, 85.39, 69.28, 59.17, 51.39, 35.01, 31.79, 31.66, 19.45. **IR (KBr, cm⁻¹):** 3447, 1653, 1071, 749. **HRMS (ESI) m/z:** [M+H]⁺ Calcd for C₃₂H₃₄NO₂ 464.2584; Found 464.2597.

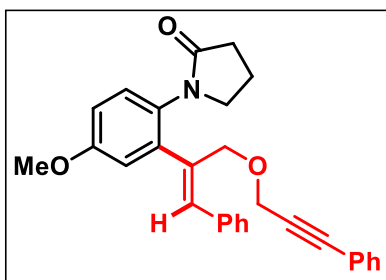


(Z)-1-(3-(1-phenyl-3-((3-phenylprop-2-yn-1-yl)oxy)prop-1-en-2-yl)-[1,1'-biphenyl]-4-yl)pyrrolidin-2-one (3ja): was prepared according to general procedure (7a.5a). The crude reaction mixture was purified by column chromatography

using silica gel (100-200 mesh size) giving (31 mg, 0.1 mmol scale) 64% yield.

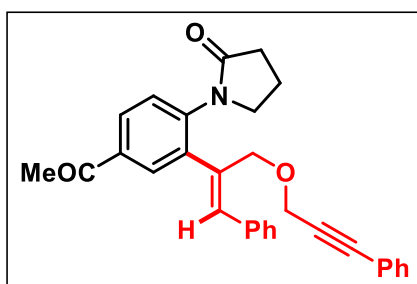
Physical State: solid brown **m.p.:** 193–195 °C **R_f-value:** 0.35 (30% EtOAc/hexane).

¹H NMR (CDCl₃, 400 MHz): δ 7.71 (s, 1H), 7.57 (t, J = 8.0Hz, 3H), 7.46 (d, J = 7.6Hz, 2H), 7.41 – 7.32 (m, 8H), 7.29 – 7.25 (m, 4H), 6.83 (s, 1H), 4.57 (s, 2H), 4.38 (s, 2H), 3.82 (t, J = 7.2Hz, 2H), 2.51 (t, J = 8.0Hz, 2H), 2.15 – 2.08 (m, 2H). **¹³C NMR (CDCl₃, 100 MHz):** δ 175.90, 141.20, 141.11, 140.79, 136.77, 136.17, 135.48, 135.37, 132.07, 129.37, 129.12, 128.87, 128.81, 128.79, 128.76, 128.60, 127.99, 127.82, 127.60, 127.49, 122.90, 87.02, 85.34, 77.36, 69.02, 59.19, 51.31, 31.78, 19.53. **IR (KBr, cm⁻¹):** 3447, 1675, 1183, 758. **HRMS (ESI) m/z:** [M+Na]⁺ Calcd for C₃₄H₂₉NO₂Na 506.2091; Found 506.2099.



(Z)-1-(4-methoxy-2-(1-phenyl-3-((3-phenylprop-2-yn-1-yl)oxy)prop-1-en-2-yl)phenyl)pyrrolidin-2-one (**3ka**): was prepared according to the general procedure (7a.5a). The crude reaction mixture was purified by column chromatography using silica

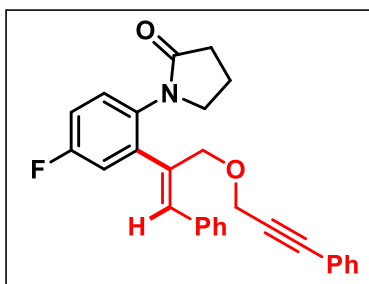
gel (100-200 mesh size) giving (29 mg, 0.1 mmol scale) 66% yield. **Physical State:** colourless liquid **R_f-value:** 0.4 (20% EtOAc/hexane). **¹H NMR (CDCl₃, 400 MHz):** δ 7.45 (d, *J* = 7.6Hz, 2H), 7.38 – 7.35 (m, 2H), 7.33 – 7.27 (m, 6H), 7.17 (d, *J* = 8.8Hz, 1H), 7.03 (d, *J* = 2.8Hz, 1H), 6.88 (d, *J* = 8.8Hz, 1H), 6.78 (s, 1H), 4.49 (s, 2H), 4.37 (s, 2H), 3.06 (s, 3H), 3.73 (t, *J* = 7.2Hz, 2H), 2.46 (t, *J* = 8.0Hz, 2H), 2.11 – 2.03 (m, 2H). **¹³C NMR (CDCl₃, 176 MHz):** δ 175.9, 159.0, 142.3, 136.7, 135.3, 135.2, 132.0, 129.7, 129.5, 129.3, 128.7, 128.7, 128.6, 127.9, 122.9, 115.2, 114.1, 86.9, 85.3, 69.0, 59.2, 55.8, 51.5, 31.6, 19.3. **IR (KBr, cm⁻¹):** 3447, 2347, 1751, 1240, 1046, 737. **HRMS (ESI) m/z:** [M+Na]⁺ Calcd for C₂₉H₂₇NO₃Na 460.1883; Found 460.1903.



(Z)-1-(4-acetyl-2-(1-phenyl-3-((3-phenylprop-2-yn-1-yl)oxy)prop-1-en-2-yl)phenyl)pyrrolidin-2-one (**3la**): was prepared according to the general procedure (7a.5a). The crude reaction mixture was purified by column

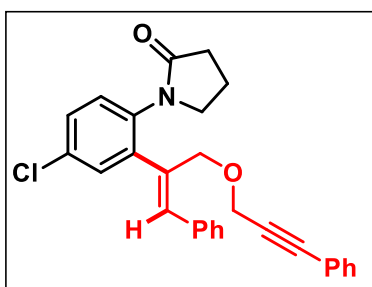
chromatography using silica gel (100-200 mesh size) giving (31 mg, 0.1 mmol scale) 69% yield. **Physical State:** yellow solid **m.p.:** 186–188 °C **R_f-value:** 0.3 (40% EtOAc/hexane). **¹H NMR (DMSO-*d*₆, 400 MHz):** δ 8.09 (d, *J* = 2.0Hz, 1H), 7.97 (d, *J* = 8.4Hz, 1H), 7.49 (t, *J* = 7.6Hz, 3H), 7.44–7.34 (m, 8H), 6.74 (s, 1H), 4.51 (s, 2H), 4.43 (s, 2H), 3.81 (t, *J* = 7.2Hz, 2H), 2.62 (s, 3H), 2.39 (t, *J* = 8.0Hz, 2H), 2.13 – 2.06

(m, 2H). **¹³C NMR (DMSO-*d*₆, 176 MHz):** δ 198.2, 175.0, 142.1, 141.1, 136.9, 136.2, 136.1, 134.7, 132.3, 130.4, 13.15, 129.8, 129.8, 129.6, 129.4, 128.8, 128.7, 128.6, 122.7, 119.3, 87.1, 86.7, 68.6, 58.9, 50.9, 31.8, 27.7, 19.8. **IR (KBr, cm⁻¹):** 3420, 2253, 1695, 1244, 1025, 763. **HRMS (ESI) m/z:** [M+Na]⁺ Calcd for C₃₀H₂₇NO₃Na 472.1883; Found 472.1866.



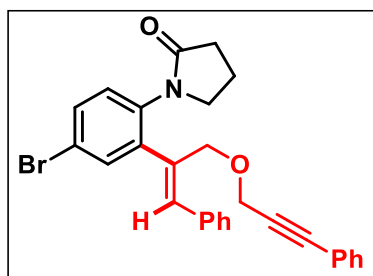
(Z)-1-(4-fluoro-2-(1-phenyl-3-((3-phenylprop-2-yn-1-yl)oxy)prop-1-en-2-yl)phenyl)pyrrolidin-2-one (3ma): was prepared according to the general procedure (7a.5a). The crude reaction mixture was purified by column chromatography using silica gel

(100-200 mesh size) giving (32 mg, 0.1 mmol scale) 75% yield. **Physical State:** colourless liquid **R_f-value:** 0.4 (30% EtOAc/hexane). **¹H NMR (CDCl₃, 400 MHz):** δ 7.43 (d, *J* = 7.2 Hz, 2H), 7.38 – 7.35 (m, 2H), 7.33 – 7.28 (m, 5H), 7.27 – 7.21 (m, 3H), 7.03 (t, *J* = 8.4Hz, 1H), 6.78 (s, 1H), 4.49 (s, 2H), 4.37 (s, 2H), 3.74 (t, *J* = 6.8Hz, 2H), 2.47 (t, *J* = 8.0Hz, 2H), 2.12 – 2.05 (m, 2H). **¹³C NMR (CDCl₃, 100 MHz):** δ 175.9, 163.1, 160.6, 143.1 (d, *J* = 34.2Hz), 136.4, 135.7, 134.4 (d, *J* = 4.4Hz), 132.9 (d, *J* = 12.0Hz), 132.0, 130.2 (d, *J* = 35.6Hz), 129.3, 128.8, 128.6, 128.1, 122.8, 116.7 (d, *J* = 90.0Hz), 115.7 (d, *J* = 88.8Hz), 87.1, 85.1, 68.8, 59.2, 51.3, 31.6, 19.4. **¹⁹F NMR (CDCl₃, 101 MHz):** δ -113.9 **IR (KBr, cm⁻¹):** 3447, 1684, 1071, 698. **HRMS (ESI) m/z:** [M+Na]⁺ Calcd for C₂₈H₂₄FNO₂Na 448.1683; Found 448.1655.



(Z)-1-(4-chloro-2-(1-phenyl-3-((3-phenylprop-2-yn-1-yl)oxy)prop-1-en-2-yl)phenyl)pyrrolidin-2-one (3na): was prepared according to the general procedure (7a.5a). The crude reaction mixture was purified by column chromatography using silica gel

(100-200 mesh size) giving (38 mg, 0.1 mmol scale) 86% yield. **Physical State:** colourless liquid **R_f-value:** 0.4 (40% EtOAc/hexane). **¹H NMR (CDCl₃, 400 MHz):** δ 7.49 (d, J = 2.0Hz, 1H), δ 7.43 (d, J = 7.6Hz, 3H), 7.38–7.27 (m, 8H), δ 7.20 (d, J = 8.4Hz, 1H), 6.76 (s, 1H), 4.48 (s, 2H), 4.37 (s, 2H), 3.75 (t, J = 7.2Hz, 2H), 2.47 (t, J = 8.0Hz, 2H), 2.12 – 2.05 (m, 2H). **¹³C NMR (CDCl₃, 100 MHz):** δ 175.7, 142.9, 136.3, 136.1, 135.9, 134.4, 132.9, 132.1, 131.75, 130.0, 129.3, 128.8, 128.6, 128.2, 122.8, 121.6, 87.1, 85.1, 77.3, 68.7, 59.2, 51.0, 31.6, 19.4. **IR (KBr, cm⁻¹):** 3446, 1700, 1070, 734. **HRMS (ESI) m/z:** [M+H]⁺ Calcd for C₂₈H₂₅ClNO₂ 442.1568; Found 442.1550.

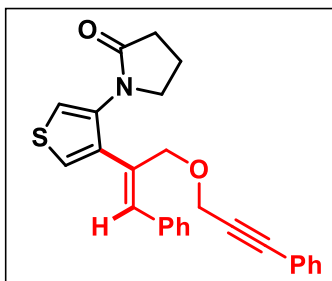


(Z)-1-(4-bromo-2-(1-phenyl-3-((3-phenylprop-2-yn-1-yl)oxy)prop-1-en-2-yl)phenyl)pyrrolidin-2-one (30a): was prepared according to the general procedure (7a.5a). The crude reaction mixture was purified by column chromatography using silica gel

(100-200 mesh size) giving (30 mg, 0.1 mmol scale) 62% yield. **Physical State:** brown liquid **R_f-value:** 0.4 (30% EtOAc/hexane). **¹H NMR (CDCl₃, 400 MHz):** δ 7.64 (d, J = 2.0Hz, 1H), 7.47- 7.42 (m, 3H), 7.39- 7.29 (m, 8H), 7.14 (d, J = 8.4Hz, 1H), 6.76 (s, 1H), 4.48 (s, 2H), 4.37 (s, 2H), 3.75 (t, J = 7.2Hz, 2H), 2.47 (t, J = 8.4Hz, 2H), 2.13 – 2.05 (m, 2H). **¹³C NMR (CDCl₃, 100 MHz):** δ 175.5, 137.3, 136.3, 135.7, 134.1, 133.7, 132.1, 130.2, 129.4, 129.3, 128.8, 128.6, 128.1, 127.9, 126.2, 123.8, 123.6, 122.9,

121.1, 87.1, 85.1, 68.8, 58.9, 50.4, 31.5, 19.4. **IR** (KBr, cm^{-1}): 3446, 1675, 1070, 757.

HRMS (ESI) m/z: $[\text{M}+\text{Na}]^+$ Calcd for $\text{C}_{28}\text{H}_{24}\text{BrNO}_2\text{Na}$ 508.0883; Found 508.0867.



(Z)-1-(4-(1-phenyl-3-((3-phenylprop-2-yn-1-

yl)oxy)prop-1-en-2-yl)thiophen-3-yl)pyrrolidin-2-one

(3pa): was prepared according to the general procedure

(2.4). The crude reaction mixture was purified by

column chromatography using silica gel (100-200 mesh

size), giving (27 mg, 0.1 mmol scale) 66% yield. **Physical State:** colourless liquid, **R_f**

-value: 0.4 (30% EtOAc/hexane). **¹H NMR (CDCl₃, 400 MHz):** δ 7.43 (d, J = 7.6Hz,

2H), 7.38 – 7.35 (m, 3H), 7.33–7.28 (m, 6H), 7.04 (d, J = 5.2Hz, 1H), 6.97 (s, 1H), 4.50

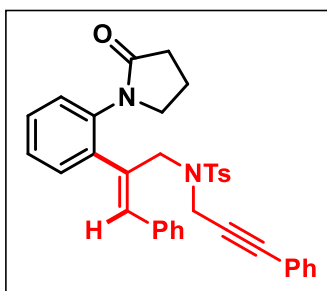
(s, 2H), 4.41 (s, 2H), 3.76 (t, J = 7.2Hz, 2H), 2.48 (t, J = 8.0Hz, 2H), 2.13 – 2.06 (m,

2H). **¹³C NMR (CDCl₃, 176 MHz):** δ 175.5, 137.3, 136.3, 135.7, 133.7, 132.1, 130.2,

129.4, 129.3, 128.8, 128.6, 128.1, 126.2, 123.8, 122.9, 93.2, 87.1, 85.1, 68.8, 58.9, 50.4,

31.5, 19.4. **IR** (KBr, cm^{-1}): 3447, 1700, 1288, 1070, 693. **HRMS (ESI) m/z:** $[\text{M}+\text{Na}]^+$

Calcd for $\text{C}_{26}\text{H}_{23}\text{NO}_2\text{SNa}$ 436.1342; Found 436.1330.



(Z)-4-methyl-N-(3-(2-(2-oxopyrrolidin-1-yl)phenyl)-

3-phenylallyl)-N-(3-phenylprop-2-yn-2-

yl)benzenesulfonamide (3ab): was prepared according

to the general procedure (7a.5a). The crude reaction

mixture was purified by column chromatography using

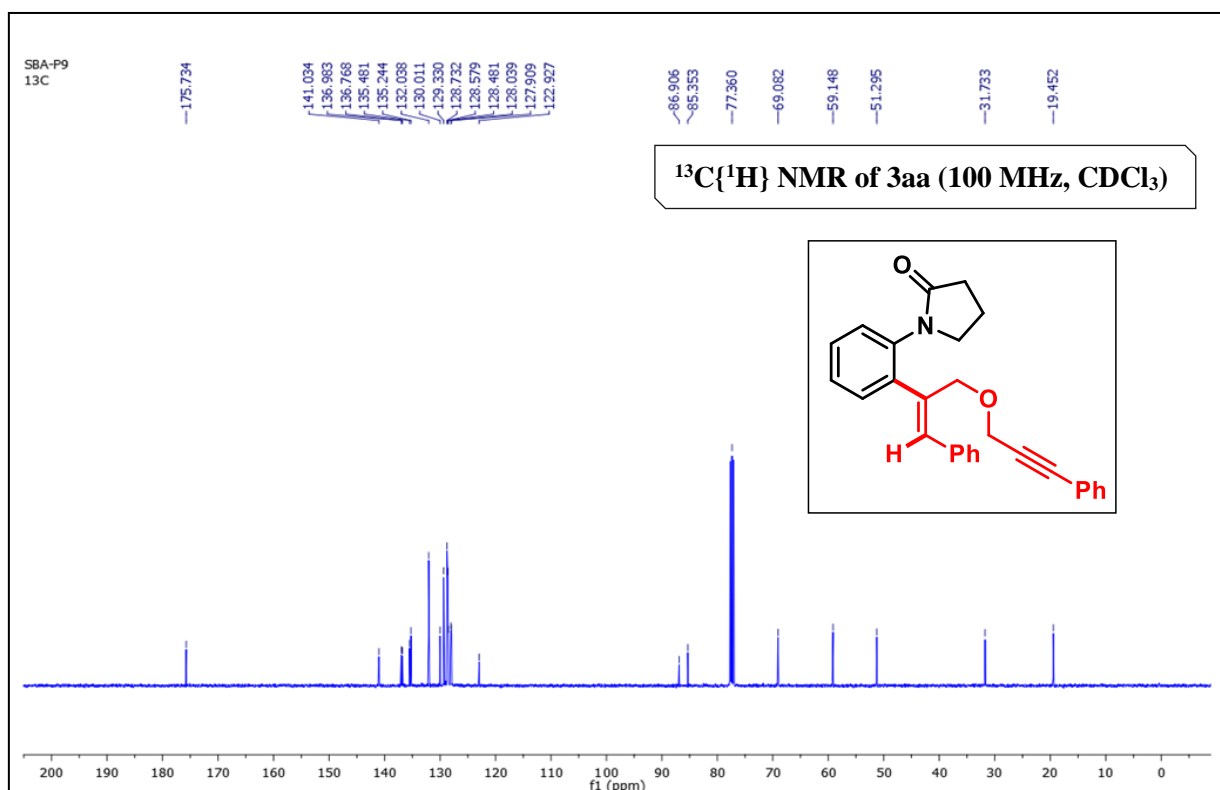
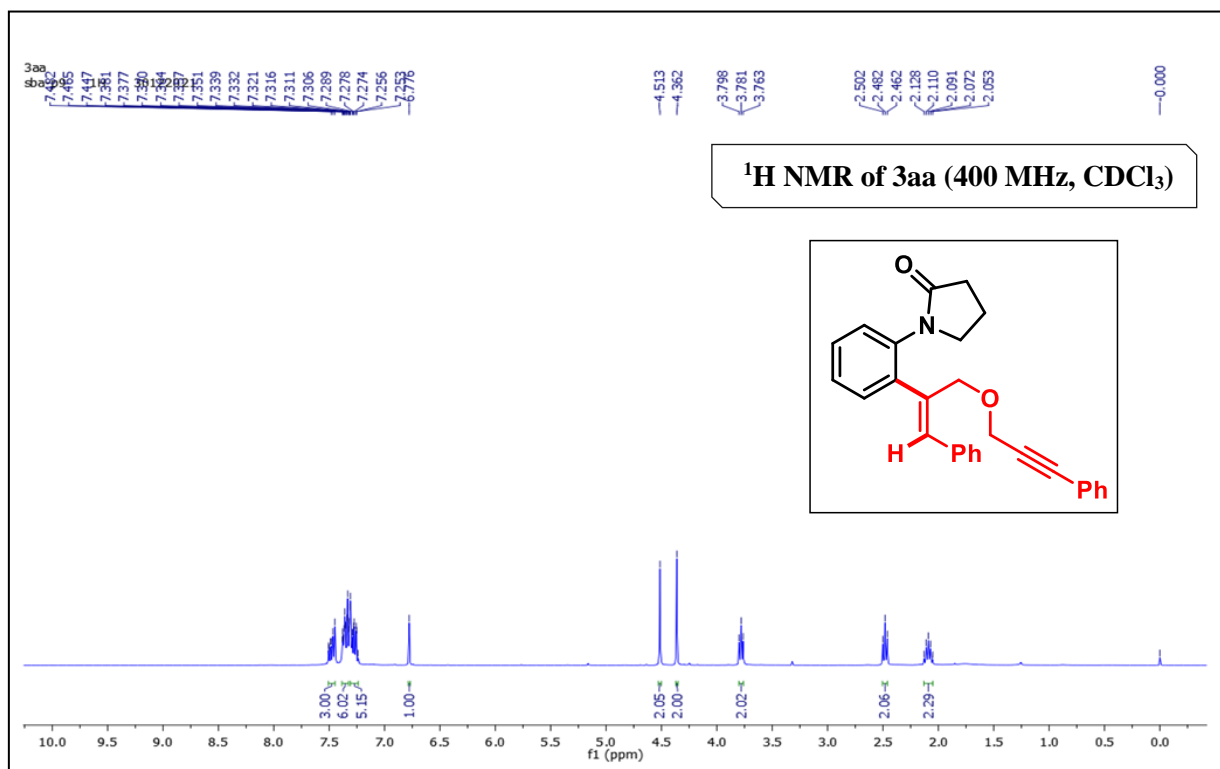
silica gel (100-200 mesh size) giving (33 mg, 0.1 mmol scale) 59% yield. **Physical**

State: solid white **m.p.:** 206–208 °C **R_f -value:** 0.35 (40% EtOAc/hexane). **¹H**

NMR (CDCl₃, 400 MHz): δ 7.57 – 7.51 (m, 3H), 7.39 – 7.27 (m, 6H), 7.24– 7.21

(m, 2H), 7.19 -7.14 (m, 3H), 7.09 (d, $J = 8\text{Hz}$, 2H), 6.83 (s, 1H), 6.78 (d, $J = 8\text{Hz}$, 2H), 4.39 (s, 2H), 4.05 (s, 2H), 3.88 (t, $J = 7.2\text{Hz}$, 2H), 2.54 (t, $J = 8.0\text{Hz}$, 2H), 2.22 (s, 3H), 2.18 (t, $J = 7.6\text{Hz}$, 2H). **^{13}C NMR (CDCl_3 , 176 MHz):** δ 175.1, 143.7, 139.1, 137.3, 136.6, 135.7, 135.1, 134.9, 131.7, 131.1, 129.6, 129.3, 128.9, 128.6, 128.4, 128.3, 128.1, 127.8, 127.5, 127.2, 122.5, 86.0, 82.1, 51.5, 46.2, 38.2, 31.8, 21.6, 19.5. **IR** (KBr, cm^{-1}): 3447, 2372, 1696, 1195, 698. **HRMS (ESI) m/z :** $[\text{M}]^+$ Calcd for $\text{C}_{35}\text{H}_{33}\text{N}_2\text{O}_3\text{S}$ 561.2206; Found 561.2239.

NMR spectra of (Z)-1-(2-(1-phenyl-3-((3-phenylprop-2-yn-1-yl)oxy)prop-1-en-2-yl)phenyl)pyrrolidin-2-one (3aa):



7a.6 REFERENCES

1. (a) Boyd, D. B.; Foster, B. J.; Hatfield, L. D.; Hornback, W. J.; Jones, N. D.; Munroe, J. E.; Swartzendruber, J. K. γ -Lactam analogues of carbapenems. *Tetrahedron Lett.* **1986**, 27, 3457–3460. (b) Baldwin, J. E., Lynch, G. P., and Pitlik, J. (1991) γ -Lactam analogues of β -lactam antibiotics. *J. Antibiot.* 44, 1–24.
2. Caruano, J.; Muccioli, G. G.; Robiette, R. Biologically active γ -lactams: Synthesis and natural sources. *Org. Biomol. Chem.* **2016**, 14, 10134–10156.
3. (a) Xi, N.; Arvedson, S.; Eisenberg, S.; Han, N.; Handley, M.; Huang, L.; Huang, Q.; Kiselyov, A.; Liu, Q.; Lu, Y.; Nunez, G.; Osslund, T.; Powers, D.; Tasker, A. S.; Wang, L.; Xiang, T.; Xu, S.; Zhang, J.; Zhu, J.; Kendall, R.; Dominguez, C. *N*-Aryl- γ -lactams as integrin $\alpha\beta 3$ antagonists. *Bioorg. Med. Chem. Lett.* **2004**, 14, 2905–2909. (b) Hanaya, K., Miller, M. K., and Ball, Z. T. (2019) Nickel(II)-Promoted Amide N–H Arylation of Pyroglutamate–Histidine with Arylboronic Acid Reagents. *Org. Lett.* **21**, 2445–2448.
4. (a) Rej, S.; Das, A.; Chatani, N. Strategic Evolution in Transition Metal-Catalyzed Directed C–H Bond Activation and Future Directions. *Coord. Chem. Rev.* **2021**, 431, 213683.
5. (b) Dalton, T.; Faber, T.; Glorius, F. C–H Activation: Toward Sustainability and Applications. *ACS Cent. Sci.* **2021**, 7, 245–261. (c) Shabani, S.; Wu, Y.; Ryan, H. G.; Hutton, C. A. Progress and perspectives on directing group-assisted palladium-catalysed C–H functionalisation of amino acids and peptides. *Chem. Soc. Rev.* **2021**, 50, 9278–9343.
6. (a) Banjare, S. K.; Chebolu, R.; Ravikumar, P. C. Cobalt Catalyzed Hydroarylation of Michael Acceptors with Indolines Directed by a Weakly Coordinating Functional Group. *Org. Lett.* **2019**, 21, 4049–4053. (b) Banjare, S.-K.; Biswal, P.; Ravikumar, P. C. Cobalt-Catalyzed One-Step Access to Pyroquilon and C-7 Alkenylation of Indoline with Activated Alkenes Using Weakly Coordinating Functional Groups. *J. Org. Chem.* **2020**, 85, 5330–5341. (c) Banjare, S. K.; Nanda, T.; Pati, B. V.; Adhikari, G. K. D.; Dutta, J.; Ravikumar, P. C. Breaking the Trend: Insight into Unforeseen Reactivity of Alkynes in Cobalt-Catalyzed Weak Chelation-Assisted Regioselective C(4)–H Functionalization of 3-Pivaloyl Indole. *ACS Catal.* **2021**, 11, 11579–11587.
7. Banjare, S. K.; Nanda, T.; Pati, B. V.; Biswal, P.; Ravikumar, P. C. O-Directed C–H functionalization via cobaltacycles: a sustainable approach for C–C and C–heteroatom bond formations. *Chem. Commun.* **2021**, 57, 3630–3647.
8. (a) Dong, Z.; Ren, Z.; Thompson, S. J.; Xu, Y.; Dong, G. Transition Metal-Catalyzed C–H Alkylation Using Alkenes. *Chem. Rev.* **2017**, 117, 9333–9403. (b) Zheng, L.; Hua, R. C–H Activation and Alkyne Annulation via Automatic or Intrinsic Directing Groups: Towards High Step Economy. *Chem. Rec.* **2018**, 18, 556–569.
9. (a) Gulías, M.; Mascareñas, J. Metal-catalyzed annulations involving the activation and cleavage of C–H bonds. *L. Angew. Chem., Int. Ed.* **2016**, 55, 11000–11019. (b) Han, X. L.; Lin, P. P.; Li, Q. Recent advances of allenes in the first-row transition metals catalyzed C–H activation reactions. *Chin. Chem. Lett.* **2019**, 30, 1495–1502.
10. Banjare, S. K.; Mahulkar, P. S.; Nanda, T.; Pati, B. V.; Najjar, L. O.; Ravikumar, P. C.; Diverse reactivity of alkynes in C–H activation reactions. *Chem. Commun.*, **2022**, 58, 10262–10289.
11. Mandal, R.; Garai, B.; Sundararaju, B. Weak-Coordination in C–H Bond Functionalizations Catalyzed by 3d Metals. *ACS Catal.* **2022**, 12, 3452–3506.
12. (a) Jang, H.-Y.; Krische, M. J. Rhodium-Catalyzed Reductive Cyclization of 1,6-Diynes and 1,6-Enynes Mediated by Hydrogen: Catalytic C–C Bond Formation via Capture of Hydrogenation Intermediates. *J. Am. Chem. Soc.* **2004**, 126, 7875. (b) Tsuchikama, K.; Kuwata, Y.; Tahara, Y.-K.;

-
- Yoshinami, Y.; Shibata, T. Rh-Catalyzed Cyclization of Diynes and Enynes Initiated by Carbonyl-Directed Activation of Aromatic and Vinylic C-H Bonds. *Org. Lett.* **2007**, *9*, 3097–3099 (c) Yamashita, K.; Yamamoto, Y.; Nishiyama, H. Ruthenium-Catalyzed Transfer Oxygenative Cyclization of α,ω -Diynes: Unprecedented [2 + 2 + 1] Route to Bicyclic Furans via Ruthenacyclopentatriene. *J. Am. Chem. Soc.* **2012**, *134*, 7660.
13. (a) Gandeepan, P.; Müller, T.; Zell, D.; Cera, G.; Warratz, S.; Ackermann, L. 3d Transition Metals for C-H Activation. *Chem. Rev.* **2019**, *119*, 2192–2452. (b) St John Campbell, S.; Bull, J. Base Metal Catalysis in Directed C (sp³)-H Functionalization. *Adv. Synth. Catal.* **2019**, *361*, 3662.
14. (a) Simmons, E. M.; Hartwig, J. F. On the Interpretation of Deuterium Kinetic Isotope Effects in C-H Bond Functionalizations by Transition-Metal Complexes. *Angew. Chem., Int. Ed.* **2012**, *51*, 3066–3072. (b) Ikemoto, H.; Yoshino, T.; Sakata, K.; Matsunaga, S.; Kanai, M. Pyrroloindolone Synthesis via a Cp*CoIII-Catalyzed Redox-Neutral Directed C-H Alkenylation/Annulation Sequence. *J. Am. Chem. Soc.* **2014**, *136*, 5424–5431. (c) Santhoshkumar, R.; Mannathan, S.; Cheng, C. H. Ligand-Controlled Divergent C—H Functionalization of Aldehydes with Enynes by Cobalt Catalysts. *J. Am. Chem. Soc.* **2015**, *137*, 16116–16120. (d) Banjare, S. K.; Nanda, T.; Ravikumar, P. C. Cobalt-Catalyzed Regioselective Direct C-4 Alkenylation of 3-Acetyldole with Michael Acceptors Using a Weakly Coordinating Functional Group. *Org. Lett.* **2019**, *21*, 8138–8143.
15. Banjare, S. K.; Biswal, P.; Ravikumar, P. C. Cobalt-Catalyzed One-Step Access to Pyroquilon and C-7 Alkenylation of Indoline with Activated Alkenes Using Weakly Coordinating Functional Groups. *J. Org. Chem.* **2020**, *85*, 5330–5341.
16. Gottlieb, H. E.; Kotlyar V.; Nudelman A.; NMR chemical shifts of common laboratory solvents as trace impurities. *J. Org. Chem.* **1997**, *62*, 7512 – 7515.

Chapter 7(B)

Weak-chelation assisted cobalt-catalyzed C-H bond activation:

*An approach towards regioselective ethynylation of N-aryl γ -
lactam*

7b.1 Abstract

7b.2 Introduction

7b.3 Results and Discussions

7b.4 Conclusions

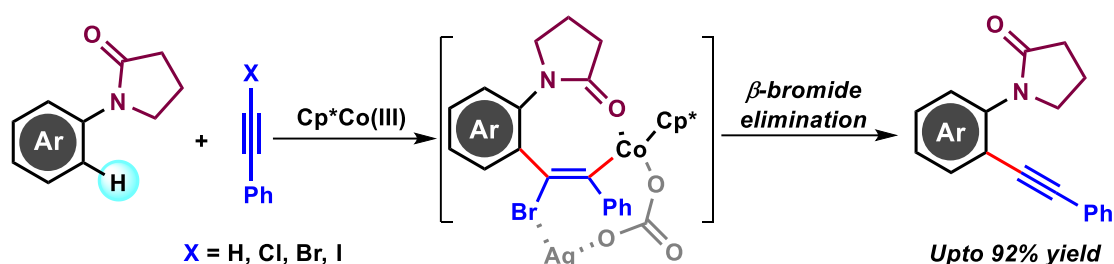
7b.5 Experimental Section

7b.6 References

Chapter 7(B)

Weak-chelation assisted cobalt-catalyzed C-H bond activation:

An approach towards regioselective ethynylation of N-aryl γ -lactam



7b.1 ABSTRACT

The sustainable C-H bond ethynylation of N-aryl γ -lactam has been achieved in a highly regioselective manner. In this protocol, earth-abundant cobalt(III)-catalyst was found to be effective, triggering the C-H metallation using a weakly coordinating lactam group. Herein, the ortho-(sp^2)-H ethynylation has been obtained regioselectively. The mechanistic studies reveal the non-involvement of the radical pathway for this conversion. However, the parallel kinetic iso-tope experiment suggests that the C-H bond activation is involved in the rate-determining step. In addition, the syn-thetic utility of ethynylated N-aryl γ -lactam has been demonstrated for many useful transformations.

7b.2 INTRODUCTION

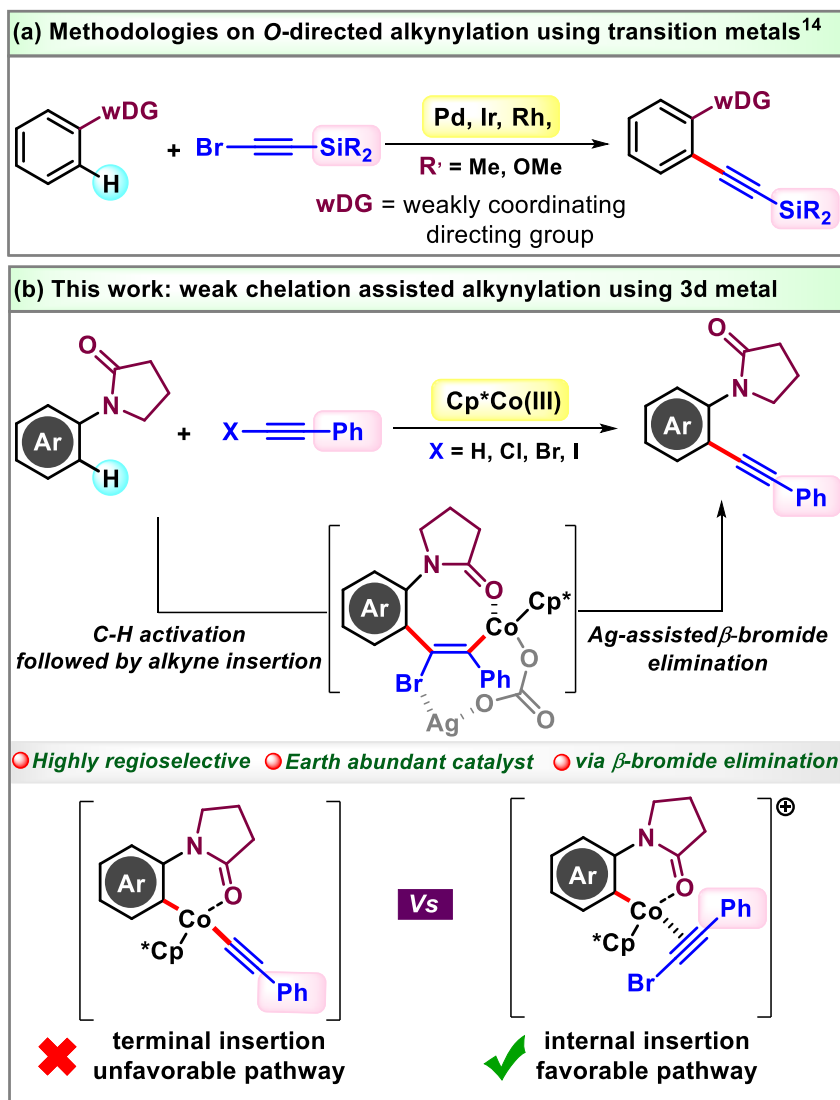
The diversification of bioactive molecular scaffolds has always been an active area of research in the search for new molecules with enhanced properties. γ -lactam is one of the essential structures present in several bioactive drugs and natural products as a core

skeleton.¹ Therefore, the functionalization of γ -lactam derivatives is important because of its potential application in medicinal chemistry.² The *N*-aryl γ -lactams are known to exhibit interesting biological activities³; therefore, diversification of *N*-aryl γ -lactams is an important research area.

The activation and functionalization of the ubiquitous C-H bonds using transition metal catalysts have gained enormous attention for the past two decades because of their step and atom economic profiles.^{4,5} Very recently, the concept of utilizing weakly chelating and easily modifiable groups such as aldehydes, ketones, esters, and lactams along with 3d metals for C-H activation has gained immense attention on account of its synthetic usefulness and sustainability.⁶ Our group has been actively working on this concept for several years.⁷

Alkyne is one of the most successful reacting partners in many C-H functionalization processes. Many useful transformations have been achieved using alkynes as coupling partners.⁸ Among all transformations of alkyne, the C-H ethynylation is one of the synthetically valuable and challenging processes.⁹⁻¹³ In this regards, chatani *et al.* reported palladium catalyzed sp^2 C-H alkynylation using triisopropylsilyl-bromoalkyne.^{14a} Antonio M. Echavarren also reported rhodium-catalyzed ethynylation of arenes using (bromoethynyl)trimethylsilane.^{14b} Further, Xianwei Li demonstrated iridium catalyzed sp^2 C-H alkynylation using ethynyltriisopropylsilane.^{14c} In continuation of this transformation, Xiaodong Shi has developed a methodology for regioselective ethynylation of arenes utilizing iridium as a catalyst where ethynyltrimethylsilane acts as an alkynylating surrogate.¹⁵

Figure 7b.1. Reactivity of transition metals towards ethynylation using various alkynylating agents.



In addition, the alkynylation was reported using various transition metals utilizing strongly *N*-coordinating directing groups.¹⁶ Although weak-chelation assisted metal catalyzed C-H ethynylation has been documented in the literature, it relies on the reactivity of expensive, less abundant 4d and 5d metals such as Pd, Rh, Ir, and silane-based ethynyl surrogates.¹⁴ Therefore, weak-chelation assisted C-H activation using first-row transition metal and subsequent functionalization with less explored ethynyl surrogates needs to be studied.¹⁶

Herein we report a methodology utilizing the reactivity of 3d metal cobalt catalyst and (bromoethynyl)benzene as reacting partners for the regioselective C-H ethynylation through weak-chelating γ -lactam as a directing group, which was never explored before. The salient features of this methodology are as follows (i) Use of γ -lactam as a weakly coordinating group along with earth-abundant cobalt catalyst for C-H ethynylation reaction. (ii) Use of non-silicon-based alkyne surrogate (iii) A mechanistic study reveals C-H bond activation is a rate-determining step (iv) The key intermediates have been detected through ESI-MS, which supports the proposed mechanism. (v) Synthetic application has been performed to make 10-phenyl-7,8-dihydropyrido[1,2-a]indol-9(6H)-one.

7b.3 I RESULTS AND DISCUSSION

Initially, we attempted to optimize the reaction conditions: After screening various parameters, a composition containing 1-phenylpyrrolidin-2-one **1a** (1 equiv), (bromoethynyl)benzene **2a** (2 equiv), Cp^{*}Co(CO)I₂ catalyst (10 mol %), AgSbF₆ (20 mol %), Ag₂CO₃ (2 equiv) as an additive and dichloroethane solvent (DCE, 0.1M) at 80 °C facilitated the desired product **3aa** in excellent yield 94 % (Table 7b.1, entry 1). Deviations from the standard reaction condition were also studied by changing several parameters to fully understand the limits of our condition. Initially, various solvents were screened instead of dichloroethane, such as methanol, benzene, tetrahydrofuran, 1,4-dioxane, and acetonitrile. However, none of these solvents produced the desired product **3aa** (Table 7b.1, entry 2). Since chlorinated solvent worked well with this method, further aromatic hydrocarbon-based chlorinated solvent, such as chlorobenzene, has been screened. However, this also failed to enhance the product yield (Table 7b.1, entry 3). Further, other silver salts, such as AgBF₄ and AgNTf₂, were

tried as halide scavengers instead of AgSbF₆, but we did not see any improvement in product yield (Table 7b.1, entries 4-5). To further check the significance of Ag₂CO₃ for this conversion, other bases, such as Li₂CO₃ and AgOAc, have been screened to understand the role of carbonate and silver. Both these bases gave only a moderate product yield (Table 7b.1, entries 6-7).

Table 7b.1. Optimization of reaction condition towards ethynylation.^{a,b,c}

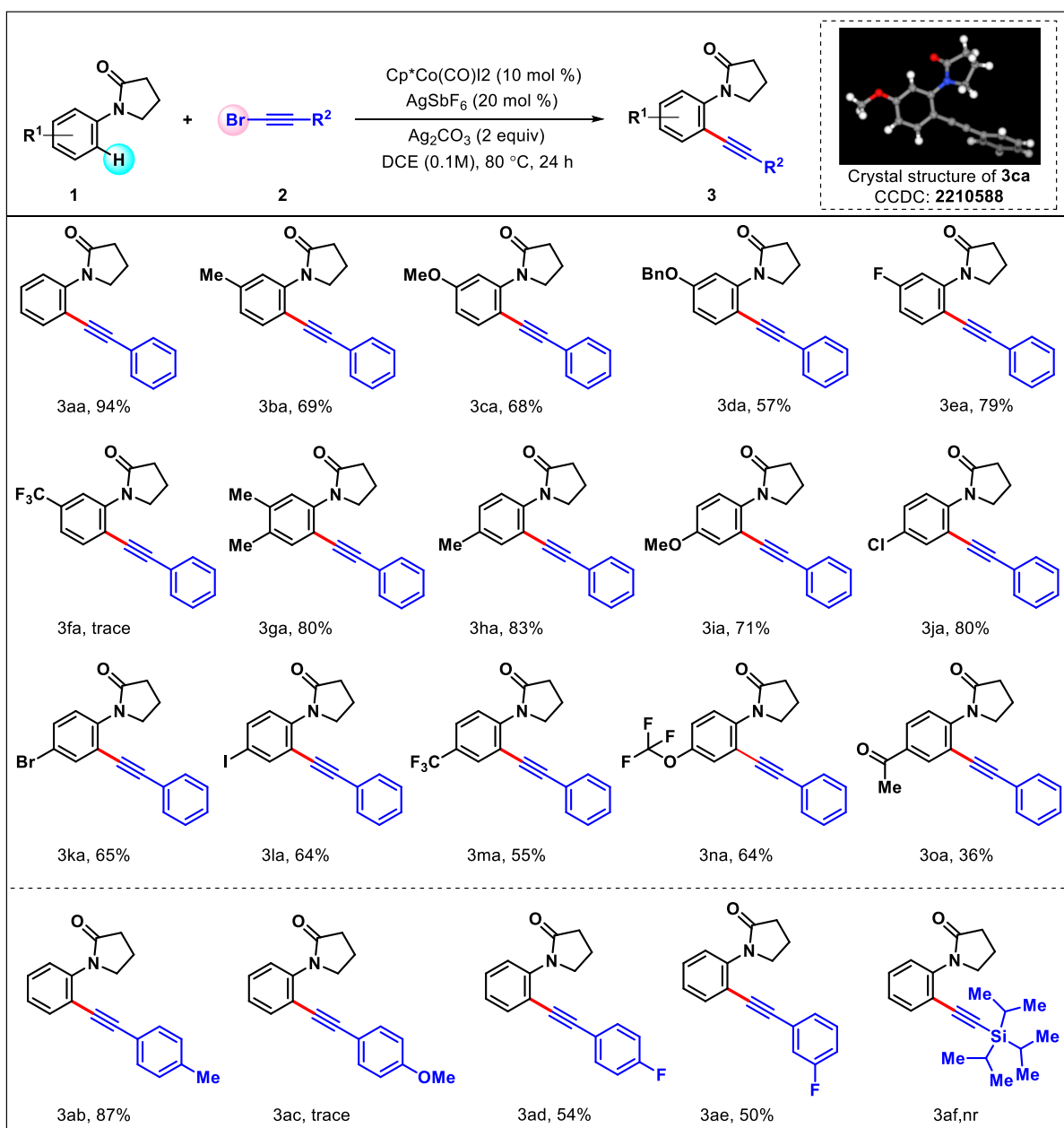
1a (1 equiv)	2a (2 equiv)	3aa
entry	deviation from the standard conditions	yield of 3aa (%) ^b
1	none	94
2 ^c	other solvents instead of DCE	0
3	chlorobenzene as a solvent instead of DCE	58
4	AgBF ₄ instead of AgSbF ₆ as a additive	24
5	AgNTf ₂ instead of AgSbF ₆ as a additive	51
6	Li ₂ CO ₃ instead of Ag ₂ CO ₃	29
7	AgOAc instead of Ag ₂ CO ₃	40
8	1 equiv instead of 2 equiv of Ag ₂ CO ₃	67
9	3 equiv instead of 2 equiv of Ag ₂ CO ₃	78
10	CoBr ₂ instead of Cp*Co(CO)I ₂ as a catalyst	0
11	Co ₂ (CO) ₈ instead of Cp*Co(CO)I ₂ as a catalyst	0
12	1 equiv instead of 2 equiv of 2a	63
13	3 equiv instead of 2 equiv of 2a	87
14	temperature 70 °C instead of 80 °C	72
15	temperature 90 °C instead of 80 °C	63
16	without Ag ₂ CO ₃ as a additive	0
17	without Cp*Co(CO)I ₂ as a catalyst	0
18	screening of other coupling partners instead of 2a :	

^aReaction conditions: **1a** (0.1 mmol), **2a** (0.2 mmol), Cp^{*}Co(CO)I₂ (10 mol %), Ag salt (20 mol %), additive (2 equiv), solvents (1 mL), 80 °C, N₂, ^bisolated yield, ^cmethanol, benzene, tetrahydrofuran, 1,4-dioxane, acetonitrile.

This suggests the critical role of silver carbonate as a basic additive. Apart from its basic property we believe silver might enhance the removal of bromide in the β -bromide elimination step. Furthermore, the amount of silver carbonate has also been screened from 2 equivalents to 1 equivalent and 3 equivalents (Table 7b.1, entry 8-9). But it turned out that 2 equivalents of silver carbonate are just optimal for this conversion. To check the crucial role of Cp^{*}Co(III) catalyst, other Co(II) and Co(0) catalyst was tested with optimized reaction condition, but both the catalysts failed to produce the desired product (Table 7b.1, entries 10,11). This suggests that the Cp^{*}Co(III) is an active catalyst and is driving the ethynylation process effectively through regioselective C-H bond activation. Also, the amount of reacting partner has varied from standard reaction conditions, which did not help to enhance the product yield (Table 7b.1, entries 12,13). Further, the physical deviation, such as temperature, has been performed from the standard condition, which was ineffective in getting an enhanced yield of the desired product **3aa** (Table 7b.1, entries 14,15). Some control experiments have been performed, such as removing additives from standard reaction conditions, but it resulted in no reaction (Table 7b.1, entry 16). Absence of Cp^{*}Co(III)-catalyst in the standard reaction failed to give the desired ethynylated product **3aa** (Table 7.1, entry 17). This suggests that this reaction is indeed catalyzed by Cp^{*}Co(III)-catalyst. Moreover, various ethynylated reacting partner derivatives have been screened, such as ethynylbenzene, (chloroethynyl)benzene, and (iodoethynyl)benzene, but all of them failed to give the desired product in good yields (Table 7b.1, entry 18).

After optimizing the reaction conditions, we stepped towards the substrate scope where various aryl substituted lactam was initially subjected to standard reaction conditions (Scheme 7b.1). It was found that *meta*-substituted electron donating groups (methyl, methoxy, -OBn) showed moderate to excellent product yield (Scheme 7b.1, **3ba-3da**). Further, the *meta*-substituted fluoro gave a very good ethynylated product yield (Scheme 7b.1, **3ea**). However, *meta*-substituted trifluoro-methyl gave only a trace yield of the product, possibly due to the high electron-withdrawing nature of the CF₃ group (Scheme 7b.1, **3fa**). The dimethyl substituted substrate 1-(3,4-dimethylphenyl)pyrrolidin-2-one was compatible with optimized reaction conditions and delivered product **3ga** in 80% yield. Further, by substituting the *para*-position, we obtained a good yield of the ethynylated product. On substituting electron donating group at the *para*-position of *N*-aryl γ -lactam such as methyl and methoxy produced their respective product in good yields (Scheme 7b.1, **3ha**, **3ia**). The halogen substituents such as chloro-, bromo-, and iodo- at the *para*-position of *N*-aryl γ -lactam gave moderate to a good yield of the desired products (Scheme 7b.1, **3ja-3la**). Notably, good product yield was obtained by substituting the *para*-position with the electron withdrawing group such as *p*-CF₃, *p*-OCF₃ (Scheme 7b.1, **3ma-3na**). However, the *para*-substituted -COMe derived product has been obtained in poor yield (Scheme 7b.1, **3oa**). Notably, *ortho*-substituted *N*-aryl γ -lactam was ineffective with optimized reaction conditions. It might be due to the steric crowding near to the directing group, thereby inhibiting the reactivity. After scrutinizing the substitution at the *N*-aryl γ -lactam's, we moved on to investigate the variations in coupling partners. On substituting the *para*-position of the arylated coupling partner with methyl, excellent yield of respective products was obtained (Scheme 7b.1, **3ab**).

Scheme 7b.1. Scope of various substrate and reacting partners towards cobalt catalyzed ethynylation.^{a,b}



^aReaction conditions: **1a** (0.1 mmol), **2a** (0.2 mmol), [Cp*Co(CO)I₂] (10 mol %), Ag salt (20 mol %), additive (2 equiv), solvents (1 mL), 80 °C, N₂, ^bisolated yield, cmethanol, benzene, tetrahydrofuran, 1,4-dioxane, acetonitrile.

However, when 1-(bromoethynyl)-4-methoxybenzene was used as a coupling partner, only a trace amount of ethynylated product was obtained (Scheme 7b.1, **3ac**). Also,

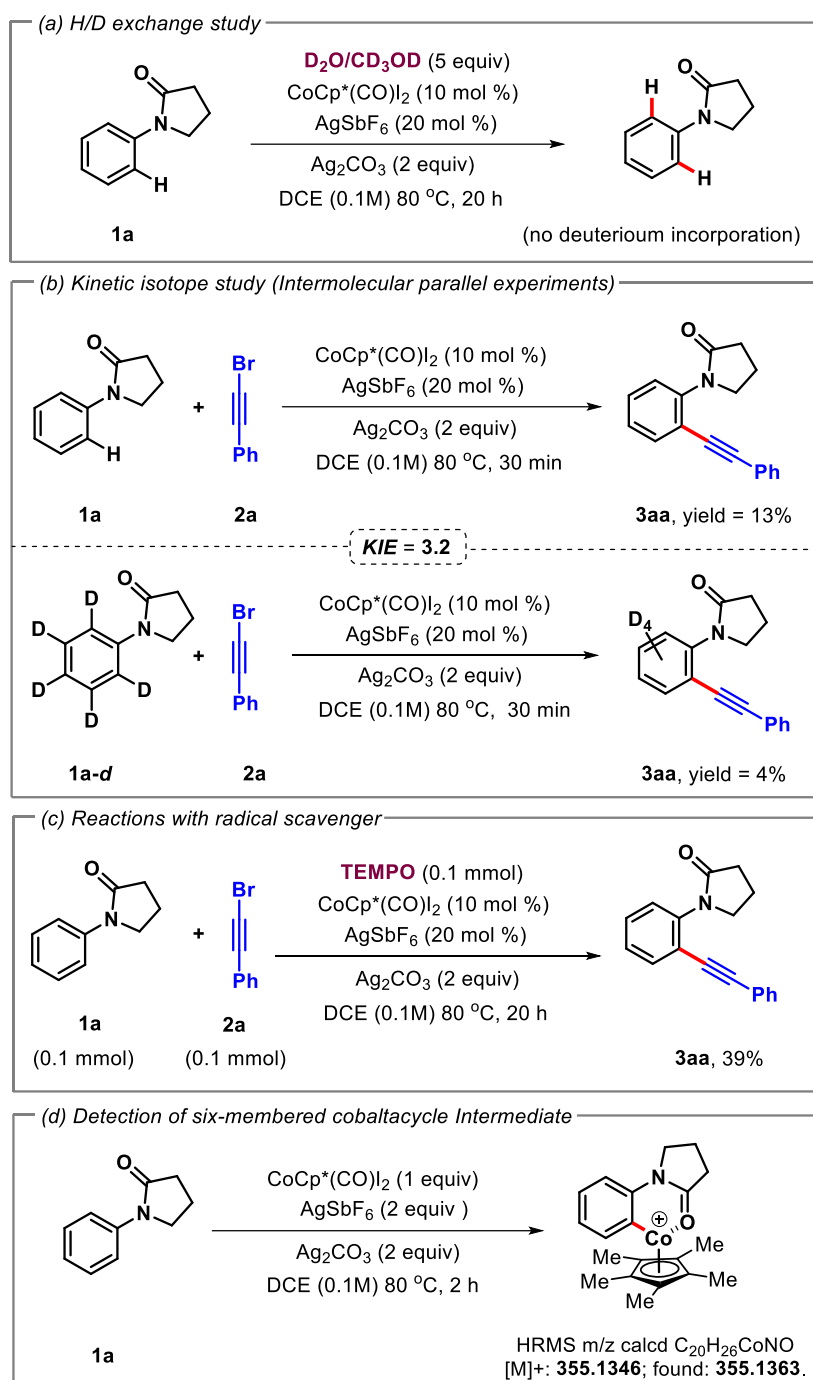
when 1-(bromoethynyl)-4-fluorobenzene was used as reacting partner, it gave 54% yield of desired product **3ad**. Further, *meta*-substituted 1-(bromoethynyl)-3-fluorobenzene coupling partner gave a moderate yield (Scheme 7b.1, **3ae**). Surprisingly, 1-(2-((triisopropylsilyl)ethynyl)phenyl)pyrrolidin-2-one has failed to react with *N*-aryl γ -lactam (Scheme 7b.1, **3af**).

Several mechanistic studies have been investigated to understand the reaction mechanism (Scheme 7b.2). Initially, the hydrogen scrambling reaction was performed by taking **1a** and D₂O/CD₃OD as deuterium sources under standard reaction conditions. We did not observe any deuterium incorporation in starting material **1a**, which indicates that the C-H metalation step may be an irreversible step (Scheme 7b.2a). Further, an intermolecular parallel kinetic isotope experiment was performed between **1a** and **1a-d** using standard reaction conditions within 30 min. The KIE value of 3.2 was observed, suggesting that the C-H activation step might be the rate-determining step (Scheme 7b.2b).¹⁸ To check whether the reaction follows an ionic or radical pathway, a radical scavenger such as TEMPO was added to the reaction mixture; however, this could not diminish the product formation (Scheme 7b.2c). This result tells the reaction is going through an anionic pathway rather than a radical pathway. In addition, the six-membered cobaltacycle intermediate has been detected in high-resolution mass spectrometry (HRMS), which confirms the metalation after C-H bond activation (Scheme 7b.2d).

Based on mechanistic studies and literature reports,^{15,22-24} a plausible catalytic cycle has been depicted in Scheme 7b.3. Initially, the active catalyst [Cp^{*}Co(CO₃)] **A** was generated in the presence of AgSbF₆, Ag₂CO₃ from [Cp^{*}Co(CO)I₂], which gives

intermediate **B** through regioselective C-H bond activation of *N*-aryl γ -lactam **1**. Intermediate **B** has been detected in high-resolution mass spectrometry (HRMS).

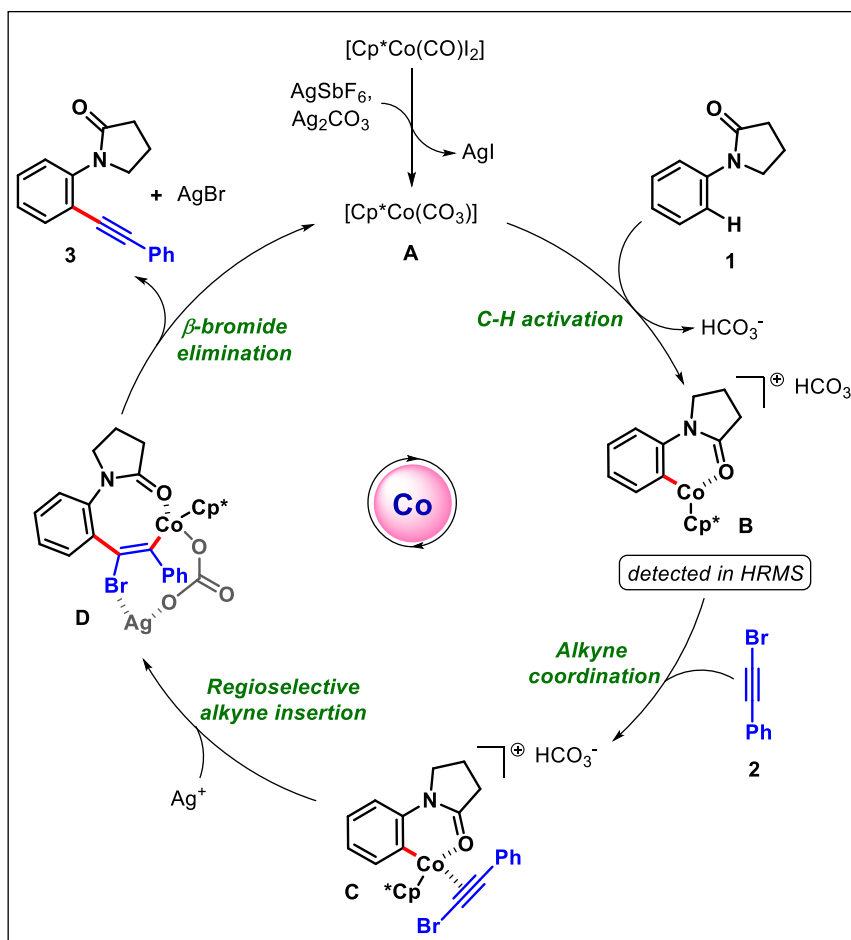
Scheme 7b.2. Mechanistic studies and control experiments



Further, intermediate **B** coordinates with bromo-alkyne **2** to generate intermediate **C**, which gives intermediate **D** after the migratory insertion of cobalt-catalyst into

alkyne. Then in the presence of silver, β -bromide elimination from intermediate **D** provides the desired ethynylated product **3** and the generation of active catalyst **A**. The process of β -bromide elimination is becoming favorable due to the coordination of silver to bromine and carbonate in intermediate **D**, which makes it possible.

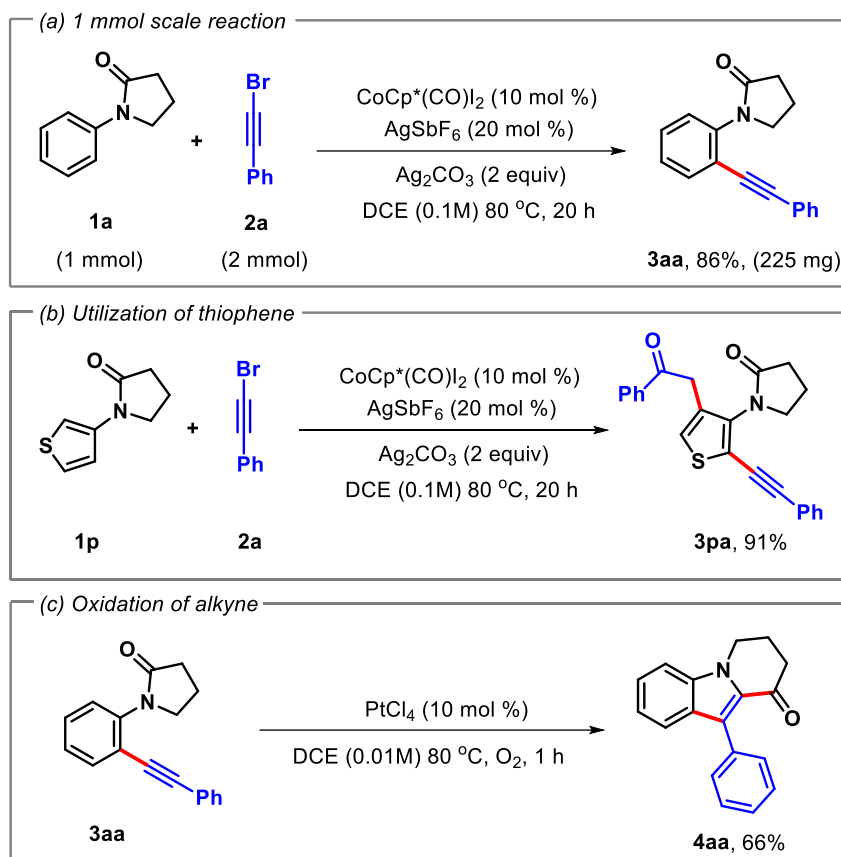
Scheme 7b.3. Catalytic cycle for regioselective Co(III)-catalysed ethynylation



The synthetic utility of obtained product has been shown in Scheme 7b.4. This desired ethynylated product has a good synthetic application because alkyne is a prominent functional group that could lead to many transformations. In these regards, initially, we have subjected a 1 mmol scale reaction to check the feasibility of this method on a large scale, which provides an excellent yield of alkynylated product in 86% (Scheme 7b.5a). Surprisingly, completely diverse product 1-(4-(2-oxo-2-phenylethyl)-2-

(phenylethynyl)thiophen-3-yl)pyrrolidin-2-one **3pa** has been obtained in excellent yield, when 1-(thiophen-3-yl)pyrrolidin-2-one **3p** was subjected with standard reaction condition (Scheme 7b.4b). This might be going through bis-ethynylation followed by selective oxidation of alkyne in the presence of mild moisture.

Scheme 7b.4. Synthetic utilization.



To check this reactivity deliberately, we added 2 equivalent water in the reaction mixture, which failed to produce **3pa**. This tells that mild moisture is beneficial in site reaction, but excess is detrimental to this conversion. Further, a cascade cyclization reaction has been performed on the product using a platinum catalyst, which provides 10-phenyl-7,8-dihydropyrido[1,2-a]indol-9(6H)-one **4aa** in good yields (Scheme 7b.4c).²⁵ This transformation increases the scope for further diversification in medicinal chemistry applications.

4.3 CONCLUSION

In summary, we have reported regioselective ethynylation of *N*-aryl γ -lactam using inexpensive first-row transition metal cobalt via weak chelation-assisted C-H bond activation. A mild reaction condition with broad substrate scope has been disclosed for C(sp²)-C(sp) coupling. Detailed mechanistic studies were performed in support of the proposed mechanism. The intermolecular parallel experiment suggests the C-H bond activation is a rate-determining step. The key intermediates have been detected through ESI-MS, which supports the proposed mechanism. Ethynylated derivatives of biologically important *N*-aryl γ -lactams were synthesized. Moreover, the reactivity of the ethynylated product was explored, which has the potential for further diversification for medicinal chemistry applications.

Limitations: *Ortho*-substituted *N*-aryl γ -lactam is incompatible with optimized reaction conditions, most likely due to steric hindrance of the *ortho*-substituents.

7b.5 EXPERIMENTAL SECTION^{7c}

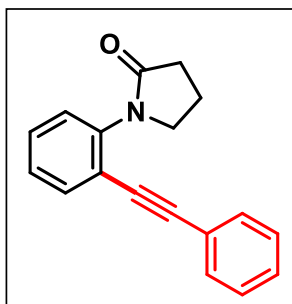
Reactions were performed using borosil Schlenk tube vial under an N₂ atmosphere. Column chromatography was done by using 100-200 & 230-400 mesh size silica gel of Acme Chemicals. Gradient elution was performed by using distilled petroleum ether and ethyl acetate. TLC plates were detected under UV light at 254 nm. ¹H NMR and ¹³C NMR were recorded on Bruker AV 400, 700 MHz spectrometers using CDCl₃ as NMR solvents. The residual CHCl₃ for ¹H NMR (δ = 7.26 ppm) and the deuterated solvent signal for ¹³C NMR (δ = 77.36 ppm) is used as reference.²⁷ Multiplicity (s = single, d = doublet, t = triplet, q = quartet, m = multiplet, dd = double doublet), integration, and coupling constants (*J*) in hertz (Hz). HRMS signal analysis was

performed using a micro TOF Q-II mass spectrometer. X-ray analysis was conducted using a Rigaku Smartlab X-ray diffractometer at SCS, NISER. Reagents and starting materials were purchased from Sigma Aldrich, Alfa Aesar, TCI, Avra, Spectrochem, Carbanio, and other commercially available sources and used without further purification unless otherwise noted.

(a) General reaction procedure for regioselective alkynylation of *N*-aryl γ -lactam:

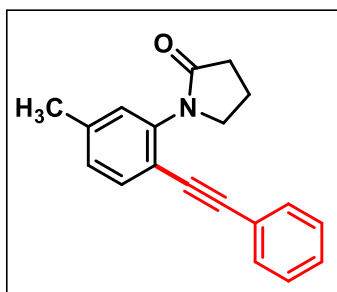
To a pre-dried sealed tube under N₂, the mixture of 1-phenylpyrrolidin-2-one **1** (0.1 mmol), (bromoethynyl)benzene **2** (0.2 mmol), [Cp*Co(CO)I₂] (10 mol %), AgSbF₆ (20 mol %), Ag₂CO₃ (2 equivalent), and dichloroethane (1 mL) were added and sealed inside the glove box. The reaction mixture was vigorously stirred at 80 °C on the preheated aluminum block for 20 h. After 20 h (completion of the reaction as monitored by TLC analysis), the reaction mixture was cooled to room temperature and diluted with ethyl acetate, and passed through a short celite pad, the solvent was evaporated under reduced pressure, and the residue was purified by column chromatography using EtOAc/hexane mixture on silica gel to give the pure product **3**.

Experimental characterization data of products:



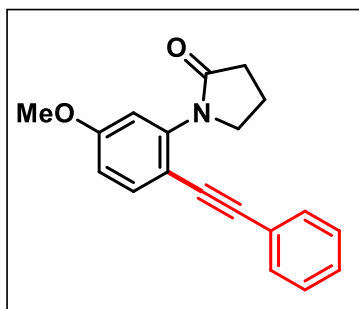
1-(2-(phenylethynyl)phenyl)pyrrolidin-2-one (3aa): was prepared according to the general procedure (7b.5a). The crude reaction mixture was purified by column chromatography using silica gel (100-200 mesh size) giving 16 mg (0.1 mmol), 94% yield. **Physical State:** yellow solid **m.p.:** 87–89 °C **R_f-value:** 0.3 (10% EtOAc/hexane). **¹H**

NMR (CDCl₃, 400 MHz): δ 7.61–7.59 (m, 1H), 7.50–7.47 (m, 2H), 7.41–7.27 (m, 6H), 3.95 (d, J = 7.6 Hz, 2H), 2.60 (d, J = 8.0 Hz, 2H), 2.23 (quint, J = 7.6 Hz, 2H). **¹³C** **NMR (CDCl₃, 100 MHz):** δ 175.2, 140.6, 133.6, 131.8, 129.6, 128.9, 128.8, 128.0, 127.7, 123.3, 121.5, 94.5, 86.3, 50.7, 31.9, 19.6. **IR (KBr, cm⁻¹):** 3447, 2924, 1675, 1206, 724. **HRMS (ESI) m/z:** [M+H]⁺ Calcd for C₁₈H₁₆NO: 262.1232; Found 262.1239.



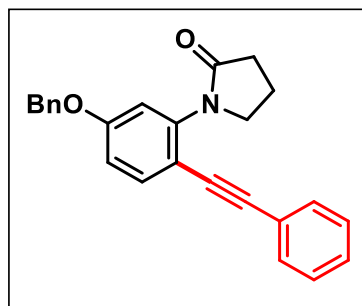
1-(5-methyl-2-(phenylethynyl)phenyl)pyrrolidin-2-one (3ba): was prepared according to the general procedure (7b.5a). The crude reaction mixture was purified by column chromatography using silica gel (100-200 mesh size) giving 19 mg (0.1mmol), 69% yield. **Physical**

State: orange liquid **R_f-value:** 0.3 (30% EtOAc/hexane). **¹H NMR (CDCl₃, 400 MHz):** δ 7.49–7.46 (m, 3H), 7.35–7.33 (m, 3H), 7.14 (s, 1H), 7.10 (d, J = 8.0 Hz, 1H), 3.93 (t, J = 7.2 Hz, 2H), 2.95 (t, J = 8.0 Hz, 2H), 3.37 (s, 3H), 2.22 (quint, J = 7.2 Hz, 2H). **¹³C** **NMR (CDCl₃, 100 MHz):** δ 175.3, 140.4, 140.2, 133.4 (2C), 131.7, 128.7, 128.7, 128.6, 123.5, 118.4, 93.8, 86.5, 50.7, 31.9, 21.7, 19.6. **IR (KBr, cm⁻¹):** 3446, 1700, 1266, 756. **HRMS (ESI) m/z:** [M+Na]⁺ Calcd for C₁₉H₁₇NONa: 298.1208; Found 298.1183.



1-(5-methoxy-2-(phenylethynyl)phenyl)pyrrolidin-2-one (3ca): was prepared according to the general procedure (7b.5a). The crude reaction mixture was purified by column chromatography using silica gel (100-200 mesh size) giving 20 mg (0.1mmol), 68%

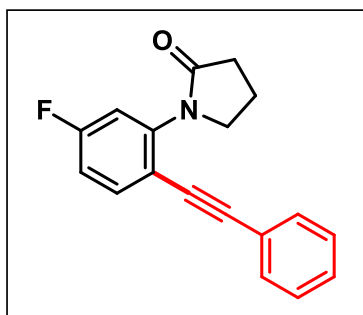
yield. **Physical State:** solid brown **m.p.:** 80–82 °C **R_f-value:** 0.3 (30% EtOAc/hexane). **¹H NMR (CDCl₃, 400 MHz):** δ 7.50 (d, J = 8.4 Hz, 1H), 7.47–7.43 (m, 2H), 7.36–7.32 (m, 3H), 6.87 (d, J = 2.4 Hz, 1H), 6.85–6.83 (m, 1H), 3.95 (t, J = 7.2 Hz, 2H), 3.82 (s, 3H), 2.60 (t, J = 8.0 Hz, 2H), 2.22 (quint, J = 7.2 Hz, 2H). **¹³C NMR (CDCl₃, 100 MHz):** δ 175.2, 160.6, 141.9, 134.6, 131.6, 128.7, 128.6, 123.6, 114.1, 113.5, 113.4, 93.1, 86.4, 55.8, 50.7, 31.9, 19.7. **IR (KBr, cm⁻¹):** 3446, 2928, 1702, 1337, 697. **HRMS (ESI) m/z:** [M+H]⁺ Calcd for C₁₉H₁₈NO₂: 292.1338; Found 292.1354.



1-(5-(benzyloxy)-2-(phenylethynyl)phenyl)pyrrolidin-2-one (3da): was prepared according to the general procedure (7b.5a). The crude reaction mixture was purified by column chromatography using silica gel (100-200 mesh size)

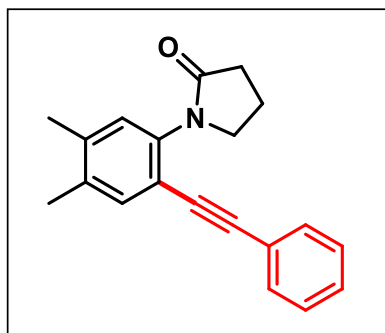
giving 21 mg (0.1mmol), 57% yield. **Physical State:** solid brown **m.p.:** 93–95 °C **R_f-value:** 0.5 (30% EtOAc/hexane). **¹H NMR (CDCl₃, 400 MHz):** δ 7.50 (d, J = 8.4 Hz, 1H), 7.47–7.45 (m, 2H), 7.43–7.37 (m, 4H), 7.35–7.32 (m, 4H), 6.97 (d, J = 2.4 Hz, 1H), 6.92–6.89 (m, 1H), 5.07 (s, 2H), 3.95 (t, J = 7.2 Hz, 2H), 2.59 (t, J = 7.6 Hz, 2H), 2.22 (quint, J = 7.6 Hz, 2H). **¹³C NMR (CDCl₃, 100 MHz):** δ 175.2, 159.7, 141.9, 136.6, 134.6, 131.6, 128.9, 128.7, 128.6, 128.5, 127.9, 123.6, 114.7, 114.3, 113.7, 93.2, 86.4,

70.6, 50.7, 31.9, 19.6. **IR** (KBr, cm^{-1}): 3446, 1697, 1203, 755. **HRMS (ESI) m/z**: $[\text{M}+\text{H}]^+$ Calcd for $\text{C}_{25}\text{H}_{22}\text{NO}_2$: 368.1650; Found 368.1661.



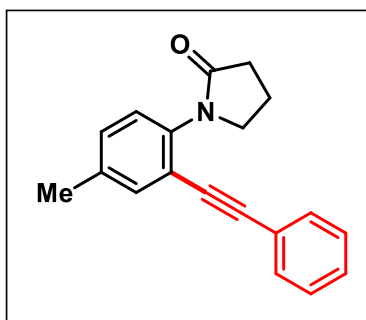
1-(5-fluoro-2-(phenylethynyl)phenyl)pyrrolidin-2-one (3ea): was prepared according to the general procedure (7b.5a). The crude reaction mixture was purified by column chromatography using silica gel (100-200 mesh size) giving 22 mg (0.1mmol), 79%

yield. **Physical State**: solid brown **m.p.**: 91–93 °C **R_f-value**: 0.2 (30% EtOAc/hexane) **¹H NMR (CDCl₃, 700 MHz)**: δ 7.52–7.51 (m, 2H), 7.36–7.32 (m, 4H), 7.15 (d, J = 7.7 Hz, 1H), 7.07 (t, J = 8.4 Hz, 1H), 3.96 (t, J = 7.0 Hz, 2H), 2.60 (t, J = 7.7 Hz, 2H), 2.23 (quint, J = 7.7 Hz, 2H). **¹³C NMR (CDCl₃, 100 MHz)**: δ 175.2, 163.6, (d, J = 7.7 Hz), 142.1 (d, J = 2.2 Hz), 131.8, 130.0, (d, J = 9.2 Hz), 129.2, 128.7, 123.5 (d, J = 9.2 Hz), 122.9, 114.7 (d, J = 21.3 Hz), 110.8, (d, J = 16.4 Hz), 99.7 (d, J = 3.5 Hz), 79.8, 50.5, 31.8, 19.6. **¹⁹F NMR (CDCl₃, 376 MHz)**: –107.59 **IR** (KBr, cm^{-1}): 3446, 2983, 1699, 1251, 757. **HRMS (ESI) m/z**: $[\text{M}+\text{H}]^+$ Calcd for $\text{C}_{18}\text{H}_{15}\text{FNO}$: 280.1138; Found 280.1154.

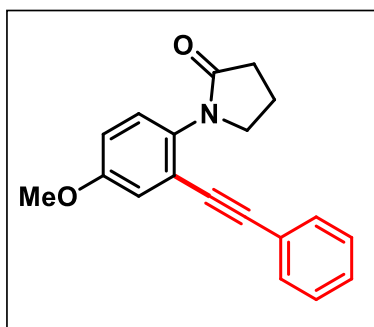


1-(4,5-dimethyl-2-(phenylethynyl)phenyl)pyrrolidin-2-one (3ga): was prepared according to the general procedure (7b.5a). The crude reaction mixture was purified by column chromatography using silica gel (100-200 mesh size) giving 24 mg (0.1mmol), 80% yield.

Physical State: yellow solid **m.p.:** 78-80 °C **R_f-value:** 0.3 (30% EtOAc/hexane) **¹H NMR (CDCl₃, 400 MHz):** δ 7.48–7.45 (m, 2H), 7.37 (s, 1H), 7.35–7.32 (m, 3H), 7.09 (s, 1H), 3.91 (t, *J* = 6.8 Hz, 2H), 2.58 (t, *J* = 7.6 Hz, 2H), 2.27 (s, 3H), 2.24 (s, 3H), 2.21 (quint, *J* = 7.6 Hz, 2H). **¹³C NMR (CDCl₃, 100 MHz):** δ 175.3, 138.8, 138.1, 136.6, 134.3, 131.7, 129.0, 128.7, 128.6, 123.6, 118.6, 93.5, 86.5, 50.8, 31.8, 20.2, 19.6, 19.5. **IR (KBr, cm⁻¹):** 3438, 1700, 1274, 763. **HRMS (ESI) m/z:** [M+H]⁺ Calcd for C₂₀H₂₀NO: 290.1545; Found 290.1566.

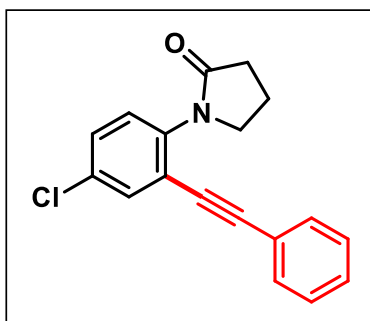


1-(4-methyl-2-(phenylethynyl)phenyl)pyrrolidin-2-one (3ha): was prepared according to the general procedure (7b.5a). The crude reaction mixture was purified by column chromatography using silica gel (100-200 mesh size) giving 23 mg (0.1mmol), 83% yield. **Physical State:** colourless liquid **R_f-value:** 0.4 (20% EtOAc/hexane). **¹H NMR (CDCl₃, 400 MHz):** δ 7.49–7.46 (m, 2H), 7.41 (s, 1H), 7.36–7.33 (m, 3H), 7.20–7.19 (m, 2H), 3.90 (t, *J* = 7.2 Hz, 2H), 2.59 (t, *J* = 7.6 Hz, 2H), 2.53 (s, 3H), 2.21 (quint, *J* = 7.6 Hz, 2H). **¹³C NMR (CDCl₃, 100 MHz):** δ 175.3, 138.0, 137.7, 134.0, 131.8, 130.5, 128.8, 128.7, 127.8, 123.4, 121.2, 94.0, 86.5, 50.7, 31.8, 21.2, 19.6. **IR (KBr, cm⁻¹):** 3446, 2924, 1700, 1301, 757. **HRMS (ESI) m/z:** [M+H]⁺ Calcd for C₁₉H₁₈NO: 276.1388; Found 276.1394.



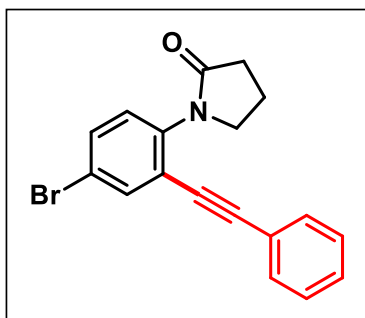
1-(4-methoxy-2-(phenylethynyl)phenyl)pyrrolidin-2-one (3ia): was prepared according to the general procedure (7b.5a). The crude reaction mixture was purified by column chromatography using silica gel (100-200 mesh size) giving 21 mg (0.1mmol), 71%

yield. **Physical State:** solid brown **m.p.:** 83–85 °C **R_f-value:** 0.4 (20% EtOAc/hexane). **¹H NMR (CDCl₃, 400 MHz):** δ 7.48–7.45 (m, 2H), 7.37–7.34 (m, 3H), 7.24 (d, J = 8.8 Hz, 1H), 7.10 (d, J = 2.8 Hz, 1H), 6.95–6.92 (m, 1H), 3.92 (t, J = 7.2 Hz, 2H), 3.82 (s, 3H), 2.66 (t, J = 8.0 Hz 2H), 2.24 (quint, J = 7.6 Hz, 2H). **¹³C NMR (CDCl₃, 100 MHz):** δ 176.7, 159.1, 132.7, 131.8, 129.1, 129.0, 128.8, 123.0, 122.4, 117.8, 116.2, 94.3, 85.8, 56.0, 51.6, 31.6, 19.4. **IR (KBr, cm⁻¹):** 3422, 1696, 1232, 758. **HRMS (ESI) m/z:** [M+H]⁺ Calcd for C₁₉H₁₈NO₂: 292.1338; Found 292.1327.



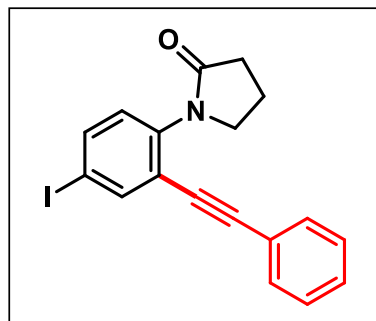
1-(4-chloro-2-(phenylethynyl)phenyl)pyrrolidin-2-one (3ja): was prepared according to the general procedure (7b.5a). The crude reaction mixture was purified by column chromatography using silica gel (100-200 mesh size) giving 24 mg (0.1mmol), 80%

yield. **Physical State:** brown liquid **R_f-value:** 0.4 (20% EtOAc/hexane). **¹H NMR (CDCl₃, 400 MHz):** δ 7.57 (d, J = 2.4 Hz, 1H), 7.49–7.46 (m, 2H), 7.38–7.34 (m, 3H), 7.33 (d, J = 2.4 Hz, 1H), 7.28 (s, 1H), 3.93 (t, J = 6.8 Hz, 2H), 2.59 (t, J = 8.4 Hz, 2H), 2.23 (quint, J = 7.6 Hz, 2H). **¹³C NMR (CDCl₃, 100 MHz):** δ 175.3, 139.1, 133.2, 133.2, 131.8, 129.7, 129.3, 129.2, 128.8, 123.0, 122.8, 95.7, 85.1, 50.5, 31.7, 19.6. **IR (KBr, cm⁻¹):** 3422, 1684, 1232, 756. **HRMS (ESI) m/z:** [M+H]⁺ Calcd for C₁₈H₁₅ClNO: 296.0842; Found 296.0834.

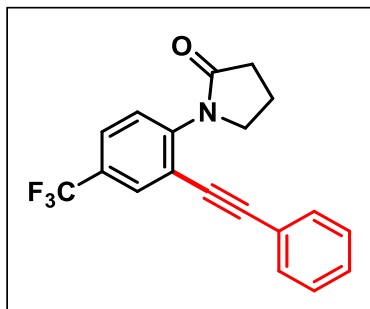


1-(4-bromo-2-(phenylethynyl)phenyl)pyrrolidin-2-one (3ka): was prepared according to the general procedure (7b.5a). The crude reaction mixture was purified by column chromatography using silica gel (100-200 mesh size) giving 22 (0.1mmol), 65% yield.

Physical State: brown liquid **R_f-value:** 0.2 (30% EtOAc/hexane) **¹H NMR (CDCl₃, 400 MHz):** δ 7.73 (d, J = 2.4 Hz, 1H), 7.50–7.46 (m, 3H), 7.37–7.36 (m, 3H), 7.21 (d, J = 8.4 Hz, 1H), 3.93 (t, J = 7.2 Hz, 2H), 2.59 (t, J = 8.0 Hz, 2H), 2.23 (quint, J = 7.6 Hz, 2H). **¹³C NMR (CDCl₃, 100 MHz):** δ 175.2, 139.6, 136.2, 132.7, 131.9, 129.4, 129.3, 128.8, 123.3, 122.8, 120.9, 95.8, 85.0, 50.5, 31.8, 19.6. **IR (KBr, cm⁻¹):** 3430, 1675, 1274, 763. **HRMS (ESI) m/z:** [M+H]⁺ Calcd for C₁₈H₁₅BrNO: 340.0337; Found 340.0316.



1-(4-iodo-2-(phenylethynyl)phenyl)pyrrolidin-2-one (3la): was prepared according to the general procedure (7b.5a). The crude reaction mixture was purified by column chromatography using silica gel (100-200 mesh size) giving 25 mg (0.1mmol), 64% yield. **Physical State:** brown solid. **m.p.:** 88–90 °C. **R_f-value:** 0.5 (30% EtOAc/hexane). **¹H NMR (CDCl₃, 400 MHz):** δ 7.93 (d, J = 2.0 Hz, 1H), 7.68 (d, J = 8.4 Hz, 1H), 7.48–7.46 (m, 2H), 7.38–7.34 (m, 3H), 7.08 (d, J = 8.4 Hz, 1H), 3.93 (t, J = 6.8 Hz, 2H), 2.58 (t, J = 7.6 Hz, 2H), 2.22 (quint, J = 8.0 Hz, 2H). **¹³C NMR (CDCl₃, 100 MHz):** δ 175.2, 142.1, 140.3, 138.6, 131.8, 129.5, 129.3, 128.8, 123.4, 122.8, 95.9, 92.0, 84.9, 50.4, 31.8, 19.6. **IR (KBr, cm⁻¹):** 3437, 1653, 1260, 749. **HRMS (ESI) m/z:** [M+H]⁺ Calcd for C₁₈H₁₅INO: 388.0198; Found 388.0215.

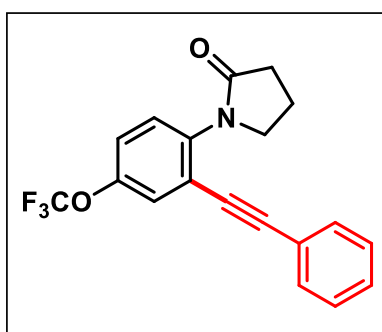


1-(2-(phenylethynyl)-4-

(trifluoromethyl)phenyl)pyrrolidin-2-one (3ma):

was prepared according to the general procedure (7b.5a). The crude reaction mixture was purified by column chromatography using silica gel (100-200

mesh size) giving 18 mg (0.1mmol) 55% yield. **Physical State:** brown solid. **m.p.:** 90–92 °C. **R_f-value:** 0.3 (40% EtOAc/hexane). **¹H NMR (CDCl₃, 400 MHz):** δ 7.86 (d, *J* = 2.0 Hz, 1H), 7.61 (q, *J* = 1.6 Hz, 1H), 7.51–7.49 (m, 3H), 7.39–7.36 (m, 3H), 4.01 (t, *J* = 7.2 Hz, 2H), 2.62 (t, *J* = 8.0 Hz, 2H), 2.26 (quint, *J* = 7.6 Hz, 2H). **¹³C NMR (CDCl₃, 100 MHz):** δ 175.2, 143.5, 131.9, 130.8 (q, *J* = 3.7 Hz), 129.9, 129.7, 129.4, 128.9, 128.3, 126.2 (q, *J* = 3.6 Hz), 122.6, 121.9, 96.2, 85.2, 50.3, 31.8, 19.7. **¹⁹F NMR (CDCl₃, 376 MHz):** –62.80. **IR (KBr, cm^{–1}):** 3437, 1638, 1274, 749. **HRMS (ESI) m/z:** [M+H]⁺ Calcd for C₁₉H₁₅F₃NO: 330.1106; Found 330.1127.



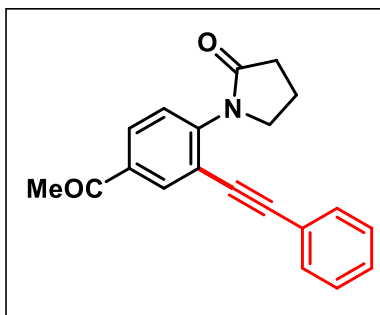
1-(2-(phenylethynyl)-4-

(trifluoromethoxy)phenyl)pyrrolidin-2-one (3na):

was prepared according to the general procedure (7b.5a). The crude reaction mixture was purified by column chromatography using silica gel (100-200

mesh size) giving 22 mg (0.1mmol), 64% yield. **Physical State:** brown solid. **m.p.:** 92–94 °C. **R_f-value:** 0.2 (30% EtOAc/hexane). **¹H NMR (CDCl₃, 400 MHz):** δ 7.50–7.48 (m, 2H), 7.44 (d, *J* = 2.0 Hz, 1H), 7.38–7.35 (m, 4H), 7.24–7.22 (m, 1H), 3.95 (t, *J* = 7.2 Hz, 2H), 2.60 (t, *J* = 7.6 Hz, 2H), 2.24 (quint, *J* = 7.6 Hz, 2H). **¹³C NMR (CDCl₃, 100 MHz):** δ 175.3, 148.0, 139.1, 131.9, 129.5, 129.4, 128.9, 125.8 (2C), 123.2, 122.6,

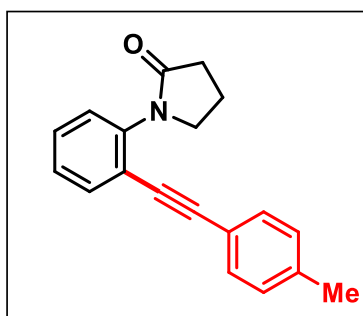
122.2, 95.9, 85.0, 50.5, 31.7, 19.6. **¹⁹F NMR (376 MHz, CDCl₃):** δ -57.88. **IR** (KBr, cm⁻¹): 3437, 1635, 1274, 748. **HRMS (ESI) m/z:** [M+H]⁺ Calcd for C₁₉H₁₅F₃NO₂: 346.1055; Found 346.1088.



1-(4-acetyl-2-(phenylethynyl)phenyl)pyrrolidin-

2-one (30a): was prepared according to the general procedure (7b.5a). The crude reaction mixture was purified by column chromatography using silica gel (100-200 mesh size) giving 11 mg (0.1mmol), 36%

yield. **Physical State:** orange solid. **m.p.:** 77–81 °C. **R_f-value:** 0.4 (20% EtOAc/hexane). **¹H NMR (CDCl₃, 400 MHz):** δ 8.17 (d, *J* = 1.4 Hz, 1H), 7.95 (d, *J* = 8.4 Hz, 1H), 7.51–7.48 (m, 3H), 7.38–7.37 (m, 3H), 4.03 (t, *J* = 7.0 Hz, 2H), 2.63–2.61 (m, 5H), 2.25 (quint, *J* = 7.7 Hz, 2H). **¹³C NMR (CDCl₃, 100 MHz):** δ 196.8, 175.2, 144.5, 135.9, 134.1, 131.8, 129.3, 129.1, 128.8, 127.8, 122.8, 121.2, 95.7, 85.8, 50.4, 31.9, 27.0, 19.8. **IR** (KBr, cm⁻¹): 3441, 1698, 1264, 746. **HRMS (ESI) m/z:** [M+H]⁺ Calcd for C₂₀H₁₈NO₂: 304.1338; Found 304.1329.

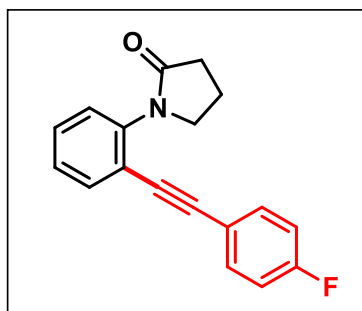


1-(2-(p-tolylethynyl)phenyl)pyrrolidin-2-one (3ab):

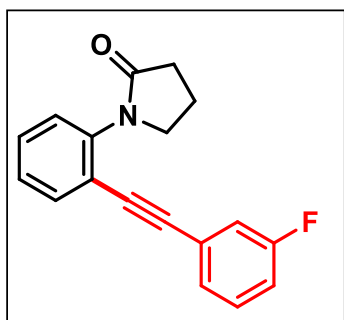
was prepared according to the general procedure (7b.5a). The crude reaction mixture was purified by column chromatography using silica gel (100-200 mesh size) giving 24 mg (0.1mmol), 87% yield.

Physical State: colourless liquid. **R_f-value:** 0.3 (40% EtOAc/hexane). **¹H NMR (CDCl₃, 400 MHz):** δ 7.58 (d, *J* = 7.6 Hz, 1H), 7.39–7.35 (m, 3H), 7.33–7.27 (m, 2H), 7.16 (d, *J* = 8.0 Hz, 2H), 3.95 (t, *J* = 7.2 Hz, 2H), 2.60 (t, *J* = 8.0 Hz, 2H), 2.23 (s, 3H), 2.22 (quint,

$J = 7.2$ Hz, 2H). **^{13}C NMR** (CDCl_3 , 100 MHz): δ 175.3, 140.5, 139.1, 133.5, 131.7, 129.5, 129.4, 128.0, 127.7, 121.1, 120.2, 94.7, 85.7, 50.6, 31.9, 21.8, 19.6. **IR** (KBr, cm^{-1}): 3437, 1686, 1266, 736. **HRMS (ESI) m/z** : $[\text{M}+\text{H}]^+$ Calcd for $\text{C}_{19}\text{H}_{18}\text{NO}$: 276.1388; Found 276.1400.

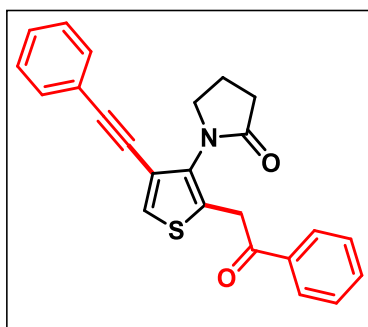


1-(2-((4-fluorophenyl)ethynyl)phenyl)pyrrolidin-2-one (3ad): was prepared according to the general procedure (7b.5a). The crude reaction mixture was purified by column chromatography using silica gel (100-200 mesh size) giving 15 mg (0.1mmol), 54% yield. **Physical State**: colourless liquid. **R_f -value**: 0.2 (30% EtOAc/hexane). **^1H NMR** (CDCl_3 , 400 MHz): δ 7.58 (d, $J = 7.4$ Hz, 1H), 7.48–7.45 (m, 2H), 7.41–7.37 (m, 1H), 7.33–7.27 (m, 2H), 7.05 (t, $J = 8.8$ Hz, 2H), 3.93 (t, $J = 7.2$ Hz, 2H), 2.59 (t, $J = 8.0$ Hz, 2H), 2.22 (quint, $J = 7.6$ Hz, 2H). **^{13}C NMR** (CDCl_3 , 100 MHz): δ 175.1, 163.0 (d, $J = 248.4$ Hz), 140.6, 133.7, 133.7, 133.6, 129.75, 127.8 (d, $J = 18.5$ Hz), 121.4, 119.4, 116.1 (d, $J = 21.9$ Hz), 93.4, 86.1, 50.7, 31.9, 19.7. **^{19}F NMR (376 MHz, CDCl_3)**: δ –110.28. **IR** (KBr, cm^{-1}): 3437, 1635, 1266, 748. **HRMS (ESI) m/z** : $[\text{M}+\text{H}]^+$ Calcd for $\text{C}_{18}\text{H}_{15}\text{FNO}_2$: 280.1138; Found 280.1161.



1-(2-((3-fluorophenyl)ethynyl)phenyl)pyrrolidin-2-one (3ae): was prepared according to the general procedure (7b.5a). The crude reaction mixture was purified by column chromatography using silica gel (100-200 mesh size) giving 14 mg (0.1mmol), 50%

yield. **Physical State:** orange liquid. **R_f-value:** 0.3 (30% EtOAc/hexane). **¹H NMR (CDCl₃, 400 MHz):** δ 7.60 (d, *J* = 7.6 Hz, 1H), 7.43–7.39 (m, 1H), 7.34–7.27 (m, 4H), 7.17 (d, *J* = 9.2 Hz, 1H), 7.08–7.04 (m, 1H), 3.94 (t, *J* = 7.2 Hz, 2H), 2.61 (t, *J* = 8.0 Hz, 2H), 2.24 (quint, *J* = 7.6 Hz, 2H). **¹³C NMR (CDCl₃, 175 MHz):** δ 175.2, 140.7, 133.7, 130.4, 130.4 (d, *J* = 8.7 Hz), 129.1, 128.0, 127.8, 127.7 (d, *J* = 2.9 Hz), 125.1 (d, *J* = 9.8 Hz), 121.1, 118.5 (d, *J* = 22.5 Hz), 116.3 (d, *J* = 21.0 Hz), 93.1, 87.3, 50.7, 31.8, 19.7. **¹⁹F NMR (376 MHz, CDCl₃):** δ –112.62. **IR (KBr, cm^{–1}):** 3437, 1635, 1274, 748. **HRMS (ESI) m/z:** [M+H]⁺ Calcd for C₁₈H₁₅FNO: 280.1138; Found 280.1127.

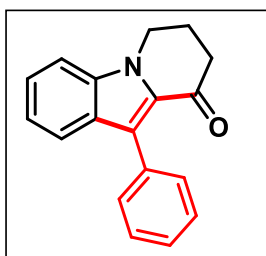


1-(2-(2-oxo-2-phenylethyl)-4-

(phenylethynyl)thiophen-3-yl)pyrrolidin-2-one (3pa):

was prepared according to the general procedure (7b.5a). The crude reaction mixture was purified by column chromatography using silica gel (100–200

mesh size) giving 35 mg (0.1 mmol), 91% yield. **Physical State:** brown liquid **R_f-value:** 0.4 (30% EtOAc/hexane). **¹H NMR (CDCl₃, 400 MHz):** δ 7.69 (s, 1H), 7.47–7.44 (m, 2H), 7.36–7.33 (m, 5H), 7.29–7.40 (m, 3H), 4.14 (m, 2H), 3.81 (t, *J* = 6.8 Hz, 2H), 2.57 (t, *J* = 8.0 Hz, 2H), 2.22 (quint, *J* = 7.2 Hz, 2H). **¹³C NMR (CDCl₃, 100 MHz):** δ 189.4, 175.7, 141.1, 135.3, 133.8, 132.7, 131.8, 129.9, 129.2, 129.0, 128.8, 127.5, 123.7, 122.6, 93.4, 81.3, 49.8, 48.0, 31.5, 19.8. **IR (KBr, cm^{–1}):** 3437, 1653, 1635, 1250, 748. **HRMS (ESI) m/z:** [M+Na]⁺ Calcd for C₁₆H₁₄NOS: 268.0796; Found 268.0825.

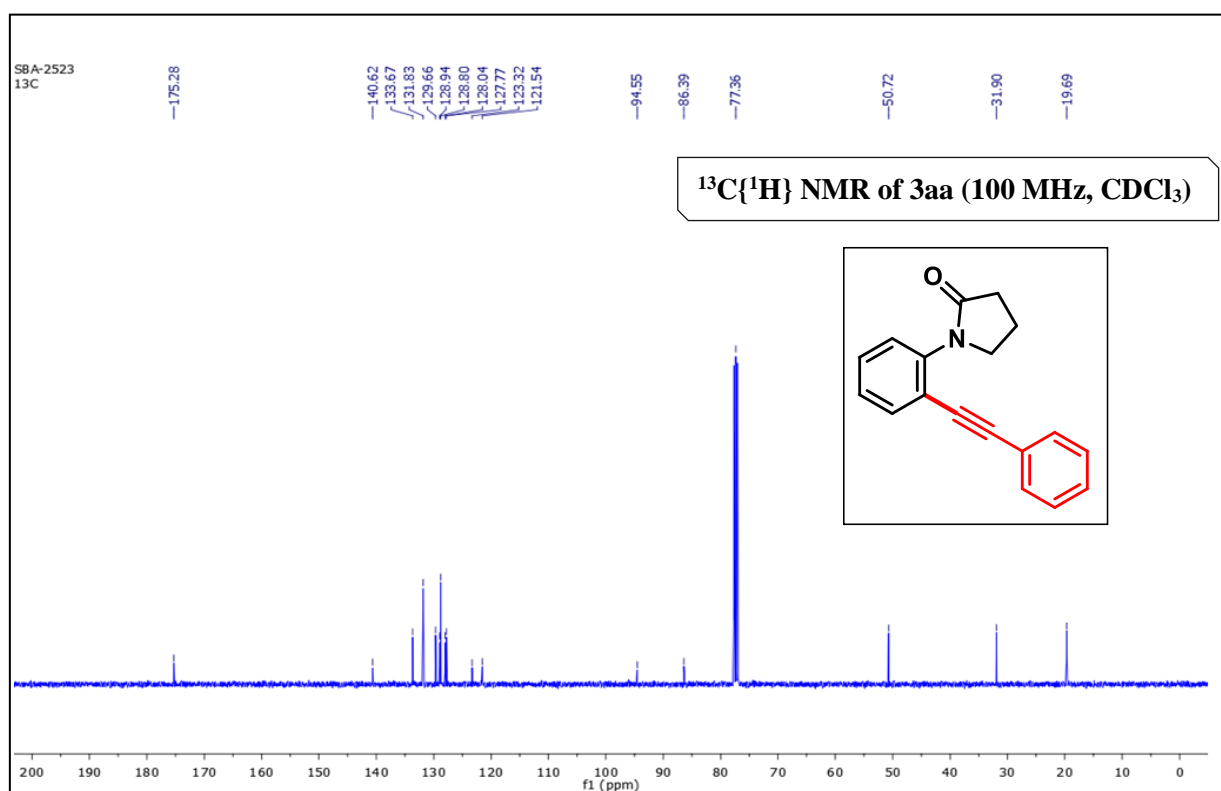
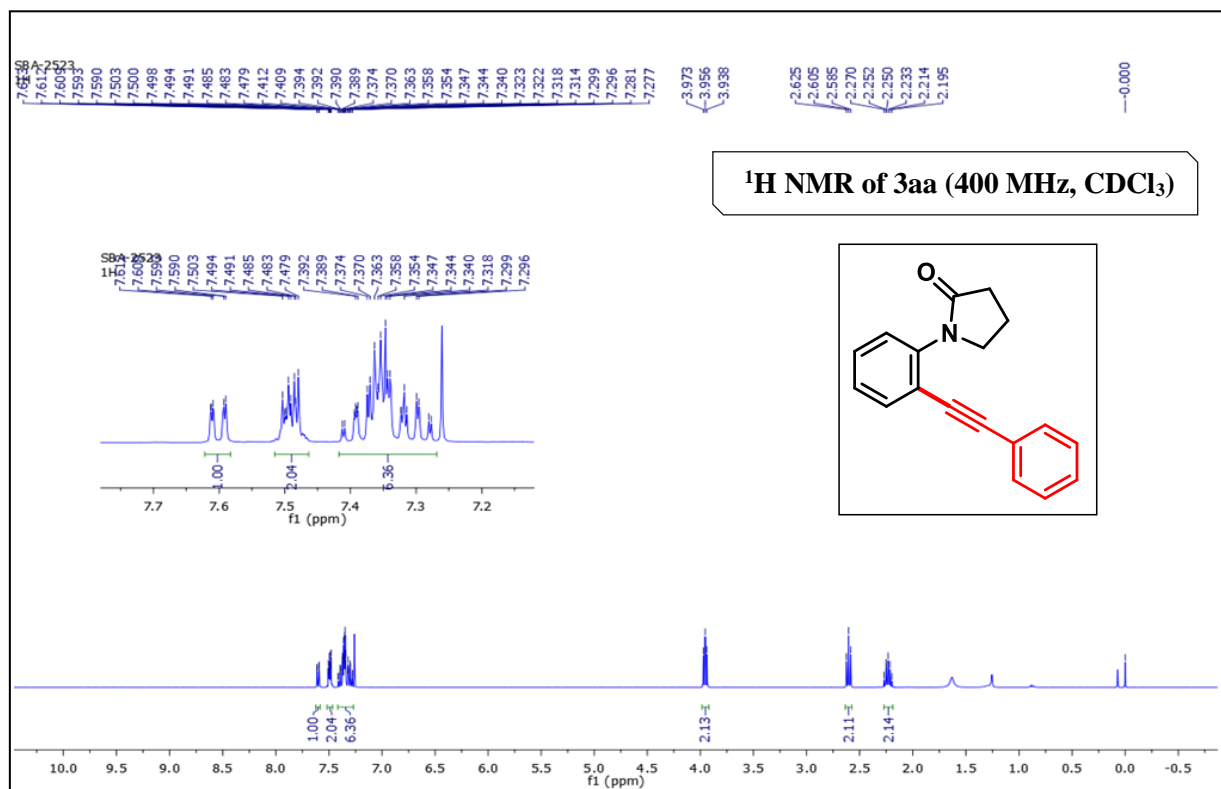


10-phenyl-7,8-dihydropyrido[1,2-a]indol-9(6H)-one (4aa):

was prepared according to reported procedure.²⁸ The crude reaction mixture was purified by column chromatography using silica gel (100-200 mesh size), giving 17 mg

(0.1mmol), 66% yield. **Physical State:** off-white solid **R_f -value:** 0.35 (30% EtOAc/hexane). **¹H NMR (CDCl₃, 400 MHz):** δ 7.71 (d, J = 8.4 Hz, 1H), 7.60 (d, J = 7.2 Hz, 2H), 7.47–7.35 (m, 5H), 7.19–7.15 (m, 1H), 4.32 (t, J = 6.0 Hz, 2H), 2.76 (t, J = 6.0 Hz, 2H), 2.43 (quint, J = 6.0 Hz, 2H). **¹³C NMR (CDCl₃, 100 MHz):** δ 190.1, 136.8, 133.8, 130.8, 128.6, 128.2, 127.6, 127.0, 126.5, 123.4, 122.8, 121.6, 110.5, 42.2, 38.4, 23.3. **HRMS (ESI) m/z:** [M+Na]⁺ Calcd for C₁₈H₁₆NO: 262.1232; Found 262.1219.

NMR spectra of 1-(2-(phenylethynyl)phenyl)pyrrolidin-2-one (3aa):



Crystals of the compounds **3ca** (1-(5-methoxy-2-(phenylethynyl)phenyl)pyrrolidin-2-one) were obtained after slow evaporation of methanol and dichloromethane.

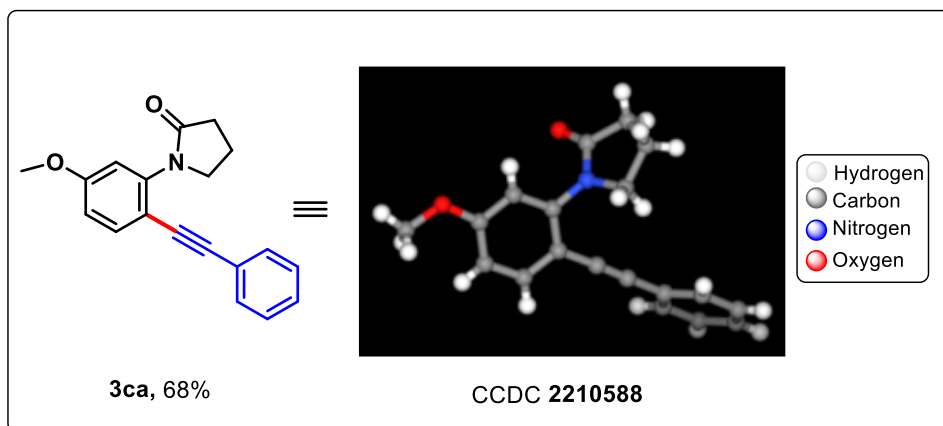
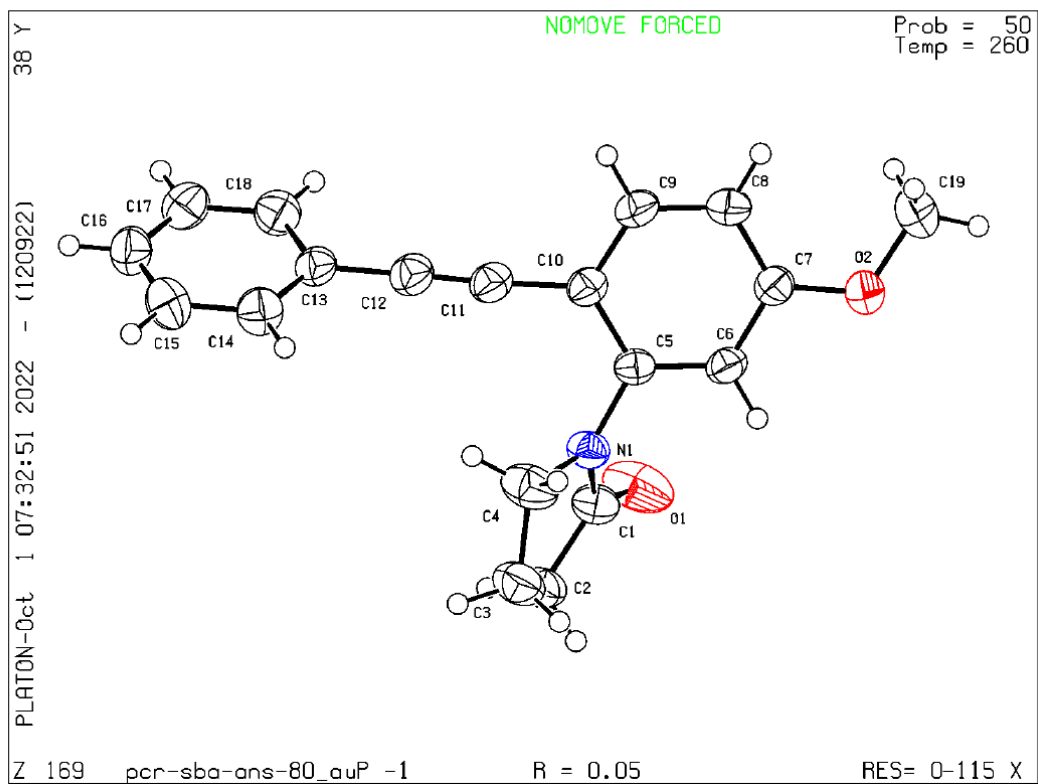


Figure 7b.2. Crystal structure of **3ca** (50% ellipsoid probability).

Datablock pcr-sba-ans-80_auto - ellipsoid plot

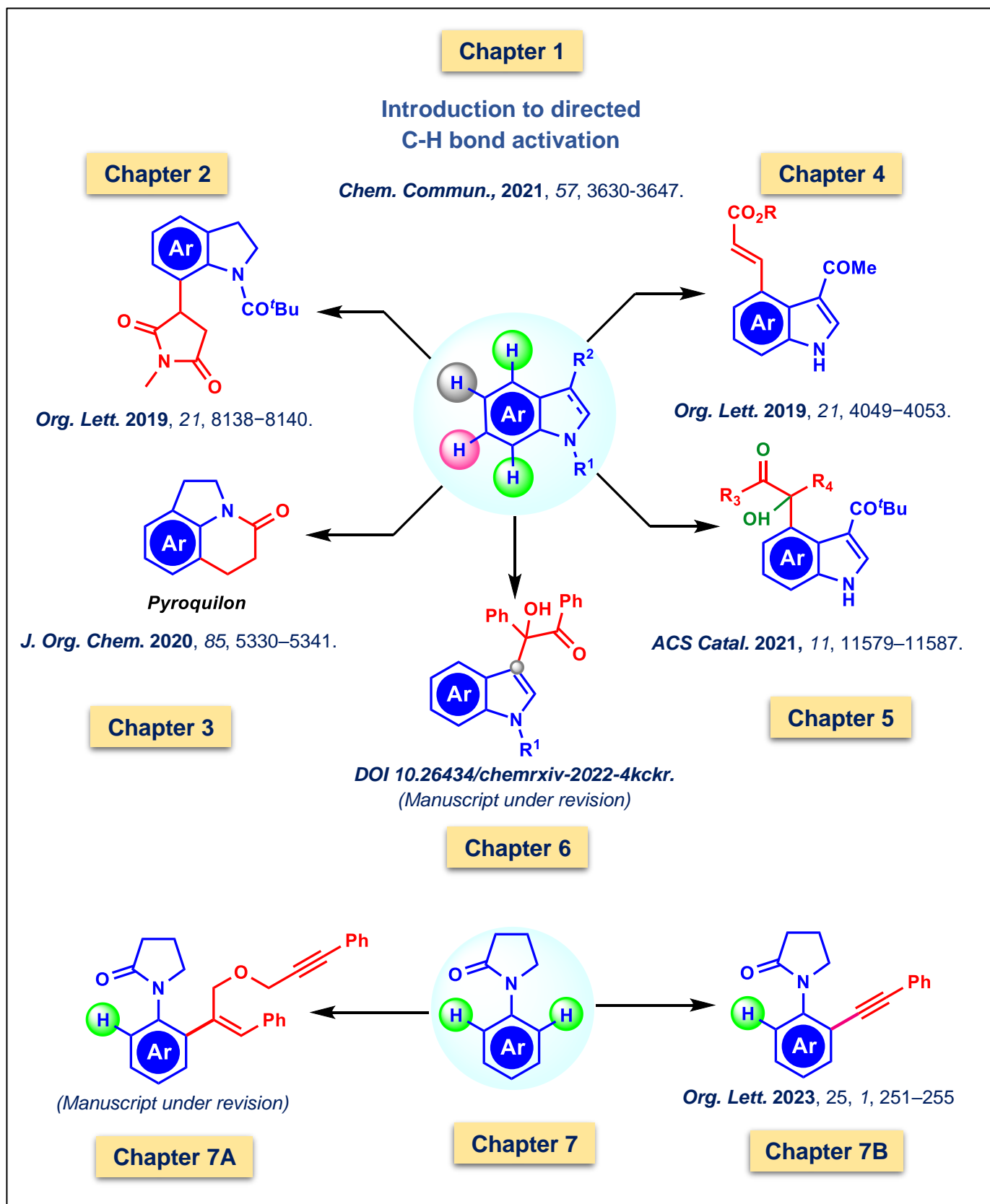


7b.5 REFERENCES

1. Boyd, D. B.; Foster, B. J.; Hatfield, L. D.; Hornback, W. J.; Jones, N. D.; Munroe, J. E.; Swartzendruber, J. K., γ -Lactam analogues of carbapenems. *Tetra. Lett.* **1986**, 27, 3457-3460.
2. Caruano, J.; Muccioli, G. G.; Robiette, R., Biologically active γ -lactams: synthesis and natural sources. *Org. Biom. Chem.* **2016**, 14, 10134-10156.
3. Xi, N.; Arvedson, S.; Eisenberg, S.; Han, N.; Handley, M.; Huang, L.; Huang, Q.; Kiselyov, A.; Liu, Q.; Lu, Y.; Nunez, G.; Osslund, T.; Powers, D.; Tasker, A. S.; Wang, L.; Xiang, T.; Xu, S.; Zhang, J.; Zhu, J.; Kendall, R.; Dominguez, C., N-Aryl- γ -lactams as integrin $\alpha v\beta 3$ -antagonists. *Bioorg. & Med. Chem. Lett.* **2004**, 14, 2905-2909.
4. Gensch, T.; Hopkinson, M. N.; Glorius, F.; Wencel-Delord, J., Mild metal-catalyzed C-H activation: examples and concepts. *Chem. Soc. Rev.* **2016**, 45, 2900-2936.
5. Roudesly, F.; Oble, J.; Poli, G., Metal-catalyzed C-H activation/functionalization: The fundamentals. *J. Mol. Catal. A: Chem.* **2017**, 426, 275-296.
6. Banjare, S. K.; Nanda, T.; Pati, B. V.; Biswal, P.; Ravikumar, P. C. O-Directed C-H functionalization via cobaltacycles: a sustainable approach for C-C and C-heteroatom bond formations. *Chem. Commun.* **2021**, 57, 3630-3647. (b) Mandal, R.; Garai, B.; Sundararaju, B. Weak-Coordination in C-H Bond Functionalizations Catalyzed by 3d Metals. *ACS Catal.* **2022**, 12, 3452-3506.
7. (a) Banjare, S. K.; Chebolu, R.; Ravikumar, P. C. Cobalt Catalyzed Hydroarylation of Michael Acceptors with Indolines Directed by a Weakly Coordinating Functional Group. *Org. Lett.* **2019**, 21, 4049-4053. (b) Banjare, S. K.; Nanda, T.; Ravikumar, P. C. Cobalt-Catalyzed Regioselective Direct C-4 Alkenylation of 3-Acetylindole with Michael Acceptors Using a Weakly Coordinating Functional Group. *Org. Lett.* **2019**, 21, 8138-8143. (c) Banjare, S.-K.; Biswal, P.; Ravikumar, P. C. Cobalt-Catalyzed One-Step Access to Py-roquilon and C-7 Alkenylation of Indoline with Activated Alkenes Using Weakly Coordinating Functional Groups. *J. Org. Chem.* **2020**, 85, 5330-5341. (d) Banjare, S. K.; Nanda, T.; Pati, B. V.; Adhikari, G. K. D.; Dutta, J.; Ravikumar, P. C. Breaking the Trend: Insight into Unforeseen Reactivity of Alkynes in Cobalt-Catalyzed Weak Chelation-Assisted Regioselective C(4)-H Functionalization of 3-Pivaloyl Indole. *ACS Catal.* **2021**, 11, 11579-11587.
8. Banjare, S. K.; Mahulkar, P. S.; Nanda, T.; Pati, B. V.; Najjar, L. O.; Ravikumar, P. C., Diverse reactivity of alkynes in C-H activation reactions. *Chem. Comm.* **2022**, 58, 10262-10289.
9. Xie, F.; Qi, Z.; Yu, S.; Li, X., Rh(III)- and Ir(III)-Catalyzed C-H Alkynylation of Arenes under Chelation Assistance. *J. Am. Chem. Soc.* **2014**, 136, 4780-4787.
10. Tan, E.; Quinone, O.; Elena de Orbe, M.; Echavarren, A. M., Broad-Scope Rh-Catalyzed Inverse-Sonogashira Reaction Directed by Weakly Coordinating Groups. *ACS Catal.* **2018**, 8, 2166-2172.
11. Tan, E.; Zanini, M.; Echavarren, A. M., Iridium-Catalyzed β -Alkynylation of Aliphatic Oximes as Masked Carbonyl Compounds and Alcohols. *Angew. Chem., Int. Ed.* **2020**, 59, 10470-10473.
12. Tan, E.; Montesinos-Magraner, M.; García-Morales, C.; Mayans, J. G.; Echavarren, A. M., Rhodium-catalyzed *ortho*-alkynylation of nitroarenes. *Chem. Sci.* **2021**, 12, 14731-14739.
13. (a) Sauermann, N.; González, M. J.; Ackermann, L., Cobalt(III)-Catalyzed C-H Alkynylation with Bromoalkynes under Mild Conditions. *Org. Lett.* **2015**, 17, 5316-5319. (b) Fang, S.; Jiang, G.; Li, M.; Liu, Z.; Jiang, H.; Wu, W., Palladium-catalyzed regioselective C-H alkynylation of indoles with haloalkynes: access to functionalized 7-alkynylindoles. *Chem. Comm.* **2019**, 55, 13769-13772.
14. (a) Tobisu, M.; Ano, Y.; Chatani, N. Palladium-Catalyzed Direct Alkynylation of C-H Bonds in Benzenes. *Org. Lett.* **2009**, 11, 3250-3252. (b) Tan, E.; Quinone, O.; Elena de Orbe, M.; Echavarren, A. M. Broad-Scope Rh-Catalyzed Inverse-Sonogashira Reaction Directed by Weakly Coordinating Groups. *ACS Catal.* **2018**, 8, 2166-2172. (c) Wu, G. C.; Ouyang, W. S.; Chen, Q.;

-
- Huo, Y. P.; Li, X. W. Cross-dehydrogenative alkynylation of sulfonamides and amides with terminal alkynes via Ir(III) catalysis. *Org. Chem. Front.* **2019**, *6*, 284–289.
15. Ye, X.; Wang, C.; Zhang, S.; Wei, J.; Shan, C.; Wojtas, L.; Xie, Y.; Shi, X. Facilitating Ir-Catalyzed C-H Alkynylation with Electrochemistry: Anodic Oxidation-Induced Reductive Elimination. *ACS Catal.* **2020**, *10*, 11693–11699.
16. (a) Wu, Y.-J.; Xie, P.-P.; Zhou, G.; Yao, Q.-J.; Hong, X.; Shi, B.-F. Atroposelective Synthesis of N-aryl Peptoid Atropisomers via a Palladium(II)-catalyzed Asymmetric C–H Alkynylation Strategy. *Chem. Sci.* **2021**, *12*, 9391–9397 (b) A. Suseelan Sarala, S. Bhowmick, R. L. de Carvalho, S. A. Al-Thabaiti, M. Mokhtar, E. N. da Silva Júnior and Maiti, D., Transition-Metal-Catalyzed Selective Alkynylation of C–H Bonds. *Ad. Syn. & Catal.*, **2021**, *363*, 4994–5027. (c) Tan, E.; Zanini, M.; Echavarren, A. M. Iridium-Catalyzed beta-Alkynylation of Aliphatic Oximes as Masked Carbonyl Compounds and Alcohols. *Angew. Chem., Int. Ed.* **2020**, *59*, 10470–10473. (d) Tan, E.; Konovalov, A. I.; Fernandez, G. A.; Dorel, R.; Echavarren, A. M. Ruthenium-catalyzed peri- and ortho-alkynylation with bromoalkynes via insertion and elimination. *Org. Lett.* **2017**, *19*, 5561–5564.
17. Simmons, E. M.; Hartwig, J. F. On the Interpretation of Deuterium Kinetic Isotope Effects in C-H Bond Functionalizations by Transition-Metal Complexes *Angew. Chem., Int. Ed.* **2012**, *51*, 3066–3072.
18. G. Li, X. Huang and L. Zhang, Platinum-Catalyzed Formation of Cyclic-Ketone-Fused Indoles from N-(2-Alkynylphenyl)lactams. *Angew. Chem., Int. Ed.*, **2008**, *47*, 346–349.

SUMMARY OF THESIS



About the Author



Shyam Kumar Banjare received his BSc and MSc degrees from Bilaspur University in the years 2013 and 2015, respectively. He served as an ad-hoc faculty in Organic Chemistry from 2016 to 2017 at Central University, GGV, Bilaspur. Then, he joined as a junior research fellow on 2nd January 2018 under the supervision of Prof. Ponneri C. Ravikumar at NISER, Bhubaneswar. He has worked as a senior research scholar January 2020 onwards. He has submitted his thesis on 9th December, 2022. His research interest is focused on catalytic chemistry for the “Development of sustainable & eco-friendly first-row transition metal-catalysed C–H/C–C bond functionalization through weak chelation.”